

University of Nottingham
UK | CHINA | MALAYSIA

Exploring the Potential of Cyanobacteria to Produce Extracellular Polymeric Substances

Thesis submitted to the University of Nottingham for the degree of Doctor of Philosophy

Christine Sophie Steffen

Supervisors: Dr Konstantina Kourmentza, Dr Yanming Wang, Professor Jon McKechnie

Department of Chemical and Environmental Engineering, Faculty of Engineering, University of Nottingham

April 2026

Table of Contents

Abstract ix

Acknowledgments xi

List of Abbreviations xii

List of Figures xv

List of Tables xxv

Chapter 1: Introduction 1

Chapter 2: Literature review 4

2.1 The Physiological Role of EPS in Natural Environments 4

2.2 Types, Composition and Properties of Cyanobacterial EPS 5

2.2.1 Composition of Cyanobacterial EPS 7

2.2.2 Characterisation Methods of EPS 15

2.2.3 Properties and Structure-Function Relationship of EPS 16

2.2.3.1 Emulsifying Activity 17

2.2.3.2 Flocculating Activity 19

2.2.3.3 Antioxidant Activity 21

2.2.3.4 Metal-Chelating Properties 24

2.2.3.5 UV-Protective Properties 26

2.2.4 Biosynthesis Pathways of Cyanobacterial EPS 28

2.3 Influence of Culture Conditions on EPS Production in Cyanobacteria 31

2.3.1 Impact of Light Intensity, Wavelength, and Photoperiod on EPS Production 33

2.3.1.1 Effect of light intensity on EPS production 33

2.3.1.2 Effect of light colour and photoperiod on EPS production 35

2.3.2 Effect of Temperature on EPS Production 36

2.3.3 Influence of pH on EPS Production 37

2.3.4 Effect of Medium Composition on EPS Production 38

2.3.4.1 Effect of Nitrogen on EPS Production 38

2.3.4.2 Effect of Phosphorus on EPS Production 40
2.3.4.3 Effect of Magnesium on EPS Production 41
2.3.4.4 Effect of Iron on EPS Production 42
2.3.4.5 Effect of Boron, Calcium and Potassium on EPS Production 43
2.3.4.6 Effect of Sodium Chloride and Ozone on EPS Production 44
2.3.5 Role of Cultivation Mode in EPS Production 46
2.3.6 Impact of Culture Conditions on EPS Composition and Properties 50
2.3.7 Complexity of Interdependent Cultivation Parameters on EPS Production 52
2.4 Industrial-Scale Production of EPS from Cyanobacteria 54
2.4.1 Upstream Processes: Cultivation Systems 54
2.4.2 Downstream Processing in Cyanobacterial EPS Production 58
2.4.3 Economic Feasibility and Market Potential 61
2.4.4 The Biorefinery Approach in EPS Production 62
2.4.1 Techno-Economic Assessments of Algal Biorefineries 63
2.4.1.1 Scenario Analysis 64
2.4.1.2 Sensitivity Analysis 64
2.4.1.3 Techno-Economic Assessments of Industrial-Scale EPS Production with Cyanobacteria in Literature 65
Chapter 3: Research Aims and Objectives 67
Chapter 4: Materials and Methodgs 73
4.1 Screening Novel Cyanobacteria for EPS and Biomass Production 73
4.1.1 Cyanobacterial Species 73
4.1.1.1 Species Selection Based on Culture Collection Availability and Literature 73
4.1.1.2 Final Selection of Species for Experimental Use 74
4.1.2 Growth Conditions of Screening Experiment 75
4.1.3 Biomass Sample Processing and Dry Cell Weight Quantification 76
4.1.4 EPS Recovery, Purification and Quantification 77
4.1.5 Characterisation of EPS 78

4.1.5.1 Carbohydrate Content determination using the Phenol-Sulphuric Acid Method ... 78
4.1.5.2 Protein Content determination using the Bradford Assay ... 78
4.1.5.3 Sulphate Content determination using the Barium Chloride Gelatine Test ... 79
4.1.5.4 Hydrolysis of EPS and Neutralisation ... 80
4.1.5.5 Monosaccharide Analysis ... 80
4.1.6 Analysis of EPS Properties ... 83
4.1.6.1 Cyanobacterial Species and Growth Conditions for EPS Properties Analysis ... 83
4.1.6.2 Emulsifying Activity Assay ... 83
4.1.6.3 Flocculating Activity Assay ... 84
4.1.6.4 Antioxidant Activity Assays ... 85
4.1.6.5 Iron-Chelating Assay ... 86
4.1.6.6 Photoprotection Assay (UV/vis Spectrophotometry) ... 87
4.1.7 Statistical Analysis ... 87
4.1.7.1 Statistical Significance ... 87
4.1.7.2 Limit of Detection (LOD) and Limit of Saturation (LOS) ... 88
4.1.7.3 Correlation between Properties and Composition ... 88
4.2 Optimisation of Cultivation Conditions ... 90
4.2.1 Single-Factor Optimisation of Light Intensity at 60% Working Volume ... 90
4.2.2 Effect of Working Volume on *C. brevissima* and *N. foliaceum* ... 90
4.2.3 Single-Factor Optimisation of Light Intensity at 25% working volume ... 91
4.2.4 Single-Factor Optimisation of BG-11 Media Components ... 91
4.2.5 Multi-Factor Optimisation using Design of Experiments (DoE) ... 92
4.2.6 Two-Factor Optimisation (Light Duration and Light Intensity) for *C. brevissima* ... 95
4.2.7 Systematic Evaluation of the Effect of Light Intensity and Temperature on EPS Production by *C. brevissima* ... 96
4.2.7.1 Validation of Optimised Conditions (Light and Temperature) for *C. brevissima* ... 97
4.2.7.2 Lipid Content Assay (Phospho-Vanillin Method) ... 97
4.3 Scale-Up to 1L Photobioreactors (PBRs) ... 98

4.3.1 Light Calibration and Equalisation of Light Intensity Across White and Coloured Light Tiles 98
4.3.2 Effects of Airflow Rate and Light Intensity on EPS Production by *C. brevissima* 98
4.3.3 Impact of CO_2 Flow Rate and Light Intensity on EPS Production by *C. brevissima* 100
4.3.4 Effect of Light Colour (Green, Blue, Red) on EPS Production by *C. brevissima* 101
4.3.5 Axenic PBR Experiment: Comparing CO_2 and Air Effects on *C. brevissima* 102
4.4 Techno-Economic Assessment 106
4.4.1 Real-Life Facility Basis for PBR Design 106
4.4.2 Baseline Scenario Process Design: Tubular PBR with Filtration 107
4.4.2.1 Upstream Process Design in SPD 109
4.4.2.2 Downstream Process Design 111
4.4.3 Calculation Methodology 114
4.4.3.1 Photobioreactor Mass Balance calculation 114
4.4.3.2 Upstream Major Equipment Cost calculation 115
4.4.3.3 Upstream Utilities calculation 116
4.4.3.3.1 Electricity Consumption of LED lights Calculation 116
4.4.3.3.2 Circulation Pump Power Calculation 117
4.4.3.3.3 Amount of Heating and Cooling Water Calculation 118
4.4.3.4 Labour Costs calculation 120
4.4.3.5 Minimum Selling Price (MSP) and Cash Flow Calculations 120
4.4.3.6 Contributing factors to MSP calculation 123
4.4.3.7 Profitability analysis 123
4.4.3.8 Price Adjustments Based on Reference Year 124
4.4.4 Scenario Analysis 124
4.4.4.1 Effect of Batch vs. Semi-Continuous on MSP 125
4.4.4.2 Effect of Downstream Processing on MSP 126
4.4.4.3 Effect of Cultivation Systems on MSP 129

4.4.4.4 Effect of Growth Mode (Photoautotrophic vs. Mixotrophic) on MSP 131
4.4.4.5 Alternative Cyanobacterial Species Scenario: *N. foliaceum* 132
4.4.4.6 Alternative Product Scenario: Cosmeceutical Product 133
4.4.5 Sensitivity Analysis 133
4.4.6 Summary of Assumptions 135
Chapter 5: Screening Novel Cyanobacteria for EPS Production 139
5.1 Chapter Overview 139
5.2 EPS and Biomass Production of Screened Cyanobacterial Species 139
5.3 Composition of EPS from Novel Species 147
5.3.1 Sugar, Protein, and Sulphate Content of Novel EPS 147
5.3.2 Monosaccharide Composition of Novel EPS 154
5.4 Selection of Seven Novel Cyanobacteria Species for EPS Properties Analysis 163
5.5 Functional Properties of Novel EPS 164
5.5.1 Emulsifying Activities 164
5.5.2 Flocculating Properties 166
5.5.3 Antioxidant Activities 171
5.5.4 Iron-Chelating Properties 176
5.5.5 UV-protective Properties 179
5.6 Correlation Between EPS Composition and Properties 183
5.7 Selection of Species for Cultivation Conditions Optimisation 187
Chapter 6: Optimisation of Cultivation Conditions 190
6.1 Chapter Overview 190
6.2 Effect of Light Intensity at 60% Working Volume *C. brevissima* 190
6.2.1 EPS and Biomass Production 190
6.2.2 Comparative Analysis of Film-like and Cotton-like Appearance of *C. brevissima* EPS 194
6.3 Impact of Light Intensity at 60% Working Volume *N. foliaceum* 198

6.4 Influence of Working Volume on *C. brevissima* and *N. foliaceum* DCW and EPS 201

6.5 Effect of Light Intensity at 25% Working Volume 207

6.6 Impact of BG-11 Media Composition and pH 210

6.7 Multi-Factor Optimisation Results for *N. foliaceum* 216

6.8 Biomass and EPS production of *N. foliaceum* under Optimised Conditions 223

6.9 Multi-Factor Optimisation Results for *C. brevissima* 226

6.10 Phototrophic Optimisation Experiments for EPS production of *C. brevissima* 234

6.10.1 Combined Effect of Light Duration and Light Intensity on *C. brevissima* DCW and EPS 234

6.10.2 Systematic Evaluation of the Effect of Light Intensity and Temperature on *C. brevissima* DCW and EPS 238

6.10.3 DCW and EPS of *C. brevissima* Under Optimised Light and Temperature Conditions over Time 241

6.10.4 Emulsifying Properties and Lipid Content of EPS under Optimised Conditions 244

6.11 Selection of Species for Scale-Up Studies 247

Chapter 7: Scale-Up to 1L Photobioreactors 249

7.1 Chapter Overview 249

7.2 Preparatory Work for 1-Litre PBRs 249

7.2.1 Light Calibration 249

7.2.2 Adjustment of PBR Aeration System, Sampling Strategy and Sterilisation and Inoculation Procedure 251

7.3 Effects of Airflow Rate and Light Intensity on EPS and DCW 251

7.4 Effects of CO_2 Flow Rate and Light Intensity on EPS and DCW in 1L PBR 255

7.5 Impact of Light Colour (Red, Green, Blue) on EPS Production in 1L PBR 259

7.6 Limitations of the Xanthella PBR System 262
7.7 Influence of CO_2 on EPS and DCW under Axenic Conditions 265
7.8 Selection of Species for Techno-Economic Assessment 269
Chapter 8: Economic Evaluation of Industrial-scale EPS Production Process .. 270
8.1 Chapter Overview 270
8.2 Market Analysis Outcomes for Bioemulsifier 270
8.3 Baseline Scenario Results 272
8.3.1 PBR Utilities of Baseline Scenario 273
8.3.2 Investment and Operating cost of Baseline Scenario 275
8.3.3 Cash Flow Analysis of Baseline Scenario 280
8.3.4 Profitability Analysis of Baseline Scenario 282
8.4 Scenario Analysis Results 283
8.4.1 Effect of Operation Mode (Batch vs. Semi-Continuous) on MSP 284
8.4.2 Effect of Downstream Processing on MSP 286
8.4.3 Effect of Cultivation Systems on MSP 290
8.4.4 Effect of Mixotrophic (Glucose) Growth Mode on MSP 294
8.4.5 Alternative Species Scenario: *Nostoc foliaceum* 302
8.4.6 Alternative Product Scenario: Cosmeceutical Product 306
8.5 Sensitivity Analysis Results 311
Chapter 9: Discussion 315
9.1 Chapter Overview 315
9.2 Screening Novel Cyanobacteria for EPS with Functional Properties 315
9.3 Culture Conditions Optimisation 320
9.4 Challenges Encountered During Scale-Up 322
9.5 Physiological Role of EPS with Emulsifying Properties in *C. brevissima* ... 325
9.6 Techno-Economic Implications and Commercial Potential 326
9.7 Future Research For Commercialising Cyanobacterial EPS 330
Chapter 10: Conclusions 333

Chapter 11: Bibliography 335

Chapter 12: Appendix 353

12.1 Calibration Curves of Detection of EPS composition and properties assays 353

12.2 Trendline Equations and Limit of Detection of EPS composition and properties assays 358

12.3 Establishing Axenic Cultures 360

12.4 Media Compositions 363

12.5 Media Compatibility Testing 367

12.6 Thermal Degradation Behaviour of Novel Cyanobacteria 369

12.7 Scanning Electron Microscopy (SEM) Pictures Novel Cyanobacteria 372

12.8 Comparative Analysis of Film-like and Cotton-like Appearance of *C. brevissima* EPS 375

12.8.1 Thermogravimetric Analysis (TGA) 375

12.8.2 Scanning Electron Microscopy (SEM) 376

12.8.1 Differential Scanning Calorimetry (DSC) 377

12.9 UV-absorbance of EPS from *Calothrix brevissima* Cultivated Under High Light 381

12.10 Sterilisation and Inoculation Procedures for PBRs 382

12.11 Conference Presentations and Posters 384

12.11.1 Oral Presentations 384

12.11.2 Conference Posters 384

Abstract

Cyanobacterial extracellular polymeric substances (EPS) are natural compounds with potential for various biotechnological applications, due to their versatile properties, including emulsifying, flocculating, gelling, and bioactive effects (e.g., antiviral, antimicrobial, immunomodulatory). The aim of this PhD thesis was to attain an economically feasible EPS production process with cyanobacteria. The research focused on screening novel cyanobacterial species regarding their EPS production, optimisation of cultivation conditions of the most promising species, scaling up EPS production in 1-litre photobioreactors (PBR), and assessing the profitability of an industrial-scale EPS production process by performing a techno-economic assessment.

During the microbial selection, the majority of the 15 novel cyanobacterial species were found to produce considerable amounts of EPS (up to 1.79 ± 0.15 g L^{-1} (n=2) after 60 days). Subsequent EPS characterisation revealed the presence of sulphate, rare monosaccharides (such as fucose and rhamnose), pentoses (arabinose, xylose) and glucuronic acid. EPS properties analysis of the seven most efficient species was performed, revealing that the EPS exhibited flocculating, emulsifying, UV-protective, metal-chelating and antioxidant properties. The results of the emulsifying assay were noteworthy, as three species reached emulsifying activities above 64%, which was similar to the synthetic emulsifier Tween20 (64 ± 1%, n=3), and 2-fold higher than xanthan gum (26 ± 1%, n=3). Two species with emulsifying properties were selected for culture condition optimisation: *Calothrix brevissima*, which reached the highest EPS concentration in the screening experiment, and *Nostoc foliaceum*, which contained the highest amount of the deoxysugar fucose.

Phototrophic single-factor optimisation of light intensity increased the EPS concentration of *C. brevissima* to 1.72 ± 0.14 g L^{-1} (n=2) on day 21, doubling the EPS productivity to 81.1 ± 6.6 mg L^{-1} d^{-1} (n=2) compared to the screening experiment. Mixotrophic multi-factor optimisation of light intensity, temperature and glucose concentration increased the concentration to 2.65 ± 0.07 g L^{-1} (n=2) on day 14, which represented a six-fold increase in the EPS productivity (189.3 ± 4.8 mg L^{-1} d^{-1}, n=2) compared to the screening experiment. In *N. foliaceum*, multi-factor optimisation of light intensity, temperature and glucose concentration resulted in an EPS

concentration of 0.70 ± 0.04 g L^{-1} (n=3) on day 14, corresponding to an EPS productivity of 49.7 ± 2.8 mg L^{-1} d^{-1} (n=3), which represented a 4-fold increase compared to the screening experiment. The combination of these three factors in a multi-optimisation is novel and represents the first approach of its kind.

Scaling-up EPS production of *C. brevissima* in 1-litre photobioreactors (PBRs) with CO_2-supplemented phototrophic growth increased biomass productivity to 361.8 ± 34.4 mg L^{-1} d^{-1} (n=2), corresponding to a dry cell weight of 2.53 ± 0.24 g L^{-1} (n=2) on day 7. However, EPS productivity decreased substantially compared to shake flasks, remaining below 45.9 ± 3.1 mg L^{-1} d^{-1} (n=2), with EPS concentrations of less than 0.51 ± 0.23 g L^{-1} (n=2). Airflow rate, CO_2 flow rate, and light colour were optimised, and modifications to maintain axenicity addressed some PBR limitations, yet EPS production remained low.

Market analysis highlighted the growth potential for EPS-based bioemulsifiers within the expanding 4.70 billion USD emulsifier market, emphasising advantages such as biodegradability and low toxicity. A screening level analysis of the techno-economics of an industrial EPS production process revealed the PBRs and lights as major cost drivers, causing 86% of equipment cost and 78% of the electricity costs. This techno-economic assessment is the first-of-its-kind. From various EPS production scenarios, outdoor production in bag PBRs using natural light and mixotrophic (aeration and glucose) conditions emerged as the only profitable scenario. This scenario led to a net present value (NPV) of 42,600,000 USD and a profitability index (PI) of 2.4. The resulting minimum selling price of 12 USD kg^{-1} EPS was below a similar commercial product, a seaweed-based bioemulsifier (73 USD kg^{-1}), but above lecithin (8.99 USD kg^{-1}) and Tween 20 (1.64 USD kg^{-1}). A cosmeceutical alternative gave a PI of 7.4 and an NPV of 892 million USD, which was about three-fold and seven-fold higher respectively.

This PhD thesis demonstrates the potential of underexplored cyanobacterial species in producing functional EPS, and suggests that, while bioemulsifier production faces economic challenges, the development of high-value cosmeceuticals may offer more promising opportunities for future research and commercialisation.

Acknowledgements

I would like to express my heartfelt gratitude to everyone who has supported me throughout my PhD journey. First and foremost, I would like to thank my supervisors, Dr Konstantina (Nadia) Kourmentza, Dr Yanming Wang, Prof Jon McKechnie and Prof Alex Conradie, for being the most supportive and motivating advisors I could have wished for. Your mentorship, guidance, insight and encouragement has been invaluable for completing this PhD and for my growth as a researcher. I would like to extend my sincere gratitude to Dr Joshua Reid, Darrell Cobon, Bradley Hopkins, and Lorelei Robertson for their expertise and dedication in performing HPAEC-PAD, DSC, TGA and SEM analyses. Their commitment and expertise provided essential data that significantly advanced my research and made a substantial contribution to my PhD. I would also like to thank Prof Gleb Yakubov for his for insights, which have greatly enriched my work. I would also like to thank Dr Simone Morra for his support, kindness, and patience, always ready to help when needed. I am grateful to Amy Pearson, Dr Lifang Zhang, and Dr Steve Hall for their technical support in the laboratory, whose expertise and dedication were essential to the success of this research. I am thankful to Prof Rachel Gomes and Donna Astill for their support, understanding, and encouragement throughout my PhD journey. Thank you to Dr Douglas McKenzie, and Alyn McKenzie from Xanthella Ltd, Dr Andrew Spicer from Algenuity and Wieger Rupert from Lgem, for their technical support with the photobioreactors and photo-incubators. I am grateful to University of Nottingham for the resources provided throughout this project, and to FROG for the financial support that made this research possible. I would like to thank my lab mates for always having an open ear and helping to collect samples during conference-related absences, ensuring my research stayed on track. I am deeply grateful for my dear friends, especially Tatiana, Robyn, Alessandro and Candice, for always making me smile; you made my time in Nottingham! My sincerest gratitude goes to my family; to my brother Lennart, my sister Carolina, my sister-in-law Xiaozao, my father Hartwig, and especially to my mother Susanne, who made me the person I am today, thank you so much for your unwavering support, encouragement and belief in me.

List of abbreviations

ABTS – 2,2'-Azino-Bis(3-Ethylbenzothiazoline-6-Sulfonic Acid)

ATCC – American Type Culture Collection

AU – Arbitrary Units

BHA – Butylated Hydroxyanisole

BHT – Butylated Hydroxytoluene

BSA – Bovine Albumin Serum

C^- – Negative Control

C^+ – Positive Control

CapEx – Capital Expenditure

CCAP – Culture Collection of Algae and Protozoa

CFA – Cash Flow Analysis

CFV – Cross Flow Velocity

CIP – Clean-In-Place

CPS – Cell-bound Extracellular Polymeric Substances

Da – Dalton

DCW – Dry Cell Weight

DFC – Discounted Cash Flow

DHA – Docosahexaenoic Acid

DoE – Design of Experiments

DPPH – 2,2-Diphenyl-1-Picrylhydrazyl

DSC – Differential Scanning Calorimetry

EDTA – Ethylenediaminetetraacetic Acid

EPS – Extracellular Polymeric Substances

GP – Gross Profit

GTs – Glycosyltransferases

HCIP – Harmonization of Consumer Index Prices

HEPES – 4-(2-Hydroxyethyl)-1-Piperazineethanesulfonic Acid

HPAEC-PAD – High-Performance Anion-Exchange Chromatography with Pulsed Amperometric Detection

HPLC – High-Performance Liquid Chromatography

IPA – Isopropyl Alcohol

LED – Light-Emitting Diode

LB – Lysogeny Broth

MAA – Mycosporine-Like Amino Acid

MEC – Major Equipment Costs

MF – Microfiltration

MQ – Milli-Q

MSC – Microbial Safety Cabinet

MSP – Minimum Selling Price

MT – Metric Ton

MWCO – Molecular Weight Cut Off

NADPH – Nicotinamide Adenine Dinucleotide Phosphate (Hydrogen)

NCF – Net Cash Flow

NCMA – National Center for Marine Algae and Microbiota

NIES – National Institute for Environmental Studies Japan

NP – Net Profit

NPV – Net Present Value

OD – Optical Density

OpEx – Operating Expenditure

OPX – Outer Membrane Polysaccharide Export

PAR – Photosynthetically Active Radiation

PBR – Photobioreactor

PCP – Polysaccharide Copolymerase

PE – Polyethylene

PI – Profitability Index

PKD – Poly-2-Keto-3-Deoxyoctulosonic Acid

ppm – Parts per million

QA – Quality Assurance

QC – Quality Control

ROS – Reactive Oxygen Species

RPM – Revolutions Per Minute

RPS – Released Extracellular Polymeric Substances

SEM – Scanning Electron Microscopy

SPF – Sun Protection Factor

TCI – Total Capital Investment

TEA – Techno-Economic Assessment

TFA - Trifluoroacetic acid

TGA – Thermogravimetric Analysis

TI – Taxable Income

TMP – Transmembrane Pressure

Tris – Tris(hydroxymethyl)aminomethane

UF – Ultrafiltration

Und-P – Undecaprenyl Diphosphate

USD - United States Dollar

UV – Ultraviolet

UV/Vis – Ultraviolet/Visible light

VVM – Volume of air per volume of culture medium per minute

XG – Xanthan Gum

List of Figures

Figure 2-1 Chelating mechanism of ethylenediaminetetraacetic acid (EDTA). 25

Figure 2-2 Illustration of the biosynthesis pathway of cyanobacterial EPS production according to Debnath, et al. [85]. 29

Figure 3-1 Graphical abstract of PhD project on exploring the potential of cyanobacteria to produce extracellular polymeric substances. 69

Figure 4-1 Elution buffer gradients used for high-performance anion exchange chromatography with pulsed-amperometric detection (HPAEC-PAD) for monosaccharide analysis. 81

Figure 4-2 Photos of *Calothrix brevissima* and *Nostoc foliaceum* cultures in SciQuip Premium Compact shaking incubator to study effect of media composition on EPS (Exp. 2-5). 92

Figure 4-3 Modified PBR setup using Duran bottles for axenic experiment (Exp. 3-4). 103

Figure 4-4 Schema and photo of a PBR module of the pre-industrial plant from the Chemical Engineering Department of the University of Almería [297]. 106

Figure 4-5 Process flow diagram of baseline scenario for extracellular polymeric substances production of *C. brevissima* modelled in SuperPro Designer®, using tubular photobioreactors as upstream, and filtration and spray drying as downstream processing. 109

Figure 4-6 Overview of relationships between scenarios for techno-economic assessment of an industrial extracellular polymeric substances (EPS) and biomass production process using cyanobacteria..... 125

Figure 4-7 Process flow diagram of scenario 3 for extracellular polymeric substances production of *C. brevissima* modelled in SuperPro Designer®, using tubular photobioreactors as upstream, and spray drying as downstream processing. 126
Figure 4-8 Process flow diagram of scenario 4 for extracellular polymeric substances production of *C. brevissima* modelled in SuperPro Designer®, using tubular photobioreactors as upstream, and ethanol precipitation with distillation for ethanol recycling and spray drying as downstream processing..... 128
Figure 5-1 Biomass and extracellular polymeric substance (EPS) production of 15 novel cyanobacterial species and *Arthrospira platensis* (positive control) over time during the screening experiment (Exp. 1). 146
Figure 5-2 Sugar, protein, and sulfate content of extracellular polymeric substances (EPS) from novel cyanobacteria after 60 days of cultivation at 25°C under 20 µmol m^{-2} s^{-1} light. 151
Figure 5-3 Chromatographs of standards for high-performance anion-exchange chromatography with pulsed-amperometric detection (HPAEC-PAD). 155
Figure 5-4 Monosaccharide composition of extracellular polymeric substances (EPS) from novel cyanobacteria based on high-performance anion-exchange chromatography with pulsed amperometric detection (HPAEC–PAD). 160
Figure 5-5 Emulsifying activities of extracellular polymeric substances (EPS) of seven novel cyanobacterial species after 50 days of cultivation at 25°C under 22 µmol m^{-2} s^{-1} light. 165
Figure 5-6 Flocculating activity of extracellular polymeric substances (EPS) from novel cyanobacterial species compared to xanthan gum (positive control, C^{+}). 169
Figure 5-7 Antioxidant activity of extracellular polymeric substances (EPS) from novel cyanobacterial species after 50 days of cultivation at 25°C under 22 µmol m^{-2} s^{-1} light. 174

Figure 5-8 Iron-chelating activity of extracellular polymeric substances (EPS) from novel cyanobacterial species after 50 days of cultivation at 25°C under 22 μmol m^{-2} s^{-1} light. 177
Figure 5-9 Ultraviolet (UV) light protection of extracellular polymeric substances (EPS) from novel cyanobacterial species compared with a commercial sunscreen (SPF 30) after 50 days of cultivation at 25°C under 22 μmol m^{-2} s^{-1} light..... 181
Figure 5-10 Transmittance of extracellular polymeric substances (EPS) from novel cyanobacterial species compared with 4000-fold diluted commercial sunscreen of sun protection factor (SPF) of 30 after 50 days of cultivation at 25°C under 22 μmol m^{-2} s^{-1} light. 183
Figure 5-11 *Nostoc foliaceum* has a thick gel-like layer on top of DCW pellet after centrifugation and decanting of supernatant. 189
Figure 6-1 Effect of light intensity (22, 50, 75, 100 μmol m^{-2} s^{-1}) on *Calothrix brevissima* dry cell weight (DCW) and extracellular polymeric substances (EPS) at 60% working volume (30 mL culture in 50 mL Erlenmeyer flasks), 25 °C, and 150 RPM shaking for 56 days. 193
Figure 6-2 Photos of extracellular polymeric substances (EPS) from *Calothrix brevissima* grown under 50-100 μmol m^{-2} s^{-1}, 25°C, 150 RPM shaking and 60% working volume (30 mL culture in 50 mL Erlenmeyer flasks)..... 195
Figure 6-3 Comparison of monosaccharide composition of cotton-like and shiny film-like extracellular polymeric substances (EPS) from *Calothrix brevissima*..... 196
Figure 6-4 Effect of light intensity (50, 75, 100, 150 μmol m^{-2} s^{-1}) on *Nostoc foliaceum* dry cell weight (DCW) and extracellular polymeric substances (EPS) at 60% working volume (30 mL culture in 50 mL Erlenmeyer flasks), 25 °C, and 150 RPM shaking for 56 days. 200

Figure 6-5 Effect of light intensity (22, 75 μmol m^{-2} s^{-1}) on *Calothrix brevissima* dry cell weight (DCW) and extracellular polymeric substances (EPS) at 25% working volume (12.5 mL culture in 50 mL Erlenmeyer flasks), 25 °C, and 150 RPM shaking for 28 days (Exp. 2-2). 204
Figure 6-6 Effect of light intensity (22, 75 μmol m^{-2} s^{-1}) on *Nostoc foliaceum* dry cell weight (DCW) and extracellular polymeric substances (EPS) at 25% working volume (12.5 mL culture in 50 mL Erlenmeyer flasks), 25 °C, and 150 RPM shaking for 28 days (Exp. 2-2). 206
Figure 6-7 Effect of light intensity (50, 75, 100, 125, 150, 175 μmol m^{-2} s^{-1}) on *Calothrix brevissima* dry cell weight (DCW) and extracellular polymeric substances (EPS) at 25% working volume (12.5 mL culture in 50 mL Erlenmeyer flasks), 25 °C, and 150 RPM shaking for 21 days (Exp. 2-3). 208
Figure 6-8 Effect of light intensity (50, 75, 100, 125, 150, 175 μmol m^{-2} s^{-1}) on *Nostoc foliaceum* dry cell weight (DCW) and extracellular polymeric substances (EPS) at 25% working volume (12.5 mL culture in 50 mL Erlenmeyer flasks), 25 °C, and 150 RPM shaking for 21 days (Exp. 2-3). 209
Figure 6-9 Effect of BG-11 composition (supplementation of acetate, glucose and 10-fold higher level of trace elements) on production of biomass and extracellular polymeric substances (EPS) of *Calothrix brevissima* and *Nostoc foliaceum* grown for 15 days at 25°C and 22 μmol m^{-2} s^{-1} without shaking. 212
Figure 6-10 Effect of magnesium, calcium, ethylenediaminetetraacetic acid (EDTA), Tris(hydroxymethyl)aminomethane (Tris) buffer and 4-(2-Hydroxyethyl)-1-Piperazineethanesulfonic Acid (HEPES) buffer in the BG-11 medium on extracellular polymeric substances (EPS) production of *Calothrix brevissima* grown for 15 days at 25°C and 22 μmol m^{-2} s^{-1} at 250 RPM. 215

Figure 6-11 Contour plots and Pareto chart of dry cell weight (DCW) production in *Nostoc foliaceum* cultivated for 14 days at 150 RPM in 50 mL Erlenmeyer flasks with 25% working volume (n=2, Experiment 2-6). 219
Figure 6-12 Contour plots and Pareto chart of extracellular polymeric substances (EPS) production in *Nostoc foliaceum* cultivated for 14 days at 150 RPM in 50 mL Erlenmeyer flasks with 25% working volume (n=2) (Experiment 2-6). 223
Figure 6-13 Experimental validation of optimal conditions for extracellular polymeric substance (EPS) production in *Nostoc foliaceum*, as predicted by Minitab software (28°C, 4.84 g L^{-1} glucose and 164 µmol m^{-2} s^{-1}). 224
Figure 6-14 Emulsifying activity of extracellular polymeric substances (EPS) from *Nostoc foliaceum* cultivated under optimised conditions (28°C, 4.84 g L^{-1} glucose and 164 µmol m^{-2} s^{-1} light) for 14 days at 150 RPM in 50 mL Erlenmeyer flasks with 25% working volume (Experiment 2-6). 225
Figure 6-15 Contour plots and Pareto chart of dry cell weight (DCW) production in *Calothrix brevissima* cultivated for 14 days at 150 RPM in 50 mL Erlenmeyer flasks with 25% working volume (n=2) (Experiment 2-6). 230
Figure 6-16 Contour plots and Pareto chart of extracellular polymeric substances (EPS) production in *Calothrix brevissima* cultivated for 14 days at 150 RPM in 50 mL Erlenmeyer flasks with 25% working volume (n=2) (Experiment 2-6). 233
Figure 6-17 Comparison of dry cell weight (DCW) and extracellular polymeric substance (EPS) productivities of *Calothrix brevissima* under phototrophic and mixotrophic growth modes. 234
Figure 6-18 Contour plots and Pareto charts of dry cell weight (DCW) and extracellular polymeric substance (EPS) production in *Calothrix brevissima* investigating the combined effect of light intensity (22 - 350 µmol m^{-2} s^{-1}) and light duration (8-24 hours). 238

Figure 6-19 Effect of temperature (25-37°C) and light intensity (25-500 μmol m^{-2} s^{-1}) on dry cell weight (DCW) and extracellular polymeric substance (EPS) production in *Calothrix brevissima* (Exp. 2-8)..... 240
Figure 6-20 Dry cell weight (DCW) and extracellular polymeric substance (EPS) production in *Calothrix brevissima* under optimised phototrophic conditions (31°C and 300 μmol m^{-2} s^{-1}) during 14 days of growth at 150 RPM in 50 mL Erlenmeyer flasks with 25% working volume (Exp-2-9). 242
Figure 6-21 Emulsifying properties of extracellular polymeric substance (EPS) from *Calothrix brevissima* grown under optimised phototrophic conditions (31°C and 300 μmol m^{-2} s^{-1}, day 10 sample, oil:water ratio of 1:1). 245
Figure 6-22 Emulsifying properties of extracellular polymeric substance (EPS) from *Calothrix brevissima* grown under optimised phototrophic conditions (31°C and 300 μmol m^{-2} s^{-1}, day 10 sample, oil:water ratio of 2:1). 246
Figure 6-23 Lipid content of extracellular polymeric substance (EPS) from *Calothrix brevissima* ($‰_{w/w}$ = gram lipid per gram EPS)..... 247
Figure 7-1 Correlation between Xanthella MicroPharos photobioreactor (PBR) light tile amperage input (mA) and light intensity output. 250
Figure 7-2 Effect of airflow rate (1-4 L min^{-1}) and light intensity (50-950 μmol m^{-2} s^{-1}) on *Calothrix brevissima* dry cell weight (DCW) and extracellular polymeric substance (EPS) production. 254
Figure 7-3 Effect of CO_2 flow rate (10-100 mL min^{-1}) and light intensity (50-950 μmol m^{-2} s^{-1}) on extracellular polymeric substance (EPS) and dry cell weight (DCW) production of *Cyanothece brevissima.*..... 258
Figure 7-4 Light tile amperage setting (mA) required to match coloured light tiles intensity to white light (500 μmol m^{-2} s^{-1}, 650 AU) in 1-litre Xanthella MicroPharos photobioreactors (PBR). 260

Figure 7-5 Effect of light colour (green, blue and red, 650 arbitrary units (AU)) on dry cell weight (DCW) and extracellular polymeric substance (EPS) of *Calothrix brevissima* grown in 1-litre Xanthella MicroPharos photobioreactors (PBR) with 1 L min^{-1} air and 55 mL min^{-1} CO_2 for 7 days (Exp. 3-3)..... 261
Figure 7-6 Photographs of Lysogeny Broth (LB) plates showing contamination levels in 1-litre Xanthella MicroPharos photobioreactors (PBRs) under different sterilisation protocols. 263
Figure 7-7 Photographs of 1-litre Xanthella MicroPharos photobioreactor (PBR) lids showing structural deformation. 264
Figure 7-8 Modified photobioreactor (PBR) setup for axenic growth. 266
Figure 7-9 Effect of CO_2 on dry cell weight (DCW) and extracellular polymeric substance (EPS) production in *Calothrix brevissima* under axenic conditions (Experiment 3-4). 268
Figure 8-1 Cost breakdown of the baseline scenario for the techno-economic assessment of an industrial extracellular polymeric substances (EPS) production process using the cyanobacterium *Calothrix brevissima*. 279
Figure 8-2 Effect of on operation mode (batch vs. semi-continuous) on minimum selling price (MSP, USD kg^{-1}) for the techno-economic assessment of an industrial extracellular polymeric substances (EPS) production process using the cyanobacterium *Calothrix brevissima*. 285
Figure 8-3 Effect of different downstream processing (DSP) equipment for extracellular polymeric substances (EPS) recovery and purification on the minimum selling price (MSP, USD kg^{-1}). 288
Figure 8-4 Effect of cultivation system on the minimum selling price (MSP, USD kg^{-1}) for the techno-economic assessment of an industrial extracellular polymeric

substances (EPS) production process using the cyanobacterium *Calothrix brevissima*. 291
Figure 8-5 Itemised costs for indoor, phototrophic growth in bag photobioreactors (PBRs) with artificial lighting (scenario 11) for the techno-economic assessment of an industrial extracellular polymeric substances (EPS) production process using the cyanobacterium *Calothrix brevissima*. 292
Figure 8-6 Effect of mixotrophic (glucose) growth mode on the minimum selling price (MSP, USD kg^{-1}) for the techno-economic assessment of an industrial extracellular polymeric substances (EPS) production process using the cyanobacterium *Calothrix brevissima*. 295
Figure 8-7 Itemised costs of indoor, mixotrophic growth in tubular photobioreactors (PBRs) with artificial lighting (scenario 13) for the techno-economic assessment of an industrial extracellular polymeric substances (EPS) production process using the cyanobacterium *Calothrix brevissima*. 297
Figure 8-8 Itemised costs of indoor, mixotrophic growth in bag photobioreactors (PBRs) with artificial lighting (scenario 14) for the techno-economic assessment of an industrial extracellular polymeric substances (EPS) production process using the cyanobacterium *Calothrix brevissima*. 298
Figure 8-9 Itemised costs of outdoor, mixotrophic growth in bag photobioreactors (PBRs) with natural light (scenario 15) for the techno-economic assessment of an industrial extracellular polymeric substances (EPS) production process using the cyanobacterium *Calothrix brevissima*. 299
Figure 8-10 Minimum selling price (MSP, USD kg^{-1}) of scenarios using alternative cyanobacterial species (*Nostoc foliaceum*) for extracellular polymeric substances (EPS) and biomass production. 303

Figure 8-11 Total capital investment (TCI), operational expenditure (OpEx), and revenues of single-product (biomass) scenarios using *Nostoc foliaceum* compared to the baseline scenario. 304
Figure 8-12 Comparison of cosmeceutical and bioemulsifier products for the techno-economic assessment of an industrial extracellular polymeric substances (EPS) production process using the cyanobacterium *Calothrix brevissima*. 308
Figure 8-13 Sensitivity analysis of the baseline scenario for phototrophic growth in tubular photobioreactors (PBRs) with artificial lighting, for the techno-economic assessment of an industrial extracellular polymeric substances (EPS) production process using the cyanobacterium *Calothrix brevissima*. 313
Figure 12-1 Standard curves for extracellular polymeric substances (EPS) composition assays. 355
Figure 12-2 Standard curves for dry cell weight (DCW) from optical density (OD) estimation, and extracellular polymeric substances (EPS) properties assays. 357
Figure 12-3 Photos of agar plates of axenisation of *Nostoc foliaceum*. 361
Figure 12-4 Thermal degradation profile obtained with Thermogravimetric Analysis of novel extracellular polymeric substances from *Anabaena oscillarioides, Calothrix brevissima, Nostoc foliaceum, Nostoc longstaffi, Nostoc zetterstedtii* and *Trichormus subtropicus*. 371
Figure 12-5 Scanning Electron Microscopy (SEM) pictures of EPS from seven novel cyanobacterial species. 374
Figure 12-6 Thermal degradation profile of shiny film-like and cotton-like extracellular polymeric substances (EPS) from *Calothrix brevissima* based on Thermogravimetric Analysis. 376
Figure 12-7 Scanning Electron Microscopy (SEM) pictures of extracellular polymeric substances (EPS) from *Calothrix brevissima*..... 377

Figure 12-8 Differential Scanning Calorimetry (DSC) of *Calothrix brevissima* extracellular polymeric substances (EPS), locust bean gum (positive control, C^+) and water (negative control, C^-). 380
Figure 12-9 Absorbance and transmittance of the supernatant (0.385 g EPS L^{-1}) of *Calothrix brevissima* grown for 7 days at 31°C and 450 µmol m^{-2} s^{-1}, and of 2000x diluted sunscreen (SPF30, 0.5 g L^{-1}). 381
Figure 12-10 Sterilisation and inoculation protocol Xanthella MicroPharos photobioreactors (PBRs). 383

List of Tables

Table 2-1 Physiological roles of extracellular polymeric substances (EPS) in cyanobacteria as reported in the literature..... 5

Table 2-2 Biochemical analyses of released extracellular polymeric substances (RPS) of cyanobacterial species reported in the literature. 10

Table 2-3 Emulsifying activities of extracellular polymeric substances (EPS) from cyanobacteria reported in the literature. 17

Table 2-4 Flocculating activity of extracellular polymeric substances (EPS) from cyanobacteria reported in the literature. 19

Table 2-5 Antioxidant activities of extracellular polymeric substances (EPS) from cyanobacteria reported in the literature, determined by 2,2-diphenyl-1-picrylhydrazyl (DPPH) scavenging assay. 23

Table 2-6 Metal-chelating activities of extracellular polymeric substances (EPS) from cyanobacteria reported in the literature. 24

Table 2-7 Ultraviolet (UV) protection level of compounds produced by cyanobacteria and algae reported in the literature. 27

Table 2-8 Effect of light intensity on extracellular polymeric substances (EPS) production of cyanobacteria as reported in the literature (non-exhaustive). 34

Table 2-9 Effect of light colour and photoperiod on extracellular polymeric substances (EPS) production of cyanobacteria as reported in the literature (non-exhaustive).... 35

Table 2-10 Effect of temperature on extracellular polymeric substances (EPS) production of cyanobacteria as reported in the literature (non-exhaustive). 37

Table 2-11 Effect of pH on extracellular polymeric substances (EPS) production of cyanobacteria as reported in the literature (non-exhaustive). 37

Table 2-12 Effect of nitrogen concentration on extracellular polymeric substances (EPS) production of cyanobacteria as reported in the literature (non-exhaustive).... 39
Table 2-13 Effect of nitrogen source type on extracellular polymeric substances (EPS) production of cyanobacteria as reported in the literature (non-exhaustive). 40
Table 2-14 Effect of phosphate concentration on extracellular polymeric substances (EPS) production of cyanobacteria as reported in the literature (non-exhaustive).... 41
Table 2-15 Effect of magnesium concentration on extracellular polymeric substances (EPS) production of cyanobacteria as reported in the literature (non-exhaustive).... 42
Table 2-16 Effect of iron concentration on extracellular polymeric substances (EPS) production of cyanobacteria as reported in the literature (non-exhaustive). 43
Table 2-17 Effect of calcium and boron concentration on extracellular polymeric substances (EPS) production of cyanobacteria as reported in the literature (non-exhaustive). 44
Table 2-18 Effect of sodium chloride concentration on extracellular polymeric substances (EPS) production of cyanobacteria as reported in the literature (non-exhaustive). 45
Table 2-19 Effect of aeration, carbon dioxide supplementation, and trophic mode (phototrophic, mixotrophic, heterotrophic) on extracellular polymeric substances (EPS) production of cyanobacteria as reported in the literature (non-exhaustive). 47
Table 2-20 Effect of cultivation mode (batch, fed-batch, continuous) and two-step cultivation on extracellular polymeric substances (EPS) production of cyanobacteria as reported in the literature (non-exhaustive). 48
Table 2-21 Effect of scale (culture volume) on extracellular polymeric substances (EPS) production of cyanobacteria as reported in the literature (non-exhaustive).... 49
Table 2-22 Effect of growth duration on extracellular polymeric substances (EPS) composition of cyanobacteria as reported in the literature (non-exhaustive). 50

Table 2-23 Effect of light colour and intensity on extracellular polymeric substances (EPS) composition of cyanobacteria as reported in the literature (non-exhaustive). 51
Table 2-24 Effect of growth condition on extracellular polymeric substances (EPS) properties of cyanobacteria as reported in the literature (non-exhaustive). 52
Table 2-25 Specifications, advantages, challenges, and applications of different cultivation systems for cyanobacteria and microalgae as reported in the literature. 55
Table 2-26 Advantages and challenges of downstream processing equipment for extracellular polymeric substances (EPS) recovery, purification, and drying as reported in the literature. 59
Table 4-1 Cyanobacterial species used in the screening experiment to investigate extracellular polymeric substances (EPS) and dry cell weight (DCW) production. .. 75
Table 4-2 Elution buffer gradient of method 1 used for high-performance anion-exchange chromatography with pulsed-amperometric detection (HPAEC-PAD) for monosaccharide analysis of extracellular polymeric substances (EPS). 82
Table 4-3 Elution buffer gradient of method 2 used for high-performance anion-exchange chromatography with pulsed-amperometric detection (HPAEC-PAD) for monosaccharide analysis of (rhamnose and arabinose) extracellular polymeric substances (EPS). 82
Table 4-4 Design of experiment (DoE) runs for 3-factor optimisation of light intensity, temperature, and glucose concentration for extracellular polymeric substances (EPS) and dry cell weight production of *Calothrix brevissima* and *Nostoc foliaceum* according to Minitab software (Exp. 2-6). 93
Table 4-5 Design of experiment (DoE) runs for 2-factor optimisation of light intensity ($\mu mol\ m^{-2}\ s^{-1}$) and light duration (hours) for extracellular polymeric substances (EPS) production of *Calothrix brevissima* according to Minitab software (randomised, Exp. 2-7). 96

Table 4-6 Cultivation parameters for photobioreactor (PBR) experiment studying the effect of airflow rate (1, 2.5, 4 L min^{-1}) and light intensity (50, 500, 950 µmol m^{-2} s^{-1}) on extracellular polymeric substances (EPS) production of *Calothrix brevissima* (Experiment 3-1). 99
Table 4-7 Cultivation parameters for photobioreactor (PBR) experiment studying the effect of carbon dioxide (CO_2) flow rate (10, 55, 100 mL min^{-1}) and light intensity (50, 500, 950 µmol m^{-2} s^{-1}) on extracellular polymeric substances (EPS) production of *Calothrix brevissima* (Experiment 3-2). 101
Table 4-8 Cultivation parameters for photobioreactor (PBR) experiments studying the effect of light colour (green, blue, red) on extracellular polymeric substances (EPS) production of *Calothrix brevissima* (Experiment 3-3). 102
Table 4-9 Cultivation parameters for photobioreactor (PBR) experiments studying the effect of CO_2 versus air on dry cell weight and extracellular polymeric substances (EPS) production of *Calothrix brevissima* under axenic conditions (Experiment 3-4). 104
Table 4-10 Specifications of a single tubular photobioreactor module from the pre-industrial plant of the Chemical Engineering Department, University of Almería. ... 110
Table 4-11 Economic parameters for utilities for non-standard equipment in SuperPro Designer® simulations of industrial-scale extracellular polymeric substance production using cyanobacteria. 111
Table 4-12 Design parameters of filtration system for extracellular polymeric substances (EPS) downstream processing including pore size, membrane cost and lifetime. 113
Table 4-13 Economic cost parameters (base cost (C_o) and base capacity (Q_o)) for non-standard equipment used in SuperPro Designer® simulations, including

photobioreactor (PBR), lights, air blower and carbon dioxide (CO_2) supply unit cost. 116
Table 4-14 Mean ($\bar{T}$), minimum (T_{min}), and maximum (T_{max}) monthly temperatures (°C) in Almería, Spain in the year 2020 [306] 119
Table 4-15 Inlet temperature (T_{inlet}), outlet temperature (T_{outlet}), temperature difference (ΔT), and price of heat transfer agents used in photobioreactor (PBR) simulations for techno-economic assessment. 119
Table 4-16 Solar irradiance (kWh m^{-2}) and daylight (hours day^{-1}) in Almería, Spain, for modelling outdoor photobioreactor scenarios. 130
Table 4-17 Input values and relative level to baseline scenario of parameters for sensitivity analysis in techno-economic assessment of extracellular polymeric substances (EPS) production using *Calothrix brevissima*. 134
Table 4-18 Summary of key assumptions for techno-economic assessment of a cyanobacterial production process of extracellular polymeric substances (EPS) using *Calothrix brevissima*. 135
Table 5-1 Composition (sugar, protein, and sulphate content) of extracellular polymeric substances (EPS) from novel cyanobacterial species. 149
Table 5-2 Monosaccharide composition of extracellular polymeric substances (EPS) of 15 novel cyanobacterial species. 157
Table 5-3 Heatmap showing Pearson correlation coefficient *r* between extracellular polymeric substances (EPS) composition and properties of seven cyanobacterial species. 185
Table 5-4 Summary of functional properties of extracellular polymeric substances (EPS) from seven novel cyanobacteria species. 188
Table 6-1 Dry cell weight (DCW) and extracellular polymeric substances (EPS) concentrations of *Calothrix brevissima* after three-factor optimisation of temperature,

light intensity, and glucose concentration using a Box-Behnken design (Experiment 2-6). 217
Table 6-2 Dry cell weight (DCW) and extracellular polymeric substances (EPS) concentrations of *Calothrix brevissima* after three-factor optimisation of temperature, light intensity, and glucose concentration using a Box-Behnken design (Experiment 2-6). 227
Table 6-3 Dry cell weight (DCW) and extracellular polymeric substances (EPS) concentrations of *Calothrix brevissima* after two-factor optimisation of light intensity and light duration using a Central-Composite-Design (Experiment 2-7). 235
Table 8-1 Monthly heating and cooling requirements and costs for a 3000 m^3 tubular photobioreactor (PBR) for industrial production of extracellular polymeric substances with cyanobacterium *Calothrix brevissima* in Almería, Spain..... 274
Table 8-2 Annual energy consumption, cost, and relative contribution of utilities for a 3000 m^3 tubular photobioreactor (PBR) for industrial production of extracellular polymeric substances with cyanobacterium *Calothrix brevissima* in Almería, Spain. 275
Table 8-3 Major equipment cost (MEC) of the baseline scenario for industrial production of extracellular polymeric substances with cyanobacterium *Calothrix brevissima*. 277
Table 8-4 Cash flow analysis (in million USD) of the baseline scenario for industrial production of extracellular polymeric substances (EPS). 281
Table 8-5 Cash flow analysis (in million USD) of the baseline scenario for industrial production of extracellular polymeric substances (EPS). 283
Table 8-6 Net present value (NPV) and profitability index (PI) of scenarios 3 to 8, which include different downstream processing strategies (DSP) for industrial production of extracellular polymeric substances (EPS). 290

Table 8-7 Net present value (NPV) and profitability index (PI) of scenarios 9 to 12, which include different cultivation systems for industrial production of extracellular polymeric substances (EPS)..... 294
Table 8-8 Net present value (NPV) and profitability index (PI) of scenarios 13 to 15, which include mixotrophic cultivation for industrial production of extracellular polymeric substances (EPS)..... 300
Table 8-9 Cash flow (in million USD), net present value (NPV), and profitability index (PI) of scenario 15 for industrial production of extracellular polymeric substances (EPS)..... 301
Table 8-10 Net present value (NPV) and profitability index (PI) of scenarios 16 to 20 for industrial production of extracellular polymeric substances (EPS) with *Nostoc foliaceum*..... 305
Table 8-11 Cash flow (in million USD), net present value, and profitability index of scenario 21 for industrial production of extracellular polymeric substances (EPS). 310
Table 9-1 Maximum extracellular polymeric substances (EPS) concentration (C_{EPS}), growth duration at which the maximum EPS concentration was obtained, and the corresponding EPS productivity (P_{EPS}) of novel cyanobacteria in screening experiment compared to literature data..... 316
Table 12-1 Trendline equations, R^2 values, standard deviation (σ) of blanks, limits of detection (LOD), and limits of saturation (LOS) for standard curves used in extracellular polymeric substances (EPS) composition and property assays. 358
Table 12-2 Retention times (minutes) and peak numbers of monosaccharides in high-performance anion-exchange chromatography with pulsed-amperometric detection ($HPAEC^-PAD$) used for monosaccharide identification and quantification of extracellular polymeric substances (EPS). 360

Table 12-3 Composition of marine media (ASN-III, ESM, L1-Si) used for cultivation of marine cyanobacteria. 363

Table 12-4 Composition of freshwater media (BG-11, BG-11_0, CB, MDM, SOT) used for cultivation of freshwater cyanobacteria..... 365

Table 12-5 Growth of novel freshwater cyanobacterial species depending on different freshwater media (BG-11, BG-11_0, CB, MDM, SOT). 368

Table 12-6 Growth of novel marine cyanobacterial species *Phormidium breve*, *Phormidium keutzingianum*, *Spirulina major*,*Acaryochloris marina*, *Oscillatoria rosea* and *Tychonema bornetii* in different marine media (ASN-III, ESM, L1-Si). 369

Table 12-7 Fibril width of extracellular polymeric substances (EPS) from seven novel cyanobacterial species. 375

Table 12-8 Onset, peak, and endset temperatures (°C) during Differential Scanning Calorimetry (DSC) of extracellular polymeric substances (EPS) from *Calothrix brevissima*, water (negative control, C^-), and locust bean gum (positive control, C^+). 380

Chapter 1: Introduction

Climate change, largely driven by anthropogenic emissions of greenhouse gases such as carbon dioxide (CO_2), represents one of the most critical challenges of our time. Reliance on fossil fuels has significantly contributed to global warming through greenhouse gas emissions and caused severe environmental issues, including air pollution, ecosystem degradation, and depletion of finite resources [1]. Fossil reserves continue to deplete, exacerbating the urgency to transition toward renewable, eco-friendly alternatives. This highlights the need to adopt biotechnological solutions based on renewable resources that ensure long-term sustainability and reduce global greenhouse gas emissions. In alignment with these goals, the European Union has committed to achieving carbon neutrality and net zero emissions by 2050, setting an ambitious standard for global sustainability efforts [2].

Meeting net zero emissions by 2050 requires innovative solutions that not only mitigate CO_2 emissions but also contribute to sustainable economic development. The use of cyanobacteria and microalgae stands out as a promising approach due to their ability to sequester atmospheric CO_2 as their primary carbon source through oxygenic photosynthesis, making them an attractive option for carbon-neutral or even carbon-negative production processes [3]. Using photoautotrophic organisms, such as plants, algae and cyanobacteria, in carbon-negative technologies is estimated to have a sequestration potential between 3.6 and 6.3 gigatons of carbon annually [4]. This can help reduce greenhouse gas emissions to counteract global warming and climate change. Among photoautotrophic organisms, cyanobacteria and algae are especially interesting as production platform, since they exhibit higher biomass productivity and photoconversion efficiency (PCE) than terrestrial plants. Regarding biomass productivity, cultivated plants typically achieve net primary productivity ranging from 10 to 40 metric tons per hectare per year, depending on species and environmental conditions. In contrast, algae can reach up to 45 MT ha^{-1} $year^{-1}$ under optimal cultivation, with even higher productivity observed in artificial systems where factors such as CO_2 enrichment and nutrient availability are controlled [5]. In terms of PCE, the best-case algae can achieve up to 6.3% PCE, as seen in outdoor cultures of *Chlorella* under reduced sunlight. Other algae cultures under full sunlight achieved around 2.6–2.7% PCE [6, 7]. In contrast, most terrestrial plants are estimated to

convert approximately 0.1% of solar energy into biomass. For crops, C3 plants can achieve up to 2.4%, while C4 crops show higher efficiency, reaching 3.7% PCE [6, 7]. Photoautotrophic production, requiring minimal inputs for growth—light, water, CO_2, and basic nutrients—offers an advantage over heterotrophic microbial cultivation, as the latter depends on glucose, which requires arable land and competes with food resources [8].

Cyanobacteria naturally produce a variety of compounds that can be exploited industrially, including pigments, bioplastics and biofuels [9, 10]. Thus, cyanobacteria offer the distinct advantage of being sustainable in a two-fold manner, by producing a bio-based product that can replace a petroleum-based product, and sequestering carbon dioxide simultaneously. A group of compounds that have gained recent attention due to their diverse functionalities, making them attractive for a variety of biotechnological applications, are extracellular polymeric substances (EPS) [11]. EPS are carbohydrate-rich compounds that form a protective layer around the cells and play a crucial physiological role for cyanobacteria, enabling them to survive in diverse and often extreme environments. This includes desiccation tolerance, protection against oxidative stress, and the adsorption of heavy metals, which reduces cellular toxicity and provides a survival advantage [12-14]. The natural protective roles of cyanobacterial EPS contribute to their distinct properties, which give them a range of biotechnologically important attributes, making them well-suited as products in the bio-based economy.

EPS functionalities range from emulsifying, flocculating, gelling and metal-absorbing properties to bioactive activities such as antiviral, antibacterial, antifungal and anticancer effects [15, 16]. Bio-polymers such as EPS from cyanobacteria offer advantages such as biodegradability, low toxicity, and good stability [17]. Compared to other organisms that produce EPS, cyanobacteria stand out as promising producers due to the unique characteristics of their EPS. Cyanobacterial EPS contain pentoses, which are absent in other microbial EPS [18]. Furthermore, cyanobacterial EPS include sulphur, an element absent in EPS from other prokaryotes and previously thought to be exclusively found in eukaryotic EPS [11, 19]. Unlike other prokaryotic EPS, which typically comprise up to four different monosaccharides, cyanobacterial EPS exhibit a more diverse monosaccharide profile, containing up to 14 different monosaccharides,

including neutral, acidic and amino sugars, adding to their functional versatility [20]. The wide range of properties makes them promising agents for developing sustainable and eco-friendly products in a variety of industries, including nutraceutical, cosmetic, and pharmaceutical [21]. The global emulsifier market alone was valued at about 4.70 billion USD in 2023 and is expected to reach approximately 7.66 billion USD by 2032, with a compound annual growth rate of 5.5% [22]. Examples for commercialised EPS from cyanobacteria include the anti-inflammatory compound *Sacran* from *Aphanothece sacrum*, and the antiviral agents *Calcium Spirulan* and *Nostoflan*, obtained from *Arthrospira platensis* and *Nostoc flagelliforme*, respectively [23-25]. An example for patented EPS is *Emulycan*, which is a bio-emulsifier obtained from *Phormidium* sp. J-1 [26]. A biopolymer produced by *Wollea saccata* showed significant antitussive and bronchodilator properties, making it suitable for medicinal applications [27].

Despite their economic potential, commercial exploitation of cyanobacterial products such as EPS remains limited. Of the estimated 200,000 – 800,000 existing species of cyanobacteria and microalgae, only 35,000 species have been identified, and merely a few hundred species have been researched regarding their valuable metabolites [28, 29]. To date, only a handful of cyanobacterial EPS, including Calcium Spirulan, Nostoflan, Sacran and Emulcyan, have been commercialised [3]. Commercialisation remains limited, as several challenges in industrial-scale production need to be overcome, particularly in upstream processing (USP) and downstream processing (DSP): Key factors such as identification of optimal production species, growth conditions, cultivation system and DSP for extraction and purification of the EPS need to be improved and optimised [11]. Addressing these bottlenecks requires a thorough understanding of EPS composition, production strategies, and current industrial approaches. Accordingly, a comprehensive literature review on cyanobacterial EPS composition, properties, and commercial production is provided in the following chapter.

Chapter 2: Literature review

2.1 The Physiological Role of EPS in Natural Environments

EPS, which are also called ‘exopolysaccharides’ or ‘extracellular polysaccharides,’ form a protective layer around the cell and have several physiological functions. EPS serve as a barrier to a multitude of unfavourable environments (Table 2-1). The desiccation-tolerance of the cyanobacterium *Nostoc commune* has been attributed to the secretion of EPS which acts as a water reserve and barrier to dry environment, stabilizing and protecting cells from desiccation [14]. Additionally, EPS produced by *Westiellopsis prolifica* ARM 366 protects from saline environments by adsorbing sodium ions and reducing the flux of these ions into the cell [30]. Similarly, EPS production in *Microcystis aeruginosa* serve as protection against toxicity and membrane damage, when exposed to soluble nanoparticles [31]. Furthermore, EPS act as a protective agent against oxidative stress in *Microcoleus vaginatus* by eliminating reactive oxygen species induced by UV-B radiation, preventing DNA strand breaks and lipid peroxidation [13]. The role of EPS as means of protection from oxidative stress has also been suggested for *Cyanothece epiphytica*, which survived prolonged exposure to ozone [32]. Similarly, EPS protect against energy stress in *Nostoc* sp. by serving as sink for excess fixed carbon under unbalanced C:N metabolism [33]. Furthermore, EPS take up pollutants such as heavy metals, to enhance the metabolism or to reduce or eliminate contaminants from the environment [12].

Table 2-1 Physiological roles of extracellular polymeric substances (EPS) in cyanobacteria as reported in the literature.

Species	Physiological role	Reference
Nostoc commune	Protection from desiccation	[14]
Westiellopsis prolifica	Protection from salinity	[30]
Microcoleus vaginatus, Cyanothece epiphytica	Protection against oxidative stress	[13, 32]
Microcystis aeruginosa	Protection against toxicity from nanoparticles	[31]
Nostoc sp.	Sink for excess fixed carbon, protection from energy stress	[33]
Microcystis aeruginosa	Colony formation	[34]
Multiple species	Accumulation of nutrients	[35]
Multiple species	Accumulation of heavy metals for metabolism or protect cells from toxicity	[12]

Another physiological function that EPS carry in cyanobacteria, is facilitating colony formation. The adhesive effect of EPS produced by *Microcystis aeruginosa* plays an important role for colony formation [36]. Large colonies represent a great advantage for *Microcystis* in competition with other phytoplankton by increasing photosynthetic efficiency, buoyancy and physiological activity [34, 37, 38]. Lastly, EPS also have the function of accumulating nutrients. This can lead to blooms which, through production of cyanotoxins, can be harmful to aquatic life and humans if present in drinking water [35].

2.2 Types, Composition and Properties of Cyanobacterial EPS

Depending on the degree of polymerisation (DP), EPS are either classified as oligosaccharides (2<DP<10) or polysaccharides (DP>10) [29]. EPS can be cell-bound EPS (Capsular polysaccharides: CPS) or released into the surrounding medium (Released polysaccharides: RPS). CPS occur as slime, sheath or capsule [20]. According to De Philippis, et al. [39] '*The sheath […] is defined as a thin, electron-*

dense layer loosely surrounding cells or cell groups and is usually visible by light microscopy without staining; the capsule […] generally consists of a thick and slimy layer intimately associated with the cell surface with sharp outlines and structurally coherent to exclude particles (e.g. India ink); the slime […] refers to the mucilaginous material dispersed around the organism but not reflecting the shape of the cells'. RPS comprise colloidal EPS and low molecular weight exudates [40].

Whether cyanobacteria produce more RPS or CPS differs among species. The RPS were more abundant than CPS in *Spirulina* sp. (family *Oscillatoriaceae*), *Oscillatoria* sp. (family *Oscillatoriaceae*), *Phormidium* sp. (family *Phormidiaceae*), *Anabaena sphaerica* (family *Nostocaceae*), *Anabaena* WSAF (family *Nostocaceae*), *Anabaena variabilis* (family *Nostocaceae*), *Fischerella muscicola* (family *Fischerellaceae*), *Chlorogloeopsis* sp. *fritschii* 6912 (family *Fischerellaceae*) [41]. In contrast, CPS were more abundant in *Tolypothrix tenuis* (family *Oscillatoriaceae*), *Nostoc linckia* (family *Nostocaceae*), *Anabaena torulosa* (family *Nostocaceae*), *Anabaena* sp. 7120 (family *Nostocaceae*), and *Scytonema hofmanni* PCC 7110 (family *Scytonemataceae*) [41].

Due to intimate association or covalent bonds with the cell walls, CPS require an extraction method, such as hot water, acid or base extraction [42]. However, only few authors examined the intactness of cells afterwards, to verify the extracellular nature of the CPS [43-45]. This might be the reason why the term 'CPS' is often misused in literature [29]. For instance, *Calcium Spirulan* and *Nostoflan*, which are polysaccharides mentioned in a literature review by Cruz, et al. [3] as examples of commercialised EPS, were extracted from dried or ground cells, leaving doubts about their extracellular nature [24, 25]. Partial cell death and lysis can result in overestimation of EPS, if no correction for potential released glycogen has been performed [46]. In this PhD thesis, a footnote behind 'CPS' or 'EPS' indicates that they were obtained using an extraction method that raises uncertainty about their extracellular nature. The extraction method can be found in the respective footnote.

From a bioprocess point of view, RPS are preferable over CPS, because RPS are easier to recover during the DSP, as they do not require the above mentioned step to break the covalent bonds between CPS and cells [3, 19-21, 47, 48]. Thus, this PhD thesis focused on RPS over CPS. A similar trend is seen for other algal products: Liu,

et al. [49] note that recovering intracellular lipids is energy and time consuming, making lipid-secreting algae strains more attractive for simpler downstream processing [49].

2.2.1 Composition of Cyanobacterial EPS

The composition of EPS is diverse and generally species-dependent [20]. Most EPS are heteropolymers, consisting of different monosaccharides and non-sugar substituents such as acetyl, methyl, pyruvyl, sulphate groups, and proteins [40]. Full characterisation of EPS is difficult due to the lack of repeating units, the complexity of sugar and non-sugar parts, and the difficulty related to EPS recovery caused by their rheological properties. Due to these reasons, fully identified structures are rare [29]. A non-exhaustive list of (partial) biochemical analyses of 61 different RPS from 21 publications, is shown in Table 2-2, to provide an overview of the compositional diversity. Further EPS compositions have been reviewed by several authors including Borowitzka [9], Cruz, et al. [3] and Prybylski, et al. [29].

Based on the data summarized in Table 2-2, carbohydrates make up the largest fraction of RPS with an average of 44.0% of RPS dry weight. The carbohydrate content of RPS varied from 9% to 93% [50, 51]. Carbohydrates comprised up to 14 different monosaccharides, including neutral sugars, uronic acids and amino sugars [52, 53]. The high number of monosaccharides differentiates cyanobacterial EPS from other prokaryotic EPS, which usually feature up to four different monosaccharides [20]. Neutral sugars found in the RPS included the hexoses glucose, galactose, mannose, fucose, rhamnose, fructose, and the pentoses arabinose, xylose and ribose. The presence of the latter is noteworthy, since pentoses are usually absent in other microbial EPS [18]. Uronic acids identified in cyanobacterial RPS are glucuronic, galacturonic and mannuronic acid [52]. Glucosamine and galactosamine are examples for amino sugars [53].

Glucose is the most prominent monosaccharide, found in most microbial and cyanobacterial EPS [11]. Exceptions are RPS from *Nostoc carneum* and *Nostoc* sp. which feature only xylose and mannose [54]. A peculiarity are the EPS[1] produced by

[1] EPS extraction method: "*The culture of Cyanothece sp. 113 was heated at 100ºC in water bath for 15 min*". [55] Cells were not examined for intactness afterward. Excluded from analysis due to not being RPS.

Cyanothece sp. 113 which consisted entirely of glucose molecules and was identified as *α*-D-1,6-homoglucan [56]. To the best knowledge of the author of this PhD thesis, *Cyanothece* sp. 113 is the only cyanobacterial species known to produce homopolymeric EPS. Monosaccharides other than glucose, that were found in the majority (>50%) of RPS, were uronic acids, mannose, xylose, galactose, rhamnose, arabinose and fucose. Fructose, ribose and amino sugars were less frequently found (Table 2-2). However, it should be noted that their analysis was omitted in most studies. Acidic sugars, in particular uronic acids, were found in most RPS (51 out of 61 species) and made up between 1.3% and 40.7% of RPS [27, 57]. An even higher content of uronic acids of 68% has been found in slime[2] from *M. flos-aquae* C3-40 [58]. Uronic acids were absent in other species [27, 59, 60]. Galacturonic acid and glucuronic acid were the most found uronic acids, making up 2.8% and 3.1% on average, respectively. However, not all studies identified the type of uronic acids present. More rarely, mannuronic acid was found, which made up 0.8% of RPS in *Microcystis aeruginosa* [52]. The last group of sugars found in RPS, are amino sugars. Glucosamine and galactosamine were found in 7 of 61 species, making up 2.5% of RPS on average (Table 2-2). However, most studies did not analyse amino sugars (54 of 61 species), with absence reported for only three species. Comparing the relative amount of each neutral sugar, glucose was the dominant neutral sugar in most species, making up the largest relative amount of monosaccharides (37 species). In other species, galactose, mannose, rhamnose were dominant neutral sugars (7, 6 and 5 species, respectively), whereas fucose, xylose and arabinose were less frequently the dominant neutral sugars. Ribose or fructose were not the dominant neutral sugar in any of the species (Table 2-2).

Proteins are commonly found in RPS (43 of 61 species), making up the second largest fraction with an average of 11.2%$_w$ of the RPS (Table 2-2). Some species produce RPS that consist predominantly of proteins (up to 55%), such as *A. platensis*, *Microcoleus vaginatus* and *Scytonema javanicum* [60, 61]. RPS of three species lack proteins, such as *Nostoc flagelliforme, Nostoc microscopica* and *Arthronema africanum* [25, 50].

[2] EPS referred to as "*slime"* [58], making them CPS [19]. Excluded from analysis due to not being RPS.

EPS of certain cyanobacteria contain sulphur, which is absent in EPS from other prokaryotes and was previously believed to only occur in EPS from eukaryotes [11, 19]. Only 11 species from Table 2-2 contained sulphate, with an average of 7%. However, most authors have not determined sulphur content of the RPS (50 out of 61 species). Cyanobacteria producing sulphated EPS are often, but not exclusively, found in saline and hypersaline habitats [19]. Conversely, the highest sulphate content (16.5%$_w$) in this literature research was found in RPS from freshwater species *Synechococcus mundulus* [62]. An even higher sulphate content (18.83%$_w$) was observed in a mixture of RPS and CPS[3] from the freshwater species *Cyanothece epiphytica* [32]. Other non-sugar constituents found in RPS are acetyl, methyl, and amide groups, pyruvate, phenolics and myristic acid [27, 52, 63, 64].

Generally, the EPS composition is species-dependent, however in some cases, culture conditions have shown to influence the biochemical composition of several EPS in a species-dependent response [20]. To a greater extent, culture conditions affect the amount of EPS produced. This will be elaborated further in section 2.3. The compositional diversity of EPS results in a wide range of properties and biotechnological applications [15]. This will be elaborated further in the next section.

[3] CPS extraction method: “With NaOH solution (pH 10) for 4 h after preheating at 45°C.” [32] Cells were not examined for intactness afterward. Excluded from analysis due to not being RPS.

Table 2-2 Biochemical analyses of released extracellular polymeric substances (RPS) of cyanobacterial species reported in the literature.Total sugar, total protein, total sulphate, total uronic acid, and total amino sugar content of released polysaccharides are shown. Relative content of neutral sugars is shown. Abbreviations: m: %mol; w: %weight; -: absence; tr: traces; Glc: glucose; Gal: galactose; Man: mannose; Rha: rhamnose; Fuc: fucose; Xyl: xylose; Ara: arabinose; Fru: fructose; Rib: ribose; Sug: Sugar; UA: uronic acid; Am.: amino sugars; Pro: protein; Sul: sulphate; Ot: other.

Species	**% Sug**	**% UA**	**% Am**	**% Pro**	**% Sul**	**% Glc**	**% Gal**	**% Man**	**% Rha**	**% Fuc**	**% Xyl**	**% Ara**	**% Oth.**	**Source**
Anacystis nidulans		-				66.0$_{m}$	14.0$_{m}$	20.0$_{m}$		-				[65]
Aphanocapsa halophytica	27.8$_{w}$	-	-	10.3$_{w}$	11.9$_{w}$	25.0	3.0	15.0	2.0	53.0	3.0			[59]
Arthronema africanum	15.0$_{w}$	13.0$_{w}$		-		10.7$_{w}$	14.6$_{w}$	7.5$_{w}$	15.3$_{w}$	30.7$_{w}$	20.5$_{w}$	0.7$_{w}$		[50]
A. platensis	13.0$_{w}$	1.9		55.0$_{w}$	0.5	15.4	17.4	0.3	4.3	15.4	16.7	1.2	29.4$_{ukn}$	[61]
A. platensis	50.2$_{w}$	1.5$_{w}$	0.8$_{w}$	1.6$_{w}$		17.0$_{w}$	19.0$_{w}$	-	41.0$_{w}$	15.0$_{w}$	8.0$_{w}$		-$_{Fru}$ -$_{Rib}$	[66]
Arthrospira sp.	71.0$_{w}$			13.1$_{w}$	2.2$_{w}$									[67]
Calothrix pulvinata		11.3$_{w}$			tr	28.0$_{m}$	16.6$_{m}$	9.7$_{m}$	14.6$_{m}$	8.2$_{m}$	15.9$_{m}$	7.1$_{m}$		[57]
Calothrix pulvinata		11.9$_{w}$			tr	23.8$_{m}$	13.5$_{m}$	13.9$_{m}$	15.9$_{m}$	14.6$_{m}$	12.7$_{m}$	5.5$_{m}$		[57]
Chroococcus minutus		3.9	7.3	3.2		24.1	12.1	13.4	11.5	5.4	11.3	5.4	16.9$_{ukn}$	[68]
Cyanothece CYY 110	70.5$_{w}$	13.7$_{w}$		4.0$_{w}$	10.6$_{w}$	24.4$_{m}$	12.2$_{m}$	24.4$_{m}$	11.0$_{m}$	9.8$_{m}$	11$_{m}$	7.3$_{m}$		[69]
Cyanothece sp.	87.0$_{w}$			1.8$_{w}$		76.7		-			16.7		6.6$_{Rib}$	[54]

(continued on next page)

Table 2-2 (continued)

Species	% Sug	% UA	% Am	% Pro	% Sul	% Glc	% Gal	% Man	% Rha	% Fuc	% Xyl	% Ara	% Oth.	Source
Leptolyngbya foveolarum		6.4$_{w}$				23.6$_{m}$	18.5$_{m}$	20.5$_{m}$	21.6$_{m}$	-	15.7$_{m}$	-		[57]
Leptolyngbya sp.	56.0$_{w}$	13.0$_{w}$		7.5$_{w}$		38.6$_{w}$	2.2$_{w}$	16.8$_{w}$	5.2$_{w}$	10.9$_{w}$	13.5$_{w}$	12.8$_{w}$		[50]
Leptolyngbya sp.	32.0$_{w}$	11.0$_{w}$		7.5$_{w}$		23.4$_{w}$	26.8$_{w}$	11.9$_{w}$	7.1$_{w}$	13.5$_{w}$	15.6$_{w}$	1.7$_{w}$		[50]
Leptolyngbya sp.	9.0$_{w}$	5.0$_{w}$		11.5$_{w}$		30.0$_{w}$	10.9$_{w}$	17.2$_{w}$	13.1$_{w}$	8.2$_{w}$	12$_{w}$	8.6$_{w}$		[50]
Leptolyngbya tenuis		12.4$_{w}$			tr	33.7$_{m}$	17.1$_{m}$	17.8$_{m}$	19.0$_{m}$	6.4$_{m}$	6.1$_{m}$	-		[57]
Microcoleus vaginatus	27.6	2.2	0.6	50.3		22.4	20.4	23. 6	6.1	4.9	9.5	10.5	2.8$_{ukn}$	[60]
Microcoleus vaginatus	52.9$_{w}$	3.5$_{w}$		14.5$_{w}$		66.4	13.9	5.0	7.6		7.1			[70]
Microcystis aeruginosa	39.2	3.9	2.3	43.6		12.6	22.6	18.5	14.2	6.6	18.0	3.0	4.5$_{ukn}$	[52]
Nostoc calcicola	40.0$_{w}$	13.0$_{w}$		1.2$_{w}$		31.1$_{w}$	6.0$_{w}$	16.8$_{w}$	0.8$_{w}$	20.2$_{w}$	12$_{w}$	13.1$_{w}$		[50]
Nostoc carneum	56.0$_{w}$			2.7$_{w}$		-		66.8			33.2			[54]
Nostoc sp.	68.5$_{w}$			4.0$_{w}$		-		68.3			31.7			[54]
Nostoc cf. *calcicola*	26.0$_{w}$	7.0$_{w}$		9.6$_{w}$		41.8$_{w}$	17.2$_{w}$	12.1$_{w}$	12.6$_{w}$	2.4$_{w}$	12.1$_{w}$	1.8$_{w}$		[50]
Nostoc cf. *linckia*	36.0$_{w}$	12.0$_{w}$		1.5$_{w}$		43$_{w}$	27.5$_{w}$	9.5$_{w}$	-	-	19.2$_{w}$	0.8$_{w}$		[50]
Nostoc flagelliforme		13.3$_{m}$		-	-	42.8	20.7	6.6			29.9			[25]

(continued on next page)

Table 2-2 (continued)

Species	% Sug	% UA	% Am	% Pro	% Sul	% Glc	% Gal	% Man	% Rha	% Fuc	% Xyl	% Ara	% Oth.	Source
Nostoc insulare		24.1	-	3.5		61.5	0.2	3.3	1.1	11.7	0.2	22.1		[68]
Nostoc microscopica	44.0$_{w}$	7.0$_{w}$		-		32.3$_{w}$	18.3$_{w}$	11.8$_{w}$	1.5$_{w}$	17.9$_{w}$	9$_{w}$	9.2$_{w}$		[50]
Nostoc muscorum	57.0$_{w}$	17.0$_{w}$		1.9$_{w}$		59.1$_{w}$	2$_{w}$	9.3$_{w}$	1.8$_{w}$	1.4$_{w}$	2.4$_{w}$	24$_{w}$		[50]
Nostoc punctiforme	37.0$_{w}$	8.0$_{w}$		11.5$_{w}$		23.2$_{w}$	14.5$_{w}$	18.1$_{w}$	8.3$_{w}$	18.3$_{w}$	8.1$_{w}$	9.5$_{w}$		[50]
Nostoc sp.	40.5	-	-	7.5		43.9	21.5	1.6	3.5	-	20.9	-	9.0$_{ukn}$	[60]
Nostoc sp.	40.0$_{w}$	18$_{w}$		3.0$_{w}$		59.5$_{w}$	5.3$_{w}$	11.7$_{w}$	2.3$_{w}$	1.5$_{w}$	19.1$_{w}$	0.7$_{w}$		[50]
Nostoc sp.	48.0$_{w}$	22$_{w}$		4.3$_{w}$		27.0$_{w}$	3.2$_{w}$	22.8$_{w}$	2.0$_{w}$	9.7$_{w}$	8.4$_{w}$	26.9$_{w}$		[50]
Nostoc sp.	37.0$_{w}$	14$_{w}$		12$_{w}$		25.0$_{w}$	20.8$_{w}$	18.6$_{w}$	4.2$_{w}$	7.1$_{w}$	14.2$_{w}$	10.1$_{w}$		[50]
Nostoc sp.	42.0$_{w}$	11$_{w}$		3.3$_{w}$		26.9$_{w}$	18.9$_{w}$	9.9$_{w}$	3.2$_{w}$	14.3$_{w}$	19.5$_{w}$	7.3$_{w}$		[50]
Nostoc sp.	45.0$_{w}$	15$_{w}$		13.8$_{w}$		21.8$_{w}$	15.1$_{w}$	23.8$_{w}$	4.8$_{w}$	10.2$_{w}$	16.1$_{w}$	8.3$_{w}$		[50]
Nostoc sp.	60.0$_{w}$	15$_{w}$		1.6$_{w}$		24.7$_{w}$	2.1$_{w}$	24.3$_{w}$	0.5$_{w}$	1.7$_{w}$	23.4$_{w}$	23.3$_{w}$		[50]
Nostoc sp.	67.0$_{w}$	9$_{w}$		5.1$_{w}$		12.9$_{w}$	26.1$_{w}$	21$_{w}$	2.9$_{w}$	13.2$_{w}$	12.3$_{w}$	11.6$_{w}$		[50]
Nostoc sp.	41.0$_{w}$	15$_{w}$		1.2$_{w}$		17.5$_{w}$	8$_{w}$	18.1$_{w}$	1$_{w}$	27.1$_{w}$	14.1$_{w}$	14.2$_{w}$		[50]
Oscillatoria sp.	70.0$_{w}$			3.4$_{w}$		73.8		-			19.3		7.0$_{Rib}$	[54]
Phormidium 94a	93.0$_{w}$	3.9$_{w}$					47.3	7.8				18.8	26.1$_{Rib}$	[51]

(continued on next page)

Table 2-2 (continued)

Species	% Sug	% UA	% Am	% Pro	% Sul	% Glc	% Gal	% Man	% Rha	% Fuc	% Xyl	% Ara	% Oth.	Source
Phormidium ambiguum		13.9$_w$			tr	19$_m$	18$_m$	6.1$_m$	23.7$_m$	10.5$_m$	15.9$_m$	6.7$_m$		[57]
Phormidium cf. *autumnale*	16.0$_w$	5$_w$		37.8$_w$		8.2$_w$	8.4$_w$	5.7$_w$	50.2$_w$	4.2$_w$	11.1$_w$	12.2$_w$		[50]
Phormidium cf. *autumnale*	62.0$_w$	9$_w$		4.0$_w$		48$_w$	9$_w$	6.6$_w$	10.9$_w$	12.8$_w$	11$_w$	1.7$_w$		[50]
Phormidium cf. *usteri*		15.4$_w$				25.8$_m$	31.2$_m$	16.6$_m$	3.9$_m$	12.5$_m$	7.4$_m$	2.6$_m$		[57]
Phormidium corium		11.1$_w$			0.7$_w$	28.5$_m$	11.6$_m$	5.9$_m$	22.1$_m$	12.7$_m$	15.3$_m$	3.9$_m$		[57]
Phormidium corium		14.6$_w$				24.1$_m$	28.3$_m$	12.9$_m$	10.4$_m$	6.3$_m$	14.3$_m$	3.8$_m$		[57]
Phormidium corium		40.7$_w$				13.4$_m$	11.7$_m$	23.9$_m$	23.6$_m$	-	27.4$_m$	-		[57]
Phormidium corium		1.3$_w$				28$_m$	16.1$_m$	21.9$_m$	17.4$_m$	-	16.6$_m$	-		[57]
Phormidium corium		17.5$_w$				31.8$_m$	14.3$_m$	15$_m$	18$_m$	4.2$_m$	12.6$_m$	4.1$_m$		[57]
Phormidium sp.	64.0$_m$	2.4$_m$	2.3		13.2$_w$	19.7$_m$	9.5$_m$	6.7$_m$	20.2$_m$	7.9$_m$	30.9$_m$	5.1$_m$		[53]
Phormidium tenue	36.1	tr	9.0	21.9		33.2	1.3	3.0	10.6	2.3	4.8	44.8		[60]

(continued on next page)

Table 2-2 (continued)

Species	% Sug	% UA	% Am	% Pro	% Sul	% Glc	% Gal	% Man	% Rha	% Fuc	% Xyl	% Ara	% Oth.	Source
Scytonema javianicum	16.6	tr	tr	50.2		24.8	23.4	22.9	7.4		6.0	9.6	6.0_{ukn}	[60]
Scytonema ocellatum	14.0_{w}	3_{w}		15_{w}		19.8_{w}	6.7_{w}	12.6_{w}	42.6_{w}	2.1_{w}	12.4_{w}	3.8_{w}		[50]
Scytonema sp.	46.0_{w}	8_{w}		10_{w}		51.3_{w}	16_{w}	5.9_{w}	1.9_{w}	10.8_{w}	6.6_{w}	7.5_{w}		[50]
Spirulina sp.		57.8	9.6						32.6			11.5		[64]
Synechococcus bigranulatus	11.0_{w}	8_{w}		6.4_{w}		36.4_{w}	6.9_{w}	6.9_{w}	4.0_{w}	17.3_{w}	21.8_{w}	6.7_{w}		[50]
Synechococcus mundulus	57.1_{w}	31.8_{w}		9.7	16.5_{w}	15.6_{w}	14.9_{w}	47.5_{w}	1.3_{w}		18.4_{w}	1.0_{w}	$1.5_{w,Fru}$	[62]
Synechococcus sp.		tr				49.0_{w}	27.0_{w}	-		20.0_{w}	-		$-_{Fru}$	[28]
Trichormus sp.	26.0_{w}	8.0_{w}		2.4_{w}		21.7_{w}	4_{w}	10.6_{w}	37.5_{w}	10.2_{w}	5.1_{w}	4.9_{w}		[50]
Trichormus variabilis	58.0_{w}	7.0_{w}		9.1_{w}		31.8_{w}	14.1_{w}	25.5_{w}	1.7_{w}	2.8_{w}	22.1_{w}	2.0_{w}		[50]
Wollea saccata	31.0	-		21.0		21.2	17.7	18.1	15	10.3	7.4	1.6	6.0_{ukn}	[27]

2.2.2 Characterisation Methods of EPS

Various methods have been employed in the literature to characterise the composition of cyanobacterial EPS, including analytical and colorimetric techniques to analyse monosaccharides, total sugars, proteins, sulphate groups, and lipids. These methods were applied to understand the molecular composition and chemical structure of EPS and are described in the following paragraphs.

To analyse the monomeric composition, the EPS are first hydrolysed to release the monosaccharides. Typically, TFA is used due to its effectiveness in hydrolysing the glycosidic bonds without destroying the monosaccharide composition [32, 71]. Gas chromatography-mass spectrometry (GC-MS) is commonly used after derivatisation to volatilise the sugars [32]. GC-MS offers high sensitivity and resolution but requires complete derivatisation to avoid sugar loss or misidentification, and uronic acids can be difficult to derivatise accurately [72]. Additionally, a single sugar can produce multiple spectra due to different derivatised forms, complicating analysis [72]. High-performance liquid chromatography (HPLC) is also one of the most commonly used methods for analysing monosaccharides due to its speed and simplicity, as it avoids the need for derivatisation if refractive index detection is used [73]. However, HPLC separates molecules primarily by polarity, which can result in poor resolution for complex mixtures where compounds of similar polarity may co-elute [72]. High-performance anion-exchange chromatography with pulsed amperometric detection (HPAEC-PAD) provides an alternative high-resolution method without derivatisation, separating sugars based on pKa differences [72, 73]. HPAEC-PAD has been shown to produce results comparable to those obtained by GC-MS for the monosaccharide composition of cyanobacterial EPS [28]. However, it is sensitive to temperature, alkalinity changes, and sample contamination by proteins or peptides [72]. Nuclear magnetic resonance (NMR) techniques, including ^{1}H-NMR, offer rapid and detailed profiling without derivatisation or extensive pre-treatment, but are costly, require specialised equipment, and demand high sample purity to ensure accurate quantification [72, 73]. Enzymatic assays (Megazyme) are another alternative, showing on average 4% variation from HPAEC-PAD, though variation for certain monosaccharides (glucuronic acid) was up to 30% [72]. Furthermore, hydrolysis efficiency may vary depending on polymer composition [72].

Total uronic acid content can be quantified by colorimetric assays such as the carbazole method or the meta-hydroxydiphenyl assay; both offering reliable detection albeit with slight variations in sensitivity and protocol complexity [32, 50, 74, 75]. For total carbohydrate content, the phenol–sulfuric acid method is extensively used due to its simplicity and robustness, although the anthrone assay provides a less toxic alternative with comparable sensitivity [32, 76-78].

Protein analysis can be conducted using several methods, including Lowry, Coomassie Brilliant Blue (Bradford), and bicinchoninic acid (BCA) assays [32, 61, 78]. The Bradford method, which is a one-step process, is commonly used because it is rapid, simple, and highly sensitive [79]. BCA method, which is a more time-consuming two-step process, offers great sensitivity and few interferences, though it is less commonly used [79]. The Lowry method is sensitive and accurate but time-consuming due to solution preparation and correction for interference with humic acids [79].

Sulfate groups, another important EPS constituent, can be quantified using the $BaCl_2$ gelatine turbidity assay, which can also be purchased as a kit from Merck [69, 80]. Finally, lipid content in EPS can be quantified via the phospho-vanillin method, which involves colorimetric detection following solvent extraction [81]. This method allows for sensitive detection of lipids [78].

2.2.3 Properties and Structure-Function Relationship of EPS

Cyanobacterial EPS exhibit distinct properties, which make them suitable as products for a wide range of applications [82]. This PhD thesis focuses on the following five properties: emulsifying, flocculating, antioxidant, metal-chelating and UV-protective activities. The relationship between these five properties and EPS composition and structure are described in the following sections. Since structure-function relationship of EPS in cyanobacteria is far from being understood, this section also includes information based on polysaccharides in general [11].

2.2.3.1 Emulsifying Activity

EPS from several cyanobacteria have shown to exhibit emulsifying activities. An emulsion is defined as a mixture of two liquids that are normally immiscible [83]. CPS[4] from *Nostoc flagelliforme* at 0.5% concentration have shown 66.39% emulsion activity, which was markedly higher than that of the positive control (C^+) xanthan gum (XG, 51%, Table 2-3). Emulsion activity was based on measuring the height of the emulsion layer compared to the overall height of the mixture [83]. Another example, the patented emulsifying EPS from *Phormidium* J-1, *Emulcyan*, was analysed using a different method based on turbidity, which was measured in Klett units. *Emulcyan* showed maximum emulsifying activity of 225 Klett units [26].

Table 2-3 Emulsifying activities of extracellular polymeric substances (EPS) from cyanobacteria reported in the literature.Abbreviations: C^+: positive control; XG: xanthan gum.

Species	Emulsifying activity	Value of C^+	Reference
Nostoc flagelliforme	66.39%	51% (XG)	[83]
Phormidium J-1	225 Klett units	N.A.	[26]

Emulsifying properties of polysaccharides depend on two features. Firstly, having their hydrophobic segments bind to oil droplets while their hydrophilic segments extend into the aqueous phase, thereby reducing the interfacial tension between oil and water and secondly, forming an effective protective layer to prevent flocculation or coalescence [84]. The first feature is crucial for the initial formation of the emulsion, while the second feature is critical for maintaining the stability of the emulsion [84].

The key factors influencing these features are molecular weight, the degree of branching, and content and distribution of hydrophobic functional groups [85]. Polysaccharides are generally hydrophilic due to the presence of hydroxyl and carboxyl groups, which makes them soluble [85]. Hydrophobic components, such as peptidic fractions, ester-linked acetyl groups, or deoxy sugars (e.g., rhamnose and fucose) are essential for binding to oil [11]. Even a small fraction of protein can suffice for this purpose [84, 86]. Low molecular weight polysaccharides could be adsorbed

[4] CPS extraction method: „*The crude CPS was obtained by extracting lyophilized cells in hot water at 80°C for 6 h*“ [83]. Cells were not examined for intactness afterward.

more quickly to the oil-water interface than higher molecular weight polysaccharides, enhancing the first feature of initial emulsifying activity [85]. However, shorter chains tend to form thin adsorbed layers, which are less effective at preventing coalescence, thus compromising the second feature of long-term stability [84]. In contrast, longer chains form thicker layers around oil droplets, better preventing coalescence and ensuring stability [84, 87]. Higher molecular weight polysaccharides provide greater steric hindrance, reducing the risk of droplet aggregation and flocculation [85]. Branching, particularly with numerous and long branches, enhances steric stabilization by increasing interactions with the aqueous phase [88]. Ionisation of carboxyl groups (e.g. in uronic acid residues), which occurs when the pH is higher than the pKa of the substance, can cause repulsion between these functional groups, which in turn leads to electrostatic stabilisation of oil droplets [84].

According to literature, it has been suggested that the physiological reason for cyanobacterium *Phormidium* J-1 to produce the emulsifying EPS, *Emulcyan*, is a dispersal strategy as it aids detachment and re-attachment to surfaces in new territories [26]. This theory was based on the observation that benthic cyanobacteria are hydrophobic whereas their hormogonia are hydrophilic. Hormogonia are small motile filaments that travel through the water current and re-gain hydrophobicity to attach to new surfaces, which is a dispersal strategy of the parent colony [26]. Production of amphiphilic EPS was theorised to be the dispersal strategy of non-hormogonia-forming cyanobacterium *Phormidium* J-1. Fattom and Shilo [26] reported that the hydrophobicity of *Phormidium* J-1 reduced as cells aged. When cells were washed and re-suspended in fresh medium, the hydrophobicity of the cell surface reoccurred. Fattom and Shilo [26] hypothesised that cells are initially attached to a surface with the aid of the hydrophobic sites of its filaments. Cells produce *Emulcyan*, which masks its hydrophobic sites, resulting in detachment and dispersal of the cells. During dispersal, *Emulcyan* is washed off, resulting in hydrophobic sites to be exposed again, which then aids re-attachment [26]. Alternatively, the authors have suggested that *Emulcyan* is produced to bind to the hydrophobic surface of the substratum [26].

EPS with emulsifying properties could find applications in food or cosmetics. In the food industry, oil-in-water emulsions find applications in dairy, candy, bakery, meat products and beverages [89]. In cosmetics, emulsifiers are used as thickening or

emulsifying agent to mix hydrocarbons and oils in liquids such as water [69]. Advantages of biosurfactants, such as bioemulsifiers, compared to chemical emulsifiers are their biodegradability and low toxicity [90].

2.2.3.2 Flocculating Activity

Another feature that cyanobacterial EPS have shown is flocculating activity. EPS obtained from *Anabaena* sp. BTA992 showed 88% flocculating activity [45]. For CPS[5] from *N. flagelliforme*, 92% flocculating activity was observed (Table 2-4) [83]. The mechanism of flocculation is complex. Polymers can act as flocculants or dispersants, depending on the dosage [91, 92]. This is due to the involvement of different mechanisms. Firstly, at low polymer concentration, bridging flocculation may occur. The polymer does not fully cover the surface of the particles, leading to bridging of only two or more droplets [93]. Secondly, at medium polymeric concentration, when there is an optimal amount of polymer for complete coverage of particles, steric stabilisation occurs [94]. Thirdly, at moderate to high polymer concentration, depletion flocculation occurs. As polymer concentration exceeds the level for complete particle coverage, polymers are present in the solution around particles except for the space between particles. This results in an osmotic effect, overcoming the repulsive interactions between particles, causing them to flocculate [94]. Lastly, at very high polymer concentration, depletion stabilisation can occur. At this point, polymer concentration is so high that the mixture resembles a colloid more than a solution [94].

Table 2-4 Flocculating activity of extracellular polymeric substances (EPS) from cyanobacteria reported in the literature.Abbreviations: C^+: Positive control; XG: Xanthan Gum.

Species	Flocculating activity	Value of C^+	Reference
Nostoc flagelliforme	91.81%	79.8% ($Al_2(SO_4)_3$), 19.9% (XG)	[83]
Anabaena sp. BTA992	88%	N.A.	[45]

[5] CPS extraction method: „*The crude CPS was obtained by extracting lyophilized cells in hot water at 80°C for 6 h*“ [83]. Cells were not examined for intactness afterward.

Several characteristics such as charge density, size and secondary structure affect flocculating properties of polymers [95, 96]. Linear chains of high molecular weight at an optimal charge density are the most effective polymers [97, 98]. The impact of each of those characteristics will be explained in the following paragraphs.

Bridging flocculation occurs when long chain polysaccharides with high molecular weights and low charge density adsorb on particles in such way that the loops and tails extend and bind to other particles [93, 97]. Due to this mechanism, longer chains (high molecular weight) should be more effective than shorter chains (low molecular weight) [99]. Branched versus linear structure also plays a role, as this impacts the effective length of the polymer chain [100].

Charge density significantly impacts flocculating activity by influencing the polymer's configuration in solution [98]. Polymers typically adopt a random coil configuration, occupying more volume than individual monomers, which affects light scattering and solution viscosity. The extent of polymer expansion is influenced by the charge on polymer segments; charged segments can repel each other, expanding the coil [98]. While higher charge density may reduce flocculation due to intramolecular repulsion, some charge is beneficial for polymer expansion, allowing it to reach other particles [101]. Therefore, an optimal charge density for effective flocculation exists [98].

Carboxylate groups and their location play a crucial role for flocculating activity of EPS. Carboxylate groups on side chains promote flocculation, while those on the backbone are less accessible, reducing the flocculation ability [101]. Uronic acids, which contain carboxylate groups, have been positively correlated to flocculating activity of cyanobacterial EPS [44]. Another influential factor is flexibility of the polymeric chain [100]. Flexible polysaccharides (e.g. alginate) facilitate bridging flocculation, whereas rigid polysaccharides (e.g. xanthan gum) promote depletion flocculation [102]. The flexibility of the macromolecular chain in microalgal glycans is influenced by the nature of the glycosidic bonds involved [29].

EPS with flocculating activity can be used in several industries. In the food and drinks industry, flocculants are used to clarify raw water [103]. EPS from cyanobacteria can be used to purify wastewater [104]. Additionally, EPS with flocculating activity find application as bioflocculants in commercial food fermentation processes, aiding the

separation of cells from the product [105]. Another application is harvesting of microalgal biomass, where positively charged polymers create bridges between negatively charged microalgal cells, overcoming the cells' electrostatic repulsion [95]. Bioflocculants represent an alternative to synthetic flocculants such as polyacrylamide, which are suspected to be carcinogenic, causing a need for non-toxic alternatives [103].

2.2.3.3 Antioxidant Activity

Another feature that EPS from cyanobacteria have shown to exhibit is antioxidant activity. Neutralisation of radicals like 2,2-diphenyl-1-picrylhydrazyl (DPPH) and 2,2'-azino-bis(3-ethylbenzothiazoline-6-sulfonic acid) cation ($ABTS^{+}$) occurs via reduction by donation of a hydrogen or electron, respectively, from an antioxidant agent [106]. The antioxidant activity of EPS is influenced by the functional groups (-COOH, $-C_2H_4O$, $-SO^{2-}$, -OH) at the interactive site [107]. Electron withdrawing groups such as sulphate, acetyl and carboxyl groups, and electron donating groups like hydroxyl groups affect water solubility, negative charge, electron density and activation of hydrogen atoms, which in turn affects hydrogen and electron donating abilities. For example, the strong radical scavenging ability of chitosan (82%) is based on its amino and hydroxyl groups [107, 108].

Multiple other characteristics of EPS are suggested to influence the antioxidant activity, such as reducing sugar content, monosaccharide composition, glycosidic linkage type, branching patterns and depolymerisation, which have been discussed in a recent study by Andrew and Jayaraman [107]. Reducing sugars with aldehyde or ketone groups can donate electrons to reduce metal ions, enhancing antioxidant potential. Monosaccharide content, through increased hydrogen donation, may elevate scavenging activity, with monomeric composition potentially having a greater impact on reducing ability than other structural features [107]. However, the antioxidant activity of polysaccharides is a function of combination of several factors such as molecular weight and content of sulphate, uronic acids and monosaccharide, rather than that of a single factor [109]. This could explain opposite trends being observed in studies when comparing antioxidant properties of EPS with composition. One study on EPS from the fungus *Hirsutella* sp. found the antioxidant activity of the EPS being positively correlated to mannose and negatively correlated to glucose [110]. Conversely, a study

on three fractions of EPS from another fungus, *Boletus aereus*, found the highest antioxidant activity (78.3%) in the fraction with the largest glucose content (51.95%) [111]. The type of glycosidic bond (*α* or *β*) has been suggested to have an influence on antioxidant properties of EPS due to the position of the hydroxyl group, flexibility and water solubility, which can affect contact and exposure of hydroxyl groups for radical neutralisation by hydrogen donation [107].

Antioxidant activity of natural polysaccharides can be further enhanced by post-production modifications of the polysaccharide [112]. Properties such as type of glycosidic bond, ways of connections and monosaccharide composition determine whether a polysaccharide has bioactive properties. However, solubility, relative molecular mass, main-chain configuration and spatial configuration affect the *level* of bioactivity [112]. This means that if bioactivity is present, it could be enhanced by modifications such as sulfation, carboxymethylation, phosphorylation selenisation, acetylation, alkylation and different methods to cleave the polysaccharides into lower molecular weight pieces [113]. The different methods were reviewed in detail by Li, et al. [112] and are summarised in the following paragraph.

Polysaccharides can be sulphated by substitution of terminal carboxyl, hydroxyl or amino groups with sulphate groups [112]. Carboxymethylation, which is the introduction of a carboxymethyl to the polysaccharide chain, increases the solubility and prevents inhibition of bioactivity caused by poor solubility [114]. Phosphorylation is the addition of charged phosphate groups, which can improve water solubility, modify chain conformation and change molecular weight of polysaccharides [112]. Selenisation is the process of forming selenide polysaccharide by using selenious acid or selenite to form selenite ester bonds with hydroxyl groups on polysaccharides [112]. Acetylation, which is the addition of acetyl groups into the polysaccharides can aid stretching the polysaccharide branches and changing orientation, resulting in improved solubility by exposure of hydroxyl groups [115]. Similarly, alkylation which involves the introduction of an alkyl group at the terminal end of the polysaccharide chain can improve solubility and decrease viscosity [112, 116]. Lastly, solubility can be enhanced by cleaving polysaccharides into smaller, lower molecular weight fractions. Cleaving methods include biological (enzymes), chemical (acid/alkali degradation for cleaving

of glycosidic bonds) and physical (ultrasonic disruption, microwave exposure or radiation-induced reaction) procedures [112].

Table 2-5 Antioxidant activities of extracellular polymeric substances (EPS) from cyanobacteria reported in the literature, determined by 2,2-diphenyl-1-picrylhydrazyl (DPPH) scavenging assay.Concentration of extracellular polymeric substances (EPS) is shown in brackets next to DPPH scavenging activity. Abbreviations: C^+: Positive control.

Species	**DPPH scavenging activity**	**Value of C^+ (Ascorbic acid)**	**Reference**
Leptolyngbya sp.	90.4% (100 g L^{-1})	80% (100 g L^{-1})	[117]
Gloeocapsa gelatinosa	95% (2 g L^{-1})	80% (2 g L^{-1})	[118]

As shown in Table 2-5, EPS of cyanobacteria in literature have shown antioxidant properties as high as 90-95%, exceeding that of the positive control, ascorbic acid [117, 118]. EPS with antioxidant activities can find applications in food, cosmetic and pharmaceutical industries. Radical scavenging activity make EPS suitable as antioxidant agents or functional food additives [105]. Antioxidants are used to improve shelf life of food, which can prevent food waste and help protect the environment [119]. Furthermore, recent interest in natural antioxidants as possible therapy for diseases related to oxidative stress, such as cardiovascular disease, diabetes, cancer and neurodegenerative disorders has emerged [120]. EPS can delay or reduce the oxidative damage to cells, while being biodegradable and non-toxic [107]. In contrast, the synthetic antioxidants butylated hydroxyanisole (BHA) and butylated hydroxytoluene (BHT) are considered carcinogenic, which is why they are strictly regulated in areas like the EU [107, 121, 122]. BHA has been shown to have carcinogenic effects on the forestomach of rodents [123]. Similarly, BHT has shown carcinogenic action depending on target organ, with adverse effects on liver, kidney and lung in rodents [124, 125]. In cosmetics, EPS with antioxidant properties can prevent reactive oxygen species (ROS) from causing skin damage and aging [126]. ROS are oxygen radicals, such as superoxide ($O_2^{\cdot -}$), hydroxyl ($OH^{\cdot}$), peroxyl ($RO_2^{\cdot}$), and hydroperoxyl ($HO_2^{\cdot}$) radicals, as well as nonradical oxidising agents like hydrogen peroxide (H_2O_2), hypochlorous acid (HOCl), and ozone (O_3), which can readily convert

into radicals [127]. A free radical is defined as any species that contains one or more unpaired electrons [127].

2.2.3.4 Metal-Chelating Properties

Cyanobacterial EPS have shown to possess metal-chelating properties, which has been theorised to have the physiological roles of accumulating the metals essential for growth and preventing cells from direct contact with toxic metals [20]. Excess of transition metals can cause damage to cells via ROS formation, which can cause damage to DNA, protein, lipids and carbohydrates [108]. In the context of lipid peroxidation, iron is particularly significant due to its high reactivity and role as a major promoter of lipid oxidation [128]. Chelating metals mediates this process by stabilizing the oxidized form of the metal ions and preventing oxidative damage, leading to some authors describing it as an antioxidant mechanism [108, 128].

Table 2-6 Metal-chelating activities of extracellular polymeric substances (EPS) from cyanobacteria reported in the literature.Abbreviations: C^+: positive control; EDTA: ethylenediaminetetraacetic acid.

Species	**Metal-chelating activity**	**Value of C^+**	**Reference**
Gloeocapsa gelatinosa	91%	75% (EDTA)	[118]
A. variabilis var. *ellipsospora*	96%	69% (Ascorbic acid), 82% (Chitosan)	[108]

Metal-chelating activities as high as 91% were observed for EPS of the cyanobacterium *Gloeocapsa gelatinosa*, exceeding that of ethylenediaminetetraacetic acid (EDTA, 75%) [118]. EPS[6] from another cyanobacterium, *A. variabilis* var. *ellipsospora*, showed an even higher chelation activity of 96%, exceeding that of the positive controls (Table 2-6) [108]. However, one of the positive controls used, ascorbic

[6] EPS extraction method: "*Two volumes of chilled acetone were added to the culture for the precipitation of EP.*" [108] Cells were not examined for intactness afterward.

acid, is considered a weak chelating agent that cannot compete with stronger chelators like EDTA [129].

Chelating properties of cyanobacterial EPS are a result of their anionic nature caused by acidic sugars (e.g. uronic acids), inorganic (e.g. sulphate groups) or organic substituents (e.g. pyruvate groups) [20]. More generally, in polysaccharides, chelating properties are a result of two or more of the following functional groups: C=O, –COOH, –O–, –OH, –SH, –S–, $–PO_3H_2$ and $–NR_2$, and a favourable structure-function-configuration [130, 131]. Glycosidic bonds are a type of ether bond (–O–), which typically link monosaccharides such as glucose, galactose and xylose together, forming the backbone of the EPS [132]. Neutral sugars contain hydroxyl (–OH) and carbonyl (C=O) groups, whereas uronic acids are formed by oxidization of the terminal hydroxyl group of an aldose to a carboxylic acid group (-COOH) [133]. Amino groups ($-NH_2$) can be present in amine sugars or in the protein fraction. The protein fraction can also contain sulfhydryl group (-SH) and disulfide linkages (–S–), as cysteine residues have sulfhydryl (thiol) groups, which can be formed into disulphide bonds [134]. Phosphate groups ($–PO_3H_2$) seem to be rare in cyanobacterial EPS, with none of the species studied in section 2.2.1 reporting presence of these groups. For illustration, the chelating mechanism of EDTA is shown in Figure 2-1.

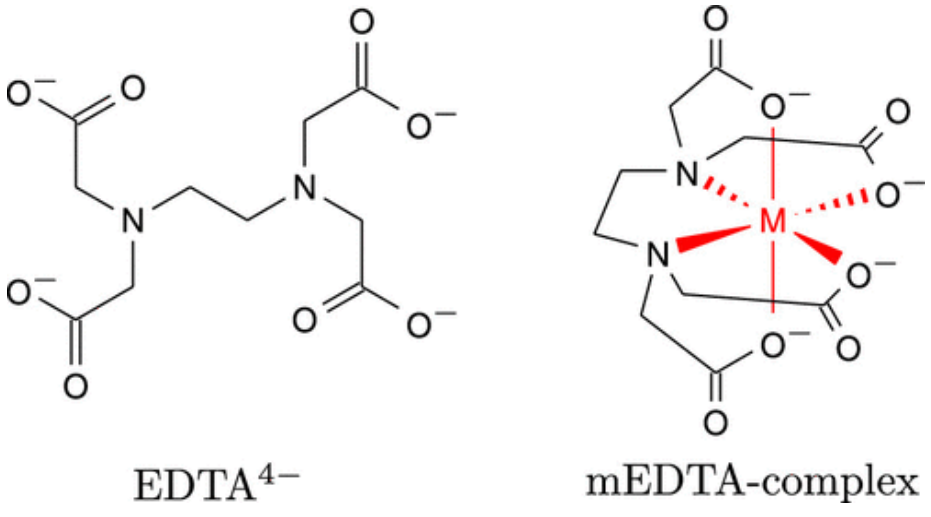


Figure 2-1 Chelating mechanism of ethylenediaminetetraacetic acid (EDTA).In solution, the carboxyl groups of EDTA are deprotonated, resulting in a negative charge. EDTA is capable of binding metal (III) ions (M) through coordination of its nitrogen and oxygen sites, forming six covalent bonds with the metal (M) [135].

EPS with chelating properties have several potential applications. Due to their protective effect against oxidation, they could be used as natural antioxidant or functional food additive [118]. Furthermore, chelating agents can find applications in wastewater treatment, e.g. to remove heavy metals from wastewater [12]. Lastly, they could be used as bio-based alternative to EDTA, which is widely used as stabiliser in cleaning products and detergents, but shows poor biodegradability in natural environments studies [136].

2.2.3.5 UV-Protective Properties

Several metabolites of cyanobacteria and microalgae have shown to exhibit photoprotective properties [137]. Photoprotection is defined as the reduction of the ultraviolet (UV) radiation damage that can lead to skin diseases and increase the risk of skin cancer [138]. UV radiation is classified into three types: UVA (320–400 nm), UVB (290–320 nm), and UVC (200–290 nm). UVA induces indirect DNA damage through the production of ROS and is linked to skin aging and pigmentation changes. UVB is primarily responsible for sunburns and DNA strand breaks, causing pyrimidine dimer mutations, which are closely associated with nonmelanoma skin cancers [139]. Driven by consumer demand, tons of UV filters are produced annually and incorporated in sunscreen lotions, facial makeup, moisturizers, and lipsticks [126, 140, 141]. Conventional sunscreens either contain inorganic or organic UV filters. Inorganic UV filters comprise of mineral particles like titanium dioxide or zinc oxide that pose a physical barrier to the UV radiation. While effective, these compounds can produce highly oxidising radicals [142]. The most common organic filters such as ethylhexylmethoxycinnamate, butyl methoxydibenzoylmethane, octocrylene and benzophenone-4 show adverse effects such as contact dermatitis [143, 144]. Additionally, an endocrine disruption effect is suggested by an increasing numbers of *in vitro* and *in vivo* studies [145]. Synthetic UV filters can also cause harmful effects on ecosystems, such as bleaching of coral reefs [146].

As a result, there is increased consumer demand for natural and sustainable cosmetic ingredients [126, 147]. A consumer study revealed that half of the participants prefer natural skincare, 60% are willing to spend more on bio-based products, and the majority are aware of the negative impact of synthetic ingredients on marine ecosystems [148]. Natural UV-protective compounds that can be found in algae and

cyanobacteria are scytonemin, mycosporine-like amino acids (MAAs), carotenoids and polyamines [137]. MAAs are small (<400 Dalton (Da)), colourless, water-soluble compounds that absorb UV and dissipate the radiation as heat without producing ROS [149-151]. The photoprotective effect of MAAs is suggested to arise from their π-electron system, which absorbs UV radiation. These π-electron systems are found in conjugated bond structures, a common characteristic of natural UV-screening molecules that enhances their UV-protective properties [152].

Table 2-7 Ultraviolet (UV) protection level of compounds produced by cyanobacteria and algae reported in the literature.Abbreviations: C^+: positive control; SPF: sun protection factor; BMDBM: butylmethoxydibenzoylmethane; OMC: octylmethoxycinnamate.

Compound	**UV-protection level**	**UV-protection level of C^+**	**Reference**
Scytonemin	SPF 33.34	N.A.	[153]
Porphyra-33	SPF 1.23	SPF 0.6 (Aloe vera gel)	[152]
Porphyra-33 + shinorine	SPF 4-6	SPF 9.54 (Reference sunscreen containing BMDBM and OMC)	[154]

Although it is less common to study EPS as a sunscreen, photoprotective compounds can be present in the EPS slime or sheath, imparting a sunscreen-like quality to EPS. For instance, the yellow-brown pigment scytonemin is predominantly produced by cyanobacteria and mostly found in the EPS sheath, functioning as a UV-protective shield around the cells that absorbs 90% of the radiation [126, 155-157]. A cream containing scytonemin from *Nostoc commune* has shown to have a sun protection factor (SPF) as high as 33.34 (Table 2-7) [153]. The MAA shinorine was found to be exclusively located in the slime layer of *Microcystis aeruginosa* strain PCC 7806. While it is not covalently bound, it remains tightly embedded within the EPS [158]. Porphyra-33, a MAA from red alga *Porphyra vietnamensis*, has shown a photoprotection level comparable to an SPF of 1.23, which was described as "*a very potent sunscreen*

compound" by the authors [152]. The combination porphyra-33 with another MAA, shinorine, was found to have an SPF of 4-6 [154].

MAAs including shinorine and porphyra-334 have been commercialised globally for incorporation into skincare and cosmetic products, including Helioguard 365, M-Rose and Fikia from BeautyLine Ltd (Rajesh Prasad Rastogi et al., 2014). Apart from photoprotection, MAAs and carotenoids are suggested to protect *Leptolyngbya* sp. from desiccation [159]. MAA production can be enhanced by changing the growth parameters, such as quantity and quality of radiation, as well as nutrient availability (e.g. ammonium chloride) [160].

2.2.4 Biosynthesis Pathways of Cyanobacterial EPS

Information on EPS biosynthesis and its regulation in cyanobacteria is limited [161]. The mechanism is very complicated and poorly understood [82]. However, due to biosynthesis pathways in bacteria being relatively conserved, it is expected that cyanobacteria would follow a similar pattern to other bacteria, including the three steps described in the following [11, 162].

1) Activation of monosaccharides and conversion into sugar nucleotides,
2) Transfer of sugar nucleotide donors to carrier molecules and assembly as repeating units,
3) Export out of the cell.

The proteins involved in polymerisation, termination and export are conserved among bacteria, whereas glycosyltransferase and the enzymes responsible for monosaccharide activation or modification are strain-dependent [20]. However, some differences to other bacteria are expected due to the unique characteristics of cyanobacterial EPS and ability of cyanobacteria to perform oxygenic photosynthesis [20].

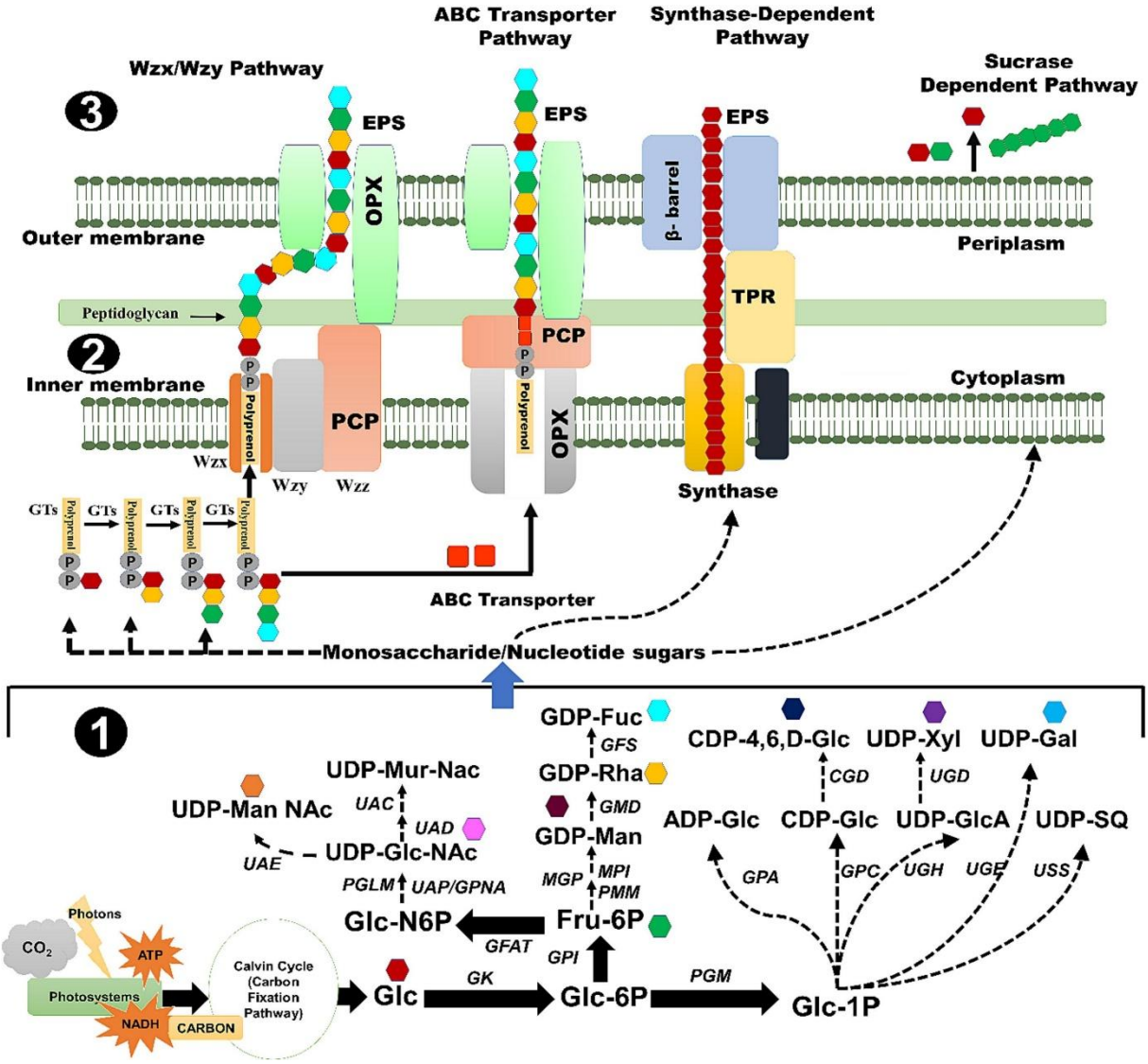


Figure 2-2 Illustration of the biosynthesis pathway of cyanobacterial EPS production according to Debnath, et al. [82].Abbreviations: 3-PG: 3-phosphoglycerate; ADP: Adenosine diphosphate; ABC: Adenosine triphosphate-binding cassette; ADP-Glc: ADP-glucose; CDP-Glc: CDP-glucose; CGD: CDP-glucose 4,6-dehydratase; CDP: Cytidine diphosphate; UDP-GlcA: UDP-d-Glucuronate; Fru-6P: Fructose-6-phosphate; GMD: GDP mannose 4,6-dehydratase; GDP-Rha: GDP-d-rhamnose; GDP-Fuc: GDP-l-fucose; GFS: GDP-l-fucose synthase; GDP-Man: GDP-mannose; GK: Glucokinase; Glc-N6P: Glucosamine 6-phosphate; GPNA: Glucosamine-1-phosphate N-acetyltransferase; Glc: Glucose; Glc-1P: Glucose 1-phosphate; Glc-6P: Glucose 6-phosphate; GPA: Glucose-1-phosphate adenylyltransferase; GPC: Glucose-1-phosphate cytidylyltransferase; GPI: Glucose-6-phosphate isomerase; GTs: Glycosyltransferases; GDP: Guanosine diphosphate; GFAT: L-glutamine:D-fructose-6-P amidotransferase; MGP: Mannose-1-phosphate guanylyltransferase; MPI: Mannose-6-phosphate isomerase; OPX: Outer membrane polysaccharide export; PGM: Phosphoglucomutase; PGLM: Phosphoglucosamine mutase; PMM: Phosphomannomutase;

PCP: Polysaccharide copolymerase; Suc-DP: Sucrase-dependent pathway; Syn-DP: Synthase-dependent pathway; TPR: Transporter protein in cell envelope; UGH: UDP glucose 6-dehydrogenase; UDP-Glc-NAc: UDP- N-Acetyl-d-glucosamine; UDP-SQ: UDP-6-sulfoquinovose; UDP-Gal: UDP-galactose; UGE: UDP-glucose 4-epimerase; UGD: UDP-glucuronate decarboxylase; UDP-Man-NAc: UDP-N-acetyl-d-mannosamine; UAC: UDP-N-acetylglucosamine 1-carboxyvinyltransferase; UAE: UDP-N-acetylglucosamine 2-epimerase; UAP: UDP-N-acetylglucosamine pyrophosphorylase; UDPMurNA: UDP-N-acetylmuramate; UAD: UDP-N-acetylmuramate dehydrogenase; USS: UDP-sulfoquinovose synthase; UDP-Xyl: UDP-xylose; UDP: Uridine diphosphate; Wzx: Wzx flippase; Wzy: Wzy polymerase; and Wzz: Wzz chain-length regulator proteins.

For cyanobacteria specifically, the proposed biosynthesis pathway is illustrated in Figure 2-2. Firstly, CO_2 is fixed via the Calvin Benson cycle to form 3-PG (3-phosphoglycerate), which is used to produce the precursor monosaccharides needed for sugar nucleotide biosynthesis, such as glucose-6-phosphate (Glc-6P), glucose-1-phosphate (Glc-1P) and fructose-6-phosphate (Fru-6P) [82]. Secondly, in the cytoplasm, glycosyltransferases (GTs) transfer the sugar nucleotides from the activated donor molecule to acceptor molecules (e.g. a lipid carrier such as polyprenol) in the plasma membrane, where the oligosaccharide chain gets extended [20]. Polymerisation and export can happen in one of four different ways [82]:

1) Wzx-Wzy pathway
2) ABC-transporter pathway
3) Synthase-dependent pathway
4) Sucrase-dependent pathway

Heteropolymers are synthesised using the Wzx-Wzy dependent pathway or the ATP-binding cassette (ABC) transporter-dependent pathway [82]. In the Wzx-Wzy dependent pathway, the monomeric nucleotide sugar molecules are connected by GTs to form hetero-oligosaccharide repeat units in the cytoplasm [20]. The composition of the hetero-oligosaccharides is based on the substrate specificity of GTs and the expressing operons. In addition, the oligosaccharides are linked to the linker molecule undecaprenyl diphosphate (Und–P) by GTs [82]. Then, the formed oligosaccharide-linker complex is flipped to the periplasm by the flippase enzyme encoded by the *wzx* gene. The oligosaccharide-linker complex are polymerised by the polymerising

enzyme encoded by the *wzy* gene to form a polysaccharide [20]. The length of the polymer chain is controlled by the polymerising enzyme encoded by *wzy* gene and the protein-polysaccharide-copolymerase enzyme unit (PCP) encoded by the *wzz* gene. Finally, the terminated polysaccharide is exported out of the cell via the non-specific outer membrane polysaccharide export (OPX) exporter located in the outer membrane [82].

CPS production is mediated by the ABC transporter pathway. Polymerisation of the nucleotide sugars occurs in the cytoplasm. Nucleotides are polymerised to linear polysaccharides attached to the Und-P linker by the GTs [82]. Besides the Und-P linker, CPS also have a unique glycolipid part made of poly-2-keto-3-deoxyoctulosonic acid (PKD) and a phosphatidylglycerol bond at the reducing terminal, which is specific for ABC transporter systems [82]. Transport to the periplasm involves a specialized protein complex that includes an ATP-binding unit and a transport permease [163]. Similar to the Wzx-Wzy pathway, the final step is export of the growing polysaccharide outside of the cell by WxPCP and OPX [82]. Termination and release can either happen coupled or uncoupled. In the coupled case, competition between assembly parts and energy components (ATP-binding parts) controls chain length. Alternatively, termination and release occurs uncoupled, in which case modification of the Und-P linker at the non-reducing terminal results in the termination of chain length extension [82].

Homopolymers such as alginates and cellulose are synthesised based on synthase-dependent pathways, where one single protein called synthase performs both, polymerization and translocation [82]. Lastly, in the sucrase-dependent pathway, the extracellular sucrase enzyme polymerizes monosaccharide units by cleaving sucrose molecules into fructose and glucose, forming the homopolymers glucans and fructans [20, 82].

2.3 Influence of Culture Conditions on EPS Production in Cyanobacteria

A wide range of cultivation parameters has shown to influence EPS production in cyanobacteria. Such parameters may include light, temperature, pH, nutrient

concentrations and cultivation mode (batch, fed-batch, continuous, phototrophic, mixotrophic and heterotrophic). This will be elaborated in the following sections.

Before describing the effect of specific cultivation parameters on EPS production, it is important to consider the different ways in which optimal conditions are expressed and quantified among various studies. Optimal EPS production is either expressed based on concentration, productivity, yield or in rare cases like by Vergnes, et al. [164] as the area covered by EPS on a microscope picture. In this PhD thesis, EPS yield (Y_{EPS}; g EPS g^{-1} biomass), EPS concentration (C_{EPS}; g L^{-1}), and EPS productivity (P_{EPS}; g L^{-1} d^{-1}) are defined according to the following two formulas, where *t* is the growth duration (days) and C_{DCW} is the concentration of dry cell weight (DCW).

$$P_{EPS} = \frac{C_{EPS}}{t}$$

Equation 2-1

$$Y_{EPS} = \frac{C_{EPS}}{C_{DCW}}$$

Equation 2-2

It is important to note that EPS concentration, productivity and yield do not always follow the same trend. This can result in different interpretations of 'optimal conditions', since a condition leading to maximum EPS concentration might not coincide with the conditions maximising EPS productivity or yield. For example, Yu, et al. [165] found that the temperature favouring the highest EPS yield (112 mg EPS g^{-1} DCW) corresponded with the lowest EPS concentration (37 mg EPS L^{-1}) in *N. flagelliforme* and vice versa. However, this relationship was not universal for all growth parameters tested: when studying the effect of $NaNO_3$ and pH on EPS, both yield and concentration showed the same trend. Finally, light intensity and K_2HPO_4 affected EPS concentration, but not EPS yield [165]. In another study it has been reported that the highest EPS yield (111 mg g^{-1}) in *A. platensis* was observed at the lowest light intensity (200 µmol m^{-2} s^{-1}) and the lowest $NaNO_3$ concentration (0.25 g L^{-1}) [166]. However, when calculating EPS concentration from the provided data based on Equation 2-2, the optimum for EPS concentration (0.0913 g L^{-1}) was found at highest $NaNO_3$ concentration (0.25 g L^{-1}) and highest light intensity (1000 µmol m^{-2} s^{-1}).

Depending on the aim of the study, different units are plausible: For studies aiming to describe the processes on a cellular level, EPS yield might be more relevant to identify possible metabolic shifts. EPS productivity is useful to compare different species and conditions regarding their EPS production efficiency. From a bioprocess point of view, EPS concentration in combination with the growth duration needed to reach this concentration is most relevant, as this is required to calculate the annual production and revenue in TEAs. This entity, the final concentration at the end of a known growth period, is also referred to as 'titre' in this thesis. Since this PhD research is focused on the bioprocess aspect of EPS production and aims to attain an economic production process, optimal conditions are considered based on EPS concentration and productivity, unless otherwise mentioned.

2.3.1 Impact of Light Intensity, Wavelength, and Photoperiod on EPS Production

2.3.1.1 Effect of light intensity on EPS production

A bibliographic meta-analysis performed by Phélippé, et al. [46], identified light as the most influential parameter on EPS[7] production in *A. platensis*. The authors emphasised the great variability of methodologies for EPS analysis and culture conditions used in the different studies [46]. Different experimental setups might be the reason for individual studies reporting different parameters being the most important one for EPS production in *A. platensis*. For example, another study stated that temperature was found to be the most important parameter for EPS production in *A. platensis* (see section 2.3.2), even though the combined effect of light intensity of temperature was also relevant [168]. It is important to note that no optimum light intensity was identified in the latter study, as the highest EPS concentration (0.294 g L^{-1}) occurred at the maximum intensity tested (180 µmol m^{-2} s^{-1}, Table 2-8). A wider range of light intensity, covering the optimum, might have led to a different ranking of parameters.

[7] The bibliographic meta-analysis performed by Phélippé, et al. [46] included results from cell extracts, which might not be extracellular. For example, the results of El-Baky, et al. [167] were based on a cell extract.

Table 2-8 Effect of light intensity on extracellular polymeric substances (EPS) production of cyanobacteria as reported in the literature (non-exhaustive).The table shows the range of light intensity tested and the optimum is highlighted in bold. The corresponding EPS concentration at the optimum is shown in the following column.

Species	**Parameter**	**Range**	**EPS concentration (g L^{-1})**	**Reference**
A. platensis	Light intensity (µmol m^{-2} s^{-1})	50; 115; **180**	0.294	[168]
Cyanobacterium aponinum	Light intensity (µmol m^{-2} s^{-1})	15; 40; 70; 100; 150; 300; **500**; 650	0.020	[169]
Scytonema tolypothrichoides	Light intensity (µmol m^{-2} s^{-1})	17.0; 22; **37.2**; 86.7[8]	0.460	[171]

Similar trends of enhanced EPS production with increased light intensity were observed in *A. maxima* IFRPD 1183, *Nostoc* PCC 8113, *Nostoc* PCC 7936, *Nostoc* PCC 7413, *Nostoc flagelliforme* and *Scytonema tolypothrichoides* [165, 171-173]. Light is a fundamental factor for photosynthesis, but above a certain level, it can lead to photoinhibition, a state when the absorbed light energy exceeds the cell's ability to use it, creating an imbalance and resulting in reduced photosynthetic activity [174]. The photoinhibition level is species-dependent and was observed in the range of between 250 and 1500 µmol m^{-2} s^{-1} [175]. Above photoinhibition level, EPS[9] productivity decreases, as reported for *Cyanothece* sp. 113 and *Cyanobacterium aponinum* [55, 169]. Increased EPS production during high light might be a response to abiotic stress, like the production of scytonenim-containing EPS in *N. flagelliforme*, which protects the cyanobacterium from UV irradiation [176]. Another hypothesis for the positive impact of high light intensity is, that when light exceeds photon saturation required for protein synthesis, production of other materials such as EPS or pigments increases [36].

[8] Light intensity converted from W m^{-2} to µmol m^{-2} s^{-1} using conversion coefficient 0.218 [170].
[9] EPS extraction method: "*The culture of Cyanothece sp. 113 was heated at 100ºC in water bath for 15 min.*" [55] Cells were not examined for intactness afterward.

2.3.1.2 Effect of light colour and photoperiod on EPS production

The wavelength of the light influenced EPS[10] production of *N. flagelliforme* [177]. Compared with white light, RPS production increased under blue, red, purple, and green light by 65%, 60%, 22%, and 11%, respectively, with the highest EPS production of 0.032 g/L obtained under blue light, but decreased under yellow light by 12% (Table 2-9). CPS[11] production increased under red and blue light by 61% and 38%, respectively, but decreased under purple, green, and yellow light by 45%, 9%, and 36%, respectively [177]. The effect of red light was further investigated in a follow-up study, concluding that red light induced photoinhibition, and therefore stimulated polysaccharide production [174].

Table 2-9 Effect of light colour and photoperiod on extracellular polymeric substances (EPS) production of cyanobacteria as reported in the literature (non-exhaustive).The table shows the range of light colour tested and the optimum is highlighted in bold. The corresponding EPS concentration at the optimum is shown in the following column.

Species	**Parameter**	**Range**	**EPS concentration ($g\ L^{-1}$)**	**Reference**
N. flagelliforme	Light colour	red 660 nm; yellow 590 nm; green 520 nm; **blue 460 nm**; purple 400 nm	0.032	[177]
Limnothrix redekei	Light:dark period	14:10; **24:0**	0.614	[178]
Anabaena WSAF	Light:dark period	12:12; **24:0**	0.056	[41]

In another follow-up study to deepen the understanding of the effect of wavelength, a mixture of red and blue light at lower light intensity (20 µmol photons $m^{-2}\ s^{-1}$) was

[10] EPS contained CPS with the following extraction method: "*extracting lyophilized cell in hot water at 80°C for 6 h*" [177]. Cells were not examined for intactness afterward.
[11] CPS extraction method used: "*extracting lyophilized cell in hot water at 80°C for 6 h*" [177]. Cells were not examined for intactness afterward.

found to be even more effective than any monochromatic light [179]. The highest RPS concentration of 86.65 mg L^{-1} was achieved when first growing *N. flagelliforme* with white light and then switching to red:blue light (ratio red:blue = 15:7). Also, the timing of the switch had an influence on the EPS production, with the optimum being identified as 9 days [179]. Additionally, a combined effect of light colour and nitrogen source on EPS production of *N. flagelliforme* was observed, which will be explained further in section 2.3.4. [179].

In addition, the light:dark regime in which the cultures are illuminated, affects EPS production. Continuous light doubled EPS[12] concentration in *Limnothrix redekei* compared to light:dark cycle of 14:10 hours [178]. Also, other cyanobacteria, such as *Phormidium* sp., *Anabaena torulosa* and *Anabaena* WSAF produced most EPS under constant illumination, whereas light:dark cycles reduced EPS production [41]. However, this effect is not universal on all cyanobacterial species as continuous light had no measurable effect on EPS production of *Oscillatoria formosa* compared to shorter illumination periods [180].

2.3.2 Effect of Temperature on EPS Production

Temperature was identified as the most important factor to enhance EPS production in *A. platensis*, reaching 0.2974 g L^{-1} at 35°C, which decreased by 40% and 10% when 40°C or 30°C were used, respectively [168]. Moreno, et al. [181] explained the positive impact of temperature on EPS from *Anabaena* sp. ATCC 33047 with the observation that cells grow faster and reach the stationary phase earlier (Table 2-10). Other species where the increase of temperature (up to a point) enhanced EPS production include *Scytonema tolypothrichoides*, *Tolypothrix bouteillei, Oscillatoria formosa*, *Arthrospira maxima* IFRPD 1183, *N. flagelliforme* and *Cyanothece* sp. 113 [55, 165, 171, 172, 180]. On the contrary, temperature had seemingly no effect on *Nostoc* PCC 7936, as EPS production was the same at 35°C and 30°C [33].

[12] CPS extraction method used: "*The pellet was treated with a mixture of 0.6 M NaCl and 0.06 M of EDTA at 50 ± 2 °C for 3 h*". [178] The cells were not examined for intactness afterwards.

Table 2-10 Effect of temperature on extracellular polymeric substances (EPS) production of cyanobacteria as reported in the literature (non-exhaustive).The table shows the range of temperature tested and the optimum is highlighted in bold. The corresponding EPS concentration at the optimum is shown in the following column.

Species	Parameter	Range	EPS concentration ($g\ L^{-1}$)	Reference
A. platensis	Temperature (°C)	30; **35;** 40	0.2974	[168]
N. flagelliforme	Temperature (°C)	15; 20; 25; **30**	0.067	[165]
Scytonema tolypothrichoides	Temperature (°C)	10; 15; 20; 25; **30;** 35	0.460	[171]

2.3.3 Influence of pH on EPS Production

The pH of the cultivation medium has shown to affect EPS production in *Anabaena* sp. BTA992, *Cyanothece* sp. ATCC 51142, *N. flagelliforme* and *A. maxima* IFRPD 1183 [45, 165, 172, 182]. For *Cyanothece* sp. ATCC 51142 and *N. flagelliforme*, the optimum pH for EPS production differed from the optimal pH for growth [165, 182].

Table 2-11 Effect of pH on extracellular polymeric substances (EPS) production of cyanobacteria as reported in the literature (non-exhaustive).The table shows the range of pH tested and the optimum is highlighted in bold. The corresponding EPS concentration at the optimum is shown in the following column.

Species	Parameter	Range	EPS concentration ($g\ L^{-1}$)	Reference
Anabaena sp. BTA992	pH	5; 5.5; 6; 6.5; 7; 7.5; 8; **8.5**; 9, 9,5;10	1.700	[45]
N. flagelliforme	pH	5; 6; 7; 8; **9**	0.106	[165]
Cyanothece sp. ATCC 51142	pH	5; **7**; 9; 11	2.000	[182]

While EPS production was highest in slightly alkaline pH for *N. flagelliforme* and *A. maxima* IFRPD 1183, for *Cyanothece* sp. ATCC 51142 the optimum was at neutral pH (Table 2-11) [165, 172, 182]. Shah, et al. [182] explained this observation in *Cyanothece* sp. ATCC 51142 with the EPS composition, as due to "*presence of anionic groups, mainly OH– and SO_2–, in EPS […] the production at a higher rate under alkaline conditions is unlikely*".

2.3.4 Effect of Medium Composition on EPS Production

2.3.4.1 Effect of Nitrogen on EPS Production

Nitrogen, one of the most essential nutrients for growth, is widely studied regarding its effect on EPS production. The response of different cyanobacterial species is complex, with some increasing EPS production in absence/limitation, and others in presence of nitrogen (Table 2-12). Absence of nitrogen enhanced EPS production in *Nostoc* sp. BTA97, *Anabaena* sp. BTA990, *Cyanothece* sp. 113 and *N. flagelliforme* [44, 55, 179]. Nitrogen limitation enhanced EPS production in *A. platensis*, *Spirulina* sp., *Oscillatoria formosa, Microcystis aeruginosa* and *Cyanothece* sp. 16Som2 [36, 41, 166, 180]. The latter, *Cyanothece* sp. 16Som2, quadrupled RPS production under nitrogen-limited conditions [183]. The enhancing effect of nitrogen starvation on EPS production is hypothesised to be caused by increased C:N ratio, promoting the incorporation of carbon into reserve molecules such as EPS [173]. In contrast, for other cyanobacteria, presence of nitrogen had a positive or neutral effect regarding EPS production: Another species of the *Cyanothece* genus, *Cyanothece* sp. ATCC 51142, produced most EPS (1.8%$_{w/v}$) under the presence of nitrogen at standard conditions ($NaNO_3$) and lowest in absence of nitrogen (0.6%$_{w/v}$) [182]. Similarly, the presence of nitrogen enhanced EPS production in *Anabaena cylindrica* 10C, *Phormidium* sp., *Anabaena torulosa, Anabaena* WSAF and *Limnothrix redekei* [41, 178, 184]. On EPS[13] production of *Cyanothece epiphytica,* $NaNO_3$ had no observable effect [32].

[13] Extraction method used: "*With NaOH solution (pH 10) for 4 h after preheating at 45°C*". [32] Cells were not examined for intactness afterward.

Table 2-12 Effect of nitrogen concentration on extracellular polymeric substances (EPS) production of cyanobacteria as reported in the literature (non-exhaustive).The table shows the range of nitrogen concentration tested and the optimum is highlighted in bold. The corresponding EPS concentration or yield at the optimum is shown in the following column.

Species	Parameter	Range	EPS yield/ concentration	Reference
A. platensis	$NaNO_3$ (g L^{-1})	**0.25**; 1.125; 2	0.111 g g^{-1}	[166]
Limnothrix redekei	KNO_3 (g L^{-1})	0.10; 0.51; **101.1**	0.032 g L^{-1}	[178]
Nostoc sp. BTA97	$NaNO_3$ (g L^{-1})	**0**; 0.75, 1.5	1.6 g L^{-1}	[44]

Furthermore, not only the nitrogen concentration but also type of nitrogen source affects EPS production. Diazotrophic growth, with N_2 gas added to the culture, resulted in increased EPS concentration (17 g L^{-1}) compared to addition of a combined nitrogen source in *Anabaena* sp. ATCC 33047, as KNO_3 and NH_4Cl resulted in 2.0 and 2.7 g L^{-1} EPS, respectively, (Table 2-13). The authors suggested that the higher EPS release was caused by nitrogen limitation stress due to lower nitrogen fixation capacity of the cells, indicated by reduction of phycobiliprotein content from 28‰$_w$ to 12‰$_w$ and decreased nitrogenase activity from 1100 to 2 µmol g^{-1} h^{-1} [181]. Similarly, diazotrophic growth of *Nostoc* sp. PCC 7936 led to formation of a thick EPS capsule compared to 'nude' nitrate grown cultures. The authors suggest that carbon fixation rate exceeded nitrogen fixation rate, and excess fixed carbon was stored as EPS [33]. However, not all nitrogen-fixing cyanobacteria produce more EPS under diazotrophic conditions. *Cyanothece* CCY 0110, *Nostoc* PCC 7413, *Nostoc* PCC 8113 and *Nostoc* PCC 7936 showed the opposite response, with more EPS being produced in presence of nitrate compared to diazotrophic growth [63, 173]. In case of combined nitrogen, different types of combined nitrogen sources resulted in different amounts of EPS. For example, *Cyanothece* sp. ATCC 51142 produced more EPS with $NaNO_3$ as nitrogen source compared to KNO_3, NH_4Cl and $CO(NH_2)_2$ [182]. A complex pattern was observed with *N. flagelliforme* depending on the wavelength of the light used: Urea resulted in the highest EPS production (0.08121 g L^{-1}) when blue light was used, whereas under red light, use of $NaNO_3$ as nitrogen source led to the highest EPS production (0.0739 g L^{-}

[1]) [179]. Evidently, species of the same genus (*Cyanothece, Anabaena)*, show opposite responses to nitrogen conditions, hence the effect of nitrogen conditions on EPS production seems to not be dependent on the genus of the cyanobacterium.

Table 2-13 Effect of nitrogen source type on extracellular polymeric substances (EPS) production of cyanobacteria as reported in the literature (non-exhaustive).The table shows the range of nitrogen sources tested and the optimum is highlighted in bold. The corresponding EPS concentration at the optimum is shown in the following column.

Species	**Parameter**	**Range**	**EPS concentration ($g\ L^{-1}$)**	**Reference**
Anabaena sp. ATCC 33047	Nitrogen source	**N_2 (air)**; KNO_3, NH_4Cl	17.2	[181]
Cyanothece CCY 0110	Nitrogen source	N_2 (air); **$NaNO_3$**	0.74[14]	[63]
N. flagelliforme	Nitrogen source	$NaNO_3$; **$CO(NH_2)$**	0.08121	[179]

2.3.4.2 Effect of Phosphorus on EPS Production

Phosphorus seems to affect EPS production in a similar complex pattern to nitrogen. Phosphate starvation stimulates EPS production in some cyanobacterial species, while it hinders EPS production in others. EPS production is stimulated by the lack or limitation of phosphate in *Spirulina* sp. and *Cyanothece* sp. 16Som2 (Table 2-14), however to a lesser extent compared to nitrogen limitation [41, 183]. On the contrary, phosphate limitation and excess both decreased EPS production in *Phormidium* sp. by 63-90% and in *N. flagelliforme* by 3-27%, where optimal phosphate concentration for EPS production coincided with phosphate optimum concentration for growth [41, 165].

[14] Mota, et al. [63] state that „*RPS constitute in average 74 ± 4% of the total carbohydrates in all conditions tested*“, which was used to calculate RPS in Table 2-13. However, the precise number was not provided in the reference.

No effect on EPS[15] production was observed when varying phosphate level for *Cyanothece* sp. 113 [55].

Table 2-14 Effect of phosphate concentration on extracellular polymeric substances (EPS) production of cyanobacteria as reported in the literature (non-exhaustive).The table shows the range of phosphate concentration tested and the optimum is highlighted in bold. The corresponding EPS concentration at the optimum is shown in the following column.

Species	**Parameter**	**Range**	**EPS concentration (g L^{-1})**	**Reference**
Spirulina sp.	K_2HPO_4 concentration (g L^{-1})	**0**; standard[16]; 1	0.030	[41]
Phormidium sp.	K_2HPO_4 concentration (g L^{-1})	0; 0.0**40;** 0.120	0.030	[41]
N. flagelliforme	K_2HPO_4 concentration (g L^{-1})	0.024; 0.238; **0.956;** 1.912	0.097	[165]

2.3.4.3 Effect of Magnesium on EPS Production

Magnesium is a key nutrient for chlorophyll synthesis and it is important for many enzymes responsible for EPS biosynthesis in heterotrophic microorganisms [32, 185]. Nonetheless, different cyanobacterial species show different response patterns to this nutrient. Lack of magnesium had a negative effect on EPS[15] production in *Cyanothece* sp. 113 and *Cyanothece epiphytica*, where the optimum was close to BG-11 standard conditions (Table 2-15) [32, 55]. EPS production for *Cyanospira capsulata* was enhanced by magnesium starvation, but it had no effect on *Cyanothece* sp. 16Som2 [183, 186].

[15] EPS extraction method: "*The culture of Cyanothece sp. 113 was heated at 100ºC in water bath for 15 min*" [55]. Cells were not examined for intactness afterward.
[16] The concentration is unknown, as the reference cited by the authors does not provide the relevant information.

Table 2-15 Effect of magnesium concentration on extracellular polymeric substances (EPS) production of cyanobacteria as reported in the literature (non-exhaustive).The table shows the range of magnesium concentration tested and the optimum is highlighted in bold. The corresponding EPS concentration or productivity at the optimum is shown in the following column.

Species	**Parameter**	**Range**	**EPS concentration/ productivity**	**Reference**
Cyanothece sp. 113	$MgSO_4$ (g L^{-1})	0; 0.1; 0.2; 0.3; 0.4; 0.5; 0.6; 0.7; 0.8, **0.9**; 1.0; 1.1; 1.2	19.1 g L^{-1}	[55]
Cyanothece epiphytica	$MgSO_4$ (g L^{-1})	0; 0.075; **0.1**; 0.3	3.18 RPS µg mL^{-1} d^{-1}	[32]
Cyanospira capsulata	$MgSO_4$ (g L^{-1})	**0.001**, 0.129	2.17 g L^{-1}	[186]

2.3.4.4 Effect of Iron on EPS Production

Less commonly studied is the effect of iron on EPS production in cyanobacteria. Iron is important for several cellular processes, in particular for chlorophyll synthesis [32]. An optimum for EPS production of *Cyanothece epiphytica* was found at an iron concentration higher than standard level (Table 2-16) [32].

Table 2-16 Effect of iron concentration on extracellular polymeric substances (EPS) production of cyanobacteria as reported in the literature (non-exhaustive).The table shows the range of iron concentration tested and the optimum is highlighted in bold. The corresponding EPS value at the optimum is shown in the following column.

Species	Parameter	Range	EPS value	Reference
Cyanothece epiphytica	Ferric ammonium citrate (g L^{-1})	0; 0.006; **0.01**; 0.03	3.18 RPS µg mL^{-1} d^{-1}	[32]
Microcystis aeruginosa	Ferric citrate (g L^{-1})	0.00068; **0.0068**	0.93 pg $cells^{-1}$	[187]

However, excess of iron can cause damage to cells due to its high reactivity and role as a major promoter of lipid oxidation [128]. Higher iron concentration in the growth medium has shown to increase CPS[17] in *Microcystis aeruginosa* strain FACHB-469 by 63%. The authors suggested that iron may regulate the expression of genes involved in polysaccharide synthesis, since the two genes of two glycosyltransferases (BH695-2217 and BH695-3696) were significantly up-regulated at the higher iron concentration [187]. As has been described in more detail in section 2.2.3.4, the EPS produced in response to elevated iron levels may help accumulate essential nutrients or protect cells by preventing direct contact with toxic metal concentrations [20].

2.3.4.5 Effect of Boron, Calcium and Potassium on EPS Production

Two essential nutrients for EPS production are boron and calcium, but their effect is less studied that other nutrients. Calcium, which is essential for nitrogen fixation, seems to play an important role for EPS production, as calcium limitation affected EPS production in *Cyanothece* sp. 16Som2 negatively [183]. An increase until 0.33 g L^{-1} $CaCl_2$ in the growth media enhanced EPS production in *Oscillatoria formosa* to 0. 0556 g L^{-1} (Table 2-17) [180]. Boron is essential for nitrogen fixation of cyanobacteria. Boron deficiency affects the ability to perform oxygenic photosynthesis, leads to decrease of phycobiliprotein and chlorophyll content, yellowing and breaking of cells [188].

[17] CPS extraction method: "*The supernatant was discarded, and the pellet was re-suspended in 15 mL 0.05% sodium chloride solution. Then, pH was adjusted to 10 using 0.5 mol L− 1 sodium hydroxide solution. The mixture was then incubated at 45 ◦C for 4 h.*" [187] Cells were not examined for intactness afterward.

Table 2-17 Effect of calcium and boron concentration on extracellular polymeric substances (EPS) production of cyanobacteria as reported in the literature (non-exhaustive).The table shows the range of calcium concentration tested and the optimum is highlighted in bold. The corresponding EPS concentration at the optimum is shown in the following column.

Species	Parameter	Range	EPS value	Reference
Oscillatoria formosa	$CaCl_2$ (g L^{-1})	0.12; 0.17; **0.33**; 0.42	0.0556 g L^{-1}	[180]
N. spongiaeforme	Calcium (g L^{-1})	0.01; **0.02**	46 µg glucose equivalent mg^{-1} dry wt.	[189]
N. spongiaeforme	Boron (mg L^{-1})	0, 0.086, 0.17, 0.35, **0.43**, 0.86	46 µg glucose equivalent mg^{-1} dry wt.	[189]

EPS production in *Nostoc spongiaeforme* declined drastically in absence of boron or calcium in the growth medium. Interestingly, when calcium was kept at a concentration of 20 mg L^{-1}, EPS production increased with increasing boron concentration, reaching 46 µg glucose equivalent mg^{-1} dry wt., at 0.43 mg L^{-1} boron, after which EPS production decreased [189]. When calcium was lacking, EPS production still increased with increasing boron concentration, but to a lower extent than observed during presence of calcium. The lower the calcium concentration, the higher was the demand for boron. These observations indicate an interactive role of the two nutrients in EPS production in *N. spongiaeforme* [189]. The authors did not mention a possible explanation for this phenomenon. Another nutrient, potassium, is rarely studied, but has shown to not affect EPS production in *Cyanothece* sp. 16Som2 [183].

2.3.4.6 Effect of Sodium Chloride and Ozone on EPS Production

Sodium chloride (NaCl) was studied by several authors based on the protective role of EPS against unfavourable environments such as saline environments, which can cause osmotic stress. For example, the marine, but not halophilic species *Cyanothece* sp. 113 produced most EPS[15] at high salt concentration, whereas absence of NaCl was optimal for growth (Table 2-18) [55]. Similarly, salinity was positively correlated to EPS production in *Synechocystis* sp. $BASO_4$44, BASO507 and BASO511, enhancing

EPS production in many different species including *Cyanothece* sp. ATCC 51142, *Microcoleus vaginatus* and *Westiellopsis prolifica* [30, 182, 190, 191]. Another species, *Oscillatoria formosa*, showed slightly reduced EPS production (0.0276 g L^{-1}) at a low NaCl concentration (0.497 g L^{-1}) but increased EPS production with higher NaCl concentration, until an optimum of 0.0552 g L^{-1} at 4.97 g L^{-1} NaCl [180]. Salinity up to 116.9 g L^{-1} NaCl resulted in slightly reduced EPS production in *Cyanothece* sp. 16Som2 to 0.28 g L^{-1}, compared to 0.42 g L^{-1} at the absence of NaCl [183]. Since this species is halotolerant, salinity might not pose a stress to this organism, omitting the need for producing EPS as a protective barrier. Contrary to expectation, also for the freshwater organism *Limnothrix redekei*, increase of salinity from 0 to 1.5 g L^{-1} led to decrease of EPS production from 0.032 to 0.0256 g L^{-1}, highlighting the complexity and unpredictability of triggers for EPS production in cyanobacteria [178]. For *Anabaena* sp. ATCC 33047, NaCl had a negative effect on EPS production, with the highest EPS concentration obtained at absence of NaCl (Table 2-18) [181].

Table 2-18 Effect of sodium chloride concentration on extracellular polymeric substances (EPS) production of cyanobacteria as reported in the literature (non-exhaustive).The table shows the range of NaCl concentration tested and the optimum is highlighted in bold. The corresponding EPS concentration at the optimum is shown in the following column.

Species	**Parameter**	**Range**	**EPS concentration (g L^{-1})**	**Reference**
Cyanothece sp. 113	NaCl (g L^{-1})	0; 20; 30; 40; 60; **70**; 80; 90; 100	8.0	[55]
Anabaena sp. ATCC 33047	NaCl (g L^{-1})	**0;** 5.0; 9.9; 19.8; 24.9; 29.7	13.5	[181]
Limnothrix redekei	NaCl (g L^{-1})	**0;** 0.5; 1.0; 2.5	0.032	[178]

Lastly, the effect of ozone in the growth medium is a rarely explored, yet has been found to be the most effective parameter for increasing EPS productivity in *Cyanothece epiphytica,* as EPS provided a protective barrier to the highly oxidising environment:

The optimum exposure was found as 0.06 mg L^{-1} ozone for 50 seconds, leading to an EPS productivity of 9.66 µg mL^{-1} day^{-1} [32].

2.3.5 Role of Cultivation Mode in EPS Production

Cultivation modes (photo-, hetero- or mixotrophic, batch, fed-batch, continuous) and bioreactor parameters (aeration) have been found to influence EPS production in different ways, as will be explained in the following paragraphs. Availability of carbon is an important factor for EPS production because excess carbon is converted into overflow products or carbon reserves like EPS due to increased C:N ratio [33, 55, 192]. Excess carbon can be introduced to the culture by increasing aeration or supplementing air with carbon dioxide (phototrophic growth), by using an organic carbon source (heterotrophic), or both (mixotrophic).

Aeration, compared to non-aeration, was reported to enhance EPS[18] production in *Cyanothece* sp. 113, *Phormidium* sp., *Anabaena torulosa* and *Anabaena WSAF* [41, 55]. However, the actual CO_2 available to the cyanobacteria was unclear, as both studies did not specify the air flowrate, leaving carbon delivery unquantified [41, 55].

Photoautotrophic growth with CO_2-supplemented air has been shown to greatly enhance EPS production in several species, including *Synechococcus* sp. BG0011, *Nostoc* sp. and *Anabaena cylindrica* 10C [33, 184, 193]. *Anabaena* sp. ATCC 33047 showed one of the highest EPS concentrations (15 g L^{-1}) reported in literature when being cultivated with carbon dioxide (6%$_{v/v}$) in air. The effect was most pronounced at the highest flowrate (Table 2-19) [181]. However, not all cyanobacterial species produce more EPS when more CO_2 is supplied. Increase of the aeration rate (containing 2%$_{v/v}$ CO_2) had a negative effect on EPS production in *A. maxima* IFRPD 1183 with most EPS (0.154 g L^{-1}) produced at the lowest aeration rate of 0.2 VVM [172].

Supplementing additional carbon sources led to enhanced EPS production in some cyanobacteria, while it caused a decrease in others. Addition of carbonates is useful, especially for alkalophilic cyanobacteria such as *A. platensis* and *Cyanobacterium* sp.

[18] EPS extraction method: "*The culture of Cyanothece sp. 113 was heated at 100ºC in water bath for 15 min.*" [55] Cells were not examined for intactness afterward.

SCSIO-45682, because it counteracts the low amount of dissolved CO_2 in alkaline environments [164, 194]. Mixotrophic conditions by adding an organic carbon source increased EPS production in *Cyanospira capsulata* and *A. platensis* by 43% and 32%, respectively [192, 195]. Addition of acetate, glucose, citrate or valerate reduced EPS production in *Anabaena cylindrica* 10C by 93.8%- 99.7% [184]. Heterotrophic mode is less commonly studied. Glucose as carbon source (in darkness) resulted in ten-fold lower EPS production in *A. platensis* (0.03 g L^{-1}) compared to photo- or mixotrophic mode (0.2905 g L^{-1}) [195].

Table 2-19 Effect of aeration, carbon dioxide supplementation, and trophic mode (phototrophic, mixotrophic, heterotrophic) on extracellular polymeric substances (EPS) production of cyanobacteria as reported in the literature (non-exhaustive).The table shows the parameter range tested and the optimum is highlighted in bold. The corresponding EPS concentration at the optimum is shown in the following column.

Species	**Parameter**	**Range**	**EPS concentration (g L^{-1})**	**Reference**
Cyanothece sp. 113	Aeration	Non-aerated; **aerated**	8.0	[55]
Anabaena sp. ATCC 33047	Airflow rate (6%$_{v/v}$ CO_2)	50; 150 and **250** L L^{-1} h^{-1}	15	[181]
A. platensis	Trophic mode	Phototrophic; **mixotrophic;** heterotrophic	0.2905	[195]

Also, the cultivation mode (batch, fed-batch, continuous) can influence EPS production. The overwhelming majority of studies are conducted in batch mode. Probably due to the reason that most cyanobacterial EPS production is linked to growth, and increases as growth progresses, with EPS production peaking during stationary phase [181]. However, there are few studies conducted in continuous or fed-batch mode. Tan, et al. [196] have successfully increased EPS production in *N. flagelliforme* by 25% (and growth by 45%) by supplementing additional nutrient medium in fed-batch compared to batch mode in a 25 L open pond. This resulted in

final concentrations of 1.16 g L^{-1} biomass and 0.124 g L^{-1} EPS [196]. Continuous cultivation has been explored with *Anabaena* sp. ATCC 33047 (Table 2-20). However, the 1.5 g L^{-1} produced in continuous mode are markedly lower than the 17 g L^{-1} produced in batch mode [181]. It is important to note that several parameters such as light intensity and air flux were not the same under continuous compared to batch mode, which makes it difficult to narrow down the decisive factor. When studying the effect of the dilution rate on EPS production in continuous cultivation of *Anabaena* sp. ATCC 33047, highest EPS production was observed at a dilution rate of 0.03 h^{-1}. At higher dilution rates (higher specific growth rates), biomass and EPS decreased by 77%-93% (Table 2-20) [181].

Table 2-20 Effect of cultivation mode (batch, fed-batch, continuous) and two-step cultivation on extracellular polymeric substances (EPS) production of cyanobacteria as reported in the literature (non-exhaustive).The table shows the parameter range tested and the optimum is highlighted in bold. The corresponding EPS concentration at the optimum is shown in the following column.

Species	Parameter	Range	EPS value	Reference
Anabaena sp. ATCC 33047	Dilution rate (h^{-1}, continuous mode)	0.013; **0.03**; 0.075; 0.15	1.5 g L^{-1}	[181]
N. flagelliforme	Fed-batch	Batch; **fed-batch**	0.124 g L^{-1}	[196]
Arthrospira sp.	Two-step cultivation	One-step; **two-step**	1.02 g g^{-1}	[67]

Two-step cultivation has been explored for species where optimal EPS production conditions have an adverse effect on growth. In the two-step cultivation process described by Chentir, et al. [67], *Arthrospira* sp. was grown at optimal growth conditions in the first batch, and then under stress conditions for EPS production in the second batch, which led to a 1.67-fold increase of EPS production compared to one step cultivation with only optimal growth conditions.

Studies examining the impact of scale-up on EPS production are scarce, with only a limited number reported in the literature [63, 64, 172]. Scale-up is the process of

increasing the size of a system from small, lab-, and pilot-scale levels up to industrial-scale levels with the goal of maintaining efficiency and performance [197]. This can, for example, be performed with a scaling factor of 10, moving from a 100 mL shake flask to lab-scale with medium-sized PBRs (1-10 L), then to pilot scale (10-100 L), and finally to industrial scale (1,000 L) [198]. As with most bioprocesses, scaling up cyanobacterial cultivation introduces several challenges that can reduce product titres. These include self-shading, poor mass transfer, and competition or inhibition arising from microbial contamination [199, 200]. The effects of these limitations are evident in reported studies: EPS production by *A. maxima* IFRPD 1183 in a 30 L pond was four times lower than in a culture tube (Table 2-21) [172]. Similarly, carbohydrate production, as well as growth of *Cyanothece* CCY 0110 was about three times lower in 10 L compared to 1L [63]. However, one promising example for industrial-scale production is *Spirulina* sp. LEB-18 cultivation in a 250 L raceway pond which produced 9.5 g EPS L^{-1}, which is higher than most cyanobacteria produce at laboratory-scale [64].

Table 2-21 Effect of scale (culture volume) on extracellular polymeric substances (EPS) production of cyanobacteria as reported in the literature (non-exhaustive).The table shows the parameter range tested and the optimum is highlighted in bold. The corresponding EPS concentration at the optimum is shown in the following column.

Species	**Parameter**	**Range**	**EPS concentration (g L-1)**	**Reference**
A. maxima IFRPD 1183	Scale	**200 mL;** 30L pond	0.1538	[172]
Cyanothece CCY 0110	Scale	**1L**; 10L	1.85[19]	[63]

[19] [63] state that „*RPS constitute in average 74 ± 4% of the total carbohydrates in all conditions tested*“, which was used to calculate RPS in Table 2-21. However, the precise number was not provided in the reference.

2.3.6 Impact of Culture Conditions on EPS Composition and Properties

In most cases EPS composition is not affected by different growth conditions. For example, the monosaccharide composition of *Anabaena cylindrica* 10C was barely affected by different carbon sources or absence of nitrogen and phosphorus [184]. However, EPS composition of some species was affected by growth conditions. One example is EPS composition changing throughout the growth duration. Longer incubation (5 vs. 3 weeks) increased rhamnose from 6.1% to 15.0% and decreased xylose content of EPS of *Wollea saccata* from 18.0% to 7.4% (Table 2-22) [27]. In *Microcystis flos-aquae* the monosaccharide composition becomes less complex over time: Glucose content increased from 15 to 60% from exponential to stationary phase, at the expense of other monosaccharides (xylose/mannose, arabinose, rhamnose, fucose, galacturonic acid, galactose) [201]. FTIR analysis of polysaccharide from *Cyanothece* sp. ATCC 51142 showed increased complexity in the 1-month culture compared to the 2-week culture, with more distinct peaks. For instance sulphite-related peaks at 1,138 and 1,120 cm^{-1} were stronger in the 1-month compared to 2-week culture, while the carboxylate peak at 1,622 cm^{-1} was absent in the 1-month compared to the 2-week culture. Monosaccharide composition was not analysed [202].

Table 2-22 Effect of growth duration on extracellular polymeric substances (EPS) composition of cyanobacteria as reported in the literature (non-exhaustive).

Species	Effect of	Response	Reference
Wollea saccata	Growth duration	Increased rhamnose and decreased xylose content	[27]
Microcystis flos-aquae	Growth duration	Increased glucose, decrease other monosaccharides	[201]
Cyanothece sp. ATCC 51142	Growth duration	More FTIR peaks, increase of sulphite-related peaks and decrease of carboxylate peak	[202]

Additionally, the different wavelengths affected the monosaccharide composition of EPS and CPS[20] in *N. flagelliforme* with the largest effect visible of yellow light increasing fructose from 10.6% to 32.0% in RPS and green light increasing the

mannose content in CPS[20] from 4.7% to 8.7% compared to white light (Table 2-23) [177]. Higher light intensity (80 vs. 40 µmol m^{-2} s^{-1}) not only increased EPS yield (134.3 vs. 97.8 mg g^{-1}) in *Nostoc* sp. but also resulted in higher protein content (19.2% vs. 11.5%) and longer chains (280–630 vs. 420–520 nm) of the EPS, whereas monosaccharide composition did not change significantly [70]. A meta-bibliographic study on light intensity on EPS composition in *A. platensis* found indication that light intensities lower than 400 µmol m^{-2} s^{-1} barely affected acidic sugars but at higher light intensities, acidic sugars, fucose and rhamnose content decreased. This was confirmed experimentally with the result that light intensity affected monosaccharide composition: High light (800 vs. 100 µmol m^{-2} s^{-1}) increased glucose content (77.7% vs. 43.3%) at the expense of other neutral sugars (20.4% vs. 49.0%) and uronic acids (1.1% vs. 6.2%). Sulfation degree was not significantly different based on light intensity [46].

Table 2-23 Effect of light colour and intensity on extracellular polymeric substances (EPS) composition of cyanobacteria as reported in the literature (non-exhaustive).

Species	Effect of	Response	Reference
N. flagelliforme	Yellow light	Increased fructose content	[177]
N. flagelliforme	Green light	Increased mannose content	[177]
Nostoc sp.	Higher light intensity	Higher protein content and longer chains	[70].
A. platensis	Higher light intensity	Increased glucose content	[46].

Growth parameters have also shown to influence the properties of some EPS. EPS obtained by salt stress from *N. flagelliforme* showed highest flocculation activity (65.95%); even higher than that of the commercial flocculants xanthan gum (19.86%) and $Al_2(SO_4)_3$ (37.3%). Furthermore, when the organism was grown under mixotrophic conditions, CPS[21] showed the highest emulsifying activity (66.39%), water (27.82 g g^{-1}) and oil holding capacities (87.97 g g^{-1}, Table 2-24) [83]. The pH influenced

[20] CPS method used: "*extracting lyophilized cell in hot water at 80°C for 6 h.*" [177] Cells were not examined for intactness afterward.
[21] CPS extraction method: „*The crude CPS was obtained by extracting lyophilized cells in hot water at 80°C for 6 h*" [83]. Cells were not examined for intactness.

flocculating activity of the EPS produced by *Anabaena* sp. BTA992 with the highest EPS flocculating activity (88%) obtained when grown at a pH value of 8.5, which coincided with the highest EPS concentration (1.27 g L^{-1}) [45].

Table 2-24 Effect of growth condition on extracellular polymeric substances (EPS) properties of cyanobacteria as reported in the literature (non-exhaustive).

Species	Effect of	Response	Reference
N. flagelliforme	Salt stress	Emulsification activity and flocculation capability	[83]
N. flagelliforme	Mixotrophic conditions	Water and oil holding capacities	[83]
Anabaena sp. BTA992	pH	Flocculating activity	[45]

2.3.7 Complexity of Interdependent Cultivation Parameters on EPS Production

Many scientific publications study the effect of one single cultivation condition at a time. However, studies that assess the combined effect of several cultivation conditions reveal the complexity and interrelated influence of different cultivation conditions on EPS production. EPS production in *Nostoc minutum* was affected by type of media used, presence/absence of nitrogen and light intensity. Use of two different media, BG-11 and BW3, showed opposite trends in influencing EPS production when varying the amount of nitrogen [203]. At high light intensity (9860 lux), the presence of nitrogen with BG-11 medium showed highest EPS production (2.87 g L^{-1}) whereas a similar EPS concentration (2.56 g L^{-1}) was achieved by using $BW3_0$ medium, which lacks nitrogen, at the same light intensity. This trend was also pronounced at intermediate light intensity (7300 lux) in both stirred and static cultures, but not at low light intensity (4530 lux) [203]. This study highlights the complexity of cultivation parameters on EPS production. Not only do different species show opposite responses to certain types of stress conditions, the study of Pereyra and Ferrari [203] shows how the same species can react in opposite ways to one nutrient when grown in different media and hence, different concentrations of other nutrients.

Most studies use the one-variable-at-a-time (OVAT) approach, which is the altering of one parameter, while the other parameters are fixed at a certain value [105]. However, OVAT does not allow the possible interactions between the different factors to be established [168]. Few studies perform multi-factor optimisation to account for these interactions using Response Surface Methodologies (RSM) such as Full-Factorial-Design (FFD), Box-Behnken Design-(BBD) and Central Composite-Design (CCD). FFD is most commonly used, being applied by Silva, et al. [166] (nitrate starvation and light), Trabelsi, et al. [168] (light and temperature) and Chentir, et al. [67] (light and NaCl). Less commonly used was CCD, which was applied by Borah, et al. [32] (magnesium and iron) and BBD, which was used by Koçer, et al. [204] to assess the impact of $NaNO_3$, Na_2CO_3 and Illumination time. Each of the three designs has distinct advantages and limitations. FFD is effective for screening but inefficient for modelling curvature [205]. CCD allows detailed optimisation of quadratic effects but may involve impractical experimental conditions, while BBD is more efficient and avoids extreme settings, though it is less effective for capturing complex interactions [205, 206].

In OVAT studies, statistical significance is often assessed using Student's t-test or one-way ANOVA with Tukey's test [117, 118, 207]. The t-test is suitable for two-group comparisons, while ANOVA handles multiple groups but both assume normality. Correlations are typically evaluated with Pearson's coefficient, which measures linear relationships, or Spearman's rank, which is used for non-linear associations [3, 28, 208].

All in all, it becomes evident that there is a variety of parameters that influence EPS production, composition, and properties. Furthermore, the effect of one parameter is not universal on all species and, depending on other conditions, can even show opposite trends within the same species. This highlights the importance of multi-factor optimisation experiments to tailor the commercial EPS production process to the specific species and desired EPS characteristics.

2.4 Industrial-Scale Production of EPS from Cyanobacteria

2.4.1 Upstream Processes: Cultivation Systems

There are various cultivation systems for cyanobacteria and microalgae, including open systems such as (raceway) ponds and closed systems such as tubular and flat-panel designs. Open systems are the most traditional and widely used ones for microalgal cultivation due to their low construction cost (270 USD m^{-3}), low operational costs and simplicity [21]. These include artificial systems such as open ponds, raceway ponds, circular ponds, and natural water bodies like lakes and lagoons. Raceway ponds, the most common artificial type, feature a shallow (15-30 cm deep), closed-loop oval channel with a paddle wheel to circulate the culture, and at times submerged aerators, maximizing light penetration and gas exchange [10].

Closed systems provide a controlled environment for the cultivation of microalgae and cyanobacteria, addressing many limitations of open ponds. Closed system designs include tubular, flat-panel, and columnar PBR configurations and bags [10, 209]. Tubular PBRs consist of transparent tubes where the culture circulates in a closed-loop system. They can be used both outdoors and indoors with natural or artificial light. These systems offer higher productivity due to a better surface-to-volume ratio (around 50) but are more expensive to construct with construction costs of 6750 USD m^{-3} [21]. The land footprint of a helical vertical tubular PBR (12.5 m^2 m^{-3}) is larger than that of a pond (4 m^2 m^{-3}), increasing costs related to land use, infrastructure, and piping distances [21]. Flat-panel PBRs feature thin, vertically oriented panels that allow efficient light penetration and gas exchange. They are suitable for high-density cultures at laboratory and industrial scale. These PBRs provide high light absorption efficiency and effective gas exchange but come with high manufacturing and maintenance costs, scaling difficulties, and potential overheating issues [210].

Table 2-25 Specifications, advantages, challenges, and applications of different cultivation systems for cyanobacteria and microalgae as reported in the literature.

Type	Design Features	Advantages	Challenges	Applications
Open Ponds	Natural/ artificial shallow pond.	Low cost, simple design	Contamination, poor control, low productivity	Low-cost products
Raceway Ponds	Shallow pond with paddle wheel, (aerator)	Improved mixing compared to static ponds, low cost	Contamination, limited control	Low-cost products, some pigments
Tubular PBRs	Transparent, closed-loop tubes	Good productivity, High control, reduced contamination risk	High costs, biofouling, scalability	High-value products
Flat-Panel PBRs	Thin, vertically oriented panels	High productivity, high light penetration	High cost, scaling challenges, potential overheating	High-value products
Bag PBRs	Vertically hung plastic bags (aerator)	Low cost, good sterility	Inadequate mixing, fragility, bag waste if single-use bags	Contamination-sensitive cultures/ products
Membrane PBRs	Closed PBR with membrane	Less shear-stress, continuous metabolite separation	Membrane fouling	Shear-sensitive cultures, extracellular metabolites

Bag PBRs consist of plastic bags (e.g. polyethylene (PE)) and a support structure, e.g. a frame from which the bags are hung, and an optional aeration system. The bags can be disposable or reusable for a certain number of years [209, 211]. The advantages of bag PBRs are low material cost and good sterility. However, disadvantages can include inadequate mixing, fragility and the disposal, in the case where single-use plastic bags are used [211]. Finally, another type of closed systems are membrane PBRs. They are suitable for shear-sensitive cultures, or to continuously separate extracellular metabolites [211]. Shear stress is a hydrodynamic force produced by mixing, pumping and aeration in microalgal cultivation. It promotes adequate culture circulation, ensuring that cells receive nutrients, carbon dioxide and light, and it also prevents sedimentation, oxygen buildup and growth on reactor walls. However, excessive shear stress can damage cells or even cause lysis [211, 212].

Each system's distinct specifications, advantages, and challenges determine its suitability for producing specific products (Table 2-25). As outlined in the previous paragraph, open ponds and raceway ponds utilize natural light but have less control over temperature and contamination. In contrast, closed systems like tubular and flat-panel PBRs offer greater control over cultivation conditions and reduced contamination risk, though they face challenges like biofouling, clogging, and scalability. Generally, open ponds are suitable for industrial-scale, low-cost production, especially for commodities like biofuels, whereas closed systems are preferable for high-value products requiring stringent quality control, such as pharmaceuticals and nutraceuticals. However, this is not always the case, as the final choice of production system depends on various factors, including the target product, desired scale, economic considerations, and specific strain characteristics. For example, *Dunaliella salina*, which was the first alga to be commercialised as a source of a high-value chemical (β-Carotene), is grown in open ponds. This is enabled by the species' ability to grow in saline brine, which limits contamination, combined with the fact that *Dunaliella salina* is having the highest β-carotene content from any species (up to 14%$_w$ of dry weight) [213, 214]. Algatechnologies is one of several companies producing the carotenoid astaxanthin and utilises outdoor tubular glass PBRs to cultivate *Haematococcus* in Israel. Production of astaxanthin from *Haematococcus* is performed in a two-stage process. The first stage (biomass accumulation) always takes place in a PBR, whereas the second stage (astaxanthin-accumulation) can take

place in a PBR or pond [9]. A commercial example for a company using a raceway pond for a high-value product such as a pigment, is Earthrise in California, which grows *A. platensis* in raceway ponds to produce the food colorant 'Lina Blue' [215]. This highlights the need to consider all relevant factors when choosing the cultivation system.

PBR materials differ in cost, durability, and effects on algal cultivation. Borosilicate glass is chemically inert, resists biofouling, and lasts up to 50 years, but is expensive, heavy, and requires a support structure [216, 217]. Plastics like polyvinyl chloride (PVC), polymethyl methacrylate (PMMA), and polyethylene (PE) are cheaper but degrade faster; PVC lasts 2–4 years and is UV-sensitive, while PMMA lasts around 10 years [217]. Plastic transparency also declines over time due to oxidation, affecting performance [216]. Optical properties, especially UV and Photosynthetically Active Radiation (PAR) transmission, influence algal growth. UVB reduces growth in species like *Dunaliella tertiolecta*, *Chlorella vulgaris*, *Nostoc* sp. (55% reduction), and *Microcystis aeruginosa* (86.2% decrease in PSII quantum yield) by damaging PSII, RuBisCO, and generating ROS [218-223]. UVA generally has less effect on biomass, though it can impair PSII and contribute to ROS via photosensitisation [222, 223]; in *Nostoc commune*, UVB induces EPS, UVA does not [224]. Glass transmits UVA but blocks most UVB, whereas PE blocks almost all UV [217, 219]. Material selection should therefore consider cost, durability, light transmission, and species-specific responses for desired products such as biomass, EPS, or UV-protective compounds.
For EPS production specifically, several factors will need to be taken into consideration. The value of the final product and amount of EPS titre will determine whether the revenues can compensate for expensive closed systems PBRs, or if cheaper ponds must be used. However, if contamination-prone systems such as open ponds are used, there could be a risk of contaminating bacteria consuming the sugar-rich EPS as carbon source. Furthermore, the suitability of the cultivation system for the species must be evaluated, as parameters such as mixing, aeration and light availability can differ among systems, which can impact EPS production as outlined in section 2.3. Lastly, the UV-transmittance of the PBR material must be taken into consideration to avoid UV-related damage or inhibition to cells in the PBR.

2.4.2 Downstream Processing in Cyanobacterial EPS Production

After cultivation in the upstream (USP) part of the process, the culture requires different DSP such as separation of biomass and supernatant, and recovery, purification and drying of EPS. Depending on the desired properties of the final product and requirements for purity, different purification techniques are applied (Table 2-26).

The first step after cultivation is to separate biomass from EPS-containing spent media by centrifugation, filtration or flocculation [21, 225]. If CPS were the target product, an additional step to break the bonds between CPS and cells would be required [42]. Following this, different steps for recovery and purification of EPS are possible. One method is recovery of EPS by alcohol precipitation and purification using dialysis [204]. The alternative method is recovery and purification using tangential filtration [21, 207]. For the first method, the addition of polar alcohol (2–3 volumes of methanol, ethanol or isopropanol per volume of supernatant) decreases the solubility of polysaccharides in water by altering their polarity [226]. Lowering the temperature further enhances this effect, causing EPS to precipitate and settle in the aqueous solution. Subsequently, the precipitated EPS are obtained by another centrifugation step [226]. The solvent used for precipitation can be recovered and reused through distillation. However, co-precipitation of different impurities with the EPS can occur, for instance the co-precipitation of salts from the growth medium in the case of marine species [40]. To avoid this, salt concentration has to be reduced before precipitating EPS [21]. An alternative EPS purification method is dialysis. Dialysis is a process where solutes diffuse across a semi-permeable membrane, allowing smaller molecules (impurities) to pass while retaining larger molecules (EPS). Over time, small molecules move across the membrane through diffusion, reaching equilibrium [227]. For *Porphyridium cruentum*, dialysis was up to three times more effective than alcohol precipitation. Furthermore, pilot-scale diafiltration was used to desalt EPS with a salt removal efficiency of 98%. EPS losses were low, with diafiltrated EPS being 46% more pure than EPS obtained by dialysis, demonstrating the potential of this technology for EPS purification [226]. Previously, another study demonstrated the feasibility of using a microfiltration/ultrafiltration system for pilot-scale EPS downstream processing [207]. The authors stated that given the nearly linear scalability of ultrafiltration (UF), this system can effectively isolate large quantities of bioactive EPS [207]. However, UF systems are prone to membrane fouling, which can reduce flux and affect long-term

performance. Therefore, an effective cleaning sequence is required after each use, typically consisting of two flushes with water, one with 0.1 M NaOH, and a final rinse with water until neutral pH [226]. To avoid irreversible fouling, which is a severe form of membrane clogging that cannot be removed by standard cleaning methods and may require membrane replacement, further strategies might be necessary. Most polymers employed in membrane production, such as polyvinylidene fluoride, polyether sulfone, and polyacrylonitrile, exhibit hydrophobic characteristics. This property promotes hydrophobic interactions, making the membranes prone to retaining hydrophobic contaminants like proteins and organic substances, which can cause fouling and compromise the membrane performance. To address this issue, one strategy involves hydrophilising and functionalising the hydrophobic membranes. For example, hydrophilic metals (e.g. Ag) and metal oxides (e.g. TiO_2, Al_2O_3, SiO2, Fe_3O_4) can be incorporated as nanoparticles to achieve the desired effect. These different anti-fouling strategies for membranes have recently been reviewed recently by Ennaceri, et al. [228].

Table 2-26 Advantages and challenges of downstream processing equipment for extracellular polymeric substances (EPS) recovery, purification, and drying as reported in the literature.

Equipment	Purpose	Advantages	Challenges
Centrifuge	Harvest, separation of biomass and EPS	Efficient separation	Added water in case of high viscosity
Filtration	Biomass separation, EPS recovery	Scalable, effective	Membrane fouling
Alcohol Precipitation	EPS recovery	Simple, solvent reuse possible	Use of solvents, co-precipitation of impurities
Freeze Dryer	EPS drying	Preserves bioactivity	High cost
Spray Dryer	EPS drying	Cost-effective	Heat-sensitive EPS may degrade

Upon recovery and purification, EPS are usually dried to obtain a powder. This can be performed with technologies such as freeze dryers or spray dryers [21]. Spray drying

involves spraying liquid or slurry into a hot gas stream, usually hot air or nitrogen. The liquid quickly evaporates in the gas stream, leaving behind fine particles of the dried material. Spray drying typically involves temperatures ranging from 150°C to 650°C, depending on the characteristics of the material being dried and the desired properties of the final product [229]. Freeze-drying, also known as lyophilization, is a dehydration process, which uses the process of sublimation. The material is cooled below freezing point and placed in a vacuum. Based on the thermodynamics of water, at low temperatures and pressure, water directly transitions from solid phase to gas phase [230]. This type of dehydration preserves the materials' properties, which makes it suitable for EPS with bioactive properties [207]. However, freeze-drying is more costly than spray drying in terms of purchase and operation costs. To make the process economical, the EPS revenue must be high, or the volume should be reduced as much as possible prior to freeze-drying to a smaller volume to be freeze-dried.

While this review focuses on EPS, it is beneficial to consider broader insights from DSP strategies used in microalgal bioprocesses. Harvesting and dewatering alone contribute 3–15% of the production costs of algae biomass [231]. Lipid extraction typically uses hexane or chloroform and methanol, which are hazardous and flammable [232]. Supercritical carbon dioxide offers solvent free, selective, and fast extraction but is costly [233]. Protein recovery relies on cell disruption methods such as bead milling, high pressure homogenization, enzymatic treatment, ultrasound, and pulsed electric field, which vary in energy use, yield, protein quality, and cell debris [234]. High pressure homogenization achieves up to 99% lysis but is energy-intensive and produces large amounts of debris, limiting industrial use [235]. Pigments such as phycocyanin and astaxanthin have been extracted using liquid-liquid, solid-liquid, or solvent methods, which are expensive [236]. Natural deep eutectic solvents offer a more sustainable and cost effective alternative, although scalability and long term feasibility remain untested [237].

These examples illustrate common DSP challenges: high costs, energy demand, solvent use, scalability, and product loss. Many constraints are relevant to EPS processing. Membrane filtration, successfully used for biomass and protein concentration, shows promise for EPS purification with advantages in scalability and

water reuse [40, 207, 238]. Learning from DSP strategies beyond EPS can inform more cost-effective and sustainable process design for EPS-based products in the future.

2.4.3 Economic Feasibility and Market Potential

As described in the introduction (Chapter 1:) only a handful of cyanobacterial EPS have been commercialised to date, including *Spirulan*, *Nostoflan*, *Sacran* and *Emulcyan* [3]. Commercialisation remains limited, as several challenges in industrial-scale production need to be overcome, particularly in USP and DSP [11]. The following paragraphs illustrate some of the most relevant challenges associated with profitability, ability to compete with other products on the market and compliance with regulations.

Compared to production from heterotrophic organisms like *Streptococcus*, *Xanthomonas* and *Leuconostoc*, there are several challenges associated with EPS production from cyanobacteria. Heterotrophic organisms can be cultivated in industrial-scale fermenters that are cheaper (3800 USD m^{-3}), have a lower footprint (0.33 m^2 m^{-3} reactor) and higher productivities (up to 180 times higher) than most algal production systems [21]. The product titre not only affects revenues and USP costs, but it also affects DSP costs. For example, a ten-fold lower microalgal titre than a bacterial one, means the product is 10-fold more diluted, resulting in 10 times more centrifugation power required to obtain the same amount of product. Overall, this results in 10–100-fold higher cost for microalgal EPS compared to bacterial or fungal polysaccharides [21]. To compensate for lower titres and higher production and processing costs, the EPS produced with cyanobacteria must be considerably more valuable than bacterial ones. However, cyanobacteria have an sustainability advantage over heterotrophic organisms as production species because they are phototrophic. In contrast, heterotrophs require glucose, which depends on arable land and competes with food production [8].

Not all markets are open to EPS products from cyanobacteria. The textures market, especially the hydrocolloid market, is closed for microalgal EPS as production costs are too high to compete with texturing agents from macroalgae and plants [21, 29]. The pharmaceutical market would match in terms of high selling prices. For example, the cost for medical device grade molecules is 170 USD kg^{-1} for a concentration of 10 g L^{-1} of pure EPS [21]. However, the strict controls that pharmaceutical products

underlie could pose a challenge. PBRs, ideally disposable ones, are compulsory to ensure batch reproducibility and microbiological quality. Furthermore, any pharmaceutical product must be very well characterised, which is rare, as for example *A. platensis* is the only species with fully characterised EPS in terms of chemistry and rheology [21]. All in all, most welcoming for novel EPS would be nutraceutical, cosmetic, and therapeutic fields but also areas like heavy metal bioremediation and green synthesis of nanomaterials and nanoparticles [21, 29].

2.4.4 The Biorefinery Approach in EPS Production

Another approach to increase profitability of EPS production processes with microalgae is to compensate for the production costs with a multi-product biorefinery concept, as opposed to trying to lower production costs [21]. Microalgae and cyanobacteria produce a variety of valuable products that can be valorised as by-products. Biomass can be used be used directly as food, for example the species *Chlorella* and *Spirulina,* which are produced as healthy food additives [239]. Furthermore, biomass can be used as feed, fertiliser or energy; or used for extraction of high-value products [240]. High-value products from microalgae and cyanobacteria comprise for example of pigments, polyhydroxyalkonates (PHA) and long-chain polyunsaturated fatty acids. Phycobilins such as phycocyanin, phycoerythrin and allophycocyanin are naturally only found in algae and cyanobacteria and have a wide range of applications, such as food and cosmetic colours. One commercial example is the phycocyanin ‘Lina Blue’ which is produced by *Arthrospira (Spirulina) platensis* and sold by DIC Corp., Japan [9]. Other high-value pigments are the carotenoids β-carotene and astaxanthin, which have been successfully commercialised in feed, food, and cosmeceutical applications due to their bioactive properties (i.e. antioxidant activity) [241, 242]. Cyanobacteria and microalgae also produce intracellular PHA as carbon and energy reserve, once nutrients such as nitrogen, phosphorus etc. become limited and if carbon is in excess. PHA is a promising bio-based, biodegradable and biocompatible polymers with similar properties to conventional synthetic polymers such as polypropylene and low-density polyethylene and could thus reduce the dependency on fossil resources, as well as the accumulation of disposed plastic waste and microplastics in the environment [243]. Moreover, compounds such as mycosporine-like amino acids (MAAs) produced by cyanobacteria and algae have gained attention for their potential applications in cosmetics, particularly as natural sunscreens. MAAs

like shinorine and porphyra-334, derived from the red macroalga *Porphyra umbilicalis*, are commercially available and used in cosmetic products. As explained in more detail in section 2.2.3.5, these compounds are valued for their ability to absorb UV radiation, thereby protecting skin from harmful effects of UV-exposure [244-246]. Another group of valuable products from algae are omega-3 fatty acids such as eicosapentaenoic acid and docosahexaenoic acid (DHA). Heterotrophic growth of *Crypthecodinium cohnii* results in a DHA-rich oil product (DHASCO™) used in infant formula [9]. Another species that is often mentioned in commercial DHA production from microalgae is the genus *Schizochytrium*. However, despite being mislabelled as such, *Schizochytrium* is in fact not an alga. It is a protist from the family of thraustochytrids, which are fungi-like heterotrophic single-celled marine eukaryotes [247].

Depending on the by-product(s) chosen, additional DSP equipment might be necessary, which in turn increases investment and operating costs. For example, the extraction and purification of DHA-rich oil from *Crypthecodinium cohnii* requires cell disruption using hexane, refining, bleaching, winterizing, deodorizing, addition of tocopherol as an antioxidant and blending with sunflower oil [248]. In the biorefinery context, the most profitable by-product can be identified by comparing the gain of additional revenues to the added costs for each scenario using Techno-Economic Analysis (TEA). TEAs, scenario analysis and sensitivity analysis of algal biorefineries are highlighted in the following section.

2.4.1 Techno-Economic Assessments of Algal Biorefineries

Techno-economic assessment (TEA) is a methodology used to evaluate the economic performance and feasibility of industrial processes. It involves process modelling, equipment sizing, cost estimation, and financial analysis to assess overall performance [249]. TEAs guide investment decisions and scaling up biotechnological processes.

TEAs of microalgal processes can be performed using spreadsheets like Microsoft Excel or process simulation software such as SuperPro Designer® (SPD) [250-252]. SPD allows modelling of batch and continuous operations, mass and energy balances, and integrated economic calculations, with extensive libraries of chemicals, equipment, and resources [253]. Its accessibility and detailed economic outputs make it widely used in bioprocess TEAs.

2.4.1.1 Scenario Analysis

Scenario analysis simulates alternative process configurations, scales, or technologies to evaluate economic impact. Vázquez-Romero, et al. [251] compared multiple microalgae species and cultivation scales and downstream processes, identifying configurations with improved cost-effectiveness and biomass titres. They found annual productivity of 12.94 tons per hectare and production costs of 60.34 USD kg^{-1} dried biomass. Extending the analysis to geographic and technological variations, production costs ranged from 50 USD kg^{-1} at 100 hectares in Norway to 26 USD kg^{-1} in Spain due to natural light availability [252]. PBR costs accounted for 76% of capital expenditure [250]. Thomassen, et al. [239] found that implementing membrane-assisted medium recycling reduced *Dunaliella salina* and *Haematococcus pluvialis* biomass costs from 74 to 46 USD kg^{-1}. Ramírez-Partida, et al. [252] showed that adding fucoidan extraction to *Sargassum* processing improved net present value from negative 2,736,000 USD to positive 3,844,000 USD. Scenario analysis identifies routes to improve profitability while maintaining technical feasibility.

2.4.1.2 Sensitivity Analysis

Sensitivity analysis evaluates how uncertainty in input parameters, such as feedstock cost, product price, or production capacity, affects key financial indicators [254]. Ramírez-Partida, et al. [252] showed that increasing production capacity directly increases net profit. In carrageenan extraction from Kappaphycus alvarezii, NPV was most sensitive to market price, less to feed cost, and least to labour cost [255]. A TEA on algal biodiesel production by Barlow, et al. [256] found productivity and biocrude yield strongly influence minimum fuel selling price (MFSP) and net energy ratio. Saral, et al. [257] identified algae productivity as a key driver of MFSP but noted income tax rate had the greatest overall effect. Integrating scenario and sensitivity analysis in TEAs, especially using SPD, allows evaluation of alternative routes, locations, and configurations, and clarifies the influence of input parameters. Together, these analyses support investment, scale-up, and commercialisation decisions in microalgal biotechnology.

2.4.1.3 Techno-Economic Assessments of Industrial-Scale EPS Production with Cyanobacteria in Literature

TEAs of industrial-scale EPS production with cyanobacteria are rare. A thorough search of the relevant literature yielded only one comprehensive TEA of microalgal EPS production conducted by Koçer, et al. [204]. The designed process consisted only a base scenario including cultivation, centrifugation, EPS recovery utilising ethanol precipitation, which was recycled via distillation, and freeze-drying of the EPS product. However, the process sheet of this study showed a conventional continuously stirred tank reactor (CSTR) as PBR, and no mentioning of adapting purchase cost to reflect PBR costs accurately. This might be the reason for the Total Capital Investment (TCI) and Operating Expenditure (OpEx) amounting to merely 11040 USD and 7028 USD y^{-1}, respectively, despite the production scale of EPS and biomass being as high as 600 and 2100 metric tons (MT) per year, respectively [204]. Based on the provided values for annual EPS production, EPS titre, growth duration and operation days per year of 600 MT y^{-1}, 0.245 g L^{-1}, 15 days and 330 days, respectively, this corresponds to a culture volume of 111,318 m^3. This in turn, corresponds to a PBR purchase price of below 0.1 USD m^{-3}, which is vastly different from any other values found in literature [21]. Another TEA seems to have been performed by Penloglou and Kiparissides [258], however this resource was not accessible to University of Nottingham. The lack of TEA studies on EPS production with cyanobacteria emphasises the need of accurate assessments of such a process.

More general TEAs of microalgal biomass production can reveal insights into cost efficiency and operational strategies. There are multiple studies based on the pre-industrial PBR facility from the Chemical Engineering Department of the University of Almería and Fundación Cajamar at PALMERILLAS Technology Demonstration Centre. The PBR facility will be described in more detail in section 4.4.1. One comprehensive TEA at this location revealed a production cost of 78 USD kg^{-1} *Scenedesmus almeriensis* biomass using tubular PBRs (PBRs), highlighting that labour and depreciation were major cost contributors. They suggested that simplifying technology and scaling up production could reduce costs to 14 USD kg^{-1}, emphasizing the need to enhance PBR efficiency and reduce production costs for economic viability [259].

A recent study found that UF was financially feasible for industrial-scale microalgae harvesting, particularly for the species *Scenedesmus acuminatus*. The researchers demonstrated that with optimal operational parameters, the UF system could achieve a high biomass recovery rate of 93% and an average membrane flux of 53.6 L m^{-2} h^{-1}. These parameters included transmembrane pressure (TMP), which is the pressure difference that drives fluid through the membrane, and cross flow velocity (CFV), which is the rate at which feed flows tangentially across the membrane surface [238]. Their TEA indicated a harvesting cost of 0.30 USD kg^{-1} of dry biomass, with the potential to reduce costs to 0.27 USD kg^{-1} through further optimisation of CFV. The study concluded that UF is a viable and efficient method for pilot-scale microalgae harvesting, supporting its application in industrial production systems [238]. The operational and economic parameters could be transferable to EPS recovery using UF, since the size of the membrane (molecular weight cut off (MWCO) = 5000 Da) was equivalent to that used for EPS purification in the study described in section 2.4.2 [207].

Chapter 3: Research Aims and Objectives

The existing literature provides insights into the composition and properties of cyanobacterial EPS, as well as the effect of cultivation conditions on the EPS titre and composition and insight into industrial-scale production of cyanobacterial EPS. However, several research gaps remain. Firstly, although between 200,000 and 800,000 cyanobacterial and microalgal species are estimated to exist, only a few hundred have been examined for their valuable metabolites. Consequently, most species remain uncharacterised, particularly concerning EPS production, highlighting a substantial research gap [28, 29]. Secondly, because the response to cultivation conditions varies between species, any newly identified EPS-producing strain requires tailored optimisation to achieve maximal EPS yields. Optimising cultivation parameters such as light intensity, temperature and nutrient availability is therefore a key challenge, as these factors strongly influence both the quantity and the quality of the EPS produced [3]. Additionally, EPS concentration affects the DSP, influencing overall costs of the process [21]. Identifying optimal cultivation conditions that can consistently produce high titres of EPS is a critical step towards commercial feasibility [11, 21]. Furthermore, despite scale-up to photobioreactors (PBRs) being essential to determine the potential for industrial-scale production, there is only a limited number of scale-up studies on EPS production [63, 64, 172]. Lastly, process design and TEAs of industrial-scale cyanobacterial EPS production processes are still lacking, with only one comprehensive TEA found in literature on microalgal EPS production by Koçer, et al. [204] despite their importance to guide research in terms of titre sufficiency and product value.

Addressing these gaps is essential to advancing the field. Given that only a small fraction of the hundreds of thousands of cyanobacterial species have been tested for their valuable metabolites and the broad range of EPS production already reported (e.g., from 0.03 to 17 g L^{-1}), it is hypothesised that the true diversity in EPS production potential across cyanobacteria is likely greater than what has been previously documented [29, 41, 181]. This hypothesis is based on the ecological and taxonomic diversity within the cyanobacterial clade, suggesting that novel, untested species may produce EPS in higher titres and with different properties than those already studied. Furthermore, it is hypothesised that optimising cultivation conditions for the most

promising EPS-producing species will significantly increase EPS titres, and that scaling up the production process will improve or maintain these titres while overcoming the challenges associated with industrial scale cultivation. Finally, it is hypothesised that through the application of techno-economic modelling, the production of cyanobacterial EPS at a commercial scale can be economically feasible, with process design and cost analysis identifying key factors for cost-effective implementation.

The overarching aim of this PhD thesis is to attain an economical EPS production process using cyanobacteria, addressing several of the key challenges described in the previous paragraph, including identification of optimal production species and growth conditions, scale-up, and economic evaluation of the production process.

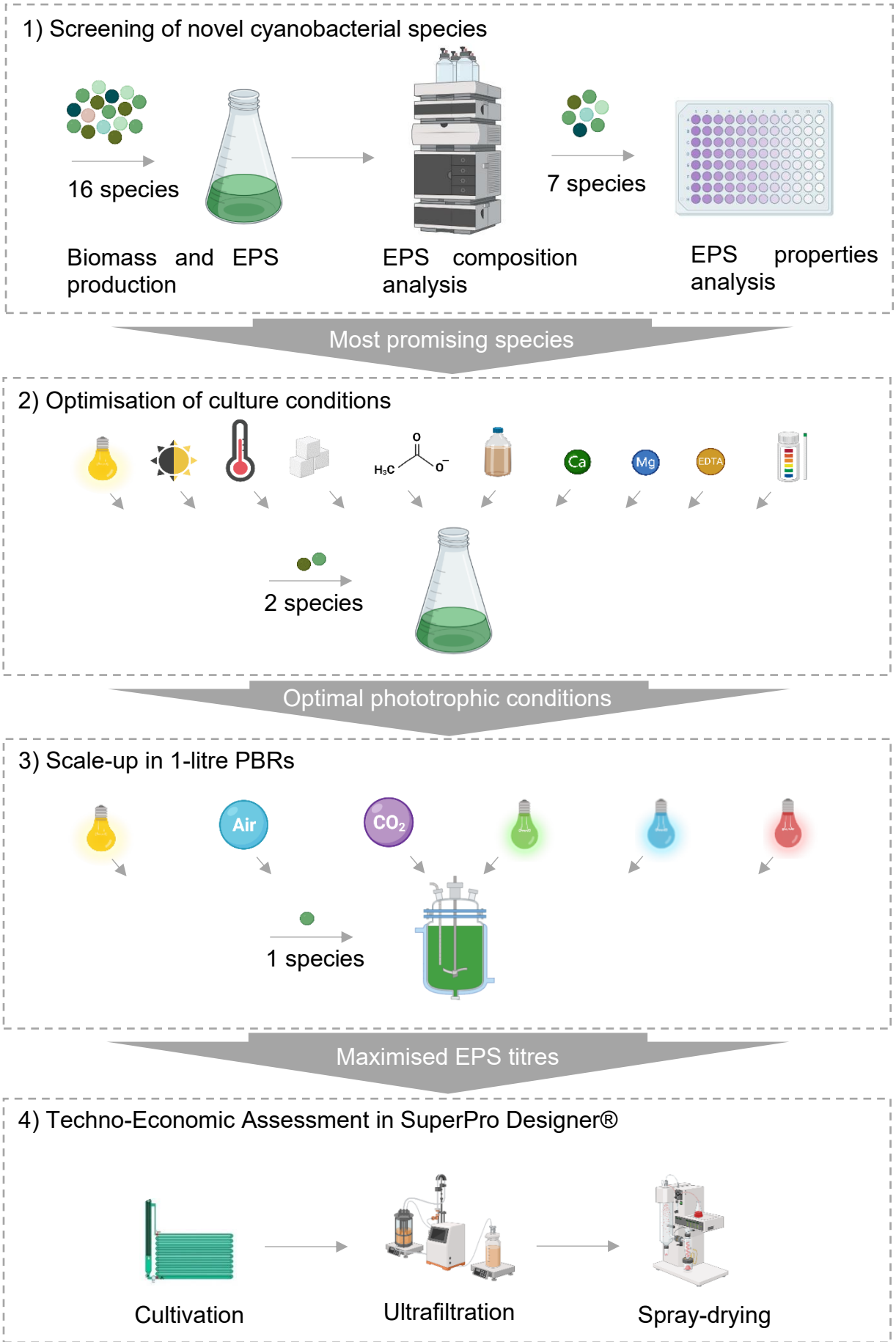


Figure 3-1 Graphical abstract of PhD project on exploring the potential of cyanobacteria to produce extracellular polymeric substances.Icons created with Biorender.com

The research (Figure 3-1) is structured around the following objectives:

1. Screening novel wild type cyanobacteria regarding EPS production to identify promising EPS producers:

   The first objective is to screen novel wild-type cyanobacteria for their EPS production potential, aiming to identify strains capable of producing ≥1 g L^{-1} of EPS. Literature values range from 0.03 to 17 g L^{-1}, though 17 g L^{-1} is likely an outlier since such levels have not been reported in the past 18 years [41, 181]. Titres above 1 g L^{-1} exceed most reported values and are considered high for this thesis. Novel cyanobacteria are cultivated, and their growth and EPS production are monitored. The EPS composition, as well as physico-chemical properties are analysed to select the most promising species. Particular interest is given to EPS containing fucose, rhamnose, and glucuronic/galacturonic acids, which are associated with bioactivity relevant to nutraceutical and pharmaceutical applications [72]. Additionally, sulphation of EPS is considered an important parameter, as sulphate content has been correlated to bioactivity, such as antiviral, antioxidant, antimicrobial and anticancer properties [15, 108, 260, 261]. Additionally, total protein content and total reducing sugar content is analysed because they are related to emulsifying and antioxidant properties, respectively [11, 84, 86, 107]. The goal is to discover a novel species producing high titres of functional EPS that can be optimised for industrial-scale production.
2. Optimisation of cultivation conditions of the most promising species for achieving higher EPS titres and productivities:

   The second objective focuses on optimising the cultivation conditions to maximise the EPS titre and productivity in shake flasks (12.5 mL culture volume). Firstly, the impact of the most relevant factors identified through literature review (section 2.3), light, temperature and carbon availability, are evaluated using single-factor optimisation to determine the most influential parameters and ranges [168]. Subsequently, the most impactful parameters and ranges are selected for multi-factor optimisation using Box–Behnken and Central Composite Designs [32, 204]. The target is to exceed the concentration obtained in the screening experiment, increasing EPS production as close as possible to 9.5 g L^{-1} and/or a productivity of 316 mg L^{-1} day^{-1}, which is the highest

value obtained in the last decade [64]. To the best knowledge of the author of this PhD thesis, the multi-factor optimisation of light, temperature and glucose concentration is the first of its kind.

3. Scaling-up to 1-litre PBRs to evaluate transition from lab-scale:
   Scale-up is implemented as third part with the objective to determine the effect of scale-up from shake flask to 1-litre PBRs on EPS production, estimating the potential of industrial-scale production. The aim is to maintain the EPS titre from the shake flask optimisation in PBRs, ideally increasing to 9.5 g L^{-1} or higher, as this was obtained at pilot-scale in literature [64].
4. Economic evaluation of a industrial-scale EPS production process:
   Based on the obtained laboratory results, an industrial-scale EPS production process is designed, using the process and economic modelling software SuperPro Designer® (SPD). A screening level analysis evaluates the economic feasibility of current production levels and identify potential adjustments needed to achieve viability. The TEA will model various production scenarios and aims to identify a process configuration that has a Profitability Index of >1.0, indicating a profitable production process. To the best knowledge of the author of this PhD thesis, this TEA of photoautotrophic EPS production is the first of its kind.

This thesis focuses on the potential of cyanobacteria as efficient producers of functional EPS, contributing to climate change mitigation through their sustainable cultivation. Microalgae, including cyanobacteria, are recognised as sustainable resources with benefits across various sectors, including carbon sequestration, bioremediation, and the production of high-value bioactive compounds. Their cultivation is environmentally sustainable, offering low carbon footprints and resource efficiency, thus supporting a green economy and contributing to Sustainable Development Goals (SDGs) [262, 263]. By developing an economically feasible process to produce cyanobacterial EPS, this research can assess current levels of production and guide future research, paving the way for the commercialisation of EPS in a range of industries. Beyond scientific innovation, this research aligns with global efforts to promote sustainability and reduce the environmental impact of industrial processes. The EPS products derived from cyanobacteria could replace petroleum-based products with renewable, bio-based alternatives, contributing to reduction of greenhouse gas emission and the preservation of natural resources. By addressing

key scientific and technological challenges, this work seeks to foster a circular bioeconomy where biological solutions play a pivotal role in mitigating climate change and advancing a sustainable, bio-based economy.

Chapter 4: Materials and Methods

4.1 Screening Novel Cyanobacteria for EPS and Biomass Production

4.1.1 Cyanobacterial Species

Cyanobacterial species were selected based on availability in culture collections and relevance in the literature (section 4.1.1.1), followed by a practical refinement for experimental use (section 4.1.1.2).

4.1.1.1 Species Selection Based on Culture Collection Availability and Literature

A list of all cyanobacterial species available in four culture collections, Culture Collection of Algae and Protozoa (CCAP), The Culture Collection of Algae at The University of Texas at Austin (UTEX), Culture Collection of Algae at the Laboratory of Algology (CCALA), and Norwegian Culture Collection of Algae (NORCCA), yielded 192 species. Each species was reviewed for prior EPS publications. Many species were identified only to genus level (e.g., *Leptolyngbya*), so their novelty compared to known species like *Leptolyngbya gelatinosa* could not be confirmed, and they were excluded from this study. Twelve identifiable species with no EPS publications were selected. Most were xenic, but purification failed for most species, and four were unsuitable after delivery: one arrived non-viable, one was never delivered, and two failed to grow under recommended conditions. This reduced the number of species to eight novel species, of which half were axenic.

The search was expanded to Microbial Culture Collection at the National Institute for Environmental Studies (NIES), Provasoli-Guillard National Center for Marine Algae and Microbiota (NCMA), Pasteur Culture Collection (PCC), and Sammlung von Algenkulturen der Universität Göttingen (SAG), yielding 162 axenic species, of which 19 had no prior EPS studies. Seven were excluded due to long delivery times, strain instability, toxicity, or cultivation requirements incompatible with laboratory facilities. *Prochlorococcus marinus* lacked key EPS biosynthesis genes and was excluded [208]. From the remaining 11 species, budget constraints allowed acquisition of 8 strains. Four belonged to the genus *Sphaerospermopsis*, so *Sphaerospermopsis reniformis*

was selected, which was available as an active subculture, while the other three were only available as cryopreserved samples requiring longer delivery times.

4.1.1.2 Final Selection of Species for Experimental Use

15 novel cyanobacterial species were selected for a screening experiment regarding their EPS production. *Arthrospira platensis* was used as positive control because the EPS are widely studied [21]. These species were obtained from the following culture collections: CCAP, UTEX, NIES and NCMA. Some species were freshwater, others marine, and some were axenic while others were xenic, as detailed in Table 4-1.

Table 4-1 Cyanobacterial species used in the screening experiment to investigate extracellular polymeric substances (EPS) and dry cell weight (DCW) production.

Species	Designation	Culture Collection	Aquatic Habitat	Axenicity
Acaryochloris marina	NIES-2412	NIES	Marine	Axenic
Anabaena oscillarioides	CCAP 1403/10	CCAP	Freshwater	Xenic[22]
Arthrospira platensis	NIES-39	NIES	Freshwater	Axenic
Calothrix brevissima	NIES-22	NIES	Freshwater	Axenic
Fremyella diplosiphon	NIES-3275	NIES	Freshwater	Axenic
Gloeocapsa alpicola	UTEX 589	UTEX	Freshwater	Axenic
Nostoc foliaceum	UTEX 1624	UTEX	Freshwater	Xenic[21]
Nostoc longstaffi	UTEX1626	UTEX	Freshwater	Xenic
Nostoc zetterstedtii	UTEX1632	UTEX	Freshwater	Axenic
Oscillatoria rosea	NIES-208	NIES	Marine	Axenic
Phormidium breve	CCAP 1406/1	CCAP	Marine	Xenic
Phormidium keutzingianum[23]	CCMP2544	NCMA	Marine	Axenic
Spirulina major	CCAP 1475/3	CCAP	Marine	Xenic
Sphaerospermopsis reniformis	NIES-1949	NIES	Freshwater	Axenic
Trichormus subtropicus	UTEX B 1618	UTEX	Freshwater	Xenic
Tychonema bornetii	CCMP2568	NCMA	Marine	Axenic

4.1.2 Growth Conditions of Screening Experiment

Pre-cultures were prepared aseptically from maintenance cultures. Maintenance cultures were agar plates or liquid cultures left on the laboratory bench at ambient light and temperature conditions. The pre-cultures of the cyanobacteria were cultivated in 250 mL Erlenmeyer flasks with 62.5 mL working volume in a shaking incubator (Excella

[22] *A. oscillarioides* and *N. foliaceum* were successfully purified and used as axenic culture for the experiments (Appendix section 12.3).
[23] The species is listed as *Phormidium keutzingianum* in the NCMA collection; however, this may be a typographical error, as only *Phormidium kuetzingianum* is present in the online database AlgaeBase.

E24R, New Brunswick) at 25°C and 250 RPM for 14 days. Freshwater species were grown in Blue-Green Algae (BG-11) medium and marine species were grown in Enriched Seawater Medium (ESM) [264, 265]. Constant illumination (20.35 ± 3.48 µmol m^{-2} s^{-2}) was provided by two light-emitting diode (LED) strips (brand unknown) affixed on the top of the incubator. Light intensity was measured at five spots in the incubator with a Li-250A light meter (LI-COR Biosciences, UK) in triplicates. The optical density (OD) was determined by measuring the absorbance at 750 nm (OD_{750}) in triplicates. The inoculation volume was calculated according to the following formula (Equation 4-1):

$$OD_{inoculum} \times V_{inoculum} = OD_{culture} \times V_{culture}$$

Equation 4-1

Where:

- $OD_{inoculum}$ is the OD_{750} of the inoculum,
- $V_{inoculum}$ is the volume (mL) of the inoculum,
- $OD_{culture}$ is the desired OD_{750} of the culture,
- $V_{culture}$ is the desired volume (mL) of the culture.

The cultures were inoculated from pre-cultures to have an OD_{750} of 0.2 at time 0, and cultivated under the same conditions as the pre-cultures for up to 60 days (Exp. 1). Culture samples of 5-10 mL were collected aseptically every 7-12 days. The samples were used to determine DCW and EPS concentration, which is described in sections 4.1.3 and 4.1.4.

4.1.3 Biomass Sample Processing and Dry Cell Weight Quantification

Biomass production was estimated by determining the DCW concentration every 7-14 days unless indicated otherwise. Culture broth (5-15 mL) was transferred aseptically from the culture flasks into pre-weighed 15 mL plastic centrifuge tubes (Falcon). The tubes were centrifuged for 15 min at 4°C and 12,841 × g (Eppendorf Centrifuge 5430

R, Eppendorf AG, Hamburg, Germany). The supernatant was filtered[24] (0.45µm, cellulose acetate), transferred to clean 50 mL plastic centrifuge tubes and stored at -20°C until EPS analysis, which will be described in the next section. The DCW pellets were dried at 80°C until constant weight for 7-14 days. The DCW was determined gravimetrically. Biomass concentration was calculated from the obtained weight and corrected for evaporation. A linear evaporation rate was assumed for simplification.

In one instance (Exp. 2-5), DCW was calculated from OD_{750} due to time limitations. The relationship between OD_{750} and DCW was estimated from an *A. oscillarioides* culture. Using centrifugation (10 min, 1,699 × g), 10mL culture was concentrated until an OD_{750} of about 20, and then serially diluted until an OD_{750} of approximately 0.25. OD_{750} was measured using a spectrophotometer (UV-1280 UV-Vis-Spectrophotometer, Shimadzu). DCW was quantified as described above. As shown Figure 12-2*a* in the appendix, DCW was strongly correlated to OD_{750} (R^2=0.9979), yielding the conversion factor of 0.3402 based on the trendline equation (Table 12-1).

4.1.4 EPS Recovery, Purification and Quantification

Cell-free supernatants from section 4.1.3 were thawed overnight at 4°C. Chilled ethanol was added in a ratio of 1:3 (volume supernatant : volume ethanol), the mixture was left overnight at 4°C and the EPS precipitate was collected the next day by centrifugation (4°C, 15 min and 12,841 × g) [266]. After discarding the ethanol, the pellet was re-suspended in 4 mL Milli-Q[25] (MQ) water and transferred into a dialysis membrane (14,000 Da, cellulose, Merck, Germany). Dialysis was performed against deionized water for 48 hours at room temperature with 50 mg L^{-1} sodium azide (Merck, Germany) as preservative [266]. The dialysed EPS were transferred into pre-weighed 15 mL plastic centrifuge tubes, freeze-dried and quantified gravimetrically. EPS concentration was calculated from the obtained weight and corrected for evaporation. A linear evaporation rate during cultivation was assumed for simplification. Media (BG-11, ESM) samples were processed in the same way and used as negative controls for the EPS composition assays.

[24] The filtration step was omitted during later experiments (optimisation and scale-up).
[25] Milli-Q water is ultrapure water showing a resistivity of 18.2 MΩ·cm at 25°C and total organic carbon (TOC) ≤ 5 ppb [267].

4.1.5 Characterisation of EPS

4.1.5.1 Carbohydrate Content determination using the Phenol-Sulphuric Acid Method

The final EPS samples of the 16 screened cyanobacteria were used for EPS characterisation (day 60). Total sugar content of the EPS was determined using the phenol-sulphuric acid method and glucose as standard (0.08 – 2.5 g L^{-1}) [78]. Freeze-dried EPS were dissolved in Milli-Q water at 2 g L^{-1}. BG-11 and ESM were used as negative controls. Assays were performed in triplicates. Based on the 96-well-format by Strieth, et al. [78], 20µL sample, 20 µL of phenol (5% in water) and 100 µL concentrated sulphuric acid were mixed in a 96-well-plate. The plate was incubated for 10 min at room temperature, followed by 15 min at 30°C, and another 10 min at room temperature. The absorbance at 490 nm was measured against MQ water as blank value. The sugar content (gram sugar per gram EPS) was calculated based on the sugar concentration (g L^{-1}) in the EPS sample and the EPS concentration (g L^{-1}) according to Equation 4-2:

$$Sugar\ content\ \left(\frac{g}{g}\right) = \frac{Sugar\ concentration\ \left(\frac{g}{L}\right)}{EPS\ concentration\ \left(\frac{g}{L}\right)}$$

Equation 4-2

The Sugar content was then converted in $\%_{w/w}$ according to Equation 4-3:

$$Sugar\ content\ (\%w/w) = Sugar\ content\ \left(\frac{g}{g}\right)\ x\ 100$$

Equation 4-3

4.1.5.2 Protein Content determination using the Bradford Assay

The Bradford assay was used to estimate the protein content of the EPS [268, 269]. Freeze-dried EPS samples were re-suspended in MQ water at a concentration of 2 g L^{-1}. Sample (5 µL) in triplicates was mixed with 250 µL Bradford reagent (Fisher Scientific, UK) in a 96-well-plate flat bottom plate (Greiner Bio-One, Germany), and incubated for 10 min at room temperature. Absorbance was measured at 595 nm. Protein content was interpolated from a standard curve of bovine albumin serum (BSA)

using water as blank for samples and standards [270]. Eight BSA standards were prepared according to the manufacturer's instructions (0.025, 0.125, 0.25, 0.5, 0.75, 1, 1.5, 2 g L^{-1}) [270]. Only the linear portion of the calibration curve (0.025–1 g L^{-1}), determined graphically with $R^2 > 0.99$, was used for interpolation of sample protein concentrations. The protein content (gram protein per gram EPS) was calculated based on the protein concentration (g L^{-1}) in the EPS sample and the EPS concentration (g L^{-1}) according to Equation 4-4:

$$Protein\ content\ \left(\frac{g}{g}\right) = \frac{Protein\ concentration\ \left(\frac{g}{L}\right)}{EPS\ concentration\ \left(\frac{g}{L}\right)}$$

Equation 4-4

The protein content was then converted in $\%_{w/w}$ according to Equation 4-5:

$$Protein\ content\ (\%w/w) = Protein\ content\ \left(\frac{g}{g}\right)\ x\ 100$$

Equation 4-5

4.1.5.3 Sulphate Content determination using the Barium Chloride Gelatine Test

Barium chloride gelatine test was used to estimate the sulphate content. Based on Torres, et al. [80], fresh barium chloride gelatine reagent was prepared by dissolution of 3 g L^{-1} gelatine in ultrapure water, incubation at 80°C for 10 min in a dry bath, and addition of 10 g L^{-1} $BaCl_2$. Samples were hydrolysed with 0.5 mol L^{-1} hydrochloric acid (HCl) for 3 hours at 105°C. Subsequently, 140 µL HCl (0.5 M in water) and 20 µL sample were added to a 96-well-plate and absorbance was measured at 440 nm (absorbance 1). Barium chloride reagent (40 µL) was added, the plate was incubated for 20 min. The absorbance was measured again (absorbance 2). Sulphate content was calculated by subtracting absorbance 1 from absorbance 2 and interpolation against a standard curve from sodium sulphate (Na_2SO_4) in 0.5 M HCl, corresponding to 0.01 to 0.34 g sulphate ion L^{-1} [80]. The sulphate content (gram sulphate per gram EPS) was calculated based on the sulphate concentration (g L^{-1}) in the EPS sample and the EPS concentration (g L^{-1}) according to Equation 4-6:

$$Sulphate\ content\ \left(\frac{g}{g}\right) = \frac{Sulphate\ concentration\ \left(\frac{g}{L}\right)}{EPS\ concentration\ \left(\frac{g}{L}\right)}$$

Equation 4-6

The sulphate content was then converted in $\%_{w/w}$ according to Equation 4-7:

$$Sulphate\ content\ (\%w/w) = Sulphate\ content\ \left(\frac{g}{g}\right)\ x\ 100$$

Equation 4-7

4.1.5.4 Hydrolysis of EPS and Neutralisation

250 µL EPS sample (2 g L^{-1}) was hydrolysed with trifluoroacetic acid (TFA) at a final concentration of 2M. Hydrolysis was performed in glass test tubes at 120°C for 2 hours. After cooling down at room temperature, sodium hydroxide was added for a final concentration of 2M. Most HPAEC-PAD monosaccharide standards (glucose, fructose, mannose, arabinose, fucose, galactose, rhamnose and xylose) were treated in the same way as samples. Five standards (fructose, ribose, glucuronic acid, galacturonic acid and glucosamine) were not subjected to TFA hydrolysis, as preliminary tests showed that no peaks were detected after TFA treatment, indicating degradation of these compounds (data not shown). The standards were prepared in two vials, hydrolysed (standards set 1) and unhydrolysed (standards set 2).

4.1.5.5 Monosaccharide Analysis

Monosaccharides were analysed with High-Performance Anion Exchange Chromatography with pulsed-amperometric detection (HPAEC-PAD), using a Thermo Scientific™ Dionex™ ICS-6000. Hydrolysed sample (20 µL, 2 g L^{-1} EPS) was diluted in 9980 µL 10mM NaOH. Injection volume into the Dionex CarboPac PA210-Fast-4µm column was 25µL.[26] The monosaccharide standards were prepared in concentrations from 0.125 to 1 mg L^{-1} in MQ water.

[26] HPAEC-PAD method development was performed in collaboration with Dr Joshua Reid (University of Nottingham). HPAEC-PAD analysis was carried out by the author of this PhD thesis.

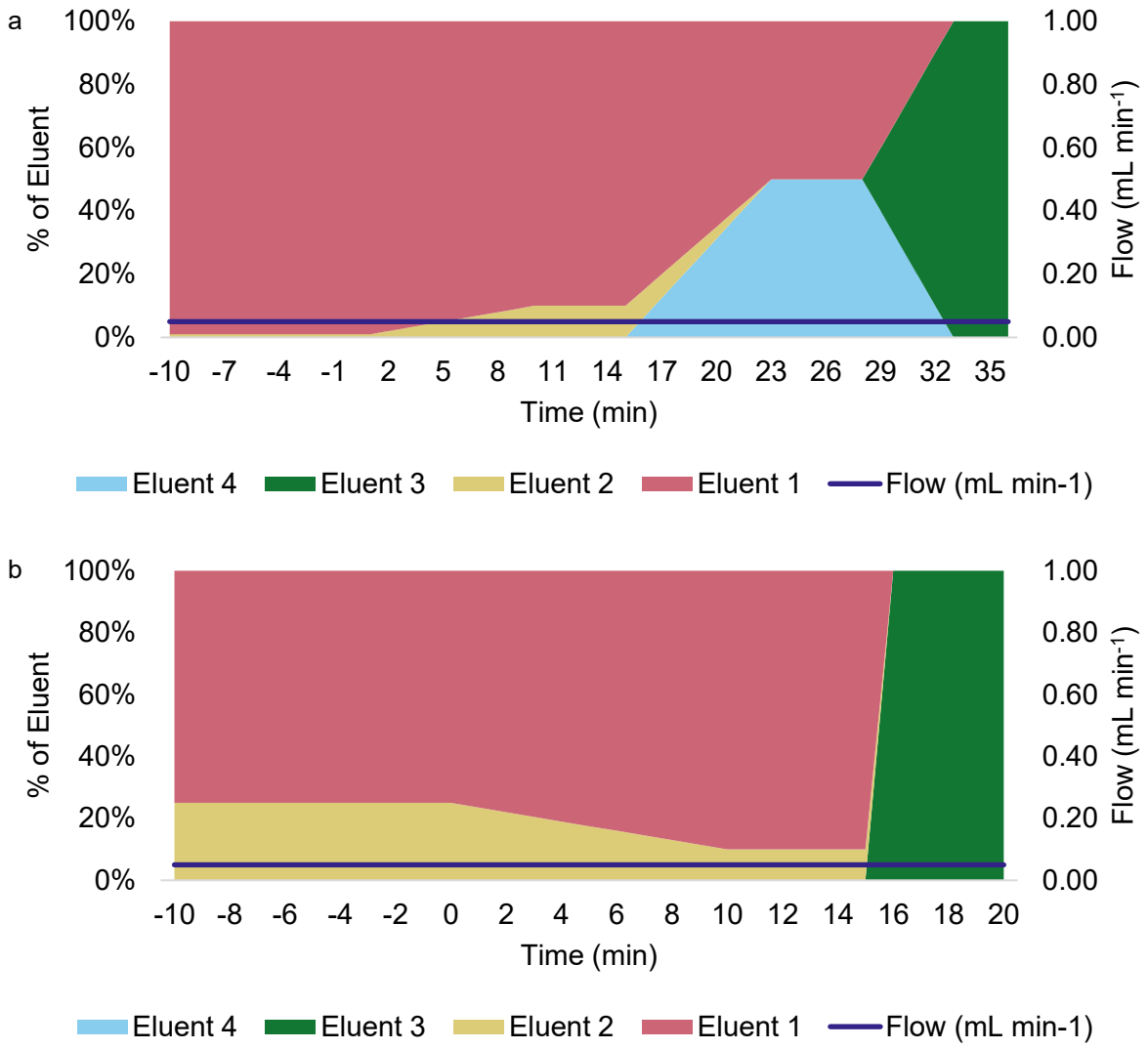


Figure 4-1 Elution buffer gradients used for high-performance anion exchange chromatography with pulsed-amperometric detection (HPAEC-PAD) for monosaccharide analysis.Eluent 1: Milli-Q water; Eluent 2: 100 mM NaOH; Eluent 3: 200 mM NaOH; Eluent 4: 100 mM NaOH + 500 mM NaOAc. (a) Method 1 used to analyse fucose, glucose, galactose, xylose, mannose, fructose, ribose, glucosamine, glucuronic acid, and galacturonic acid. (b) Method 2 used to analyse rhamnose and arabinose.

Each sample was run with two different methods at a flowrate of 0.05 mL min^{-1}.[26] Most standards (fucose, glucose, galactose, xylose, mannose, fructose, ribose, glucosamine, glucuronic and galacturonic acid) were analysed with method 1. Method 1 used an elution buffer gradient consisting of mainly Eluent 1 (MQ water) for 10 min, after which Eluent 2 (100 mM NaOH) was slowly added, and Eluent 4 (200 mM NaOH) was added more rapidly. In method 2 (Figure 4-1*c*), a decrease method of Eluent 2

(100 mM NaOH) compared to Eluent 1 (MQ water) was used. Both methods ended with Eluent 3 (200mM NaOH) for approximately 5 min. The details of the elution buffer gradients of method 1 and method 2 can be found in Table 4-2 and Table 4-3, respectively. This method was developed by Yakubov, et al. [271] and refined for this PhD project in collaboration with one of the authors, Dr Joshua Reid (University of Nottingham). HPAEC-PAD analysis was carried out by the author of this PhD thesis.

Table 4-2 Elution buffer gradient of method 1 used for high-performance anion-exchange chromatography with pulsed-amperometric detection (HPAEC-PAD) for monosaccharide analysis of extracellular polymeric substances (EPS).Method 1 was used for analysis of Fucose, galactose, glucose, xylose, mannose, glucosamine, fructose, ribose, galacturonic acid and glucuronic acid.

Time from injection (min)	**Eluent 1 (MQ water)**	**Eluent 2 (100 mM NaOH)**	**Eluent 3 (200mM NaOH)**	**Eluent 4 (200mM NaOH)**	**Flow (mL min^{-1})**
-10.0	99%	1%	0%	0%	0.05
0.0	99%	1%	0%	0%	0.05
10.0	90%	10%	0%	0%	0.05
15.0	90%	10%	0%	0%	0.05
22.5	50%	0%	0%	50%	0.05
27.5	50%	0%	0%	50%	0.05
32.5	0%	0%	100%	0%	0.05
36.0	0%	0%	100%	0%	0.05

Table 4-3 Elution buffer gradient of method 2 used for high-performance anion-exchange chromatography with pulsed-amperometric detection (HPAEC-PAD) for monosaccharide analysis of (rhamnose and arabinose) extracellular polymeric substances (EPS).

Time from injection (min)	**Eluent 1 (MQ water)**	**Eluent 2 (100 mM NaOH)**	**Eluent 3 (200mM NaOH)**	**Eluent 4 (200mM NaOH)**	**Flow (mL min^{-1})**
-10.0	75%	25%	0%	0%	0.05
0.0	75%g	25%	0%	0%	0.05
10.0	90%	10%	0%	0%	0.05
15.0	90%	10%	0%	0%	0.05
16.0	0%	0%	0%	100%	0.05
20.0	0%	0%	0%	100%	0.05

Fucose, galactose, glucose, xylose and mannose were analysed based on the chromatograph of standards set 1 under method 1. Glucosamine, fructose, ribose, galacturonic acid and glucuronic acid were analysed based on the chromatograph of standards set 2 under method 1. Arabinose and rhamnose were analysed based on standards set 1 under method 2.

The monosaccharide content (gram monosaccharide per gram EPS) was calculated based on the monosaccharide concentration (g L^{-1}) in the EPS sample and the EPS concentration (g L^{-1}) according to Equation 4-8:

$$Monosaccharide\ content\ \left(\frac{g}{g}\right) = \frac{Monosaccharide\ concentration\ \left(\frac{g}{L}\right)}{EPS\ concentration\ \left(\frac{g}{L}\right)}$$

Equation 4-8

The monosaccharide content was then converted in $\%_{w/w}$ according to Equation 4-9:

$$Monosaccharide\ content\ (\%w/w) = Monosaccharide\ content\ \left(\frac{g}{g}\right)\ x\ 100$$

Equation 4-9

4.1.6 Analysis of EPS Properties

4.1.6.1 Cyanobacterial Species and Growth Conditions for EPS Properties Analysis

The properties of the EPS of seven species were analysed. *A. marina*, *A. oscillarioides*, *C. brevissima*, *N. foliaceum*, *N. longstaffi*, *N. zetterstedtii* and *T. subtropicus* were cultivated for 50 days at 22 µmol m^{-2} s^{-1} and 25°C in a shaking incubator (SciQuip Premium Compact). EPS were processed as described in section 4.1.4 and used for EPS properties analysis.

4.1.6.2 Emulsifying Activity Assay

The emulsifying activity of the EPS was measured based on the method of Cooper and Goldenberg [272] with modifications [105]. Freeze-dried EPS were resuspended in MQ water at a concentration of 2 g L^{-1}. EPS solution (2 mL) and 2 mL olive oil were vortexed for 2 min, resulting in a final EPS concentration of 1 g L^{-1}. After 24 hours, the height

(H) in millimetres (mm) of the oil, emulsion and aqueous layer was measured using a ruler. MQ water was used as negative control, whereas Tween20 (final concentration of 0.0001 – 137.5 g L^{-1}) and xanthan gum (1 g L^{-1}) were used as positive controls [105]. The emulsifying rate was calculated based on the following formula (Equation 4-10) [105]:

$$Emulsifying\ rate\ (\%) = \frac{H_{emulsion}}{H_{emulsion} + H_{oil} + H_{aqueous}} \times 100$$

Equation 4-10

Where:

- $H_{emulsion}$ is the height of the emulsion layer (mm),
- H_{oil} is the height of the oil layer (mm),
- $H_{aqueous}$ is the height of the aqueous layer (mm).

At a later stage, 1.3 mL EPS (6 g L^{-1}) were mixed with 2.6 mL olive oil, resulting in a final concentration of 2 g L^{-1} EPS and an oil:water ratio of (2:1). The test was performed as described above.

4.1.6.3 Flocculating Activity Assay

The flocculating assay was based on Kurane, et al. [273] with modifications [105]. $CaCl_2.2H_2O$ (4.9 mL) was mixed with 0.1 mL EPS (2 g L^{-1}) and 45 mL kaolin clay solution (5 g L^{-1}, pH 7). The mixture was vortexed for 20 seconds and left for 5 minutes at room temperature. One millilitre of the top layer was removed to measure the absorbance (A) at 550 nm. Xanthan gum (2 g L^{-1}), BG-11 and water were used as positive control, negative control and blank, respectively [105]. The flocculating activity was calculated according to the following formula [105]:

$$Flocculating\ rate\ (\%) = \frac{A_{blank} - A_{sample}}{A_{blank}} \times 100$$

Equation 4-11

Where:

- A_{blank} is the absorbance at 550 nm of the blank (water),
- A_{sample} is the absorbance at 550 nm of the sample.

4.1.6.4 Antioxidant Activity Assays

The antioxidant activity of the EPS was determined using two different radicals, 2,2-diphenyl-1-picrylhydrazyl (DPPH) and 2,2'-azino-bis(3-ethylbenzothiazoline-6-sulfonic acid) cation ($ABTS^+$) [106]. The DPPH antioxidant assay was based on Shimada, et al. [274] with slight modifications [105]. Samples of EPS at different concentrations (2, 1, 0.5, 0.25, 0.125 g L^{-1}; 150 µL each) were mixed with 150 µL DPPH solution (0.05 g L^{-1} in ethanol) in microcentrifuge tubes (Eppendorf) and incubated at 30°C in the dark. Background absorbance values were obtained using 150 µL ethanol. After 1 hour incubation, the tubes were centrifuged at 4°C and 16,873 × g for 20 min (Eppendorf Centrifuge 5418 R, Eppendorf AG, Hamburg, Germany). Samples, background samples, standards, controls and blanks were treated in the same way. Of the supernatant, 200 µL were transferred to a 96-well-plate and the absorbance was read at 570 nm. Ascorbic acid (0.013 – 2 g L^{-1}) was used as a positive control [105]. The residual concentration of DPPH (C_{DPPH}) was interpolated from a standard curve of 150 µL DPPH (0.00313 – 0.05 g L^{-1} in ethanol) mixed with 150 µL water. Water (150 µL) mixed with 150 µL ethanol was used as blank. After subtraction of the background value, the DPPH removal activity was calculated based on Equation 4-12 [105]:

$$DPPH\ scavenging\ activity\ (\%) = \frac{C_{DPPH,reagent} - C_{DPPH,sample}}{C_{DPPH,reagent}} \times 100$$

Equation 4-12

Where:

- $C_{DPPH,\ reagent}$ is the concentration of DPPH in the reagent,
- $C_{DPPH,\ sample}$ is the concentration of DPPH in the sample.

According to Re, et al. [275] with modifications, ABTS (3.6 g L^{-1}) was mixed with ammonium persulphate (0.56 g L^{-1}) in sodium phosphate buffer (pH 7.4) and incubated overnight in the dark at room temperature [105]. After 10-fold dilution, the $ABTS^+$ solution was used as the reagent and as standard curve of the assay. $ABTS^+$ reagent (30 µL) was mixed with 270 µL EPS sample. Phosphate buffer (30 µL)

instead of reagent was used to obtain background values. Ascorbic acid, BG-11 and water were used as positive control, negative control and blank, respectively [105]. The tubes were incubated at 30°C for 5 min in the dark and subsequently centrifuged for 20 min at 4°C and 16,873 × g. Samples, background samples, standards, controls and blanks were treated in the same way. Of the supernatant, 200 µL were measured in a 96-well-plate at 750 nm. The residual $ABTS^+$ concentration (C_{ABTS+}) was interpolated from a standard curve. The $ABTS^+$ removal activity was calculated based on Equation 4-13 after subtraction of the background value [105].

$$ABTS^+ \; scavenging \; activity \; (\%) = \frac{C_{ABTS+,reagent} - C_{ABTS+,sample}}{C_{ABTS+,reagent}} \times 100$$

Equation 4-13

Where:

- $C_{ABTS+,\ reagent}$ is the concentration of $ABTS^+$ in the reagent,
- $C_{\ ABTS+,\ sample}$ is the concentration of $ABTS^+$ in the sample.

4.1.6.5 Iron-Chelating Assay

The iron-chelating activity of the EPS was determined with a Fe^{2+}-binding assay using $FeCl_2.4H_2O$ and ferrozine (5,6-Diphenyl-3-(2-pyridyl)-1,2,4-triazine-4′,4″-disulfonic acid sodium salt) based on Chun-hui, et al. [276] with modifications [277]. Briefly, 3 µL $FeCl_2.4H_2O$ (0.4 g L^{-1}) was mixed with 300 µL EPS (2, 1, 0.5, 0.25, 0.125 g L^{-1}) and vortexed. Ferrozine (2.6 g L^{-1}, 12 µL) was added and the tubes were vortexed. After 10 min of incubation at room temperature, the tubes were centrifuged at 4°C and 16,873 × g for 20 min. The absorbance of 200 µL of the supernatant was measured at 570 nm. MQ water (15 µL) with 300 µL EPS sample was used to obtain background absorbance values. EDTA, BG-11 and water were used as positive control, negative control and blank, respectively. The concentration of ferrous ferrozine complex (Fe complex) was interpolated using a standard curve of 3 µL $FeCl_2.4H_2O$ (0.4 g L^{-1}) and 12 µL ferrozine (2.6 g L^{-1}) in 300 µL water. The chelating activity was calculated based on the following formula after subtraction of the background value:

$$Chelating\ rate\ (\%) = \frac{C_{Fe\ complex,reagent} - C_{Fe\ complex,sample}}{C_{Fe\ complex,reagent}} \times 100$$

Equation 4-14

Where:

- $C_{Fe\ complex,\ reagent}$ is the concentration of Fe complex in the reagent,
- $C_{Fe\ complex,\ sample}$ is the concentration Fe complex in the sample.

4.1.6.6 Photoprotection Assay (UV/vis Spectrophotometry)

The UV/vis spectrum of 1 mL EPS samples at different concentrations (2, 1, 0.5, 0.25, 0.125 g L^{-1}) was measured at 185 – 800 nm in quartz cuvettes, using a Shimadzu UV-2600 spectrophotometer and water as baseline. Commercial sunscreen (SPF30) was diluted 500, 1000, 2000, 4000, 8000 and 16000-fold in water and analysed in the same manner. The absorbance values of interest are the UV region (200 - 400 nm) [139]. According to Chou, et al. [278], transmittance (Tr) was calculated from each absorbance (A) value by applying Equation 4-15. UV-protection level was expressed as the fraction that does not get transmitted according to Equation 4-16.

$$A = -log\ (Tr)$$

Equation 4-15

$$UV - protection\ level\ (\%) = 100\% - Tr$$

Equation 4-16

4.1.7 Statistical Analysis

Data are presented as mean ± standard deviation (σ). Mean and standard deviation were calculated using the AVERAGE and STDEV.S function of MS Excel, respectively [279].

4.1.7.1 Statistical Significance

Statistical analysis was conducted using Microsoft Excel. Statistical significance was assessed using an unpaired t-test assuming unequal variances [117, 118, 207]. P-

values are indicated by the following symbols: * $p < 0.05$, ** $p < 0.01$, and *** $p < 0.001$, with significance set at $p < 0.05$ [53].

4.1.7.2 Limit of Detection (LOD) and Limit of Saturation (LOS)

Limit of Detection (LOD) was calculated based on the following formula [280]:

$$LOD = \frac{3.3 * \sigma}{s}$$

Equation 4-17

Where:

- s is the slope of the calibration curve,
- σ is the standard deviation of the lowest standard concentration (calculated from triplicates) [281-283].

The LOD values of all EPS composition and EPS properties assays can be found in the Appendix (Table 12-1). The Limit of Saturation (LOS) was determined by the graphical method as the highest standard concentration showing a linear response in peak area (HPAEC-PAD) or absorbance (colorimetric and turbidimetric assays) [28]. The detection range is defined as analyte concentrations between the LOD and LOS. Values below the LOD were displayed as "<LOD" in tables and excluded from graphs. However, for antioxidant and iron-chelating assays, which calculate removal as a percentage of radical or Fe-complex reduction, the lowest measured concentrations correspond to the highest removal values. Concentrations below the LOD were capped at the LOD. For example, the LOD for $ABTS^{+}$ radical is 0.0011 g L^{-1} (Table 12-1), which corresponds to a maximum quantifiable scavenging activity of 97% (based on Equation 4-13). Any antioxidant activity above this (e.g., 99%) is reported as 97%.

4.1.7.3 Correlation between Properties and Composition

The Pearson correlation coefficient *r* between EPS properties and composition was calculated using the associated Microsoft (MS) Excel function to measure the linear correlation between each of the property with each of the compositional aspects [284].

Each composition datapoint *x* (sugar, protein, sulphate and monosaccharide content) was correlated to each of the properties datapoint *y* (emulsifying, flocculating, antioxidant, metal-chelating and UV-protective activity). For properties with non-linear dose-dependent response (e.g. flocculating, DPPH scavenging, $ABTS^+$ scavenging, UV-protecting activity), the maximum obtained activity was used. Values below the LOD, were replaced with LOD/√2 [285]. A heatmap was created using conditional formatting in MS Excel.

Spearman rank was not used because it is not available as function in MS Excel. Instead, data were plotted to visually inspect for potential non-linear trends that might not be captured by the Pearson correlation coefficient alone. Additionally, species were ranked by each compositional variable *x* and by each property *y*, and the two sets of ranks were compared side by side to look for matching or contrasting orderings.

4.2 Optimisation of Cultivation Conditions

Optimisation of growth conditions of *C. brevissima* and *N. foliaceum* was performed under the following conditions, unless specified otherwise. BG-11 medium with 1mM 4-(2-hydroxyethyl)-1-piperazineethanesulfonic acid (HEPES) buffer (pH 7.5) was used as growth medium. Species were grown in 50 mL Erlenmeyer flasks in the Algem HT24 (Algenuity Ltd, UK), that were placed in a Stuart SI-600 incubator (Cole Palmer, UK) for shaking at 150 RPM. Experiments were performed in biological duplicates. Pre-cultures were cultivated under the same conditions than the actual cultures. Cultures and samples were handled aseptically and checked for contamination by streaking onto an LB plate. Obtained EPS and DCW concentrations were corrected for evaporation.

4.2.1 Single-Factor Optimisation of Light Intensity at 60% Working Volume

C. brevissima and *N. foliaceum* pre-cultures were prepared in 50 mL Erlenmeyer flasks filled with 30 mL volume. Pre-cultures were grown in unbuffered BG-11 medium for 14 days at 25°C and different light intensities, *2*2, 50, 75 and 100 µmol m^{-2} s^{-1} for *C. brevissima* and 50, 75, 100 and 150 µmol m^{-2} s^{-1} for *N. foliaceum*. Cultures were inoculated from pre-cultures according to Equation 4-1 at a start OD_{750} of 0.2 and a volume of 30 mL. Cultures were grown in triplicates for 56 days, with sampling every 14 days (Exp. 2-1). This duration was chosen to align with the 60-day screening experiment for direct comparison, with sampling every 14 days and four sampling points, leading to 56 days duration. The culture samples were processed for DCW and EPS production based on sections 4.1.3 and 4.1.4.

4.2.2 Effect of Working Volume on *C. brevissima* and *N. foliaceum*

C. brevissima and *N. foliaceum* were grown in two different light intensities (22 and 75 µmol m^{-2} s^{-1}) at a lower working volume of 25% (12.5mL in 50 mL flask) and 25°C. Pre-cultures were grown in unbuffered BG-11 medium for 14 days and used to inoculate cultures at a start OD_{750} of 0.2, according to Equation 4-1. Cultures were grown for 28 days with sampling every 6-15 days (Exp. 2-2). The culture samples were processed for DCW and EPS production based on sections 4.1.3 and 4.1.4.

4.2.3 Single-Factor Optimisation of Light Intensity at 25% working volume

C. brevissima and *N. foliaceum* pre-cultures (12.5 mL) were grown in unbuffered BG-11 medium for 10 days at 25°C and 6 different light intensities (50, 75, 100, 125, 150 and 175 µmol m^{-2} s^{-1}, Exp. 2-3). The pre-cultures were used to inoculate the cultures at an initial OD_{750} of 0.5, according to Equation 4-1. After 21 days of growth, the cultures were processed for DCW and EPS production based on sections 4.1.3 and 4.1.4.

4.2.4 Single-Factor Optimisation of BG-11 Media Components

Two shake flasks experiments were performed in a shaking incubator (Premium Compact, SciQuip Ltd, UK) to study the effect of media composition on EPS production of *C. brevissima* and *N. foliaceum.* First, the two species were grown in four different types of medium: standard BG-11, BG-11 supplemented with 5 g L^{-1} acetate, BG-11 supplemented with 5 g L^{-1} glucose [184], and BG-11 with 10-fold higher trace metals (Exp. 2-4). For the latter, 10 mL trace metal solution was added per litre BG-11 medium instead of the standard level of 1 mL L^{-1}. A maintenance culture (ambient light and temperature) was used as inoculum at an initial OD_{750} of 1.6 and 1.1 for *C. brevissima* and *N. foliaceum*, respectively. The cultures were incubated at 25°C for 15 days at 22 µmol m^{-2} s^{-1} without shaking (Figure 4-2*a*). Cultures were used for OD_{750} measurement, and supernatants were processed for EPS quantification as described in section 4.1.4. DCW was estimated by multiplying OD_{750} with the factor 0.3402 (Table 12-1).



Figure 4-2 Photos of *Calothrix brevissima* and *Nostoc foliaceum* cultures in SciQuip Premium Compact shaking incubator to study effect of media composition on EPS (Exp. 2-5).(a) Cultivation with different BG-11 compositions (standard, + glucose, + acetate, + 10x TM) (Exp. 2-4). (b) Cultivation with different levels of $MgSO_4$, $CaCl_2$, EDTA and pH (Exp. 2-5).

C. brevissima and *N. foliaceum* were grown in BG-11 with different levels of magnesium, $CaCl_2$ and EDTA, and at different pH using Tris(Hydroxymethyl)aminomethane (Tris) buffer (Exp. 2-5). BG-11 was prepared with $CaCl_2$, magnesium and EDTA at 50%, 100%, 250% and 500% of standard BG-11 level. Additionally, BG-11 with Tris buffer (1.21 g L^{-1}) instead of HEPES was prepared at pH 7.5 and pH 9. Cultures (12.5 mL) were inoculated from a maintenance culture (room temperature, ambient light) for a start OD_{750} of 0.5 in 50 mL Erlenmeyer flasks. Cultures were cultivated at 75 µmol m^{-2} s^{-1}, 25°C and 250 RPM for 2 weeks (Figure 4-2*b*). EPS samples of *C. brevissima* were processed according to section 4.1.4.

4.2.5 Multi-Factor Optimisation using Design of Experiments (DoE)

Minitab software was used to design multi-factor optimisation of glucose concentration, light intensity and temperature. Response Surface Design (Box Behnken) with 3 continuous factors (unblocked) was used [204]. The centre points and replicates were set to 2. Factors were defined as temperature (low: 20, high: 30°C), light intensity (low: 75, high: 225 µmol m^{-2} s^{-1} for *C. brevissima*; low: 25, high: 175 µmol m^{-2} s^{-1} for *N. foliaceum*), glucose concentration (low: 0, high: 5 g L^{-1}). In Minitab, the experimental range is defined by the selected low and high values, which are then coded as −1 (low), 0 (centre), and +1 (high). The experiments were carried out at the actual values, while Minitab uses the coded (normalised) values for the statistical analysis. In Minitab, runs

were randomised, however, they were sorted by temperature due to the equipment (Algem HT24, Table 4-4).

Table 4-4 Design of experiment (DoE) runs for 3-factor optimisation of light intensity, temperature, and glucose concentration for extracellular polymeric substances (EPS) and dry cell weight production of *Calothrix brevissima* and *Nostoc foliaceum* according to Minitab software (Exp. 2-6).Other growth conditions: 50 mL Erlenmeyer flasks with 25% working volume, shaking at 150 RPM. Runs were sorted by temperature and were carried out in three separate batches because temperature cannot be individually controlled in the equipment (Algenuity Algem HT24).

Flask #	**Temp.**	**Glucose**	**Light intensity**		**Run #**
(-)	(°C)	(g L^{-1})	(µmol m^{-2} s^{-1})		(-)
			C. brevissima	*N. foliaceum*	
1	25	0	75	25	Run 1 (25°C)
2	25	0	75	25	Run 1 (25°C)
3	25	0	225	175	Run 1 (25°C)
4	25	0	225	175	Run 1 (25°C)
5	25	2.5	150	100	Run 1 (25°C)
6	25	2.5	150	100	Run 1 (25°C)
7	25	2.5	150	100	Run 1 (25°C)
8	25	2.5	150	100	Run 1 (25°C)
9	25	5	75	25	Run 1 (25°C)
10	25	5	225	175	Run 1 (25°C)
11	25	5	75	25	Run 1 (25°C)
12	25	5	225	175	Run 1 (25°C)
13	28	0	150	100	Run 2 (28°C)
14	28	0	150	100	Run 2 (28°C)
15	28	2.5	225	175	Run 2 (28°C)
16	28	2.5	75	25	Run 2 (28°C)
17	28	2.5	225	175	Run 2 (28°C)
18	28	2.5	75	25	Run 2 (28°C)
19	28	5	150	100	Run 2 (28°C)
20	28	5	150	100	Run 2 (28°C)

(continued on next page)

Table 4-4 (continued)

Flask # (-)	**Temp.** (°C)	**Glucose** (g L^{-1})	**Light intensity** (µmol m^{-2} s^{-1})		**Run #** (-)
			C. brevissima	*N. foliaceum*	
21	22	0	150	100	Run 3 (22°C)
22	22	0	150	100	Run 3 (22°C)
23	22	2.5	75	25	Run 3 (22°C)
24	22	2.5	225	175	Run 3 (22°C)
25	22	2.5	75	25	Run 3 (22°C)
26	22	2.5	225	175	Run 3 (22°C)
27	22	5	150	100	Run 3 (22°C)
28	22	5	150	100	Run 3 (22°C)

In the laboratory, the 3-factor optimisation experiment (light intensity, temperature, glucose) was performed in three separate runs based on the three different temperatures. For each run, pre-cultures were grown for 10 days in the conditions specified in Table 4-4 (Exp. 2-6). For inoculation, pre-cultures were gently harvested by centrifugation (10 min, room temperature, 1,699 × g), re-suspended in fresh medium and used as inoculum for cultures at a start OD_{750} of 0.5. After 14 days of growth, the culture samples were processed for DCW and EPS production based on sections 4.1.3 and 4.1.4.

The final DCW and EPS results (day 14) were analysed with Minitab software to model the response surface of the parameters and determine the level of significance of the impact of each parameter on EPS and DCW. The optimal conditions were identified using the Minitab Response Optimiser feature. Subsequently, *N. foliaceum* pre-cultures were grown under the optimal conditions (4.84 g L^{-1} glucose, 28°C and 164 µmol m^{-2} s^{-1}) for 10 days and used for inoculation of cultures at a start OD_{750} of 0.5. After 7 and 14 days of growth, biological triplicates of cultures were processed for DCW and EPS production based on sections 4.1.3 and 4.1.4.

4.2.6 Two-Factor Optimisation (Light Duration and Light Intensity) for *C. brevissima*

Central Composite design (Minitab software) was used to design a 2-factor optimisation experiment of *C. brevissima* (Exp. 2-7) [32]. Factors were defined as light intensity (low: 20, high: 350 µmol m^{-2} s^{-1}) and light duration (low: 8, high: 24 hours), which is in accordance with literature [28, 41, 178]. Parameter values were rounded to the nearest integer based on the setting range of the equipment (Algem HT24). Pre-cultures were grown under the conditions and randomised order specified in Table 4-5 for 10 days and used to inoculate cultures at a start OD_{750} of 0.5. After 7 days of growth, the cultures were processed for DCW and EPS production based on sections 4.1.3 and 4.1.4.

Table 4-5 Design of experiment (DoE) runs for 2-factor optimisation of light intensity (µmol m^{-2} s^{-1}) and light duration (hours) for extracellular polymeric substances (EPS) production of *Calothrix brevissima* according to Minitab software (randomised, Exp. 2-7).Other growth conditions: 25 °C, 50 mL Erlenmeyer flasks with 25% working volume, shaking at 150 RPM.

Flask # (-)	**Light intensity (µmol m^{-2} s^{-1})**	**Light duration** (hours)
1	68	10
2	302	10
3	68	21
4	302	21
5	20	16
6	350	16
7	185	8
8	185	24
9	185	16
10	68	10
11	302	10
12	68	21
13	302	21
14	20	16
15	350	16
16	185	8
17	185	24
18	185	16

4.2.7 Systematic Evaluation of the Effect of Light Intensity and Temperature on EPS Production by *C. brevissima*

C. brevissima was grown at up to 12 different light intensities (25, 50, 75, 100, 150, 185, 225, 265, 300, 350, 400, 450, 500 µmol m^{-2} s^{-1}) and at five different temperatures (25, 28, 31, 34, 37°C, Exp. 2-8). Pre-cultures were grown for 10 days to inoculate cultures at OD_{750} of 0.5. After 7 days of growth, the cultures were processed for DCW and EPS production based on sections 4.1.3 and 4.1.4.

4.2.7.1 Validation of Optimised Conditions (Light and Temperature) for C. brevissima

C. brevissima pre-cultures were grown at 31°C and 300 µmol m^{-2} s^{-1} for 10 days. Cultures (12.5 mL culture volume in 50 mL flasks) were inoculated at OD_{750} of 0.5 and grown for 14 days, sampling every 1-3 days (Exp. 2-9). Samples were processed according to section 4.1.3 for DCW and 4.1.4 for EPS. Additionally, the emulsifying properties and lipid content was estimated of the day 10 sample according to sections 4.1.6 and 4.2.7.2.

4.2.7.2 Lipid Content Assay (Phospho-Vanillin Method)

According to Park, et al. [81], for lipid content estimation, 2 mL chloroform:methanol solution (2:1 ratio) was added to 2 mg freeze-dried EPS from *C. brevissima* in glass tubes and vortexed for 1 min. NaCl solution (1.5 mL, 0.9% in MQ water) was added and the tubes were centrifuged at 1,301 × g for 15 seconds. The lower phase containing chloroform and extracted lipids was transferred into clean glass tubes with glass Pasteur pipettes. The tubes were placed in a heat block to evaporate the solvent (10 min, 90°C). Subsequently, 0.1 mL concentrated sulphuric acid was added, and the tubes were incubated at 90°C. After 10 min, the glass tubes were cooled on ice for 5 min. Phospho-vanillin reagent was freshly prepared by dissolving 72 mg vanillin in 12 mL hot water and adding 48 mL phosphoric acid (85%). Phospho-vanillin reagent (2.4 mL) was added per tube and allowed to develop a pink colour for 10 min [81]. Absorbance was measured at 530 nm and the concentration of lipids was interpolated using a standard curve of 0.0125 to 0.2 g L^{-1} olive oil in methanol. Olive oil was used as positive control and methanol was used as negative control for lipid extraction and quantification.

4.3 Scale-Up to 1L Photobioreactors (PBRs)

4.3.1 Light Calibration and Equalisation of Light Intensity Across White and Coloured Light Tiles

Light calibration of the MicroPharos PBRs (Xanthella Ltd, UK) was performed by measuring the light intensity (µmol m^{-2} s^{-1}) with a Li-250A light meter (Li-Cor) at different amperages (mA). Amperage and light intensity were correlated using MS Excel. The light intensity of the coloured light tiles (red, blue, green) was measured with two different sensors. Firstly, with the Li-250A light meter (Li-Cor) and secondly, with the internal light sensor of the PBRs, which measures light in 'arbitrary units' (AU).

4.3.2 Effects of Airflow Rate and Light Intensity on EPS Production by *C. brevissima*

C. brevissima inoculum was grown for 14 days in 250 mL shake flasks filled with 62.5 mL BG-11 + 10mM HEPES in SciQuip Premium Compact incubator at 31°C and 220 µmol m^{-2} s^{-1} constant light. For each PBR, the contents of four shake flasks were aseptically pooled into a sterile 1 litre bottle. The OD_{750} of each bottle was measured in triplicates and the inoculation volume was adapted based on Equation 4-1. The bottles were filled to 750 mL with BG-11 for an initial OD_{750} of 0.5. HEPES buffer (10mM) was used for pH control instead of CO_2 due to a malfunctioning pH sensor.

PBRs were inoculated aseptically with *C. brevissima* as described in the Appendix (section 12.10). The species was cultivated in duplicates at 31 °C for 7 days, varying two parameters, airflow and light intensity, at three levels, minimum, intermediate, and maximum. Airflow was tested at 1, 2.5, and 4 L min^{-1}, and light intensity at 50, 500, and 950 µmol m^{-2} s^{-1}, corresponding to light tile settings of 16, 197, and 378 mA, respectively (Table 4-6, Exp. 3-1). The minimum and maximum values were determined by equipment ranges: Airflow setting ranged from 0.6 to 5 L min^{-1}, with no bubbles forming below 1 L min^{-1} and foaming pushing liquid through filters at 5 L min^{-1}. Light intensity ranged from 0 to 1000 µmol m^{-2} s^{-1}, with a linear response during calibration between 50 and 1000 µmol m^{-2} s^{-1} (section 7.2.1). CO_2 flowrate setting was 10 to 100 mL min^{-1}, which was used in the next experiments (Exp. 3.2 to Exp. 3.4). The CO_2 level in parts per million (ppm) was estimated by considering both the CO_2 in ambient air and the pure CO_2 from the gas cylinder, using the ratio of their respective

flow rates to the total gas flow, and multiplying by 1,000,000. CO_2 in ambient air is estimated to be 410 ppm [286].

Table 4-6 Cultivation parameters for photobioreactor (PBR) experiment studying the effect of airflow rate (1, 2.5, 4 L min^{-1}) and light intensity (50, 500, 950 µmol m^{-2} s^{-1}) on extracellular polymeric substances (EPS) production of *Calothrix brevissima* (Experiment 3-1).Growth conditions: 1 L Xanthella MicroPharos photobioreactors with 750 mL culture, 31 °C. CO_2 level (ppm) based on air is shown.

PBR run #	**Run order**	**PBR #**	**Light colour**	**Light intensity**	**Light tile setting**	**Airflow rate**	**CO_2 flow rate**	**CO_2 level**
Unit	(-)	(-)	(-)	µmol m^{-2} s^{-1}	mA	L min^{-1}	mL min^{-1}	ppm
1	6	4	White	500	197	1	0	410
2	10	4	White	500	197	1	0	410
3	4	2	White	50	16	2.5	0	410
4	8	2	White	50	16	2.5	0	410
5	3	1	White	500	197	2.5	0	410
6	7	1	White	500	197	2.5	0	410
7	1	1	White	950	378	2.5	0	410
8	2	2	White	950	378	2.5	0	410
9	5	3	White	500	197	4	0	410
10	9	3	White	500	197	4	0	410

EPS samples were taken every 1-3 days through the sampling port and processed according to section 4.1.4. On day 7, the culture was filled into a clean bottle. Biofilm was removed manually from PBR walls and sensors and added to the bottle. After mixing, samples were taken in triplicates from the bottle and processed for biomass and EPS quantification as described in sections 4.1.3 and 4.1.4. Liquid volumes on the sampling day were noted to correct EPS concentration calculated from dried EPS weight for evaporation according to Equation 4-18. DCW concentration was corrected in the same manner.

$$C_t = \frac{W_t}{V_{Sample,t}} \times \frac{V_{PBR,t}}{V_{PBR,0}}$$

Equation 4-18

Where:

- C_t is the concentration of EPS or DCW on day *t* (mg mL^{-1}),
- W_t is the weight of dried EPS or DCW sample on day *t* (mg),
- $V_{sample,t}$ is the volume of the sample of day *t* (mL),
- $V_{PBR,t}$ is the volume of the PBR on day *t* (mL),
- $V_{PBR,0}$ is the volume of the PBR on day 0 (mL).

4.3.3 Impact of CO_2 Flow Rate and Light Intensity on EPS Production by *C. brevissima*

C. brevissima was cultivated in duplicates at 31°C, a fixed airflow rate at 1 L min^{-1}, three different CO_2 flow rates (10, 55 and 100 mL min^{-1}) and three different light intensities (50, 500, 950 µmol m^{-2} s^{-1}), as specified in Table 4-7 for 7 days (Exp. 3-2). Sampling was performed in the same manner as the previous experiment.

Table 4-7 Cultivation parameters for photobioreactor (PBR) experiment studying the effect of carbon dioxide (CO_2) flow rate (10, 55, 100 mL min^{-1}) and light intensity (50, 500, 950 µmol m^{-2} s^{-1}) on extracellular polymeric substances (EPS) production of *Calothrix brevissima* (Experiment 3-2).Growth conditions: 1 L Xanthella MicroPharos photobioreactors with 750 mL culture, 1 L min^{-1} airflow rate, 31 °C. Shown are CO_2 levels (ppm) combining the supplemented CO_2 and that from air.

PBR run #	**Run order**	**PBR #**	**Light colour**	**Light intensity**	**Light tile setting**	**Airflow rate**	**CO_2 flow rate**	**CO_2 level**
Unit	(-)	(-)	(-)	µmol m^{-2} s^{-1}	mA	L min^{-1}	mL min^{-1}	ppm
11	11	1	White	500	197	1	10	10,307
12	15	1	White	500	197	1	10	10,307
13	12	2	White	50	16	1	55	52,521
14	24	2	White	50	16	1	55	52,521
15	14	4	White	500	197	1	55	52,521
16	18	4	White	500	197	1	55	52,521
17	16	2	White	950	378	1	55	52,521
18	20	2	White	950	378	1	55	52,521
19	13	3	White	500	197	1	100	91,282
20	17	3	White	500	197	1	100	91,282

4.3.4 Effect of Light Colour (Green, Blue, Red) on EPS Production by *C. brevissima*

C. brevissima was cultivated in duplicates at a fixed airflow rate of 1 L min^{-1} and a fixed CO_2 flow rate of 55 mL min^{-1} for 7 days at 31°C with green, blue and red light tiles set at 240 mA, as specified in Table 4-8 (Exp. 3-3). Sampling was performed in the same manner as the previous experiments.

Table 4-8 Cultivation parameters for photobioreactor (PBR) experiments studying the effect of light colour (green, blue, red) on extracellular polymeric substances (EPS) production of *Calothrix brevissima* (Experiment 3-3).Growth conditions: 1 L Xanthella MicroPharos photobioreactors with 750 mL culture, 1 L min^{-1} airflow rate, 55 L min^{-1} carbon dioxide (CO_2) rate, 31 °C. Shown are CO_2 levels (ppm) combining the supplemented CO_2 and that from air.

PBR run #	**Run order**	**PBR #**	**Light colour**	**Light intensity**	**Light tile setting**	**Airflow rate**	**CO_2 flow rate**	**CO_2 level**
Unit	(-)	(-)	(-)	AU	mA	L min^{-1}	mL min^{-1}	ppm
21	19	1	Green	650	240	1	55	52,521
22	23	1	Green	650	240	1	55	52,521
23	21	3	Blue	650	240	1	55	52,521
24	25	3	Blue	650	240	1	55	52,521
25	22	4	Red	650	240	1	55	52,521
26	26	4	Red	650	240	1	55	52,521

4.3.5 Axenic PBR Experiment: Comparing CO_2 and Air Effects on *C. brevissima*

C. brevissima was run under axenic conditions in a modified setup (PBR run# 27-30, Table 4-6, Exp. 3-4). The setup can be seen in Figure 4-3*a*. A 750 mL Duran bottle (borosilicate glass) with a cylinder-shaped bubble diffuser was used as culture bottle (Figure 4-3*b*). A second Duran bottle (500 mL) was used as foam trap. The two bottles were fitted with 2-hose connector screw cap lids and connected with silicone tubing (5mm I.D x 6mm O.D). Each bottle was fitted with a filter (Polydisc™ AS, Whatman™ 0.2 µm, VWR) and autoclaved. Four of these bottle setups were prepared to run four axenic PBRs. The bottles were left in a drying cabinet until completely dry.



Figure 4-3 Modified PBR setup using Duran bottles for axenic experiment (Exp. 3-4).(a) Overview of modified PBR setup using a Duran bottle instead of the original Xanthella container. (b) Autoclaved Duran bottle for growth with foam trap. (c) Duran bottle with culture placed in Xanthella housing.

The sterile Duran bottles were wiped down with IPA, placed in a MSC and exposed to UV light for 5 min. The inoculum was prepared as described in the Appendix (section

12.10) and used to inoculate at OD_{750} of 0.5. The culture bottles were filled up to 375 mL with BG-11 containing 10mM HEPES buffer (pH 7.5). Contamination checks of the inoculum, empty bottles and samples were performed. The culture bottles were placed in the Xanthella MicroPharos housings (Figure 4-3*c*). The housings were filled with water and used as a heat bath. The thermometers were placed at the front of the bottles. The tubes from gas board 1 were split into two tubes each using a Y splitter, and one tube was placed into each PBR heat bath for mixing. Similarly, the two tubes from gas board 2 were split using another Y splitter, and one tube was connected to the filter of each culture bottle.

Table 4-9 Cultivation parameters for photobioreactor (PBR) experiments studying the effect of CO_2 versus air on dry cell weight and extracellular polymeric substances (EPS) production of *Calothrix brevissima* under axenic conditions (Experiment 3-4).Growth conditions: 1 L autoclaved Duran bottles with 375 mL culture in Xanthella housing, 31 °C, 0.5 L min^{-1} airflow rate, 31 °C. Shown are CO_2 levels (ppm) combining the supplemented CO_2 and that from air.

PBR run #	**Run order**	**PBR #**	**Light colour**	**Light intensity**	**Light tile setting**	**Airflow rate**	**CO_2 flow rate**	**CO_2 level**
Unit	(-)	(-)	(-)	µmol m^{-2} s^{-1}	mA	L min^{-1}	mL min^{-1}	ppm
27	27	1	White	500	197	1	0	410
28	28	2	White	500	197	1	0	410
29	29	3	White	500	197	1	55	52,521
30	30	4	White	500	197	1	55	52,521

The airflow rate on the gas board was set to 1 L min^{-1}, corresponding to a flow of 0.5 L min^{-1} per culture bottle. This was equivalent to a volume of air per volume of culture medium per minute (VVM) value of 1.33, corresponding to the value used for Exp. 3-1 to Exp. 3-4 (1 L min^{-1} per 0.75 L = 1.33 VVM). PBR 1 and PBR 2 were grown with air, whereas PBR 3 and PBR 4 were supplemented with 5.5% CO_2. A tube was connected to the vent filter of PBR 3 and 4 and taped to an extractor. The cultures were grown for 14 days as specified in Table 4-9. Samples were taken aseptically every 2-3 days. During sampling, the culture was mixed by shaking and pipetting. Samples were

processed for DCW and EPS analysis as described in section 4.1.3 and 4.1.4. After the day 7 sample, the CO_2 flow rate of PBRs 3 and 4 was set to zero.

4.4 Techno-Economic Assessment

4.4.1 Real-Life Facility Basis for PBR Design

For a screening level analysis of the techno-economics of a large-scale EPS production process, the tubular PBRs were modelled based on the pre-industrial plant from the Chemical Engineering Department of the University of Almería and Fundación Cajamar at PALMERILLAS Technology Demonstration Centre which consists of ten modules (3 m^3) of tubular PBRs for a total volume of 30 m^3. Each module consists of one bubble (airlift) column for mixing and degassing and one solar receiver for growth made of transparent plastic tubes (Figure 4-4*b*) [287, 288].

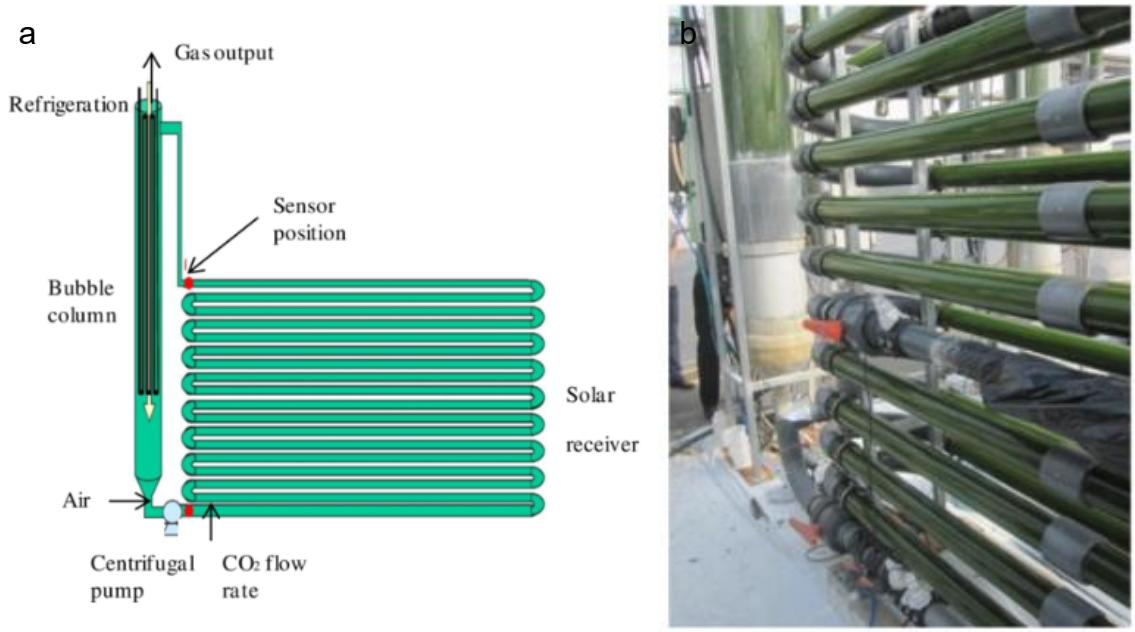


Figure 4-4 Schema and photo of a PBR module of the pre-industrial plant from the Chemical Engineering Department of the University of Almería [287].(a) Schema of one PBR module. (b) Photo of a PBR module.

At the bottom of the solar receiver, pure CO_2 is supplied on-demand for pH control. A centrifugal pump moves the culture upwards through the external loop (solar receiver) at a speed of 0.9 m s^{-1} [287]. When the culture flows downwards through the bubble column, oxygen accumulated from photosynthesis is stripped from the liquid by air being supplied at the bottom of the bubble column. The bubble column contains a heat exchange coil for temperature control. An optical sensor is located in the mixing unit to

determine the progress of the growth. In the external loop there are two dissolved oxygen sensors, three pH sensors and three temperature sensors: one at the beginning, one at the halfway point of the loop and one at the end point [287].

4.4.2 Baseline Scenario Process Design: Tubular PBR with Filtration

A industrial-scale EPS production process scenario was designed and modelled in SPD. The values were left at default unless mentioned otherwise. The process flow diagram, shown in Figure 4-5, contains five sections: cultivation, harvest, filtration, drying and storage. The process was run in semi-continuous mode. The PBRs themselves have to be operated in batch mode as cells produced most EPS in stationary phase (Exp. 2-9). However, due to the modular nature of PBRs, allowing staggered inoculation and harvesting, semi-continuous operation of the DSP equipment (centrifuge and spray dryer) and some USP equipment (media and bleach tank) was assumed. The filtration systems were run in batch mode to schedule filtration, backwashing and cleaning-in-place (CIP). The USP process and DSP are described in more detail in the following sections.

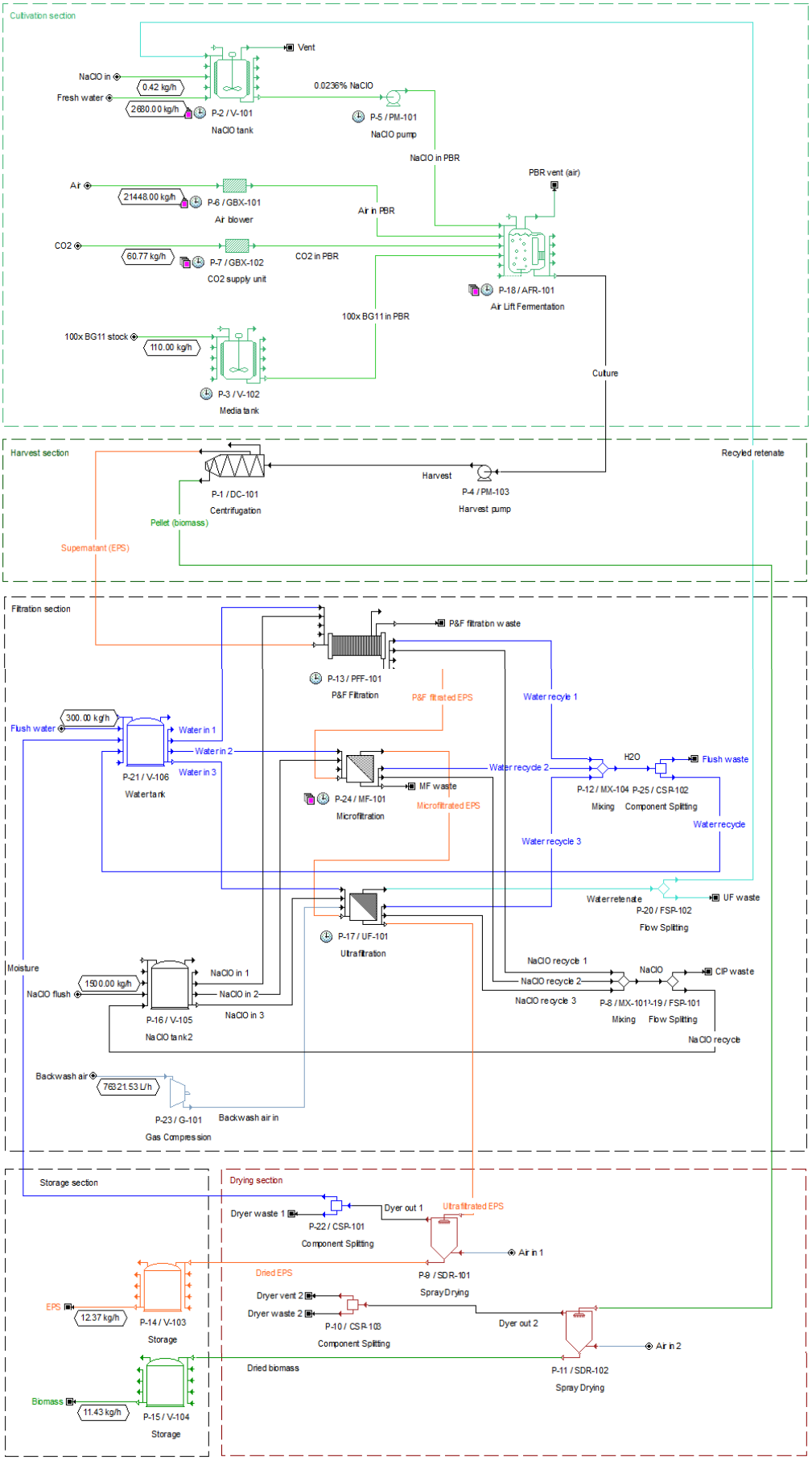

Cultivation section
Vent
NaClO in
0.42 kg/h
Fresh water
2680.00 kg/h
P-2 / V-101
NaClO tank
0.0236% NaClO
P-5 / PM-101
NaClO pump
NaClO in PBR
PBR vent (air)
Air
21448.00 kg/h
P-6 / GBX-101
Air blower
Air in PBR
CO2
60.77 kg/h
P-7 / GBX-102
CO2 supply unit
CO2 in PBR
P-18 / AFR-101
Air Lift Fermentation
100x BG11 in PBR
100x BG11 stock
110.00 kg/h
P-3 / V-102
Media tank
Culture
Harvest section
Recyled retenate
P-1 / DC-101
Centrifugation
Harvest
P-4 / PM-103
Harvest pump
Pellet (biomass)
Supernatant (EPS)
Filtration section
P&F filtration waste
P-13 / PFF-101
P&F Filtration
P&F filtrated EPS
Water recyle 1
300.00 kg/h
Flush water
Water in 1
Water in 2
Water in 3
P-21 / V-106
Watertank
H2O
Flush waste
Water recycle 2
P-12 / MX-104
Mixing
P-25 / CSR-102
Component Splitting
MF waste
P-24 / MF-101
Microfiltration
Microfiltrated EPS
Water recycle
Water recycle 3
Water retenate
UF waste
P-20 / FSP-102
Flow Splitting
P-17 / UF-101
Ultrafiltration
Moisture
NaClO recycle 1
NaClO
CIP waste
150.00 kg/h
NaClO flush
NaClO in 1
NaClO in 2
NaClO in 3
NaClO recycle 2
NaClO recycle 3
P-8 / MX-101
P-19 / FSP-101
Mixing
Flow Splitting
P-16 / V-105
NaClO tank2
NaClO recycle
Backwash air
76321.53 L/h
P-23 / G-101
Gas Compression
Backwash air in
Storage section
Drying section
Dryer waste 1
P-22 / CSR-101
Component Splitting
Dyer out 1
Ultrafiltrated EPS
Air in 1
P-9 / SDR-101
Spray Drying
Dried EPS
Dryer vent 2
Dryer waste 2
P-10 / CSR-103
Component Splitting
Dyer out 2
Air in 2
EPS
12.37 kg/h
P-14 / V-103
Storage
Dried biomass
P-11 / SDR-102
Spray Drying
Biomass
11.43 kg/h
P-15 / V-104
Storage

Figure 4-5 Process flow diagram of baseline scenario for extracellular polymeric substances production of *C. brevissima* modelled in SuperPro Designer®, using tubular photobioreactors as upstream, and filtration and spray drying as downstream processing.

4.4.2.1 Upstream Process Design in SPD

The USP of the EPS production process comprised of PBRs, air blowers, CO_2 supply units, sodium hypochlorite (NaClO) tanks and BG-11 medium tanks. The dimensions and features of the modular PBR system were based on the facility in Almería. It was assumed that sensors, centrifugal pump, bubble column and solar receiver were part of the purchase of one PBR module. A higher number of PBR modules (1,100 units) was used for a scale of 3300 m^3 culture, which was in the range of literature values of 30 m^3 to 122,000 m^3 [204, 259]. As will be described in section 6.10.2, EPS production was highly dependent on culture conditions, with the highest EPS concentration under phototrophic conditions (1.26 g L^{-1}) observed at 31°C and constant light at 300 µmol m^{-2} s^{-1} (Exp. 2-8). Therefore, the PBRs were designed for indoor operation with artificial lighting to allow control of temperature and light at these levels. It was assumed that LED light tiles were constructed vertically on each side of the solar receiver. Based on the dimensions of the solar receiver, two light tiles of 2.2 m height and 19 m length per module were required. Purchase costs of light tiles were estimated as 170 USD m^{-2} illuminated surface [170]. Since SPD did not feature a PBR as unit operation, an air-lift fermenter was used to model the PBR due to the similarity with the bubble column. Dimensions were changed to match the footprint of the PBRs defined in section 4.4.1, to accurately account for land use. It was assumed that 10% of the PBRs were used for the seed train to prepare the inoculum [250]. This was taken into account in the mass balance, as will be outlined later (Equation 4-20). Electricity consumption associated with LED lights and culture circulation was added as power consumption to the PBRs to match the calculated annual amount shown in Table 4-11. Similarly, the amount of heating and cooling water was added as auxiliary utilities.

Table 4-10 Specifications of a single tubular photobioreactor module from the pre-industrial plant of the Chemical Engineering Department, University of Almería.This module forms the basis of the techno-economic assessment of industrial-scale extracellular polymeric substance production using cyanobacteria.

PBR specifications	**Amount**	**Unit**	**Source**
Bubble column height	3.5	m	[287]
Bubble column diameter	0.4	m	[287]
Solar receiver length	400	m	[287]
Solar receiver diameter	0.09	m	[287]
Footprint	20	m^2	[289]
Volume	3	m^3	[287]
Light tiles	84	m^2	Calculated
LED area to volume ratio	28	$m^2\ m^{-3}$	Calculated

As shown in Figure 4-5, first sodium hypochlorite (NaClO) and water were mixed in the NaClO tank and pumped into the PBRs. The concentration of 0.0236% was based on the laboratory sterilisation protocol (Appendix section 12.10). Sterilisation was scheduled for 24 hours with aeration. It was assumed that NaClO fully de-chlorinated in the given timeframe. BG-11 medium was prepared as 10-fold concentrated stock in the medium tank and pumped into the PBRs. The BG-11 stock was allowed to disperse evenly with the aid of aeration and centrifugal pumping for an hour. The culture was cultivated at 31°C and 300 µmol $m^{-2}\ s^{-1}$ for 10 days according to Exp. 2-9.

Table 4-11 Economic parameters for utilities for non-standard equipment in SuperPro Designer® simulations of industrial-scale extracellular polymeric substance production using cyanobacteria.

Equipment	Amount	Unit	Source
PBR lights	95,300,000	kWh y^{-1}	Calculated based on Kratky, et al. [170]
PBR circulation pump	2,450,000	kWh y^{-1}	Calculated based on Dormido, et al. [287]
PBR hot water	2,850,000	MT y^{-1}	Calculated based on Acién, et al. [259]
PBR cooling water	266,000	MT y^{-1}	Calculated based on Acién, et al. [259]
Air blower	0.01	kW kg^{-1} h^{-1}	[259]
CO_2 supply unit	0.5	kW kg^{-1} h^{-1}	[259]

CO_2 and air were supplied to the PBRs using CO_2 supply units and air blowers. The airflow rate was assumed to be 0.11 VVM (volume of air sparged per unit volume of growth medium per minute) based on Acién, et al. [259]. CO_2 flowrate was based on the mass balance, which will be described later (Equation 4-20). Raw materials such as CO_2 and their respective prices are shown in Table 4-18. The CO_2 supply unit and air blower were modelled with the unit procedure 'Pass Through Generic Box'. Power consumption, sizing and purchase costs of Pass Through Generic Boxes were based on throughput (kg h^{-1}), matching the units of specification of air blower and CO_2 supply unit in literature [259]. This made Pass Through Generic Boxes preferable to other equipment like compressors, which were modelled based on their power (W). Table 4-11 shows the power consumptions of the CO_2 supply unit and the air blower, which were based on literature [259]. Utility calculations will be elaborated later (section 0).

4.4.2.2 Downstream Process Design

The DSP equipment comprised of centrifugation, filtration, drying and storage. At the end of the growth duration, biomass was separated from the EPS-containing supernatant by centrifugation with a solid stream concentration of 200 g L^{-1}. A series

of filtrations was utilised to purify the EPS. The filtration system was designed based on a pilot-scale study isolating bioactive microalgal EPS using tangential-flow UF [207]. Economic input parameters were based on two other studies, TEAs of microalgal harvesting using UF and microfiltration (MF) [231, 238]. First, the cell-free supernatant was plate-and-frame filtrated (P&F) to remove residual cells and cellular debris. Subsequently, MF was performed using a MF membrane [231]. The specifications of the membranes and process parameters are shown in Table 4-12. Lastly, the EPS were concentrated using ultrafiltration [207]. Membrane backwashing and CIP were incorporated to prevent clogging and biofouling, introducing downtime for cleaning and backwashing. For every 24 hours of operation, filtration occurred for 19.7 hours, backwashing for 1.3 hours, and CIP for 3 hours [238]. Backwashing was designed using water and compressed air [238]. As backwashing is not a feature in SPD, it was modelled as forward flushing; this is assumed not to affect costs, as only the flow direction was changed while all other factors (pumps, energy, water, chemicals, and associated operational requirements) were accounted for. CIP was designed using sodium hypochlorite (NaClO), including one hour of flushing and two hours of soaking [238]. The ratios of filtrate volume, CIP solution, air, and water were 1:1:3:0.2, respectively [238]. The flushing and CIP procedures were also added to the P&F and MF. The flush water and NaClO solutions are stored in two separate tanks and circulated between the three systems, assuming 5% waste of each stream. The filtrate from the UF system was sent to the NaClO tank in the cultivation section, to be reused for sterilisation and cultivation of the PBRs (assuming 5% waste).

Table 4-12 Design parameters of microfiltration (MF) and ultrafiltration (UF) system for extracellular polymeric substances (EPS) downstream processing including pore size, membrane cost and lifetime.

Item	Amount	Unit	Source
MF membrane size	0.45	µm	[290]
MF membrane cost	129	USD m^{-2}	[231]
MF membrane lifetime	3	years	[231]
UF molecular weight cutoff	5000	Da	[207]
UF Average flux	44.1	L m^{-2} h^{-1}	[238]
UF volumetric reduction factor	50	(-)	[238]
UF membrane price	60	USD m^{-2}	[238]
UF membrane lifetime	5	years	[238]
Backwashing pressure	175	kPa	[238]
Compressor efficiency	90	%	[238]
NaClO concentration	0.4	g L^{-1}	[238]

The filtrated EPS were spray dried. The moisture content of the EPS after spray drying was set to 5% [251]. The wastewater from the EPS drying was recycled as flush water for the membrane system (5% waste assumed). Due to the high temperature of water exiting the spray dryer (70°C), the flush water storage tank was set to cool its content to 45°C with cooling water to avoid damage to the membranes. Subsequently, the solid stream containing the biomass was spray dried using the same spray dryer. A small fraction (0.4%) of the EPS was assumed to be lost in the solid stream with the biomass. The water fraction from the spray drying of the biomass was discarded. It was assumed that the same spray dryer was used consecutively for EPS and biomass. However, since it was not possible to share equipment in semi-continuous mode, the purchase cost of the biomass spray dryer was set to zero to model consecutive use. The dried EPS and DCW were stored in storage tanks.

The EPS stream was classified as main product stream, and the biomass stream was classified as an additional revenue stream. Waste streams were classified as such. The waste products and their respective treatment/disposal costs are shown in Table 4-18.

4.4.3 Calculation Methodology

TCI, OpEx and revenues of the process were estimated using SPD. TCI include major equipment costs (MEC), as well as costs associated with installation, construction etc., which are defined Table 4-18. OpEx are costs associated with operating the facility, including raw materials costs, consumables costs, waste treatment/disposal costs, labour-dependent costs and facility-dependent costs. Facility-dependent costs are a percentage of the TCI to account for costs associated with equipment maintenance, depreciation, insurance, local (property) taxes and factory expenses [291]. Factory expenses are the overhead costs associated with the operation of non-production facilities and services, including functions like accounting, payroll, fire protection, security and cafeteria services [291]. Local (property) taxes and insurance costs were set at 1% and 0.6% of TCI, respectively [251]. Factory expenses were estimated as 2% of TCI, based on a microalgal production process in literature [251]. Equipment maintenance cost was estimated as 4% of equipment purchase cost, as defined in Table 4-18 [251].

4.4.3.1 Photobioreactor Mass Balance calculation

The mass balance for the PBR of the baseline scenario can be found in Equation 4-19. The mass balance was based on 1 litre BG-11 growth medium with an assumed density of 1 kg L^{-1}. The concentrations of EPS (1.26 g L^{-1}) and biomass (1.08 g L^{-1}) were taken from Exp. 2-9 (day 10). The CO_2 demand was calculated based on the experimentally obtained substrate yield coefficient of 2.3 kg CO_2 kg^{-1} biomass [259]. This substrate yield coefficient was assumed for both, biomass and EPS. Produced oxygen was based on the theoretical O_2 evolution rate (0.73 kg O_2 kg^{-1} CO_2) obtained from the basic stoichiometric photosynthesis equation. The product side was balanced with water. Evaporation was omitted as it is negligible in closed systems [292].

$$1000g\ BG11 + 5.4\ g\ CO_2 \rightarrow 1.3\ g\ EPS + 1.1\ g\ biomass + 4.0\ g\ O_2 + 999.1\ g\ H_2O$$

Equation 4-19

The mass balance was adapted to account for biomass produced for the seed train. Adding the seed train as separate unit procedures was not possible because the version of SPD was limited to 25 unit procedures. Ten percent of the culture grown in the PBR was assumed to be used as seed train to produce inoculum [259]. It was assumed that the seed train influences the sizing of USP equipment, which affects TCI and OpEx of the overall process. However, the seed train was assumed to not transition into the DSP, meaning it does not generate revenue or affect sizing of DSP equipment. To account for this, the products (growth medium and CO_2) were increased by 10% to account for material costs and USP equipment sizing. On the reactants side, to remove 10% of the products, they were modelled as nitrogen which vents out of the PBR, to prevent them from affecting DSP costs and revenues. This method attempts to accurately account for costs associated with producing the seed train in the USP, without affecting revenues or costs of the DSP. The modified mass balance is shown below (Equation 4-20):

$$1100g\ BG11 + 5.96\ g\ CO_2$$
$$\rightarrow 1.26\ g\ EPS + 1.08\ g\ DCW + 4.33\ g\ O_2 + 989.36\ g\ H_2O + 109.93\ g\ N_2$$

Equation 4-20

4.4.3.2 Upstream Major Equipment Cost calculation

The 'Power law cost estimation' formula of SPD was used to calculate equipment cost Equation 4-21 below [291]:

$$Cost = C_0 \times \frac{Q}{Q_0}^{a}$$

Equation 4-21

Where:

- C_0 is the Base Cost,
- Q is the capacity,
- Q_0 is the Base Capacity,
- a is the scaling factor.

In Table 4-13, these values can be found for the PBR, lights, air blower and CO_2 supply unit, as those were not standard equipment in SPD. A scaling factor (a) of 1 was assumed due to the modular nature of the PBR and gas systems.

Table 4-13 Economic cost parameters (base cost (C_o) and base capacity (Q_o)) for non-standard equipment used in SuperPro Designer® simulations, including photobioreactor (PBR), lights, air blower and carbon dioxide (CO_2) supply unit cost.Scaling factor is assumed to be 1 due to the modular nature of PBRs and auxiliary equipment.

Equipment	**Base Cost (C_o)**	**Unit**	**Base Capacity (Q_o)**	**Unit**	**Source**
PBR	16,000	USD	3	m^3	[259]
PBR lights	14,000	USD	3	m^3	Calculated based on Kratky, et al. [170]
Air blower	2,500	USD	250	kg h^{-1}	[259]
CO_2 supply unit	500	USD	4	kg h^{-1}	[259]

4.4.3.3 Upstream Utilities calculation

Utility consumption of the PBRs was calculated in Excel and added to the airlift fermenter in SPD. Costs included electricity for LED lighting and the circulation pump, and water for heating and cooling. The following paragraphs detail each aspect.

4.4.3.3.1 Electricity Consumption of LED lights Calculation

The annual electricity demand (kWh $year^{-1}$) of the LED lights was calculated according to the formula below. The electricity price is given in Table 4-18.

$$E_{LED} = \frac{I_{LED} \times A_{LED} \times t}{\eta_{LED}} : 1000$$

Equation 4-22

Where:

- E_{LED} is the electricity consumption of the LED lights (kWh year^{-1}),
- I_{LED} is the intensity of the LED lights = 65 W m^{-2}, converted from µmol m^{-2} s^{-1} using the conversion factor of 0.218 [170],
- A_{LED} is the area of the LED lights = 84 m^2 (calculated),
- t is the operating time = 7920 hours year^{-1},
- η_{LED} is the efficiency of the LED lights = 50% [293].

4.4.3.3.2 Circulation Pump Power Calculation

The power (W) required for the circulation pump was calculated based on the formula below [294]. The power of the pump was multiplied by the number of modules and annual operating hours and divided by 1000 to obtain the annual electricity for culture circulation (kWh y^{-1}), which is shown in Table 4-11.

$$P_{Pump} = \frac{\rho \times g \times Q_{pump} \times h}{\eta}$$

Equation 4-23

Where:

- P_{Pump} is the power of the pump (W)
- ρ is the density of the fluid (kg m^{-3}), assumed 1,
- g is the gravitational constant = 9.8 m s^{-2},
- Q is the flowrate of the pump (m^3 s^{-1}),
- h is the head of the pump = 3.5 m [287],
- η is the efficiency of the pump, assumed to be the SPD of 70% [291].

The flowrate of the pump Q was calculated according to the following formula:

$$Q = \pi \times \left(\frac{d}{2}\right)^2 \times v$$

Equation 4-24

Where:

- d is the diameter of the PBR tube = 0.09 m [287],
- v is the circulation velocity = 0.9 m s^{-1} [287].

4.4.3.3.3 Amount of Heating and Cooling Water Calculation

The heating/cooling requirement of the PBR was calculated as following. Based on the monthly average temperatures in Almería, Spain, which are shown in Table 4-14, the heating/cooling requirements for the PBRs were calculated considering heat gain from LED lights and heat loss via convection of the PBR surface. Metabolic heat generation and heat loss via evaporation was omitted due to the use of a closed system [292]. A recent study provided detailed temperature control calculations in the supplementary materials [250]. In this PhD thesis, the formula was simplified to Equation 4-25.

$$\dot{Q} = \dot{Q}_{gain} - \dot{Q}_{loss} = I_{LED} \times (1 - \eta_{LED}) \times \alpha \times \tau \times A_{SR} - U_{PBR} \times A_{PBR} \times (T_{desired} - T_{ambient})$$

Equation 4-25

Where:

- $\dot{Q}$ is the amount of heating or cooling needed (W),
- $\dot{Q}_{gain}$ is the amount of energy gained from the LED lights (W),
- $\dot{Q}_{loss}$ is the amount of energy lost via convection (W)
- α is the absorbance of the culture = 0.9 [250],
- τ is the transmissivity of the PBR tubes = 0.9 [250],
- A_{SR} is the area of the solar receiver = 113 m^2, calculated based on [287],
- U_{PBR} is the U-value of the PBR (W m^{-2} °C^{-1}) = 3.83 [295],
- A_{PBR} is the area of the PBR in contact with the surrounding air (solar receiver and bubble column) = 118 m^2, calculated based on [287],
- $T_{desired}$ is the cultivation temperature = 31°C (this study),
- $T_{ambient}$ is the ambient temperature in Almería, Spain = variable (Table 4-14).

The mean, minimum and maximum temperatures for Almería, Spain can be found in Table 4-14. The monthly mean temperatures were used for $T_{ambient}$. The heating/cooling requirement was calculated for each month. The sum of all 12 heating/cooling requirements were used for the annual heating/cooling requirement. For simplification, daily and within-month temperature differences were not considered in this PhD thesis.

Table 4-14 Mean ($\bar{T}$), minimum (T_{min}), and maximum (T_{max}) monthly temperatures (°C) in Almería, Spain in the year 2020 [296]

Month	**J**	**F**	**M**	**A**	**M**	**J**	**J**	**A**	**S**	**O**	**N**	**D**
T_{min} (°C)	5.0	5.6	7.5	10.3	13.9	17.8	20.8	20.7	17.2	13.6	8.8	6.1
T_{max} (°C)	13.8	14.2	16.8	19.3	23.4	27.7	31.0	30.5	26.2	22.2	17.0	14.4
$\bar{T}$ (°C)	8.8	12.4	12.6	14.3	20	23.1	26.7	26	22	16.4	13.4	9.4

According to Bergman [297], the obtained heating/cooling requirement (kW) for each month was converted into kg h^{-1} of heating or cooling water based on the specific heat formula (Equation 4-26):

$$\dot{m} = \frac{Q}{C \times \Delta T}$$

Equation 4-26

Where:

- $\dot{m}$ is the kg h^{-1} flow of the heating or cooling water,
- Q is the heating or cooling requirement (kJ h^{-1}), obtained by multiplying $\dot{Q}$ (W) with 3.6,
- C the specific heat capacity of water = 4.186 kJ kg^{-1} $°C^{-1}$,
- ΔT the difference in inlet and outlet temperature of the heating/cooling water (Table 4-15).

Table 4-15 Inlet temperature (T_{inlet}), outlet temperature (T_{outlet}), temperature difference (ΔT), and price of heat transfer agents used in photobioreactor (PBR) simulations for techno-economic assessment.

Heat transfer agent	**T_{inlet}** °C	**T_{outlet}** °C	**ΔT** °C	**Price** USD MT^{-1}	**Source**
Hot water	40	30	10	0.05	[291]
Cooling water	25	30	5	0.05	[291]

4.4.3.4 Labour Costs calculation

In literature, the number of operators varies greatly with values ranging from one operator per 25 ha to 8 operators per one hectare [251, 298]. Based on PBR volumes per hectare of 5000 m^3 and 380 m^3, respectively, this corresponds to one operator per 5000 m^3 and 48 m^3, respectively [251, 298]. For this study, it was assumed that a minimum of two operators must always be present for culture volumes up to 3000 m^3, after which one additional operator was required per 1500 m^3 of culture volume. The salary of the operators was left at the default value (69 USD h^{-1}). SPD by default assumed labour costs for operation, as well as an additional 15% of labour for laboratory, Quality Control (QC) and Quality Assurance (QA) [291].

4.4.3.5 Minimum Selling Price (MSP) and Cash Flow Calculations

The Minimum Selling Price (MSP) was defined as the selling price (SP) in USD kg^{-1} required to achieve a non-negative Net Present Value (NPV) at the end of the project life. The MSP value was rounded to zero digits. NPV was determined from summing up the Discounted Cash Flow (DCF) over the project lifetime using the following formula [291]:

$$NPV = \sum_{t=1}^{N} DCF = \sum_{t=1}^{N} \frac{NCF}{(1+i)^t}$$

Equation 4-27

Where:

- NPV is net present value (USD),
- DSF is the Discounted Cash Flow,
- NCF is the Net Cash Flow,
- *N* is the project life, set to 15 years [251, 291],
- *i* is the interest rate, set at 8% [251, 291],
- *t* is the year.

The NCF for each year (*t*) was calculated as: [291]

$$NCF_t = Net\ profit_t - CapEx_t$$

Equation 4-28

Capital expenses (CapEx) were calculated as a percentage of the TCI according to the formula below, which was a simplification of the formula provided in the SPD manual [291]:

$$CapEx_t = (1 - f_s) \times f_{c,t} \times TCI$$

Equation 4-29

Where:

- $CapEx_t$ is the CapEx of year t,
- t = year; $1 \leq t \leq N$,
- f_s = 5% is the salvage value factor,
- $f_{c,1} = f_{c,3}$ = 30% (for years 1 and 3),
- $f_{c.2}$ = 40% (for year 2) is the capital expenses fraction,
- TCI = Total Capital Investment.

Net profit for year t was determined as following: [291]

$$Net\ Profit_t = Gross\ profit_t - Taxes_t + Depreciation_t$$

Equation 4-30

Taxes were calculated as 40% of gross profit, but only applied if the gross profit was positive:

$$Taxes_t = 40\% \times Gross\ Profit_t\ ;\ if\ Gross\ Profit_t > 0$$

Equation 4-31

Depreciation is a tax deduction that accounts for the loss in value of fixed capital, primarily caused by equipment wear and obsolescence. It was calculated as a fraction of the TCI for years 3 to 12: [291]

$$Depreciation_t = \frac{TCI}{10}\ ;\ for\ 3 < t < 12$$

Equation 4-32

Gross profit was calculated as revenues minus operational expenditures (OpEx): [291]

$$Gross\ Profit_t = Revenues_t - OpEx_t$$

Equation 4-33

Revenues were derived from the sales of biomass and EPS according to the formula below:

$$Revenues_t = AP_{biomass,t} \times SP_{biomass} + AP_{EPS,t} \times SP_{EPS}$$

Equation 4-34

Where:

- $SP_{biomass}$ is the selling price of biomass = 56 USD kg^{-1} [299],
- SP_{EPS} is the selling price of EPS (USD kg^{-1}) = variable,
- $AP_{biomass,t}$ is the annual biomass production of year t (kg $year^{-1}$) = variable; taken from the Cash Flow Analysis (CFA) Report of SPD,
- $AP_{EPS,t}$ is the annual EPS production of year t (kg $year^{-1}$) = variable; taken from the CFA Report of SPD.

$OpEx_t$ and annual production of biomass and EPS were taken from the CFA Report from SPD. In short, no OpEx were assumed during the startup time of the process (30 months), which resulted in absence of OpEx in year 1 and 2 and lower OpEx in year 3 than in year 4 to 15. Additionally, SPD assumes depreciation as cost added to OpEx, which is later subtracted according to Equation 4-30. As depreciation only applies to

year 3 to 12, as described earlier, OpEx were lower for year 12 to 15. Similarly, there was no biomass and EPS production assumed during the startup time.

The MSP of EPS (MSP_{EPS}) was defined as the selling price of EPS when the NPV is greater than or equal to zero:

$$MSP_{EPS} = SP_{EPS};\ when\ NPV \geq 0$$

Equation 4-35

4.4.3.6 Contributing factors to MSP calculation

To illustrate the contribution of OpEx, CapEx, tax and interest to the MSP in figures, the fraction of each cost was calculated. The fraction of OpEx (f_{OpEx}), contributing to MSP was calculated according to the formula below. The fractions of CapEx (f_{CapEx}), tax (f_{tax}) and interest ($f_{interest}$) were calculated in the same manner.

$$f_{OpEx} = \frac{\sum_{t=1}^{N} OpEx_t}{\sum_{t=1}^{N} OpEx_t + \sum_{t=1}^{N} CapEx_t + \sum_{t=1}^{N} tax_t + \sum_{t=1}^{N} interest_t} * MSP$$

Equation 4-36

The fractions of each type of OpEx cost were calculated in a similar manner. For example, the fraction of labour cost (f_{labour}), was calculated as shown below. The fractions of facility-dependent cost ($f_{facility}$), raw materials ($f_{materials}$), utilities ($f_{utilities}$), consumables ($f_{consumables}$) and waste disposal cost (f_{waste}) were calculated in the same way.

$$f_{labour} = \frac{\sum_{t=1}^{N} Labour\ cost_t}{\sum_{t=1}^{N} OpEx_t} \times f_{OpEx}$$

Equation 4-37

4.4.3.7 Profitability analysis

Profitability analysis was performed by calculating the Profitability Index (PI) according to Equation 4-38 [300]. For profitability analysis, the selling price of EPS was fixed at 73 USD kg^{-1} [301]. NPV was calculated as described in the previous section.

$$PI = 1 + \frac{NPV}{CapEx}$$

Equation 4-38

4.4.3.8 Price Adjustments Based on Reference Year

Prices (e.g. raw materials, disposal, wastewater treatment etc.) from sources from previous years were adjusted to 2024 according to the Harmonization of Consumer Index Prices (HCIP) [302] using the following formula according to Vázquez-Romero, et al. [251]:

$$Price_{2024} = \frac{HCIP_{2024}}{HCIP_{reference\ year}} \times Price_{reference\ year}$$

Equation 4-39

4.4.4 Scenario Analysis

Scenario analysis was used to determine the effect of different scales, operation modes, DSP equipment, cultivation systems, growth mode, cyanobacterial species and type of product on the MSP. Twenty-one different scenarios were designed. An overview of the relationships between the different scenarios is shown in Figure 4-6. The detailed design descriptions will be elaborated in the following sections.

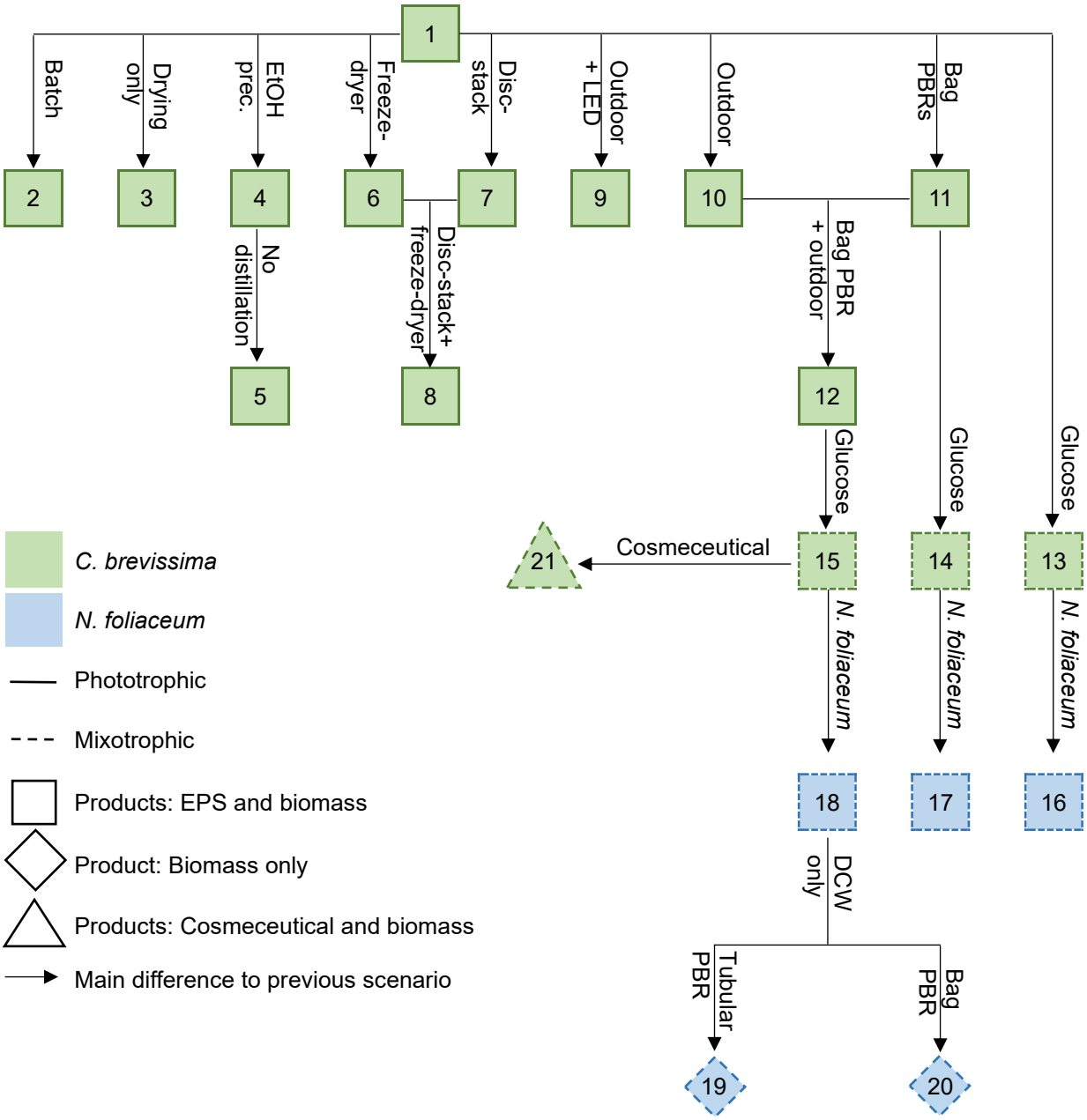


Figure 4-6 Overview of relationships between scenarios for techno-economic assessment of an industrial extracellular polymeric substances (EPS) and biomass production process using cyanobacteria.The numbers represent scenarios 1 to 21.Key differences between scenarios are displayed as text on arrows. Details such as trophic mode, type(s) of product(s), cyanobacterial species, are indicated by shape, colour and line style (see legend).

4.4.4.1 Effect of Batch vs. Semi-Continuous on MSP

The effect of batch vs. semi-continuous mode was investigated. As mentioned in section 4.4.2, the baseline scenario (scenario 1) was designed in semi-continuous mode, with PBRs running in batch mode and DSP equipment running in semi-

continuous mode. In scenario 2, the entire plant (USP and DSP) was operated in batch mode by switching the operation mode in SPD.

4.4.4.2 Effect of Downstream Processing on MSP

To study the effect of different DSP types on MSP, scenario 1 was compared to two other EPS purification scenarios: spray drying without any EPS purification (scenario 3) and ethanol precipitation as purification step (scenario 4 and scenario 5). In scenario 3, supernatant and pellet were sent directly to the spray dryer, omitting the filtration steps. After drying, the vapour from the supernatant was recycled back to the PBR (Figure 4-7).

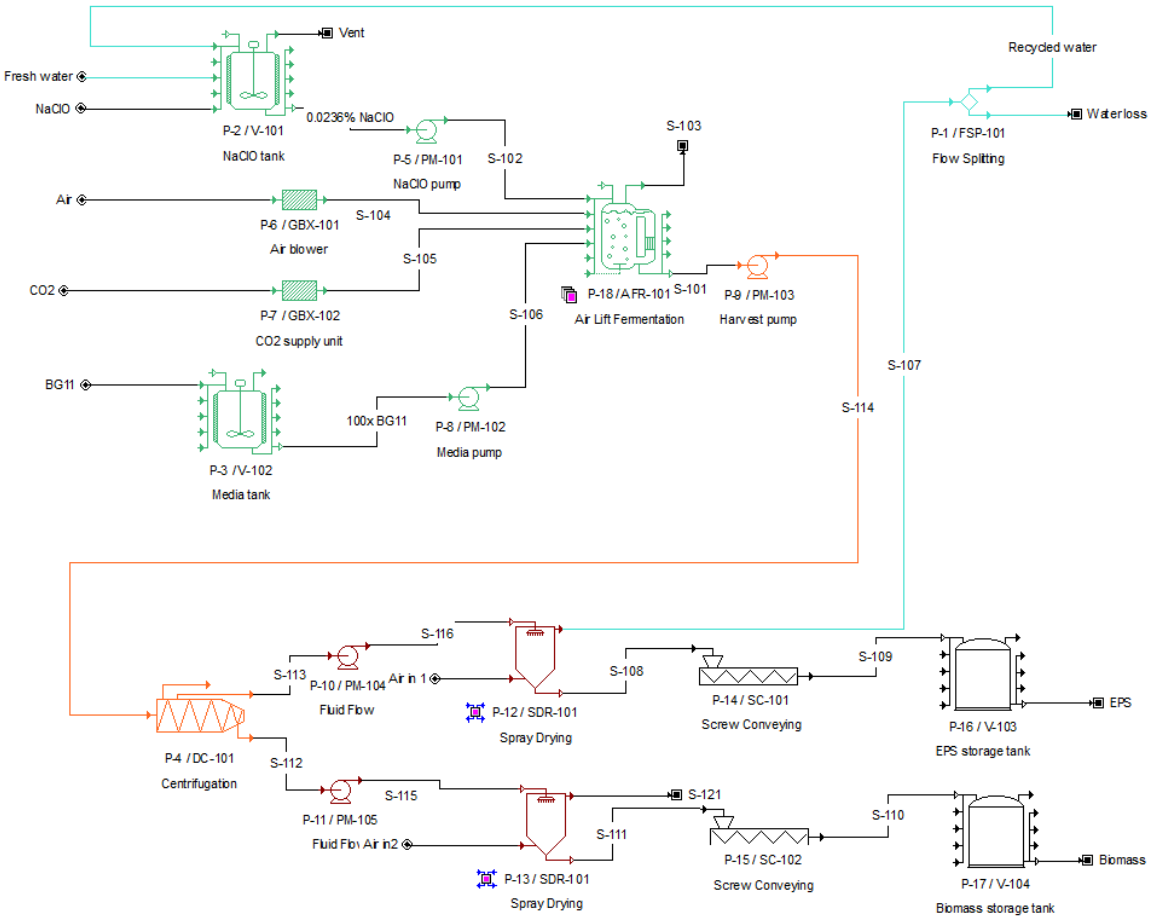


Figure 4-7 Process flow diagram of scenario 3 for extracellular polymeric substances production of *C. brevissima* modelled in SuperPro Designer®, using tubular photobioreactors as upstream, and spray drying as downstream processing.

Scenario 4 (ethanol precipitation with solvent recycling) included purification of EPS using ethanol precipitation instead of filtration (Figure 4-8). In a mixer-settler extraction, ethanol was added to the cell-free supernatant at a ratio of 2:1 (volume ethanol:volume supernatant) and mixed for 10 minutes [303]. Subsequently, the mixture was allowed to settle for 12 hours at 8°C, and the supernatant was transferred to the distillation column to separate ethanol from the spent medium. The ethanol fraction was cooled to 25°C using a heat exchanger and sent to a storage tank for solvent recycling, assuming 5% ethanol waste. The water fraction was recycled back to the PBR (assuming 5% waste). The pellet containing the precipitated EPS was spray-dried and stored in a storage tank. In scenario 5 (ethanol precipitation without solvent recycling), the ethanol-water mixture was discarded instead of being recycled, omitting the distillation and ethanol storage steps.

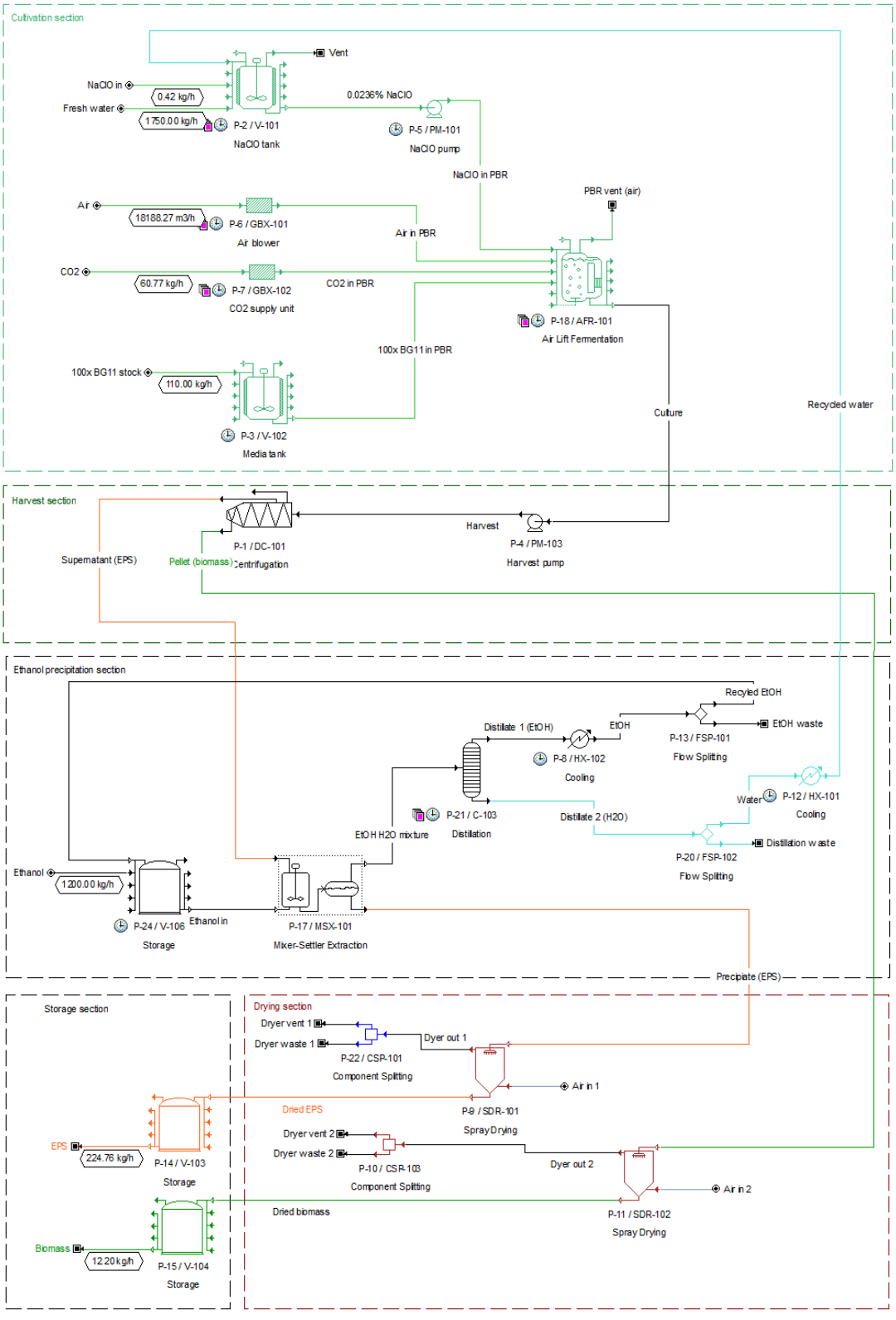


Figure 4-8 Process flow diagram of scenario 4 for extracellular polymeric substances production of *C. brevissima* modelled in SuperPro Designer®, using tubular photobioreactors as upstream, and ethanol precipitation with distillation for ethanol recycling and spray drying as downstream processing.

Different DSP variations of the baseline scenario were tested. Firstly, the effect of using a freeze dryer instead of a spray dryer was tested (scenario 6). Moisture content after spray drying and freeze drying was set to be 5.0% and 1.5%, respectively [251]. Additionally, the effect of using a disc-stack centrifuge instead of decanter centrifuge was tested (scenario 7). Lastly, the effect of both, a disc-stack centrifuge and a freeze dryer, was investigated (scenario 8).

4.4.4.3 Effect of Cultivation Systems on MSP

The effect of different cultivation systems on MSP was investigated. Four different USP variations of the baseline scenario were designed. Firstly, the PBR was designed outdoors with artificial LED lighting (scenario 9). The solar irradiation data of Almería, Spain was utilised to adjust the lighting and heating/cooling requirement under outdoor conditions. The solar irradiation data was converted to different units as shown in the following formulas.

$$I_{sun,PAR} = a \times I_{sun,\mu E}$$

Equation 4-40

Where:

- $I_{sun,PAR}$ = Solar irradiation (Unit: PAR) = variable (Table 4-16),
- $I_{sun,\mu E}$ = Solar irradiation (µmol m^{-2} s^{-1}) = variable (Table 4-16),
- a = conversion factor µmol m^{-2} s^{-1} into PAR ≈ 43% [304].

$$I_{sun,\mu E} = I_{kWh} \times \frac{b \times c}{L_m \times D_m \times 3600}$$

Equation 4-41

Where:

- $I_{sun,kWh\ m\text{-}2}$ = Solar irradiation (kWh m^{-2}) = variable (Table 4-16),
- b = conversion factor = 3.6 × 10^6 J kWh^{-1},
- L_m = daylight duration of the month (hours per month) = variable (Table 4-16),
- D_m = days per month = variable (Table 4-16),
- c = Conversion factor ≈ 4.6 µE W^{-1} m^2 [170].

As all PAR values were above the required 300 μmol m^{-2} s^{-1}, it was assumed that LED lighting was only needed during dark hours.

Table 4-16 Solar irradiance (kWh m^{-2}) and daylight (hours day^{-1}) in Almería, Spain, for modelling outdoor photobioreactor scenarios.

Month	**Daylight**	**Days per month**	**Solar irradiation**	**Solar irradiation**	**Solar irradiation**
Unit	h day^{-1}	(-)	kWh m^{-2}	μmol m^{-2} s^{-1}	PAR
Jan	14	31	86.4	1278	550
Feb	13	28	116.8	1739	748
Mar	12	31	135.1	1666	716
Apr	11	30	165.8	1950	839
May	10	31	227.0	2399	1032
Jun	9	30	239.4	2440	1049
Jul	10	31	237.6	2511	1080
Aug	11	31	212.7	2421	1041
Sep	11	30	160.1	1883	810
Oct	13	31	132.4	1781	766
Nov	14	30	88.7	1356	583
Dec	15	31	85.0	1397	601
Reference	[296]	Calculated	[296]	Calculated	Calculated

The heating/cooling requirement was re-calculated considering the heat gain from natural sunlight (in μmol m^{-2} s^{-1}) during day light hours, and from an artificial light flux of 300 μmol m^{-2} s^{-1} with 50% efficiency during dark hours. The utility costs of the PBR were adjusted to match electricity consumption of LEDs, heating water and cooling water of 55,600,000 kWh y^{-1}, 0 MT y^{-1} and 33,700,000 MT y^{-1}, respectively. The buildings cost for the USP was removed as the PBRs were designed outdoors.

Similarly, the scenario of outdoor cultivation using only natural light (scenario 10) was investigated. The PBR utilities were adjusted, now only considering heating/cooling based on the heat gain from natural sunlight. This resulted in 0 kWh y^{-1} needed for

LED lights, 0 MT y^{-1} hot water and 22,400,000 MT y^{-1} cooling water. The purchase cost of LED lights was removed as no LEDs were used in this scenario.

The use of a hanging plastic bag PBRs (scenario 11) instead of tubular PBRs (indoors) was investigated. The PBR bags (50 L) were treated as consumable with 5 years lifetime and a purchasing price of 10 USD per bag [209]. The bags were hung in a support structure, which cost 20 USD per bag [209]. To match the bag case scenario to the tubular case scenario, 74,000 bags were needed to accommodate culture and seed train. As the bags were reusable, it was assumed that the sterilisation protocol remained the same. The utility cost of the baseline scenario was assumed for scenario 11. Lastly, a combination of scenario 10 and 11 was designed: Scenario 12 was designed as outdoor cultivation in hanging bags. The utility cost from scenario 10 were assumed for scenario 12 due to outdoor cultivation with natural light.

4.4.4.4 Effect of Growth Mode (Photoautotrophic vs. Mixotrophic) on MSP

As will be explained in section 6.9, the highest EPS titre was achieved under mixotrophic conditions (glucose) in shake flasks (Exp. 2-6). Scenarios 13, 14 and 15 were based on the results and conditions of the mixotrophic experiment (Exp. 2-6). Mixotrophic scenario 13 was designed with indoor tubular PBRs with artificial lighting, based on scenario 1. Mixotrophic scenario 14 was designed with indoor bag PBRs with artificial lighting, based on scenario 11. Lastly, scenario 15 was designed as mixotrophic growth in bag PBRs in outdoor conditions (no artificial lighting) based on scenario 12. For all mixotrophic scenarios, the CO_2 supply unit was removed, since only aeration was used. Glucose was added to the BG-11 medium for a final concentration of 5 g L^{-1}. The cultivation time was adjusted to 14 days. The mass balance was adjusted based on the EPS and biomass titres obtained in experiment 2-6 as shown below:

$$1100 g\ BG11 + 5.50\ g\ glucose \rightarrow 2.65\ g\ EPS + 2.2\ g\ DCW + 990.58\ g\ H_2O + 110.06\ g\ N_2$$

Equation 4-42

According to the experimental conditions, the utilities of the PBR for scenarios 13 and 14 were adjusted by re-calculating power consumption of LEDs for 150 µmol m^{-2} s^{-1} and heating/cooling requirement for 28°C. This resulted in 47,600,000 kWh y^{-1} for lights, 2,950,000 MT y^{-1} hot water and 225,000 MT y^{-1} cooling water. Due to the lower

light intensity used, cheaper LEDs were used. The purchase costs were calculated at 3,000 USD m^{-3} culture based on the given values in literature for LED lights with maximum intensity of 250 µmol m^{-2} s^{-1} [250]. For scenario 15, no purchase cost and electricity costs were required for LED lights, no hot water but 24,600,000 MT y^{-1} cooling water were needed.

4.4.4.5 Alternative Cyanobacterial Species Scenario: N. foliaceum

The effect of using an alternative cyanobacterial species, *Nostoc foliaceum*, was investigated. The highest EPS titre of 0.70 g L^{-1} was obtained under 28°C, 4.8 g L^{-1} glucose and 164 µmol m^{-2} s^{-1} (Exp. 2-6, section 6.7). DCW production under these conditions was 4.41 g L^{-1}. Based on these conditions, PBR utilities were recalculated as 52,100,000 kWh y^{-1} for LED lighting, 2,850,000 MT y^{-1} hot water and 265,000 MT y^{-1} cooling water. Four different scenarios with *Nostoc foliaceum* were investigated. Scenario 16 was based on scenario 13, including cultivation in indoor tubular PBRs with two products, DCW and EPS, which were purified by filtration. In scenario 17, tubular PBRs were replaced with bag PBRs, similar to scenario 14. Scenario 18 included outdoor cultivation with natural light in bag PBRs, based on scenario 15. The resulting mass balance for scenarios 16, 17 and 18 was the following:

$$1100 g\ BG11 + 5.3\ g\ glucose \rightarrow 0.70\ g\ EPS + 4.4\ g\ DCW + 990.2\ g\ H_2O + 110.0\ g\ N_2$$

Equation 4-43

Additionally, scenarios 19 and 20 were designed to produce biomass as the sole product. These scenarios were based on scenario 18. In these two scenarios, the DSP consisted only of harvesting by centrifugation, recirculation of the supernatant into the PBR, and spray drying of biomass, which was then stored. The mass balance was adjusted to the following:

$$1100 g\ BG11 + 5.32\ g\ glucose \rightarrow 4.41\ g\ DCW + 990.82\ g\ H_2O + 110.09\ g\ N_2$$

Equation 4-44

The single-product (biomass) outdoor natural light scenario was once designed with tubular PBRs (scenario 19) and bag PBRs (scenario 20).

4.4.4.6 Alternative Product Scenario: Cosmeceutical Product

The effect of producing an alternative product was explored in scenario 21. This scenario was based on scenario 15, which consisted of outdoor cultivation in bag PBRs under mixotrophic conditions. The spray dryer was replaced with a freeze dryer and the EPS selling price was adjusted to 1,460 USD kg^{-1}.

4.4.5 Sensitivity Analysis

A sensitivity analysis was carried out to identify the key cost drivers in the techno-economic assessment by varying the purchase price of a PBR module (including lighting), electricity price, EPS titre, and production scale. For each parameter, five different input values based on typical ranges in literature were applied (Table 4-17). To test the effect of PBR (with lights) purchase cost, the price for one module (USD m^{-3}) was adapted according to PBR prices in literature and suppliers (Table 4-17). To study the effect of electricity price (USD kWh^{-1}), the cost was adapted to the range, in which the electricity price has varied in Spain over the last 5 years [305]. The electricity price was adjusted in the process options of SPD. When varying the EPS titre (kg L^{-1}), the mass balance of the PBR was re-calculated and CO_2 inflow stream were adapted according to section 4.4.3.1. When studying the effect of scale (PBR volume in m^3), two operators were added for scales of 30 – 3,000 m^3, whereas 26 and 90 operators were added for 38,000 m^3 and 122,000 m^3, respectively, based on the labour requirement defined in section 4.4.3.4. The simulations were run in SPD and the results were plotted in MS Excel.

Table 4-17 Input values and relative level to baseline scenario of parameters for sensitivity analysis in techno-economic assessment of extracellular polymeric substances (EPS) production using *Calothrix brevissima*.

Input #	Input value	Relative level	Reference
Price of one PBR module with lights (USD unit^{-1})			
1	0.345	0%	[204]
2	29,700	85%	[21]
3	30,500	87%	[250]
4	31,400	90%	Baseline scenario
5	34,900	100%	[306]
6	64,400	185%	[239]
Electricity price (USD kWh^{-1})			
1	0.08	79%	[305]
2	0.09	87%	[305]
3	0.11	100%	Baseline scenario
4	0.12	112%	[305]
5	0.16	152%	[305]
6	0.22	206%	[305]
Scale (m^3 PBR volume)			
1	30	1%	[259]
2	45	2%	[306]
3	380	13%	[251]
4	3,000	100%	Baseline
5	38,000	1267%	[251]
6	122,000	4082%	[204]
EPS titre (kg m^{-3})			
1	0.25	19%	[204]
2	0.58	45%	[50]
3	1.3	100%	Baseline
4	2.5	192%	[50]

(continued on next page)

Table 4-17 (continued)

Input #	Input value	Relative level	Reference
5	17.2	1369%	[181]
6	19.1	1521%	[55]

4.4.6 Summary of Assumptions

The key assumptions for the techno-economic assessment are summarised in Table 4-18.

Table 4-18 Summary of key assumptions for techno-economic assessment of a cyanobacterial production process of extracellular polymeric substances (EPS) using *Calothrix brevissima*.Abbreviations: total capital investment (TCI); major equipment cost (MEC); metric ton (MT); photobioreactor (PBR); dry cell weight (DCW); quality analysis (QA); quality control (QC).

Material	Value	Unit	Source
Sodium hypochlorite (13%)	1.92	USD L^{-1}	[250]
Fresh water	0.54	USD m^{-3}	[250]
Glucose	0.27	USD kg^{-1}	[307]
Ethanol	0.34	USD kg^{-1}	[21]
BG-11	0.02	USD kg^{-1}	[308]
CO_2	1.32	USD kg^{-1}	[250]
Consumable cost	**Value**	**Unit**	**Source**
PBR bag support structure	10	USD bag^{-1}	[209]
PBR bag	20	USD bag^{-1}	[209]
MF membrane	129	USD m^{-2}	[231]
UF membrane	60	USD m^{-2}	[238]

(continued on next page)

Table 4-18 (continued)

Consumable lifetime	**Value**	**Unit**	**Source**
PBR bag	5	years	[209]
MF membrane	3	years	[231]
UF membrane	5	years	[238]
Utility	**Value**	**Unit**	**Source**
Electricity	0.1	USD kWh^{-1}	[291]
Hot water	0.05	USD MT^{-1}	[291]
Cooling water	0.05	USD MT^{-1}	[291]
Disposal Costs	**Value**	**Unit**	**Source**
Wastewater	0.73	USD m^{-3}	[251]
Ethanol waste	5.77	USD kg^{-1}	[309]
Price	**Value**	**Unit**	**Source**
Biomass	56	USD kg^{-1}	[299]
EPS	73	USD kg^{-1}	[301]
Cosmeceutical	1460	USD kg^{-1}	Calculated based on [310]
Product Titre	**Value**	**Unit**	**Source**
EPS	1.26	g L^{-1}	This study
DCW	1.08	g L^{-1}	This study

(continued on next page)

Table 4-18 (continued)

Major Equipment Cost	**Value**	**Unit**	**Source**
PBR module	16000	USD per 3 m^3 PBR	[259]
PBR lights (max. 500 µmol m^{-2} $s^{-2)}$	14000	USD per 3 m^3 PBR	Calculated based on Kratky, et al. [170]
PBR lights (max. 250 µmol m^{-2} $s^{-2)}$	9000	USD per 3 m^3 PBR	[250]
Process Parameters	**Value**	**Unit**	**Source**
Cultivation temperature (baseline scenario)	31	°C	This study
Light intensity (baseline scenario)	300	µmol m^{-2} s^{-2}	This study
Batch time	10	days	This study
Operating time per year	330	days	[291]
Waste from each stream	5	%	Assumption
EPS losses in the solid stream	0.4	%	[291]
Finanical Assumptions	**Value**	**Unit**	**Source**
Local (property) taxes	1	%	[251]
Insurance costs	0.6	%	[251]
Factory expenses	2	% of TCI	[251]
Number operators (minimum: 2)	1	Per 1500 m^3 PBR volume	Assumption based on [251, 298]

(continued on next page)

Table 4-18 (continued)

Labour costs	**69**	**USD h^{-1}**	**[291]**
Labour operation	85	%	[291]
Labour QA,QC etc	15	%	[291]
Salvage value factor f_s	5	%	[291]
Taxes on profits	40	%	[291]
Interest rate	8	%	[251, 291]
CapEx fraction f_c (year 1 and 3)	30	% of TCI	[291]
CapEx fraction f_c (year 2)	40	% of TCI	[291]
Start-up period	30	months	[291]

Lang Factors	**Value**	**Unit**	**Source**
Piping	20	% of MEC	[251]
Instrumentation	15	% of MEC	[251]
Insulation	0	% of MEC	[251]
Electrical Facilities	10	% of MEC	[251]
Buildings	23	% of MEC	[251]
Yard Improvements	12	% of MEC	[251]
Auxiliary Facilities	20	% of MEC	[251]
Engineering	30	% of MEC	[251]
Construction	10	% of MEC	[251]
Contractor’s Fee	5	% of MEC	[251]
Contingency	15	% of MEC	[251]
Installation cost	20	% of MEC	[251]
Maintenance cost	4	% of MEC	[251]

Chapter 5: Screening Novel Cyanobacteria for EPS Production

5.1 Chapter Overview

Sixteen cyanobacterial species were studied regarding their EPS and biomass production. The novel cyanobacteria were selected based on genera that have been shown to produce EPS in literature (e.g. *Anabaena*, *Nostoc* and *Phormidium*) (Chapter 2:), and the criterium that they have not been previously studied regarding their EPS production in the literature. Prior to the screening, two xenic species were purified for axenic cultivation (Appendix section 12.3). Furthermore, the compatibility of different freshwater and marine media was investigated to perform the screening experiment in the same medium for the two groups (Appendix section 12.5). Characterisation of EPS regarding sugar, protein, sulphate and monosaccharide content of 16 species was performed. Besides, the emulsifying, flocculating, antioxidant, metal-chelating and UV-protective properties of EPS from seven species were analysed. In the following sections, the results of the screening are described in detail, after which two species were selected for culture conditions optimisation (Chapter 6:).

5.2 EPS and Biomass Production of Screened Cyanobacterial Species

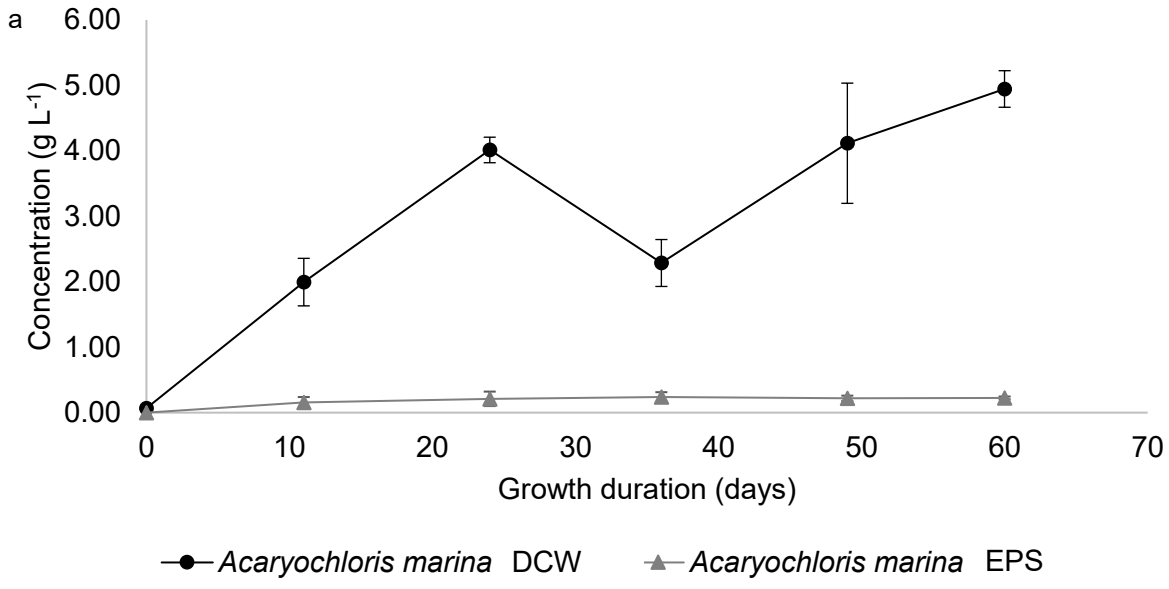
Production of DCW and EPS of the 15 novel cyanobacterial species and the control species, *A. platensis*, are shown in Figure 5-1. The 16 species reached maximum DCW concentrations between 0.83 ± 0.32 g L^{-1} (n=3, *O. rosea*) and 4.95 ± 0.28 g L^{-1} (n=3, *A. marina*). Species with high final DCW were *A. marina*, *P. breve*, *N. longstaffi*, *T. subtropicus* and *N. foliaceum*, reaching at least 3.61 ± 0.50 g L^{-1} (n=3) DCW (*T. subtropicus*) after 60 days of incubation. For most species, DCW steadily increased throughout the growth duration, reaching DCW_{Max} at the final sample (day 60). The typical pattern of microbial growth, including lag, exponential, stationary and decay phase was only partially visible [311]: There seemed to be a lag phase for the first 10 to 15 days for most species, followed by an exponential phase, in which most species seemed to remain until the end of the experiment. The DCW of some species, such as *A. oscillarioides* and *N. zetterstedtii*, stabilised around day 36 and remained stable until

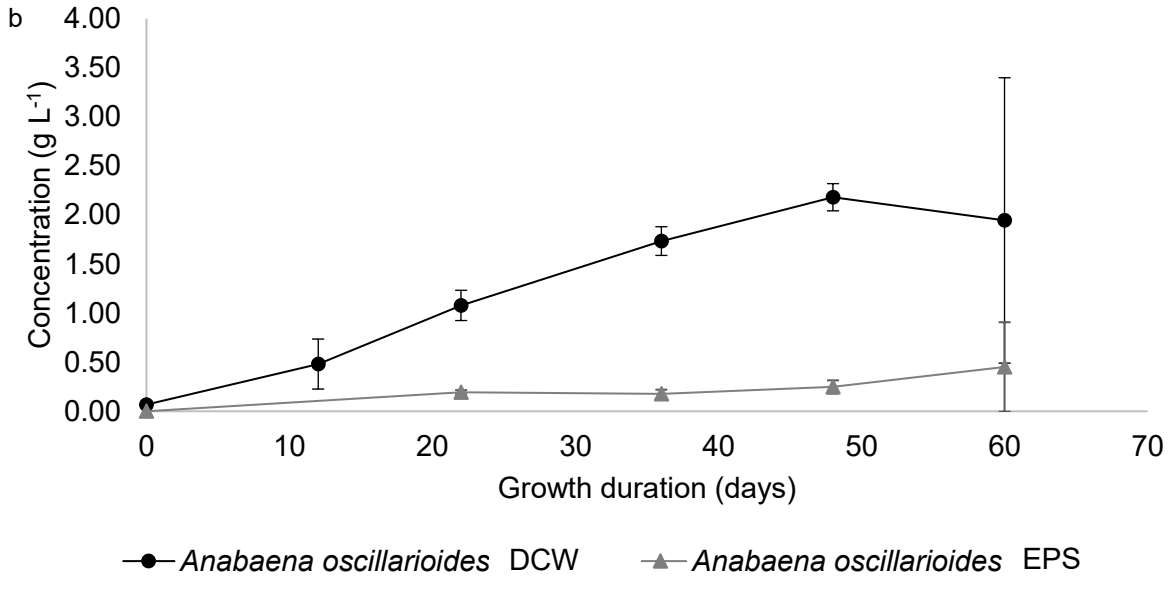
day 48, indicating stationary phase, after which DCW decreased, indicating decay phase. One species that showed a strong increase later in the growth duration was *S. reniformis*: It remained around the same DCW value of 0.82 ± 0.30 g L^{-1} (n=3) to 0.85 ± 0.07 g L^{-1} (n=3) between day 12 and 36, after which DCW rose sharply to DCW_{Max} (2.78 ± 0.35 g L^{-1}, n=3) on day 48, after which it decreased to 1.25 ± 0.35 g L-1 (n=3, day 60). As described in the Materials and Methods chapter (section 4.1.3), DCW was obtained by centrifugation of culture samples. Obtaining cell pellets from *S. reniformis* culture was difficult, as cells floated instead of pelleting, possibly resulting in inaccurate DCW results. The floating was likely due to presence of gas vacuoles, as observed in *Sphaerospermopsis aphanizomenoides* [312]. Several species such as *N. foliaceum, T. subtropicus, P. keutzingianum, F. diplosiphon* and *C. brevissima* showed a strong increase in DCW at the very end of the experiment (day 48 to 60). An atypical growth pattern was visible for *S. major*, which reached a high DCW value on day 12 (1.93 ± 0.19 g L^{-1}, n=2) at which value the species remained until the end of the experiment. Similarly, *A. platensis* reached DCW_{Max} earlier than most species (day 24, 1.43 ± 0.33 g L^{-1}, n=2), after which it decreased to 0.42 ± 0.01 g L^{-1} (n=2) on day 60. The observation that the studied species did not follow a typical bacterial growth curve is consistent with reports for other cyanobacteria producing large amounts of extracellular polysaccharides [63, 165, 313].

Some species such as *G. alpicola*, *O. rosea* and *T. bornetii* did not exceed DCW values of 1.15 ± 0.14 g L^{-1} (n=2, *T. bornetii*). *O. rosea* stopped growing after day 12. This was in contrary to the behaviour observed in the media compatibility experiment, where *O. rosea* exhibited strong growth, obtaining the highest OD_{750} value of all marine species (1.033 ± 0.028, n=3, Table 12-6). Since the media compatibility experiment was conducted at room temperature and natural light (natural dark/light cycle), it is possible that the conditions used in the screening experiment (25°C, constant light at 20 µmol m^{-2} s^{-2}) were unsuitable for this species. Too high light irradiation can lead to photoinhibition [174]. However, for most cyanobacteria species, photoinhibition occurs in a much higher light intensity range of 250 – 1500 µmol m^{-2} s^{-1} [175].

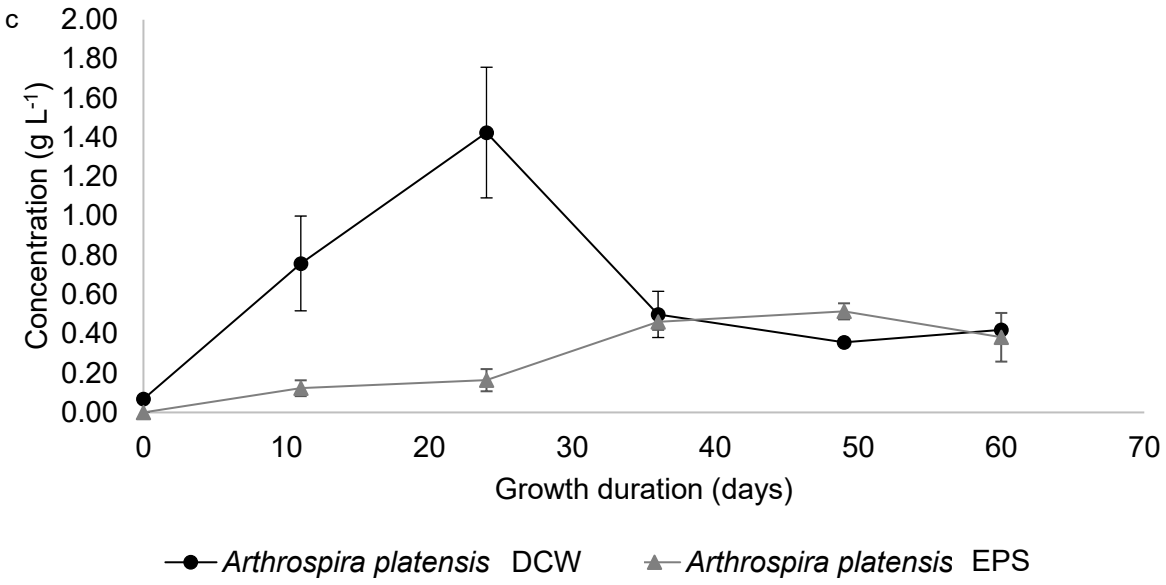
The highest DCW of 4.95 ± 0.28 g L^{-1} (n=3) was reached by *A. marina*. This species showed a ‘dip’ in the DCW data of the sample from day 36. Centrifuged samples of this species seemed to have a gel-like layer on top of the DCW pellet. This gel-like

layer possibly consisted of accumulated EPS, which might have led to an overestimation of DCW and an underestimation of EPS. For the day 36 sample, the gel-like layer of this species was removed for separate analysis, causing the 'dip' in Figure 5-1*a*. However, distinguishing and separating the gel-like layer from the DCW pellet turned out to be very difficult, which is why this step was omitted for later samples. Two other species, *N. foliaceum* and *T. subtropicus,* also showed this type of gel-like layer on top of the pellet, which could result in the same overestimation of DCW for those two species. Other factors that could have affected DCW measurements were environmental influences such as varying humidity, temperature and draught in the lab.



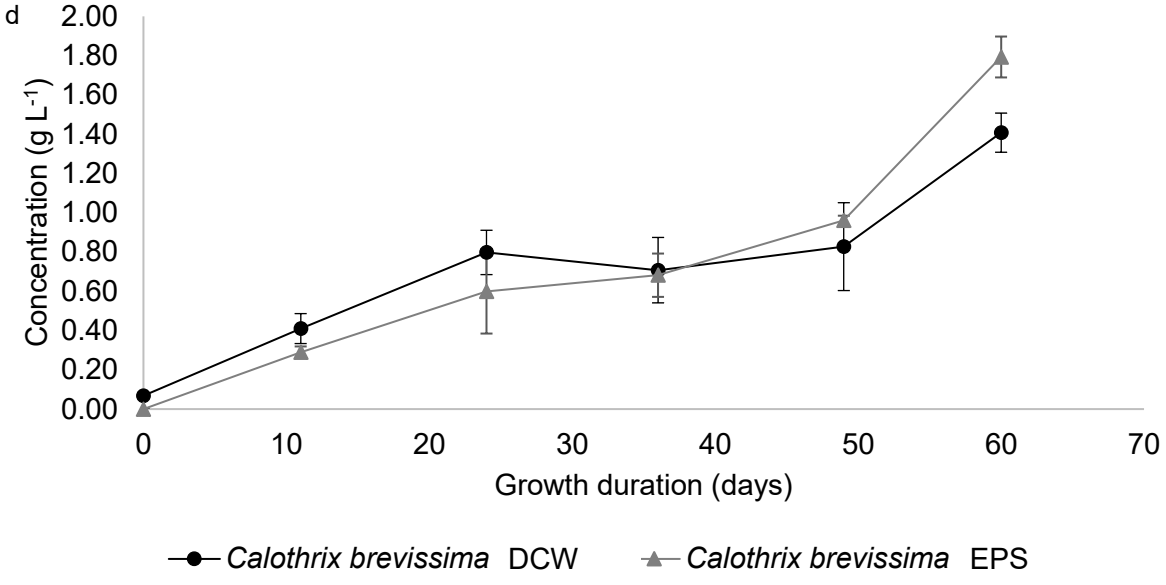


c



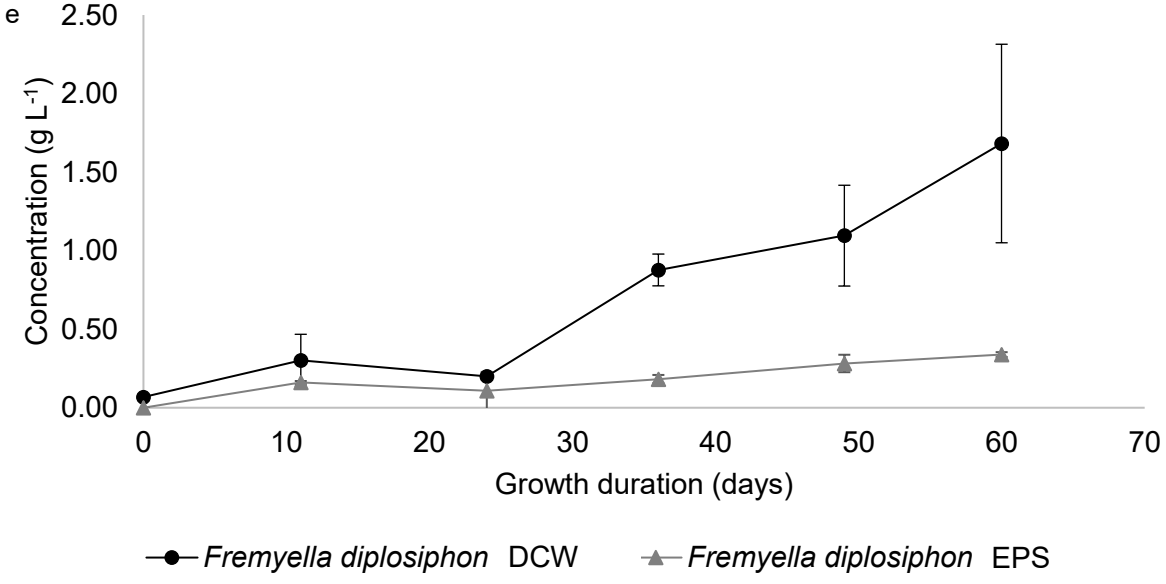
Arthrospira platensis DCW *Arthrospira platensis* EPS

d



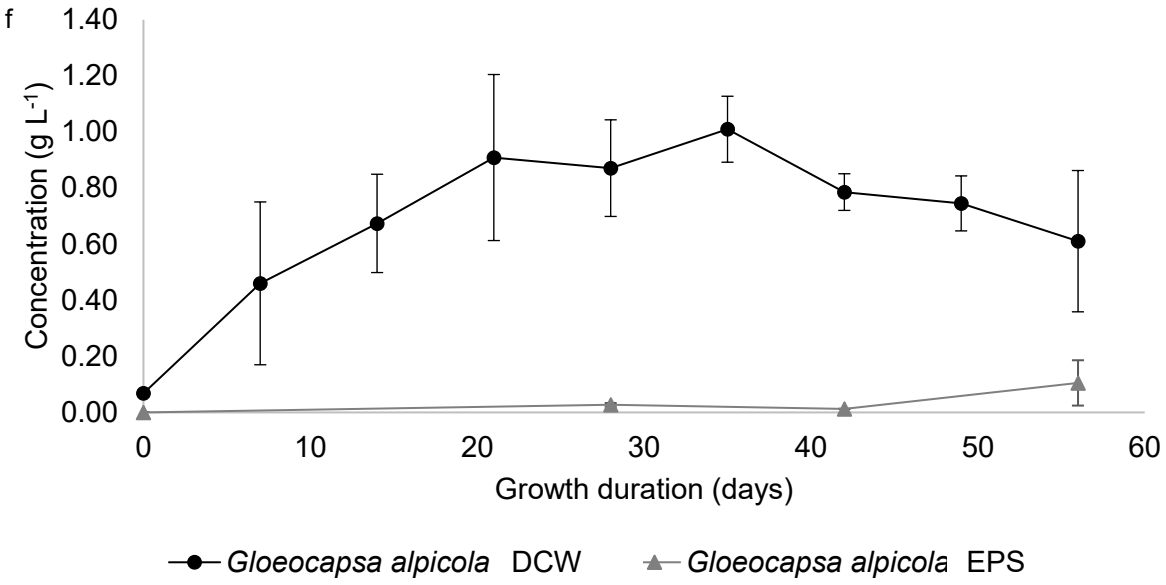
Calothrix brevissima DCW *Calothrix brevissima* EPS

e

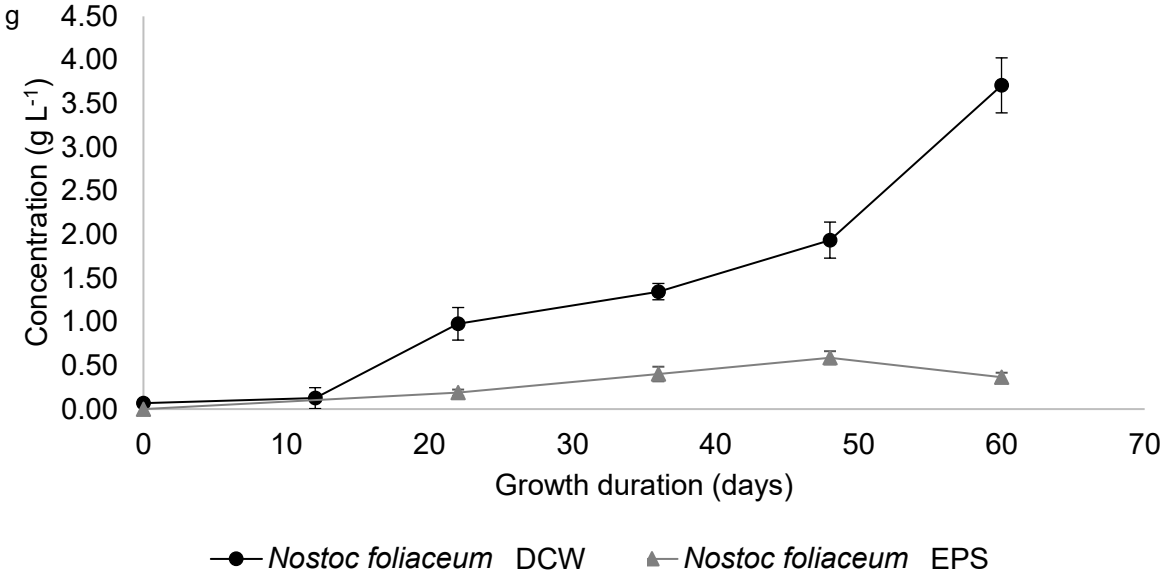


Fremyella diplosiphon DCW *Fremyella diplosiphon* EPS

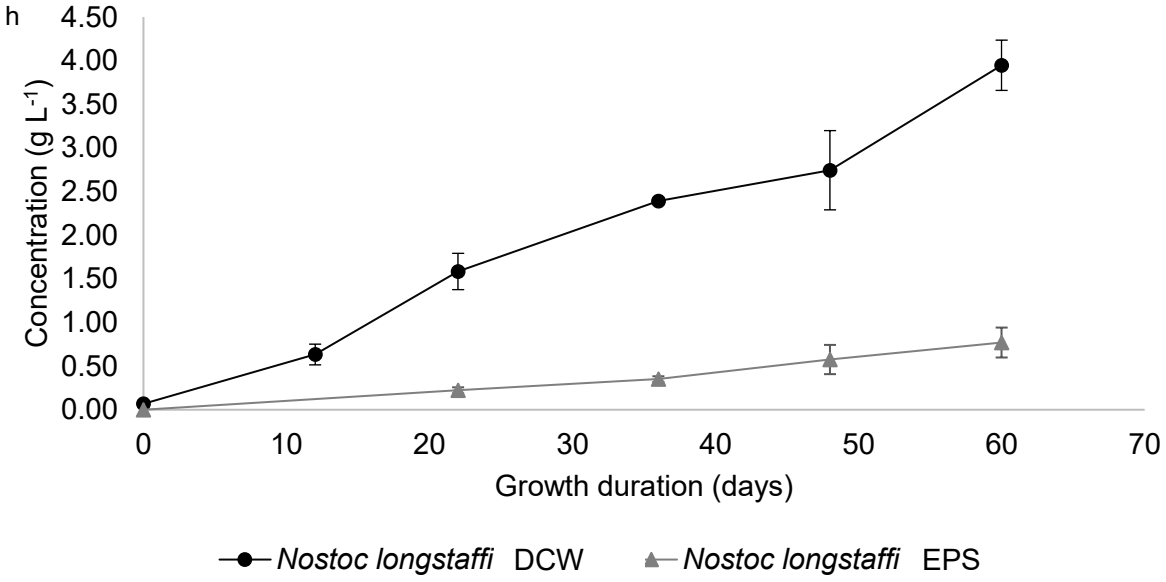
f


1.40
1.20
1.00
0.80
0.60
0.40
0.20
0.00
Concentration (g L-1)
0
10
20
30
40
50
60
Growth duration (days)
Gloeocapsa alpicola DCW
Gloeocapsa alpicola EPS

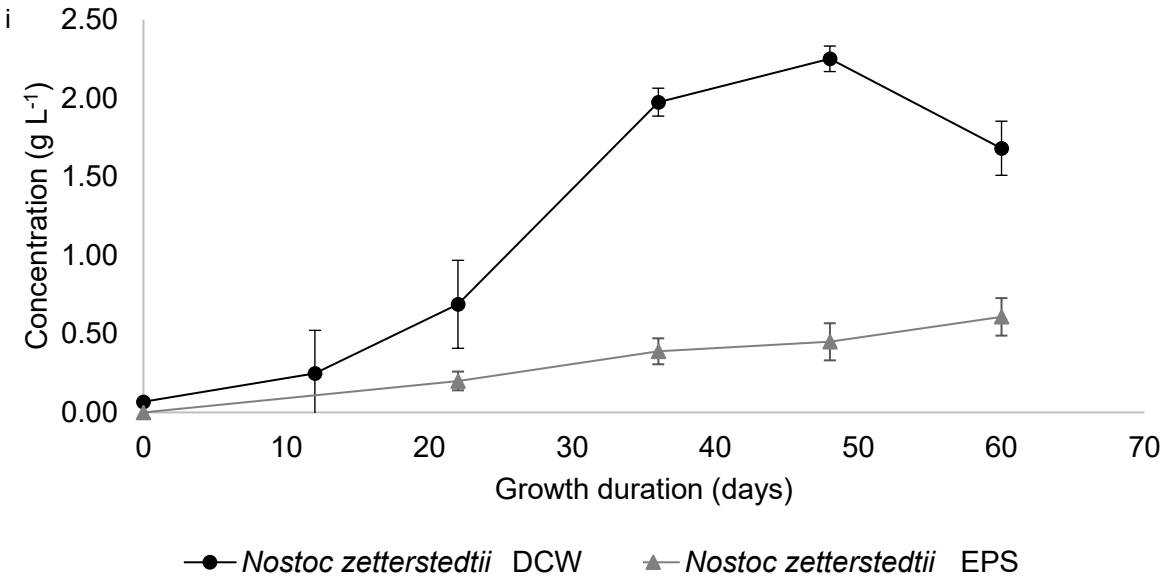
g


4.50
4.00
3.50
3.00
2.50
2.00
1.50
1.00
0.50
0.00
Concentration (g L-1)
0
10
20
30
40
50
60
70
Growth duration (days)
Nostoc foliaceum DCW
Nostoc foliaceum EPS

h

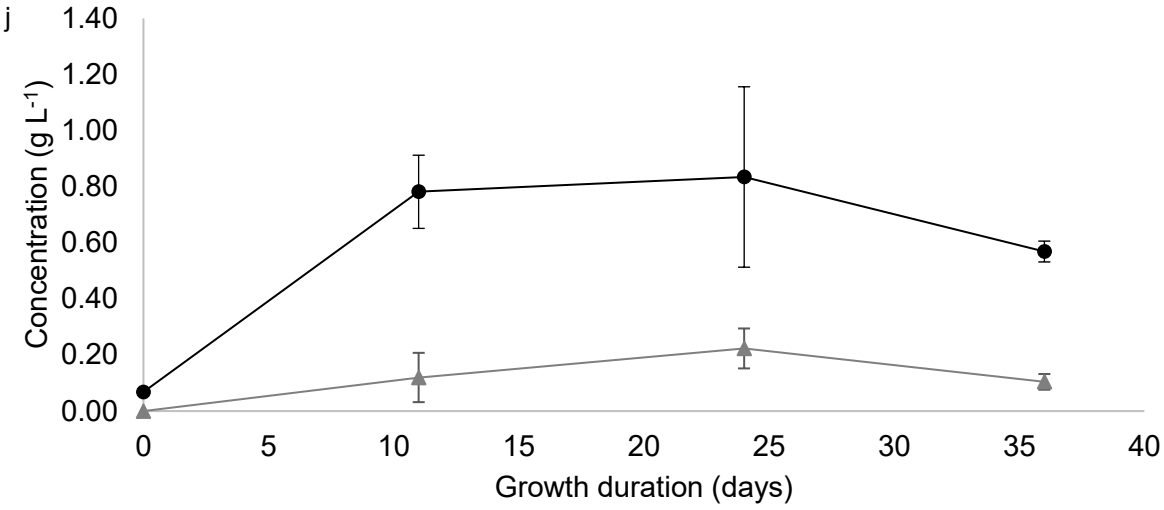

4.50
4.00
3.50
3.00
2.50
2.00
1.50
1.00
0.50
0.00
Concentration (g L-1)
0
10
20
30
40
50
60
70
Growth duration (days)
Nostoc longstaffi DCW
Nostoc longstaffi EPS

i



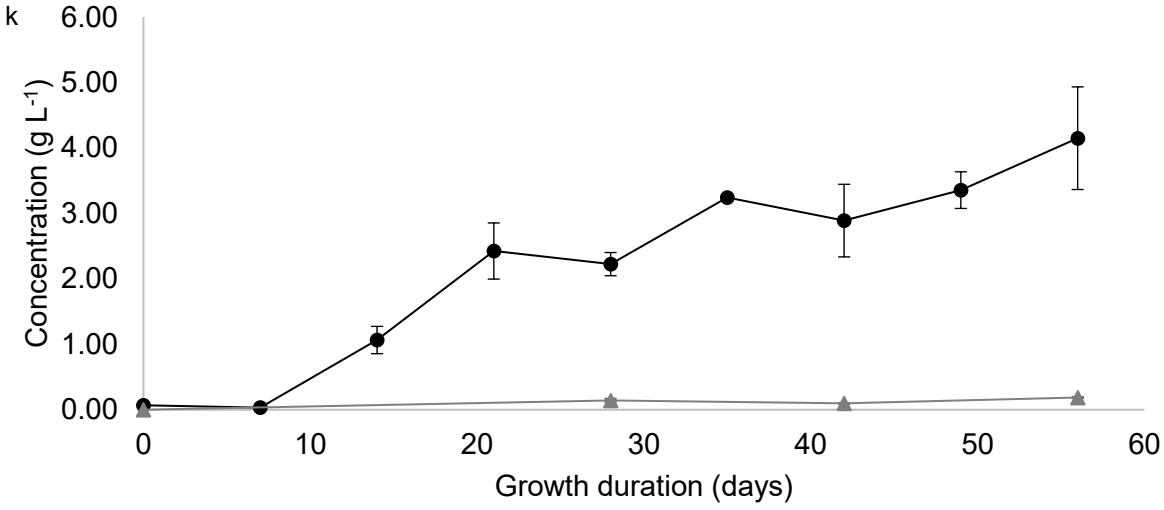
Nostoc zetterstedtii DCW *Nostoc zetterstedtii* EPS

j



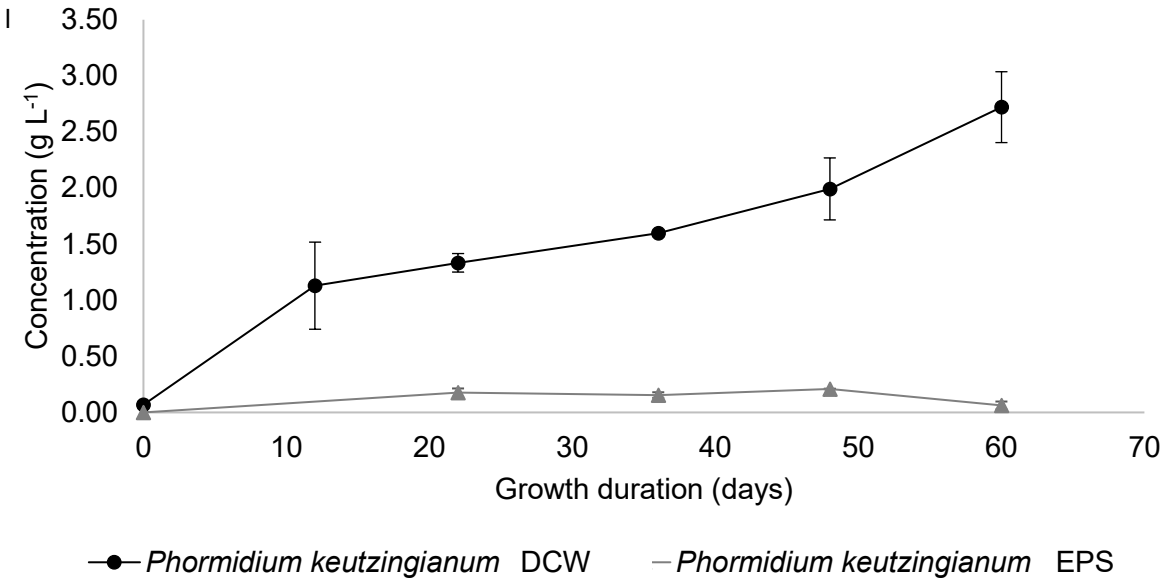
Oscillatoria rosea DCW *Oscillatoria rosea* EPS

k



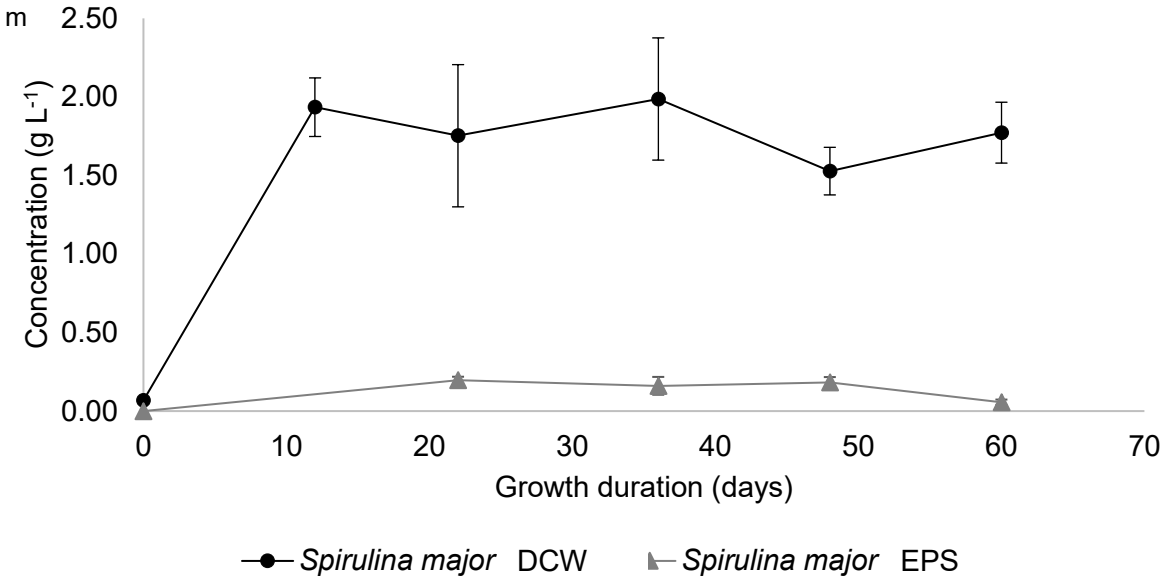
Phormidium breve DCW *Phormidium breve* EPS

l



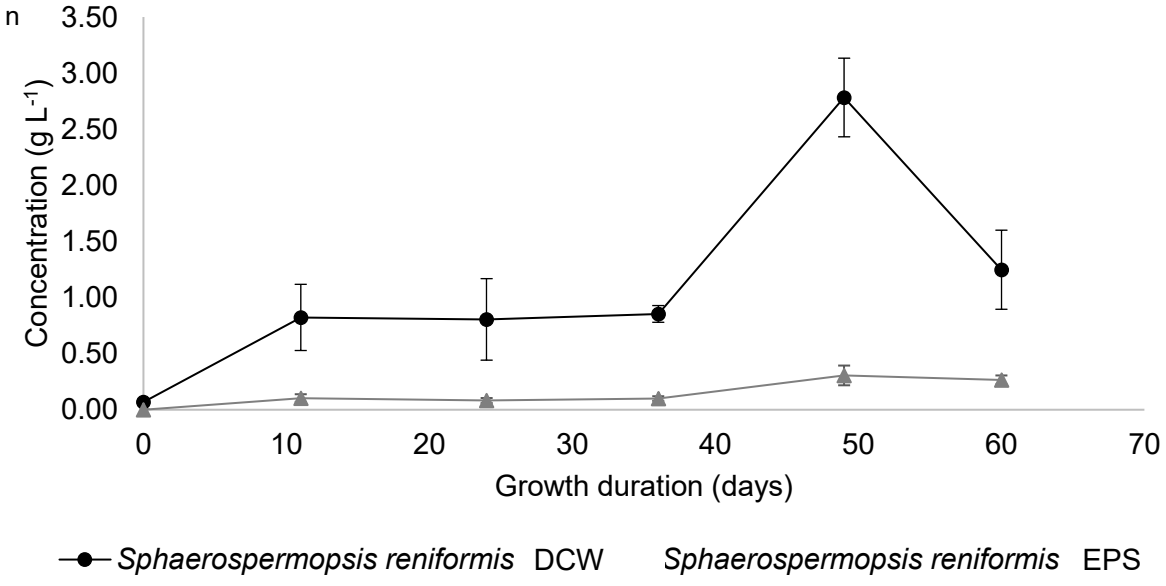
Phormidium keutzingianum DCW *Phormidium keutzingianum* EPS

m



Spirulina major DCW *Spirulina major* EPS

n



Sphaerospermopsis reniformis DCW *Sphaerospermopsis reniformis* EPS

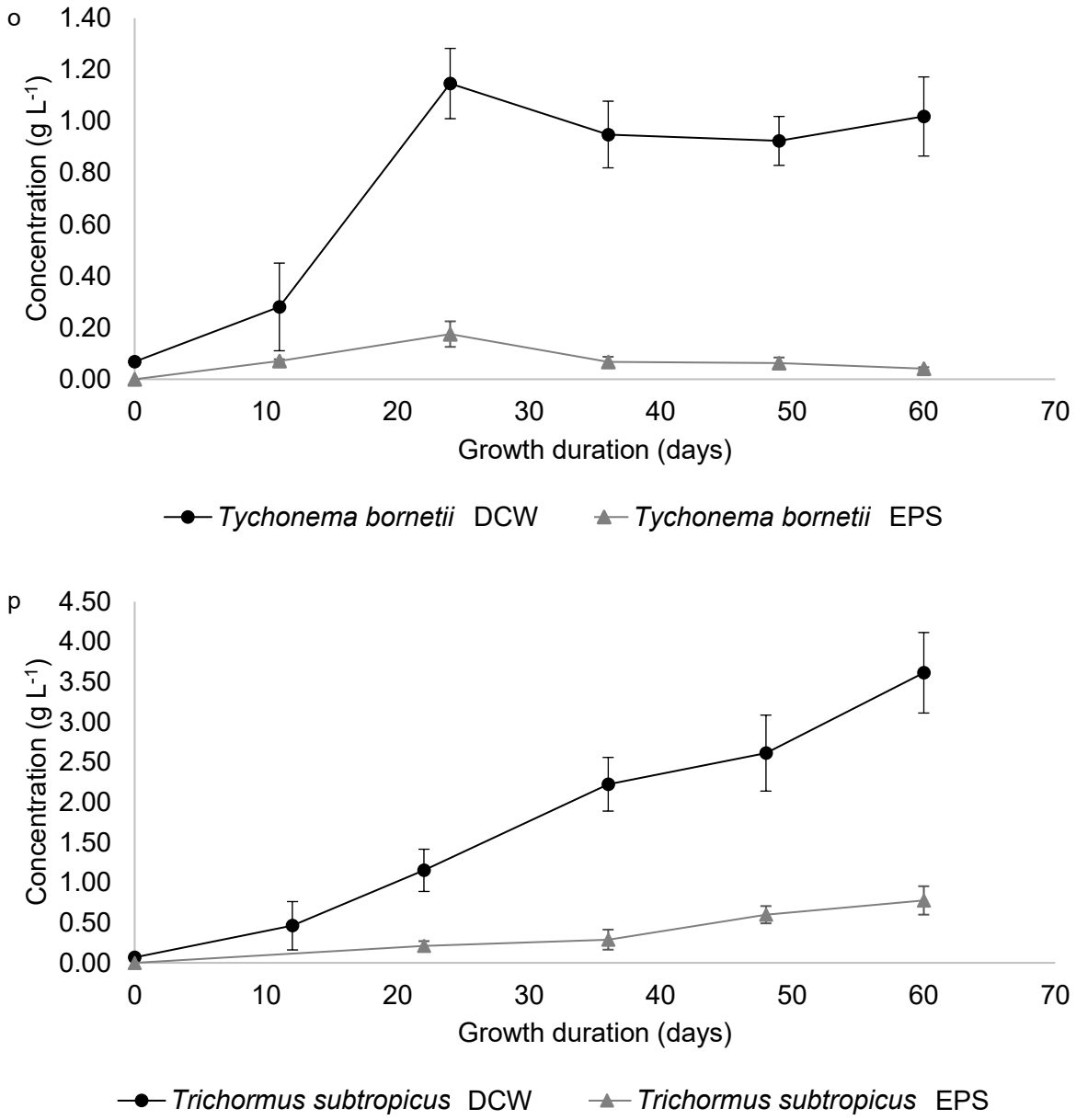


Figure 5-1 Biomass and extracellular polymeric substance (EPS) production of 15 novel cyanobacterial species and *Arthrospira platensis* (positive control) over time during the screening experiment (Exp. 1).Cultures were grown at 25°C under 20 µmol m^{-2} s^{-1} light in 250 mL Erlenmeyer flasks with 62.5 mL working volume, agitated at 250 RPM in a shaking incubator. Data points represent mean values ± 1 standard deviation of biological replicates. Species with triplicate datasets: *Acaryochloris marina* (a), *Calothrix brevissima* (d), *Fremyella diplosiphon* (e), *Gloeocapsa alpicola* (f), *Nostoc foliaceum* (g), *Nostoc longstaffi* (h), *Nostoc zetterstedtii* (i), *Oscillatoria rosea* (j), *Phormidium breve* (k), *Sphaerospermopsis reniformis,* and *Trichormus subtropicus* (p). For *Anabaena oscillarioides* (b), *Phormidium keutzingianum* (l), and *Spirulina major* (m), triplicates were used from day 0–36 and duplicates from day 36–60 due to incubator space limitations. Data for *Arthrospira platensis* (c) and *Tychonema*

bornetii (o) were obtained from duplicates. The day 60 EPS value for *Calothrix brevissima* is based on two measurements, as one replicate was lost due to centrifuge tube breakage.

As displayed in Figure 5-1*b*, there was one species in particular that produced high amounts of EPS: *C. brevissima* consistently produced more EPS than any other species throughout the growth duration, reaching a maximum EPS concentration of 1.79 ± 0.15 g L^{-1} (n=2, day 60), which was more than twice as much as the second highest producer (*T. subtropicus*, 0.78 ± 0.18 g L^{-1}, n=3). Other species producing considerable amounts of EPS (> 0.51 g L^{-1}) were *N. longstaffi*, *N. foliaceum*, *N. zetterstedtii* and *A. platensis*. Low amounts of EPS (< 0.17 g L^{-1}) were produced by *G. alpicola*, *S. major*, *P. keutzingianum*, *P. breve* and *O. rosea*. Most species increased EPS steadily during their growth duration, resulting in the highest EPS value obtained at the last sample (day 60). Many cyanobacteria produce the largest amounts of EPS in the late stationary phase [181]. A few species such as *T. bornetii*, *P. breve* and *G. alpicola* did not show a clear trend, with EPS production staying around the same (low) value of less than 0.18 ± 0.05 g L^{-1} (n=2, *T. bornetii*). Similarly, EPS production *P. keutzingianum* and *S. major* remained relatively stable at around 0.18 ± 0.03 g L^{-1} (n=2, *S. major,* day 48), except for a decrease to 0.06 ± 0.02 g L^{-1} (n=2, *S. major*, day 60) at the end of the growth duration.

5.3 Composition of EPS from Novel Species

5.3.1 Sugar, Protein, and Sulphate Content of Novel EPS

The sugar, protein and sulphate content of the EPS of the novel species are displayed in Figure 5-2. Sugars were found in EPS from 15 out of 16 species, forming the largest fraction of the novel EPS, making up 41%$_{w/w}$ (gram sugar per gram EPS) on average. This was similar to the average value found for 61 cyanobacterial EPS in literature (44%$_{w/w}$, section 2.2.1), based on values ranging from 9% to 93% [50, 51]. High sugar content was found in *F. diplosiphon* (87 ± 12%$_{w/w}$, n=3), *N. zetterstedtii* (82 ± 14%$_{w/w}$, n=3) and *N. longstaffi* (63 ± 21%$_{w/w}$, n=3). No sugar was detected in the negative controls (BG11, ESM). Two species, *O. rosea* and *G. alpicola*, showed unusually low sugar content of 8 ± 2% (n=3) and 8 ± 3%$_{w/w}$ (n=2), respectively. Combined with the observation that these species produced only small amounts of EPS (Figure 5-1*f,* Figure 5-1*j*), an explanation could be that the obtained EPS primarily consisted of

impurities rather than polysaccharide components. Co-precipitation of impurities with ethanol can occur [40]. For one species, *S. major*, sugar content was below the limit of detection (LOD). LODs can be found in Table 12-1.

Table 5-1 Composition (sugar, protein, and sulphate content) of extracellular polymeric substances (EPS) from novel cyanobacterial species.The table shows sugar, protein, and sulphate concentrations (g L^{-1}) in extracellular polymeric substances (EPS) samples dissolved at 2 g L^{-1} in Milli-Q water, determined using phenol-sulfuric acid assay, Bradford assay, and barium chloride gelatin test, respectively.Using Equation 4-2 to Equation 4-7 (see section 4.1.5), the sugar, protein and sulfate content ($\%_{w/w}$) was calculated from each concentration (g L^{-1}). Data represent mean ± standard deviation of biological duplicates (n=2) or triplicates (n=3) as indicated in the second column. Calibration curves can be found in Figure 12-1, trendline equations, limit of detection (LOD) and limit of saturation (LOS) can be found in Table 12-1. Abbreviations: n: number of replicates; conc.: concentration; <LOD: below detection limit.

Sample	**n**	**Sugar conc.**	**Protein conc.**	**Sulphate conc.**	**Sample conc.**	**EPS sugar content**	**EPS protein content**	**EPS sulphate content**
Unit	N.A.	g L^{-1}	g L^{-1}	g L^{-1}	g L^{-1}	$\%_{w/w}$	$\%_{w/w}$	$\%_{w/w}$
A. marina	3	0.49 ± 0.05	<LOD	0.16 ± 0.01	2	24 ± 3%	<LOD	8 ± 1%
A. oscillarioides	2	0.53 ± 0.40	0.11 ± 0.08	<LOD	2	27 ± 20%	5 ± 4%	<LOD
A. platensis	2	1.24 ± 0.21	0.07 ± 0.00	<LOD	2	62 ± 11%	3 ± 0.2%	<LOD
C. brevissima	3	1.24 ± 0.05	0.17 ± 0.06	<LOD	2	62 ± 2%	9 ± 3%	<LOD
F. diplosiphon	3	1.74 ± 0.24	0.19 ± 0.05	<LOD	2	87 ± 12%	10 ± 3%	<LOD
G. alpicola	2	0.15 ± 0.07	0.15 ± 0.05	<LOD	2	8 ± 3%	8 ± 2%	<LOD
N. foliaceum	3	0.89 ± 0.23	<LOD	<LOD	2	44 ± 12%	<LOD	<LOD
N. longstaffi	3	1.26 ± 0.43	<LOD	<LOD	2	63 ± 21%	<LOD	<LOD
N. zetterstedtii	3	1.65 ± 0.27	<LOD	<LOD	2	82 ± 14%	<LOD	<LOD
O. rosea	3	0.17 ± 0.03	<LOD	0.15 ± 0.06	2	8 ± 2%	<LOD	7 ± 3%
P. breve	3	0.92 ± 0.31	<LOD	0.03 ± 0.00	2	46 ± 15%	<LOD	1 ± 0.2%

(continued on next page)

Table 5-1 (continued)

Sample	**n**	**Sugar conc.**	**Protein conc.**	**Sulphate conc.**	**Sample conc.**	**EPS sugar content**	**EPS protein content**	**EPS sulphate content**
Unit	N.A.	g L^{-1}	g L^{-1}	g L^{-1}	g L^{-1}	$\%_{w/w}$	$\%_{w/w}$	$\%_{w/w}$
P. keutzingianum	3	0.24 ± 0.17	<LOD	0.26 ± 0.05	2	12 ± 9%	<LOD	13 ± 2%
S. major	3	<LOD	<LOD	0.23 ± 0.03	2	<LOD	<LOD	11 ± 1%
S. reniformis	3	0.73 ± 0.19	0.23 ± 0.11	<LOD	2	37 ± 9%	12 ± 5%	<LOD
T. bornetii	2	0.21 ± 0.02	<LOD	0.06 ± 0.00	2	11 ± 1%	<LOD	3 ± 0.2%
T. subtropicus	3	0.82 ± 0.33	<LOD	<LOD	2	41 ± 16%	<LOD	<LOD
BG-11	3	<LOD	<LOD	0.02 ± 0.00	2	<LOD	<LOD	1 ± 0.1%
ESM	3	<LOD	<LOD	0.05 ± 0.02	2	<LOD	<LOD	2 ± 1%

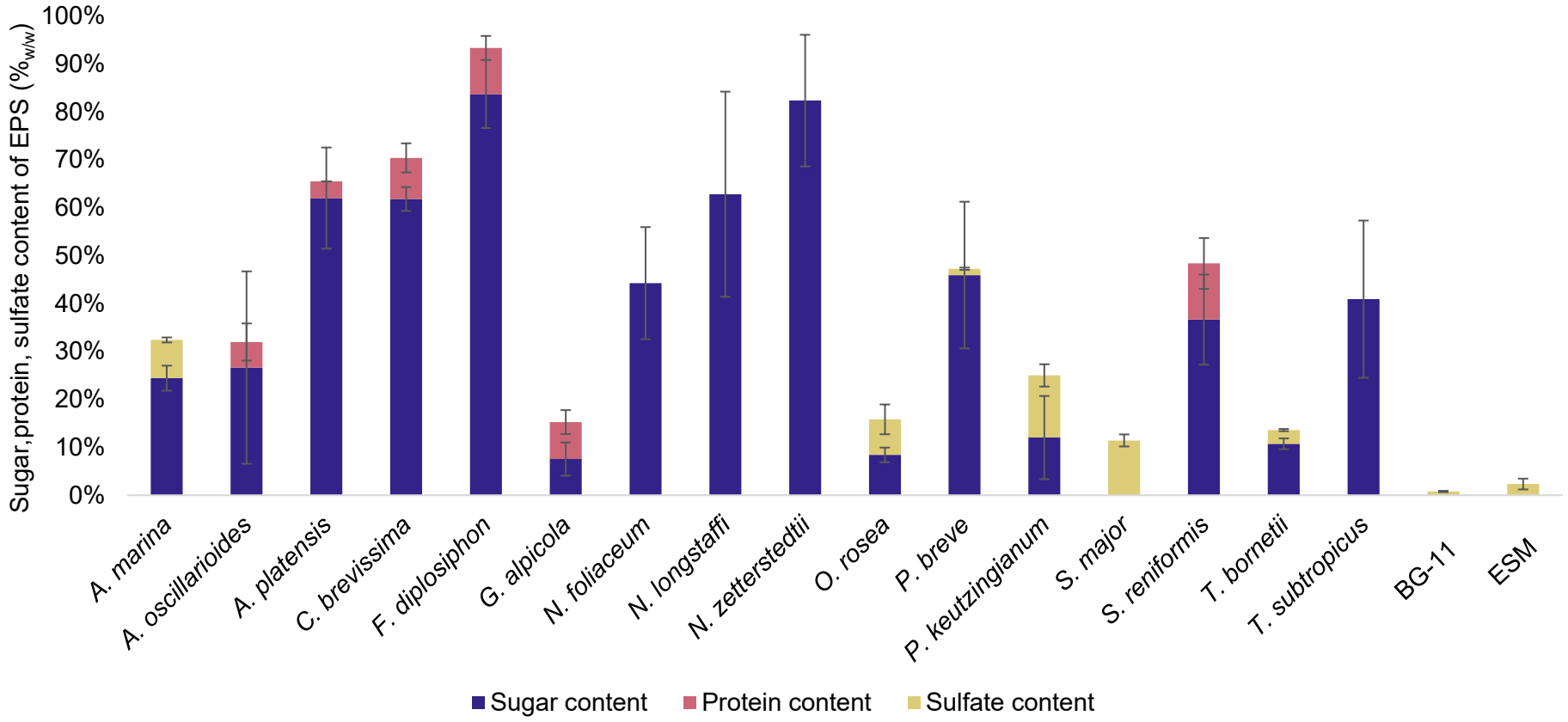


Figure 5-2 Sugar, protein, and sulfate content of extracellular polymeric substances (EPS) from novel cyanobacteria after 60 days of cultivation at 25°C under 20 µmol m^{-2} s^{-1} light.EPS were analysed using the phenol-sulfuric acid method (sugars), Bradford assay (proteins), and barium chloride–gelatin test (sulfates). Bars represent the proportion of each component in total EPS composition (g sugar/protein/sulfate per g EPS, % $_{w/w}$) as stacked bars (not accumulated values). Data points represent mean ± 1 standard deviation. Species with triplicate datasets (n=3): *Acaryochloris marina*, *Calothrix brevissima*, *Fremyella diplosiphon*, *Nostoc foliaceum*, *Nostoc longstaffi*, *Nostoc zetterstedtii*, *Oscillatoria rosea*, *Phormidium breve*,

Sphaerospermopsis reniformis and *Trichormus subtropicus*. Species with duplicate datasets (n=2): *Anabaena oscillarioides*, *Arthrospira platensis*, *Gloeocapsa alpicola*, *Phormidium keutzingianum*, *Spirulina major* and *Tychonema bornetii*. Calibration curves can be found in Figure 12-1, trendline equations, limit of detection (LOD) and limit of saturation (LOS) can be found in Table 12-1.

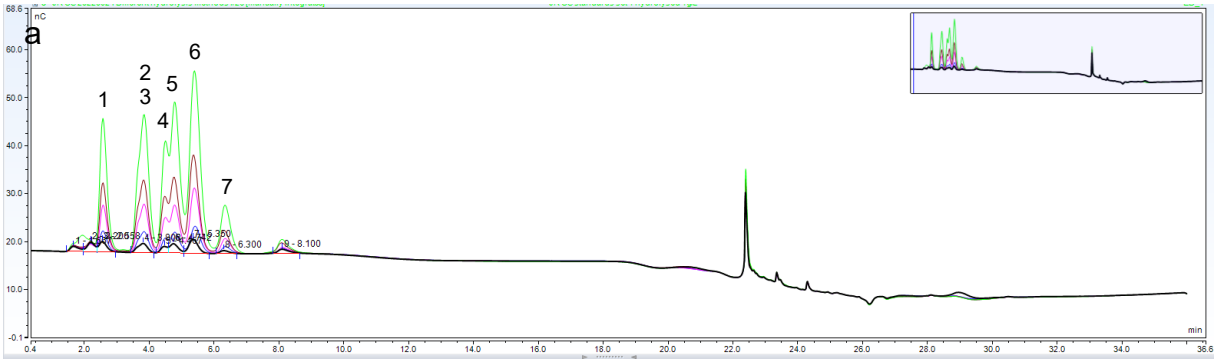
Protein was found in six out of 16 novel EPS, making up 8%$_{w/w}$ (gram protein per gram EPS) on average. The highest amount was found in EPS from *S. reniformis* (12 ± 5%$_{w/w}$, n=3). Other species with high protein content were *F. diplosiphon* (10 ± 3%$_{w/w}$ (n=3) and *C. brevissima* (9 ± 3%$_{w/w}$, n=3), whereas only 3 - 5%$_{w/w}$ were found in other species (Table 5-1). The values were within the range of literature data, where proteins make up between 0% and 55% of cyanobacterial EPS [61, 314]. No protein was detected in *A. marina, N. foliaceum, N. longstaffi, N. zetterstedtii, O. rosea, P. breve, P. keutzingianum, S. major, T. bornetii*, *T. subtropicus* and the negative controls, BG-11 and ESM. Measured EPS protein concentrations ranged from 0.07 to 0.23 g L^{-1} (Table 5-1), and lie within the linear calibration range of 0.025–1 g L^{-1} (R^2 = 0.992, Table 12-1). These samples are bracketed by three calibration points (0.025, 0.125, 0.25 g L^{-1}) and are above the LOD of 0.069 g L^{-1} (Table 12-1), allowing interpolation from the linear portion of the calibration curve. As these samples fall in the lower range of the curve, additional standards in this region could further improve measurement resolution.

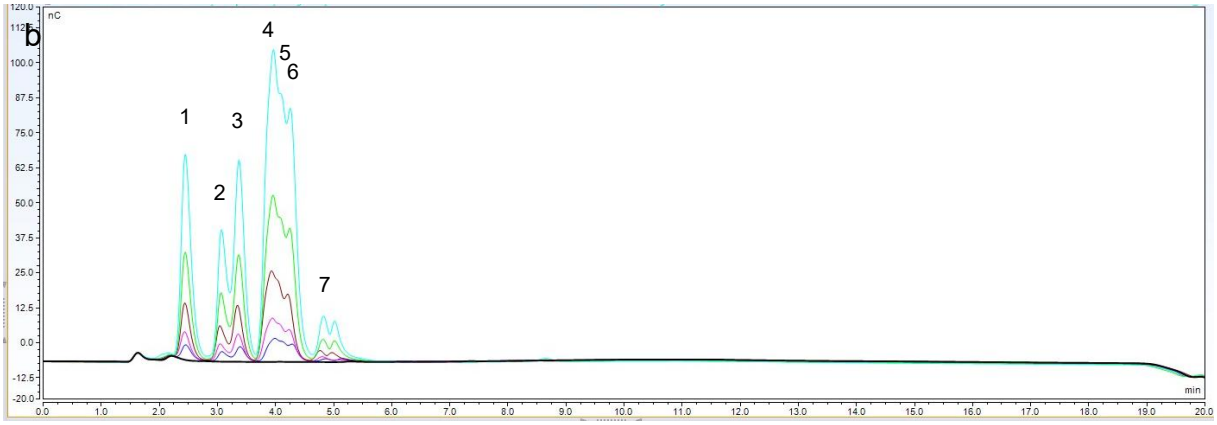
Sulphate was detected in six out 16 species, making up 7%$_{w/w}$ (gram sulphate per gram EPS) on average. The highest amount of sulphate of 13 ± 2%$_{w/w}$ (n=2) was present in EPS from *P. keutzingianum*. The second highest amount was found in EPS from *S. major* (11 ± 1%$_{w/w}$, n=3). In EPS from, *P. breve*, *A. marina*, *O. rosea* and *T. bornetii* between 1 ± 0.2%$_{w/w}$ (n=3, *P. breve*) and 8 ± 1%$_{w/w}$ (n=3, *A. marina*) sulphate was found. The sulphate content of the novel EPS were within the range of literature values (0 to 18%) [32, 315]. All species with sulphated EPS were marine species, consistent with previous findings that sulphated EPS are frequently, though not exclusively, found in saline and hypersaline habitats [39]. Low amounts were also detected in the negative controls, BG-11 (1 ± 0.1%$_{w/w}$, n=3) and ESM (2 ± 1%$_{w/w}$, n=3).

A. platensis, which served as positive control in this experiment, consisted of 62 ± 11%$_{w/w}$ (n=2) sugar, 3 ± 0.2%$_{w/w}$ (n=2) protein and no sulphate. In literature, EPS from *A. platensis* were found to contain 50.2% sugar, 1.62% protein and low amounts of sulphate (0.5%) [61, 66].

5.3.2 Monosaccharide Composition of Novel EPS

The monosaccharide composition of novel EPS was analysed using HPAEC-PAD as described in section 4.1.5.5. The HPAEC-PAD chromatographs are shown in Figure 5-3. As can be seen, using method 1, there was overlap of the peaks of arabinose and rhamnose (Figure 5-3*a*). Hence, another method (method 2) was applied to separate these two monosaccharides (Figure 5-3*b*). In Figure 5-3*c*, the chromatograph of standard set 2 under method 1 is shown. The standards for glucosamine, fructose, ribose, galacturonic acid and glucuronic acid showed degradation after TFA hydrolysis (data not shown), and were therefore used without being subjected to TFA hydrolysis. The retention times and trendline equations of each monosaccharide can be found in Table 12-2.





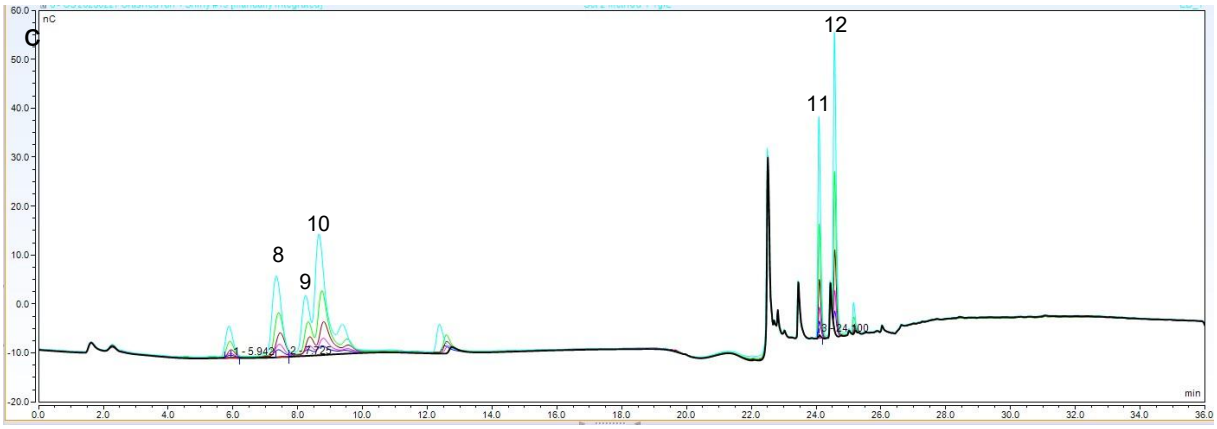


Figure 5-3 Chromatographs of standards for high-performance anion-exchange chromatography with pulsed-amperometric detection (HPAEC-PAD).(a) Chromatograph of standards set 1 under method 1 (hydrolysed). (b) Chromatograph of standards set 1 under method 2 (hydrolysed). (c) Chromatograph of standards set 2 under method 1 (unhydrolysed). Peaks numbered by monosaccharide: fucose, 1; rhamnose, 2; arabinose, 3; galactose, 4; glucose, 5; xylose, 6; mannose, 7; glucosamine, 8; fructose, 9; ribose, 10; galacturonic, 11; glucuronic acid, 12. Calibration curves can be found in Figure 12-1; trendline equations, limit of detection (LOD) and limit of saturation (LOS) can be found in Table 12-1.

As shown in Figure 5-4, glucose was found in the majority of EPS from the novel cyanobacterial species (10 species). This is in accordance with literature, as glucose is the most prominent monosaccharide in cyanobacterial EPS [28]. The highest glucose content (gram glucose per gram EPS) was found in *F. diplosiphon*, *A. platensis* and *C. brevissima*, amounting to 60 ± 6%$_{w/w}$(n=3), 49 ± 1%$_{w/w}$ (n=2) and 31 ± 6%$_{w/w}$ (n=3), respectively. The pentose arabinose was present in EPS from seven out of the 16 species, with the highest content found in EPS from *T. subtropicus* and *A. marina* with 6 ± 3%$_{w/w}$ (n=2) and 3 ± 0.2%$_{w/w}$ (n=2), respectively. Another common monosaccharide was galactose, which was found in EPS of six out of 16 species. The highest amounts of galactose were present in *N. longstaffi*, *N. foliaceum* and *A. marina* with 34 ± 4%$_{w/w}$ (n=3), 16 ± 4%$_{w/w}$ (n=3) and 12 ± 1%$_{w/w}$ (n=2), respectively. Mannose was present in EPS of three out of 16 species. *N. longstaffi*, *N. zetterstedtii* and *C. brevissima* contained 16 ± 2%$_{w/w}$ (n=3), 14 ± 5%$_{w/w}$ (n=3) and 8 ± 2%$_{w/w}$ (n=3) mannose, respectively. High amounts of xylose were found in *N. zetterstedtii* and *N. longstaffi* with 16 ± 5%$_{w/w}$ (n=3) and 11 ± 1%$_{w/w}$ (n=3), respectively. EPS from *F. diplosiphon* and *A. platensis* had the highest amounts of fructose with 11 ± 2%$_{w/w}$ (n=3)

and 6 ± 0.5%$_{w/w}$ (n=2), respectively. The deoxy sugar fucose was only found in *N. foliaceum*, amounting to 13 ± 3%$_{w/w}$ (n=3). Another deoxy sugar, rhamnose, was detected in *S. reniformis, N. foliaceum* and *A. platensis*, making up and 4 ± 1%$_{w/w}$ (n=2), 3 ± 1%$_{w/w}$ (n=3) and 2 ± 0.4%$_{w/w}$ (n=3), respectively. Additionally, the HPAEC-PAD chromatograph of *N. foliaceum* showed three unidentified peaks, possibly indicating the presence of three additional unknown monosaccharides (data not shown). Ribose was not detected.

Uronic acids were rarer than neutral sugars. Glucuronic acid was found in three out of 16 species, with the highest amounts present in *T. subtropicus* and *A. marina* 13 ± 0.3%$_{w/w}$ (n=2) and 10 ± 2%$_{w/w}$ (n=2), respectively. Another uronic acid, galacturonic acid and the amino sugar glucosamine were not detected. No sugars were detected in the negative controls, BG-11 and ESM.

Table 5-2 Monosaccharide composition of extracellular polymeric substances (EPS) of 15 novel cyanobacterial species.The table presents analyte concentrations (g L^{-1} monosaccharide) measured in EPS samples dissolved at 2 g L^{-1} in Milli-Q water using high-performance anion-exchange chromatography with pulsed-amperometric detection (HPAEC-PAD).Using Equation 4-8 and Equation 4-9 (see section 4.1.5.5), the monosaccharide content ($\%_{w/w}$) was calculated by dividing the measured monosaccharide concentration (in g L^{-1}) by the EPS sample concentration (2 g L^{-1}). Data represent mean ± standard deviation of biological duplicates (n=2) or triplicates (n=3) as indicated in the second column. Negative controls (BG-11 and ESM media) were analysed in technical triplicates (n=3). Calibration curves can be found in Figure 12-1, trendline equations, limit of detection (LOD) and limit of saturation (LOS) can be found in Table 12-1. Ribose, glucosamine and galacturonic acid were below the LOD in all samples and were excluded from the table. Abbreviations: $C_{Analyte}$: Concentration of analyte; C_{EPS}: Concentration of EPS; n: number of replicates; <LOD: below detection limit; *A. m.*: *Acaryochloris marina*; *A. o.*: *Anabaena oscillarioides*; *A. p.*: *Arthrospira platensis*; *C. b.*: *Calothrix brevissima*; *F. d.*: *Fremyella diplosiphon*; *G. a.*: *Gloeocapsa alpicola*; *N. f.*: *Nostoc foliaceum*; *N. l.*: *Nostoc longstaffi*; *N. z.*: *Nostoc zetterstedtii*; *O. r.*: *Oscillatoria rosea*; *P. b.*: *Phormidium breve*; *P. k.*: *Phormidium keutzingianum*; *S. m.*: *Spirulina major*; *S. r.*: *Sphaerospermopsis reniformis*; *T. b. Tychonema bornetti*; *T. s.*: *Trichormus subtropicus*; GlcAc: glucuronic acid.

$C_{Analyte}$	**n**	**Glucose**	**Galactose**	**Mannose**	**Fructose**	**Rhamnose**	**Fucose**	**Xylose**	**Arabinose**	**GlcAc**
Unit	(-)	g L^{-1}	g L^{-1}	g L^{-1}	g L^{-1}	g L^{-1}	g L^{-1}	g L^{-1}	g L^{-1}	g L^{-1}
A. m.	2	0.08±0.01	0.24±0.03	<LOD	<LOD	<LOD	<LOD	<LOD	0.05±0.00	0.21±0.03
A. o.	2	0.33±0.30	<LOD	<LOD	<LOD	<LOD	<LOD	<LOD	<LOD	<LOD
A. p.	2	0.98±0.02	<LOD	<LOD	0.12±0.01	0.04±0.01	<LOD	<LOD	<LOD	<LOD
C. b.	3	0.62±0.12	<LOD	0.16±0.03	0.10±0.01	<LOD	<LOD	<LOD	0.03±0.01	<LOD
F. d.	3	1.21±0.12	<LOD	<LOD	0.23±0.04	<LOD	<LOD	<LOD	0.03±0.01	<LOD
G. a.	2	<LOD	<LOD	<LOD	<LOD	<LOD	<LOD	<LOD	<LOD	<LOD
N. f.	3	0.27±0.06	0.31±0.07	<LOD	0.11±0.03	0.07±0.02	0.26±0.06	<LOD	0.03±0.00	<LOD

(continued on next page)

Table 5-2 (continued)

$C_{Analyte}$	n	Glucose	Galactose	Mannose	Fructose	Rhamnose	Fucose	Xylose	Arabinose	GlcAc
Unit	(-)	g L^{-1}	g L^{-1}	g L^{-1}	g L^{-1}	g L^{-1}	g L^{-1}	g L^{-1}	g L^{-1}	g L^{-1}
N. l.	3	<LOD	0.68±0.08	0.32±0.04	<LOD	<LOD	<LOD	0.22±0.02	<LOD	<LOD
N. z.	3	<LOD	0.22±0.06	0.27±0.09	<LOD	<LOD	<LOD	0.31±0.10	0.03±0.00	<LOD
O. r.	3	<LOD	<LOD	<LOD	<LOD	<LOD	<LOD	<LOD	<LOD	<LOD
P. b.	3	0.27±0.05	<LOD	<LOD	<LOD	<LOD	<LOD	<LOD	<LOD	<LOD
P. k.	2	0.23±0.01	<LOD	<LOD	<LOD	<LOD	<LOD	<LOD	<LOD	<LOD
S. m.	2	<LOD	<LOD	<LOD	<LOD	<LOD	<LOD	<LOD	<LOD	<LOD
S. r.	3	0.08±0.02	0.10±0.01	<LOD	<LOD	0.07±0.01	<LOD	<LOD	0.02±0.00	<LOD
T. b.	2	<LOD	<LOD	<LOD	<LOD	<LOD	<LOD	<LOD	<LOD	<LOD
T. s.	3	0.18±0.08	0.14±0.05	<LOD	<LOD	<LOD	<LOD	<LOD	0.12±0.06	0.26±0.01
BG11	3	<LOD	<LOD	<LOD	<LOD	<LOD	<LOD	<LOD	<LOD	<LOD
ESM	3	<LOD	<LOD	<LOD	<LOD	<LOD	<LOD	<LOD	<LOD	<LOD

Content (‰w/w)	C_{EPS}	Glucose	Galactose	Mannose	Fructose	Rhamnose	Fucose	Xylose	Arabinose	GlcAc
Unit	g L^{-1}	‰w/w	‰w/w	‰w/w	‰w/w	‰w/w	‰w/w	‰w/w	‰w/w	‰w/w
A. m.	2	4±0.3%	12±1%	<LOD	<LOD	<LOD	<LOD	<LOD	3±0.2%	10±2%
A. o.	2	17±15%	<LOD	<LOD	<LOD	<LOD	<LOD	<LOD	<LOD	<LOD
A. p.	2	49±1%	<LOD	<LOD	6±0.5%	2±0.4%	<LOD	<LOD	<LOD	<LOD

(continued on next page)

Table 5-2 (continued)

Content ($\%_{w/w}$)	C_{EPS}	Glucose	Galactose	Mannose	Fructose	Rhamnose	Fucose	Xylose	Arabinose	GlcAc
C. b.	2	31±6%	<LOD	8±2%	5±1%	<LOD	<LOD	<LOD	1±0.4%	5±1%
F. d.	2	60±6%	<LOD	<LOD	11±2%	<LOD	<LOD	<LOD	1±0.5%	<LOD
G. a.	2	<LOD	<LOD	<LOD	<LOD	<LOD	<LOD	<LOD	<LOD	<LOD
N. f.	2	14±3%	16±4%	<LOD	5±1%	3±1%	13±3%	<LOD	2±0.2%	<LOD
N. l.	2	<LOD	34±4%	16±2%	<LOD	<LOD	<LOD	11±1%	<LOD	<LOD
N. z.	2	<LOD	11±3%	14±5%	<LOD	<LOD	<LOD	16±5%	2±0.1%	<LOD
O. r.	2	<LOD	<LOD	<LOD	<LOD	<LOD	<LOD	<LOD	<LOD	<LOD
P. b.	2	13±2%	<LOD	<LOD	<LOD	<LOD	<LOD	<LOD	<LOD	<LOD
P. k.	2	12±1%	<LOD	<LOD	<LOD	<LOD	<LOD	<LOD	<LOD	<LOD
S. m.	2	<LOD	<LOD	<LOD	<LOD	<LOD	<LOD	<LOD	<LOD	<LOD
S. r.	2	4±1%	5±1%	<LOD	<LOD	4±1%	<LOD	<LOD	1±0.2%	<LOD
T. b.	2	<LOD	<LOD	<LOD	<LOD	<LOD	<LOD	<LOD	<LOD	<LOD
T. s.	2	9±4%	7±3%	<LOD	<LOD	<LOD	<LOD	<LOD	6±3%	13±0.3%
BG11	2	<LOD	<LOD	<LOD	<LOD	<LOD	<LOD	<LOD	<LOD	<LOD
ESM	2	<LOD	<LOD	<LOD	<LOD	<LOD	<LOD	<LOD	<LOD	<LOD

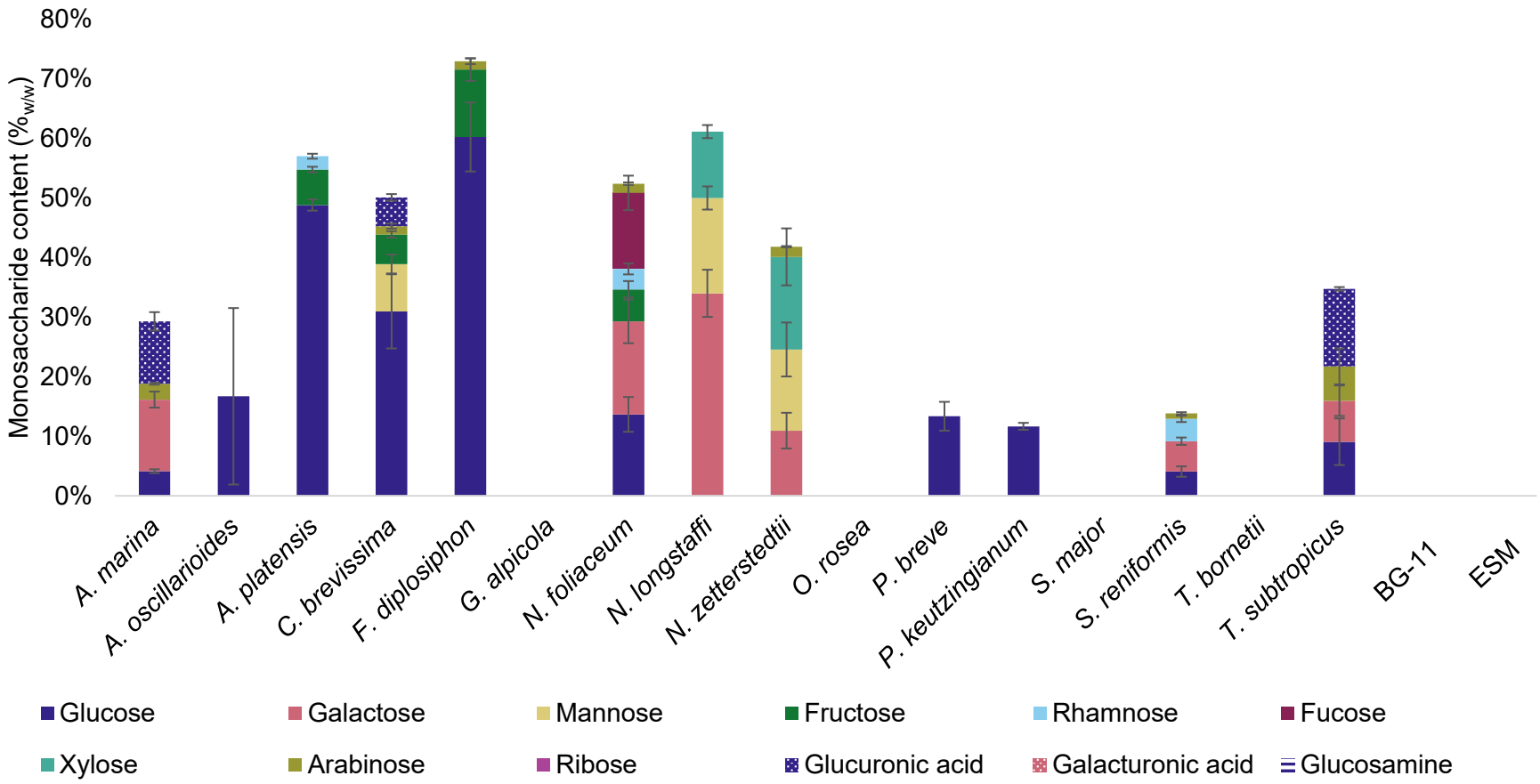


Figure 5-4 Monosaccharide composition of extracellular polymeric substances (EPS) from novel cyanobacteria based on high-performance anion-exchange chromatography with pulsed amperometric detection (HPAEC–PAD).EPS were obtained after 60 days of cultivation at 25°C and 20 µmol m^{-2} s^{-1} light. Bars represent the proportion of each monosaccharide (g monosaccharide per g EPS, $\%_{w/w}$) as stacked bars (not accumulated values). Data points represent mean ± 1 standard deviation. Species with triplicate datasets (n=3): *Acaryochloris marina*, *Calothrix brevissima*, *F. diplosiphon*,

Nostoc foliaceum, *Nostoc longstaffi*, *Nostoc zetterstedtii*, *Oscillatoria rosea*, *Phormidium breve*, *Sphaerospermopsis reniformis* and *Trichormus subtropicus*. Species with duplicate datasets (n=2): *Anabaena oscillarioides*, *Arthrospira platensis*, *Gloeocapsa alpicola*, *Phormidium keutzingianum*, *Spirulina major* and *Tychonema bornetii*. Calibration curves can be found in Figure 12-1; trendline equations, limit of detection (LOD) and limit of saturation (LOS) can be found in Table 12-1.

The positive control, *A. platensis* consisted of 49 ± 1%$_{w/w}$ (n=2) glucose, 6 ± 0.5%$_{w/w}$ (n=2) fructose, 2 ± 0.4%$_{w/w}$ (n=2) rhamnose. In literature, monosaccharides composition of *A. platensis* varied depending on the study. As shown in Table 2-2, two publications identified the EPS from *A. platensis* as being predominantly composed of glucose, galactose, and fucose, with both studies reporting comparable results. However, for other sugars, such as xylose and galacturonic acid, the numbers varied considerably more. This was most pronounced for rhamnose content, which ranged from 3.7%$_{w/w}$ to 41%$_{w/w}$ [61, 66].

Generally, HPAEC-PAD is a reliable method to determine the monosaccharide composition of microalgae as it provides high-resolution analysis for the most commonly occurring monosaccharides [72]. However, the accuracy of the results could be further improved by optimising the hydrolysis protocol. Suboptimal hydrolysis conditions can result in incomplete release of monosaccharides from the EPS, whereas supraoptimal hydrolysis can lead to degradation of monosaccharides. For instance, pentoses were shown to degrade more rapidly after release from the polymer due to them being less stable than hexoses [72]. As shown by Decamp, et al. [72], hydrolysis kinetics are polymer-dependent, so the best results can be obtained by optimising the hydrolysis protocol for each EPS individually. In this study, no peaks were detected after TFA hydrolysis for the monosaccharide standards glucosamine, ribose, fructose, galacturonic acid and glucuronic acid, indicating degradation (data not shown). In particular for these monosaccharides, an optimised hydrolysis protocol could further improve results.

Visually comparing Figure 5-2 and Figure 5-4, it can be seen that the sums of monosaccharides obtained from HPAEC-PAD (represented by the height of the stacked bars) were similar to the results of the total sugar results (phenol-sulphuric acid method). For most species, the sugar content was slightly higher than the sum of identified monosaccharides. Discrepancies may stem from inaccuracies inherent in the phenol-sulphuric acid method, in addition to the non-optimal hydrolysis conditions mentioned in the previous paragraph. The phenol-sulphuric acid method can lead to an over- or underestimation due to the use of one standard (glucose) for a complex mixture [316]. Furthermore, many substances can interfere with colorimetric

carbohydrate assays and result in false readings [317]. All things considered the two independent methods were in agreement.

5.4 Selection of Seven Novel Cyanobacteria Species for EPS Properties Analysis

Seven species from the 15 novel species of the screening experiment were selected for properties analysis. Selection was based on several criteria, considering the final aim of identifying a species and product suitable for commercial production. Freshwater species are preferable over marine species to avoid the desalting need [21]. Axenic species are advantageous over xenic mixtures, as other species can interfere with the observed EPS by consuming or producing EPS themselves. High EPS titre is desirable to facilitate the industrial development of cyanobacterial EPS [21]. EPS compositions and applications with higher economical value are beneficial to increase revenues and attain an profitable produciton process.

As detailed in section 2.2.3, several structural features of cyanobacterial EPS correlate with their functional properties. The anionic nature, mainly due to uronic acids and other acidic substituents, promotes metal binding and adhesion, while higher uronic acid content is linked to flocculating activity [39, 44, 63, 318]. Hydrophobic groups such as acetyl groups, deoxy sugars, and peptides contribute to emulsifying and rheological behavior, and sulphate substitution has been associated with various bioactivities, including antiviral and antioxidant effects [11, 15, 108, 260, 261, 319, 320].

Based on this information, *T. bornetii*, *P. breve*, *G. alpicola*, *F. diplosiphon*, *S. reniformis, S. major*, *P. keutzingianum* and *O. rosea* were considered unsuitable due to their low EPS titre (< 0.34 g L^{-1}). Seven other species with high EPS titre and/or interesting composition were selected for properties testing. *A. marina* produced the highest titre of the marine species (sulphated EPS, 0.24 ± 0.07 g EPS L^{-1}, n=3), making it interesting to test for bioactive properties. The axenic *N. zetterstedtii* was interesting due to the high sugar content (82 ± 14%, n=3), since high reducing sugar content can affect antioxidant activity of EPS [107]. The deoxy sugars fucose (13 ± 3%, n=3), and rhamnose (3 ± 1%, n=3), found in *N. foliaceum* could be related to emulsifying and rheological properties of EPS [11, 319, 320]. The axenic *A. oscillarioides* showed high EPS titre of 0.45 ± 0.46 g L^{-1} (n=2). *N. longstaffi* and *T. subtropicus* showed high EPS

production of 0.78 ± 0.18 g L^{-1} (n=3) and 0.77 ± 0.17 g L^{-1} (n=3) respectively, despite them being xenic. The emulsification, flocculation, metal-chelating, antioxidant and UV-protective properties of the EPS of these seven species were investigated. Thermal degradation behaviour and SEM pictures of the EPS can be found in the appendix in sections 12.6 and 12.7, respectively.

5.5 Functional Properties of Novel EPS

5.5.1 Emulsifying Activities

As shown in Figure 5-5*a*, the EPS of three species, *A. oscillarioides*, *C. brevissima* and *T. subtropicus*, showed emulsifying activities of about 65%, which was as efficient as the synthetic emulsifier Tween20 (64 ± 1%, n=3), and 2-3 times stronger than xanthan gum (26 ± 1%, n=3), which is a natural emulsion stabiliser used as positive control for emulsifying activity [83]. *N. foliaceum* showed moderate emulsifying activity (25 ± 11%, n=3), similar to xanthan gum. *A. marina*, *N. longstaffi* and *N. zetterstedtii* showed negligible activity similar to the negative control, water (3 ± 0.1%, n=3). In literature, 66.39% emulsion activity has been observed for EPS from *Nostoc flagelliforme* at 0.5% concentration [83].

As can be seen in Figure 5-5*b*, the emulsifying activity of the positive control, Tween20, did not increase past 65%, even when a 138-fold higher concentration of Tween20 was used. This was due to the oil:water ratio used (1:1), since at a later stage of the PhD, a larger oil:water ratio (3:2) was used, resulting in a higher emulsifying activity (80 ± 1% (n=2) with Tween20, section 6.10.4). It is expected that a 100% emulsifying activity can be achieved with EPS from *A. oscillarioides*, *C. brevissima* and *T. subtropicus* by optimising the oil:water ratio.

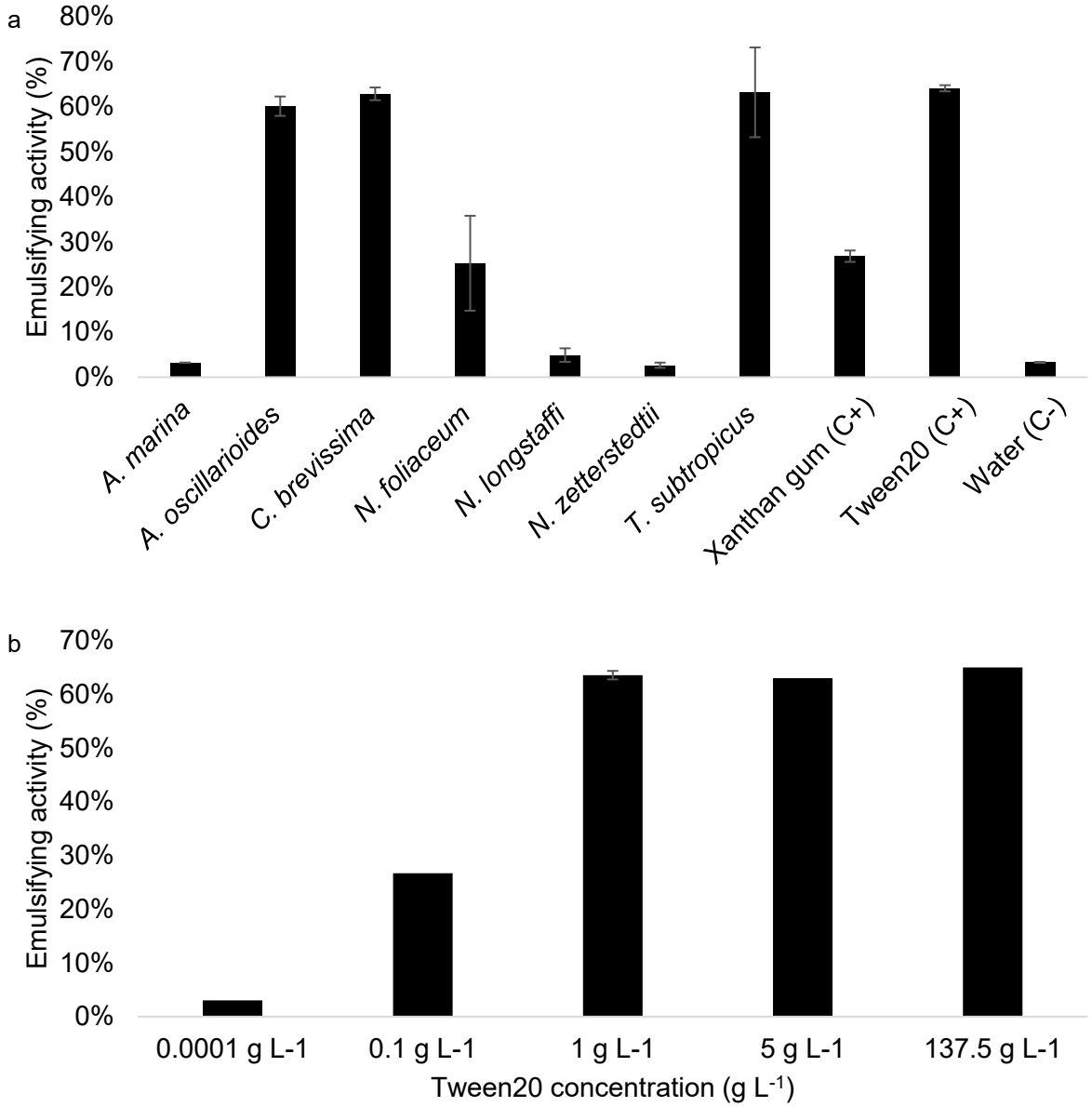


Figure 5-5 Emulsifying activities of extracellular polymeric substances (EPS) of seven novel cyanobacterial species after 50 days of cultivation at 25°C under 22 µmol m^{-2} s^{-1} light.(a) Emulsifying activity of EPS at 1 g L^{-1} compared to xanthan gum (C^+, positive control), Tween 20 (C^+, positive control), and water (C^-, negative control). Data points represent mean values of biological triplicates, and error bars indicate ± 1 standard deviation (n=3). (b) Concentration-dependent emulsifying activity of Tween 20 (C^+).

According to literature, emulsifying activity is a result of the hydrophobicity of the EPS caused by ester-linked acetyl groups, deoxy sugars (e.g., rhamnose and fucose) and peptidic fractions, and degree of branching [11, 85]. For *C. brevissima*, the emulsifying

properties might stem from the protein (9 ± 3%, n=3) content. The high emulsifying activity in *A. oscillarioides*, despite deoxy sugars content below the LOD, is likely caused by presence of proteins (5 ± 4%, n=2), of which even a small fraction can suffice [84, 86]. EPS from *T. subtropicus* showed high emulsifying activity (63 ± 10%, n=3), despite absence of deoxy sugars and proteins. EPS from *N. foliaceum* showed lower emulsifying activity (25 ± 11%, n=3) than other species, despite containing the highest deoxy sugar content of 13 ± 3% (n=3) fucose and 3 ± 1% (n=3) rhamnose. However, as will be described later (section 6.7), when a higher concentration of EPS of *N. foliaceum* was used (4 g L^{-1}), a higher emulsion activity (70 ± 1%, n=2) was obtained. No significant correlation between emulsifying properties and EPS composition (sugar, protein, sulphate or monosaccharide content) could be found (section 5.6).

One possible physiological reason cyanobacteria produce emulsifying EPS is to support attachment and dispersal, as suggested by studies on *Phormidium* J-1 [26]. This was discussed in the literature review (section 2.2.3.1), with the specific relationship to the species studied in this PhD project elaborated in the Discussion chapter (section 9.5).

5.5.2 Flocculating Properties

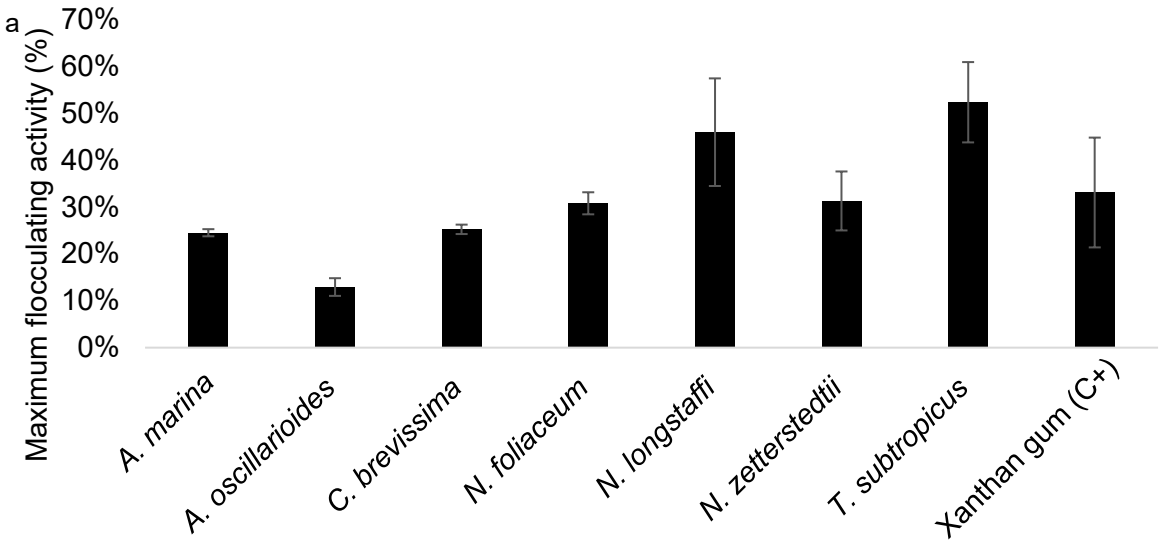
The novel EPS exhibited flocculating activity, which varied greatly, based on species and concentration (Figure 5-6). *T. subtropicus* and *N. longstaffi* showed the highest maximum flocculating activities of 52 ± 9% (n=3) and 46 ± 11% (n=3), respectively, exceeding that of the positive control, xanthan gum (33 ± 12%, n=3). *N. foliaceum* and *N. zetterstedtii* showed flocculating activities of 31 ± 2% (n=3), similar to that of xanthan gum. Slightly lower flocculating activity was found in *A. marina* (25 ± 1%, n=2) and *C. brevissima* (25 ± 1%, n=2). The lowest flocculating activity was found in *A. oscillarioides* (13 ± 2%, n=2).

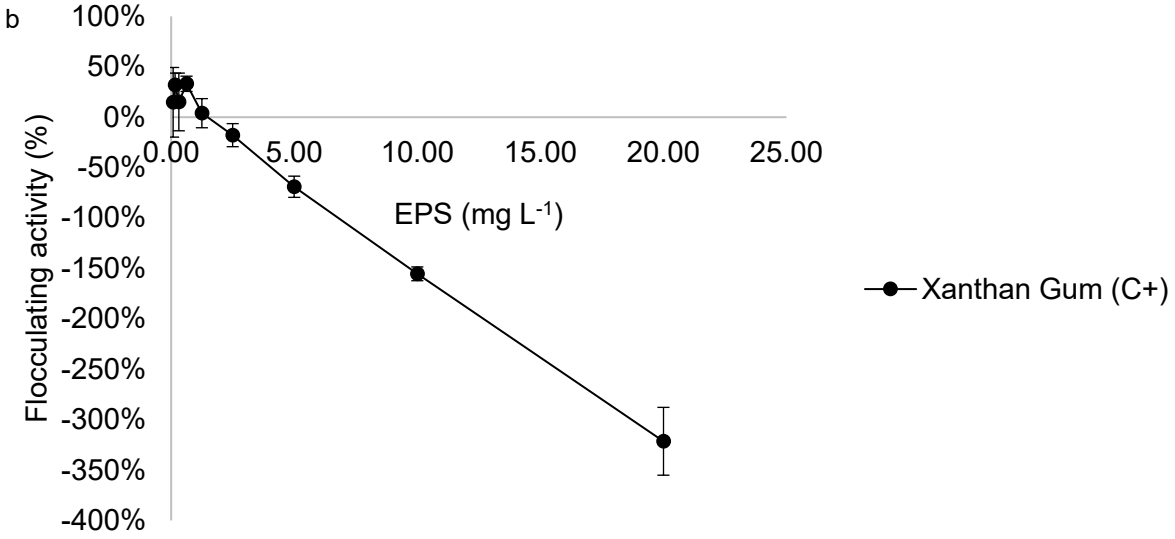
Interesting was the non-linear pattern of flocculation activity based on concentration. *C. brevissima* (Figure 5-6*c*) and *A. marina* (not shown) followed a similar pattern to the positive control, xanthan gum (Figure 5-6*b*): At lower concentrations, the flocculating activity increased until a maximum value, after which it declined drastically into negative values. A different pattern was visible for *T. subtropicus*, which showed the

highest maximum flocculating activity (52 ± 9, n=3, Figure 5-6*d*): The flocculating activity increased at lower concentrations until a first peak, followed by a strong decrease, after which it increased again and flattened out at around 50%. The graphs of *N. longstaffi, A. oscillarioides, N. foliaceum* and *N. zetterstedtii* were highly irregular, with large error bars making it difficult to discern clear trends (data not shown).

A possible explanation for the non-linear flocculation activity profiles is the complex mode of action of flocculation, which can lead to flocculation at certain concentrations and dispersion at others [91]. Negative flocculation values are obtained when kaolin particles are remaining in suspension longer than in the blank, which indicates EPS cause dispersion rather than flocculation. Negative flocculation rates have been reported in the literature by Bonilla T and Allen [92].

As described in section 2.2.3.2, with increasing polymer concentration the observed flocculation mechanisms are: 1) bridging, 2) steric stabilisation, 3) depletion flocculation and 4) depletion stabilisation [94]. For *C. brevissima*, *A. marina* and xanthan gum, at low concentration, bridging occurred leading to an increase of the flocculation activity until reaching the maximum peak, which corresponded to the optimal flocculant concentration for ideal coverage of the kaolin clay particles. At higher polymer concentration, the coverage of the particle was too thick, resulting in steric stabilisation, visible as the decreasing flocculation activity. For *T. subtropicus*, *N. longstaffi, N. foliaceum* and *N. zetterstedtii*, the bridging and steric stabilisation effects were also observed, which is visible as the first peak. However, instead of continuing into the negative part of the y-axis, the flocculating activity of EPS of these species increased again. This increase could be a result of depletion flocculation. Depletion flocculation occurs when polymers are present in the solution around particles except for the space between particles, resulting in an osmotic effect that attracts the particles to each other [94].


a
Maximum flocculating activity (%)
70%
60%
50%
40%
30%
20%
10%
0%
A. marina
A. oscillarioides
C. brevissima
N. foliaceum
N. longstaffi
N. zetterstedtii
T. subtropicus
Xanthan gum (C+)


b
Flocculating activity (%)
100%
50%
0%
-50%
-100%
-150%
-200%
-250%
-300%
-350%
-400%
0.00
5.00
10.00
15.00
20.00
25.00
EPS (mg L-1)
Xanthan Gum (C+)

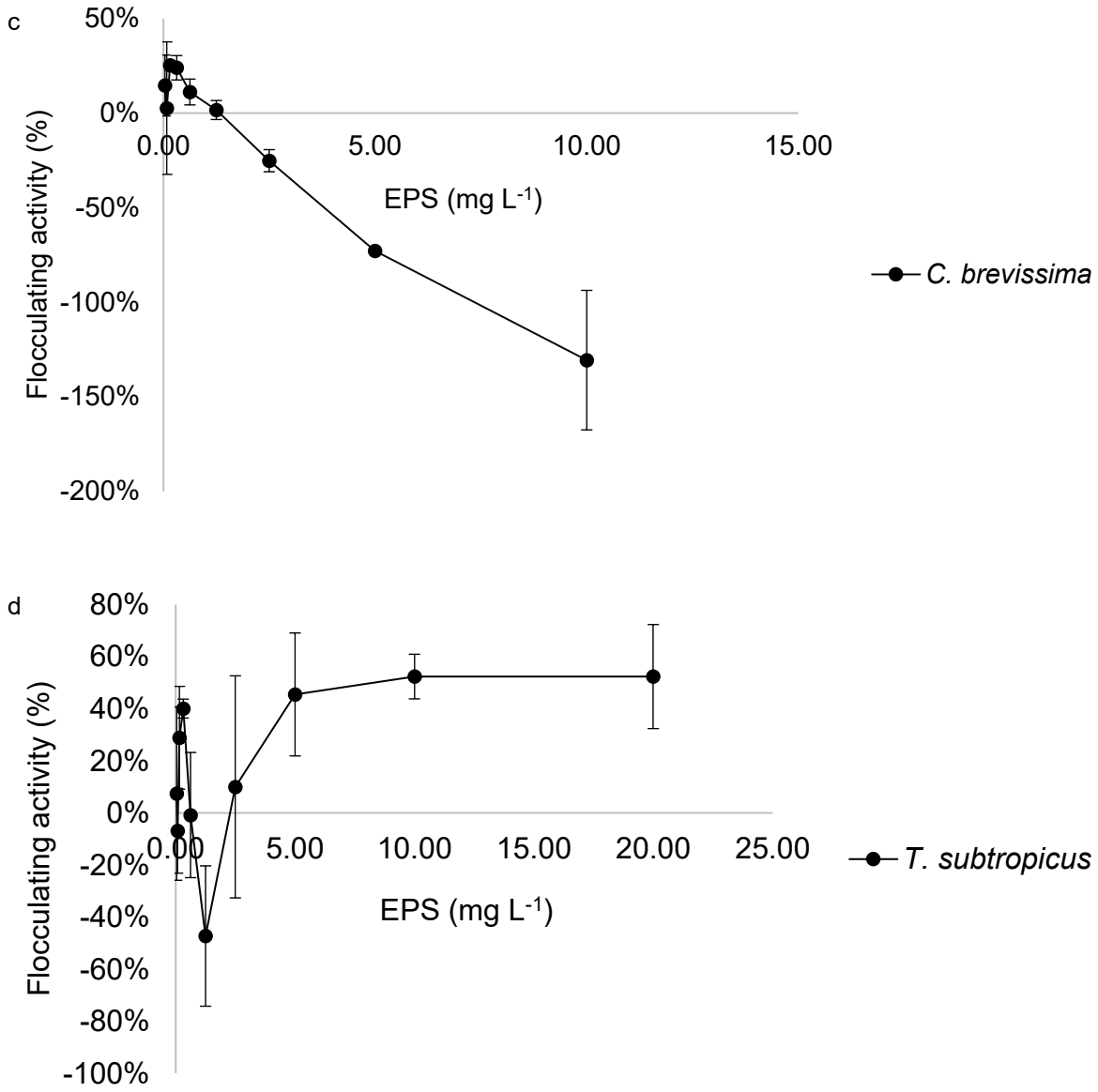


Figure 5-6 Flocculating activity of extracellular polymeric substances (EPS) from novel cyanobacterial species compared to xanthan gum (positive control, C^+).EPS were obtained after 50 days of cultivation at 25°C under 22 µmol m^{-2} s^{-1} light. Data points represent mean ± 1 standard deviation. Species with triplicate datasets (n=3): *Anabaena oscillarioides*, *Calothrix brevissima*, *Nostoc foliaceum*, *Nostoc longstaffi*, *Nostoc zetterstedtii*, and *Trichormus subtropicus*; species with duplicate dataset (n=2): *Acaryochloris marina*. (a) Maximum obtained flocculating activity of species and xanthan gum (C^+). (b) Flocculating activity of xanthan gum depending on concentration (mg L^{-1}). (c) Flocculating activity of EPS from *C. brevissima* depending on EPS concentration (mg L^{-1}). (d) Flocculating activity of EPS from *T. subtropicus* depending on EPS concentration (mg L^{-1}).

Comparing the maximum obtained flocculation activity with the respective EPS composition, which will be described in more detail in section 5.6, it is noticeable that *T. subtropicus*, which showed the strongest flocculating activity (52 ± 9%, n=3) also had the highest content of uronic acids (13 ± 0.3%, n=2), which is correlated to flocculating activity [44]. However, the second highest flocculating activity (46 ± 11%, n=3) was obtained with EPS from *N. longstaffi*, which contained no uronic acids. In fact, taking all seven species into consideration, no correlation between flocculation and uronic acid content or any other composition (sugar, protein, sulphate or monosaccharide content) was found (section 5.6). The reason for flocculating activity in *N. longstaffi* might be caused by other characteristics such as charge density caused by groups other than carboxylate groups of uronic acids. EPS of *A. marina* showed low flocculating activity (26 ± 1%, n=2) despite high uronic acids content (10 ± 2%, n=2). As described in section 2.2.3.2, too high electron density can lead to intramolecular repulsion of polysaccharide fragments, preventing bridging flocculation. Furthermore, even if charge density is optimal, if the polysaccharide is branched, too short or inflexible, this also prevents bridging flocculation (section 2.2.3.2). For instance, EPS of *C. brevissima* showed high emulsifying (63 ± 1%, n=3) but moderate flocculating activity (25 ± 1%, n=3) despite an uronic acid content of 5 ± 1% (n=3). This could indicate branched rather than linear structure, as branched structure is beneficial for emulsifying properties by causing steric stabilisation, which in turn is disadvantageous for flocculating properties [88, 94]. Further analysis would be interesting to relate flocculating activity with EPS characteristics. Polysaccharides with higher molecular weight, longer chains and lower charge density are more effective in bridging flocculation [93, 97, 99]. Gel permeation chromatography or size exclusion chromatography are commonly used to determine the molar mass of polysaccharide fractions [100]. To determine charge density, colloid titration can be used to identify the mole percent of charged groups [321]. Additionally, zeta-potential measurements would reveal surface charge and help link EPS charge to flocculating performance [322]. However, these analyses were not performed due to time constraints.

It was promising that two novel EPS performed better than the positive control, however, the values were lower than flocculating activities of EPS from cyanobacteria in literature: EPS from *Anabaena* sp. BTA992 have shown flocculating activities as high as 90% [45]. Another type of flocculating assay might provide more accurate

results with lower variation in the replicates, as there were obstacles with the kaolin clay assay, such as heterogeneity in the clay suspension and disturbance of the settling process caused by drops from the falling into the plastic tubes. However, most authors appear to use turbidity-based flocculation assays [45, 83]. Furthermore, it would be interesting to see how the EPS compare to industrially used flocculants and behave with real-world applications (e.g. flocculation of wastewater). Flocculating EPS can find application in food, water purification and microalgae harvesting as described in section 2.2.3.2.

A possible physiological role of producing flocculating EPS could be to flocculate suspended particles to increase light availability in the water column. This was described in literature to explain the reason of *Phormidium* J-1 to produce the emulsifying EPS *Emulcyan*, however it would also make sense as a reason to produce EPS with flocculating properties [323].

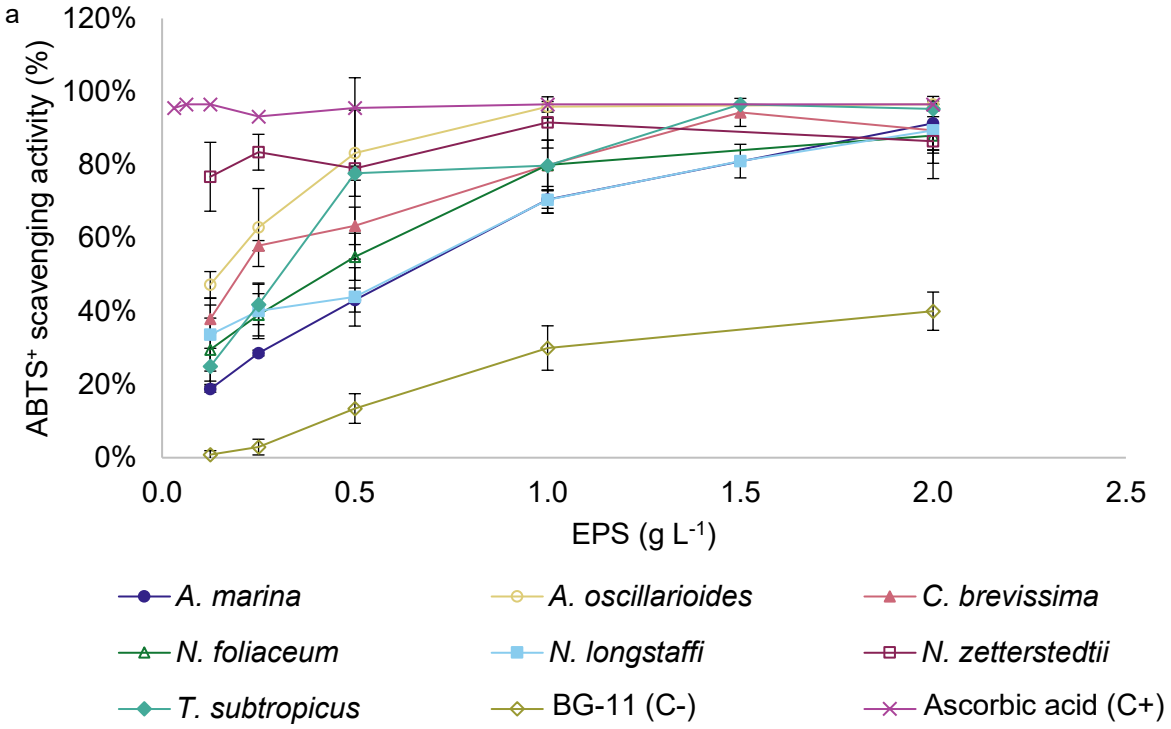
5.5.3 Antioxidant Activities

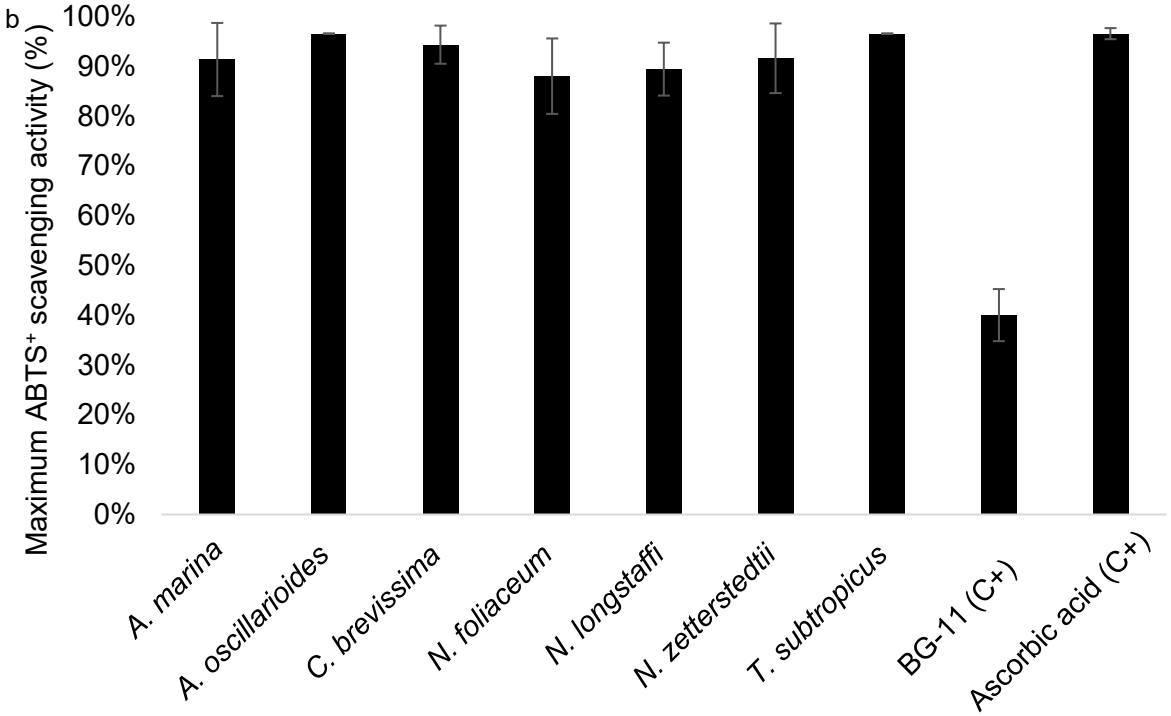
The antioxidant capacity of the novel EPS was evaluated by quantifying the scavenging activity of two radicals, 2,2-diphenyl-1-picrylhydrazyl (DPPH) and 2,2'-azino-bis(3-ethylbenzothiazoline-6-sulfonic acid) cation ($ABTS^+$). DPPH and $ABTS^+$ are dark coloured radicals, purple and green, respectively, whereas the neutral forms are yellow (DPPH-H) and colourless (ABTS). The colour change results in a decrease of the absorbance, which is proportional to the antioxidant capacity of the sample [106].

The DPPH and $ABTS^+$ scavenging activities depending on EPS concentration are shown in Figure 5-7. The $ABTS^+$ removal capacity was dose-dependent, increasing with higher EPS concentrations. All species reached high $ABTS^+$ scavenging activities (89-97%) at high enough EPS concentrations. *N. zetterstedtii* exhibited high $ABTS^+$ scavenging efficiency, reaching 77 ± 9% (n=3) removal at the lowest EPS concentration tested (0.0125 g L^{-1}), which increased to 92 ± 12% (n=2) at 1 g L^{-1}. *A. oscillarioides*, *C. brevissima, T. subtropicus* and *N. foliaceum* showed slightly less removal at the lowest EPS concentration with removal activities between 25 ± 5% (n=3, *T. subtropicus*) to 47 ± 4% (n=3, *A. oscillarioides*), but also removed nearly all the $ABTS^+$ radical at the highest EPS concentration tested (2 g L^{-1}). *A. marina* and *N. longstaffi* showed the lowest $ABTS^+$ scavenging activities at lowest EPS concentration,

gradually increasing until reaching a maximum of 89 ± 5% (n=3, *N. longstaffi*) and 91 ± 7% (n=2, *A. marina*), when the EPS concentration was sufficiently high (2 g L^{-1} EPS). However, the EPS were less effective than the positive control, ascorbic acid, which removed nearly all (96 ± 1%, n=3) of the $ABTS^+$ radical at the lowest concentration tested (0.009 g L^{-1}). Interestingly, even BG-11 showed a maximum $ABTS^+$ scavenging activity of 40 ± 5% (n=3). However, the values of all species were significantly different to BG-11 ($p \leq 0.023$). The scavenging potential of BG-11 could stem from compounds such as citric acid, which functions as an antioxidant [324].

DPPH scavenging activities were observed to be lower than those for $ABTS^+$. DPPH removal increased with increasing concentrations but flattened out at a maximum value of 20-45%, depending on the species. Interestingly, *N. longstaffi* exhibited the highest DPPH removal activity (45 ± 6%, n=3), despite obtaining the lowest $ABTS^+$ scavenging activity (89 ± 5%, n=3). *A. oscillarioides*, *C. brevissima, T. subtropicus, N. zetterstedtii* and *N. foliaceum* removed DPPH to a similar extent, reaching maximum activities of 24-30%. *A. marina* showed the lowest maximum DPPH scavenging activity (20 ± 8%, n=2), similar to the $ABTS^+$ results. The DPPH removal activity of the positive control, ascorbic acid, was considerably higher than that of the novel EPS, reaching 93 ± 1% (n=3) of DPPH removal at a concentration as low as 0.01 g L^{-1}. DPPH scavenging activity of the negative control, BG-11, was negligible (1 ± 2%, n=3).


a
120%
100%
80%
60%
40%
20%
0%
ABTS+ scavenging activity (%)
0.0
0.5
1.0
1.5
2.0
2.5
EPS (g L-1)
A. marina
A. oscillarioides
C. brevissima
N. foliaceum
N. longstaffi
N. zetterstedtii
T. subtropicus
BG-11 (C-)
Ascorbic acid (C+)


b
100%
90%
80%
70%
60%
50%
40%
30%
20%
10%
0%
Maximum ABTS+ scavenging activity (%)
A. marina
A. oscillarioides
C. brevissima
N. foliaceum
N. longstaffi
N. zetterstedtii
T. subtropicus
BG-11 (C+)
Ascorbic acid (C+)

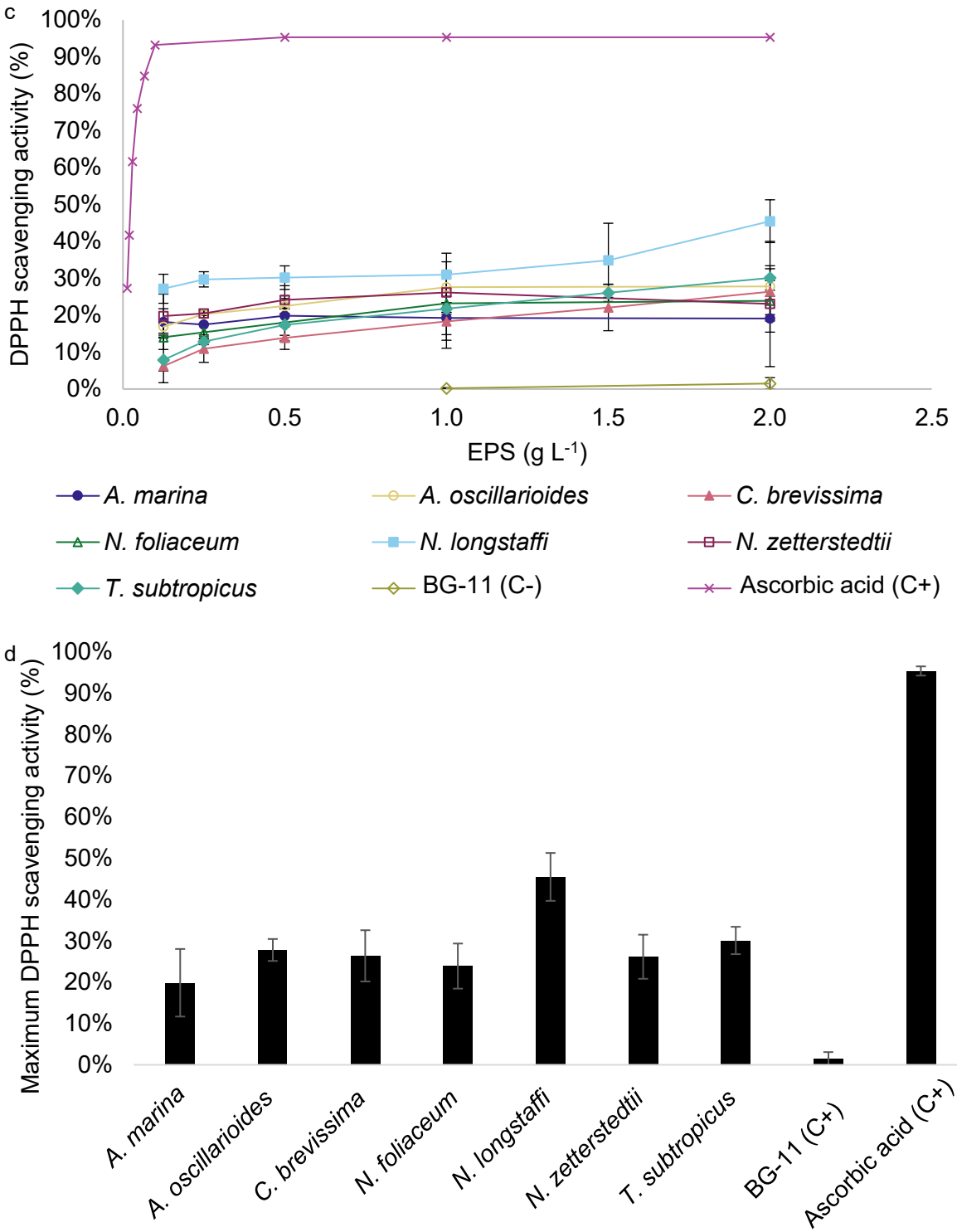


Figure 5-7 Antioxidant activity of extracellular polymeric substances (EPS) from novel cyanobacterial species after 50 days of cultivation at 25°C under 22 µmol m^{-2} s^{-1} light.(a) 2,2'-Azino-bis(3-ethylbenzothiazoline-6-sulfonic acid) cation ($ABTS^{+}$) radical scavenging activity as a function of EPS concentration (g L^{-1}). (b) Maximum $ABTS^{+}$ scavenging activity. (c) 2,2-Diphenyl-1-picrylhydrazyl (DPPH) radical scavenging activity as a function of EPS concentration (g L^{-1}). (d) Maximum DPPH scavenging activity. Data points represent mean ± 1

standard deviation. Species with triplicate datasets (n=3): *Anabaena oscillarioides*, *Calothrix brevissima*, *Nostoc foliaceum*, *Nostoc longstaffi*, *Nostoc zetterstedtii*, and *Trichormus subtropicus*; species with duplicate datasets (n=2): *Acaryochloris marina*. Calibration curves can be found in Figure 12-1, trendline equations, limit of detection (LOD) and limit of saturation (LOS) can be found in Table 12-1.

The dose-dependent response is commonly seen for antioxidant activities of EPS from cyanobacteria and other bacteria, flattening out at values between 45-95% [117, 118, 325, 326]. Neutralisation of the radicals $ABTS^+$ and DPPH occurs by transformation into ABTS and DPPH-H, respectively, which indicates that the novel EPS were good electron and hydrogen donors [106, 110]. *N. longstaffi*, which exhibited the highest DPPH (46 ± 6%, n=3) but lowest $ABTS^+$ scavenging activity (89 ± 5%, n=3), might be a good hydrogen donor but a poorer electron donor. In species from literature studies, bioactive properties like antioxidant capacity were positively correlated to the sulphate (r = 0.878) and mannose content of EPS (r = 0.942) and negatively to the glucose content (r = −0.905) [108, 110]. However, as can be seen in section 5.3.1, *A. marina* has the highest sulphate content among the seven species (8 ± 1%, n=3) yet shows the lowest DPPH scavenging capacity (20 ± 8%, n=2). In fact, no correlation between antioxidant properties and EPS composition (sugar, protein, sulphate or monosaccharide content) was found in this study (r < 0.95). The $ABTS^+$ scavenging activities were generally higher than DPPH scavenging activities, which was observed for other EPS in literature and suggested to be attributed to their affinity differences, with $ABTS^+$ being hydrophilic and DPPH hydrophobic [327, 328].

Antioxidant properties can make the EPS functional ingredients for food, cosmetics and pharmaceutical products, as described in section 2.2.3.3. However, the obtained $ABTS^+$ and DPPH removal activities were lower than those of ascorbic acid and of EPS in literature. As described in the literature review (section 2.2.3.3), EPS from other cyanobacteria have shown antioxidant properties as high as 90-95%, exceeding that of the positive control (ascorbic acid) [117, 118]. It is uncertain whether the antioxidant activity observed in the novel EPS is sufficiently strong to compete with other natural antioxidant agents.

As described in the literature review (section 2.2.3.3), characteristics such as type of glycosidic bond, ways of connections and monosaccharides composition determine whether or not a polysaccharide has bioactive properties, whereas solubility, relative molecular mass, main-chain configuration and spatial configuration affect the level of bioactivity. The bioactivity of the novel EPS could possibly be enhanced by the modifications described in section 2.2.3.3.

5.5.4 Iron-Chelating Properties

Iron-chelating activity was tested by mixing the EPS solution with Fe^{2+} ions and subsequent addition of ferrozine, which forms a ferrous ferrozine complex (magenta colour) with any residual Fe^{2+} ions, resulting in an increase of absorbance [276]. As shown in Figure 5-8*b*, EPS from *A. oscillarioides* showed the highest chelating activity (78 ± 18%, n=2, at 2 g L^{-1} EPS). Moderate chelating activity was observed in EPS from *N. zetterstedtii* (46 ± 7%, n=2)*, N. foliaceum* (55 ± 11%, n=3)*, C. brevissima* (43 ± 12%, n=3)*,* and *A. marina* (63 ± 0.3%, n=2). The positive control, EDTA, showed higher chelating activity than any of the species, binding 96 ± 1% (n=3) of the ferric ions from concentrations as low as 0.4 g L^{-1} EDTA. As described in the literature review (section 2.2.3.4), the chelating activity of EPS of another cyanobacterium, *Gloeocapsa gelatinosa*, (91%) has shown to exceed that of EDTA (75%) [118]. EPS[27] from another cyanobacterium, *A. variabilis* var. *ellipsospora*, showed an even higher chelation activity of 96% [108].

[27] EPS extraction method: "*Two volumes of chilled acetone were added to the culture for the precipitation of EP.*" [108] Cells were not examined for intactness afterward.

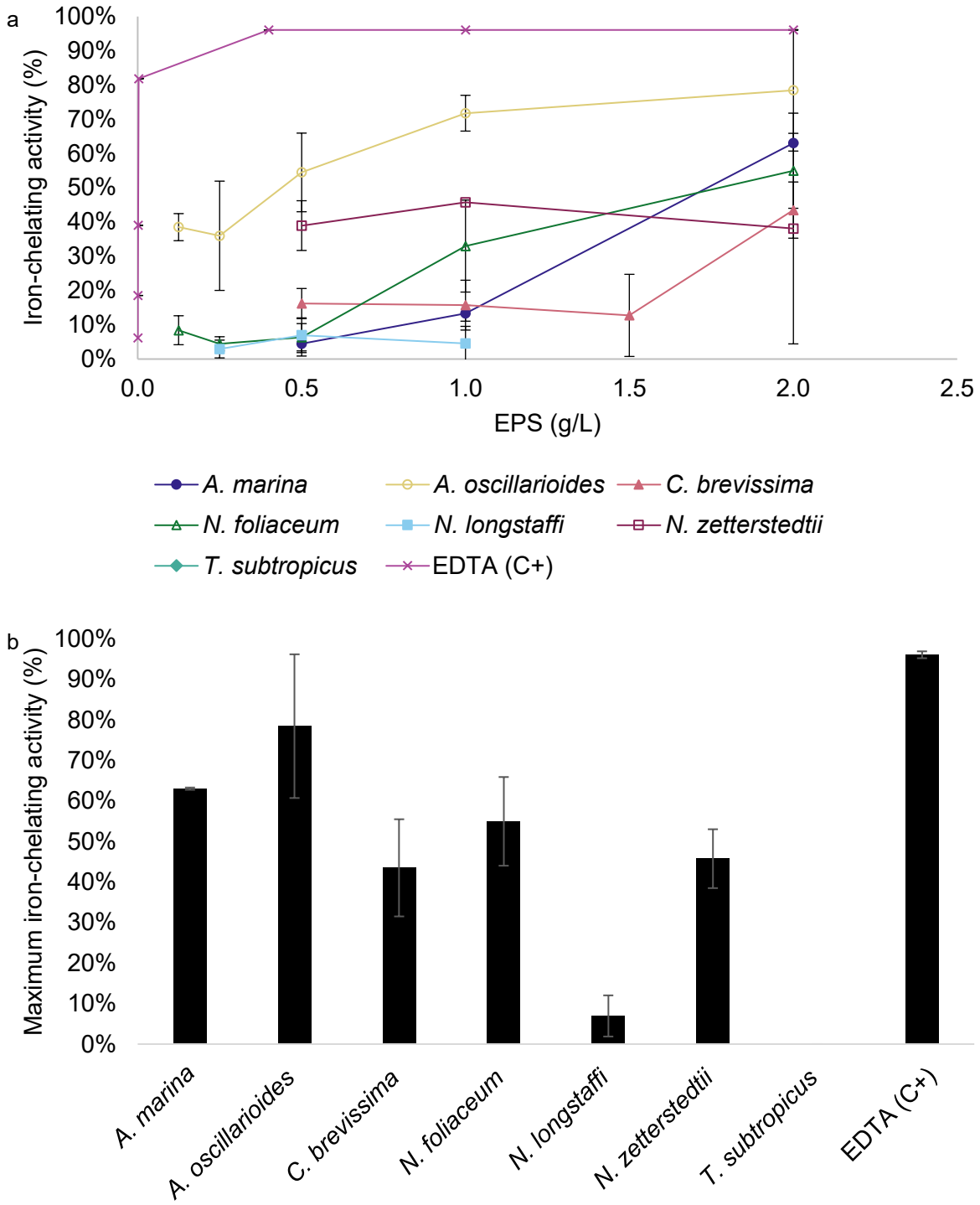


Figure 5-8 Iron-chelating activity of extracellular polymeric substances (EPS) from novel cyanobacterial species after 50 days of cultivation at 25°C under 22 µmol m^{-2} s^{-1} light.(a) Iron-chelating activity of EPS as a function of concentration (g L^{-1}) compared with the positive control Ethylenediaminetetraacetic Acid (EDTA, C^{+}). (b) Maximum iron-chelating activity obtained. Data points represent mean ± 1 standard deviation. Species with triplicate datasets (n=3): *Anabaena oscillarioides*, *Calothrix brevissima*, *Nostoc foliaceum*, *Nostoc longstaffi*, *Nostoc zetterstedtii*, and *Trichormus subtropicus*; species with duplicate datasets (n=2):

Acaryochloris marina. Calibration curves can be found in Figure 12-1; trendline equations, limit of detection (LOD) and limit of saturation (LOS) can be found in Table 12-1.

As shown in Figure 5-8*a*, chelating activity of EPS varied between species. EPS from *A. oscillarioides, N. zetterstedtii* and *C. brevissima* showed a dose-dependent response, with chelating activity increasing with higher EPS concentrations until flattening out at a maximum value. This pattern is coherent with cyanobacterial EPS in literature [108, 118]. EPS from *N. foliaceum* and *A. marina* showed a more gradual increase, whereas no iron-chelating activity could be detected in *T. subtropicus,* even at the highest EPS concentration (2 g L^{-1}). EPS from *N. longstaffi* showed low iron-chelating activity (7 ± 5%, n=3, at 0.5 g L^{-1} EPS).

Binding of cations (e.g. Fe^{2+}) can be a result of the negative charge of EPS caused by acidic sugars like uronic acids, inorganic substituents (e.g. sulphate groups) and/or organic acids such as pyruvate groups [20, 313]. More specifically, as mentioned in the literature review (section 2.2.3.4), chelating properties are a result of two or more of the following functional groups: C=O, –COOH, –O–, –OH, –SH, –S–, $–PO_3H_2$ and $–NR^2$, and a favourable structure–function configuration [130, 131]. For EPS from *A. oscillarioides*, which showed the highest chelating activity (78 ± 18%, n=2), the responsible functional groups could be hydroxyl groups from the neutral monosaccharides (glucose) and amino, thiol groups or disulfide linkage of the protein fraction (5 ± 4%, n=2). However, as most of the *A. oscillarioides* EPS was unidentified (68%), other groups from the non-identified part could play a role too. The second highest chelating activity, observed in EPS from *A. marina* (63 ± 0%, n=2), could be a result of carboxyl groups being present in the uronic acid content (10 ± 2%, n=2) and hydroxyl groups from the neutral monosaccharides, e.g. galactose (12 ± 1%, n=2). Moderate activity was observed in EPS from *N. foliaceum* and *N. zetterstedtii*, despite absence of uronic acids and proteins. Other functional groups could be present in the unidentified fraction. In contrast, EPS from *C. brevissima*, which contains moderate amounts of uronic acids (5 ± 2%, n=3) and proteins (9 ± 3%, n=3), only showed moderate chelating activity (43 ± 8%, n=3). Similarly, EPS from *T. subtropicus* did not exhibit chelating activity despite having the highest uronic acid content (13 ± 0%, n=2), possibly due to the absence of protein. EPS from these species might contain the required functional groups, but not in a favourable structure–function configuration for

effective chelation. Lastly, EPS from *N. longstaffi* showed low chelating activity (7 ± 0%, n=3), which could be explained by the absence of uronic acids and proteins. Based on the compositions of all seven species, no significant correlation between chelating properties and EPS composition (sugar, protein, sulphate or monosaccharide content) could be found (section 5.6). Analyses such as Nuclear magnetic resonance (NMR) could provide more insight into the spatial configuration of the EPS [329]. EPS with chelating properties can serve as natural antioxidants, functional food additives, and bio-based alternatives to EDTA in cleaning products, while also aiding in heavy metal removal from wastewater [12, 118].

5.5.5 UV-protective Properties

Absorbance measurements can give an indication of the UV-protective properties, as the transmittance, which is the percentage of the UV-radiation that is not blocked or filtered out by a sunscreen, can be calculated from the absorbance according to Equation 4-15 [278].

Figure 5-9*a* shows the UV/vis absorbance spectrum of the novel EPS dissolved in water at a concentration of 1 g L^{-1}. EPS of all species, except *A. marina*, showed a peak around 190-230 nm, as well as a shoulder around 280 nm. EPS from *N. zetterstedtii*, *N. foliaceum*, *A. oscillarioides, T. subtropcius* and *C. brevissima* also showed absorbance in the 300-400 nm region. EPS from *A. oscillarioides* showed the highest absorbance, followed by *N. zetterstedtii, C. brevissima, N. foliaceum* and *T. subtropicus.* EPS from *A. marina* and *N. longstaffi* showed the lowest absorbance. The shoulder at 300-400 nm was most pronounced in EPS from *C. brevissima*.

The UV/vis absorbance spectrum was similar to that of *A. platensis* in literature. As the authors state, the first peak (190-230 nm) can be caused by a variety of functional groups, including amine, carboxyl, carbonyl, and ester groups [61]. All screened species are expected to have at least one of these groups, since carbonyl, carboxyl and amino groups are found in the sugar, uronic acid and protein fraction, respectively. Ester-linked acetyl groups have been identified in other cyanobacterial EPS [11]. No correlation between UV absorbance values and EPS composition (sugar, protein, sulphate or monosaccharide content) was found ($r < 0.95$). The second peak around 260-280 nm could be caused by aromatic and polyaromatic compounds, found e.g. in

proteins, which were identified in EPS six species (section 5.3.1) [61]. Most interesting was the region between 300-400 nm, which could indicate the presence of MAAs or scytonemin [61]. MAAs are promising alternatives to commercial sunscreens, avoiding adverse health effects, such as endocrine dysfunction of the reproductive and developmental systems as well as ecological effects (e.g. coral bleaching) of conventional products [138, 146]. Especially compounds that protect from UV rays in the area of 285–350 nm would be most valuable, as near-UV light is the most detrimental to DNA and RNA [330]. Another photoprotective compound produced by cyanobacteria is the pigment scytonemin, which absorbs 90% of the radiation [156]. The UV/vis absorbance spectrum of the EPS had similarities with commercial sunscreen (SPF30, Figure 5-9*b*), which also showed a first peak (190-230 nm), a second peak around 280 nm and a shoulder between 300 and 400nm.

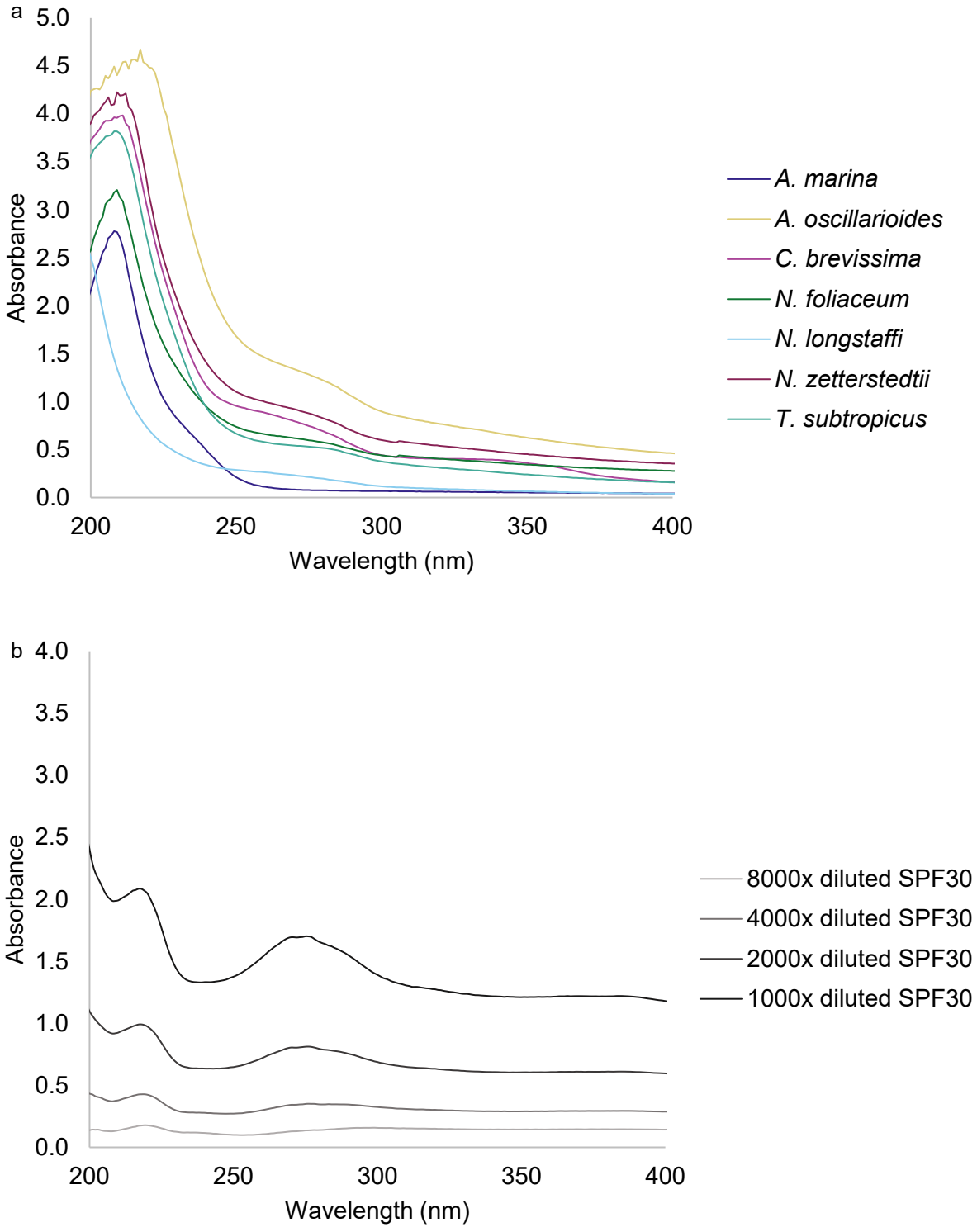


Figure 5-9 Ultraviolet (UV) light protection of extracellular polymeric substances (EPS) from novel cyanobacterial species compared with a commercial sunscreen (SPF 30) after 50 days of cultivation at 25°C under 22 µmol m^{-2} s^{-1} light.(a) Absorbance spectrum of EPS at 1 g L^{-1} in the UV range (200–400 nm). (b) Absorbance spectrum of commercial sunscreen in the UV

range (200–400 nm) at different dilutions. Data points represent mean values of biological replicates. Species with triplicate datasets (n=3): *Calothrix brevissima*, *Nostoc foliaceum*, *Nostoc longstaffi*, and *Trichormus subtropicus*; species with duplicate datasets (n=2): *Anabaena oscillarioides*, *Acaryochloris marina*; species without replicate: *Nostoc zetterstedtii*, SPF30.

The transmittance of the absorbance of the novel EPS was calculated according to Equation 4-15. UV-protection level was expressed as the fraction that does not get transmitted according to Equation 4-16. The transmittance of the EPS (1 g L^{-1}) compared to 4000-fold diluted sunscreen (SPF30) is shown in Figure 5-10. Considering only the relevant wavelength region (200-400 nm), most species, including *A. marina*, *C. brevissima*, *N. foliaceum*, *N. longstaffi* and *T. subtropicus* showed higher transmittance than 4000-diluted SPF30, indicating a lower UV-protection level. However, EPS from *A. oscillarioides* and *N. zetterstedtii* showed lower transmittance for each datapoint than SPF30, indicating potentially higher UV-protection. Given that the 4000-fold diluted SPF30 corresponds to a concentration of 0.25 g L^{-1}, while the EPS was at 1 g L^{-1}, this could indicate that the EPS from *A. oscillarioides* and *N. zetterstedtii* would need to be approximately four times more potent to achieve UV-protection comparable to SPF30. Even at a high EPS concentration, such as 500 g L^{-1}, an 8-fold increase in UV-absorbing properties would still be required to match the UV protection level of SPF30. If the UV-protective properties stem from the presence of MAAs, the production of MAAs could be enhanced by cultivating the species with UV-irradiation [224].

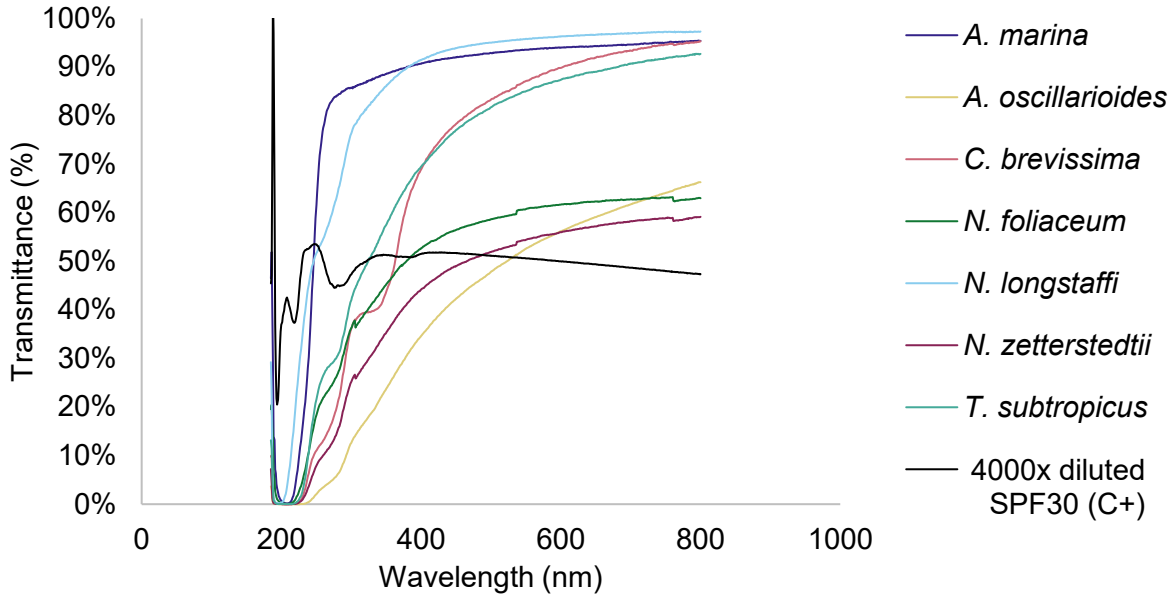


Figure 5-10 Transmittance of extracellular polymeric substances (EPS) from novel cyanobacterial species compared with 4000-fold diluted commercial sunscreen of sun protection factor (SPF) of 30 after 50 days of cultivation at 25°C under 22 µmol m^{-2} s^{-1} light.Transmittance was calculated based on absorbance according to Equation 4-15. Data points represent mean values of biological replicates. Species with triplicate datasets (n=3): *Calothrix brevissima*, *Nostoc foliaceum*, *Nostoc longstaffi*, and *Trichormus subtropicus*; species with duplicate datasets (n=2): *Anabaena oscillarioides*, *Acaryochloris marina*; species without replicate: *Nostoc zetterstedtii*, SPF30.

Once an adequate protection level is reached, several other challenges need to be addressed before the product can be commercialised. Firstly, the EPS have to be characterised, e.g. identifying the types of MAA present using HPLC [154]. Secondly, testing efficacy *in-vivo* is necessary to assess whether the EPS are suitable as UV-protective compounds [331]. Lastly, the safety of the product for humans has to be assured by testing cytotoxicity, skin penetration and skin tolerance [332].

5.6 Correlation Between EPS Composition and Properties

The correlation coefficient (Pearson) between compositional components (sugar, protein, sulphate and monosaccharide content) and the functional properties of the EPS were studied. Table 5-3 shows the results of the correlation coefficients *r* as a

heatmap. No significant correlations could be found, with all *r* values being lower than 0.95.

Glucose (r = 0.757) and protein (r = 0.646) content showed the strongest positive correlation with the emulsifying activity, indicating their potential to enhance emulsification, whereas galactose (r = -0.677) and xylose (r = -0.631) negatively impacted this property. Emulsifying properties are associated to amphiphilic character [11]. Glucose, the most prominent monosaccharide in cyanobacterial EPS, is hydrophilic and interacts with water, while proteins are hydrophobic and can bind to oil particles [28, 84]. The flocculating activity was positively influenced by arabinose (r = 0.579) and galactose (r = 0.5), suggesting that these sugars contributed to improved flocculation, while protein (r = -0.496) and glucose (r = -0.419) content had a negative effect. As proteins and glucose were positively influencing emulsifying properties, this could indicate that proteins rather contribute to stabilisation than flocculation. However, since the correlation coefficients are not significant, it is difficult to draw final conclusions.

When examining antioxidant activities, glucuronic acid (r = 0.418), arabinose (r = 0.392) and protein (r = 0.467) positively influenced $ABTS^+$ scavenging activity, whereas galactose and mannose (r = 0.723 and 0.704, respectively) showed positive correlation with DPPH scavenging activities. Mannose has been attributed to higher antioxidant activity, i.e. hydroxyl radical (•OH) scavenging activity in literature [110]. However, the observed correlations contradict the expected chemical behavior. $ABTS^+$ is neutralised by electron transfer, while DPPH is neutralised by hydrogen donation [106]. Mannose and galactose are reducing sugars capable of donating electrons, whereas glucuronic acid and proteins contain carboxyl groups that can donate hydrogen to neutralise DPPH. Since the correlation coefficients are not significant and the sample size is small (n=7), it is difficult to draw final conclusions. Despite Parwani, et al. [108] reporting positive correlation of antioxidant property with sulphate content, in this study sulphate content was slightly negatively correlated (r = -0.156 for $ABTS^+$ and r = -0.470 for DPPH).

Table 5-3 Heatmap showing Pearson correlation coefficient *r* between extracellular polymeric substances (EPS) composition and properties of seven cyanobacterial species.Results colour-coded for strongest positive correlation (blue) and strongest negative correlation (red). Values show mean ± 1 standard deviation. Species with triplicate datasets (n=3): *Calothrix brevissima*, *Nostoc foliaceum*, *Nostoc longstaffi* and *Nostoc zetterstedtii*. Species with duplicate datasets (n=2): *Acaryochloris marina*, *Anabaena oscillarioides* and *Trichormus subtropicus*. Abbreviations: Sug: sugar content; Pro: protein content; Sul: sulphate content; Glc: glucose; Fru: fructose; Man: mannose; Ara: arabinose; Gal: galactose; Fuc: fucose; GlcAc: glucuronic acid; Rha: rhamnose; Xyl: xylose; Emul: maximum emulsifying activity; Floc: maximum flocculating activity; ABTS: maximum azino-bis(3-ethylbenzothiazoline-6-sulfonic acid) cation ($ABTS^{+}$) scavenging activity; DPPH: maximum 2,2-diphenyl-1-picrylhydrazyl (DPPH) scavenging activity; Chel: maximum iron-chelating activity; UV260-300: UV-protection level of the 260-300 nm region, calculated from absorbance; UV301-400: UV-protection level of the 301-400 nm region, calculated from absorbance.

Pearson Coefficient	**Emul**	**Floc**	**ABTS**	**DPPH**	**Chel**	**$UV_{260-300}$**	**$UV_{301-400}$**
Sug	-0.296	0.316	-0.289	0.356	-0.384	0.244	0.186
Pro	0.646	-0.496	0.467	-0.131	0.282	0.369	0.384
Sul	-0.428	-0.242	-0.156	-0.470	0.326	-0.749	-0.673
Glc	0.757	-0.419	0.391	-0.246	0.265	0.518	0.517
Fru	0.239	-0.180	-0.343	-0.293	0.189	0.351	0.352
Man	-0.558	0.352	-0.399	0.704	-0.429	-0.234	-0.275
Ara	0.282	0.579	0.392	-0.220	-0.495	0.122	0.003
Gal	-0.677	0.500	-0.725	0.723	-0.462	-0.611	-0.659
Fuc	-0.097	-0.035	-0.595	-0.251	0.202	0.210	0.239
GlcAc	0.239	0.382	0.418	-0.276	-0.342	-0.208	-0.297
Rha	-0.097	-0.035	-0.595	-0.251	0.202	0.210	0.239
Xyl	-0.631	0.244	-0.345	0.399	-0.246	-0.056	-0.058

The iron-chelating activity did not show any strong positive correlation with any of the compositional aspects. Instead, it was negatively correlated with arabinose (r = -0.495)

and galactose (r = -0.462). Monosaccharides contain the necessary functional groups for metal-chelation. However, the literature highlights the importance of a favourable structure-function relationship, which might explain the low correlation score with the composition in this case [130, 131]. The maximum absorbance value in the area of 260-300 nm and 300-400 nm was related to glucose content, though the nature of this relationship remains unclear (r = 0.518 for 260-300nm and r = 0.517 for 300-400nm). Despite peaks in this area are associated with aromatic and polyaromatic compounds, found e.g. in proteins, the correlation with proteins was weak (r = 0.369 and r = 0.384, respectively) [61].

No significant correlation between composition and property was found using the Pearson coefficient, which investigates linear correlations only. Furthermore, no trends were identified when visually comparing trendlines (data not shown) of plotting each compositional aspect depending on each property, to account for non-linear trends. Additionally, no compositional variable showed the same ranking as any of the functional properties (rankings not shown). Possibly, the dataset was too small, as only seven species were tested regarding their properties. Additionally, the relationship between structure and function may be more nuanced than a straightforward one-to-one correspondence between composition and property. For example, antioxidant activity is a function of combination of several factors, rather than that of a single factor [109]. Lastly, a different incubator was used to grow the cultures to obtain the EPS used for the properties analysis (SciQuip Premium Compact) compared to the EPS used for composition analysis (New Brunswick Excella E24R). Possibly, equipment-specific differences, e.g. light quality or shaking diameter have led to differences in the produced EPS. Light colour has shown to influence EPS composition [177]. To better understand the correlation between composition and properties, one could either study a larger selection of EPS or focus on EPS from a single species. For the latter approach, this might involve analysing EPS fractions of different molecular weight, if present, or specifically modifying individual structural components to observe their impact on the overall properties. For example, in literature, different EPS fractions were isolated from the fungus *Hirsutella* sp. by using varying alcohol concentrations, resulting in strong correlations between antioxidant activity and monosaccharide type [110].

5.7 Selection of Species for Cultivation Conditions Optimisation

The seven novel EPS exhibited flocculating, emulsifying, UV-protective, metal-chelating and antioxidant properties. A summary of EPS and DCW titre, as well as functional properties of EPS can be found in Table 5-4. Most of these properties were moderate or low compared to the positive controls used. However, the results of the emulsifying assay were noteworthy, as three species showed emulsifying properties similar to the synthetic emulsifier Tween20 and 2-3x higher than xanthan gum at a concentration of 1 g L^{-1}. *C. brevissima* was presumed to be the most promising species due to the highest EPS titre (1.8 ± 0.10 g L^{-1}, n=2), its axenicity, and the high emulsifying activity (63 ± 1%, n=3), making it a potential production species for a bioemulsifier. In addition, the moderate antioxidant and UV-protective properties were interesting to explore a bioactive product as alternative.

Table 5-4 Summary of functional properties of extracellular polymeric substances (EPS) from seven novel cyanobacteria species.Table displays maximum EPS and dry cell weight (DCW) concentrations obtained, as well as emulsifying, flocculating, antioxidant (2,2'-azino-bis(3-ethylbenzothiazoline-6-sulfonic acid ($ABTS^+$) and 2,2-diphenyl-1-picrylhydrazyl (DPPH) scavenging), iron-chelating and ultraviolet (UV) protective activities and axenicity status.UV-protection was calculated from transmittance according to Equation 4-15 and Equation 4-16. Data represent mean ± standard deviation of biological triplicates (n=3) for most measurements, except for *A. m.* (flocculating, $ABTS^+$, DPPH, iron-chelating, UV-protection), *A.o.* (EPS_{Max}, DCW_{Max}, iron-chelating, UV-protection), *C.b.* (flocculating, iron-chelating), *N.z.* (iron-chelating) and *A.p.* (EPS_{Max}, DCW_{Max}), which were performed in duplicates (n=2). UV-protection assay of *N.z.* and SPF30 were performed without replicates (n=1). Values are colour-scaled (light to dark green), where darker green corresponds to higher values. Abbreviations: *A.m.: Acaryochloris marina; A.o.: Anabaena oscillarioides; C.b.: Calothrix brevissima; N.f.: Nostoc foliaceum; N.l.: Nostoc longstaffi; N.z.: Nostoc zetterstedtii; T.s.: Trichormus subtropicus; A.p.: Arthrospira platensis*; C^+: positive control; EDTA: ethylenediaminetetraacetic acid; SPF: sun protection factor; Ax.: axenic; X.: xenic.

	EPS_{max}	**DCW_{max}**	**Emulsifying activity**	**Flocculating activity**	**$ABTS^+$ scavenging activity**	**DPPH scavenging activity**	**Iron-chelating activity**	**UV-protection 260-300 nm**	**UV-protection 301-400 nm**	**Ax.**
Unit	g L^{-1}	g L^{-1}	%	%	%	%	%	%	%	
A. m.	0.24±0.07	4.95±0.28	3 ± 0.0%	25 ± 1%	91 ± 7%	20 ± 8%	63 ± 0.3%	22 ± 3%	14 ± 3%	Ax.
A. o.	0.45±0.46	2.18±0.14	60 ± 2%	13 ± 2%	97 ± 0.0%	28 ± 3%	78 ± 18%	96 ± 3%	87 ± 3%	Ax.
C. b.	1.79±0.15	1.41±0.10	63 ± 1%	25 ± 1%	94 ± 4%	26 ± 6%	43 ± 12%	87 ± 2%	63 ± 3%	Ax.
N. f.	0.59±0.08	3.71±0.32	25 ± 11%	31 ± 2%	88 ± 8%	24 ± 5%	55 ± 11%	78 ± 4%	63 ± 7%	Ax.
N. l.	0.77±0.17	3.95±0.29	5 ± 2%	46 ± 11%	89 ± 5%	45 ± 6%	7 ± 5%	44 ± 14%	23 ± 9%	X.
N. z.	0.61±0.12	2.25±0.08	3 ± 1%	31 ± 6%	92 ± 7%	26 ± 5%	46 ± 7%	90%	74%	Ax.
T. s.	0.78±0.18	3.61±0.50	63 ± 10%	52 ± 9%	97 ± 0.0%	30 ± 3%	N.A.	73 ± 5%	57 ± 5%	X.
C^+	*A. p.*	*A. p.*	Tween20	Xanthan gum	Ascorbic acid	Ascorbic acid	EDTA	SPF30	SPF30	N.A.
Value of C^+	0.51±0.04	1.43±0.33	64 ± 1%	33 ± 12%	97%+1%	95%+1%	96 ± 1%	96%	93%	N.A.

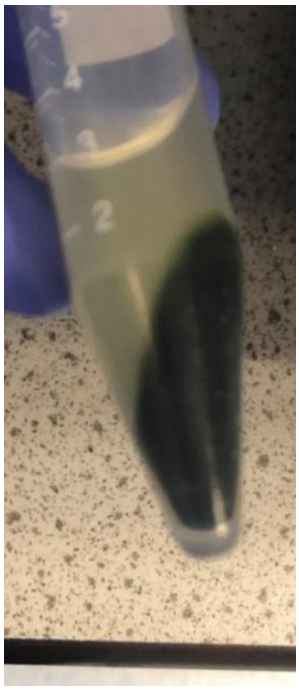


Figure 5-11 *Nostoc foliaceum* has a thick gel-like layer on top of DCW pellet after centrifugation and decanting of supernatant.

Additionally, *N. foliaceum* was selected for optimisation. *N. foliaceum* showed interesting EPS composition with high amounts of fucose (13 ± 3%, n=3), and three unknown sugars. Furthermore, there was one observation made during sample processing that could indicate potential for commercial value. When centrifuging and decanting the supernatant, *N. foliaceum* carried a thick gel-like layer on top of the DCW pellet. This layer sometimes appeared in other species as well, however the largest amount was observed in *N. foliaceum* cultures. In case this layer consisted of EPS, it could mean that the EPS have gelling properties. Additionally, the fact that the compounds sedimented could indicate they had higher molecular weight than other EPS staying in solution. High molecular weight in EPS is a key feature, "*which determines most of the properties generally considered to be useful for industrial applications*" [20]. Lastly, *N. foliaceum* produced a high amount of biomass of 3.7 ± 0.3 g L^{-1} (n=3) placing it near the upper end of the observed range, as *A. marina* showed the highest dry cell weight at 5.0 ± 0.3 g L^{-1} (n=3) while *A. platensis* only reached 0.42 ± 0.0 g L^{-1} (n=2). Such biomass levels could generate substantial by-product revenues because several *Nostoc* species are edible and contain bioactive compounds with antioxidant, anti-inflammatory, or antitumor properties [333].

Chapter 6: Optimisation of Cultivation Conditions

6.1 Chapter Overview

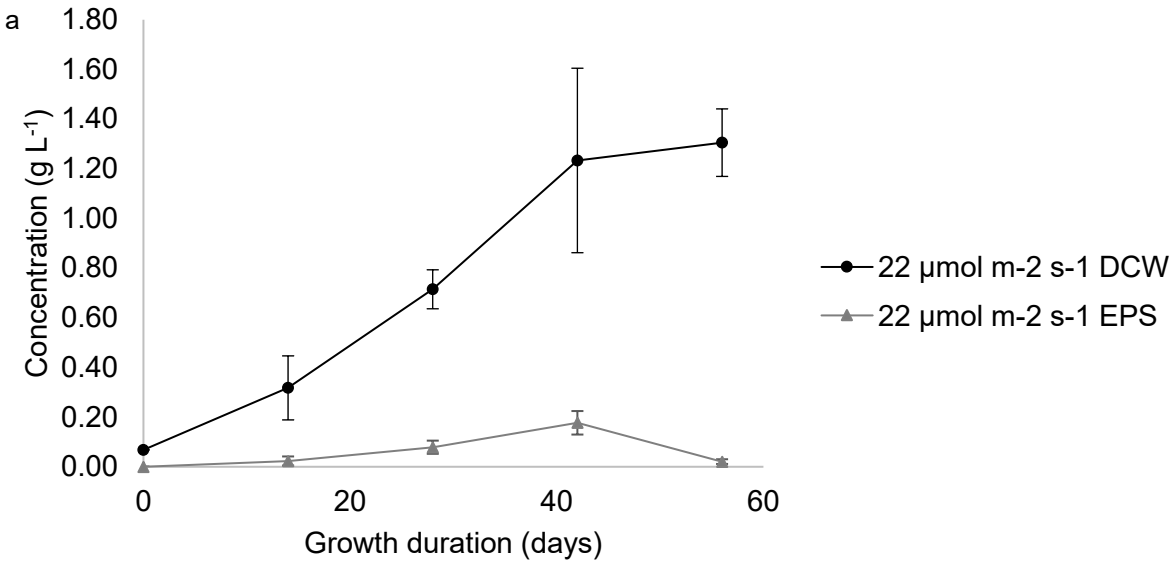
After the screening (Chapter 5:), the two most promising species, *C. brevissima* and *N. foliaceum* were selected for the optimisation of cultivation conditions, which consisted of a series of optimisation studies. In short, single-factor optimisation of light intensity was initially performed at 60% working volume, which was recommended by the manufacturer for the equipment (Algem HT24) [334]. The working volume was then reduced to 25% due to an observed negative effect on DCW and EPS. Simultaneously, the effect of media components (glucose, acetate, trace metals, magnesium, EDTA and calcium chloride) and pH on EPS production was studied. Based on the obtained results, multi-factor optimisation experiments were designed using the DoE function of Minitab software. Initially, 3-factor optimisation (light intensity, temperature and glucose) was performed, followed by validation of the identified optimal conditions for *N. foliaceum*. However, due to inconclusive results for *C. brevissima*, further experiments at higher light intensities were conducted. Firstly, 2-factor optimisation of light duration and light intensity was performed. Subsequently, an extensive experiment studying the effect of temperature and light intensity was systematically conducted, in which the light intensity range was increased even further, until the maximum of the equipment was reached. Finally, the optimised conditions identified for *C. brevissima* and desired property of the obtained EPS product were validated.

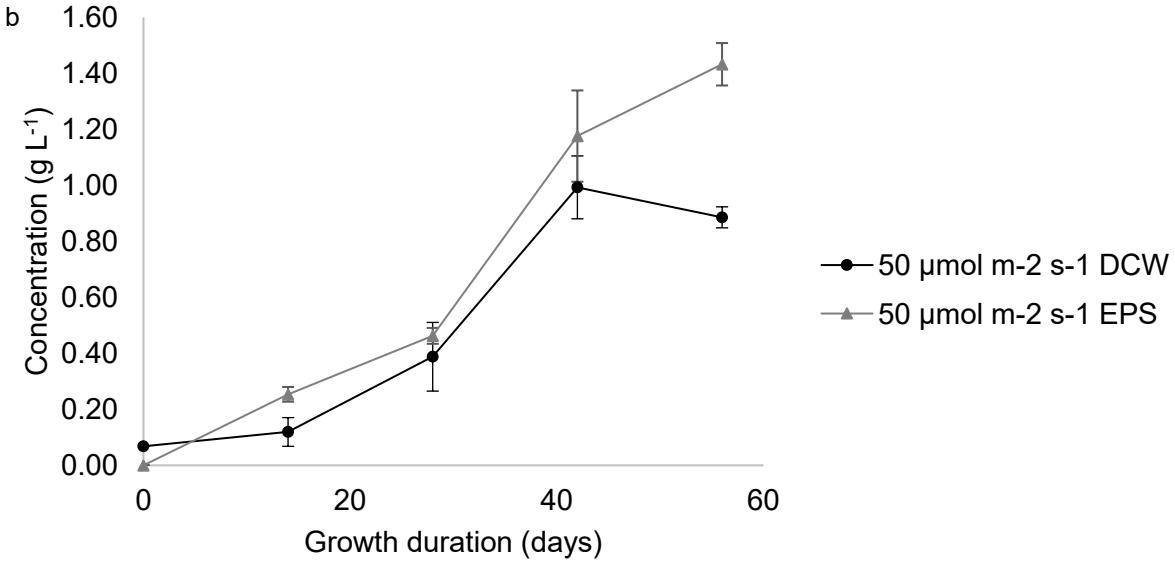
6.2 Effect of Light Intensity at 60% Working Volume *C. brevissima*

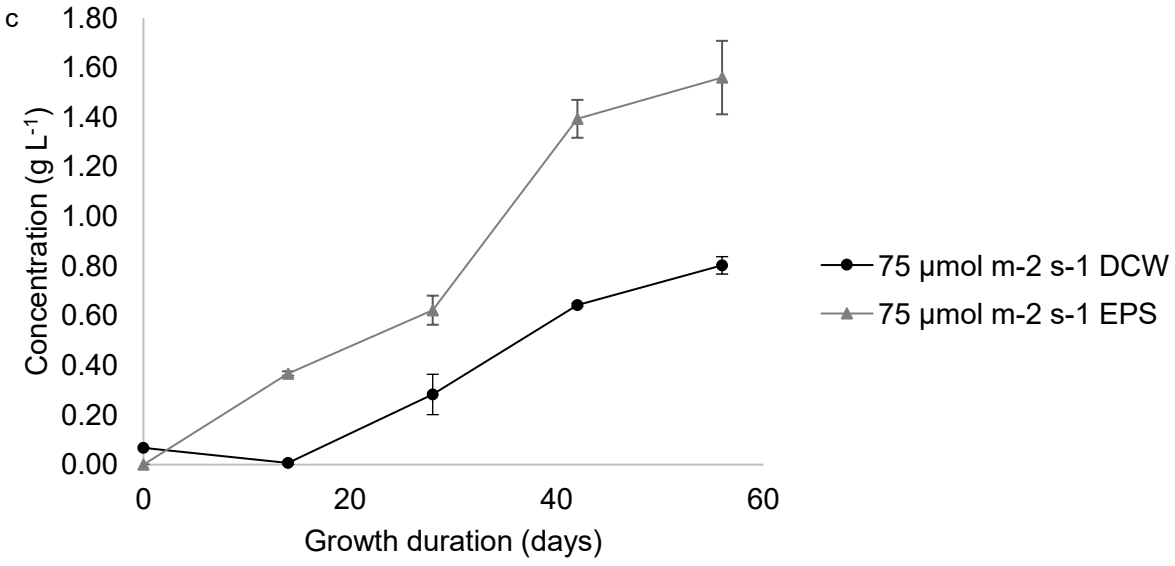
6.2.1 EPS and Biomass Production

The effect of four different light intensities (22, 50, 75, 100 µmol m^{-2} s^{-1}) on EPS and biomass (DCW) production of *C. brevissima* was studied at 60% working volume. The light intensity of 22 µE was selected to benchmark the optimisation experiment to the screening experiment (Exp. 1), while three higher light intensities were used to investigate the effect of increased light levels on EPS production, as higher light intensity is known to enhance EPS production (section 2.3.1.1). The upper limit of the range (100 µmol m^{-2} s^{-1}) was based on literature [168, 171].

The biomass and EPS production of *C. brevissima* under four different light intensities at 60% working volume is shown in Figure 6-1. The highest DCW was observed at the lowest light intensity (22 µmol m^{-2} s^{-1}) with cells increasing from day 28 (exponential phase) until day 42, at which DCW_{Max} (1.31 ± 0.14 g L^{-1}, n=3) was reached (Figure 6-1*a*). Afterwards, cells remained in stationary phase until the end of the experiment (day 60). The 50 µmol m^{-2} s^{-1} *C. brevissima* culture followed a similar trend regarding timing of growth phases but plateaued at a lower DCW value (0.99 ± 0.11 g L^{-1}, n=3) followed by a slight decrease. Even higher light intensities (75 and 100 µmol m^{-2} s^{-1}) resulted in even less growth, plateauing at values of around 0.71 ± 0.04 g L^{-1} (n=3, 100 µmol m^{-2} s^{-1}).


a
1.80
1.60
1.40
1.20
1.00
0.80
0.60
0.40
0.20
0.00
Concentration (g L-1)
0
20
40
60
Growth duration (days)
22 µmol m-2 s-1 DCW
22 µmol m-2 s-1 EPS


b
1.60
1.40
1.20
1.00
0.80
0.60
0.40
0.20
0.00
Concentration (g L-1)
0
20
40
60
Growth duration (days)
50 µmol m-2 s-1 DCW
50 µmol m-2 s-1 EPS


c
1.80
1.60
1.40
1.20
1.00
0.80
0.60
0.40
0.20
0.00
Concentration (g L-1)
0
20
40
60
Growth duration (days)
75 µmol m-2 s-1 DCW
75 µmol m-2 s-1 EPS

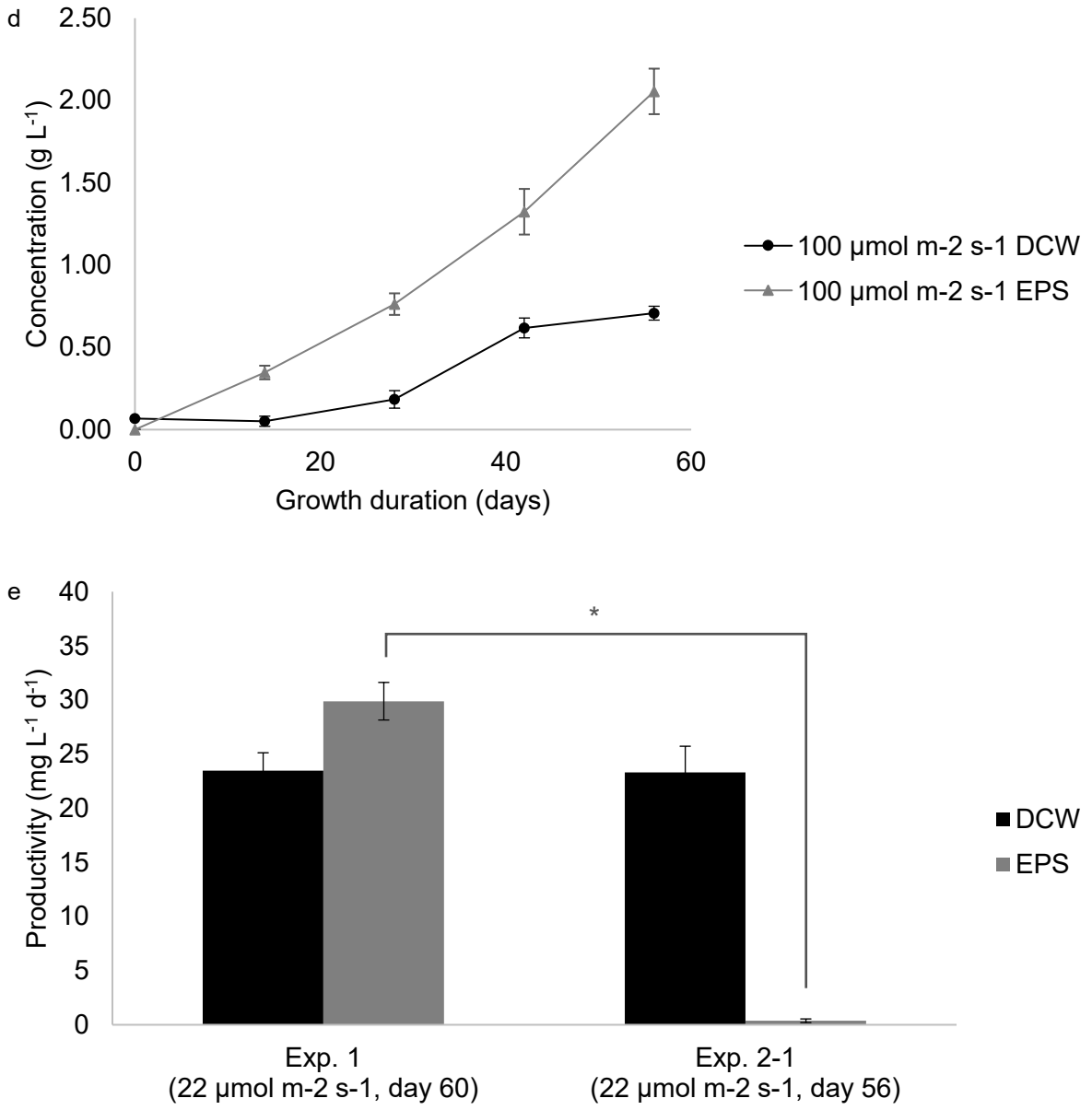


Figure 6-1 Effect of light intensity (22, 50, 75, 100 µmol m^{-2} s^{-1}) on *Calothrix brevissima* dry cell weight (DCW) and extracellular polymeric substances (EPS) at 60% working volume (30 mL culture in 50 mL Erlenmeyer flasks), 25 °C, and 150 RPM shaking for 56 days.(a) DCW and EPS concentration over time at 22 µmol m^{-2} s^{-1}. (b) DCW and EPS concentration over time at 50 µmol m^{-2} s^{-1}. (c) DCW and EPS concentration over time at 75 µmol m^{-2} s^{-1}. (d) DCW and EPS concentration over time at 100 µmol m^{-2} s^{-1}. (e) Comparison of DCW and EPS productivity of this experiment (Exp. 2-1, 22 µmol m^{-2} s^{-1}) with the screening experiment (Exp. 1). Conditions of Exp. 1: 22 µmol m^{-2} s^{-1}, 25% working volume (62.5 mL culture in 250 mL Erlenmeyer flasks), 25 °C, and 250 RPM shaking for 60 days. Values represent mean ± 1 standard deviation of biological triplicates (n=3). Asterisks indicate statistically significant differences: * ($p < 0.05$); ** ($p < 0.01$); *** ($p < 0.001$).

EPS production showed the opposite trend to DCW, with most EPS (2.05 ± 0.14 g L^{-1}, n=3) being produced at the highest light intensity (100 µmol m^{-2} s^{-1}, Figure 6-1*d*). EPS concentration of 50, 75 and 100 µmol m^{-2} s^{-1} cultures consistently increased and peaked at the end of the experiment (day 60). This resulted in final EPS titres of 1.56 ± 0.15 g L^{-1} (n=3) and 1.43 ± 0.08 g L^{-1} (n=3) for 75 and 50 µmol m^{-2} s^{-1}, respectively. The 22 µmol m^{-2} s^{-1} culture showed nearly no EPS production. This was a significant (p=0.003) difference to the screening experiment (Exp. 1) which was conducted at the same light intensity (22 µmol m^{-2} s^{-1}). The comparison of the final samples of the two experiments can be seen in Figure 6-1*e*. In the screening experiment, EPS increased consistently throughout the growth duration, reaching the maximum concentration at the end of the experiment (day 60, 1.79 ± 0.15 g L^{-1}, n=2), whereas in this optimisation experiment (Exp. 2-1), the culture showed barely any EPS production, with the maximum EPS of only 0.18 ± 0.05 g L^{-1} (n=3) obtained on day 42, after which it declined to 0.02 ± 0.01 g L^{-1} (n=3) on day 60. The biomass production of the two experiments appeared more similar, with comparable results being obtained for the first 28 days, after which the optimisation experiment culture (Exp. 2-1) increased rapidly and reached stationary phase on day 42, whereas the screening experiment (Exp. 1) culture remained in exponential phase throughout the experiment.

Comparison of the productivity of the end point samples showed that the culture from the single-factor optimisation of light (Exp. 2-1) showed a 99% reduction of EPS and 1% decrease of DCW compared to the screening experiment (Figure 6-1*e*). The EPS difference was statistically significant (p=0.036). These results led to another experiment, studying the effect of the working volume on EPS and DCW production (Exp. 2-2), which will be presented in section 6.4.

6.2.2 Comparative Analysis of Film-like and Cotton-like Appearance of *C. brevissima* EPS

An interesting observation was made regarding the appearance of the EPS of *C. brevissima* in the single-factor optimisation of light intensity experiment at 60% working volume (Exp. 2-1). Figure 6-2 shows photos of EPS of earlier samples that appeared as a shiny film, whereas later samples appeared as cotton-like fibres. The freeze-dried EPS of day 14 and day 28 under light intensities 50, 75 and 100 µmol m^{-2} s^{-1} showed the shiny film appearance. On the contrary, the freeze-dried EPS of day 42 and 56 of

these light intensities appeared cotton-like. The EPS of the 22 µmol m^{-2} s^{-1} light intensity were negligible in earlier samples (day 14 and 28) and looked cotton-like but with a red/brown colour on day 42 and 56 (photos not shown).

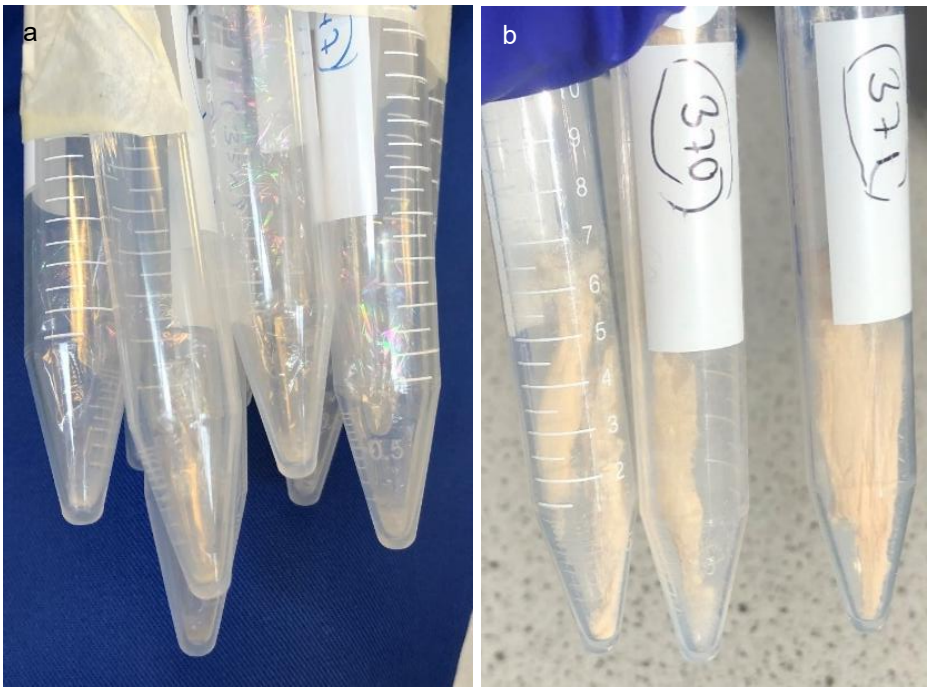


Figure 6-2 Photos of extracellular polymeric substances (EPS) from *Calothrix brevissima* grown under 50-100 µmol m^{-2} s^{-1}, 25°C, 150 RPM shaking and 60% working volume (30 mL culture in 50 mL Erlenmeyer flasks).(a) *Calothrix brevissima* early samples appear like a shiny film (day 14 and 28). (b) Later samples of *Calothrix brevissima* appear like cotton (day 42 and 56).

This shiny film appearance was observed once before in *C. brevissima* during the screening experiment: One of the triplicates of the final EPS samples (day 60, Exp. 1) showed the same shiny film-like appearance. Initially, this was suspected to be an outlier, until it was a consistent observation in Exp. 2-1. Most EPS in the screening experiment appeared cotton-like. The only exception were two triplicates of the day 60 sample of *A. marina* during the screening experiment, which appeared film-like, however the film did not show the different colours observed for *C. brevissima.* Film-like EPS might find application for use as bioplastic. To investigate difference in these two appearances, the two types of EPS were compared based on monosaccharide composition (HPAEC-PAD) and freezing behaviour (DSC).

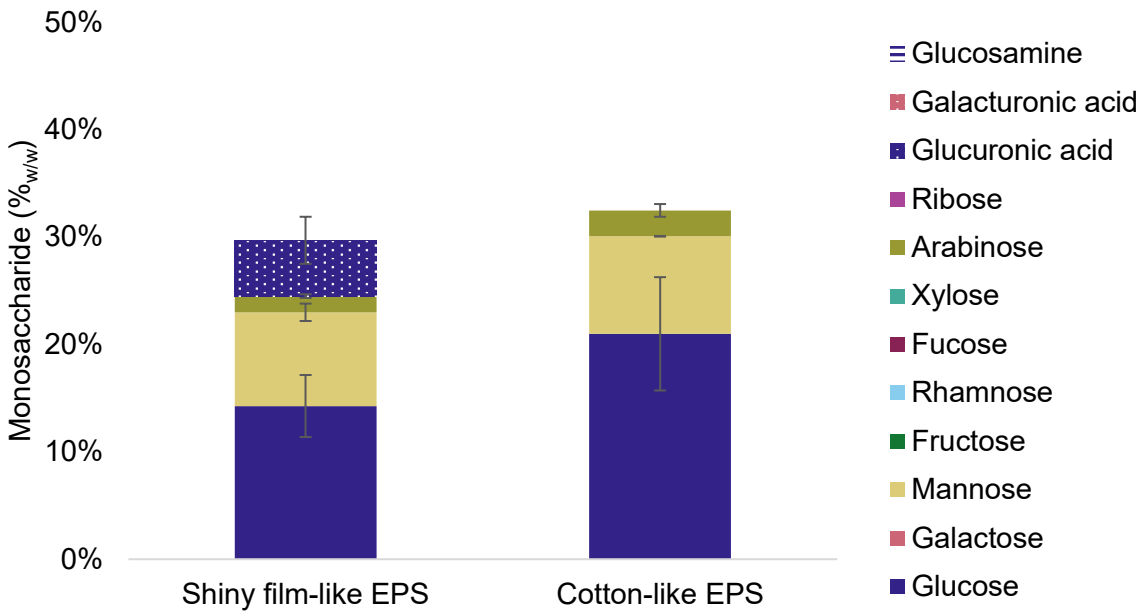


Figure 6-3 Comparison of monosaccharide composition of cotton-like and shiny film-like extracellular polymeric substances (EPS) from *Calothrix brevissima*. Monosaccharide composition based on High-Performance Anion-Exchange Chromatography with Pulsed Amperometric Detection. Data represent mean ± standard deviation of biological triplicates (n=3). Calibration curves can be found in Figure 12-1; trendline equations, limit of detection (LOD) and limit of saturation (LOS) can be found in Table 12-1.

As can be seen in Figure 6-3, the monosaccharide composition of the shiny-film EPS and cotton-like EPS were similar. Both types of EPS consisted of mainly glucose (14 ± 3% (n=3) and 21 ± 5% (n=3), respectively), mannose (7 ± 2% (n=3) and 6 ± 2% (n=3), respectively) and arabinose (2 ± 0.2% (n=3) and 2 ± 0.6% (n=3), respectively). The main difference was presence of 5 ± 2% (n=3) glucuronic acid in the shiny-film EPS, which were lacking in the cotton-like EPS. In the cotton-like EPS, instead, a higher amount of glucose was found, which was not statistically significant (p=0.15). However, it is unlikely that the uronic acids were the cause for the difference in appearance, since all three replicates of the screening experiment contained glucuronic acid (5 ± 0.6%, n=3), but only one replicate showed the shiny-film appearance. Based on HPAEC-PAD, 31-32% of the EPS was identified, leaving most of the EPS unidentified. As described in the literature review, fully identified structures of cyanobacterial EPS are rare due to their complex sugar and non-sugar components and lack of repeating units [29]. The reason for the observed difference could be

related to the unidentified fraction of the EPS, or other aspects such as structural configuration.

When EPS solutions are frozen prior to freeze-drying, they usually freeze from the walls towards the centre of the tube due to the outside surface area being in contact with the lower temperature. Similarly, when being freeze-dried, the outside parts dry first. These processes push the EPS to the centre of the tube, leading them to appear as rod-shaped fibrous material in the centre of the tube after freeze-drying [335]. The appearance as a film on the walls of the tube was peculiar as the EPS did not get pushed towards the centre of the tube. One explanation for this phenomenon could be that EPS could cause freezing point depression, which is the reduction of the maximum temperature at which a substance freezes [335, 336]. If EPS from *C. brevissima* cause freezing point depression, this could explain an observation made with *C. brevissima*: It was possible to resurrect *C. brevissima,* which was frozen at -20°C without cryoprotective agent. Possibly, the EPS were protecting the cells from freeze-related death due to the freezing point depression properties. Molecules with this property could find application as functional food additive in the ice cream industry to keep ice cream soft at negative temperatures [335, 336].

To investigate whether freezing point depression was occurring, DSC measurements were performed. However, problems with the DSC instrument became apparent in the control samples of locust bean gum and water, where some thermograms appeared as flat lines and the freezing point of water was recorded far below its expected value. The source of these issues remains unknown, and the measurements could not be repeated due to time constraints. The shiny film and cotton-like EPS did not exhibit distinguishable differences in freezing behavior, providing no evidence that the observed phenomena were related to differences in freezing characteristics; nevertheless, the reliability of these results is uncertain given the equipment malfunction. The DSC data is included in the appendix, together with the TGA analyses and SEM images of the shiny-film and cotton-like EPS.

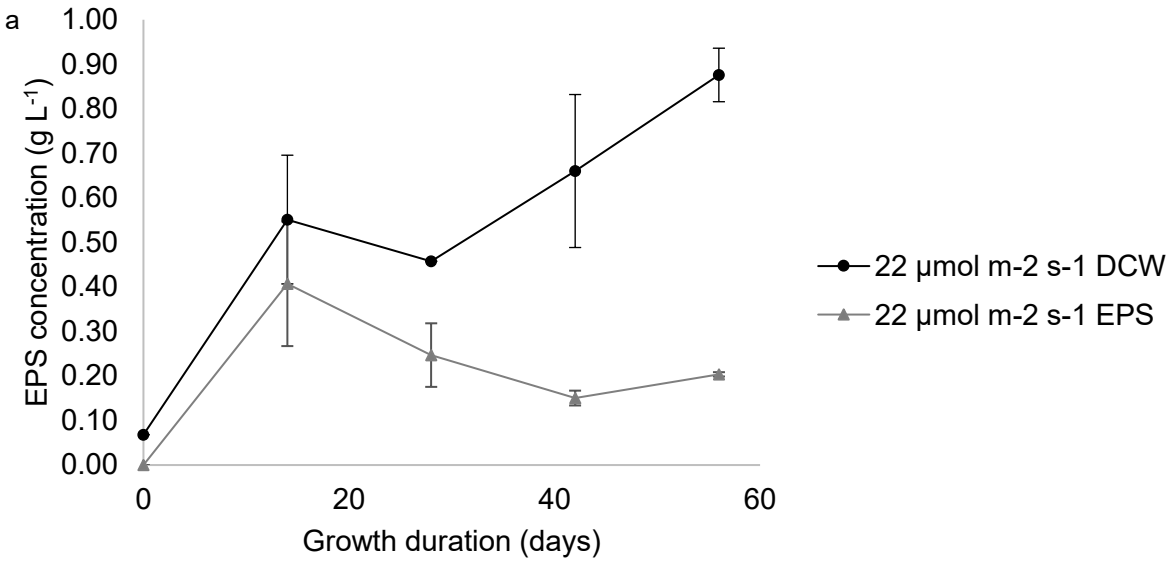
The cause of the appearance differences remains unknown, possibly stemming from untested compositional or functional variations or even from equipment-related issues. One hypothesis is that equipment malfunction, such as the freeze dryer failing to

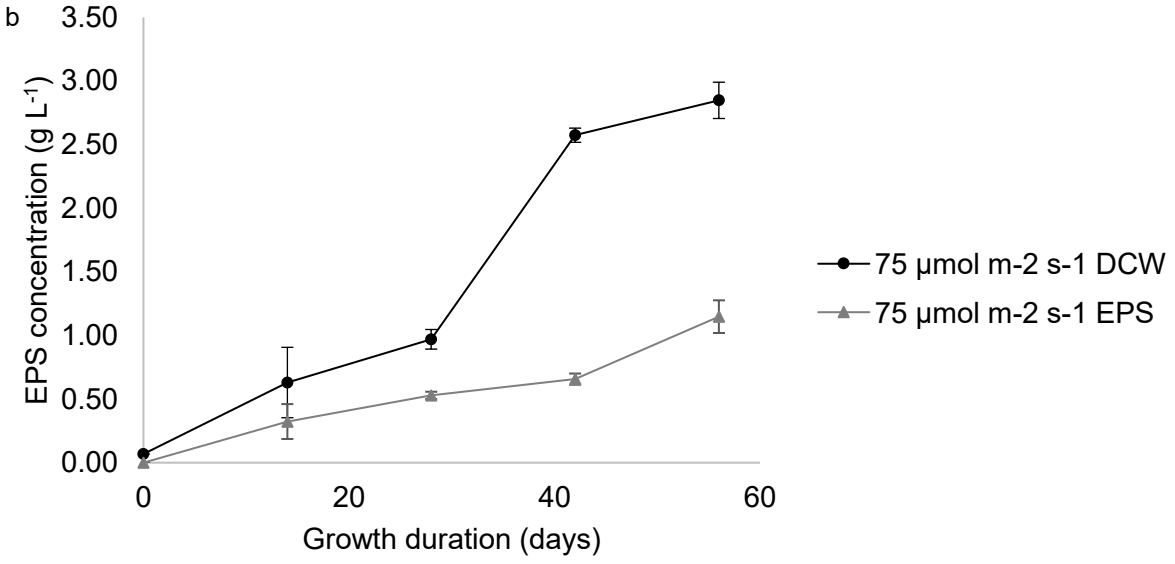
maintain the required temperature of -35°C, could have led to temporary thawing. This would allow the EPS to move freely in solution, adhering to the walls of the plastic tube and contributing to the film-like appearance. Following this experiment, a different freeze dryer was used (-55°C operating temperature), and no further occurrences of the film-like EPS appearance were observed.

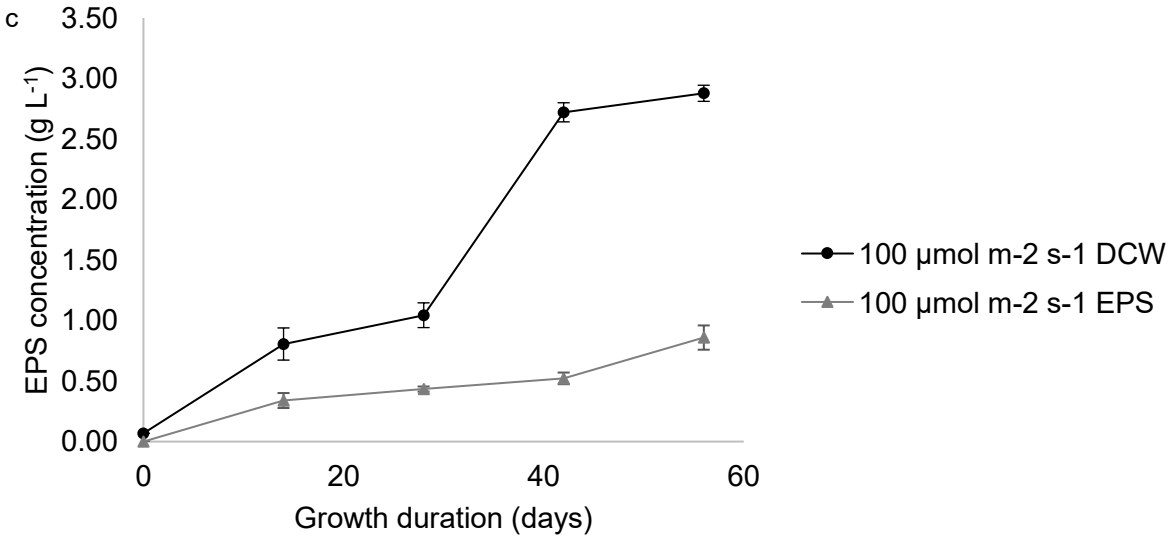
6.3 Impact of Light Intensity at 60% Working Volume *N. foliaceum*

Studying the effect of four different light intensities (50, 75, 100 and 150 µmol m^{-2} s^{-1}) on EPS and biomass (DCW) production at 60% working volume (Exp. 2-1) was also performed with another species, *N. foliaceum*. As explained in section 6.2.1, EPS production for *C. brevissima* was highest at 100 µmol m^{-2} s^{-1}. Therefore, the light range was extended to 150 µmol m^{-2} s^{-1} for *N. foliaceum* to capture a potential higher optimum, while avoiding photoinhibition, since levels of 250 µmol m^{-2} s^{-1} can inhibit some species [175]. In the screening experiment (Exp. 1), one species was already inhibited under continuous illumination at 22 µmol m^{-2} s^{-1} (*O. rosea*, section 5.2).

N. foliaceum EPS (Figure 6-4) increased steadily throughout the growth duration for all higher light intensities (75, 100, 150 µmol m^{-2} s^{-1}), whereas the EPS at 22 µmol m^{-2} s^{-1} peaked early in the growth (day 14, 0.41 ± 0.14 g L^{-1}, n=3) and then decreased. Most EPS (1.15 ± 0.13 g L^{-1}, n=3) were produced at 75 µmol m^{-2} s^{-1} at the end of the experiment (day 56). Higher light intensities (100 and 150 µmol m^{-2} s^{-1}) resulted in moderately high EPS_{Max} (0.86 ± 0.10 g L^{-1} (n=3) and 0.82 ± 0.03 g L^{-1} (n=3), respectively).


a
1.00
0.90
0.80
0.70
0.60
0.50
0.40
0.30
0.20
0.10
0.00
EPS concentration (g L-1)
0
20
40
60
Growth duration (days)
22 µmol m-2 s-1 DCW
22 µmol m-2 s-1 EPS


b
3.50
3.00
2.50
2.00
1.50
1.00
0.50
0.00
EPS concentration (g L-1)
0
20
40
60
Growth duration (days)
75 µmol m-2 s-1 DCW
75 µmol m-2 s-1 EPS


c
3.50
3.00
2.50
2.00
1.50
1.00
0.50
0.00
EPS concentration (g L-1)
0
20
40
60
Growth duration (days)
100 µmol m-2 s-1 DCW
100 µmol m-2 s-1 EPS

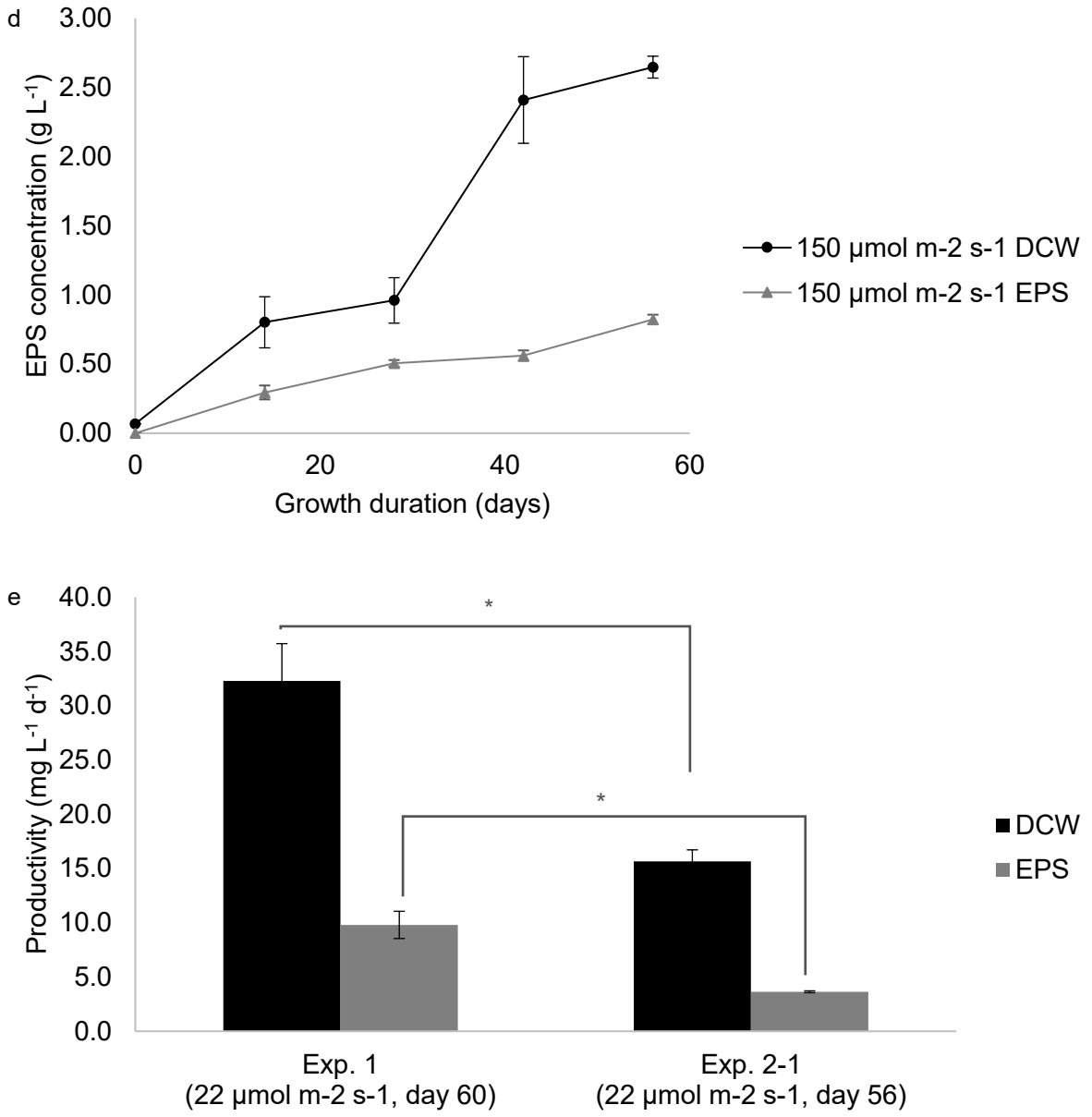


Figure 6-4 Effect of light intensity (50, 75, 100, 150 µmol m^{-2} s^{-1}) on *Nostoc foliaceum* dry cell weight (DCW) and extracellular polymeric substances (EPS) at 60% working volume (30 mL culture in 50 mL Erlenmeyer flasks), 25 °C, and 150 RPM shaking for 56 days.(a) DCW and EPS concentration over time at 50 µmol m^{-2} s^{-1}. (b) DCW and EPS concentration over time at 75 µmol m^{-2} s^{-1}. (c) DCW and EPS concentration over time at 100 µmol m^{-2} s^{-1}. (d) DCW and EPS concentration over time at 150 µmol m^{-2} s^{-1}. (e) Comparison of DCW and EPS productivity of this experiment (Exp. 2-1, 22 µmol m^{-2} s^{-1}) with the screening experiment (Exp. 1). Conditions of Exp. 1: 22 µmol m^{-2} s^{-1}, 25% working volume (62.5 mL culture in 250 mL Erlenmeyer flasks), 25 °C, and 250 RPM shaking for 60 days. Values represent mean ± 1 standard deviation of biological triplicates (n=3). Asterisks indicate statistically significant differences: * ($p < 0.05$); ** ($p < 0.01$); *** ($p < 0.001$).

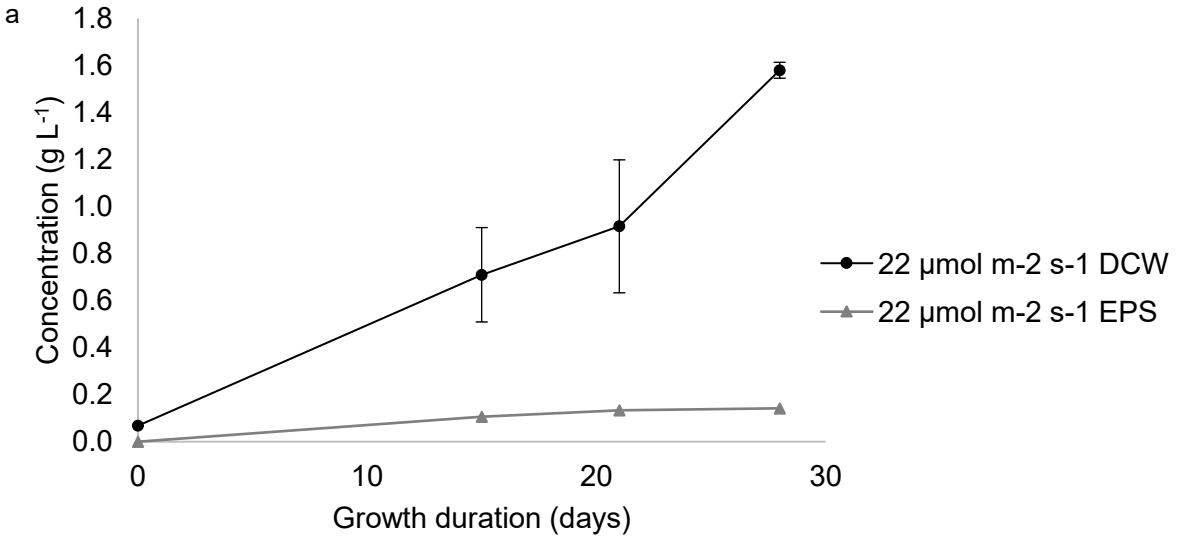
N. foliaceum biomass grown at 50, 75 and 100 µmol m^{-2} s^{-1} increased exponentially between day 28 and 42, after which the cells remained in stationary phase until the end of the experiment (Figure 6-4*b-d*). The maximum DCW of 2.88 ± 0.07 g L^{-1} (n=3, 100 µmol m^{-2} s^{-1}) was reached on day 56, and was at a similar value for all three higher light intensities. Lower light (22 µmol m^{-2} s^{-1}) resulted in significantly lower final biomass concentration (DCW_{Max} = 0.88 ± 0.06 g L^{-1}, n=3) than 50, 75 and 100 µmol m^{-2} s^{-1}, with p-values of 4.1 x 10^{-4}, 3.0 x 10^{-6} and 1.2 x 10^{-5}, respectively. The three higher light intensities followed a similar pattern to each other. This could indicate that another factor than light was limiting, leading to the cells not being able to use all the energy provided by the light. One possibility could be low carbon availability due to inefficient gas transfer based on the 60% working volume.

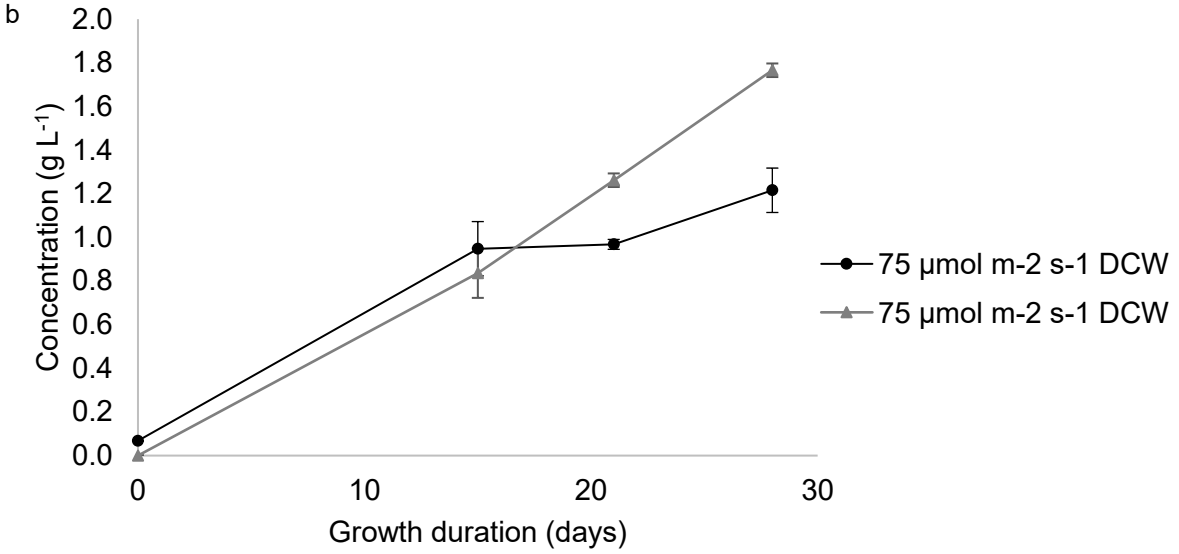
Similarly to *C. brevissima*, DCW and EPS productivities of *N. foliaceum* at 22 µmol m^{-2} s^{-1} in the optimisation experiment (Exp. 2-1) were lower than in screening experiment (Exp. 1). As shown in Figure 6-4*e*, DCW productivity was 15.6 ± 1.1 mg L^{-1} d^{-1} (n=3), which represents a significant reduction to the screening experiment of 52% (p=0.036). EPS productivity was 3.6 ± 0.1 mg L^{-1} d^{-1} (n=3), which was a 63% reduction (Figure 6-4*e*), and also statistically significant (p=0.013).

6.4 Influence of Working Volume on *C. brevissima* and *N. foliaceum* DCW and EPS

It was hypothesised that the 60% working volume, which was recommended by the manufacturer, was too high, resulting in unfavourable conditions for EPS production, i.e. less efficient gas transfer, reduced carbon availability and less light penetration. A follow-up experiment was performed to study the effect of lower working volume (25%) on DCW and EPS (Exp. 2-2). This experiment was conducted at two different light intensities. Firstly, 22 µmol m^{-2} s^{-1} was selected to benchmark the screening experiment to the optimisation experiment, since different equipment was used. Secondly, a higher light intensity was chosen as this resulted in an enhancement of EPS in Exp. 2-1. Even though the highest EPS (2.05 ± 0.14 g L^{-1}, n=3) were observed at 100 µmol m^{-2} s^{-1}, 75 µmol m^{-2} s^{-1} was selected instead. The reason was that reduction in working volume also reduced the light penetration path, which meant cells were more exposed to light and less protected from self-shading. Consequently, it was

considered that 100 µmol m^{-2} s^{-1} may be too intense, potentially leading to photoinhibition.


a
Concentration (g L-1)
1.8
1.6
1.4
1.2
1.0
0.8
0.6
0.4
0.2
0.0
0
10
20
30
Growth duration (days)
22 µmol m-2 s-1 DCW
22 µmol m-2 s-1 EPS


b
Concentration (g L-1)
2.0
1.8
1.6
1.4
1.2
1.0
0.8
0.6
0.4
0.2
0.0
0
10
20
30
Growth duration (days)
75 µmol m-2 s-1 DCW
75 µmol m-2 s-1 DCW

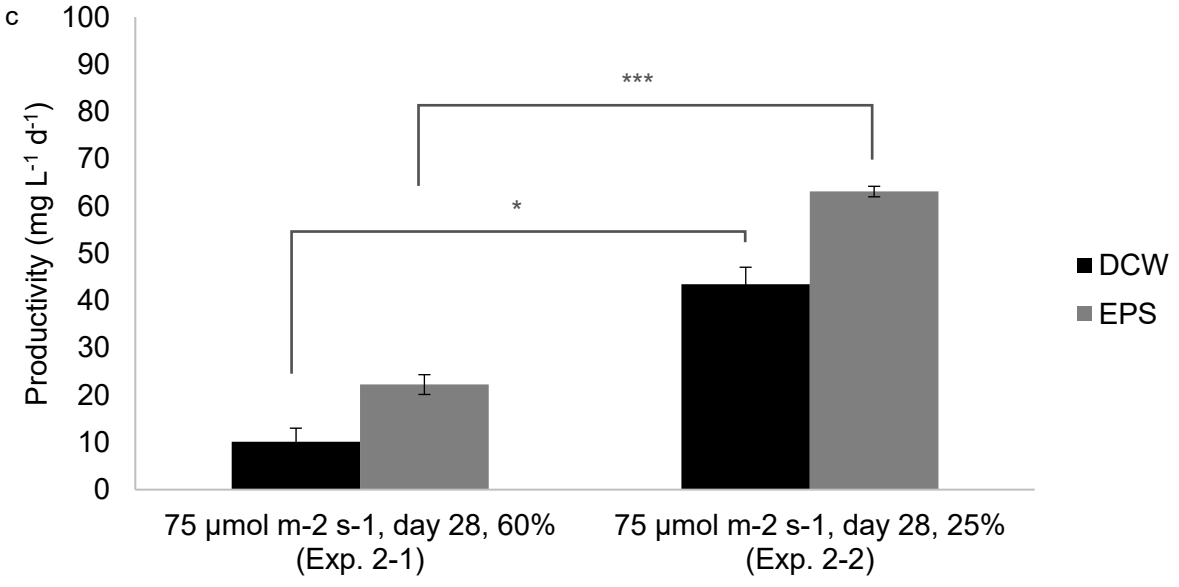
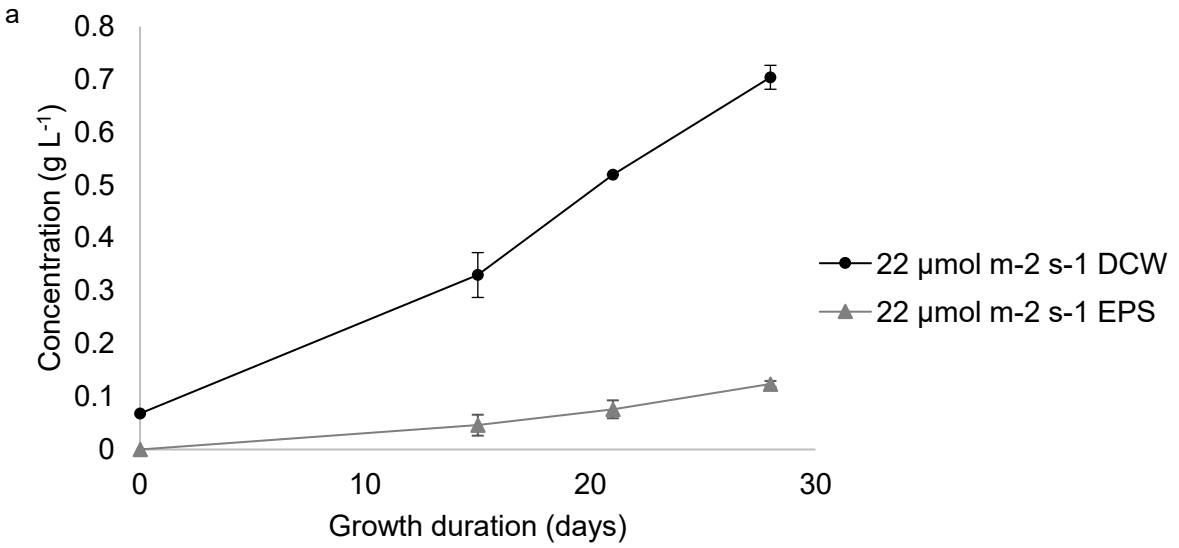
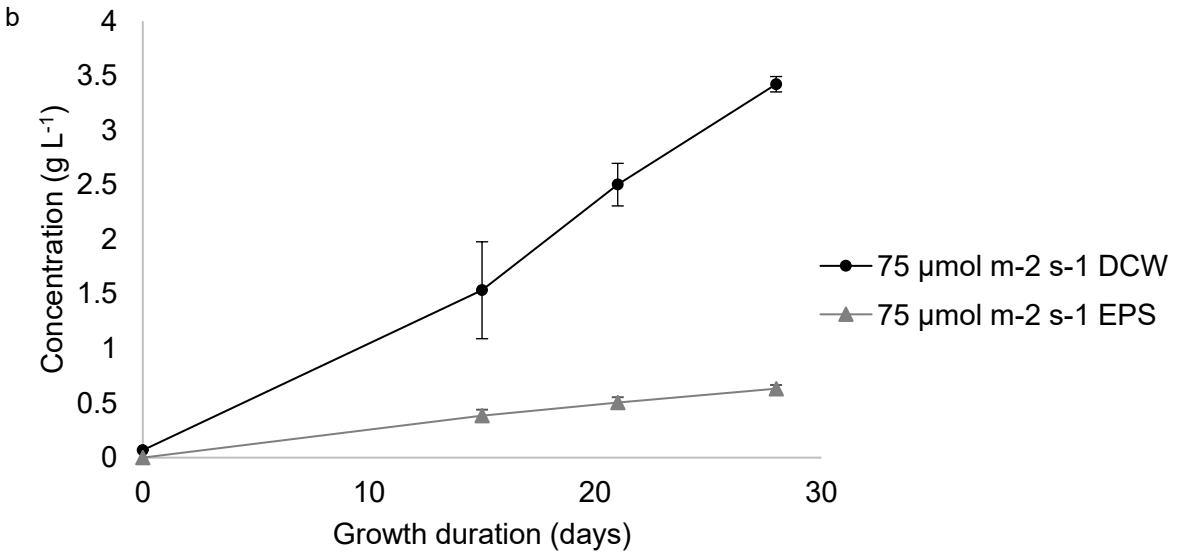

c
Productivity (mg L-1 d-1)
100
90
80
70
60
50
40
30
20
10
0
***
*
75 µmol m-2 s-1, day 28, 60%
(Exp. 2-1)
75 µmol m-2 s-1, day 28, 25%
(Exp. 2-2)
DCW
EPS

Figure 6-5 Effect of light intensity (22, 75 µmol m^{-2} s^{-1}) on *Calothrix brevissima* dry cell weight (DCW) and extracellular polymeric substances (EPS) at 25% working volume (12.5 mL culture in 50 mL Erlenmeyer flasks), 25 °C, and 150 RPM shaking for 28 days (Exp. 2-2).(a) DCW and EPS concentration over time at 22 µmol m^{-2} s^{-1}. (b) DCW and EPS concentration over time at 75 µmol m^{-2} s^{-1}. (c) Comparison of DCW and EPS productivity in this experiment (25% working volume, 75 µmol m^{-2} s^{-1}, day 28) with Exp. 2-1 (60% working volume, 75 µmol m^{-2} s^{-1}, day 28). Values represent mean ± 1 standard deviation of biological replicates (n=2 in Exp. 2-2; n=3 in Exp. 2-1). Asterisk (*) shows statistically significant difference: * ($p<0.05$); ** ($p<0.01$); *** ($p<0.001$).

The results are depicted in Figure 6-5. At 25% working volume, DCW production was similar at 22 µmol m^{-2} s^{-1} and 75 µmol m^{-2} s^{-1}, reaching maximum values of 1.58 ± 0.03 g L^{-1} (n=2) and 1.22 ± 0.10 g L^{-1} (n=2) on day 28, respectively. None of the samples from the two light intensities were significantly different from each other ($p>0.05$). However, EPS production was drastically different. *C. brevissima* reached 1.77 ± 0.03 g L^{-1} (n=2) on day 28 when grown in 75 µmol m^{-2} s^{-1}, whereas the 22 µmol m^{-2} s^{-1} culture reached merely 0.14 ± 0.04 g L^{-1} (n=2). This difference was statistically significant for day 21 and day 28 samples ($p\leq0.012$). Comparing these results to Exp. 2-1, it becomes evident that decreasing the working volume from 60% to 25% quadrupled DCW productivity and tripled the EPS productivity at 75 µmol m^{-2} s^{-1} (Figure 6-5*c*). This resulted in a DCW productivity of 43.4 ± 3.6 mg L^{-1} d^{-1} (n=2), which was significantly different from the result obtained with 60% working volume ($p=0.011$). The EPS productivity was 63.1 ± 1.1 mg L^{-1} d^{-1} (n=2), which was also significantly different from the result with 60% working volume ($p=0.00010$). This indicates that the high working volume (60%) had inhibited EPS and biomass production, as hypothesised in the previous paragraph.


a
0.8
0.7
0.6
0.5
0.4
0.3
0.2
0.1
0
Concentration (g L-1)
0
10
20
30
Growth duration (days)
22 μmol m-2 s-1 DCW
22 μmol m-2 s-1 EPS


b
4
3.5
3
2.5
2
1.5
1
0.5
0
Concentration (g L-1)
0
10
20
30
Growth duration (days)
75 μmol m-2 s-1 DCW
75 μmol m-2 s-1 EPS

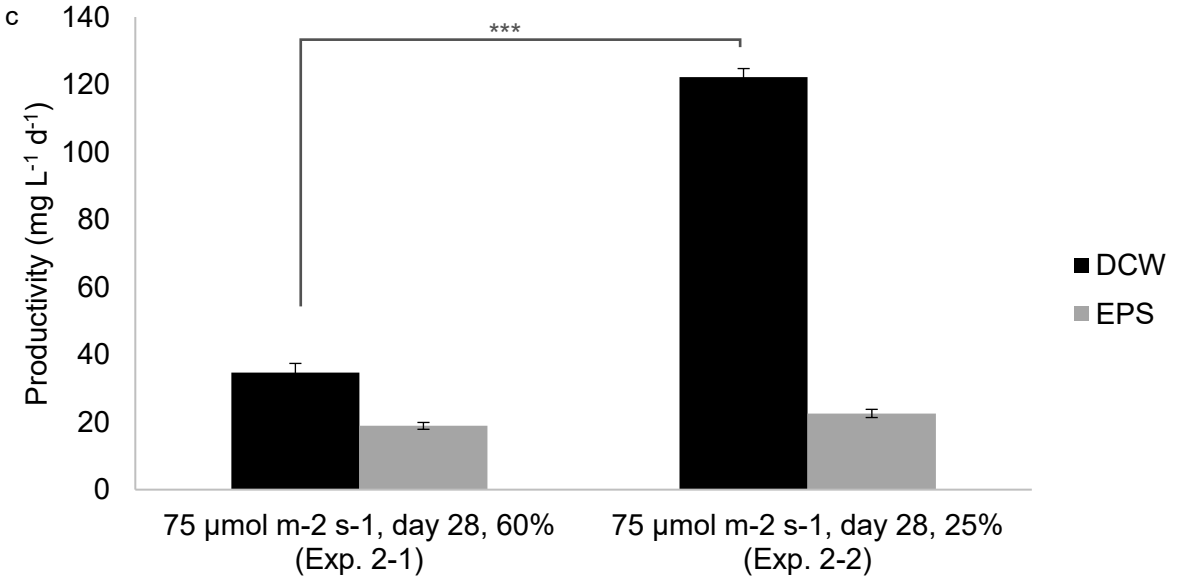

c
140
120
100
80
60
40
20
0
Productivity (mg L-1 d-1)
***
75 μmol m-2 s-1, day 28, 60%
(Exp. 2-1)
75 μmol m-2 s-1, day 28, 25%
(Exp. 2-2)
DCW
EPS

Figure 6-6 Effect of light intensity (22, 75 µmol m^{-2} s^{-1}) on *Nostoc foliaceum* dry cell weight (DCW) and extracellular polymeric substances (EPS) at 25% working volume (12.5 mL culture in 50 mL Erlenmeyer flasks), 25 °C, and 150 RPM shaking for 28 days (Exp. 2-2).(a) DCW and EPS concentration over time at 22 µmol m^{-2} s^{-1}. (b) DCW and EPS concentration over time at 75 µmol m^{-2} s^{-1}. (c) Comparison of DCW and EPS productivity in this experiment (25% working volume, 75 µmol m^{-2} s^{-1}, day 28) with Exp. 2-1 (60% working volume, 75 µmol m^{-2} s^{-1}, day 28). Values represent mean ± 1 standard deviation of biological replicates (n=2 in Exp. 2-2; n=3 in Exp. 2-1). Asterisk (*) shows statistically significant difference: * ($p<0.05$); ** ($p<0.01$); *** ($p<0.001$).

Similarly, *N. foliaceum* also showed improved DCW and EPS production at smaller working volume (25%). As shown in Figure 6-6*a-b*, DCW increased steadily, with cells remaining in exponential phase. The higher light intensity, 75 µmol m^{-2} s^{-1} resulted in a maximum DCW of 3.42 ± 0.07 g L^{-1} (n=2) compared to 0.70 ± 0.02 g L^{-1} (n=2) at 22 µmol m^{-2} s^{-1}, a statistically significant difference ($p=0.0058$). EPS production of *N. foliaceum* showed a similar trend, with EPS concentration increasing throughout the experiment. On day 28, the highest EPS concentrations were obtained, amounting to 0.63 ± 0.03 g L^{-1} (n=2) and 0.12 ± 0.01 g L^{-1} (n=2) for 75 and 22 µmol m^{-2} s^{-1}, respectively. The differences in EPS production based on light intensity were statistically significant for all samples ($p\leq0.046$). Compared to the previous experiment (Exp. 2-1), DCW productivity tripled at lower working volume, resulting in 122.2 ± mg L^{-1} d^{-1} (n=2), which was statistically significant ($p=0.00021$, Figure 6-6*c*). However, EPS production increased merely by 19% to 22.6 ± 1.2 mg L^{-1} d^{-1} (n=2), which was not a significant difference.

Interestingly, the 22 µmol m^{-2} s^{-1} EPS results of *C. brevissima* in Exp. 2-2 were still lower than those obtained in the screening experiment (Exp. 1), indicating that the 60% working volume was not solely responsible for the observed differences. Parameters that differ in the equipment used for the optimisation experiment (Algem HT24, Algenuity) compared to the screening experiment (Excella E24R, New Brunswick) are shaking speed, flask size and light source. The smaller flask size of the Algem HT24 (50 mL) might result in more efficient gas transfer, explaining the improved DCW and higher overall carbon fixation in this experiment compared to the screening experiment. However, it does not explain the lower EPS production. Possibly, the higher shaking

speed in the screening experiment (250 rpm), compared to the 150 rpm used in the optimisation experiments, led to increased shear stress, to which the cells might have reacted with EPS production at the expense of DCW. Increased shear can lead to cell damage, and shear stress has shown to increase EPS secretion in biofilms [211, 337]. Furthermore, different light sources could mean different light colour (warm vs. cool white), which could affect the photon energy delivered to the cells. Also, the distance to the lamp was smaller in the Algem HT24 compared to the Excella E24R incubator, possibly resulting in different light penetration depth or even indirectly warming the culture temperature.

Due to the enhancement of EPS production at 25% working volume, this was adopted for further experiments. Since 75 µmol m^{-2} s^{-1} enhanced EPS production, the following experiment using even higher light intensities (175 µmol m^{-2} s^{-1}) was performed (Exp. 2-3). The objective was to determine the optimal light intensity to be applied during the multi-factor optimisation (section 6.5).

6.5 Effect of Light Intensity at 25% Working Volume

To select suitable light conditions for the multi-factor optimisation experiment, preliminary experiments with six different light intensities were performed with *C. brevissima* and *N. foliaceum* (Exp. 2-3).

As shown in Figure 6-7*a*, *C. brevissima* showed more biomass production at lower light intensities (DCW_{Max} of 1.26 ± 0.23, n=2, at 50 µmol m^{-2} s^{-1}), whereas more EPS were produced at higher light intensities (EPS_{Max} of 1.72 ± 0.14, n=2, at 150 µmol m^{-2} s^{-1}). Also, the specific EPS yield (g EPS g^{-1} DCW) of *C. brevissima* was heavily influenced by light intensity. At the lowest light intensity (50 µmol m^{-2} s^{-1}), *C. brevissima* produced biomass and EPS in similar amounts (EPS_{Yield} = 0.73 ± 0.13 g EPS g^{-1} DCW), whereas at higher light intensities (150 µmol m^{-2} s^{-1}) *C. brevissima* produced 2.6 times as much EPS as DCW (EPS_{yield} = 2.59 ± 0.05 g EPS g^{-1} DCW). The difference between the yields was statistically significant (p=0.029, data not shown). Increasing the light intensity from 75 µmol m^{-2} s^{-1} to 150 µmol m^{-2} s^{-1} resulted in a 36% increase in EPS productivity of *C. brevissima* to 81.8 ± 6.6 mg L^{-1} d^{-1} (n=2, Figure 6-7*b*). However, this occurred alongside a significant reduction of DCW by 32% to 31.6 ± 2.0 mg L^{-1} d^{-1} (n=2, p=0.022, Figure 6-7*b*).

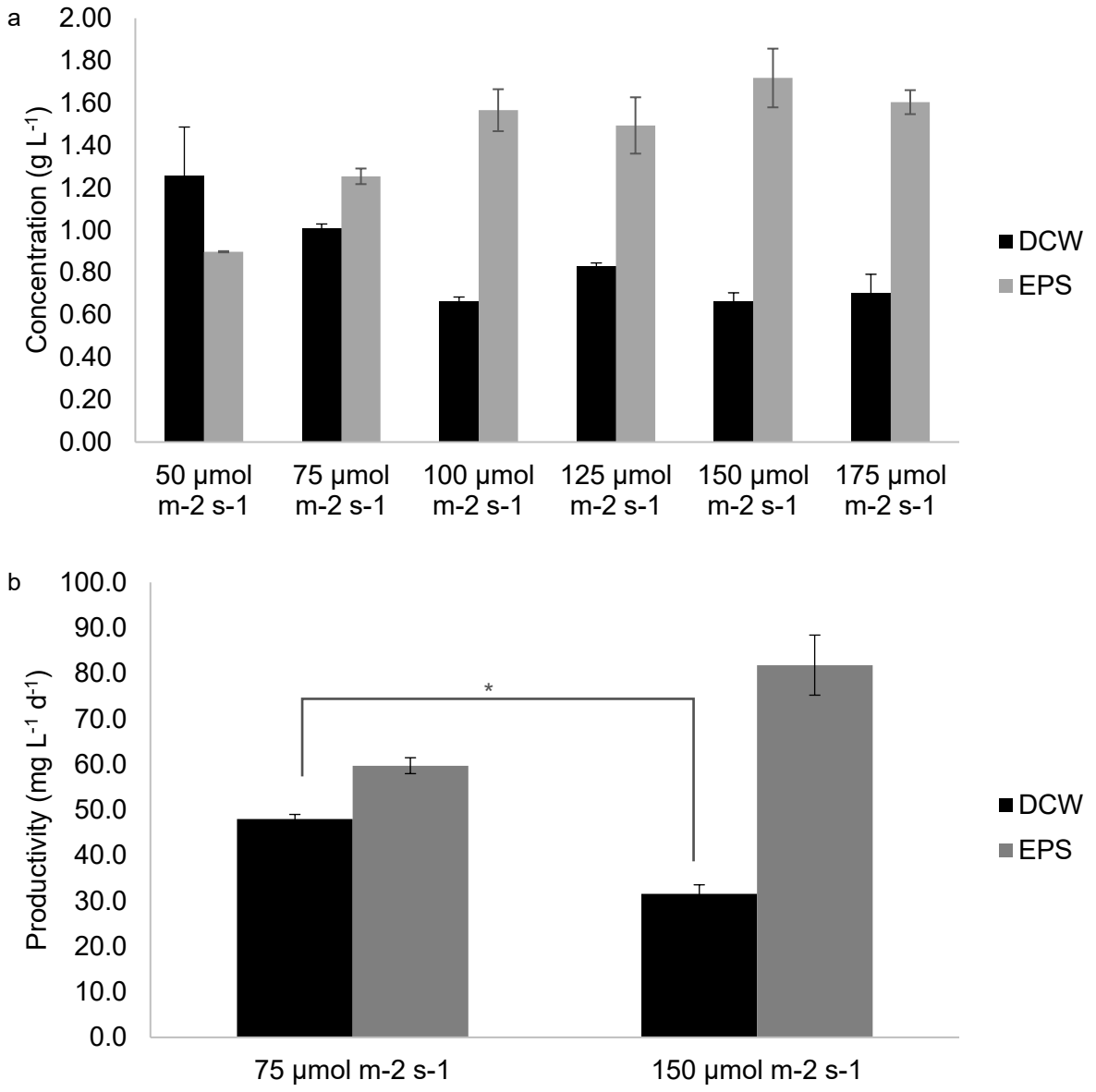


Figure 6-7 Effect of light intensity (50, 75, 100, 125, 150, 175 µmol m^{-2} s^{-1}) on *Calothrix brevissima* dry cell weight (DCW) and extracellular polymeric substances (EPS) at 25% working volume (12.5 mL culture in 50 mL Erlenmeyer flasks), 25 °C, and 150 RPM shaking for 21 days (Exp. 2-3).(a) DCW and EPS concentration depending on light intensity on day 21. (b) Comparison of DCW and EPS productivity under 75 and 150 µmol m^{-2} s^{-1}. Values represent mean ± 1 standard deviation of biological duplicates (n=2). Asterisk (*) shows statistically significant difference: * ($p<0.05$); ** ($p<0.01$); *** ($p<0.001$). µmol m^{-2} s^{-1})

N. foliaceum produced more biomass (DCW max = 3.11 ± 0.15 g L^{-1}, n=2) than EPS (EPS_{max} = 0.42 ± 0.03 g L^{-1}, n=2) for all light intensities studied, as shown in Figure 6-8*a*. As a result, most of the EPS yields were not significantly different from each other

(data not shown). The optimal light intensity for EPS production of *N. foliaceum* was 100 µmol m^{-2} s^{-1}, whereas 150 µmol m^{-2} s^{-1} was optimal for biomass production. Comparing the results from 75 to 100 µmol m^{-2} s^{-1}, DCW and EPS productivities were not significantly different, amounting to 135.7 ± 14.2 mg L^{-1} d^{-1} (n=2) and 20.2 ± 1.3 mg L^{-1} d^{-1} (n=2), respectively (Figure 6-8*b)*.

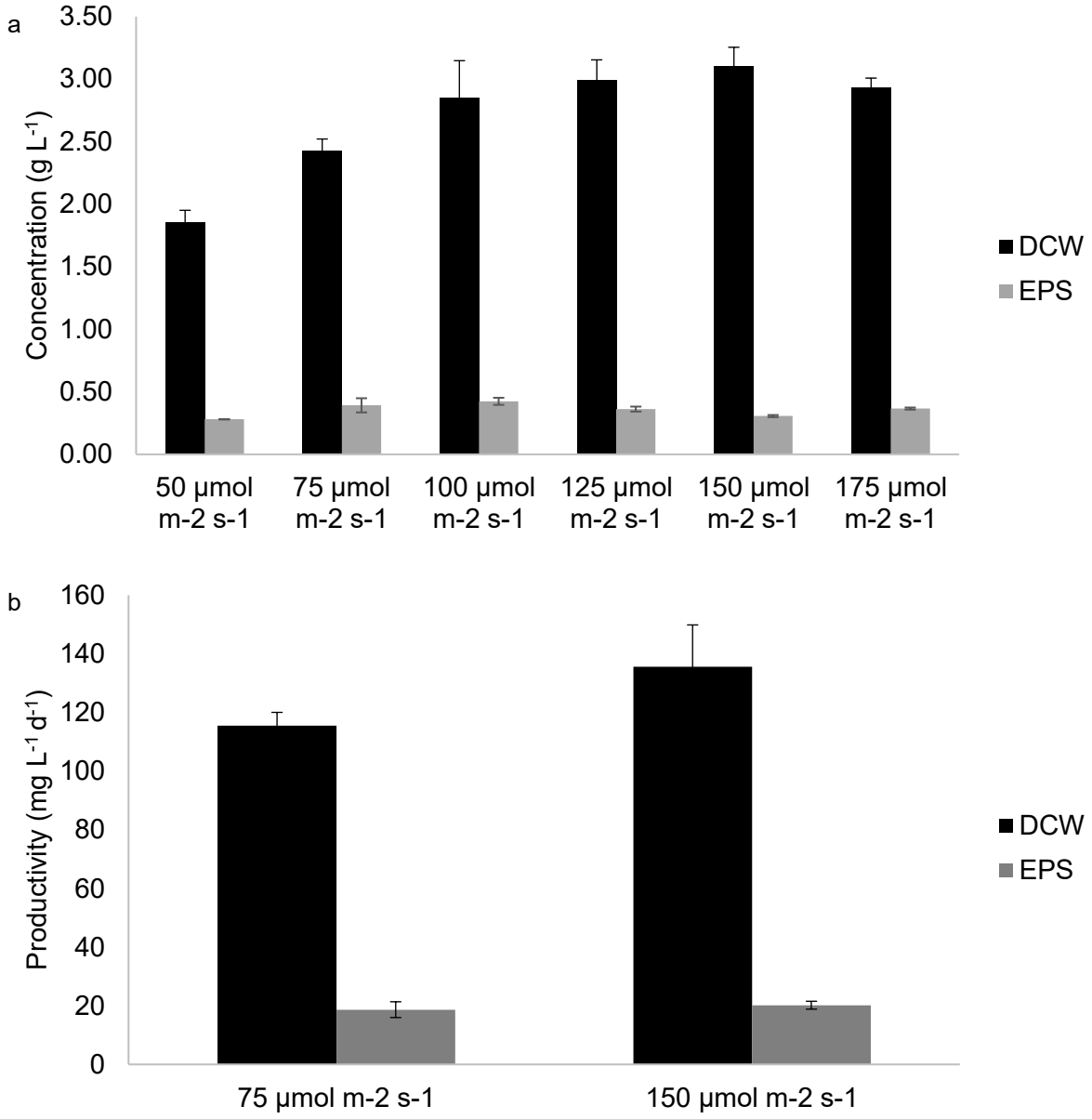


Figure 6-8 Effect of light intensity (50, 75, 100, 125, 150, 175 µmol m^{-2} s^{-1}) on *Nostoc foliaceum* dry cell weight (DCW) and extracellular polymeric substances (EPS) at 25% working volume (12.5 mL culture in 50 mL Erlenmeyer flasks), 25 °C, and 150 RPM shaking for 21 days (Exp. 2-3).(a) DCW and EPS concentration depending on light intensity on day 21. (b) Comparison of DCW and EPS productivity under 75 and 150 µmol m^{-2} s^{-1}. Values represent mean ± 1

standard deviation of biological duplicates (n=2). Asterisk (*) shows statistically significant difference: * ($p<0.05$); ** ($p<0.01$); *** ($p<0.001$). µmol m^{-2} s^{-1})

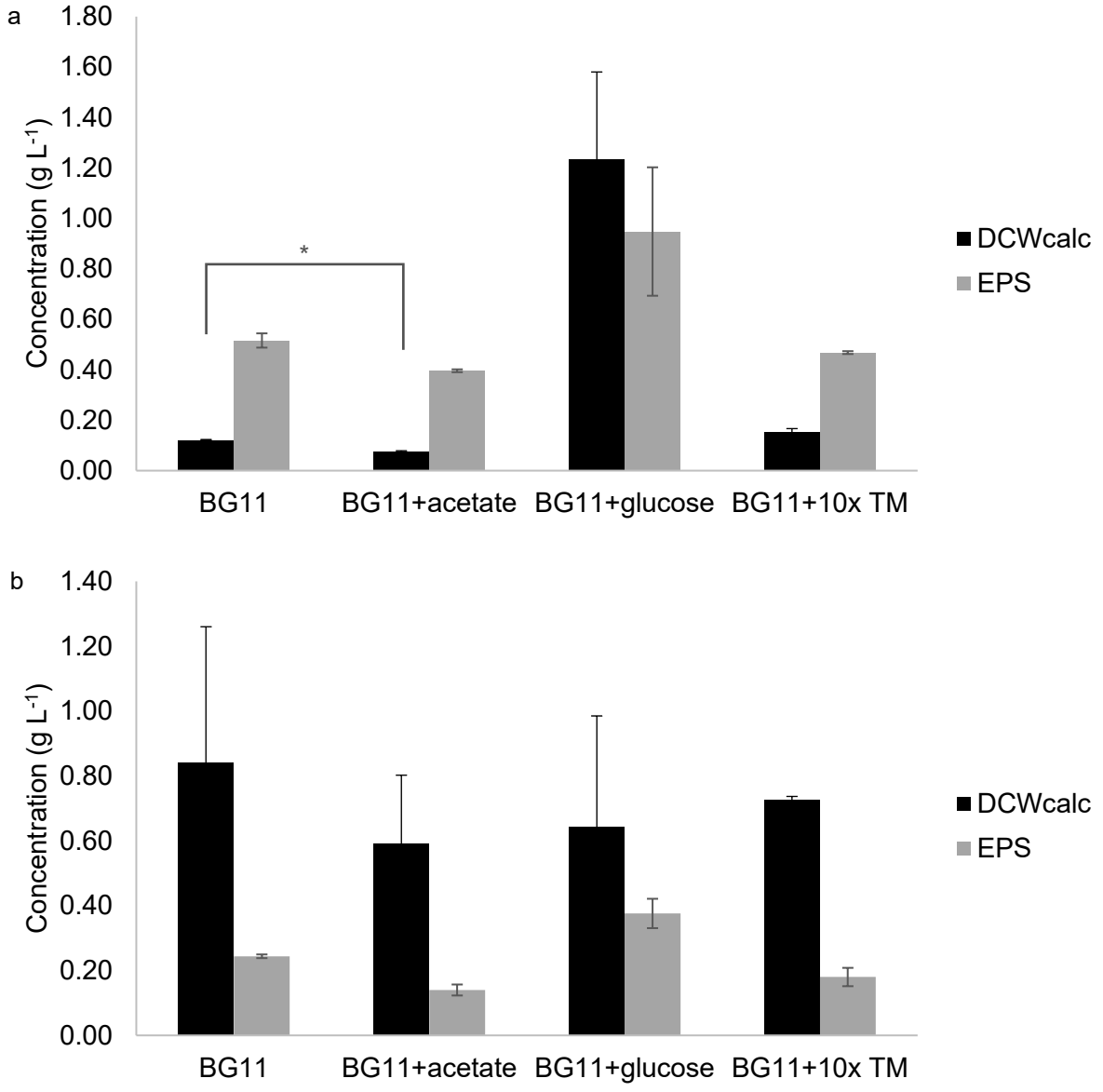
Based on the obtained results, the optima of 100 and 150 µmol m^{-2} s^{-1} were concluded for *C. brevissima* and *N. foliaceum*, respectively, and applied for the multi-factor optimisation experiment (sections 6.7 and 6.9, Exp. 2-6).

6.6 Impact of BG-11 Media Composition and pH

To select suitable media conditions for the multi-factor optimisation experiments, two experiments with different BG-11 medium compositions were performed. Firstly, the effect of glucose, acetate and trace metals supplementation on *C. brevissima* and *N. foliaceum* was studied (Exp. 2-4). As described in section 2.3.5, the C:N ratio is an important factor to increase EPS production, hence the amount of carbon was increased in the medium by addition of glucose or acetate [173]. Figure 6-9*a-b* shows that BG-11 supplemented with 5 g L^{-1} glucose resulted in highest EPS production in both species. The effect was more pronounced in *C. brevissima*, reaching 1.23 ± 0.35 g L^{-1} (n=2) DCW_{Max} and 0.95 ± 0.25 g L^{-1} (n=2) EPS_{Max} in the glucose-supplemented BG-11. *N. foliaceum* reached 0.38 ± 0.05 g L^{-1} (n=2) EPS_{Max} in glucose- supplemented BG-11. However, the highest DCW was obtained under standard conditions (0.84 ± 0.42 g L^{-1}, n=2). In contrast, 5 g L^{-1} acetate had a negative impact on DCW and EPS of both species. Ten-fold higher trace element levels lead to an increase of biomass but a decrease of EPS in *C. brevissima*, whereas it reduced both, DCW and EPS in *N. foliaceum*. However, most of these results were not statistically significant. The only significant difference in respect to standard BG-11 was the DCW value obtained from *C. brevissima* grown in BG-11 with 5 g L^{-1} acetate ($p=0.0075$).

The positive effect of glucose-supplemented BG-11 was also visible in the appearance of the cultures. As can be seen in Figure 6-9*c-d*, *C. brevissima* appeared as dark green culture in BG-11 with glucose, whereas it appeared brownish in BG-11 and BG-11 with higher trace metals, and light green in BG-11 with acetate. *N. foliaceum* appeared similar for all media, except slightly more biomass in the glucose flask. Possibly, the positive effect of glucose on biomass and EPS production on both species was more pronounced due to absence of shaking. Repetition of the experiment in aerated cultures could have provided more clarity but was not performed due to time

constraints. The glucose that was supplemented to the BG-11 medium was not detectable as a false-positive in the EPS quantification due to the dialysis step described in section 4.1.4. The dialysis, using a membrane with a 14,000 Da cutoff, removes glucose (180 Da) from the samples before the assay, preventing any interference with the EPS measurement.



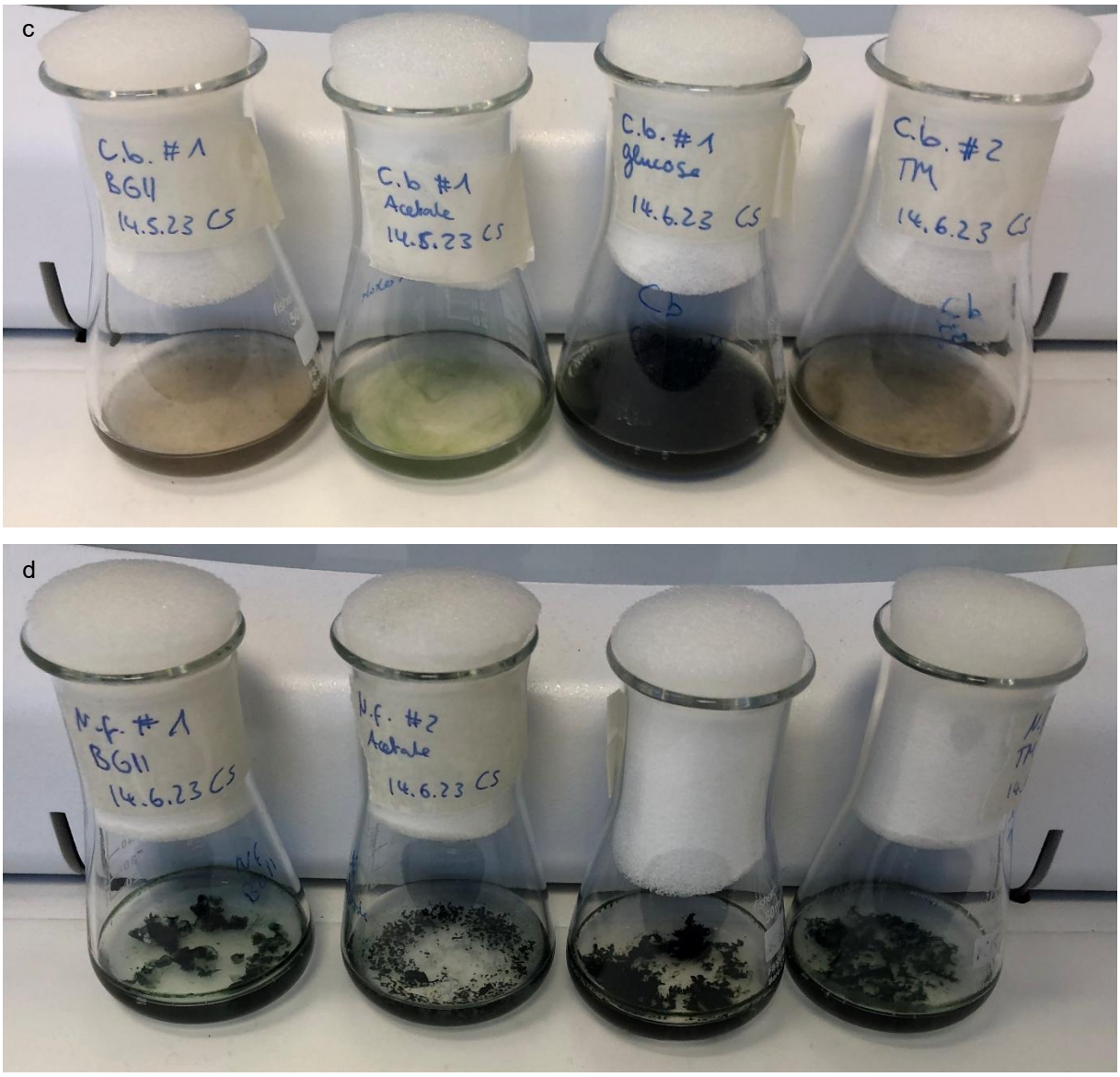
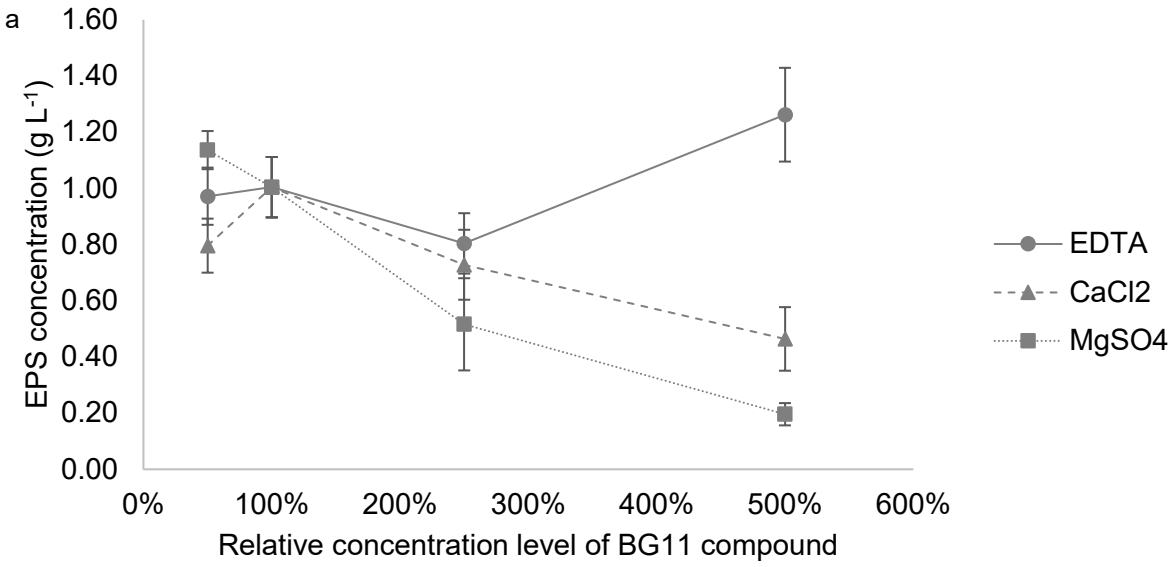
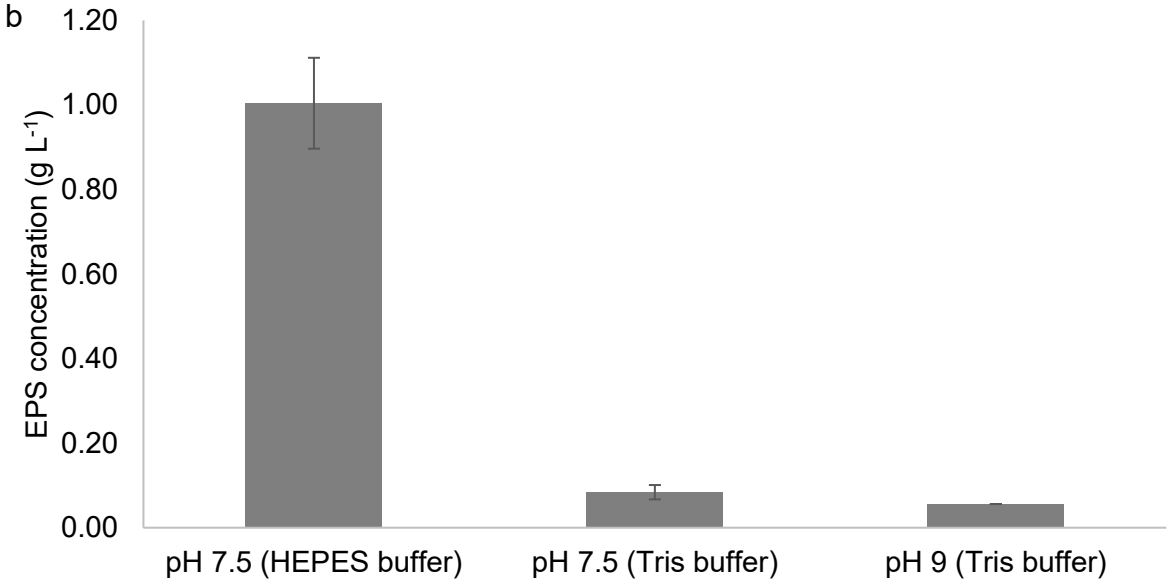


Figure 6-9 Effect of BG-11 composition (supplementation of acetate, glucose and 10-fold higher level of trace elements) on production of biomass and extracellular polymeric substances (EPS) of *Calothrix brevissima* and *Nostoc foliaceum* grown for 15 days at 25°C and 22 µmol m^{-2} s^{-1} without shaking.(a) Dry cell weight (DCWcalc, calculated from OD_{750} based on Equation 4-1) and EPS concentration of *Calothrix brevissima* depending on different media conditions: BG-11 (standard), BG-11 supplemented with 5 g L^{-1} acetate, BG-11 supplemented with 5 g L^{-1} glucose, and BG-11 supplemented with 10-fold higher level of trace elements. (b) DCW calculated from OD_{750} and EPS concentration of *Nostoc foliaceum* depending on the different media conditions. Values show mean ± 1 standard deviation (n=2). (c) Photo of *Calothrix brevissima* cultures on day 15. (d) Photo of *Nostoc foliaceum* cultures on day 15. Asterisk (*) shows statistically significant difference: * ($p<0.05$); ** ($p<0.01$); *** ($p<0.001$).

The effect of media components $MgSO_4$, EDTA, $CaCl_2$ at different levels of standard BG-11 level (50%, 100%, 250% and 500%) as well as the effect of pH using Tris buffer (pH 7.5 and pH 9) was studied (Exp. 2-5). As shown in Figure 6-10*a*, the higher the $MgSO_4$ level, the less EPS was produced. Reducing the $MgSO_4$ to 50%, increased EPS by 12.3% to 1.14 ± 0.07 g L^{-1} (n=2) compared to standard BG-11 level. However, this difference was not statistically significant. 500% $MgSO_4$ resulted in the lowest EPS (0.20 ± 0.04 g L^{-1}, n=2) obtained in this experiment, which was significantly different from standard BG-11 (1.00 ± 0.11 g L^{-1}, n=2, p=0.037). Increase and decrease of the concentration of $CaCl_2$ had a negative impact on EPS, with the highest EPS being found at standard BG-11 level (1.00 ± 0.11 g L^{-1}, n=2). EPS at 500% $CaCl_2$ were significantly lower than standard level (0.80 ± 0.10 g L^{-1}, n=2, p=0.040). Calcium has been suggested to be essential for EPS production, especially in the absence of boron [189]. It has been observed that EPS increase with increasing $CaCl_2$ concentration, contrary to the obtained results in this PhD thesis [180]. However, optima likely differ from species to species.


a
1.60
1.40
1.20
1.00
0.80
0.60
0.40
0.20
0.00
EPS concentration (g L-1)
0%
100%
200%
300%
400%
500%
600%
Relative concentration level of BG11 compound
EDTA
CaCl2
MgSO4


b
1.20
1.00
0.80
0.60
0.40
0.20
0.00
EPS concentration (g L-1)
pH 7.5 (HEPES buffer)
pH 7.5 (Tris buffer)
pH 9 (Tris buffer)

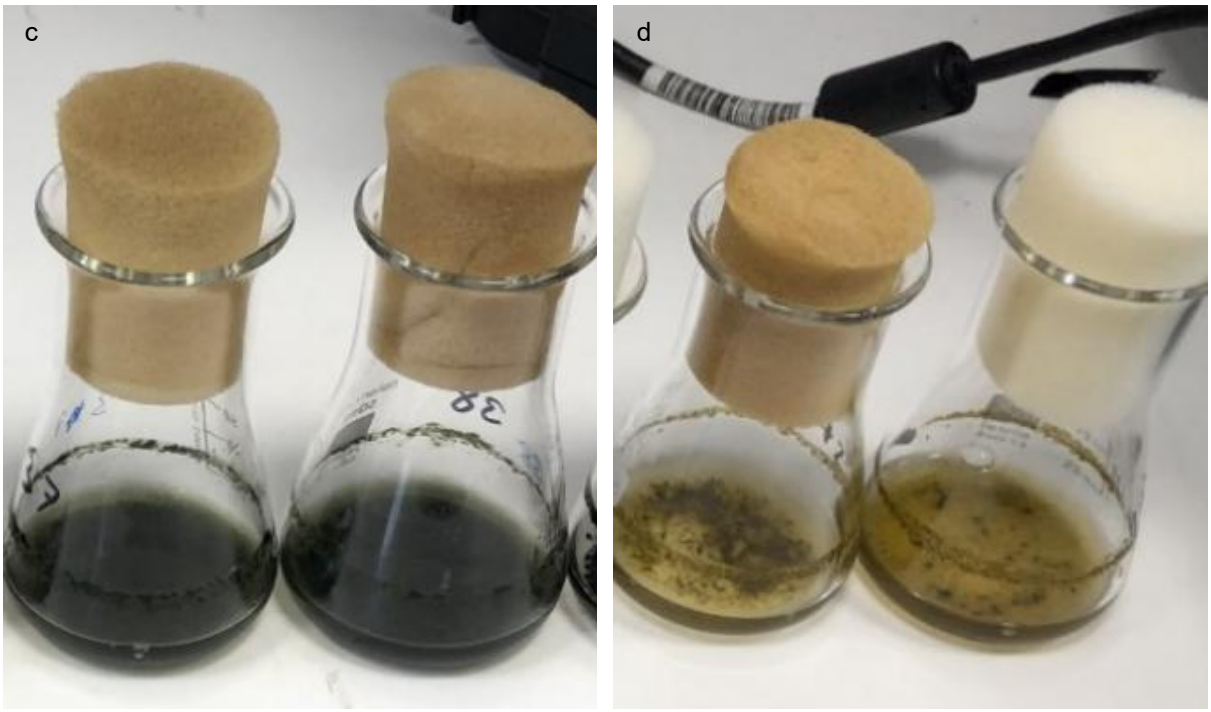


Figure 6-10 Effect of magnesium, calcium, ethylenediaminetetraacetic acid (EDTA), Tris(hydroxymethyl)aminomethane (Tris) buffer and 4-(2-Hydroxyethyl)-1-Piperazineethanesulfonic Acid (HEPES) buffer in the BG-11 medium on extracellular polymeric substances (EPS) production of *Calothrix brevissima* grown for 15 days at 25°C and 22 µmol m^{-2} s^{-1} at 250 RPM.(a) EPS concentration of *Calothrix brevissima* based on $MgSO_4$, $CaCl_2$, EDTA level in the medium compared to BG-11 standard level. (b) Effect of pH (pH 7.5 vs. pH 9) and type of buffer (Tris-buffered vs. HEPES-buffered) medium on EPS production of *Calothrix brevissima*. (c) Photo of *Calothrix brevissima* culture grown in HEPES-buffered medium (day 15). (d) Photo of *Calothrix brevissima* culture grown in Tris-buffered medium (day 15). Values show mean ± 1 standard deviation (n=2). Asterisk (*) shows statistically significant difference: * ($p<0.05$); ** ($p<0.01$); *** ($p<0.001$).

Initially, increasing EDTA had a negative effect on EPS (up until 250% EDTA), but at 500% EDTA, the highest EPS concentration was obtained (1.26 ± 0.17 g L^{-1}, n=2), which exceeded standard BG-11 by 30%. However, this difference was not statistically significant. Due to EDTA being a chelating agent, too high concentrations could potentially deplete essential metal ions from the cells, leading to deficiencies and impaired cellular functions [135]. The production of EPS could be a cellular response to capture nutrients during conditions of nutrient deficiency. For example, Mg^{2+} is a cation that can be effectively chelated by EDTA [338]. The EDTA results in combination

with the magnesium results could indicate that *C. brevissima* produced EPS to capture nutrients such as magnesium. Potentially, when magnesium was abundant, EPS were not required, and production was decreased. When magnesium was less available, either by lowering the concentration to 50%, or by making it unavailable using chelating agents, the cells produced more EPS. In literature, EPS production of *Cyanospira capsulata* was enhanced by magnesium starvation [186]. However, more research would be required to test this hypothesis, before definite conclusions can be drawn.

As shown in Figure 6-10*b*, Tris buffer had a negative effect on EPS, leading to a significant reduction (90%) to 0.08 ± 0.02 g L^{-1} (n=2) compared to HEPES buffer (pH=7.5, p=0.047). This was likely caused by the negative effect of Tris buffer on *C. brevissima* culture shown in Figure 6-10*d*, which shows *C. brevissima* culture appearing as deeply yellow colour. In literature, use of Tris buffer has shown a 'deleterious effect' on growth, phycoerythrin content and chlorophyll *a* content of red algae *Gracilaria birdie*. The authors suggested that this effect may be related to disruptions in nitrogen acquisition or assimilation [339]. Regarding the effect of pH on EPS from Tris-grown cells, neutral pH (7.5) resulted in slightly more EPS than a basic pH of 9 (0.06 ± 0.01 g L^{-1}, n=2, Figure 6-10*b*). However, the difference was not statistically significant, and inconclusive due to the use of an unsuitable buffer.

Based on the results of these two experiments, glucose showed the most drastic increase in EPS and was hence selected as the third factor for multi-factor experiment to be tested alongside of light intensity and temperature. Light intensity and temperature were chosen since those two parameters were most relevant in literature for the cyanobacterium *A. platensis*, as described in the literature review (section 2.3.1) [46, 168].

6.7 Multi-Factor Optimisation Results for *N. foliaceum*

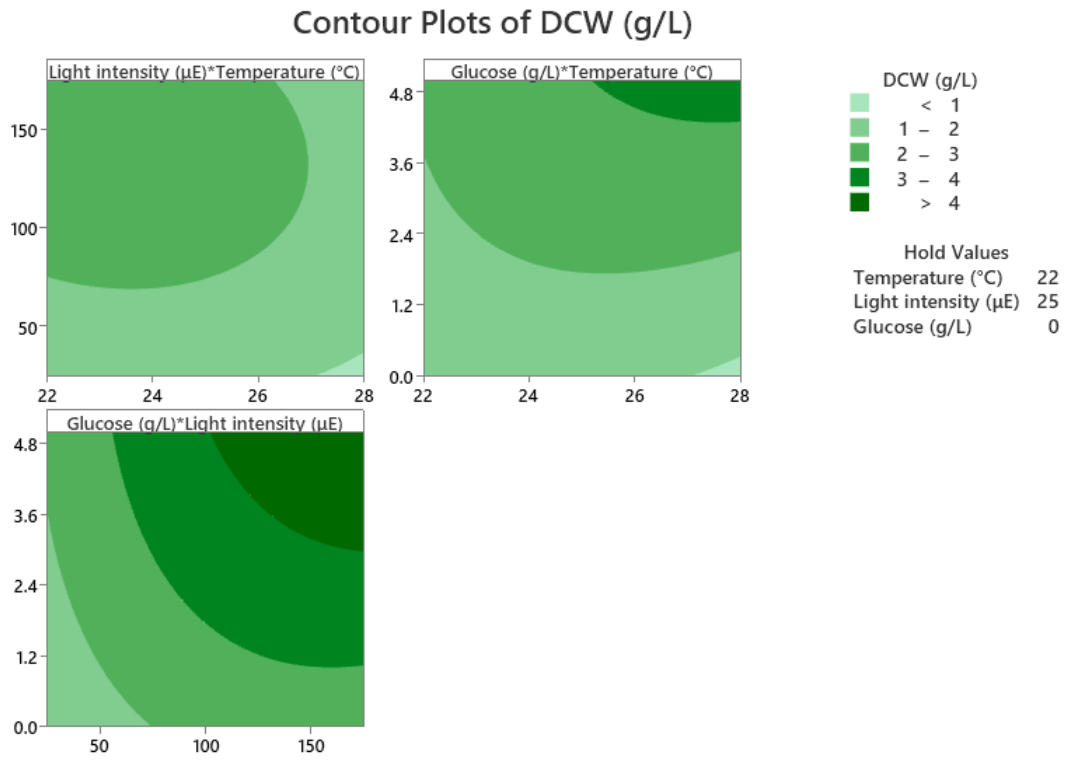
Multi-factor optimisation for maximum EPS production in *N. foliaceum* was performed using DoE with Minitab software. A Box-Benken-Design was used to study light intensity, temperature, and glucose concentration to examine their individual and combined effects on DCW and EPS production. The experimental results obtained are shown in Table 6-1. Depending on the conditions, *N. foliaceum* produced up to 5.96 ± 0.80 g L^{-1} (n=2) DCW and up to 0.64 ± 0.04 g L^{-1} (n=2) EPS.

Table 6-1 Dry cell weight (DCW) and extracellular polymeric substances (EPS) concentrations of *Calothrix brevissima* after three-factor optimisation of temperature, light intensity, and glucose concentration using a Box-Behnken design (Experiment 2-6).Cultures were grown for 14 days at 150 RPM in 50 mL Erlenmeyer flasks with 25 % working volume at three levels of temperature (22, 25, 28 °C), light intensity (75, 150, 225 µmol m^{-2} s^{-1}), and glucose concentration (0, 0.25, 5 g L^{-1}). Values represent mean ± 1 standard deviation (n=2).

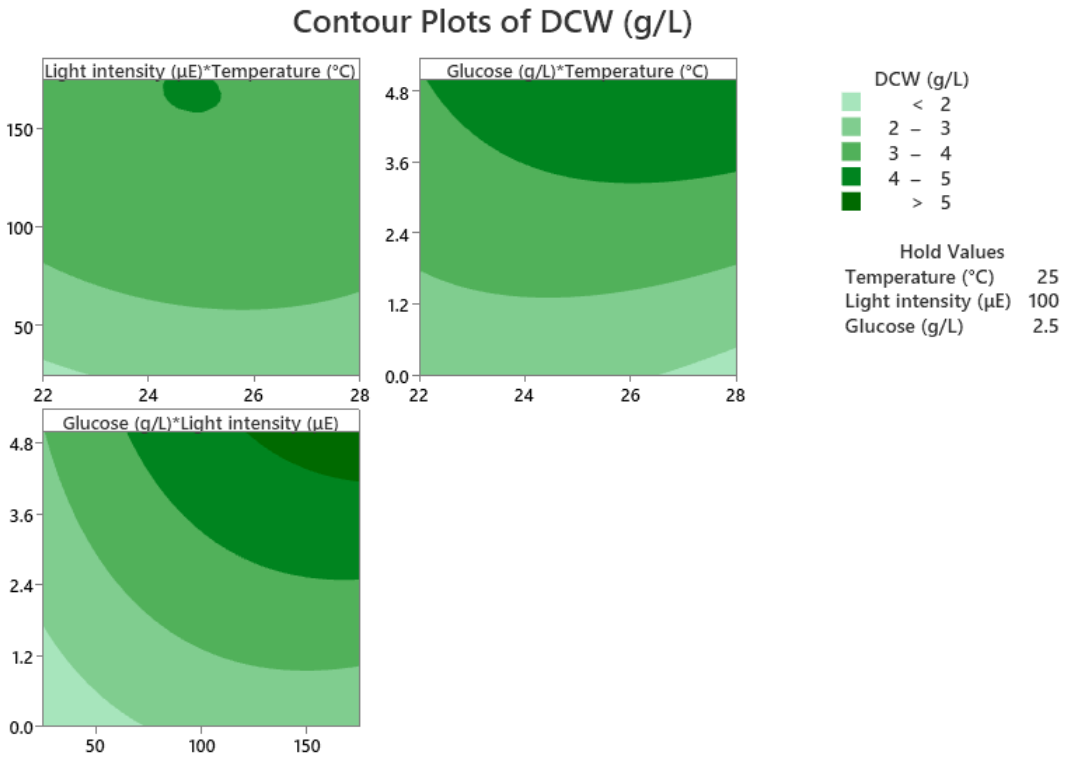
Temperature	**Light intensity**	**Glucose**	**DCW**	**EPS**
°C	µmol m^{-2} s^{-1}	g L^{-1}	g L^{-1}	g L^{-1}
22	150	0	2.12 ± 0.10	0.28 ± 0.12
22	75	2.5	2.27 ± 0.12	0.23 ± 0.11
22	225	2.5	3.88 ± 0.23	0.37 ± 0.02
22	150	5	3.51 ± 0.23	0.39 ± 0.03
25	75	0	0.76 ± 0.09	0.08 ± 0.00
25	225	0	2.27 ± 0.06	0.25 ± 0.02
25	150	2.5	3.71 ± 0.09	0.51 ± 0.01
25	150	2.5	3.43 ± 0.14	0.50 ± 0.02
25	75	5	2.93 ± 0.19	0.30 ± 0.02
25	225	5	5.96 ± 0.80	0.54 ± 0.03
28	150	0	2.10 ± 0.23	0.40 ± 0.05
28	75	2.5	2.08 ± 0.05	0.16 ± 0.01
28	225	2.5	3.22 ± 0.20	0.64 ± 0.04
28	150	5	5.01 ± 0.27	0.53 ± 0.02

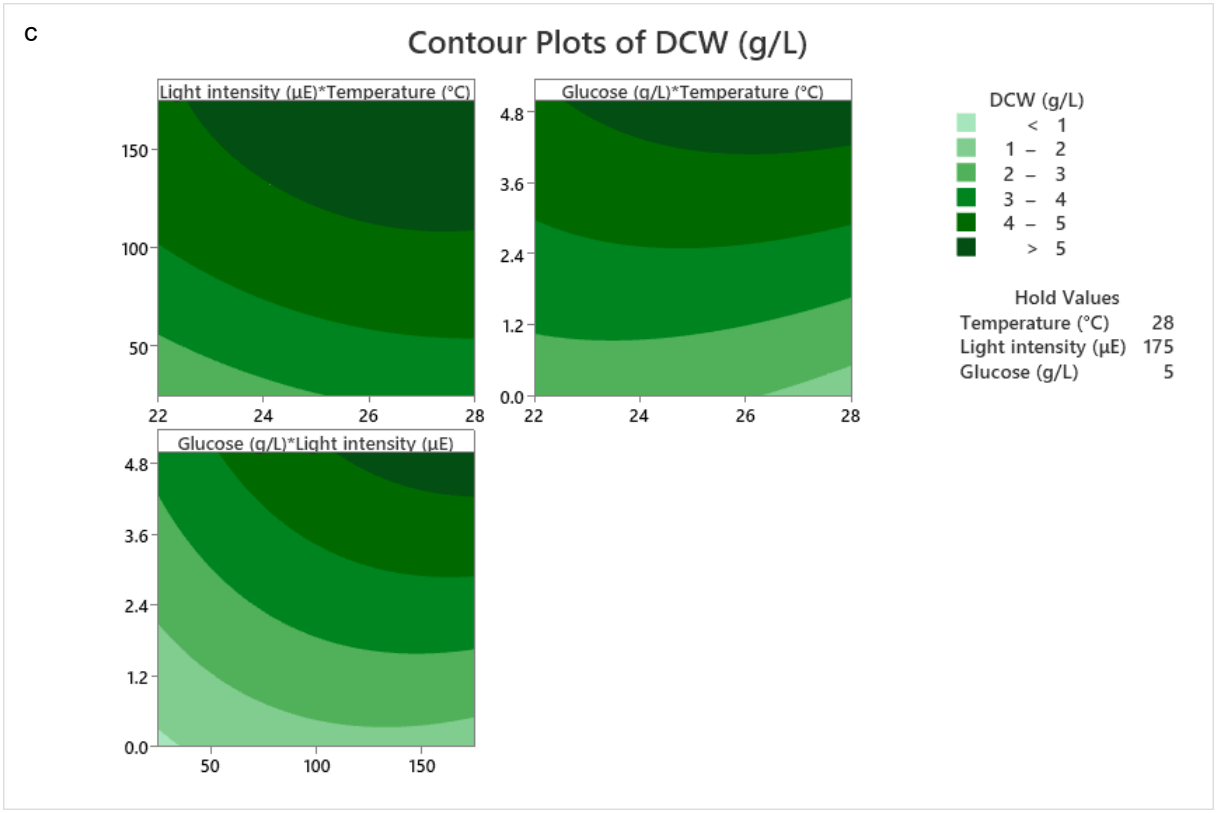
As shown in Figure 6-11*d*, for DCW production of *N. foliaceum*, glucose was the most influential factor, followed by light intensity and several combinations of factors. All three factors had a positive effect on DCW with the highest DCW values being obtained at the upper limit of the ranges (Figure 6-11*a-c*). The optimal conditions were calculated by Minitab as 27.75°C, 175 µmol m^{-2} s^{-1} and 5 g L^{-1} glucose, at which a DCW value of 5.60 g L^{-1} was predicted. This indicates that the true DCW optimum is likely to lie outside of the tested conditions. Response Surface Regression Analysis of the DCW data of *N. foliaceum* with Minitab software showed an R^2 value of 90.83%, showing a strong fit with the experimental data.

a


Contour Plots of DCW (g/L)
Light intensity (µE)*Temperature (°C)
Glucose (g/L)*Temperature (°C)
Glucose (g/L)*Light intensity (µE)
DCW (g/L)
< 1
1 – 2
2 – 3
3 – 4
> 4
Hold Values
Temperature (°C) 22
Light intensity (µE) 25
Glucose (g/L) 0

b


Contour Plots of DCW (g/L)
Light intensity (µE)*Temperature (°C)
Glucose (g/L)*Temperature (°C)
Glucose (g/L)*Light intensity (µE)
DCW (g/L)
< 2
2 – 3
3 – 4
4 – 5
> 5
Hold Values
Temperature (°C) 25
Light intensity (µE) 100
Glucose (g/L) 2.5



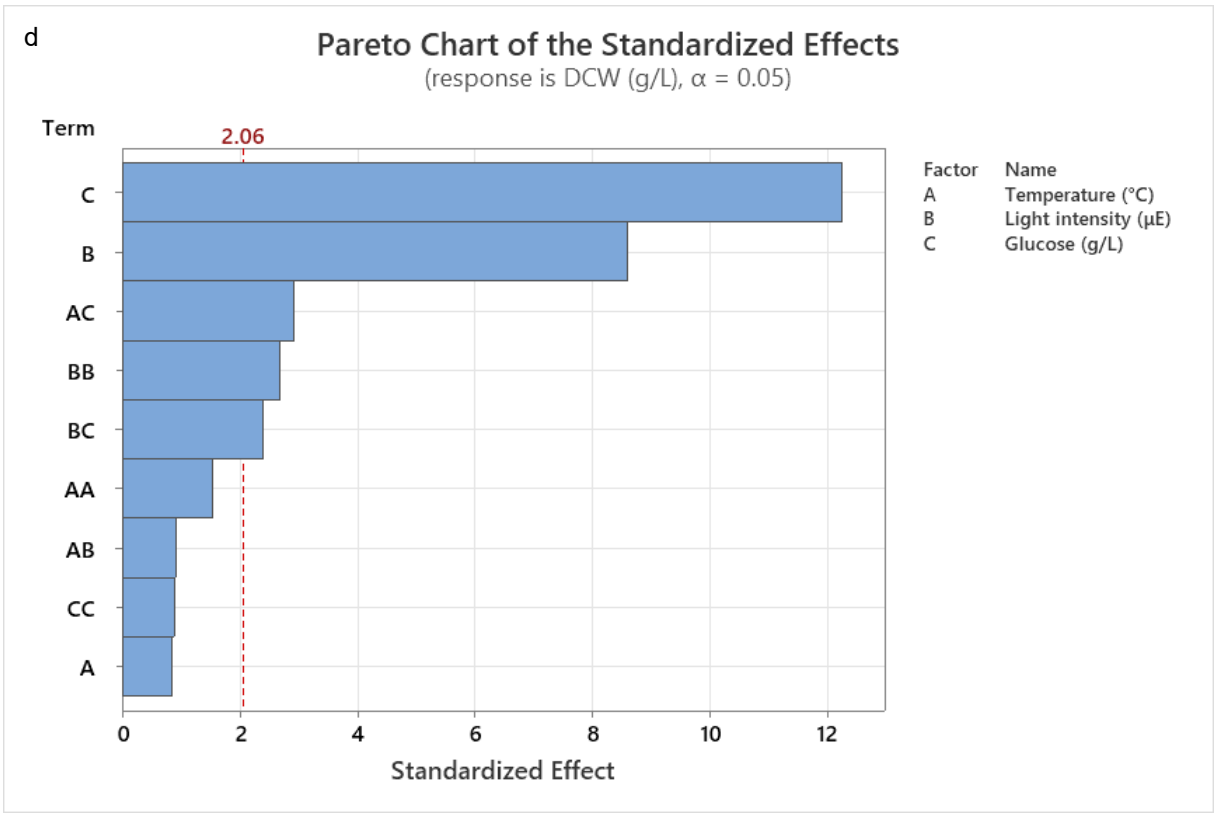
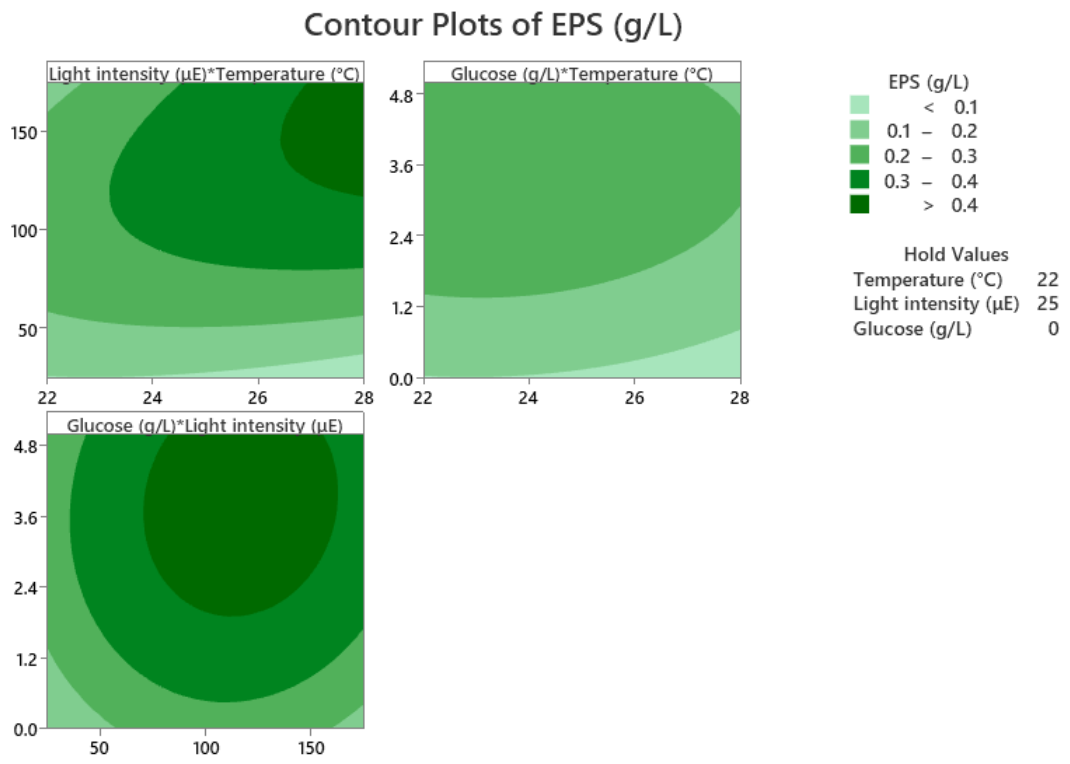


Figure 6-11 Contour plots and Pareto chart of dry cell weight (DCW) production in *Nostoc foliaceum* cultivated for 14 days at 150 RPM in 50 mL Erlenmeyer flasks with 25% working volume (n=2, Experiment 2-6).(a) Contour plot of DCW at hold values of 22°C, 25 µmol m^{-2} s^{-1} light intensity, and 0 g L^{-1} glucose. (b) Contour plot of DCW at hold values of 25°C, 100 µmol

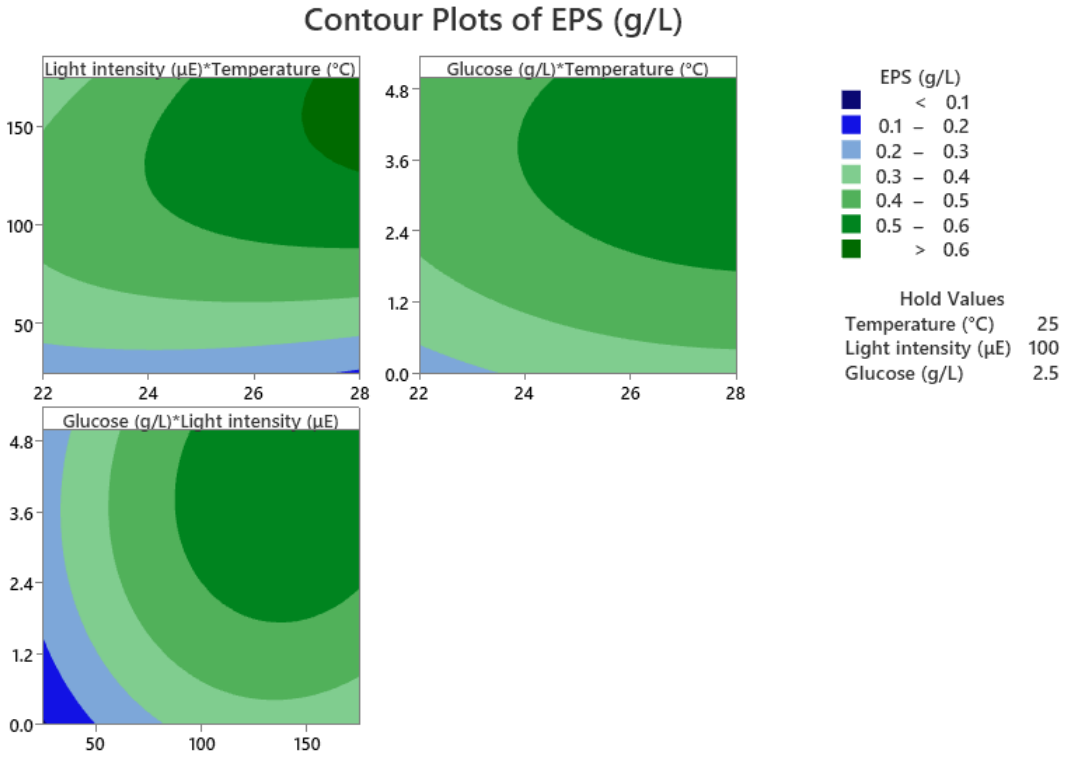
m^{-2} s^{-1} light intensity, and 2.5 g L^{-1} glucose. (c) Contour plot of DCW at hold values of 28°C, 175 µmol m^{-2} s^{-1} light intensity, and 5 g L^{-1} glucose. (d) Pareto chart showing the relative influence of individual parameters and their interactions on DCW concentration.

For EPS production in *N. foliaceum*, the analysis showed that all three factors, as well as certain combinations of them, were significantly correlated with EPS production (Figure 6-12*d*). Among these, light intensity had the greatest impact, followed by glucose concentration and temperature. Higher levels of each factor consistently led to increased EPS concentrations, with the highest titre observed at the upper limits of light intensity, temperature, and glucose concentration (Figure 6-12*a*-*c*). The EPS production showed a slightly lower R^2 value of 88.68%.

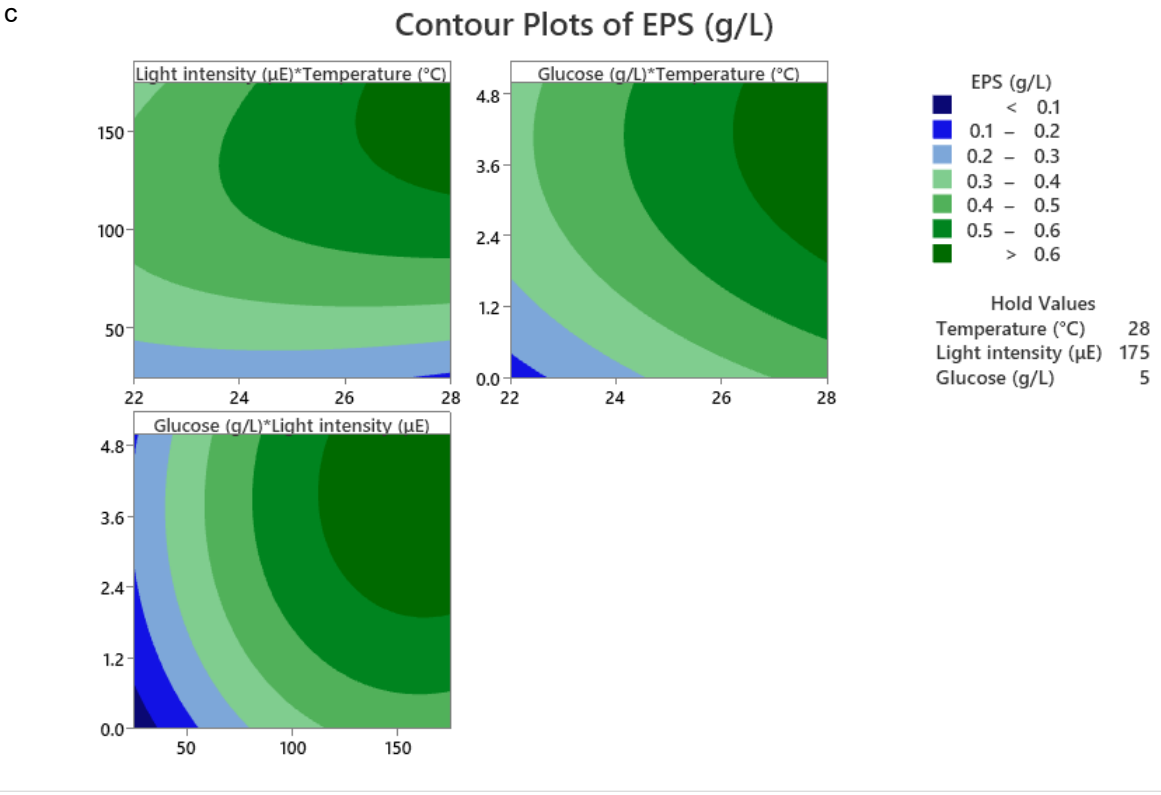
a


Contour Plots of EPS (g/L)
Light intensity (µE)*Temperature (°C)
Glucose (g/L)*Temperature (°C)
Glucose (g/L)*Light intensity (µE)
EPS (g/L)
< 0.1
0.1 – 0.2
0.2 – 0.3
0.3 – 0.4
> 0.4
Hold Values
Temperature (°C) 22
Light intensity (µE) 25
Glucose (g/L) 0

b


Contour Plots of EPS (g/L)
Light intensity (µE)*Temperature (°C)
Glucose (g/L)*Temperature (°C)
Glucose (g/L)*Light intensity (µE)
EPS (g/L)
< 0.1
0.1 – 0.2
0.2 – 0.3
0.3 – 0.4
0.4 – 0.5
0.5 – 0.6
> 0.6
Hold Values
Temperature (°C) 25
Light intensity (µE) 100
Glucose (g/L) 2.5

c


Contour Plots of EPS (g/L)
Light intensity (µE)*Temperature (°C)
Glucose (g/L)*Temperature (°C)
Glucose (g/L)*Light intensity (µE)
EPS (g/L)
< 0.1
0.1 – 0.2
0.2 – 0.3
0.3 – 0.4
0.4 – 0.5
0.5 – 0.6
> 0.6
Hold Values
Temperature (°C) 28
Light intensity (µE) 175
Glucose (g/L) 5

d

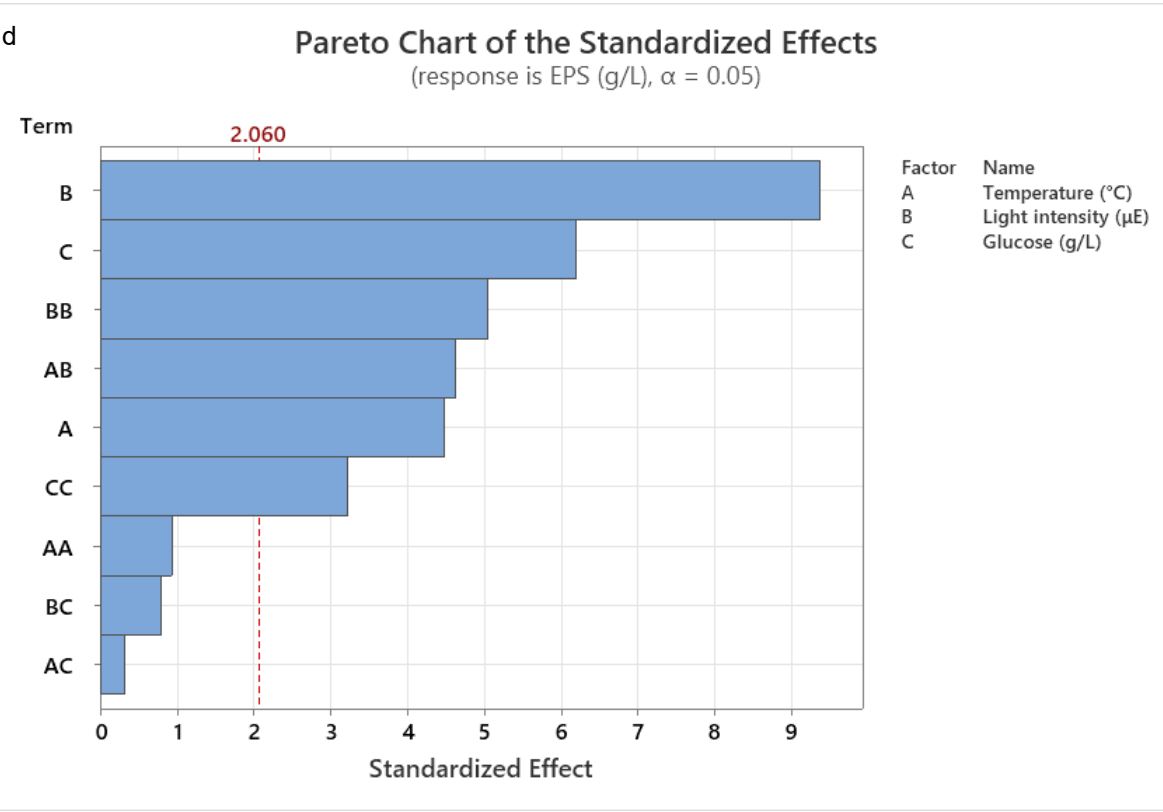

Pareto Chart of the Standardized Effects
(response is EPS (g/L), α = 0.05)
Term
2.060
B
C
BB
AB
A
CC
AA
BC
AC
Standardized Effect
Factor Name
A Temperature (°C)
B Light intensity (µE)
C Glucose (g/L)

Figure 6-12 Contour plots and Pareto chart of extracellular polymeric substances (EPS) production in *Nostoc foliaceum* cultivated for 14 days at 150 RPM in 50 mL Erlenmeyer flasks with 25% working volume (n=2) (Experiment 2-6).(a) Contour plot of EPS at hold values of 22°C, 25 µmol m^{-2} s^{-1} light intensity, and 0 g L^{-1} glucose. (b) Contour plot of EPS at hold values of 25°C, 100 µmol m^{-2} s^{-1} light intensity, and 2.5 g L^{-1} glucose. (c) Contour plot of EPS at hold values of 28°C, 175 µmol m^{-2} s^{-1} light intensity, and 5 g L^{-1} glucose. (d) Pareto chart showing the relative influence of individual parameters and their interactions on EPS concentration.

Minitab's optimisation feature suggested that the ideal conditions for EPS production were 28°C, 164 µmol m^{-2} s^{-1} and 4.84 g L^{-1} glucose, predicting an EPS concentration of 0.67 g L^{-1}. This was slightly higher than the maximum EPS concentration observed during the experiments, which was 0.64 ± 0.04 g L^{-1} (n=2), obtained at 28°C, 225 µmol m^{-2} s^{-1} and 2.5 g L^{-1} glucose. The upper limits of the experimental design may have restricted the ability to explore even higher values, possibly preventing the identification of a true optimum. However, the calculated optimal conditions were largely within the tested range, except for temperature. To explore this further, experiments at higher temperatures could help determine whether EPS production increases; however, this was not performed due to time constraints.

6.8 Biomass and EPS production of *N. foliaceum* under Optimised Conditions

The conditions to maximise EPS production in *N. foliaceum* were identified as 28°C, 4.84 g L^{-1} glucose and 164 µmol m^{-2} s^{-1}. Subsequently, these conditions were validated experimentally. As shown in Figure 6-13*a, N. foliaceum* reached 4.41 ± 0.24 g L^{-1} DCW and an EPS value of 0.70 ± 0.04 g L^{-1} (n=3) on day 14, slightly exceeding Minitab's predicted value of 0.67 g L^{-1}. Notably, this EPS titre surpassed any value observed under different combinations of temperature, light intensity, and glucose concentration during the multi-factor optimisation experiment, demonstrating the efficacy of Minitab in identifying optimal conditions. However, the obtained EPS productivity of 49.7 ± 2.8 mg L^{-1} d^{-1} (n=3), was not significantly different from the previously highest recorded EPS productivity (Figure 6-13*b*). All in all, optimised conditions led to a 5-fold enhancement of EPS production in *N. foliaceum* compared to the screening experiment (Exp. 1).

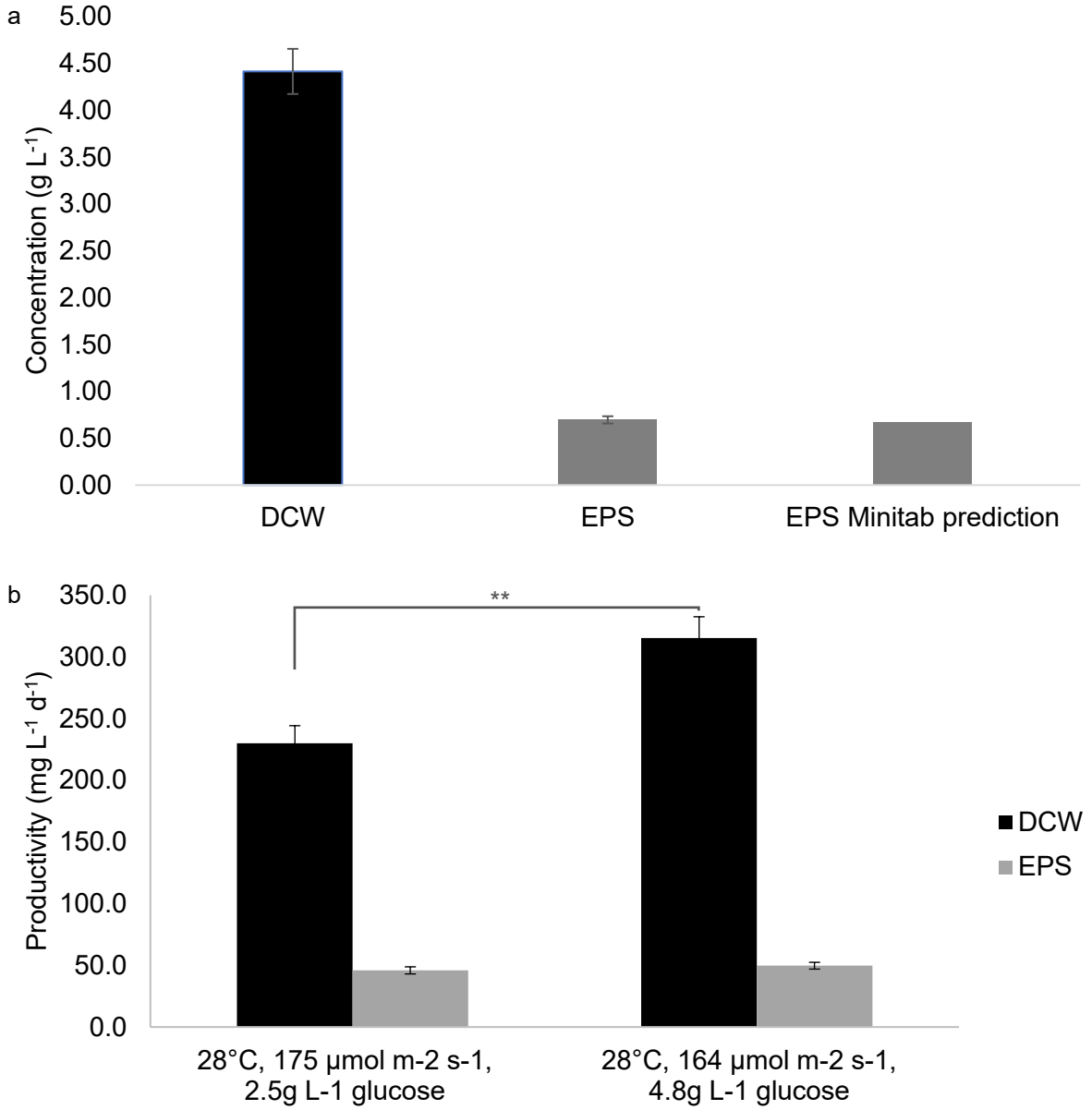


Figure 6-13 Experimental validation of optimal conditions for extracellular polymeric substance (EPS) production in *Nostoc foliaceum*, as predicted by Minitab software (28°C, 4.84 g L^{-1} glucose and 164 µmol m^{-2} s^{-1}).Cultures were grown for 14 days at 150 RPM in 50 mL Erlenmeyer flasks with 25% working volume (Experiment 2-6). (a) Dry cell weight (DCW) and EPS concentration on day 14 compared to predcted EPS values. (b) Comparison of measured DCW and EPS productivities (day 14) with the highest EPS productivity previously obtained for *Nostoc foliaceum* (Experiment 2-3). Values show mean ± 1 standard deviation, n=3 for Exp. 2-6 data and n=2 for Exp. 2-3 data. Asterisk (*) shows statistically significant difference: * ($p<0.05$); ** ($p<0.01$); *** ($p<0.001$).

It is noteworthy that the optimal conditions for EPS did not correspond to those for DCW production. While the highest EPS value of 0.70 ± 0.04 g L^{-1} (n=3) was achieved, DCW production remained at around 4.41 ± 0.24 g L^{-1} (n=3). This was lower than DCW values obtained under different conditions, such as 25°C, 175 µmol m^{-2} s^{-1} light intensity, and 5 g L^{-1} glucose concentration, where DCW had reached 5.96 ± 0.80 g L^{-1} (n=2). However, DCW productivity (315.3 ± 17.2 mg L^{-1} d^{-1} (n=2), was significantly enhanced under optimised conditions (p=0.0031, Figure 6-13*b*). Optima for EPS and DCW production differ for several species (section 2.3) because growth and carbon-based EPS metabolism competing for assimilated carbon and energy source [168]. Further research could increase understanding of the relationship between growth and EPS in *N. foliaceum* cultures.

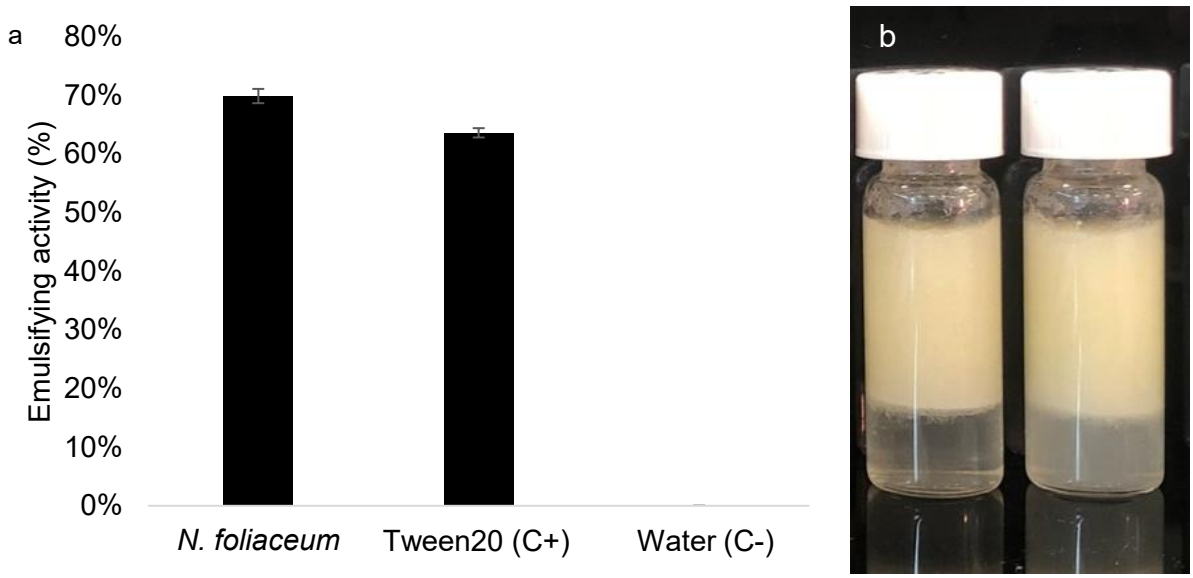


Figure 6-14 Emulsifying activity of extracellular polymeric substances (EPS) from *Nostoc foliaceum* cultivated under optimised conditions (28°C, 4.84 g L^{-1} glucose and 164 µmol m^{-2} s^{-1} light) for 14 days at 150 RPM in 50 mL Erlenmeyer flasks with 25% working volume (Experiment 2-6).(a) Emulsifying activity of EPS at 4 g L^{-1} compared with Tween 20 (positive control, C^+) and water (negative control, C^-). Values show mean ± 1 standard deviation (n=2). (b) Photograph of EPS-based emulsions from *Nostoc foliaceum*.

Additionally, the emulsifying properties of *N. foliaceum* EPS under optimised conditions were tested (Figure 6-14*a*). As only a partial emulsion was observed in the EPS

properties analysis in the screening experiment, a higher EPS concentration (4 g L^{-1}) was used. This led to a 70 ± 1% (n=2) emulsifying activity, exceeding that of Tween20 (64 ± 1%, n=2, 2 g L^{-1}, section 5.5.1). This indicated that *N. foliaceum* EPS could find application as an effective bioemulsifier.

6.9 Multi-Factor Optimisation Results for *C. brevissima*

The multi-factor optimisation of light intensity, glucose and temperature was also performed for *C. brevissima*. The experimental results are shown in Table 6-2. *C. brevissima* reached DCW concentrations of up to 3.24 ± 0.26 g L^{-1} (n=2), when grown in high temperature (28°C), low light (75 µmol m^{-2} s^{-1}) and medium glucose concentration (2.5 g L^{-1}). The highest EPS titre of 2.65 ± 0.07 g L^{-1} (n=2) was obtained under 28°C, 150 µmol m^{-2} s^{-1} and 5 g L^{-1} glucose.

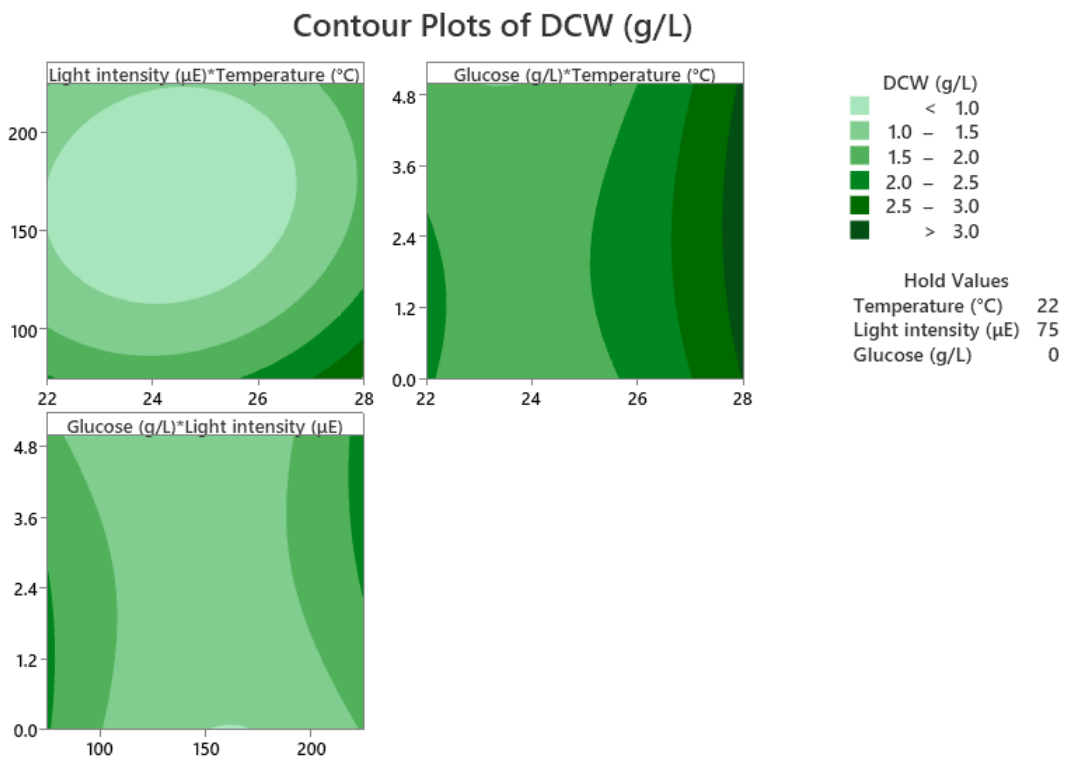
Table 6-2 Dry cell weight (DCW) and extracellular polymeric substances (EPS) concentrations of *Calothrix brevissima* after three-factor optimisation of temperature, light intensity, and glucose concentration using a Box-Behnken design (Experiment 2-6).Cultures were grown for 14 days at 150 RPM in 50 mL Erlenmeyer flasks with 25 % working volume at three levels of temperature (22, 25, 28 °C), light intensity (75, 150, 225 µmol m^{-2} s^{-1}), and glucose concentration (0, 0.25, 5 g L^{-1}). Values represent mean ± 1 standard deviation (n=2).

Temperature	**Light intensity**	**Glucose**	**DCW**	**EPS**
°C	µmol m^{-2} s^{-1}	g L^{-1}	g L^{-1}	g L^{-1}
22	150	0	1.04 ± 0.08	1.00 ± 0.06
22	75	2.5	2.29 ± 0.14	1.50 ± 0.09
22	225	2.5	2.04 ± 1.06	1.39 ± 0.31
22	150	5	0.81 ± 0.03	1.43 ± 0.09
25	75	0	1.42 ± 0.10	0.65 ± 0.06
25	225	0	0.98 ± 0.05	1.02 ± 0.01
25	150	2.5	1.05 ± 0.23	1.51 ± 0.15
25	150	2.5	1.01 ± 0.08	1.32 ± 0.01
25	75	5	2.33 ± 0.04	2.31 ± 0.05
25	225	5	1.74 ± 0.32	1.80 ± 0.07
28	150	0	1.96 ± 0.07	0.38 ± 0.04
28	75	2.5	3.24 ± 0.26	0.51 ± 0.16
28	225	2.5	2.37 ± 0.18	1.50 ± 0.07
28	150	5	2.20 ± 0.55	2.65 ± 0.07

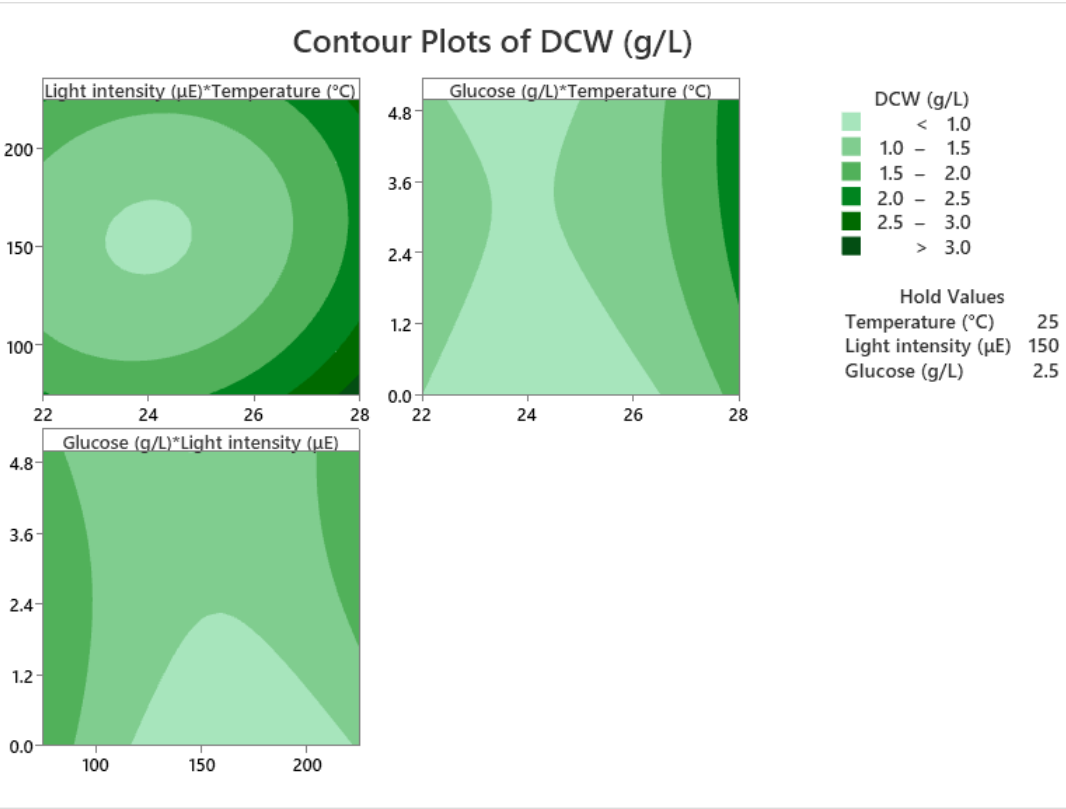
Higher temperature (28°C) and lower light intensity (75 µmol m^{-2} s^{-1}) favoured higher DCW production in *C. brevissima* (Figure 6-15*a*-*c*). For glucose concentration, the contour plots showed pessima rather than optima. From all three factors, temperature was the only statistically significant parameter for DCW production in *C. brevissima* (Figure 6-15*d*). The optimiser feature revealed the upper limit of temperature (28°C) and lower limit of light intensity (75 µmol m^{-2} s^{-1}) as well as medium glucose concentration (2.7 g L^{-1}) as optimum conditions for DCW. This could indicate that the real optimum was outside the tested range of temperature and light intensity. The R^2 score of the model (76.43%) was lower than for *N. foliaceum*, indicating a worse fit of the model. Some cultures showed a brownish yellow tint, possibly indicating they had

entered decay phase at the time of the endpoint sample (day 14). Different growth phases might have skewed the DCW data, resulting in a lower R^2 score.

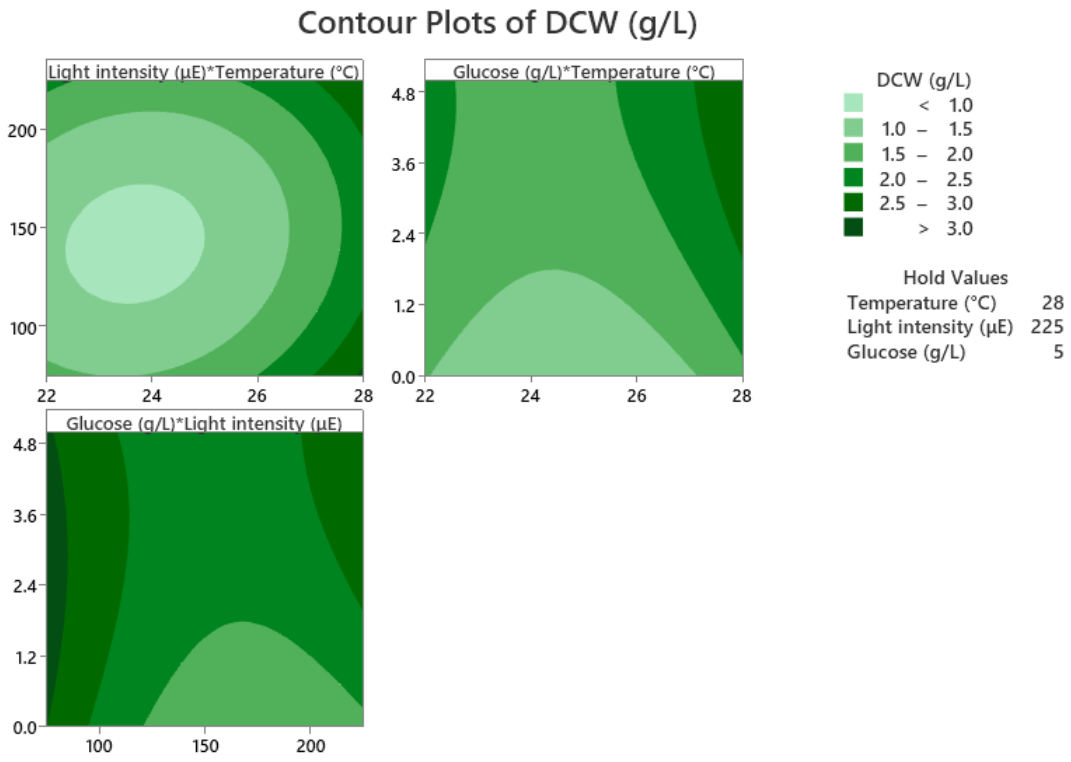
a



b



c


Contour Plots of DCW (g/L)
Light intensity (µE)*Temperature (°C)
Glucose (g/L)*Temperature (°C)
Glucose (g/L)*Light intensity (µE)
DCW (g/L)
< 1.0
1.0 – 1.5
1.5 – 2.0
2.0 – 2.5
2.5 – 3.0
> 3.0
Hold Values
Temperature (°C) 28
Light intensity (µE) 225
Glucose (g/L) 5

d

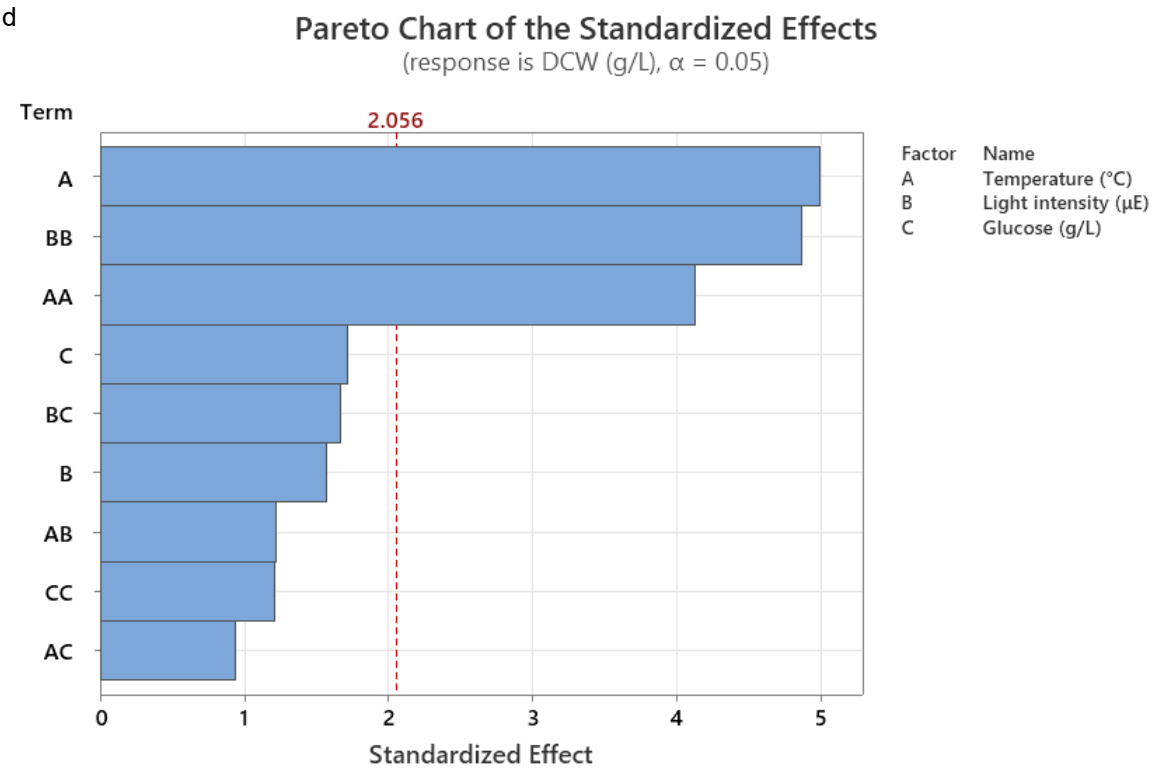
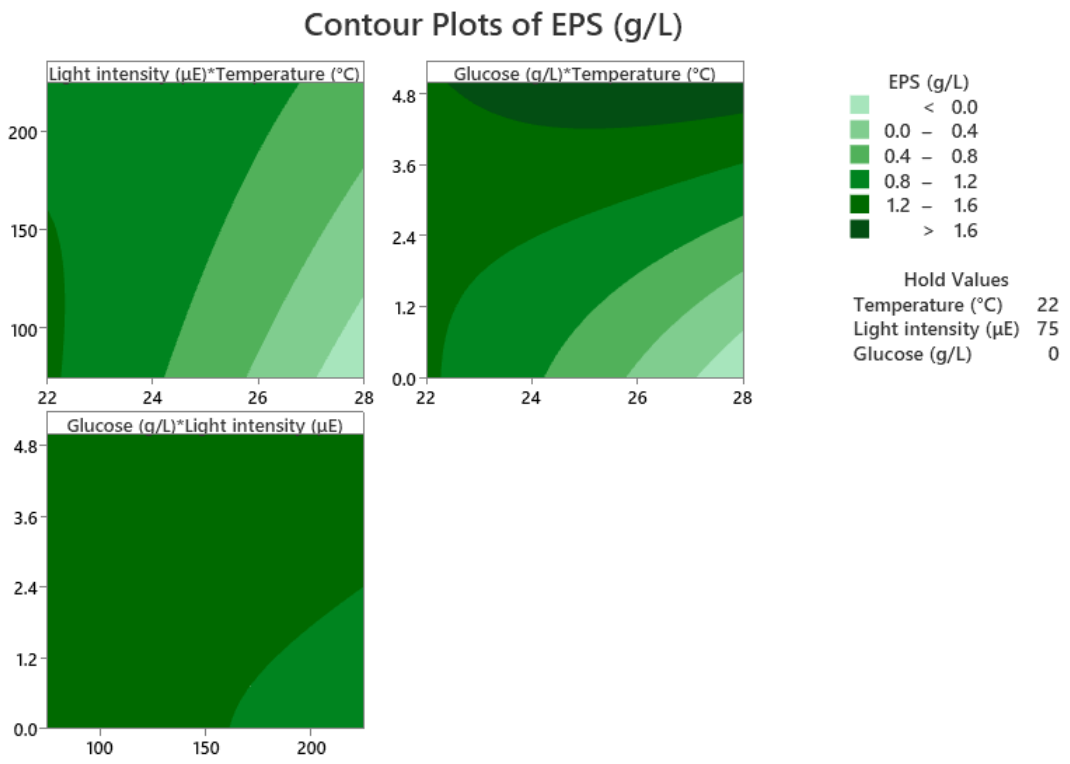

Pareto Chart of the Standardized Effects
(response is DCW (g/L), α = 0.05)
Term
2.056
A
BB
AA
C
BC
B
AB
CC
AC
Standardized Effect
Factor Name
A Temperature (°C)
B Light intensity (µE)
C Glucose (g/L)

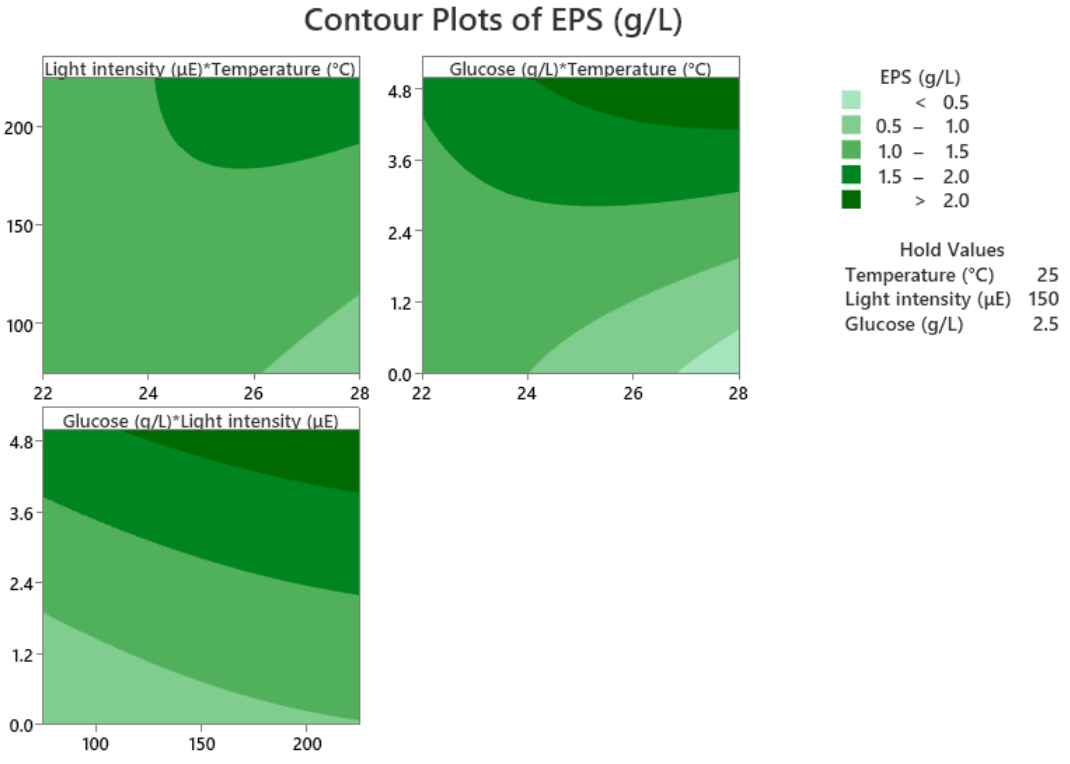
Figure 6-15 Contour plots and Pareto chart of dry cell weight (DCW) production in *Calothrix brevissima* cultivated for 14 days at 150 RPM in 50 mL Erlenmeyer flasks with 25% working volume (n=2) (Experiment 2-6).(a) Contour plot of DCW at hold values of 22°C, 75 µmol m^{-2} s^{-1} light intensity, and 0 g L^{-1} glucose. (b) Contour plot of DCW at hold values of 25°C, 150 µmol m^{-2} s^{-1} light intensity, and 2.5 g L^{-1} glucose. (c) Contour plot of DCW at hold values of 28°C, 225 µmol m^{-2} s^{-1} light intensity, and 5 g L^{-1} glucose. (d) Pareto chart showing the relative influence of individual parameters and their interactions on EPS concentration.

C. brevissima produced most EPS at highest glucose concentration (5 g L^{-1}) and highest temperature (28°C). This trend applied to all three light intensities (Figure 6-16*a-c*). Glucose concentration was the most influential factor for EPS production, followed by light intensity and several combinations of factors (Figure 6-16*d)*. Contrary to DCW production, temperature was not significantly related to EPS. Analysing the EPS concentrations with Minitab software resulted in a R^2 of 91.55%, indicating a much better fit for EPS than for DCW. Applying the EPS optimiser function, the software identified 28°C, 225 µmol m^{-2} s^{-1} and 5 g L^{-1} as the optimum conditions, predicting 2.9 g L^{-1} EPS. This value was slightly higher than the maximum experimental EPS concentration obtained, which was 2.65 ± 0.07 g L^{-1} (n=2) EPS at 28°C, 150 µmol m^{-2} s^{-1} and 5 g L^{-1} glucose. It should be noted that the optimum conditions calculated by Minitab represented the upper limits of each parameter, meaning the true optimum likely lay outside of the tested conditions, similar to the DCW results.

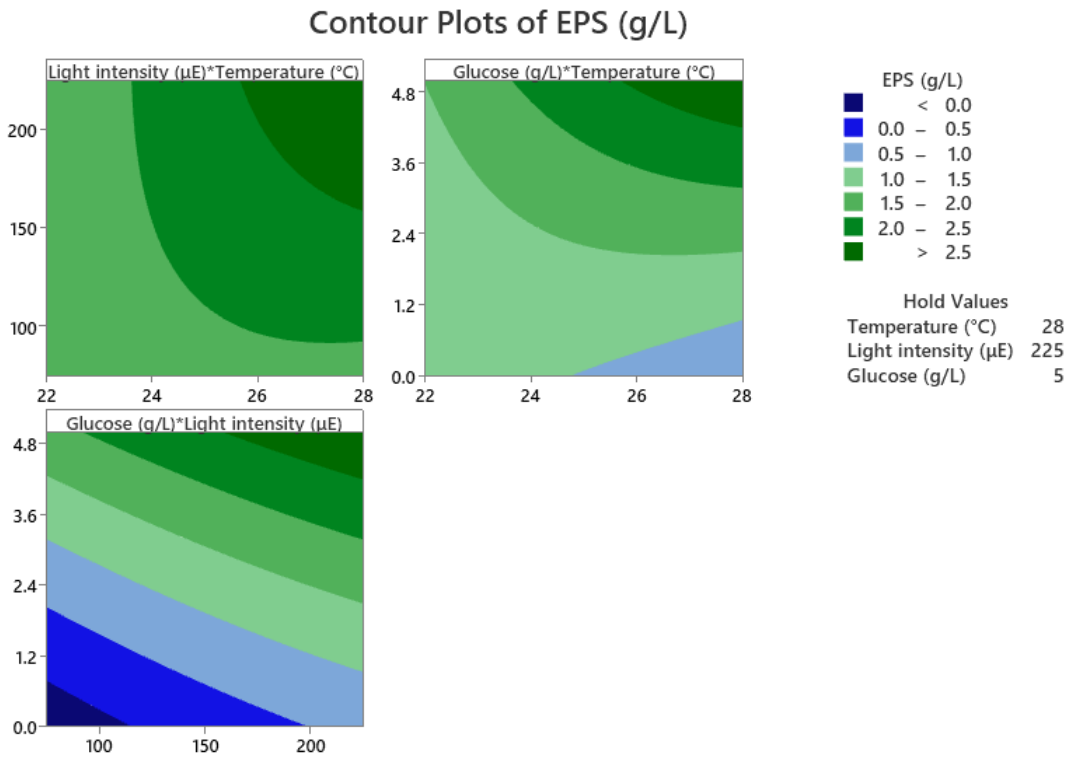
a


Contour Plots of EPS (g/L)
Light intensity (µE)*Temperature (°C)
Glucose (g/L)*Temperature (°C)
Glucose (g/L)*Light intensity (µE)
EPS (g/L)
< 0.0
0.0 – 0.4
0.4 – 0.8
0.8 – 1.2
1.2 – 1.6
> 1.6
Hold Values
Temperature (°C) 22
Light intensity (µE) 75
Glucose (g/L) 0

b


Contour Plots of EPS (g/L)
Light intensity (µE)*Temperature (°C)
Glucose (g/L)*Temperature (°C)
Glucose (g/L)*Light intensity (µE)
EPS (g/L)
< 0.5
0.5 – 1.0
1.0 – 1.5
1.5 – 2.0
> 2.0
Hold Values
Temperature (°C) 25
Light intensity (µE) 150
Glucose (g/L) 2.5

c


Contour Plots of EPS (g/L)
Light intensity (µE)*Temperature (°C)
Glucose (g/L)*Temperature (°C)
Glucose (g/L)*Light intensity (µE)
EPS (g/L)
< 0.0
0.0 – 0.5
0.5 – 1.0
1.0 – 1.5
1.5 – 2.0
2.0 – 2.5
> 2.5
Hold Values
Temperature (°C) 28
Light intensity (µE) 225
Glucose (g/L) 5

d

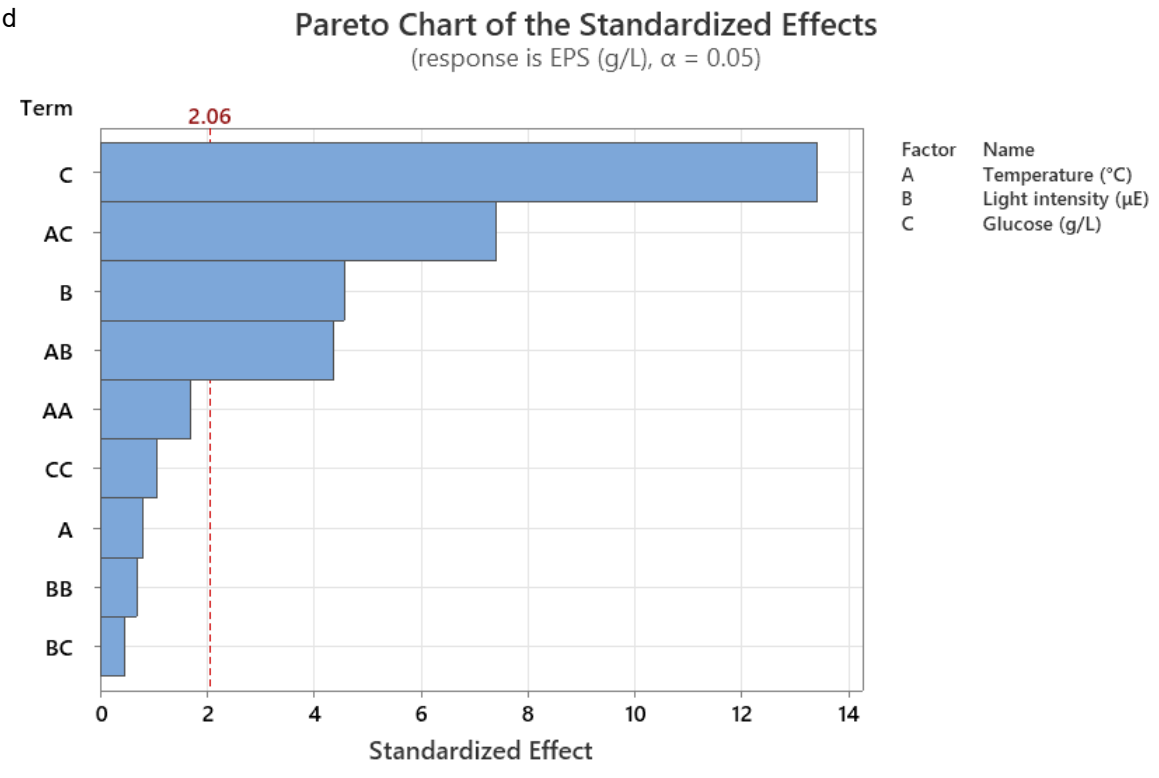

Pareto Chart of the Standardized Effects
(response is EPS (g/L), α = 0.05)
Term
2.06
C
AC
B
AB
AA
CC
A
BB
BC
Standardized Effect
Factor Name
A Temperature (°C)
B Light intensity (µE)
C Glucose (g/L)

Figure 6-16 Contour plots and Pareto chart of extracellular polymeric substances (EPS) production in *Calothrix brevissima* cultivated for 14 days at 150 RPM in 50 mL Erlenmeyer flasks with 25% working volume (n=2) (Experiment 2-6).(a) Contour plot of EPS at hold values of 22°C, 75 µmol m^{-2} s^{-1} light intensity, and 0 g L^{-1} glucose. (b) Contour plot of EPS at hold values of 25°C, 150 µmol m^{-2} s^{-1} light intensity, and 2.5 g L^{-1} glucose. (c) Contour plot of EPS at hold values of 28°C, 225 µmol m^{-2} s^{-1} light intensity, and 5 g L^{-1} glucose. (d) Pareto chart showing the relative influence of individual parameters and their interactions on EPS concentration.

Supplementing *C. brevissima* with glucose and increasing light intensity and temperature resulted in the highest amount of EPS obtained in this PhD thesis (2.65 ± 0.07 g L^{-1}, n=2) in only 14 days, resulting in a productivity of 189.3 ± 4.8 mg L^{-1} d^{-1} (n=2). This represented a doubling compared to the previous experiment (Exp. 2-3, Figure 6-17) and a 6-fold increase compared to the screening experiment (Exp. 1). However, growing cyanobacteria mixotrophically with glucose might not be suitable for industrial scale. The main sustainability advantage of cyanobacteria over heterotrophs is their non-reliance on arable land [8]. However, using glucose to grow cyanobacteria negates this benefit, as heterotrophs, with up to 180 times higher productivity, could then be used directly [21]. Further experiments were conducted to explore the potential for achieving such high EPS titres under phototrophic conditions, as outlined in the following sections.

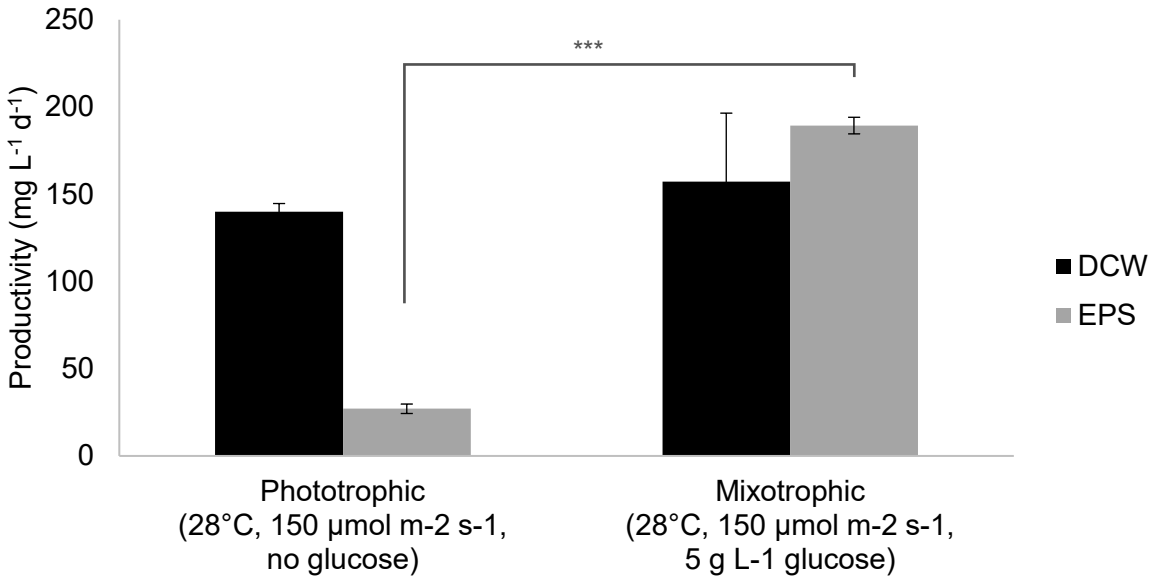


Figure 6-17 Comparison of dry cell weight (DCW) and extracellular polymeric substance (EPS) productivities of *Calothrix brevissima* under phototrophic and mixotrophic growth modes.Cultures were grown for 14 days at 28°C, 150 µmol m^{-2} s^{-1} and 150 RPM in 50 mL Erlenmeyer flasks with 25% working volume (Experiment 2-6). Values represent mean ± 1 standard deviation. Asterisk (*) shows statistically significant difference: * ($p<0.05$); ** ($p<0.01$); *** ($p<0.001$).

6.10 Phototrophic Optimisation Experiments for EPS production of *C. brevissima*

Further experiments were conducted to study the effect of light intensity on EPS production under phototrophic conditions. As described in section 4.2.6, the light intensity range was increased to 350 µmol m^{-2} s^{-1}, as previous intensities were too low (section 6.9). The growth duration was shortened to 7 days to avoid the decay phase, and glucose was not supplemented due to its disadvantages for industrial-scale production, as discussed earlier.

6.10.1 Combined Effect of Light Duration and Light Intensity on *C. brevissima* DCW and EPS

The combined effect of light intensity and light duration was studied to find optimal light duration and light intensity for EPS production under photoautotrophic conditions (Exp. 2-7). The experimental results based on the conditions are shown in Table 6-3. Under

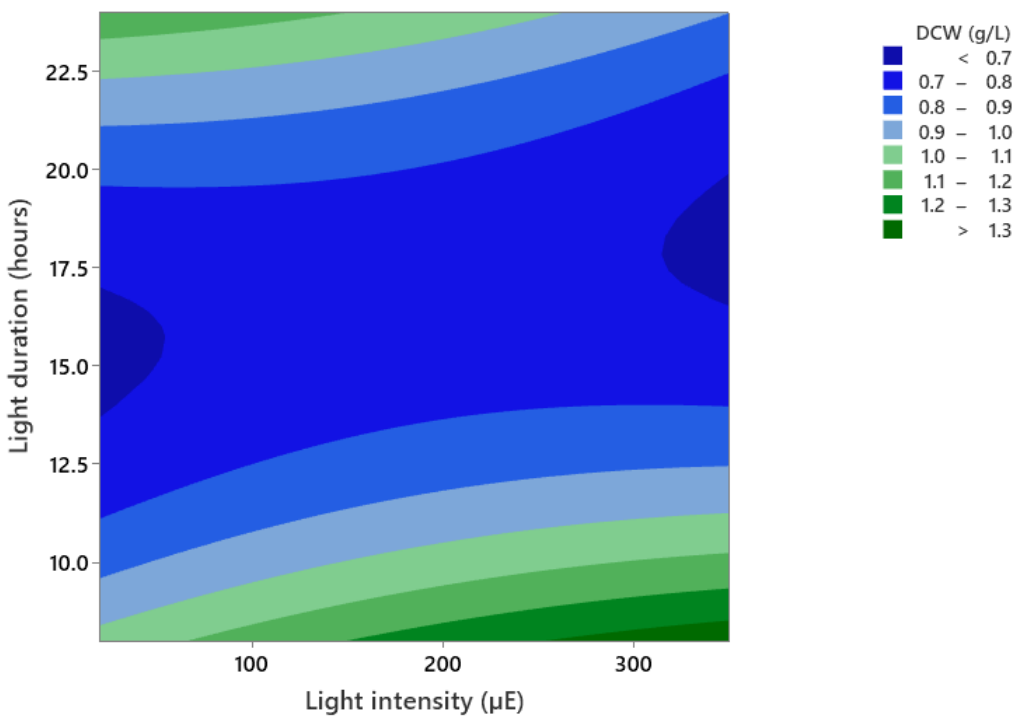
phototrophic conditions, *C. brevissima* reached DCW and EPS concentration of up to 1.18 ± 0.06 g L^{-1} (n=2) and 0.22 ± 0.01 g L^{-1} (n=2), respectively.

Table 6-3 Dry cell weight (DCW) and extracellular polymeric substances (EPS) concentrations of *Calothrix brevissima* after two-factor optimisation of light intensity and light duration using a Central-Composite-Design (Experiment 2-7).Cultures were grown for 7 days at 150 RPM in 50 mL Erlenmeyer flasks with 25 % working volume at different levels of light intensity (22 - 350 µmol m^{-2} s^{-1}) and light duration (8-24 hours). Values represent mean ± 1 standard deviation (n=2).

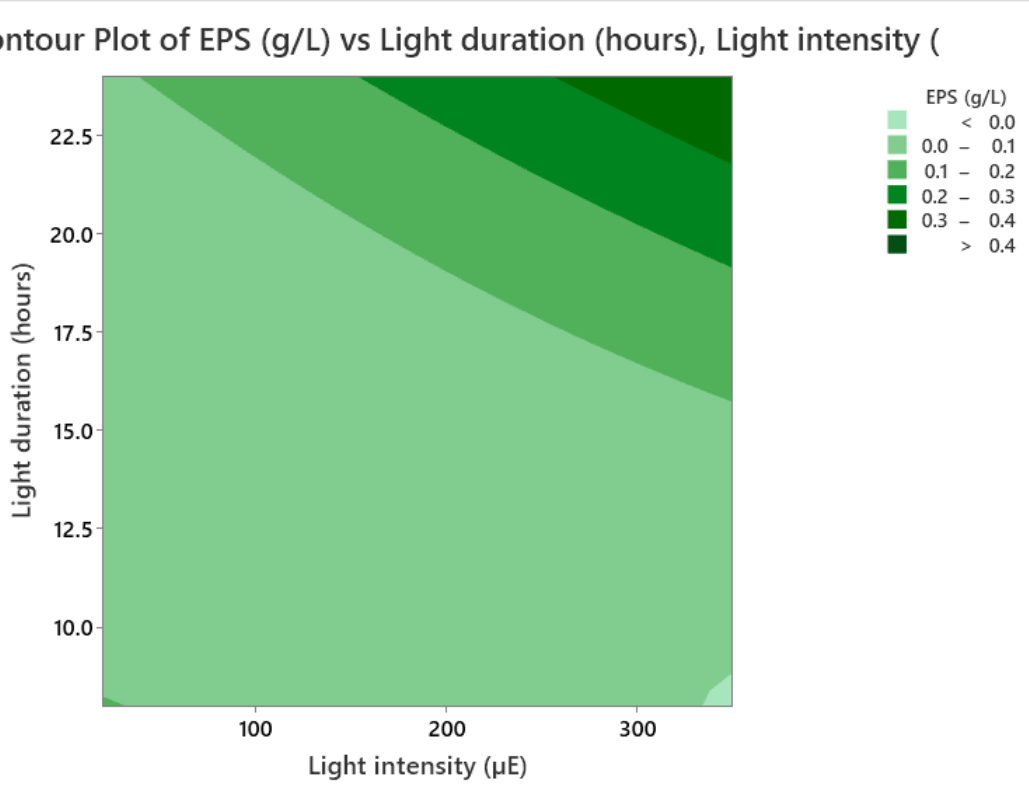
Light intensity µmol m^{-2} s^{-1}	**Light duration** hours	**Dark duration** hours	**DCW** g L^{-1}	**EPS** g L^{-1}
68	10	14	1.16 ± 0.09	0.01 ± 0.00
302	10	14	1.01 ± 0.06	0.06 ± 0.00
68	22	2	1.03 ± 0.45	0.04 ± 0.01
302	22	2	0.57 ± 0.03	0.30 ± 0.01
20	16	8	0.44 ± 0.07	0.05 ± 0.02
350	16	8	0.93 ± 0.01	0.04 ± 0.03
185	8	16	1.10 ± 0.16	0.03 ± 0.01
185	24	0	1.18 ± 0.06	0.22 ± 0.01
185	16	8	0.73 ± 0.13	0.04 ± 0.01

The contour plots for EPS production based on light duration and light intensity are shown in Figure 6-18*b*. It appeared that a threshold of light intensity and duration must be exceeded for *C. brevissima* to initiate EPS production. At light durations of 16 hours and light intensities of 25 µmol m^{-2} s^{-1} and more, EPS production rapidly increased, with the highest EPS found under constant light at the highest light intensity tested (350 µmol m^{-2} s^{-1}). Both parameters, light intensity and photoperiod were statistically significant for EPS production (Figure 6-18*d*). The model showed a high R^2 score of 82.57%.

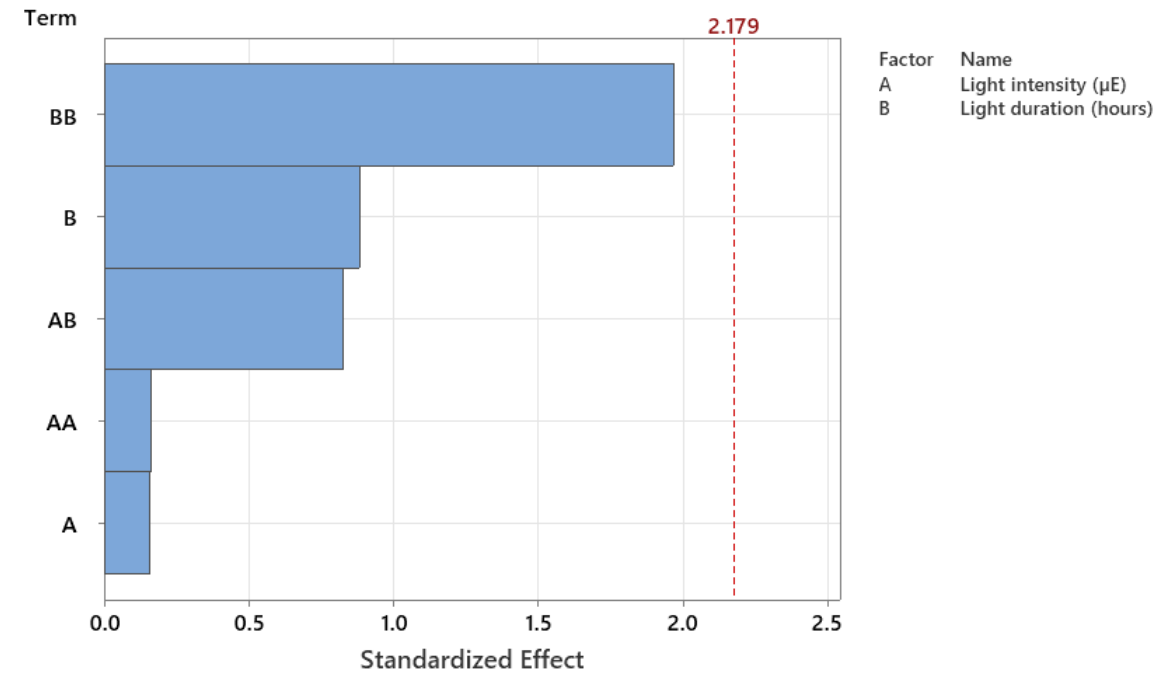
a


Contour Plot of DCW (g/L) vs Light duration (hours), Light intensity (
Light duration (hours)
22.5
20.0
17.5
15.0
12.5
10.0
100
200
300
Light intensity (µE)
DCW (g/L)
< 0.7
0.7 – 0.8
0.8 – 0.9
0.9 – 1.0
1.0 – 1.1
1.1 – 1.2
1.2 – 1.3
> 1.3

b


Contour Plot of EPS (g/L) vs Light duration (hours), Light intensity (
Light duration (hours)
22.5
20.0
17.5
15.0
12.5
10.0
100
200
300
Light intensity (µE)
EPS (g/L)
< 0.0
0.0 – 0.1
0.1 – 0.2
0.2 – 0.3
0.3 – 0.4
> 0.4

c


Pareto Chart of the Standardized Effects
(response is DCW (g/L), α = 0.05)
Term
2.179
BB
B
AB
AA
A
0.0
0.5
1.0
1.5
2.0
2.5
Standardized Effect
Factor Name
A Light intensity (µE)
B Light duration (hours)

d

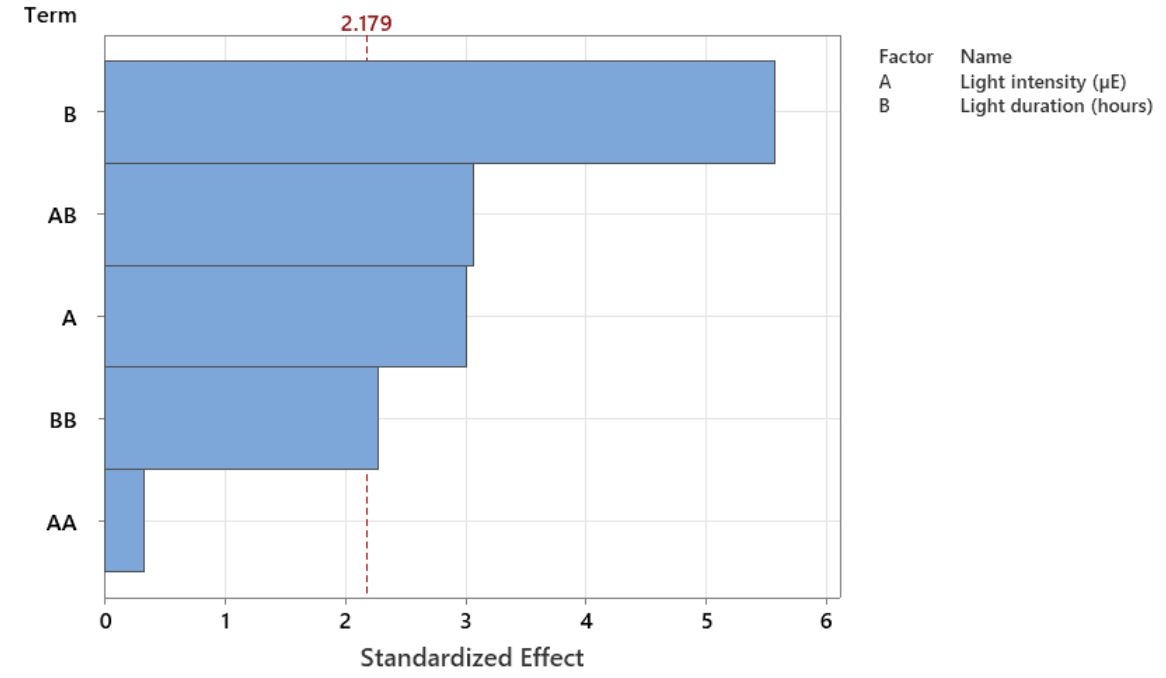

Pareto Chart of the Standardized Effects
(response is EPS (g/L), α = 0.05)
Term
2.179
B
AB
A
BB
AA
0
1
2
3
4
5
6
Standardized Effect
Factor Name
A Light intensity (µE)
B Light duration (hours)

Figure 6-18 Contour plots and Pareto charts of dry cell weight (DCW) and extracellular polymeric substance (EPS) production in *Calothrix brevissima* investigating the combined effect of light intensity (22 - 350 µmol m^{-2} s^{-1}) and light duration (8-24 hours).Cultures were cultivated under phototrophic conditions for 14 days at 150 RPM in 50 mL Erlenmeyer flasks with 25% working volume (n=2; Experiment 2-7). (a) Contour plot showing the effect of light intensity and light duration on DCW. (b) Contour plot showing the effect of light intensity and light duration on EPS. (c) Pareto chart illustrating the relative influence of light intensity, light duration, and their interaction on DCW. (d) Pareto chart illustrating the relative influence of light intensity, light duration, and their interaction on EPS.

According to the contour plots for DCW, the highest concentration was obtained at highest light intensity and shortest photoperiod, with a second area of high DCW being visible at lowest light intensity and longest photoperiod. This trend could potentially be explained by the combined effects of energy stress induced by both light intensity and light duration, which may result in *C. brevissima* being capable of tolerating high light intensities only for short periods or lower light intensities for extended durations. However, since the OD_{750} values of the pre-cultures exhibited a clear optimum under constant high light (350 µmol m^{-2} s^{-1}, data not shown), which also coincided with the peak EPS production, it's possible that practical issues, such as inaccuracies in the balance when weighing the DCW samples, could be responsible for the observed variation. None of the parameters was significant for DCW (Figure 6-18*c*), and the model had a low prediction score (R^2 = 42.09%).

Contrary to expectations, increasing the light intensity range to 350 µmol m^{-2} s^{-1} was not sufficient to cover the optimum light intensity. As a result, an extensive experiment systematically studying EPS and DCW at a wide range of temperatures and light intensities was performed (Exp. 2-8) and the results are described in the next section.

6.10.2 Systematic Evaluation of the Effect of Light Intensity and Temperature on *C. brevissima* DCW and EPS

Due to inconclusive results regarding optimal light intensity and temperature for *C. brevissima*, this species was grown under up to 12 different light intensities and 5 different temperatures (Exp. 2-8). Increasing light intensity strongly enhanced DCW production, which nearly tripled from 25 to 75 µmol m^{-2} s^{-1} (Figure 6-19). However,

beyond 75 µmol m^{-2} s^{-1}, DCW plateaued, maintaining a relatively consistent level until 500 µmol m^{-2} s^{-1}, which was the upper limit of the equipment, resulting in no light intensity optimum for DCW being identified. This trend was the same for all temperature tested. Increasing the temperature also enhanced DCW, despite a slight drop at 31°C compared to 28°C. The optimal temperature appeared to be 34°C at all light intensities, with the highest DCW (1.54 ± 0.06 g L^{-1}, n=2) obtained at 500 µmol m^{-2} s^{-1} and 34°C. At higher temperatures (37°C), DCW declined to 1.41 ± 0.01 g L^{-1} (n=2, 450 µmol m^{-2} s^{-1}). This supports the results of the multi-factor optimisation analysis from section 6.9, which identified temperature as the most significant factor for DCW. It also confirmed that the range for the multi-factor optimisation (22-28°C, 75-150 µmol m^{-2} s^{-1}) had been set too low, possibly explaining why the contour graphs in Figure 6-15 showed pessima rather than optima. *C. brevissima* was able to grow at very high light intensities (≥ 500 µmol m^{-2} s^{-1}). Photoinhibition of algae has been observed at light intensities between 250 and 1500 µmol m^{-2} s^{-1} [175]. The simplest explanation could be that production of EPS protects the cells from light stress, enabling growth at high light intensities. However, EPS followed a different response pattern to light intensity, decreasing at higher light intensities, as described in the next paragraph.

The highest EPS concentration (0.44 ± 0.01 g L^{-1}, n=2) was observed as 300 µmol m^{-2} s^{-1} and 31°C, indicating these conditions represent the optimum for EPS production (Figure 6-19). The EPS optimum differed from the DCW optimum, with cells producing most EPS when temperatures were suboptimal for growth. This could indicate that EPS were produced as a response to cold stress. Higher or lower temperatures resulted in lower EPS production. Possibly, at higher temperatures EPS might not be needed, leading to the cells diverting resources to cell growth, resulting in the higher DCW, whereas at much lower temperatures reduced metabolic rates might limit EPS and DCW production. According to Trabelsi, et al. [168], "*temperature is undoubtedly the most fundamental factor that affects all metabolic activities and nutrient uptake"*. However, the precise relationship in the case of *C. brevissima* remains unclear.

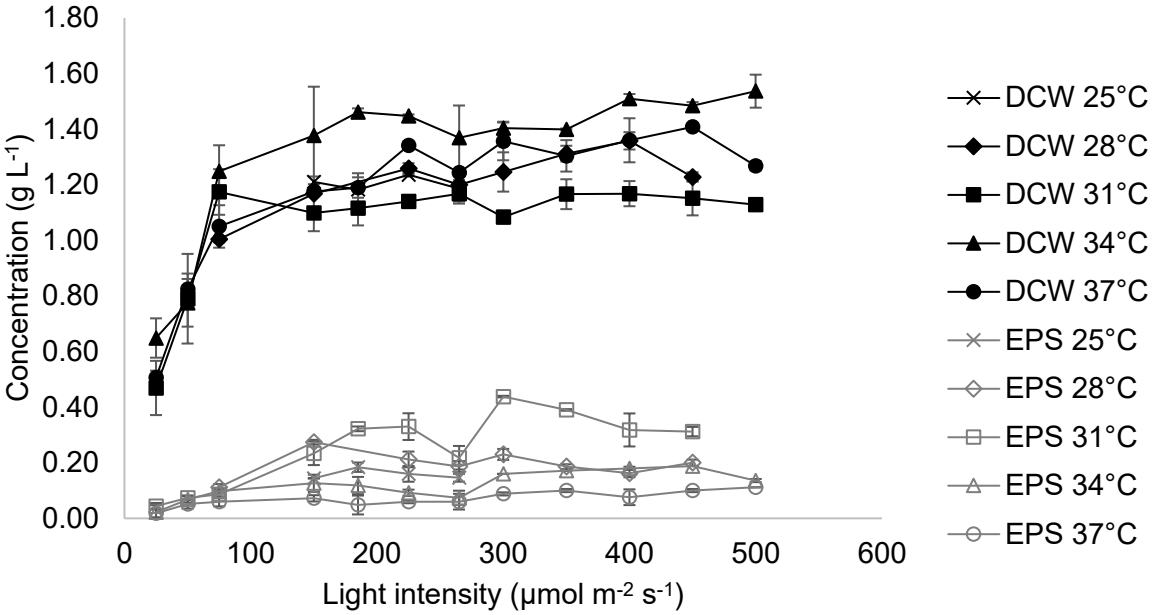


Figure 6-19 Effect of temperature (25-37°C) and light intensity (25-500 µmol m^{-2} s^{-1}) on dry cell weight (DCW) and extracellular polymeric substance (EPS) production in *Calothrix brevissima* (Exp. 2-8).Cultures were grown in BG-11 medium at 150 RPM in 50 mL Erlenmeyer flasks with 25% working volume for 7 days. Values show mean ± 1 standard deviation (n=2).

An anomaly was observed at 265 µmol m^{-2} s^{-1} across all temperatures, where a decrease in EPS production occurred before the expected increase (Figure 6-19). This decrease was also observed in a previous experiment (Exp. 2-3, section 6.5), where EPS were observed to increase between 50 µmol m^{-2} s^{-1} and 150 µmol m^{-2} s^{-1} and decreasing between 150 µmol m^{-2} s^{-1} and 175 µmol m^{-2} s^{-1}. This had resulted in 150 µmol m^{-2} s^{-1} being incorrectly interpreted as the optimal light intensity in Exp. 2-3. A similar decrease prior to the optimum was seen in DCW data with increasing temperature. The anomaly could represent either a biological threshold response or an unexplained variation. Equipment error was ruled out, though confirmatory tests on alternative systems were not possible due to light intensity limits. The cause for the observed anomaly remains unclear. No evidence was found in the literature to suggest that a specific threshold effect occurs at this light intensity, so this result should be interpreted with caution.

Excluding the observed anomaly, the pattern of DCW in Figure 6-19 was similar to literature studies estimating growth or biomass production of cyanobacteria. Growth rate of *Synechocystis* GT-L and oxygen evolution rate of *S. almeriensis* followed the same pattern [340, 341]. The sharp increase at lower light intensities is described as light-limited growth and the observed plateauing is referred to as light-saturated growth [340]. In this experiment, the two growth regimes occurred in regions of 25-100 µmol m^{-2} s^{-1} and 100-500 µmol m^{-2} s^{-1}, respectively. At higher radiances (above 500 µmol m^{-2} s^{-1}), light-inhibited growth is expected to occur, but this point was not reached in this experiment. Possibly, at light-saturated growth, another limiting factor may exist. This could potentially be related to availability of carbon or other nutrients, suggesting that although there is abundant light energy, the insufficient nutrient supply possibly hinders its utilisation [340]. Enhancing carbon availability through increased shaking speed for improved gas transfer was considered, but the maximum recommended shaking speed of the equipment (Algem HT24) of 150 RPM had been reached.

Recognising these limitations, the study transitioned to the 1-litre PBRs. The MicroPharos PBRs offer light intensities up to 1000 µmol m^{-2} s^{-1} and the option to supplement CO_2 to the culture, addressing potential limitations encountered with the Algem HT24.

6.10.3 DCW and EPS of *C. brevissima* Under Optimised Light and Temperature Conditions over Time

DCW and EPS concentration of *C. brevissima* under optimised conditions (31°C and 300 µmol m^{-2} s^{-1}) over time was studied (Exp. 2-9). As shown in Figure 6-20*a*, *C. brevissima* grew rapidly, reaching its DCW_{Max} of 1.08 ± 0.02 g L^{-1} (n=2) on day 7. During the exponential phase, the culture appeared green which got progressively darker as the culture continued to grow (Figure 6-20*c*). From day 7 to day 10, *C. brevissima* was plateauing at its maximum DCW value, marking the stationary phase. On day 10, the culture started to appear with an orange tint and the DCW started to decrease, as cells entered the decay phase. On day 12, the culture appeared less dense, with solitary green cell flocs within an orange coloured spent medium. On day 14, the culture appeared orange/yellow with white cell flocs, accompanied by an even lower DCW value of 0.60 ± 0.04 g L^{-1} (n=2).

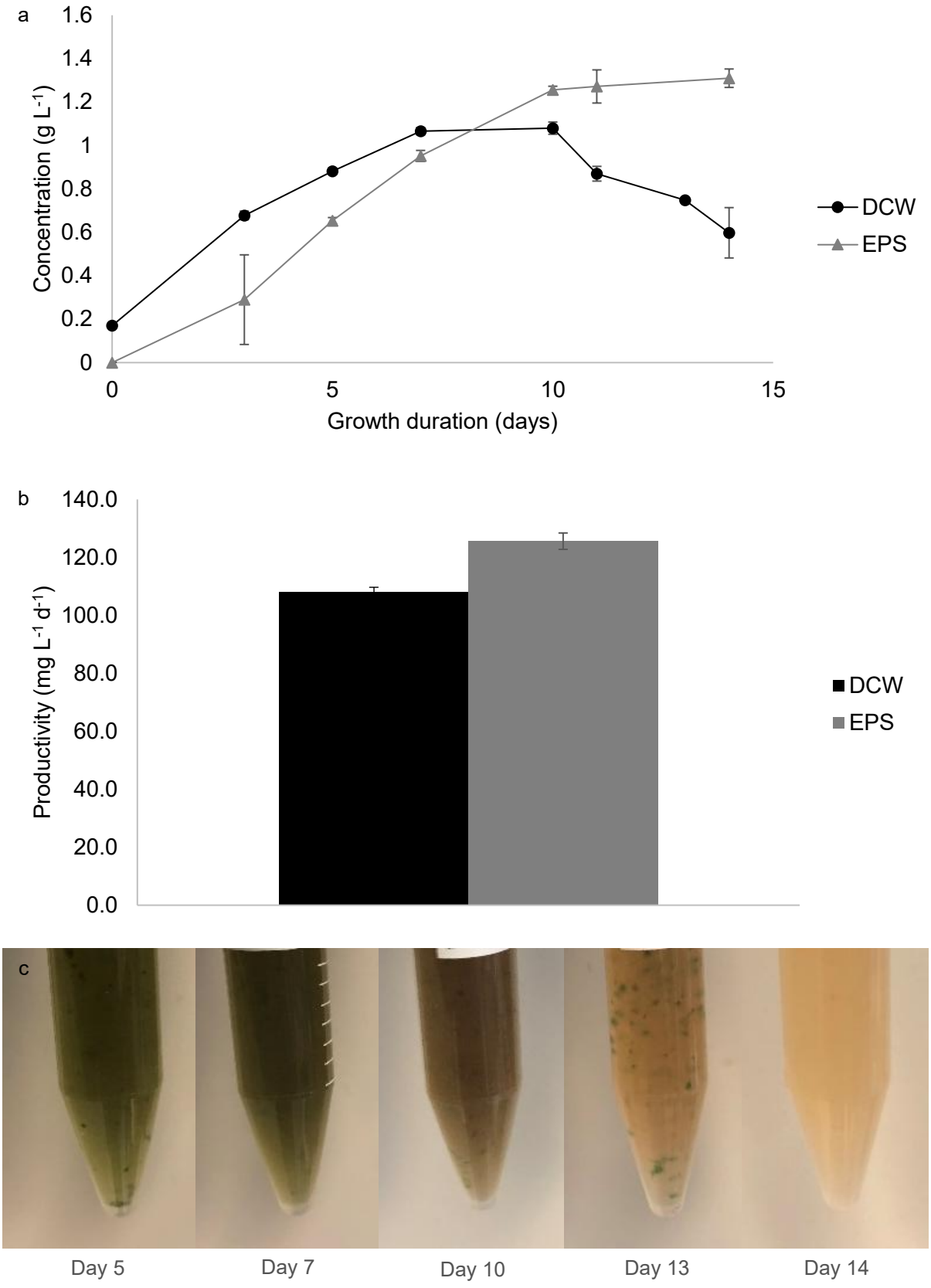


Figure 6-20 Dry cell weight (DCW) and extracellular polymeric substance (EPS) production in *Calothrix brevissima* under optimised phototrophic conditions (31°C and 300 µmol m^{-2} s^{-1}) during 14 days of growth at 150 RPM in 50 mL Erlenmeyer flasks with 25% working volume

(Exp-2-9).(a) DCW and EPS concentration over time. (b) DCW and EPS productivity (day 10). (c) Photos of cultures at different time points. Values show mean ± 1 standard deviation (n=2).

The EPS production increased progressively during exponential and stationary phase, surpassing DCW on day 8 and reaching 1.26 ± 0.03 g L^{-1} (n=2) at the end of stationary phase (day 10). Until the end of the experiment, the EPS concentration remained around this value, reaching 1.31 ± 0.12 g L^{-1} (n=2) on day 14. This is noteworthy as it indicates that using end point samples in the previous experiments was a valid approach, assuming that the EPS production followed a similar trend at different conditions. It also shows that the decrease of DCW was not accompanied by an increase of EPS, which indicates that the EPS are truly of extracellular nature and were not a result of intracellular polysaccharides (e.g. glycogen) from lysed cells. Additionally, the fact that the EPS concentration did not decrease during stationary and decay phase, indicates that *C. brevissima* did not consume EPS to survive. This could indicate that EPS had another function than carbon storage, and/or that the cells could not utilise EPS for cell growth, e.g. because other nutrients were lacking. It is known that the C:N ratio plays a role for EPS accumulation in a lot of species [55, 173]. However, *C. brevissima* has shown to grow in nitrogen-free BG-11_0 medium, and is known to be a nitrogen-fixing species [342]. This could mean that nutrients other than nitrogen might be limiting. Exp. 2-5 showed that for example magnesium limitation increased EPS production (section 6.6). This could be tested by supplementing different nutrients when the cells are in stationary phase to see whether the EPS are being consumed and whether the DCW increases again. If that is not the case, the EPS might have another physiological role than carbon storage. Notably, the EPS concentration on day 7 (0.95 ± 0.02 g L^{-1}, n=2) was higher than the values obtained in the previous experiment under the same condition: In Exp. 2-8, 0.44 ± 0.01 g L^{-1} (n=2) EPS was obtained. This was potentially caused by elevated CO_2 levels in the laboratory due to the PBRs being operated with CO_2 in close proximity to the incubator used for the optimisation experiments (Algem HT24).

Under optimised phototrophic conditions, DCW and EPS productivity amounted to 108.0 ± 1.7 g L^{-1} d^{-1} (n=2) and 125.6 ± 2.8 mg L^{-1} d^{-1} (n=2), respectively (Figure 6-20*b*). Compared to mixotrophic conditions (Exp. 2-6, section 6.9), DCW and EPS productivity was reduced by 31% and 34%, respectively. The difference in EPS productivity was

significant (p=0.0003). However, the EPS productivity was the highest achieved in this PhD thesis under phototrophic conditions, exceeding that of Exp. 2-3 (81.8 ± 6.6 mg L^{-1} d^{-1}, n=2) by 54%.

The high EPS titres obtained in Exp. 2-6 under mixotrophic conditions could not be reproduced under phototrophic conditions. It is unclear what prevented *C. brevissima* from reaching higher DCW and EPS titres before reaching decay phase. Possibly, resources were needed for other cellular processes, or stress factors were lowering the metabolic rate of *C. brevissima.* Future research into the specific factors limiting *C. brevissima* EPS production under phototrophic conditions could help increase EPS titres. Potentially, optimising the medium composition could lead to further enhancements of EPS titres under photoautotrophic conditions.

6.10.4 Emulsifying Properties and Lipid Content of EPS under Optimised Conditions

The emulsifying properties of EPS under optimised conditions (day 10) was used to investigate whether the EPS retained the desired properties. As can be seen in Figure 6-21*a*, the EPS showed a 64 ± 2% (n=2) emulsion activity at a concentration of 1 g L^{-1}, similar to the values obtained in section 5.5.1. This shows that optimising the cultivation conditions has not affected the properties of the EPS.

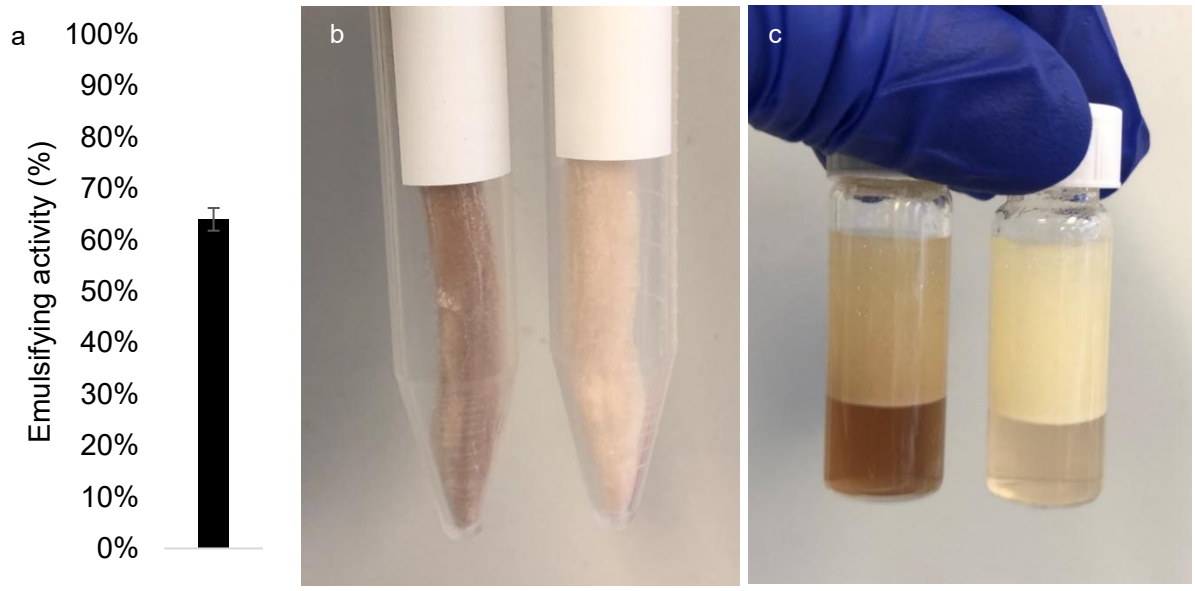


Figure 6-21 Emulsifying properties of extracellular polymeric substance (EPS) from *Calothrix brevissima* grown under optimised phototrophic conditions (31°C and 300 µmol m^{-2} s^{-1}, day 10 sample, oil:water ratio of 1:1).a) Emulsifying activity of 1 g L^{-1} EPS with an oil:water ratio of 1:1. Values show mean ± 1 standard deviation (n=2). (b) Photo of EPS from day 10. (c) Photo of emulsions.

Additionally, the emulsifying activity at a different oil:water ratio was tested, since the screening experiment showed excess water at the bottom of the glass vial. As shown in Figure 6-22*a*, a solution of EPS from *C. brevissima* with olive oil at a 2:1 ratio resulted in near-complete emulsion (94 ± 1%, n=2), exceeding that of the positive control (Tween20, 80 ± 1%, n=2). This was considerably higher than the emulsifying activity observed for another cyanobacterium in literature, *Nostoc flagelliforme,* which showed 66.39% emulsion activity at 5 g L^{-1} concentration and a 3:2 oil:water ratio [83].

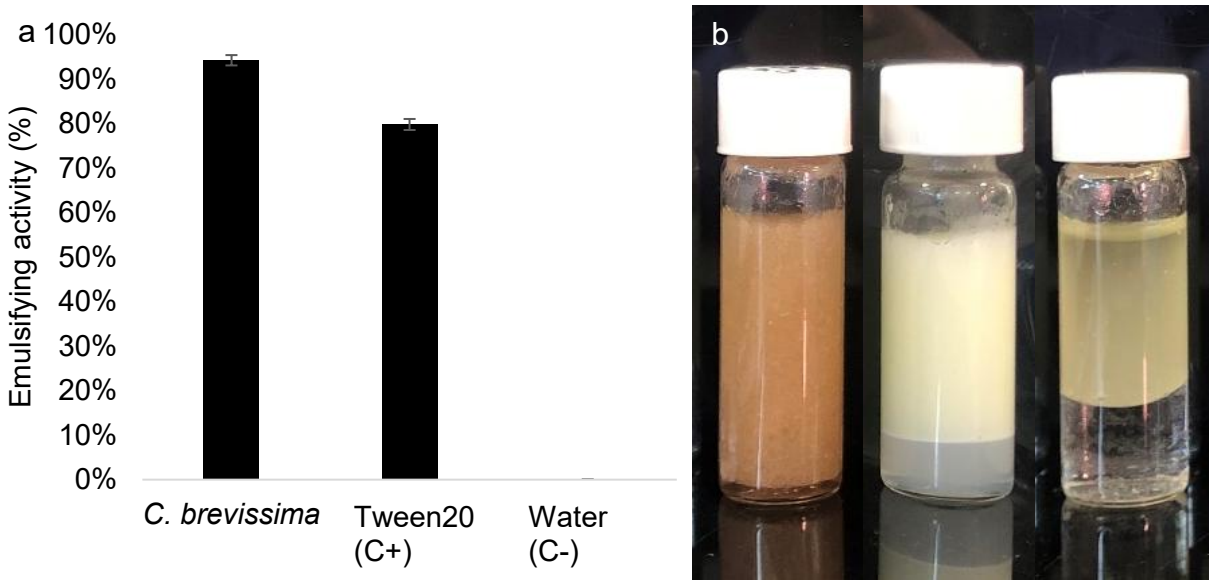


Figure 6-22 Emulsifying properties of extracellular polymeric substance (EPS) from *Calothrix brevissima* grown under optimised phototrophic conditions (31°C and 300 µmol m^{-2} s^{-1}, day 10 sample, oil:water ratio of 2:1).a) Emulsifying activities of 1 g L^{-1} EPS, 1 g L^{-1} Tween20 (positive control, C^+) and water (negative control, C^-). Values show mean ± 1 standard deviation (n=2). (b) Photos of emulsions of EPS, Tween20 (C^+) and water (C^-).

As mentioned in section 2.2.3.1, emulsifying properties of EPS are related to hydrophobic groups, such as the protein fraction (9 ± 3%, n=3) [11]. However, the identified hydrophobic groups only made up 9% of the EPS, so the EPS were also tested for presence of another groups of hydrophobic compounds, lipids, using the phospho-vanillin method. The results are depicted in Figure 6-23*a*, which revealed that *C. brevissima* EPS contained 2.5 ± 0.5%$_{w/w}$ lipids. In literature, lipids have been identified in RPS and CPS of *Nostoc spec.* Values as high as 30% of EPS were obtained in early stages of the growth, which was theorised by the author to be due to the role of lipids in the surface in the beginning of biofilm formation, as it is the case for fungal species [78, 343]. Based on these results, the EPS consisted to 9.5% of hydrophobic compounds.

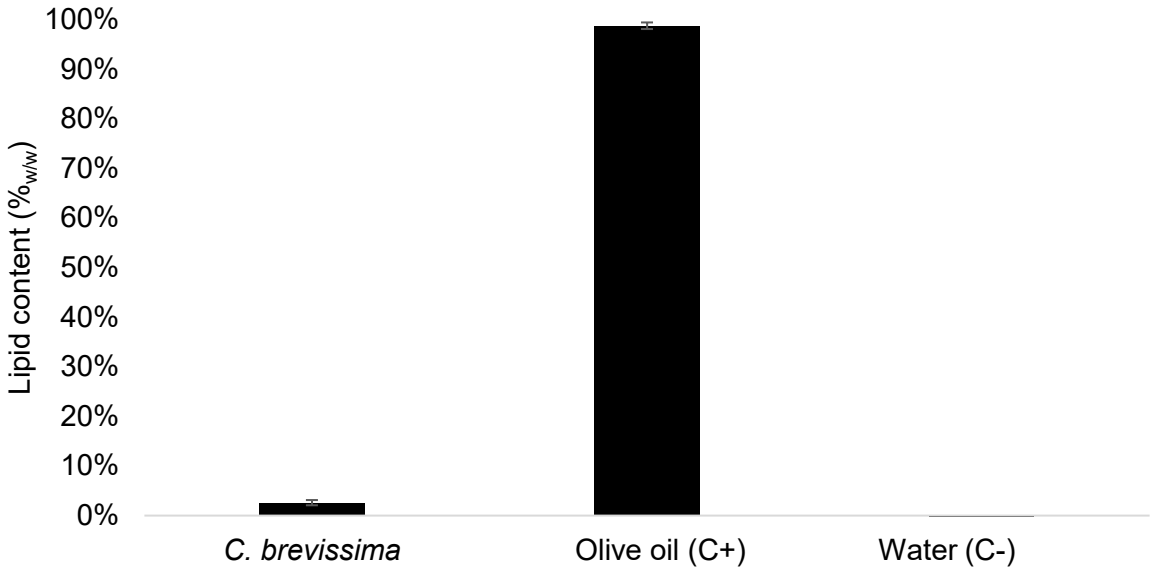


Figure 6-23 Lipid content of extracellular polymeric substance (EPS) from *Calothrix brevissima* ($\%_{w/w}$ = gram lipid per gram EPS).Cultures were grown under optimised phototrophic conditions (31°C and 300 µmol m^{-2} s^{-1}, day 10 sample), olive oil (positive control, C^+) and methanol (negative control, C^-). Values show mean ± 1 standard deviation (n=2). Calibration curves can be found in Figure 12-1; trendline equations, limit of detection (LOD) and limit of saturation (LOS) can be found in Table 12-1.

The hydrophobic fractions in combination with hydrophilic fractions such as glucose (31 ± 6%, n=3) are responsible for the amphiphilic nature of the EPS, resulting in emulsifying properties. Amphiphilic behaviour is an industrially-desirable feature [11]. Possibly, emulsifying properties could be further improved, e.g. by studying the effect of pH, temperature and presence of cations, as this has shown to affect the emulsifying activity of *Emulcyan* [26]. Additionally, analyses such as zeta potential and droplet size can provide further insight into the mechanism and interaction of droplets of the bioemulsifier [344].

6.11 Selection of Species for Scale-Up Studies

Based on the results of the optimisation experiment, *C. brevissima*, was selected for scale-up in 1-litre PBRs. EPS of *C. brevissima*, showed high emulsifying properties, (94 ± 1%, n=2) in 2:1 oil water ratio, exceeding that of the control (Tween20, 80 ± 1%, n=2). The amphiphilic character of the molecule, resulting from the presence of hydrophobic and hydrophilic parts, is an industrially-desirable feature [11]. *N. foliaceum* was not selected for scale-up due to lower EPS production and worse performance of

the bioemulsifier, which required a higher concentration (4 g L^{-1}) to result in a similar emulsifying activity. Furthermore, the EPS production in *C. brevissima* was highly enhanceable, allowing for substantial increase through optimisation. Single-factor optimisation resulted in a doubling of EPS productivity, while multi-factor optimisation achieved a 6-fold increase compared to the screening experiment. The highest EPS titre of 2.65 ± 0.07 g L^{-1} (n=2) was obtained under mixotrophic conditions at 28°C, 150 µmol m^{-2} s^{-1} and 5 g L^{-1} glucose for 14 days. It was attempted to achieve a similar titre under phototrophic conditions by systematically optimising temperature and light intensity. However, the optimal phototrophic conditions resulted in merely 1.26 ± 0.03 g L^{-1} (n=2) EPS on day 10. Phototrophic growth is preferable to mixotrophic growth, as glucose requires arable land, which competes with food resources [8]. In the scale-up experiment, it will be tested whether CO_2 can achieve the same EPS increase as glucose.

Chapter 7: Scale-Up to 1L Photobioreactors

7.1 Chapter Overview

Based on the results of the optimisation experiment, *C. brevissima* was selected for scale-up in 1-litre PBRs. Prior to the scale-up experiments, light calibration was performed, and the effect of different spargers on culture homogeneity, growth and EPS production was evaluated. Subsequently, four different experiments were carried out. Firstly, the effect of airflow rate at different light intensities was studied. Secondly, fixing the airflow rate at the obtained value, the effect of the CO_2 flow rate at different light intensities was evaluated. Thirdly, the effect of different light colours (green, blue, red) at fixed airflow, fixed CO_2 rate and equivalent light intensity was studied. Lastly, the effect of CO_2 under axenic conditions was evaluated by replacing the PBR vessels with Duran bottles to ensure axenity.

7.2 Preparatory Work for 1-Litre PBRs

7.2.1 Light Calibration

The amperage input of the PBR light tiles was correlated to the light intensity output (Figure 7-1). The light intensity was measured with two devices, the Li-Cor light meter (µmol m^{-2} s^{-1}, Figure 7-1*a*-*b*) and the internal light tracker (AU, Figure 7-1*c*-*d*). Light intensity in µmol m^{-2} s^{-1} was highly correlated with amperage (R^2= 0.9998), however there was high variation between the replicates of this measurement, which was visible as large error bars. This can likely be explained due to differences in distance from sensor to light tile and angle of sensor (Figure 7-1*b*), all of which seemed to highly affect the light intensity measured. Despite the high variation, the average measured maximum light intensity (1004 ± 196 µmol m^{-2} s^{-1}, n=2) matched the specifications of the manufacturer (1000 µmol m^{-2} s^{-1}) [345]. The trendline equation was used to calculate the required amperage to match the desired intensity (µmol m^{-2} s^{-1}).

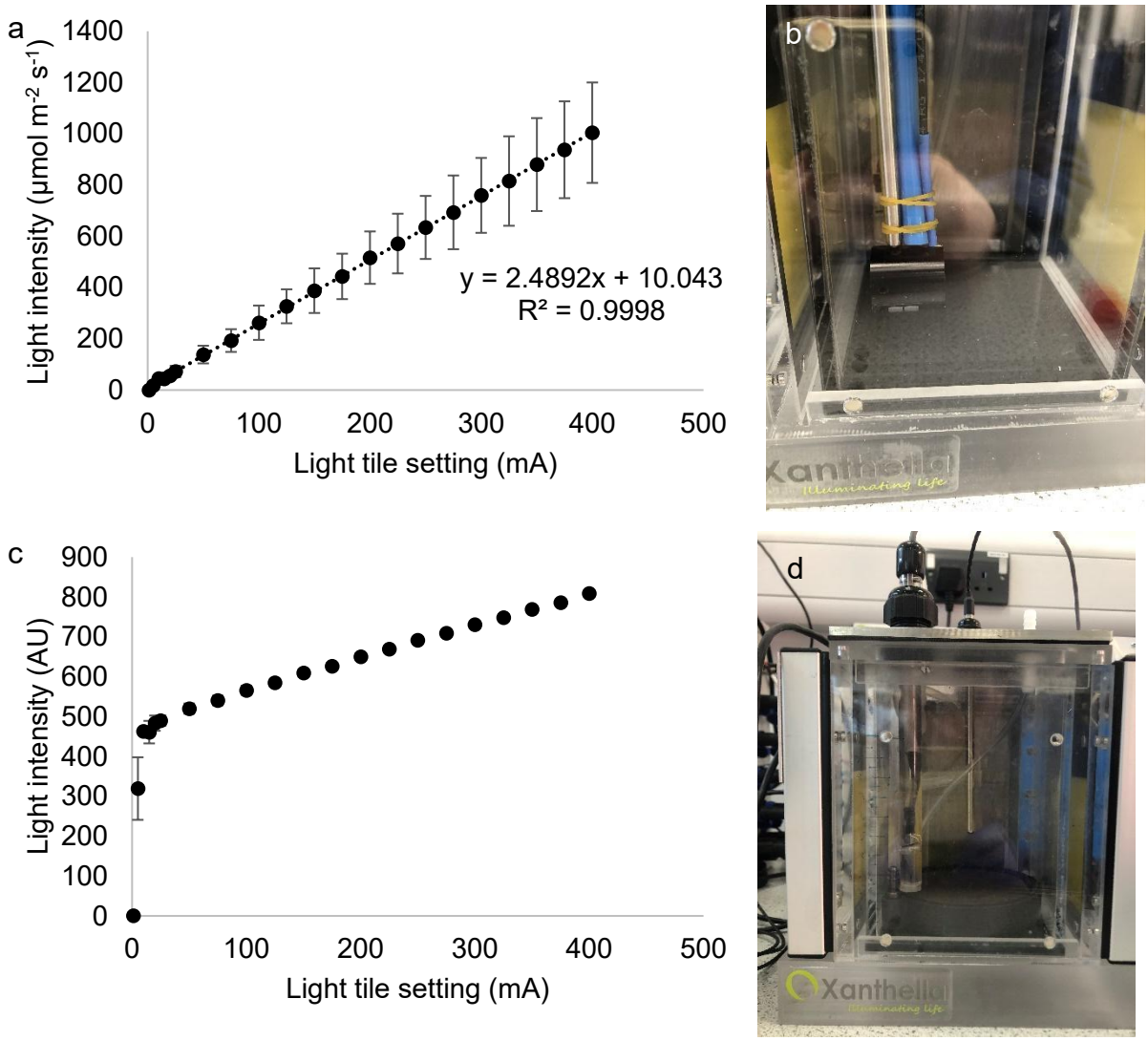


Figure 7-1 Correlation between Xanthella MicroPharos photobioreactor (PBR) light tile amperage input (mA) and light intensity output.(a) Light intensity output (µmol m^{-2} s^{-1}) to Li-Cor light meter depending on amperage input (mA). (b) Photo of Li-Cor light meter inside PBR. c) Light intensity output (AU) according to internal light tracker depending on amperage input (mA). d) Photo of Xanthella internal light tracker inside of PBR. Values show mean measurements of the four different PBRs ± 1 standard deviation.

The internal light tracker (AU) was also correlated to amperage, but only from 25 mA onwards (Figure 7-1*c*). In conclusion, µmol m^{-2} s^{-1} and AU were also correlated for values higher than 25mA, which corresponded to 490 ± 13 AU (n=7) or 72 ± 22 µmol m^{-2} s^{-1} (n=2, data not shown).

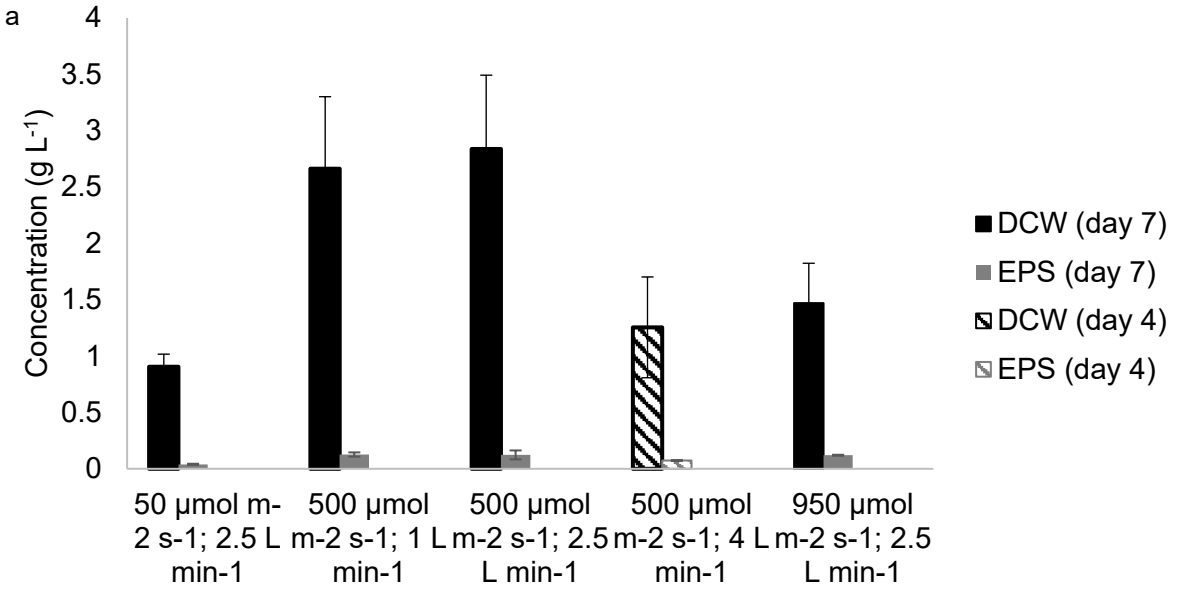
7.2.2 Adjustment of PBR Aeration System, Sampling Strategy and Sterilisation and Inoculation Procedure

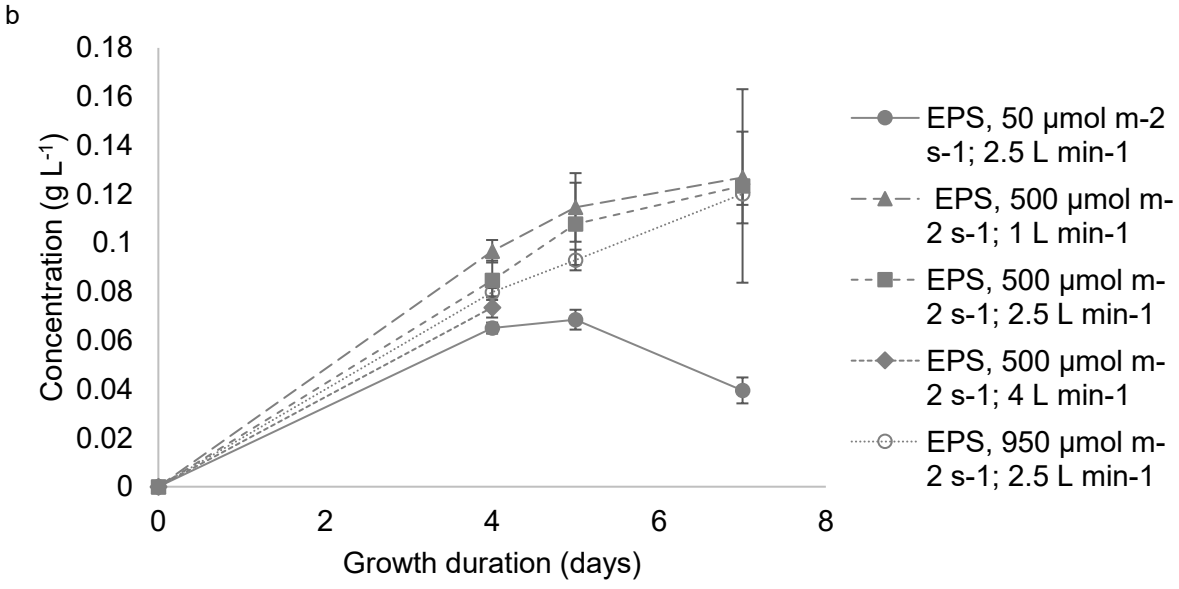
Adjustments were made to the PBR sparger design to improve mixing and homogeneous culture for representative samples. The original aeration setup, consisting of a silicon tube and single cylindrical air stone, was replaced with a disc-shaped sparger (10 cm diameter, Boxtech). A leak was identified in one of the gas boards using leak detector spray (Rocol). The issue appeared to be resolved by rearranging the tubes on the gas board. However, as will be described in section 7.6, there was a persistent problem with PBR 2, which could indicate the issue was not entirely resolved or that an additional problem went unnoticed. Different sampling methods showed that EPS measurements were accurate through the sampling port, but DCW results were near-zero (data not shown). Consequently, only end-point samples (day 7) after mixing the entire culture in a clean bottle were used for DCW measurements. Additionally, the sterilisation and inoculation procedure was adapted and the final method is described in the Appendix (section 12.10). However, as will be described in more detail in section 7.6, while the sterilisation procedure was successful, the PBRs could not maintain axenicity throughout the run.

7.3 Effects of Airflow Rate and Light Intensity on EPS and DCW

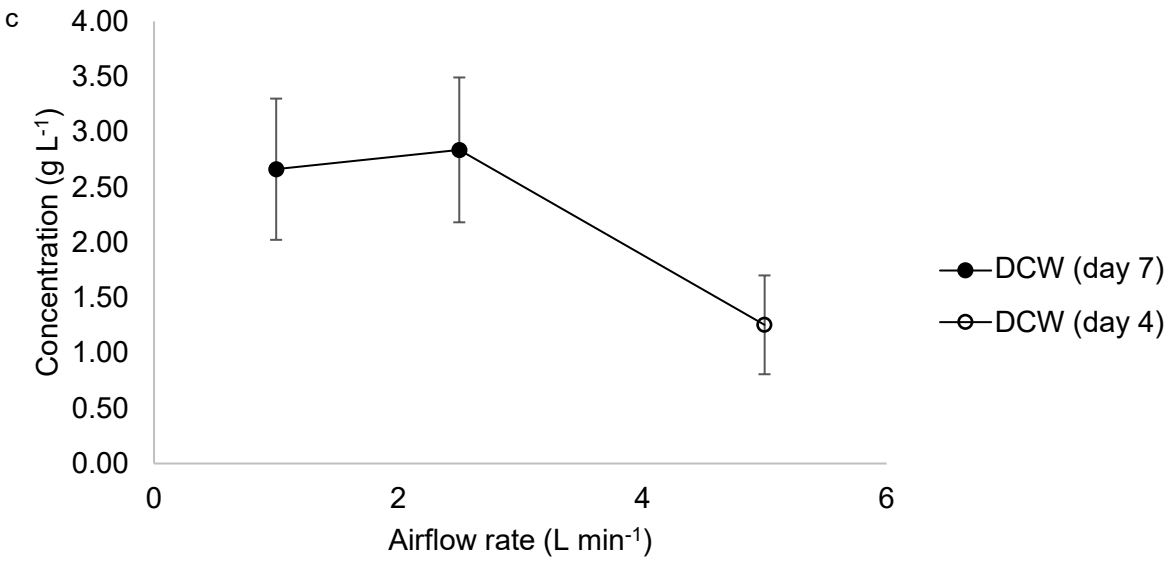
The effect of airflow rate (1, 2.5 and 4 L min^{-1}, 410 ppm) at three different light intensities (50, 500 and 950 µmol m^{-2} s^{-1}) on EPS and DCW production of *C. brevissima* was investigated (Exp. 3-1). Figure 7-2*b* shows the production of EPS over time based on different airflow rates and light intensities. Under most conditions, EPS increased steadily over the growth duration, reaching their maximum of up to 0.13 ± 0.02 g L^{-1} (n=2, 500 µmol m^{-2} s^{-1}) at the end of the growth duration (day 7). The only exception was low light (50 µmol m^{-2} s^{-1}, 2.5 L min^{-1}) which plateaued at around 0.07 ± 0.10 g L^{-1} (n=2) EPS between day 4 and 6, after which it decreased. High airflow rate (4 L min^{-1}) resulted in rapid evaporation and drying out of the PBR by day 4. Due to this occurrence, day 4 results were included in Figure 7-2*c-f* for more accurate comparison of different conditions.

The highest EPS production was observed at lowest airflow rate (1 L min^{-1}) and medium light intensity (500 µmol m^{-2} s^{-1}), resulting in 0.13 ± 0.02 g L^{-1} (n=2) (Figure 7-2*d*). The day 4 trend of EPS depending on airflow rate (L min^{-1}) showed that increasing the airflow rate led to a decrease in EPS (Figure 7-2*d)*. The difference between EPS obtained at 1 L min^{-1} compared to 4 L min^{-1} on day 4 was statistically significant (p=0.035). Regarding the effect of light intensity, similar EPS concentrations were obtained for 500 µmol m^{-2} s^{-1} (0.12 ± 0.04 g L^{-1}, n=2) and 950 µmol m^{-2} s^{-1} (0.12 ± 0.01 g L^{-1}, n=2), whereas low light (50 µmol m^{-2} s^{-1}) strongly reduced EPS to 0.04 ± 0.01 g L^{-1} (n=2). The difference in EPS between 950 and 50 µmol m^{-2} s^{-1} light was significant (p=0.0042).

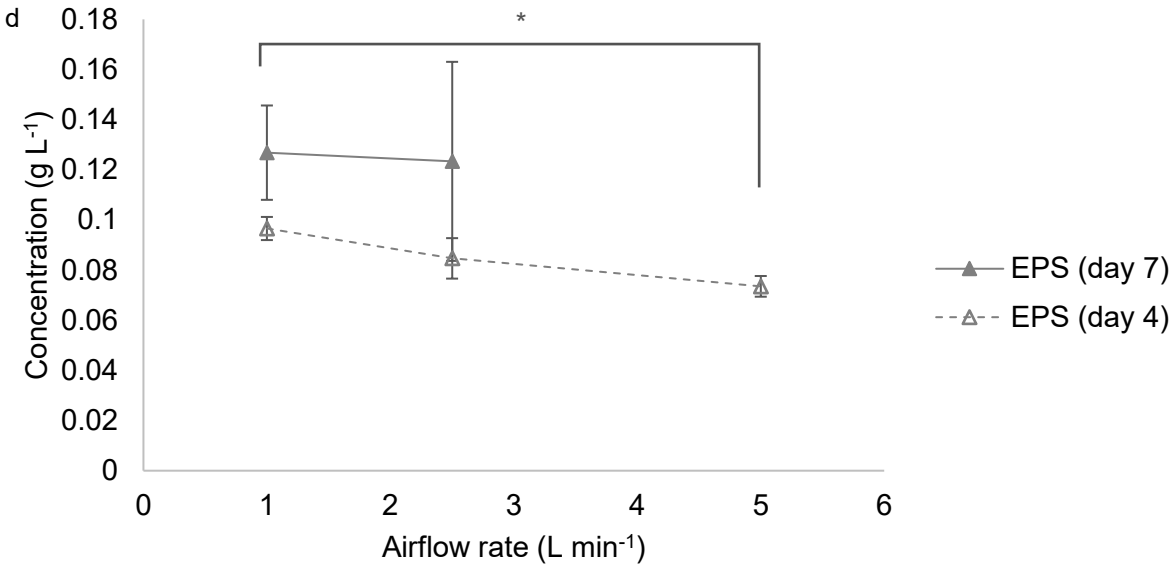




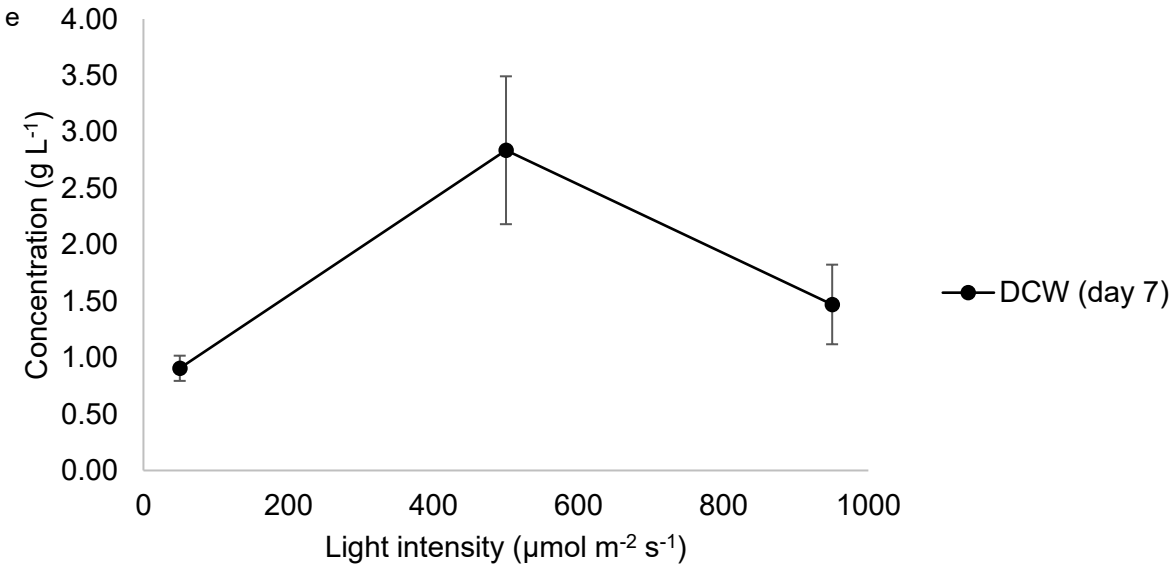
c


4.00
3.50
3.00
2.50
2.00
1.50
1.00
0.50
0.00
Concentration (g L-1)
0
2
4
6
Airflow rate (L min-1)
DCW (day 7)
DCW (day 4)

d


*
0.18
0.16
0.14
0.12
0.1
0.08
0.06
0.04
0.02
0
Concentration (g L-1)
0
1
2
3
4
5
6
Airflow rate (L min-1)
EPS (day 7)
EPS (day 4)

e


4.00
3.50
3.00
2.50
2.00
1.50
1.00
0.50
0.00
Concentration (g L-1)
0
200
400
600
800
1000
Light intensity (µmol m-2 s-1)
DCW (day 7)

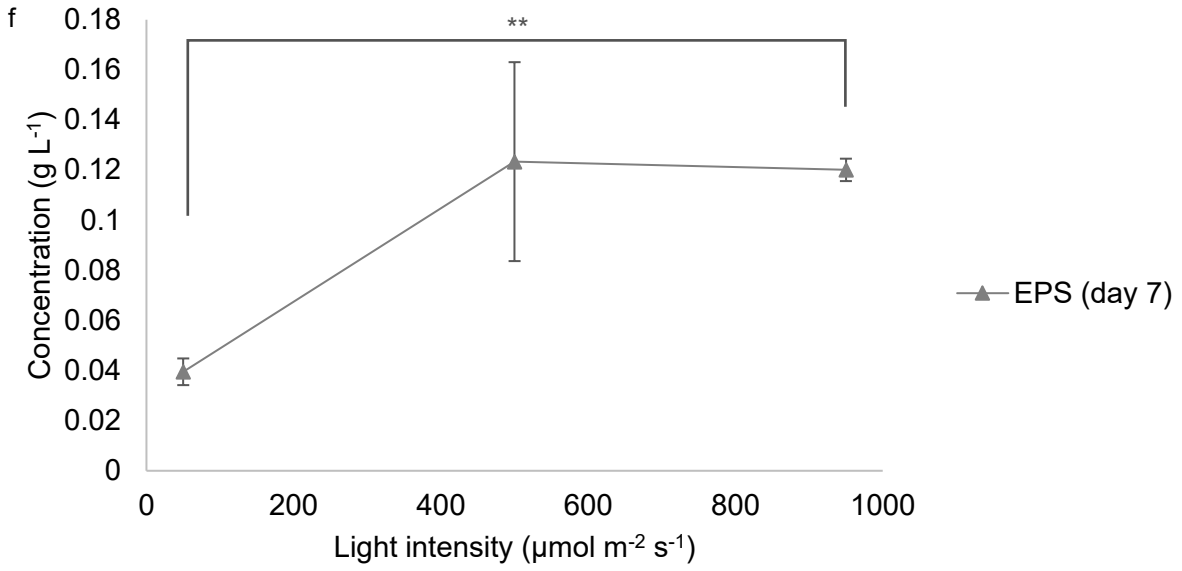


Figure 7-2 Effect of airflow rate (1-4 L min^{-1}) and light intensity (50-950 µmol m^{-2} s^{-1}) on *Calothrix brevissima* dry cell weight (DCW) and extracellular polymeric substance (EPS) production.*C. brevissima* was grown in 1-litre Xanthella MicroPharos photobioreactors (PBR) for 7 days (Exp. 3-1). (a) DCW and EPS on day 7. (b) EPS concentration over time. (c) DCW as a function of airflow rate. (d) EPS as a function of airflow rate. (e) DCW as a function of light intensity. (f) EPS as a function of light intensity. Values show mean ± 1 standard deviation (n=2). Due to PBR3 having dried out on day 4, day 4 sample is included as dashed line, column or empty datapoint. Asterisk (*) shows statistically significant difference: * ($p<0.05$); ** ($p<0.01$); *** ($p<0.001$).

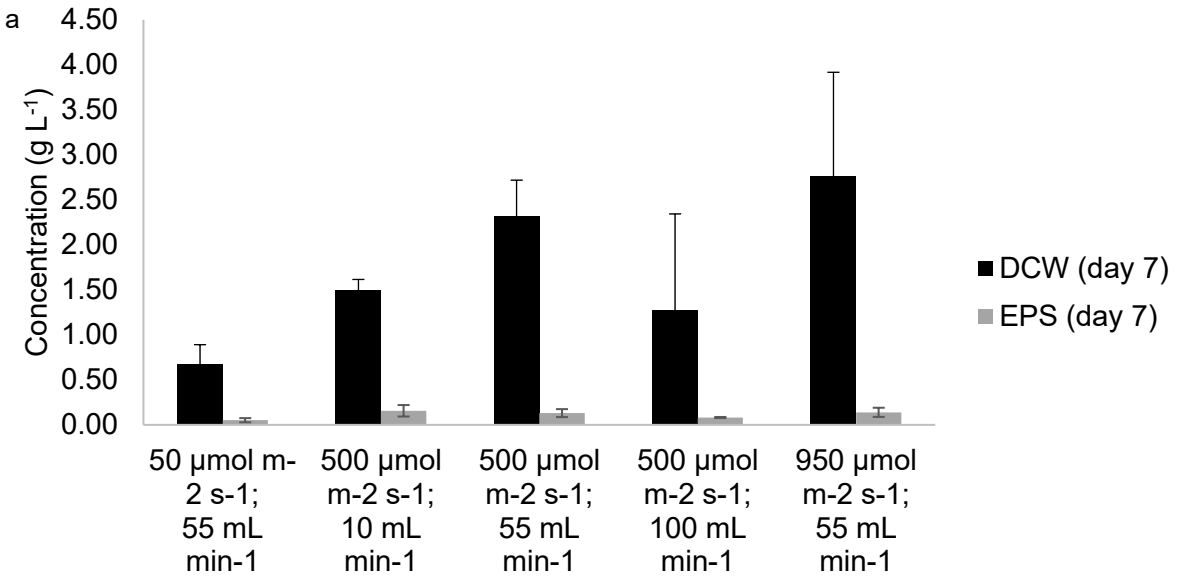
Most DCW (2.84 ± 0.66 g L^{-1}, n=2) was produced at medium light intensity (500 µmol m^{-2} s^{-1}) and medium airflow (2.5 L min^{-1}, Figure 7-2*e)*. A similar amount (2.66 ± 0.64 g L^{-1}, n=2) was obtained at low airflow (1 L min^{-1}) and medium light (500 µmol m^{-2} s^{-1}). However, high airflow resulted in only 1.25 ± 0.45 g L^{-1} (n=2) DCW before the PBR dried out (Figure 7-2*c)*. Possibly, at too high airflow rates, the volume reduction due to rapid evaporation led to up-concentration of cells, causing self-shading and less efficient photosynthetic activity. Potentially, DCW production could be improved by testing lower airflow rates than 1 L min^{-1}, which corresponds to 1.33 VVM. For the green alga *Scenedesmus quadricauda,* 0.6 VVM was identified as the optimum, with biomass concentration increasing from 0.45 g L^{-1} to 0.553 g L^{-1} when VVM was increased from 0.2 to 0.6; an increase to 1 VVM led to a decrease in the biomass concentration to 0.343 g L^{-1} [346]. Higher (950 µmol m^{-2} s^{-1}) and lower (50 µmol m^{-2} s^{-1}) light intensity reduced DCW to 1.47 ± 0.35 g L^{-1} (n=2) and 0.91 ± 0.11 g L^{-1} (n=2),

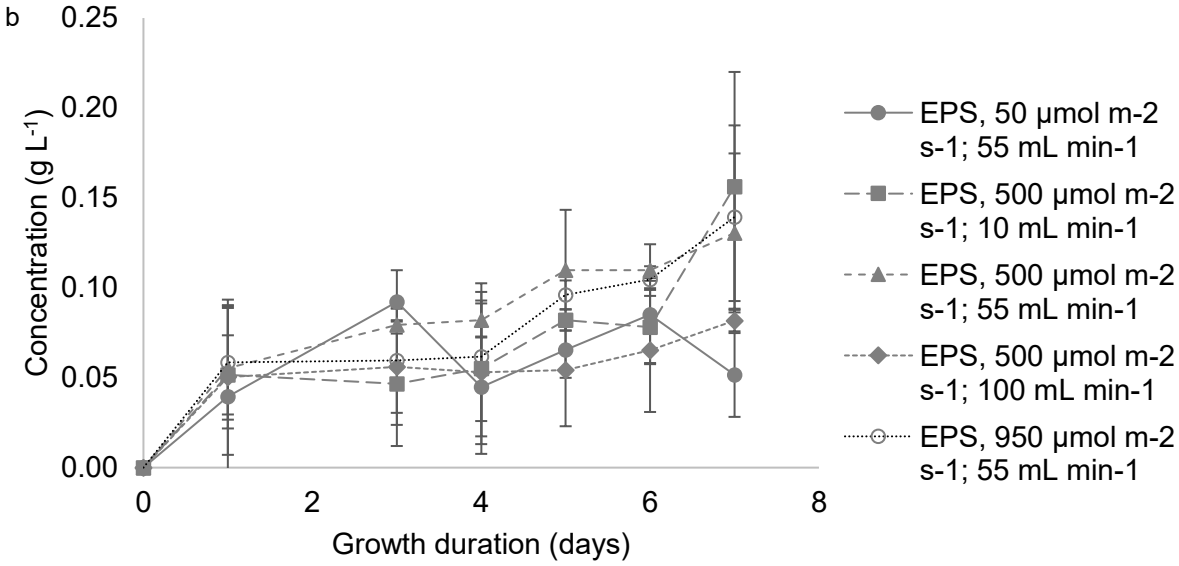
respectively. Insufficient light delivers inadequate energy to the cells, while excessive light can cause photoinhibition (section 2.3.1.1) [340]. Due to 1 L min^{-1} resulting in the highest EPS 0.13 ± 0.02 g L^{-1} (n=2) and the second-highest DCW (2.84 ± 0.66 g L^{-1}, n=2) result, 1 L min^{-1} was selected for further experiments.

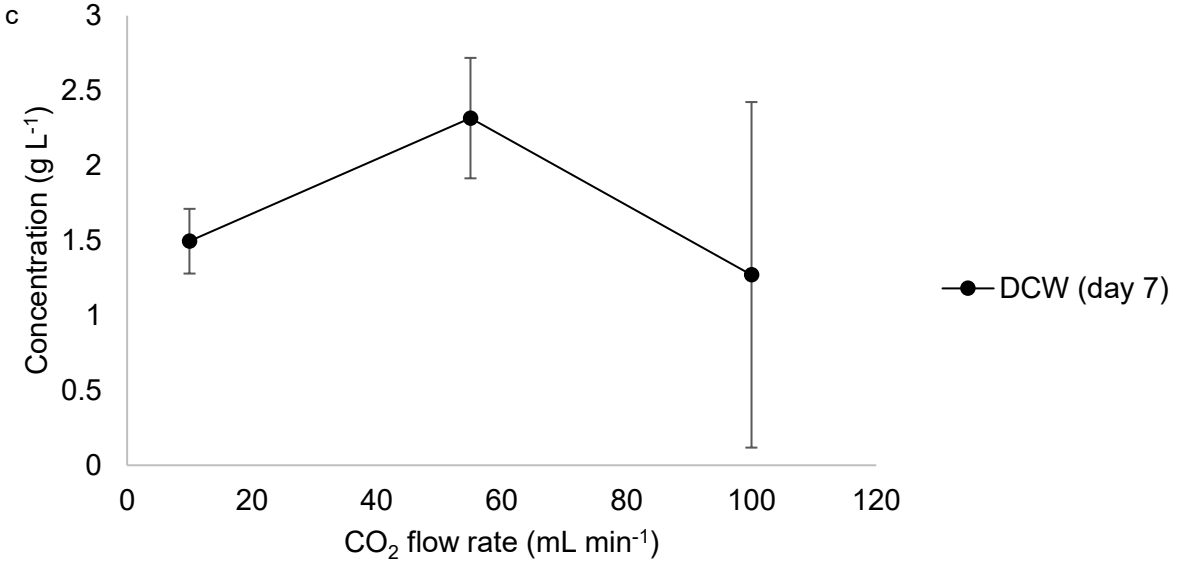
7.4 Effects of CO_2 Flow Rate and Light Intensity on EPS and DCW in 1L PBR

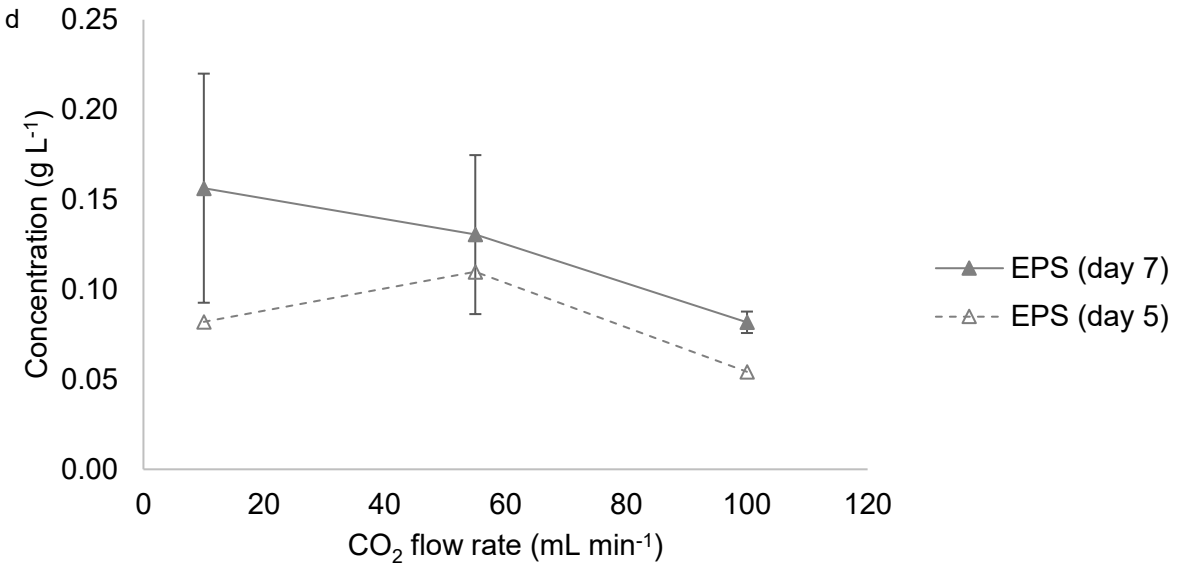
The effect of the CO_2 flow rate (10, 55 and 100 mL min^{-1} corresponding to 10,307, 52,133 and 91,282 ppm CO_2) and light intensity (50, 500 and 950 µmol m^{-2} s^{-1}) on *C. brevissima* EPS and DCW was investigated (Exp. 3-2). As depicted in Figure 7-3*b*, EPS increased throughout the growth duration with the highest value being obtained at the end of the growth duration (day 7, 0.16 ± 0.06 g L^{-1}, n=2). This was the case for most conditions except low light (50 µmol m^{-2} s^{-1}) which peaked on day 3 (0.09 ± 0.02 g L^{-1}, n=2) after which it declined, similar to the PBR experiments with air (Exp. 3-1). For all other conditions, a sudden spike in EPS occurred after day 5. This event only happened in the second replicate of the experiment. It appeared, that the CO_2 cylinder had finished and the PBRs were only supplied with air for the last 24-48 hours during the second replicate. Due to this reason, day 5 samples are depicted in Figure 7-3*d* and Figure 7-3*f*, to provide a more accurate comparison of different conditions. None of the differences in EPS production was statistically significant.

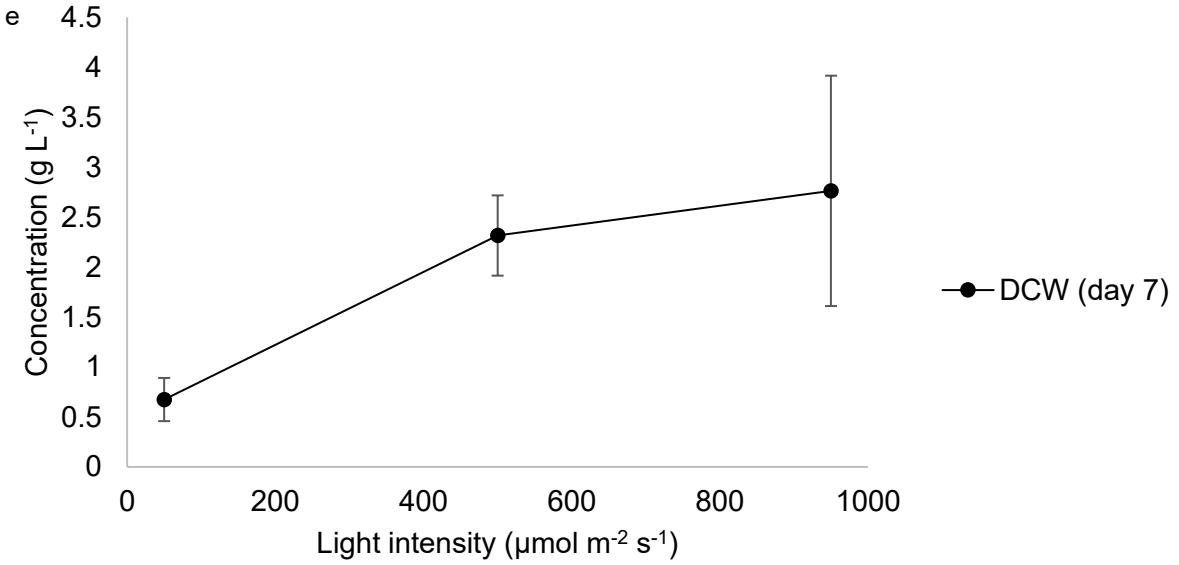
Highest DCW was observed with high light (950 µmol m^{-2} s^{-1}, 2.76 ± 1.15 g L^{-1}, n=2). However, the replicates showed high variation, which resulted in no statistically significant differences between the DCW results. The optimal CO_2 flow rate for DCW appeared to be 55 mL min^{-1} (52,521 ppm) resulting in 2.32 ± 0.40 g L^{-1} (n=2). Regarding EPS, medium CO_2 flow (55mL min^{-1}, 52,521 ppm) and medium light intensity (500 µmol m^{-2} s^{-1}) resulted in the highest EPS (0.11 ± 0.03 g L^{-1}, n=2), based on the day 5 sample. Increase or decrease of CO_2 flow rate or light intensity resulted in lower EPS. Since medium CO_2 flow (55 mL min^{-1}, 52,521 ppm) resulted in the highest EPS (0.11 ± 0.03 g L^{-1}, n=2) and the second highest DCW (2.32 ± 0.40 g L^{-1}, n=2), 55 mL min^{-1} CO_2 (52,521 ppm) was selected for the following experiments.


a
Concentration (g L-1)
4.50
4.00
3.50
3.00
2.50
2.00
1.50
1.00
0.50
0.00
50 µmol m-2 s-1; 55 mL min-1
500 µmol m-2 s-1; 10 mL min-1
500 µmol m-2 s-1; 55 mL min-1
500 µmol m-2 s-1; 100 mL min-1
950 µmol m-2 s-1; 55 mL min-1
DCW (day 7)
EPS (day 7)


b
Concentration (g L-1)
0.25
0.20
0.15
0.10
0.05
0.00
0
2
4
6
8
Growth duration (days)
EPS, 50 µmol m-2 s-1; 55 mL min-1
EPS, 500 µmol m-2 s-1; 10 mL min-1
EPS, 500 µmol m-2 s-1; 55 mL min-1
EPS, 500 µmol m-2 s-1; 100 mL min-1
EPS, 950 µmol m-2 s-1; 55 mL min-1


c
Concentration (g L-1)
3
2.5
2
1.5
1
0.5
0
0
20
40
60
80
100
120
CO2 flow rate (mL min-1)
DCW (day 7)


d
0.25
0.20
0.15
0.10
0.05
0.00
Concentration (g L-1)
0
20
40
60
80
100
120
CO2 flow rate (mL min-1)
EPS (day 7)
EPS (day 5)


e
4.5
4
3.5
3
2.5
2
1.5
1
0.5
0
Concentration (g L-1)
0
200
400
600
800
1000
Light intensity (µmol m-2 s-1)
DCW (day 7)

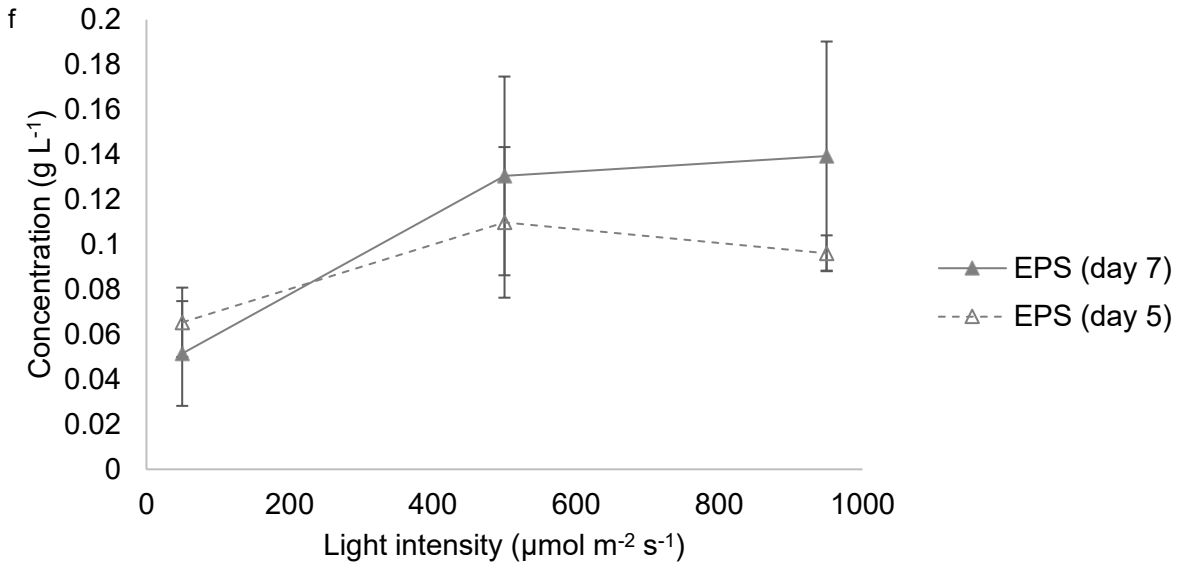


Figure 7-3 Effect of CO_2 flow rate (10-100 mL min^{-1}) and light intensity (50-950 µmol m^{-2} s^{-1}) on extracellular polymeric substance (EPS) and dry cell weight (DCW) production of *Cyanothece brevissima.C. brevissima* was grown in 1-litre Xanthella MicroPharos photobioreactors (PBR) with 1 L min^{-1} airflow rate for 7 days (Exp. 3-2). (a) DCW at day 7. (b) EPS concentration over time. (c) DCW as a function of CO_2 flow rate. (d) EPS as a function of CO_2 flow rate. (e) DCW as a function of light intensity. (f) EPS as a function of light intensity. Values represent mean ± 1 standard deviation (n=2). Day 5 results are shown as dashed lines to allow comparison before depletion of the CO_2 cylinder.

The observation that the 2nd replicate of all four PBRs showed a spike of EPS after the system accidentally switched from CO_2 to air, could indicate that a two-stage culture (first CO_2, then air) might enhance EPS production. This hypothesis was investigated in another experiment (Exp. 3-4) and the results will be described in section 7.7. As mentioned previously, the CO_2 cylinder was finished quicker than calculated. This supported a previous suspicion that there was a leak in one of the gas boards (gas board 1). This might explain some of the observed variation. Unfortunately, this issue might have affected the results from the start of the PBR experiment, leading to false conclusions being drawn along the way and implemented into the next experiments.

7.5 Impact of Light Colour (Red, Green, Blue) on EPS Production in 1L PBR

Before investigating the effect of light colour on EPS production of *C. brevissima*, the red, green, and blue light tiles were calibrated to match the white light tiles, as their light intensities could vary [345]. As described in section 4.3.1, the coloured light tiles were measured in two different ways, firstly with the Li-COR light meter and secondly with the internal light sensor.

Figure 7-4 shows the amperage setting (mA) required to match the coloured light tiles to the intensity of white light, according to the internal light tracker or the Li-COR light meter. White light at 197mA corresponded to 650 AU (internal tracker) or 550 µmol m^{-2} s^{-1} (Li-COR). According to the internal light tracker, all coloured light tiles have to be set at 240 mA to achieve 650 AU. However, according to the Li-COR light meter, green, red and blue tiles have to be set at 300, 700 and 165 mA, respectively. The Li-COR sensor measured light intensity as µmol m^{-2} s^{-1}, which is a measurement of photons per time and area. Blue light has a lower wavelength and carries more energy, whereas red light has longer wavelength and carries less energy [347]. As a consequence, blue light required a lower amperage and red light required a higher amperage to deliver the same amount of photons.

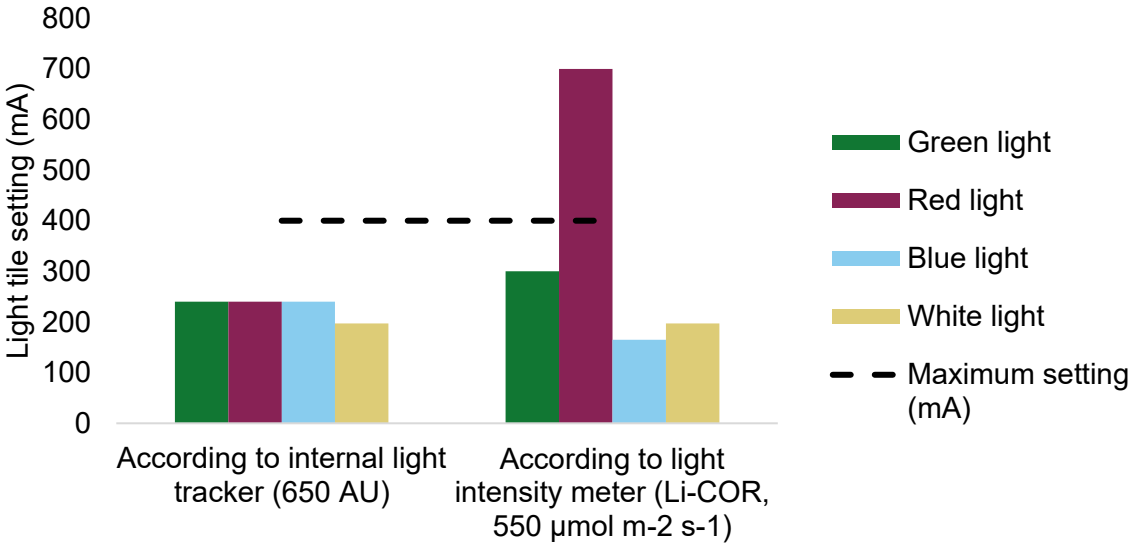


Figure 7-4 Light tile amperage setting (mA) required to match coloured light tiles intensity to white light (500 µmol m^{-2} s^{-1}, 650 AU) in 1-litre Xanthella MicroPharos photobioreactors (PBR).(a) Amperage setting of coloured light tiles according to internal light tracker (arbitrary units, AU). (b) Amperage setting of coloured light tiles according to Li-COR light intensity meter (µmol m^{-2} s^{-1}). Dashed black line shows upper limit of amperage setting.

For the light colour experiments, it was decided to set the amperage according to the internal light tracker. The reason was that according to the alternative, the Li-COR light intensity meter, the red light would have to be set at 700 mA to reach 500 µmol m^{-2} s^{-1}, which was outside of the setting range (1-400 mA). Since this setting was outside of the range, all coloured light tiles would have to be set at a lower light intensity (< 500 µmol m^{-2} s^{-1}) to compare the coloured light tiles to each other. Additionally, the results of the coloured light tiles have to be compared to the white light tiles. Since white light experiments had only been performed at 50, 500 and 950 µmol m^{-2} s^{-1}, this only left 50 µmol m^{-2} s^{-1} as an option. However, 50 µmol m^{-2} s^{-1} had resulted in the lowest DCW and EPS production and was not a promising choice. Besides, the internal light tracker had the advantage that the light tiles were not only comparable based on light intensity (AU), but also based on amperage (240 mA). To avoid these issues, a possibility to gain a better understanding of the effects of light colour on EPS would be to study the different colours at different light intensities. However, this was not performed due to time constraints.

C. brevissima was grown under red, green and blue light with constant air and CO_2 flow of 1 L min^{-1} and 55 m L min^{-1} (52,521 ppm CO_2) (Exp. 3-3). As shown in Figure 7-5*b*, EPS generally increased throughout the growth duration despite some fluctuations. Green light resulted in most EPS (0.10 ± 0.01 g L^{-1}, n=2) and blue light in the least (0.06 ± 0.03 g L^{-1}, n=2), however none of the EPS results were statistically significant from each other. Green light also resulted in most DCW (2.53 ± 0.13 g L^{-1}, n=2), whereas blue light resulted in the least DCW (1.18 ± 0.02 g L^{-1}, n=2). This difference was statistically significant (p=0.040).

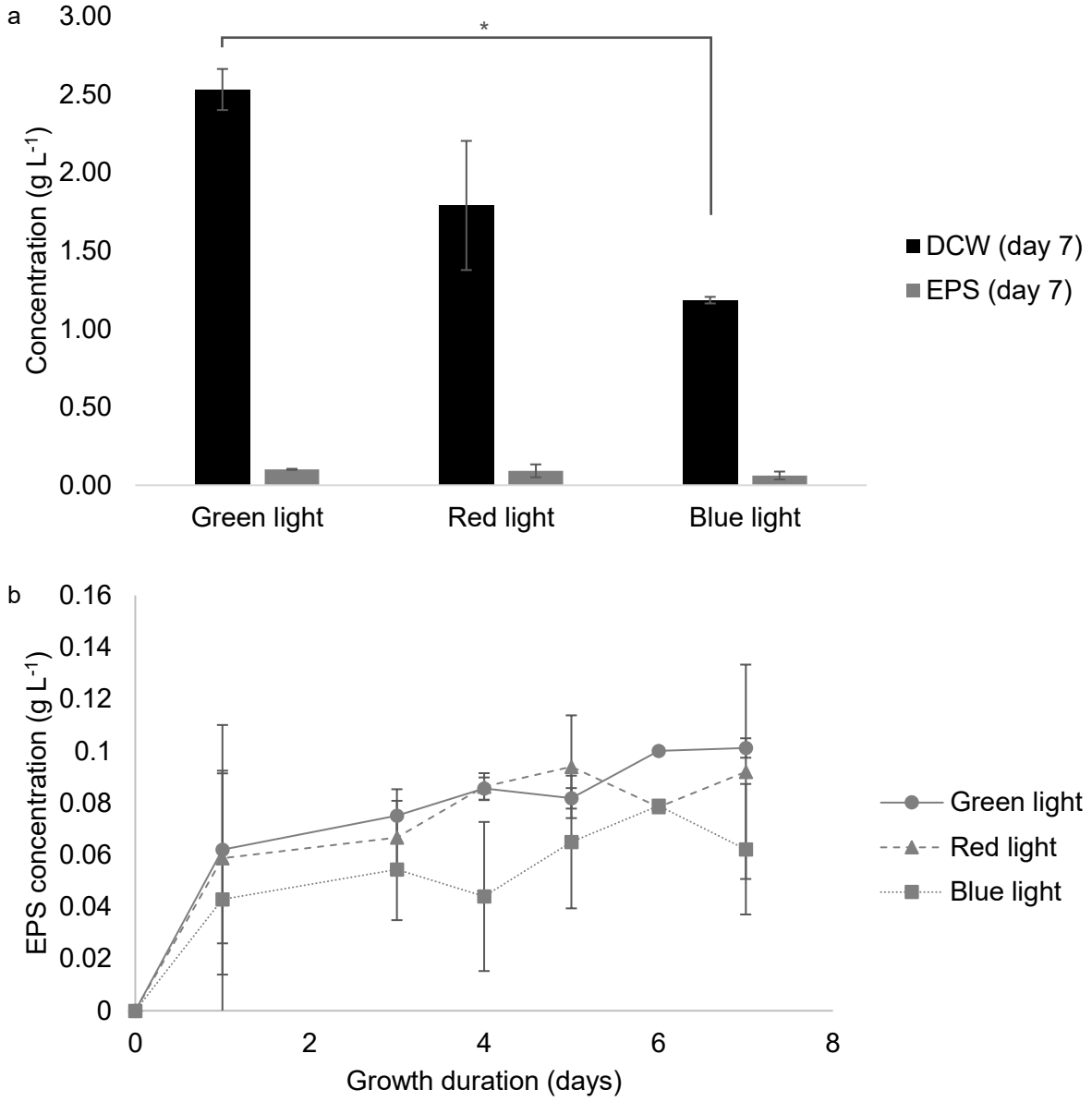


Figure 7-5 Effect of light colour (green, blue and red, 650 arbitrary units (AU)) on dry cell weight (DCW) and extracellular polymeric substance (EPS) of *Calothrix brevissima* grown in 1-litre Xanthella MicroPharos photobioreactors (PBR) with 1 L min^{-1} air and 55 mL min^{-1} CO_2 for 7 days (Exp. 3-3).(a) DCW concentration depending on light colour (day 7) (b) EPS concentration over time based on light colour. Values show mean ± 1 standard deviation (n=2). Asterisk (*) shows statistically significant difference: * ($p<0.05$); ** ($p<0.01$); *** ($p<0.001$).

As can be seen in Figure 7-4, the measurement of light intensity with the Li-Cor light intensity meter showed that red light provided the least amount of photons (µmol m^{-2}

s^{-1}), which could mean the cells grown under red light received less photon energy, reducing their photosynthetic activity. Despite green light showing the best results among the different light colours, the results were lower than white light (section 7.4). The lower DCW values could be the result of a lag phase, as the inoculum was grown with white light. The lag phase could be a result of the cells needing time to perform chromatic acclimation, which is the process of changing the activities of genes encoding specific phycobiliproteins depending on the light wavelength [348]. The most common type of chromatic acclimation is type III, where pigments are mainly regulated by a green/red light response. Red light promotes a greater accumulation of pigments such as phycocyanin, allophycocyanin, and overall carotenoids, whereas green light enhances the production of chlorophyll and, when present, phycoerythrin [349, 350].

In literature, red and blue light have shown to enhance both, biomass and EPS, to a larger extent than green light in *N. flagelliforme* [177]. It is important to note that Han, et al. [177] equalised the light intensities based on µmol m^{-2} s^{-1}, whereas in this study, AU were used. This difference might explain the discrepancy between this study and the literature. To draw reliable conclusions about the effect of light colour on *C. brevissima*, it would be beneficial to repeat this experiment at equal µmol m^{-2} s^{-1} in the future.

7.6 Limitations of the Xanthella PBR System

There were several challenges and limitations associated with the Xanthella PBRs: During the experiments with the PBRs, it became evident that all samples tested positive for contamination, visible by colonies on LB plates. To determine at which stage contamination got introduced, contamination checks were performed at different stages and under different conditions. Figure 7-6 shows photos of the LB plates used as contamination checks. For each PBR (1 to 4), the inoculum was tested before addition to the PBR (top row), as well as the empty PBR right after sterilisation and neutralisation (day 0, middle row), and the PBR culture at the end of the growth duration (day 7, bottom row).

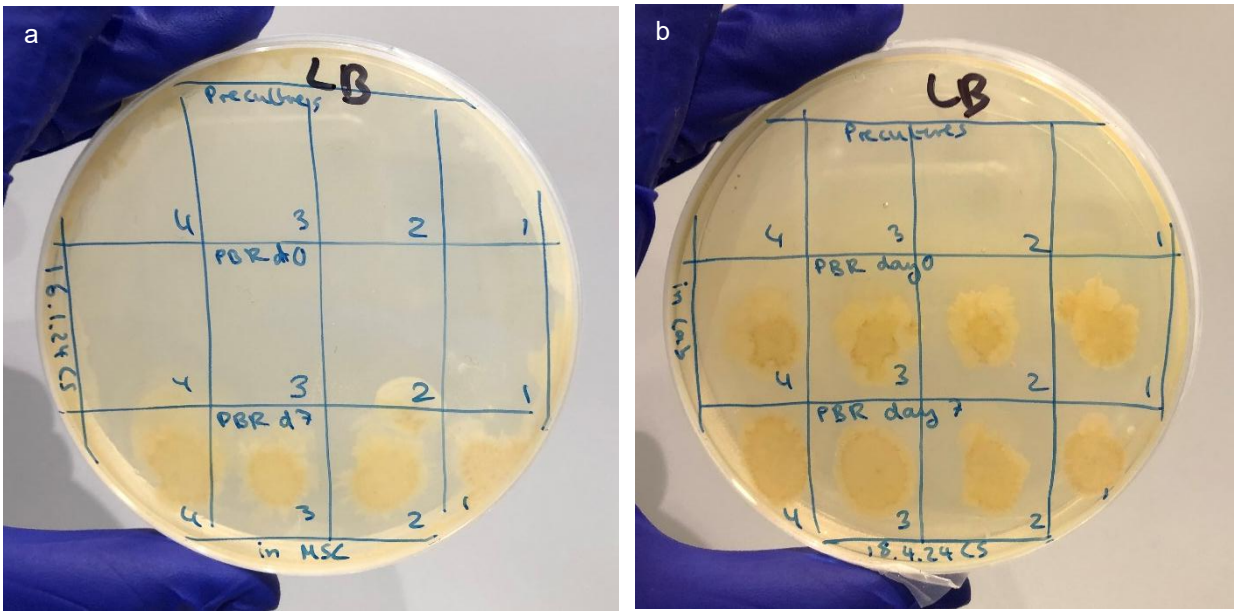


Figure 7-6 Photographs of Lysogeny Broth (LB) plates showing contamination levels in 1-litre Xanthella MicroPharos photobioreactors (PBRs) under different sterilisation protocols.(a) PBRs sterilised and neutralised in a sterile environment (microbial safety cabinet) using 0.003% sodium hypochlorite for 24 h with aeration, followed by neutralization with 0.003% sodium thiosulfate for 24 h with aeration. (b) PBRs sterilised and neutralised in a standard laboratory environment using the same protocol. Individual checks include inoculum (top row), empty PBRs after sterilisation and neutralisation at day 0 (middle row), and PBRs with culture at the end of the run (day 7, bottom row). Numbers 1–4 correspond to PBRs 1–4.

Figure 7-6*a* shows the contamination level when the PBRs were left in a sterile environment (MSC) during the 48 hours of sterilisation and neutralisation. Figure 7-6*b* shows the contaminating level when the PBRs were moved to regular laboratory environment after aseptic addition of sterilising or neutralising agent. The inoculum sample showed no growth on LB, suggesting it was not the source of contamination. When the PBRs were placed in a sterile environment (MSC) during the sterilisation and neutralisation process, they were sterile at day 0, which indicated that the sterilisation protocol was sufficient. However, day 7 culture showed contamination, suggesting that the PBRs could not maintain axenicity throughout the growth duration (Figure 7-6*a*). This hypothesis was supported by the case of leaving PBRs in regular laboratory environment during the 24 hours of sterilisation and 24 hours of neutralisation (Figure 7-6*b*). In that case, the PBRs were already contaminated on day zero (after sterilisation and neutralisation, before inoculation). These results indicate

that despite the successful sterilisation procedure, the neutralised PBRs contracted contamination as soon as they were exposed to regular laboratory environment.

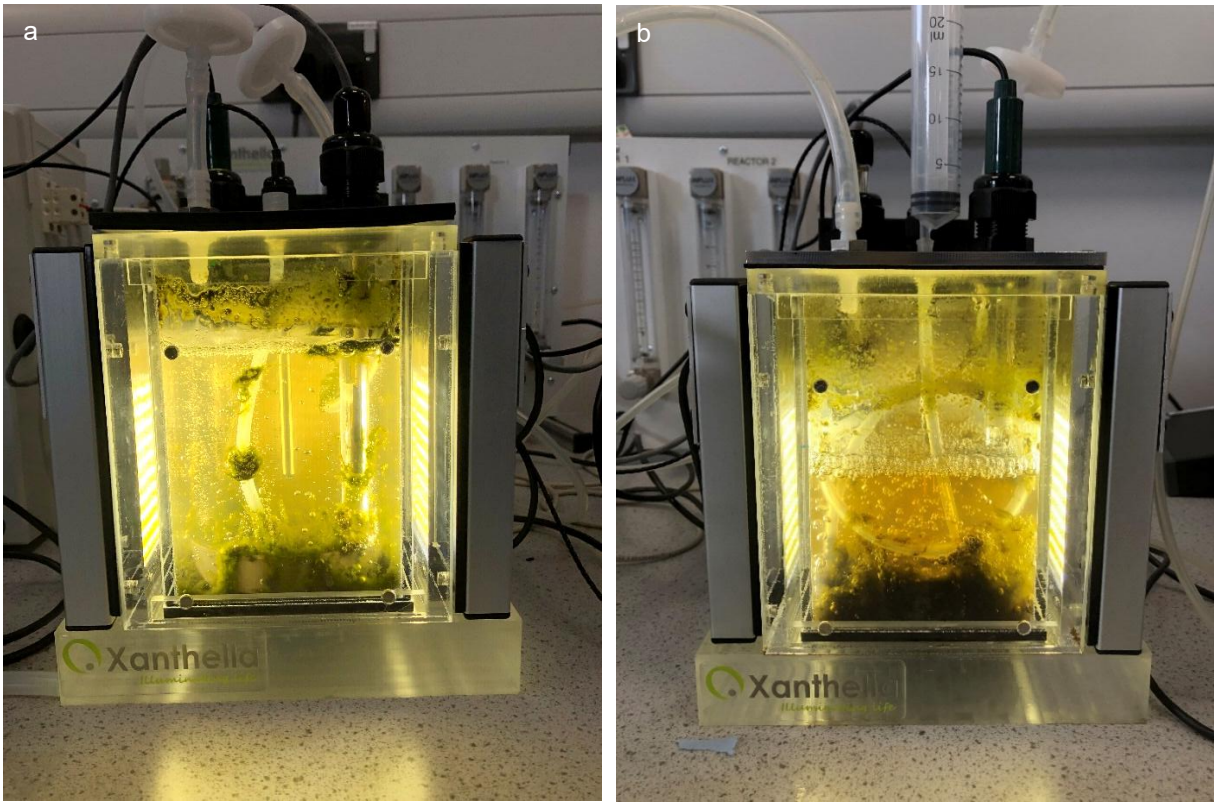


Figure 7-7 Photographs of 1-litre Xanthella MicroPharos photobioreactor (PBR) lids showing structural deformation.(a) Acrylic lid with edges bending upwards. (b) Steel lid retaining its original shape.

Several adjustments were undertaken to prevent contamination. Firstly, as described in section 12.10, an extensive adaptation of the sterilisation protocol and setup was performed. One adaptation was the use of foam traps that were connected to the PBR vents. The vent in the original Xanthella setup consisted only of a short silicon tube that was open to the surrounding. Initially, this was closed using a filter. However, the filter was rapidly getting blocked by culture being pushed out through the vent. Therefore, a Duran bottle with 2-hose connector screw cap lid with a vent filter was autoclaved and connected to the PBR with a silicon tube in the MSC. Secondly, it was noticed that the original acrylic lid had bent under the weight of the sensors and other lid components. The lid bent upwards on the edges, leading to an open gap between lid and PBR (Figure 7-7*a*). The lid was replaced by Xanthella with steel lids that keep their form and do not bend upwards on the edges (Figure 7-7*b*). Unfortunately, those

adjustments did not lead to an axenic vessel, as the contamination problem persisted. It was observed that the seal under the lid was always soaking wet, likely making it more prone to contamination. At high airflow rate (4 L min^{-1}), it was both visible and audible that the lid, which was held in place by small magnets, was pushed open repeatedly to release the pressure. This indicated that pushing the lid upwards represented less resistance than the air being pushed through the filter of the foam trap. When attempting to clamp the lid in place, the culture got pushed out through the sensor openings, despite the nuts being screwed as tight as possible. This indicated the sealing of sensors was not sufficient.

Possible improvements to the design could include screwing or clamping the lid instead of using magnets, replacing the acrylic screws and nuts of the lid components with metal ones and using more effective O-rings and seals. In other words, the design could be improved by aiming for the PBR to be hermetically sealed, with the only exception being the inlets and outlets covered with filters. A design like that could possibly result in an axenic system. For example, an autoclavable vessel out of borosilicate glass and steel instead of acrylic material could improve sterility, as well as time-efficiency, as the 48-hour sterilisation and neutralisation became redundant. Alternatively, a lower airflow rate could improve the system by causing less culture splashing, hopefully maintaining the integrity of the seal. Additionally, a lower airflow rate would mean less pressure, resulting in less culture being lost through the vent. A lower airflow rate could also potentially enhance biomass and EPS production, based on the results in Figure 7-2. However, this would require a different gas board, as the setting range of the Xanthella gas board was 0.6 to 5 L min^{-1}, with no bubble formation being observed at settings lower than 1 L min^{-1}. In addition to the contamination issue and gas board leak, one of the pH electrodes did not function. This malfunction hindered the system's ability to use on-demand CO_2 injection based on the pH level. HEPES buffer was used instead to maintain stable pH.

7.7 Influence of CO_2 on EPS and DCW under Axenic Conditions

As elaborated in the previous section, the PBRs did not remain contamination-free throughout the growth duration. Due to the EPS results being considerably lower than

in the axenic shake flasks experiments, a modified setup was created to test the effect of CO_2 on *C. brevissima* EPS under axenic conditions. As much as possible from the original Xanthella MicroPharos was utilised. However, the PBR containers were replaced with Duran bottles, as those can be autoclaved for sterility (Figure 7-8*a*).

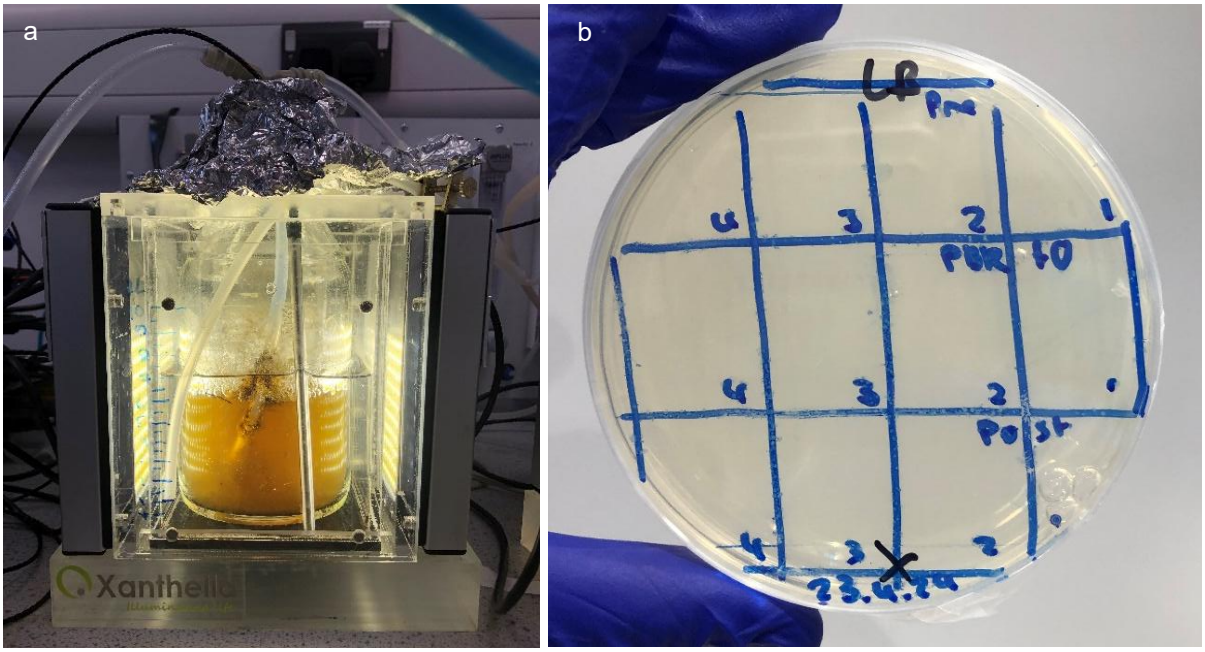


Figure 7-8 Modified photobioreactor (PBR) setup for axenic growth.(a) Photograph of the modified setup using an autoclaved Duran bottle instead of the original Xanthella MicroPharos PBR vessel. (b) Lysogeny Broth (LB) plate showing contamination levels of the modified setup. Individual checks include inoculum (top row), empty Duran bottles just before inoculation, and bottles with culture at the end of the run (day 7, bottom row). Numbers 1–4 correspond to PBRs 1–4.

As shown in Figure 7-8*b*, using autoclaved Duran bottles instead of the Xanthella PBR vessel resulted in an axenic culture. Inoculum and the empty, autoclaved bottle were contamination-free and remained axenic until the end of the experiment. This supported the hypothesis from section 7.6 that the reason for the contamination in the Xanthella PBRs was the integrity of the PBR vessel which made it not being able to remain contamination-free.

The results from this axenic run are shown in Figure 7-9. The cultures grown with air (410 ppm CO_2) grew rapidly until reaching stationary phase on day 4 (DCW_{Max} = 1.27 ± 0.84 g L^{-1}, n=2, Figure 7-9*a*). They remained in stationary phase until day 9, after

which DCW decreased to 0.79 ± 0.41 g L^{-1} (n=2) at the end of the experiment (day 14). EPS increased throughout the growth duration, until reaching the maximum on day 11 (0.51 ± 0.23 g L^{-1}, n=2), followed by a slight decrease. Under axenic conditions, *C. brevissima* cultivated with air containing 5.5% CO_2 (52,521 ppm) showed a lag phase of about 2 days compared to *C. brevissima* cultivated with air only (Figure 7-9*b*). Subsequently, the cells grew exponentially until day 7 (DCW_{Max} = 2.53 ± 0.24 g L^{-1}, n=2), at which point the CO_2 was removed. DCW plateaued until day 9, indicating that cells were in stationary phase. Decay phase lasted from day 9 until the end of the experiment (day 14) at which point DCW had dropped to 1.48 ± 0.02 g L^{-1} (n=2). With CO_2 supplementation, *C. brevissima* produced less EPS compared to only air, with the EPS concentration staying below 0.13 ± 0.01 g L^{-1} (n=2) until day 7.

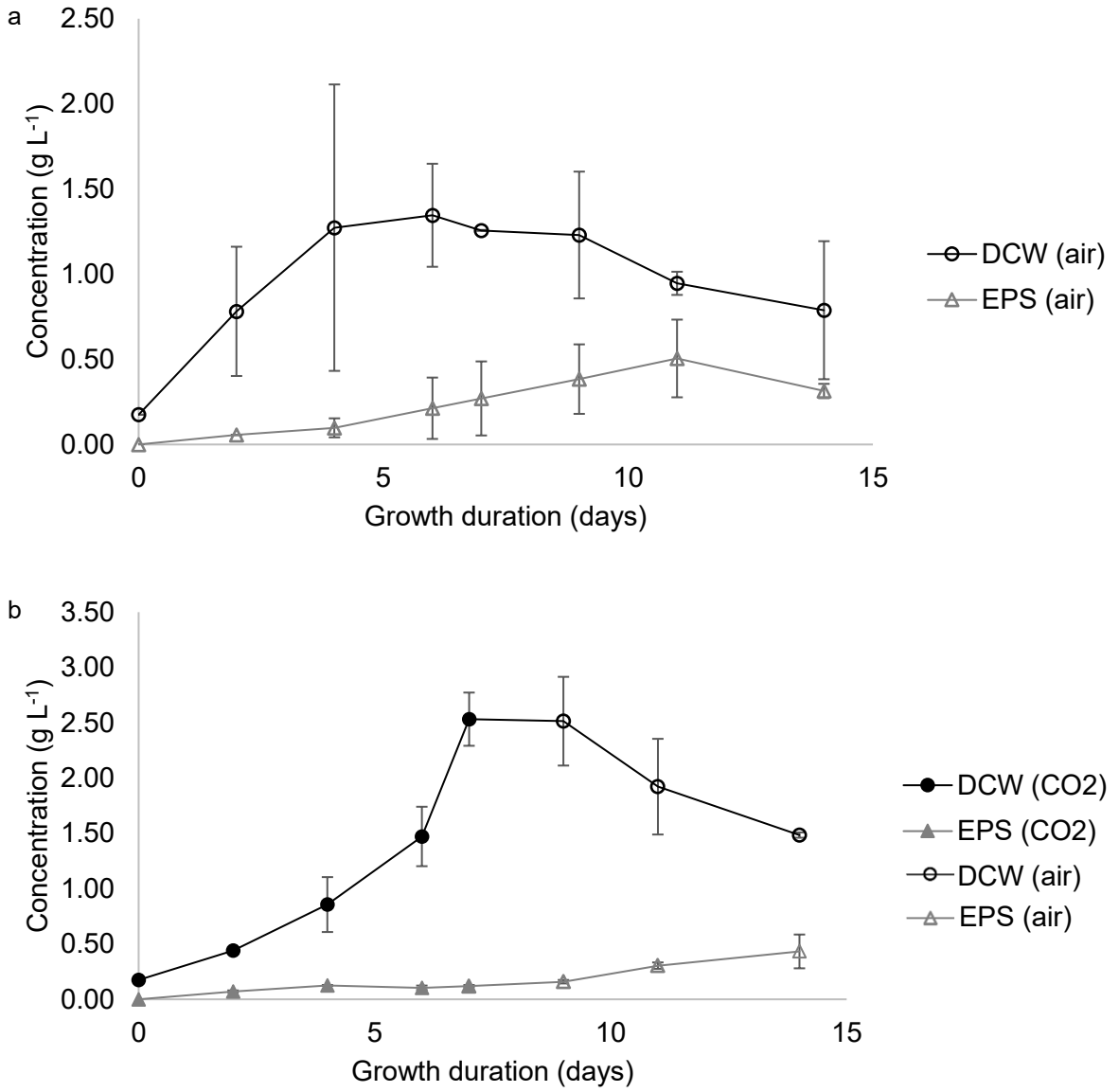


Figure 7-9 Effect of CO_2 on dry cell weight (DCW) and extracellular polymeric substance (EPS) production in *Calothrix brevissima* under axenic conditions (Experiment 3-4).(a) DCW and EPS concentrations over time when grown with air only (410 ppm CO_2). (b) DCW and EPS concentrations over time when grown with air containing 5.5% CO_2 (52,521 ppm CO_2). CO_2 was disconnected after the day 7 sample. Solid fill indicates CO_2 supplementation; no fill indicates air only. Values show mean ± 1 standard deviation (n=2).

The observation that supplementing *C. brevissima* with CO_2 increased DCW at the expense of EPS was consistent with the results of the previous experiments (Exp. 3-1 and Exp. 3-2). Based on Figure 7-9, one explanation for this observation could be that on *C. brevissima* grown in air already entered stationary phase on day 7 and

accumulated EPS, whereas the culture supplemented with CO_2 was still in exponential phase, resulting in more cells and less EPS.

As described in section 7.4, during the 2nd replicate of Exp. 3-2, the CO_2 cylinder was depleted after day 5, resulting in the PBRs being supplied only with air for the last two days, which was accompanied by a spike in EPS in all four reactors from day 6 to day 7. This led to the hypothesis that a two-stage cultivation (first CO_2, then only air) might trigger EPS to accumulate earlier. To test this hypothesis, the CO_2 was removed after the day 7 sample (Figure 7-9*b*). EPS concentration initially increased slowly after CO_2 removal (day 7), and nearly doubled at the end of stationary phase (from day 9 to 11), reaching the maximum (0.43 ± 0.15 g L^{-1}, n=2) at the end of the experiment (day 14). This event might be the reason for the cells to enter stationary phase and increase EPS. However, the increase in EPS was not drastic, leading the results being inconclusive. An additional experiment comparing one-stage cultivation (CO_2) to two-stage cultivation (CO_2, then air) would be required to directly study the effect of switching from CO_2 to air mid-run.

7.8 Selection of Species for Techno-Economic Assessment

The scale-up studies did not result in higher EPS titres, as production in the PBRs was lower than in the shake flasks. A potential physiological explanation is discussed in section 9.5, and the challenges encountered with the PBRs are outlined in section 9.4. Due to these challenges and the low EPS production observed in the PBRs, the shake flask data were used to carry out a screening-level techno-economic analysis of an industrial-scale EPS process to identify key cost drivers. *C. brevissima* was chosen as the baseline organism for the TEA, with *N. folicaeum* included as an alternative species.

Chapter 8: Economic Evaluation of Industrial-scale EPS Production Process

8.1 Chapter Overview

To assess whether current product titres are sufficient for economic viability or require improvement, the techno-economics of a large-scale EPS production process was conducted. A baseline scenario, featuring *C. brevissima*, tubular PBRs, and tangential-flow UF, was evaluated to identify major cost drivers, profitability and key economic factors. Alternative scenarios explore variations in cultivation systems, DSP methods, species, and products to assess their impact on economic performance. A sensitivity analysis highlights the influence of critical parameters on production viability. This chapter aims to identify the most cost-effective strategies for scaling up production while maintaining competitive pricing. The Discussion chapter will place these findings within the broader market context, outlining the main challenges and potential opportunities for commercialisation.

8.2 Market Analysis Outcomes for Bioemulsifier

Bio-surfactants such as bioemulsifiers derived from EPS from cyanobacteria represent a promising alternative to synthetic emulsifiers. They offer advantages such as biodegradability, low toxicity, increased environmental compatibility, higher specificity and good stability [17]. This market analysis evaluates the potential market size, demand, competition, and pricing strategy for EPS-derived bioemulsifiers.

Global emulsifier market was valued at approximately 4.70 billion USD in 2023 and is projected to reach around 7.66 billion USD by 2032, growing at a compound annual growth rate (CAGR) of 5.5% [22]. Bioemulsifiers represent a niche within this larger market but have significant growth potential due to growing consumer awareness on using natural ingredients over synthetic additives. Bioemulsifiers find applications in many industries such as food, cosmetics, pharmaceuticals and agriculture [351]. In the food industry, emulsifiers are used to stabilise emulsions to prevent the separation of oil and water, as well as controlling oxygen and humidity transport [352]. The global

demand for emulsifiers in the food industry alone is expected to be above 1.3 million tons by 2025 [353].

Drivers of demand to use natural ingredients instead of synthetic ones are growing consumer awareness for natural ingredients, corporate sustainability goals, and the implementation of regulations (e.g. for food safety) [351, 354]. Challenges are associated with the current high production costs, low production titres, and potentially regulatory approvals and compliance requirements. Also, performance of bioemulsifiers compared to synthetic emulsifiers is an important factor.

The major producers of emulsifiers include companies such as BASF SE, DuPont, Kerry Inc., Akzo Nobel N.V., and Corbion, among others [355]. Competitive products are synthetic emulsifier such as polysorbate 20, and natural emulsifiers such as lecithin [356]. The most similar competitive product on the market is a seaweed-derived cosmetic emulsifier by biotech company Carbonwave, which is commercially available under the name SeaBalance 2000. The company has sold half a ton of the product, which was named as ‘Best Functional Ingredient’ at In-Cosmetics Global in 2022. In an interview, the company stated it had secured funding for a new biorefinery in Puerto Rico, scaling the process up to hundreds of tons annually [357].

Competitive advantages of EPS-derived emulsifiers to synthetic emulsifiers are that they are bio-based products, which are preferable over synthetic emulsifiers due to biodegradability and lower toxicity. A recent study has shown that the dietary emulsifiers carboxymethylcellulose and polysorbate 80 promote intestinal inflammation. The authors stated that the emulsifiers “*induced a lasting seemingly detrimental impact on microbiota composition and function*” [358]. This was observed for many of the tested emulsifiers, with the exception of lecithin [358]. Furthermore, the production process of EPS with cyanobacteria is more sustainable than other bio-based emulsifiers. Cyanobacterial cultivation relies primarily on sunlight, carbon dioxide and water. This represents an advantage over heterotrophic microbial cultivation, which uses glucose as feedstock, which requires arable land and competes with food resources [8]. Similarly, the natural emulsifier lecithin is usually sourced from soy bean, which is often associated with ecological damage to the rain forest due to deforestation and mono-culturing [359]. Furthermore, cyanobacterial EPS exhibit

unique properties due to their complex structure and composition. For example, the antioxidant properties can be advantageous in food or cosmetic products. A competitive advantage of the emulsifier produced by *C. brevissima* over the seaweed-derived cosmetic emulsifier SeaBalance 2000 is that it is effective at concentrations as low as 0.2%w v^{-1} (this study), compared to the 3–6% use level of SeaBalance 2000 [301].

The prices of competing products range from 1.64 USD kg^{-1} to 73 USD kg^{-1}: The natural emulsifier lecithin and the synthetic emulsifier Tween20 are estimated at 1.64 USD kg^{-1} and 8.99 USD kg^{-1}, respectively [360, 361]. Given that the majority of consumers are willing to pay more for a bio-based product, a premium pricing strategy may be adopted that presents the bioemulsifier as a more environmentally conscious choice [148]. A premium pricing strategy can compensate for the higher production costs. The seaweed-derived cosmetic emulsifier SeaBalance 2000 from the company Carbonwave is available commercially as 85-90% solution with xanthan gum and pentylene glycol for 150 USD for 5lb (≈ 2.27 kg), resulting in a emulsifier price of 73 USD kg^{-1} [301]. Given the commercial success of this product, a bioemulsifier derived from cyanobacteria should aim for a similar selling price. Another comparable product is *Emulcyan*, an emulsifying EPS from *Phormidium* J-1 [362]. However, it is no longer available, as the patent expired due to fee-related issues [363]. This could indicate the challenges with introducing this type of product into the market.

8.3 Baseline Scenario Results

A baseline production scenario (scenario 1) was designed using tubular photobioreactors (PBRs) as cultivation system and a series of filtration systems as EPS downstream processing. Filtration was chosen as the baseline downstream process because several studies identify it as suitable for EPS recovery, with one pilot-scale study showing that microfiltration–ultrafiltration can efficiently recover EPS while preserving bioactivity [21, 207]. While one study demonstrated the techno-economic feasibility of ultrafiltration for harvesting of microalgal biomass, no previous study has assessed the techno-economics of filtration specifically for EPS, highlighting the gap addressed in this study [238]. The TEA results of this scenario are presented in the following sections. The utilities of the baseline scenario were calculated with MS Excel and the overall process economics were determined with SuperPro Designer® (SPD).

8.3.1 PBR Utilities of Baseline Scenario

The utility cost of a PBR in Almería, Spain was estimated by calculating costs for LED lighting, heating water, cooling water and culture circulation. As shown in Table 8-1, the monthly average temperatures in Almería range from 8.8°C in January to 26.7°C in July. Based on heat gain from LED lights and heat gain or loss via convection, the culture required heating from September to June and cooling from July to August. Heating requirement for a culture volume of 3300 m^3 varied between 624,000 W (June) and 7,720,000 W (January), whereas cooling requirement ranged from 914,000 W (August) to 1,160,000 (July).

Table 8-1 Monthly heating and cooling requirements and costs for a 3000 m^3 tubular photobioreactor (PBR) for industrial production of extracellular polymeric substances with cyanobacterium *Calothrix brevissima* in Almería, Spain.The table includes average ambient temperature (°C), heating and cooling energy (W), hot and cooling water amounts (kg h^{-1}), and total annual energy use (MT y^{-1}) with corresponding costs (USD y^{-1}).

Month	**Temp.**	**Heating required**	**Cooling required**	**Hot water amount**	**Cooling water amount**
	°C	W	W	kg h^{-1}	kg h^{-1}
Jan	8.8	7,720,000	0	665,000	0
Feb	12.4	5,930,000	0	511,000	0
Mar	12.6	5,830,000	0	502,000	0
Apr	14.3	4,990,000	0	430,000	0
May	20.0	2,160,000	0	186,000	0
Jun	23.1	624,000	0	53,700	0
Jul	26.7	0	1,160,000	0	200,000
Aug	26.2	0	914,000	0	157,000
Sep	21.7	1,320,000	0	114,000	0
Oct	16.4	3,950,000	0	340,000	0
Nov	13.4	5,440,000	0	468,000	0
Dec	9.4	7,420,000	0	639,000	0
			Sum (MT y^{-1})	2,850,000	266,000
			Cost (USD y^{-1})	142,000	13,300
		Total cost for heating and cooling (USD y^{-1})			**156,000**

As described in section 0, heating and cooling was designed to be performed by circulating hot or cold water through the heat exchanger coil in the bubble column. Hot water flow rates ranged from 53,700 kg h^{-1} (June) and 665,000 kg h^{-1} (January), and cooling water flow rates varied between 157,000 kg h^{-1} (August) and 200,000 kg h^{-1} (July). This resulted in 2,850,000 (metric tons, MT) hot water and 266,000 MT cooling water being required per year, costing 142,000 and 13,300 USD y^{-1}, respectively, resulting in total temperature control cost of 156,000 USD y^{-1}. For simplification, temperature variance throughout the day and month was not considered. If maximum monthly temperatures had been used instead of mean values, cooling demand would

likely be higher than estimated, increasing the required water flow and associated costs. Conversely, operation in colder regions, such as Iceland, would reduce the cooling requirement but substantially increase the heating demand during winter. This highlights the importance of location-specific climate considerations when designing industrial-scale cultivation systems.

Table 8-2 Annual energy consumption, cost, and relative contribution of utilities for a 3000 m^3 tubular photobioreactor (PBR) for industrial production of extracellular polymeric substances with cyanobacterium *Calothrix brevissima* in Almería, Spain.Utilities include LED lighting, centrifugal pump for culture circulation, hot water, and cooling water. Costs are shown in USD y^{-1} and percentage contribution to total PBR utility costs.

Utility	**Amount**	**Unit**	**Cost ($ y^{-1})**	**Cost (%)**
LED lights	95,300,000	kWh	9,530,000	94.5%
Centrifugal pump	2,450,000	kWh	245,000	2.4%
Hot water	2,850,000	MT y^{-1}	285,000	2.8%
Cooling water	266,000	MT y^{-1}	26,600	0.3%
	Total PBR utilities		**10,086,600**	100.0%

Table 8-2 shows the PBR utilities associated with lights, culture circulation and heating/cooling during cultivation. The largest cost driver for the PBR utilities were electricity costs associated with the LED lighting (94.5%), costing 9,530,000 USD annually. Electricity costs caused by the centrifugal pump (245,000 USD y^{-1}) made up merely 2.8%. Heating and cooling performed by hot water and cooling water, respectively, were the lowest cost drivers, causing 2.8% and 0.3%, respectively.

8.3.2 Investment and Operating cost of Baseline Scenario

Phototrophic growth in tubular PBRs with filtration as downstream processing (DSP) (scenario 1) resulted in Total Capital Investment (TCI) and Operating Expenditure (OpEx) of 176,000,000 USD and 23,800,000 USD y^{-1}, respectively. Dry cell weight (DCW) production and EPS production were 86,100 and 89,400 kg y^{-1}, respectively. As shown in Table 8-3, the cultivation section of the process contained 1,100 PBR modules with LEDs, 83 air blowers, 16 CO_2 supply units, four NaClO tanks, one media tank and one upstream processing (USP) pump. The harvest section contained one harvest pump and one decanter centrifuge. The filtration section contained one plate

and frame (P&F) filtration unit, seven microfiltration (MF) units and one ultrafiltration (UF) unit. Furthermore, the drying section contained the spray dryer. Lastly, the storage section contained a storage tank for EPS and an additional one for biomass. The equipment amounted to a total Major equipment cost (MEC) of 44,800,000 USD. The PBRs with LEDs were the most expensive equipment (38,500,000 USD), making up 86% of MEC. The tubular PBRs themselves cost 22,400,000 USD, whereas the lights cost 15,900,000 USD. The PBR cost was followed by tanks (7%), filtration units (4%), centrifuge (1%), air blowers (1%), spray dryer (0.5%), pumps (0.1%) and CO_2 supply units (0.0%).

Table 8-3 Major equipment cost (MEC) of the baseline scenario for industrial production of extracellular polymeric substances with cyanobacterium *Calothrix brevissima*.The baseline scenario (scenario 1) includes indoor phototrophic growth with artificial lighting in tubular photobioreactors with filtration as downstream processing for the EPS.

Section	**Item**	**Unit Cost**	**Quantity**	**Cost**
Unit	(-)	USD	(-)	USD
Cultivation	PBRs + LEDs	35,000	1,100	38,500,000
Cultivation	NaClO tank 1	670,000	4	2,680,000
Cultivation	Media tank	344,000	1	344,000
Cultivation	Air blower	4,000	83	332,000
Cultivation	CO_2 supply unit	1,000	16	16,000
Cultivation	NaClO pump	14,000	1	14,000
Harvest	Centrifuge	404,000	1	404,000
Harvest	Harvest pump	14,000	1	14,000
Filtration	Microfilter	196,000	7	1,400,000
Filtration	Ultrafilter	327,000	1	332,000
Filtration	P&F filter	273,000	1	283,000
Filtration	Air compressor	112,000	1	112,000
Filtration	NaClO tank 2	82,000	1	82,000
Filtration	Flush water tank	48,000	1	48,000
Drying	Spray dryer	206,000	1	207,000
Storage	Biomass tank	48,000	1	48,000
Storage	EPS tank	48,000	1	48,000
		Total MEC (USD)		**44,800,000**

The baseline scenario resulted in a minimum selling price (MSP) of 539 USD kg^{-1}. As described in the Materials and Methods chapter (4.4.3.5), the MSP was calculated as the selling price for EPS to reach a non-negative net present value (NPV). The detailed cash flow analysis (CFA) will be discussed later (section 8.3.3). OpEx were the largest contributor to MSP (43%), followed by Capital Expenditure (CapEx, 26%), interest (19%) and tax (13%) (Figure 8-1*a*). The largest cost-driver for both, TCI and OpEx, were the PBRs. Due to their high purchase cost, the PBRs were not only the main contributor to the high TCI, but they also increased OpEx via utilities and facility-

dependent cost. The largest cost factor of total OpEx were utilities (51%, Figure 8-1*b*), which were mostly caused by the cultivation stage (98%). Utilities were predominantly electricity (98%), with heat transfer agents making up merely 2%. Within the cultivation stage, the PBR was the main contributor to the electricity cost (83%) compared to other equipment such as air blower, CO_2 supply unit, NaClO and media tank. As mentioned in the previous section, the PBR utilities were mainly caused by LED lights (96%), followed by the centrifugal pump (3%), heating (1%) and cooling (0.2%). Facility-dependent cost (7,800,000 USD), which were estimated as a percentage of the TCI (section 4.4.3), was the second largest cost factor of total OpEx, making up 33%. As can be seen in the itemised cost (Figure 8-1*c*), the facility-dependent cost was almost entirely caused by the cultivation section (92%).

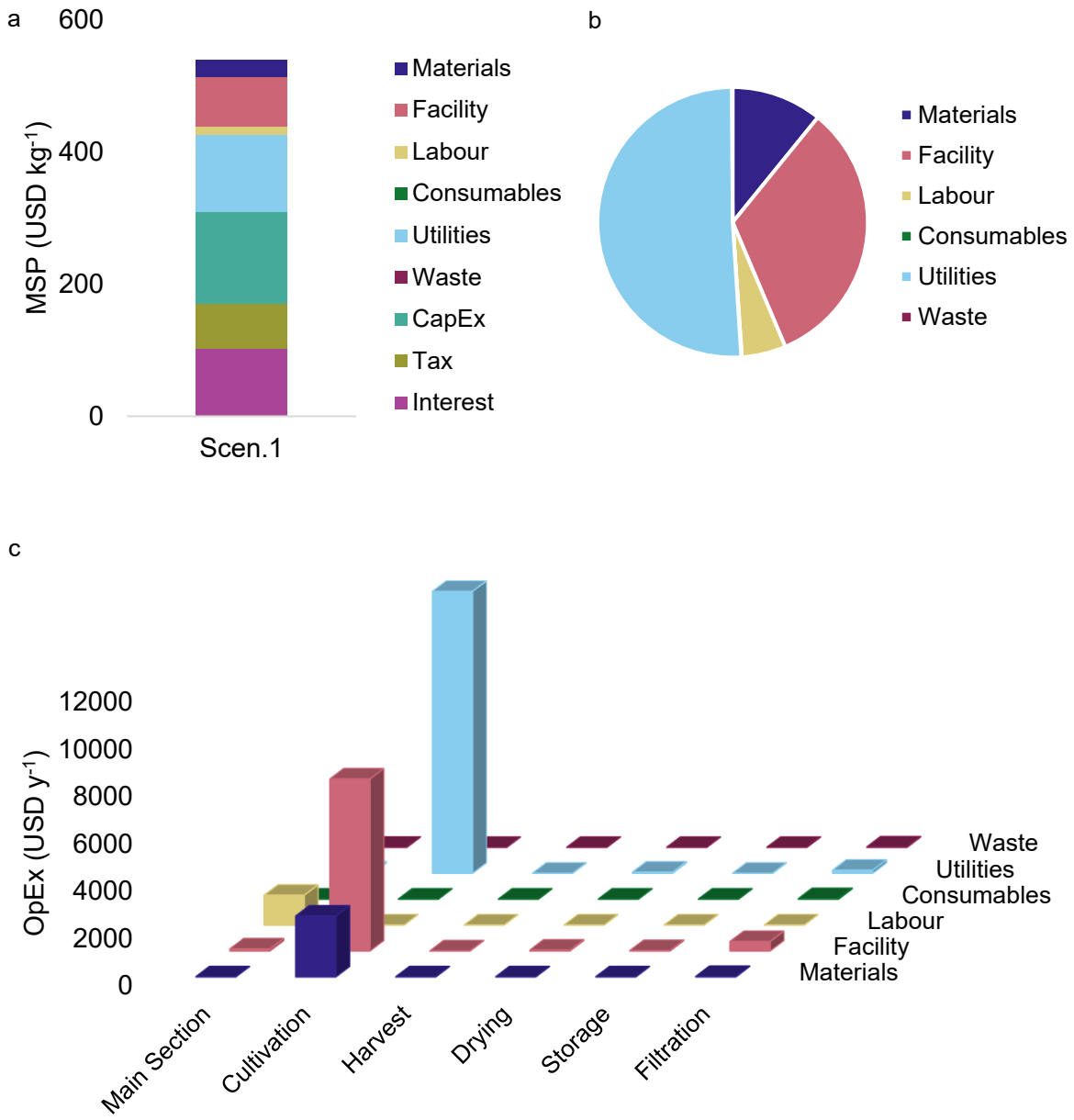


Figure 8-1 Cost breakdown of the baseline scenario for the techno-economic assessment of an industrial extracellular polymeric substances (EPS) production process using the cyanobacterium *Calothrix brevissima*.The baseline scenario includes phototrophic growth in tubular photobioreactors (PBRs) in semi-continuous mode with filtration as EPS downstream processing (DSP). (a) Contribution of capital expenditure (CapEx), facility-dependent costs, labour-dependent costs, raw materials, utilities, consumables, waste, tax, and interest to the minimum selling price (MSP, USD kg^{-1}). (b) Contribution of facility-dependent costs, labour-dependent costs, raw materials, utilities, and consumables to operational expenditure (OpEx). (c) Itemised OpEx based on section and cost type.

Raw materials and labour-dependent cost made up 11% and 5%, respectively, whereas consumables and waste treatment were negligible (<1%). Similarly, raw

materials were mainly used by the cultivation stage (99%), with BG-11 stock (100-fold concentrated) being the main contributor (75%), followed by carbon dioxide (25%). Fresh water and sodium hypochlorite merely contributed 0.3% and 0.5%. Main section (labour) was the second largest contributor to the OpEx (5%), followed by filtration (3%). Harvest, drying and storage sections contributed less than 1%. Within the filtration stage, the facility-dependent costs were the most influential (90%). Utilities such as power consumption of the filtration units and auxiliary equipment such as the compressor made up 7%. The replacements of the filtration membranes made up 1%. The MF membrane caused considerably more (88%) consumables costs than the UF membrane (12%) due to the higher purchasing cost per area (129 USD m^{-2}) and shorter lifetime (3 years). Waste disposal of a fraction of recycled flush water, CIP water and retentate contributed 0.9%. Raw materials of the filtration section such as freshwater and NaClO contributed a similar amount (0.9%).

There are several advantages and disadvantages of the filtration system in terms of product purity and product losses. Due to the multiple filtration steps, it is expected that the EPS product exhibits high purity due to the removal of residual cells, debris and spent media components, and the absence of solvents. Furthermore, as only the filtrate of the UF system was recycled back to the PBRs, it is expected that it was of high purity and suitable for reuse for cultivation, while reducing the risk of accumulation of inhibitory compounds. The main disadvantage of the filtration scenario was high product losses as EPS were lost at each of the filtration steps, resulting 9% of EPS being lost in total.

8.3.3 Cash Flow Analysis of Baseline Scenario

As described in the method section, the MSP (USD kg^{-1}) was calculated based on a cash flow where the process reaches a non-negative NPV. The CFA of this scenario with an MSP of 539 USD kg^{-1} is shown in Table 8-4.

Table 8-4 Cash flow analysis (in million USD) of the baseline scenario for industrial production of extracellular polymeric substances (EPS).The baseline scenario (scenario 1) comprises indoor phototrophic growth of cyanobacterium *Calothrix brevissima* with artificial lighting in tubular photobioreactors, with filtration for EPS downstream processing and use of the EPS as bio-emulsifier. An EPS minimum selling price (MSP) of 539 USD kg^{-1} and an interest rate of 8% were used. The MSP corresponds to the value at which the plant achieves a non-negative net present value. Abbreviations: CapEx, capital expenditure; Rev, revenues; OpEx, operating expenditure; GP, gross profit; Dep, depreciation; TI, taxable income; Tax, taxes; NP, net profit; NCF, net cash flow; DCF, discounted cash flow.

Year	CapEx	Rev	OpEx	GP	Dep	TI	Tax	NP	NCF	DCF
1	-50	0	0	0	0	0	0	0	-50	-50
2	-67	0	0	0	0	0	0	0	-67	-57
3	-50	9	27	-18	18	0	0	-1	-51	-40
4	0	53	40	13	18	13	5	26	26	19
5	0	53	40	13	18	13	5	26	26	17
6	0	53	40	13	18	13	5	26	26	16
7	0	53	40	13	18	13	5	26	26	15
8	0	53	40	13	18	13	5	26	26	14
9	0	53	40	13	18	13	5	26	26	13
10	0	53	40	13	18	13	5	26	26	12
11	0	53	40	13	18	13	5	26	26	11
12	0	53	40	13	18	13	5	26	26	10
13	0	53	24	29	0	29	12	18	18	6
14	0	53	24	29	0	29	12	18	18	6
15	9	53	24	29	0	29	12	18	26	8
									NPV	0
									PI	1.0

According to the definition in the Materials and Methods chapter, CapEx was assumed to be 30%, 40% and 30% of TCI in years 1, 2 and 3, respectively, with a salvage value of 5% of TCI (9 MM USD). During the startup period, which was assumed to be 30 months (SPD default value), no revenues or OpEx are generated. This resulted in a negative NCF of about -53 MM USD annually in the first two years. The plant was assumed to be operational within the third year, generating 9 MM USD of revenues

and causing 27 MM USD OpEx. This resulted in a negative gross profit for year 3 (-18 MM USD). As depreciation was assumed to be applied in year 3 to 12, depreciation was 18 MM USD for year 3. However, taxable income was still zero, resulting in no tax being paid in year 3. This resulted in a negative NCF in year 3 of -51 MM USD, which corresponded to a discounted NCF of -40 MM USD. In years 4 to 15 the plant was operational and generating 53 MM USD revenues annually. Years 4 to 12, OpEx were 40 MM USD annually, resulting in gross profit of 13 MM USD. After adding depreciation (18 MM USD) and deducting taxes (5 MM USD), the net profit amounted to 26 MM USD. This resulted in a NCF of 26 MM USD and a DCF between 10 and 19 MM USD in years four to 12. In year 13 and 14, the plant was fully depreciated, resulting in 24 MM USD OpEx and a higher gross profit of 29 MM USD, resulting in more tax being paid (12 MM USD). This resulted in a net profit and NCF of 18 MM USD annually, which corresponded to a DCF of 6 MM USD. In year 15, the salvage value of the plant was considered, resulting in a NCF of 26 MM USD, which corresponded to a DCF of 8 MM USD. As per design, this resulted in a NPV of zero USD. Evidently, to generate actual profits in terms of positive NPV, an even higher EPS selling price than 539 USD kg^{-1} would have to be applied.

8.3.4 Profitability Analysis of Baseline Scenario

For the profitability analysis, the target EPS selling price of 73 USD kg^{-1} was applied. The cash flow of that case is shown in Table 8-5. As can be seen, the revenues are considerably less due to the lower selling price, resulting in only 11 MM USD annually. As this could not compensate for the OpEx of 40 MM USD, a negative net profit (-11 MM USD), NCF (-11 MM USD) and negative DCF of between -1 and -8 MM USD was observed during operational years. This resulted in a negative NPV of -215 MM USD, indicating the plant would lose money rather than generating profits at an EPS selling price of 73 USD kg^{-1}.

The PI, calculated based on NPV and total investment, was negative (-0.2), indicating that the baseline scenario was not profitable if the target EPS selling price of 73 USD kg^{-1} was applied. A scenario analysis of different production scenarios and their effect on MSP (USD kg^{-1}) is presented in the next subchapter.

Table 8-5 Cash flow analysis (in million USD) of the baseline scenario for industrial production of extracellular polymeric substances (EPS).The baseline scenario (scenario 1) comprises indoor phototrophic growth of cyanobacterium *Calothrix brevissima* with artificial lighting in tubular photobioreactors, with filtration for EPS downstream processing and use of the EPS as bio-emulsifier. An EPS minimum selling price (MSP) of 73 USD kg^{-1} and an interest rate of 8% were used. The MSP corresponds to the value of a similar product on the market (seaweed-based emulsifier) [301]. Abbreviations: CapEx, capital expenditure; Rev, revenues; OpEx, operating expenditure; GP, gross profit; Dep, depreciation; TI, taxable income; Tax, taxes; NP, net profit; NCF, net cash flow; DCF, discounted cash flow.

Year	CapEx	Rev	OpEx	GP	Dep	TI	Tax	NP	NCF	DCF
1	-50	0	0	0	0	0	0	0	-50	-50
2	-67	0	0	0	0	0	0	0	-67	-57
3	-50	2	27	-25	18	0	0	-8	-58	-46
4	0	11	40	-28	18	0	0	-11	-11	-8
5	0	11	40	-28	18	0	0	-11	-11	-7
6	0	11	40	-28	18	0	0	-11	-11	-7
7	0	11	40	-28	18	0	0	-11	-11	-6
8	0	11	40	-28	18	0	0	-11	-11	-6
9	0	11	40	-28	18	0	0	-11	-11	-5
10	0	11	40	-28	18	0	0	-11	-11	-5
11	0	11	40	-28	18	0	0	-11	-11	-5
12	0	11	40	-28	18	0	0	-11	-11	-4
13	0	11	24	-12	0	0	0	-12	-12	-5
14	0	11	24	-12	0	0	0	-12	-12	-4
15	9	11	24	-12	0	0	0	-12	-4	-1
									NPV	-215
									PI	-0.2

8.4 Scenario Analysis Results

Twenty additional scenarios were designed and compared based on their MSP (USD kg^{-1}). The effect of DSP equipment, cultivation systems, trophic mode, cyanobacterial species and type of product was investigated. Regarding DSP, ethanol precipitation was included because it is the downstream process used in the only published techno-

economic analysis of microalgal EPS production [204]. That study did not consider a phototrophic PBR process and likely underestimated costs, so this thesis combines ethanol precipitation of EPS with an actual phototrophic cultivation. Freeze-drying and spray-drying were compared following the approach of Vázquez-Romero, et al. [251] for a microalgal biomass production process. Regarding centrifuges, two types were compared because the only TEA on microalgal EPS used a decanter [204]. A different type of centrifuge was included to evaluate performance and costs, in case a decanter would not be sufficient to separate biomass from EPS. A disc stack centrifuge was chosen as the alternative based on previous studies on microalgal biomass [250]. Different cultivation systems were examined because PBRs are more expensive than conventional reactors, representing a major barrier to profitability, so cheaper cultivation systems were tested to assess the extent to which profitability could be improved [21, 211]. Different growth modes, phototrophic and mixotrophic were compared based on laboratory results that the highest EPS were obtained under mixotrophic conditions (5 g L^{-1} glucose, 28°C, 150 µmol m^{-2} s^{-1}), to assess the impact of higher EPS titre on revenues and the effect of using of glucose instead of CO_2 on costs. *N. foliaceum* was explored as an alternative species because experimental data showed it produced more biomass but less EPS than *C. brevissima.* This allowed investigation of how different ratios of biomass and EPS affect overall process techno-economics and comparison of the impact of producing both products versus biomass alone. A cosmeceutical product was explored as an alternative product to investigate the effect of producing a higher-value product compared with a lower-value product such as an emulsifier because the literature suggests focusing on high-value products to compensate for the high production costs [11, 21].

8.4.1 Effect of Operation Mode (Batch vs. Semi-Continuous) on MSP

As can be seen in Figure 8-2*a*, batch mode operation (scenario 2) resulted in a 3-fold higher MSP (1,750 USD kg^{-1}) compared to the semi-continuous mode of the baseline scenario (scenario 1). TCI and OpEx were 707,000,000 USD and 47,600,000 USD, respectively, which was 3 times higher than semi-continuous mode. This was mainly caused by larger DSP equipment. In batch mode, the DSP equipment had to be large enough to process one entire batch volume, whereas in case of semi-continuous mode, smaller equipment was sufficient. MEC was 181,000,000 USD, which was four times higher than in semi-continuous mode.

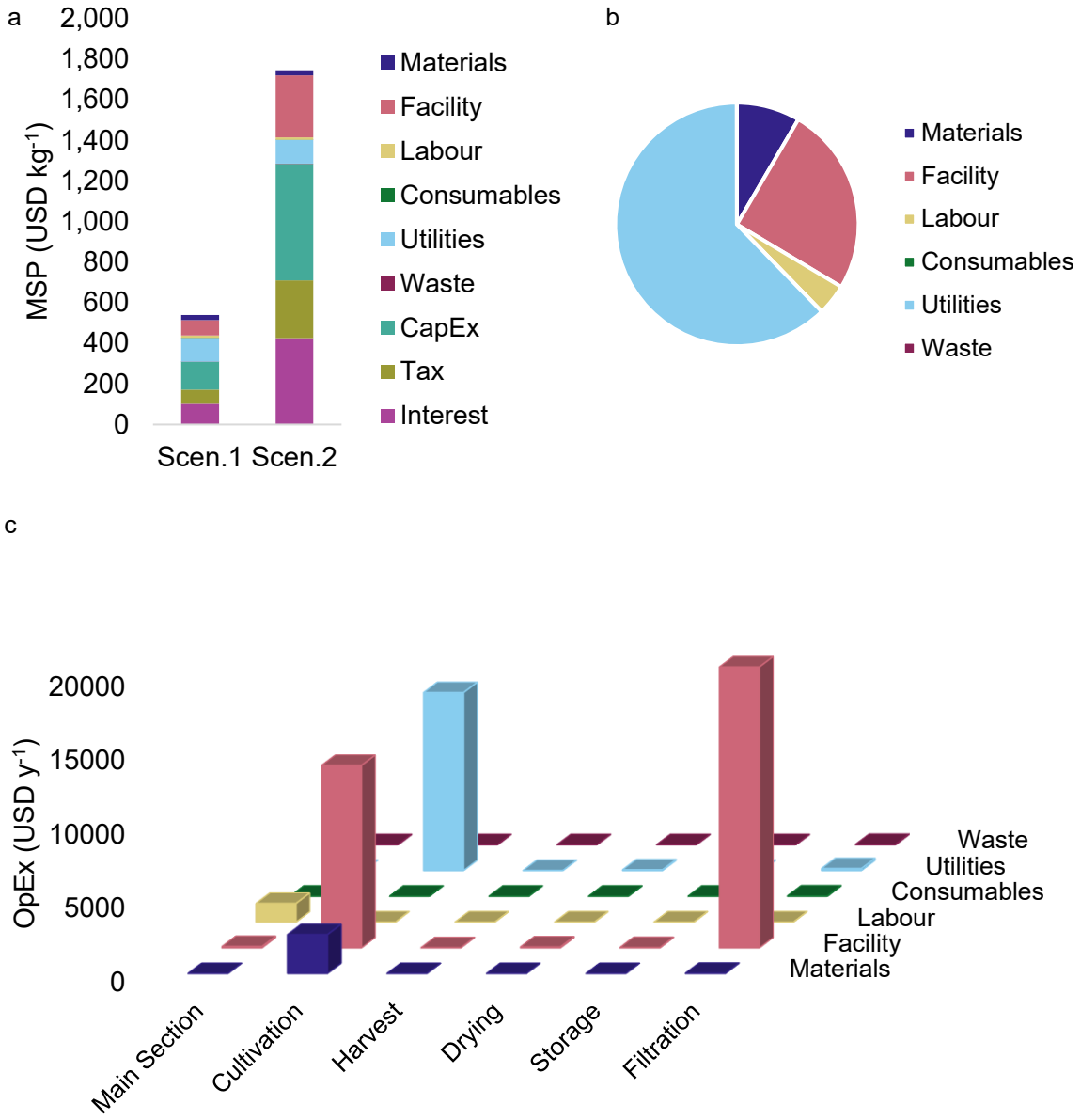


Figure 8-2 Effect of on operation mode (batch vs. semi-continuous) on minimum selling price (MSP, USD kg^{-1}) for the techno-economic assessment of an industrial extracellular polymeric substances (EPS) production process using the cyanobacterium *Calothrix brevissima*.The baseline scenario (scenario 1) involves phototrophic growth in tubular photobioreactors (PBRs) in semi-continuous mode with filtration for EPS downstream processing (DSP), while scenario 2 is in batch mode. (a) Contribution of capital expenditure (CapEx), facility-dependent costs, labour-dependent costs, raw materials, utilities, consumables, waste, tax, and interest to the minimum selling price (MSP, USD kg-1) depending on operation mode (batch, scenario 2 vs. semi-continuous, scenario 1). (b) Contribution of facility-dependent costs, labour-dependent costs, raw materials, utilities, and consumables to operational expenditure (OpEx) to scenario 2 (batch mode). (c) Itemised OpEx based on section and cost type for scenario 2 (batch mode).

Larger equipment had higher purchase costs, which increased TCI, as well as OpEx cost via facility-dependent costs. As can be seen in Figure 8-2*b*, in batch mode, the facility-dependent cost was considerably higher than in semi-continuous mode (4-fold) and made up 85% of OpEx. Figure 8-2*c* shows that the facility-dependent cost was mainly caused by the filtration section, even exceeding that of the cultivation section. This was mainly caused by an increase of MF units from 7 (semi-continuous) to 425 units (batch), costing 88,000,000 USD in total, which made up 49% of the MEC. Furthermore, ten times more NaClO tanks were needed in the cultivation section, costing 31,400,000 USD in total, making them nearly as expensive as the PBRs themselves. Facility-dependent cost of other storage tanks such as the water and NaClO tanks for flushing the filtration systems increased by a factor 9 and 4, respectively, due to the larger size. Other OpEx costs such as labour, material, waste and utilities remained the same as in batch mode. Calculating the cash flow at the target EPS selling price of 73 USD kg^{-1} revealed a negative NPV (-782,000,000 USD) and negative PI (-0.1), indicating that batch mode (scenario 2) was not profitable.

8.4.2 Effect of Downstream Processing on MSP

The effect of different DSP on MSP (USD kg^{-1}) was investigated and the results are shown in Figure 8-3. The cheapest DSP was scenario 3, which comprised only of centrifugation and spray drying, resulting in an MSP of 547 USD kg^{-1}. Since only two unit procedures were required, the MEC was lower than in the baseline scenario. However, the difference was only 1% due to the most expensive equipment, the PBR, remaining at the same value. Furthermore, a much larger spray dryer was required, as there was no concentration step of the supernatant. This resulted in the spray dryer in scenario 3 being 76-fold larger (142 m^3) than in baseline scenario (1.8 m^3), resulting in twice as expensive equipment. Furthermore, without an EPS concentration step, a large amount of water had to be evaporated, resulting in higher utilities cost caused by the power consumption of the spray dryer (2,980,000 USD y^{-1}) which caused 10% of the total OpEx. In other words, the difference in MSP compared to the baseline scenario was merely 8 USD, as the lower facility-dependent cost were balanced out by higher utility costs. The type of DSP also affected EPS purity and product losses. EPS product losses were lower in scenario 3, as the only loss occurred through the biomass stream after centrifugation, which amounted to 0.3% of total EPS being lost. However, since the entire supernatant was dried without any purification step, different

impurities such as residual cells, debris and spent media components are expected to be present in the EPS product. Furthermore, the water recycled back to the cultivation section was not subjected to any purification, leaving its suitability for reuse uncertain.

Ethanol precipitation (scenario 4) resulted in a MSP of 1,090 USD kg^{-1}, which was nearly twice as expensive as the baseline scenario. The increase was largely driven by the size of equipment such as distillation column, ethanol storage tank and mixer-settler extraction unit. Due to the ratio of ethanol to supernatant of 2:1, the DSP equipment needed to process triple the volume compared to the filtration system [303]. The DSP equipment led to a two-fold increase in utilities (22,600,000 USD), whereas TCI (177,000,000 USD) and facility-dependent cost (7,640,000 USD) were similar to the baseline scenario. The largest contribution to OpEx, however, was waste disposal/treatment cost with 55%. Due to the high solvent disposal costs, waste costs amounted to 45,600,000 USD y^{-1}, which was 2,000-fold more than in the baseline scenario. This was even more pronounced when the solvent was not recycled (scenario 5), which increased waste costs and MSP 35,600-fold and 16-fold compared to baseline scenario and scenario 4, respectively. Due to this drastic difference in MSP, Figure 8-3 was displayed with a discontinuous axis. The ethanol precipitation scenario did not only result in the highest MSP from the three different purification methods, but it also had the disadvantage that ethanol traces remained in the EPS product, present in the 5% moisture of the product. Additionally, in case of malfunctioning of the distillation column, ethanol could enter the PBR via the water recycling stream and cause harm to the cyanobacterial culture. Furthermore, co-precipitation of different impurities can occur with use of ethanol [40]. Ethanol precipitation was used in this study because it was applied in the only TEA found in the literature for microalgal EPS production [204]. Other solvents such as methanol, isopropyl alcohol, acetone, and dimethyl sulfoxide (DMSO) could also be used, with acetone showing the highest EPS recovery yield in literature [54]. In the EU, industrial use of ethanol is regulated under Council Directive 92/83/EEC and requires a license in many European countries, whereas acetone is regulated under REACH (Registration, Evaluation, Authorisation and Restriction of Chemicals) and does not require a license [364, 365]. In this study, solvent extraction did not present any clear advantages over filtration as a downstream processing method. However, if this changes in future work, the advantages and disadvantages of different solvents should be carefully evaluated, considering factors

such as recovery efficiency, licensing requirements, health and safety implications, and overall costs.

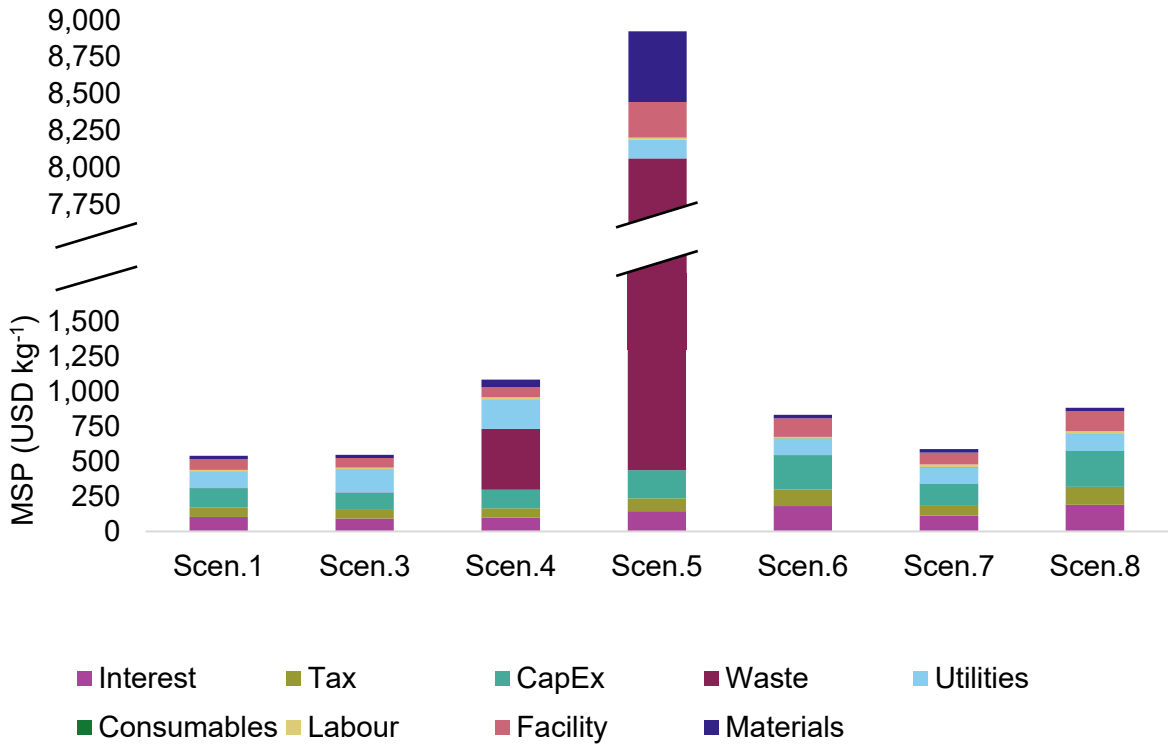


Figure 8-3 Effect of different downstream processing (DSP) equipment for extracellular polymeric substances (EPS) recovery and purification on the minimum selling price (MSP, USD kg^{-1}).The baseline scenario (scenario 1) involves phototrophic growth in tubular photobioreactors (PBRs) in semi-continuous mode with filtration as DSP. Scenario 3-8 explore different DSP compared to the baseline scenario. Scenario 3: only spray drying. Scenario 4: ethanol precipitation with solvent recycling. Scenario 5: ethanol precipitation without solvent recycling. Scenario 6: freeze-dryer instead of spray dryer. Scenario 7: disc-stack centrifuge instead of decanter centrifuge. Scenario 8: freeze-dryer and disc-stack centrifuge. Costs are broken down into capital expenditure (CapEx), facility-dependent costs, labour-dependent costs, raw materials, utilities, consumables, waste, tax, and interest contributing to the minimum selling price (MSP, USD kg^{-1}). Figure is displayed with a discontinuous y-axis due to the high waste costs of scenario 5.

Lastly, three variations of the baseline scenario were explored. Firstly, the spray dryer was replaced by a freeze dryer (scenario 6). Secondly, the decanter centrifuge was replaced by a disc-stack centrifuge (scenario 7). Lastly, both the disc-stack centrifuge and the freeze dryer were applied (scenario 8). It is assumed that spray drying does not affect the emulsifying properties of the EPS. However, if it became apparent that

spray drying affected the emulsifying properties, a freeze dryer could be used instead (scenario 6). Lyophilisation is known to preserve properties of a compound, even characteristics such as bioactivity [207]. Due to higher purchase costs of the freeze dryer (4,040,000 USD) and the smaller capacity of one unit (530 kg), eight freeze driers were required instead of one spray dryer, increasing MEC to 76,900,000 USD, which resulted in 42% higher TCI (300,000,000 USD) and facility-dependent costs (13,400,000 USD) than the baseline scenario. This resulted in a 35% higher MSP (832 USD kg^{-1}) of scenario 6 compared to the baseline scenario. Another variation of the baseline scenario was the use of a disc-stack centrifuge instead of a decanter centrifuge (scenario 7). If the decanter centrifuge appeared to be insufficient in separating biomass from cell-free supernatant, five disc-stack centrifuges (764,000 USD per item) could be used instead which would increase the MSP by 8% to 589 USD kg^{-1}. Using both, disc-stack centrifuge and freeze dryer (scenario 8) would lead to a price increase of 39% (MSP of 883 USD kg^{-1}). The utility cost of scenario 6, scenario 7 and scenario 8 were similar to that of the baseline scenario.

Table 8-6 Net present value (NPV) and profitability index (PI) of scenarios 3 to 8, which include different downstream processing strategies (DSP) for industrial production of extracellular polymeric substances (EPS).An EPS minimum selling price (MSP) of 73 USD kg^{-1} and an interest rate of 8% were used. Baseline scenario (scenario 1): centrifugation, filtration and spray-drying for EPS downstream processing (DSP) from *Calothrix brevissima*. Scenario 3: centrifugation and spray-drying. Scenario 4: centrifugation, ethanol precipitation with solvent recycling and spray-drying. Scenario 5: centrifugation, ethanol precipitation (without solvent recycling) and spray-drying. Scenario 6: centrifugation, filtration and freeze-drying. Scenario 7: centrifugation using a disc-stack centrifuge instead of decanter centrifuge. Scenario 8: centrifugation using a disc-stack centrifuge instead of decanter centrifuge and a freeze-dryer instead of a spray-dryer.

Scenario	**NPV**	**PI**
Scenario 3	-216,000,000	-0.4
Scenario 4	-782,000,000	-2.2
Scenario 5	-249,000,000	-19.5
Scenario 6	-571,000,000	-0.2
Scenario 7	-4,830,000,000	-0.3
Scenario 8	-349,000,000	-0.2

The NPV and PI of scenario 3 to 8 at an EPS selling price of 73 USD kg^{-1} are shown in Table 8-6. All different DSP scenarios showed negative NPVs varying between -216,00,000 USD and -4,830,000,000 USD. This resulted in negative PIs between -0.2 and -19.5, indicating none of the scenarios was profitable.

8.4.3 Effect of Cultivation Systems on MSP

The effect of different cultivation systems in the USP on MSP was investigated. Firstly, outdoor cultivation with artificial LEDs (scenario 9) resulted in 14% lower MSP (466 USD kg^{-1}, Figure 8-4). Outdoor cultivation did not require buildings, which reduced TCI and facility-dependent costs by 10%. Furthermore, since natural light could be used during daytime, LEDs were designed to only operate during nighttime, reducing LED electricity cost by 42% and overall utilities by 35%. Solar radiation appeared to heat the culture more than LEDs, reducing hot water requirement to zero, instead requiring more cooling, causing 127-fold higher cooling water need in scenario 9 compared to baseline. The cost reduction through reduced electricity need was further enhanced

when using outdoor cultivation with natural light (scenario 10). Due to the absence of LEDs, TCI and facility-dependent costs reduced 43% compared to the baseline scenario. Utility cost showed the strongest decrease of 85%, due to the LEDs being the main contributor to electricity cost in the baseline scenario. This resulted in a MSP of 262 USD kg^{-1} for scenario 10, which was 51% cheaper than the baseline scenario.

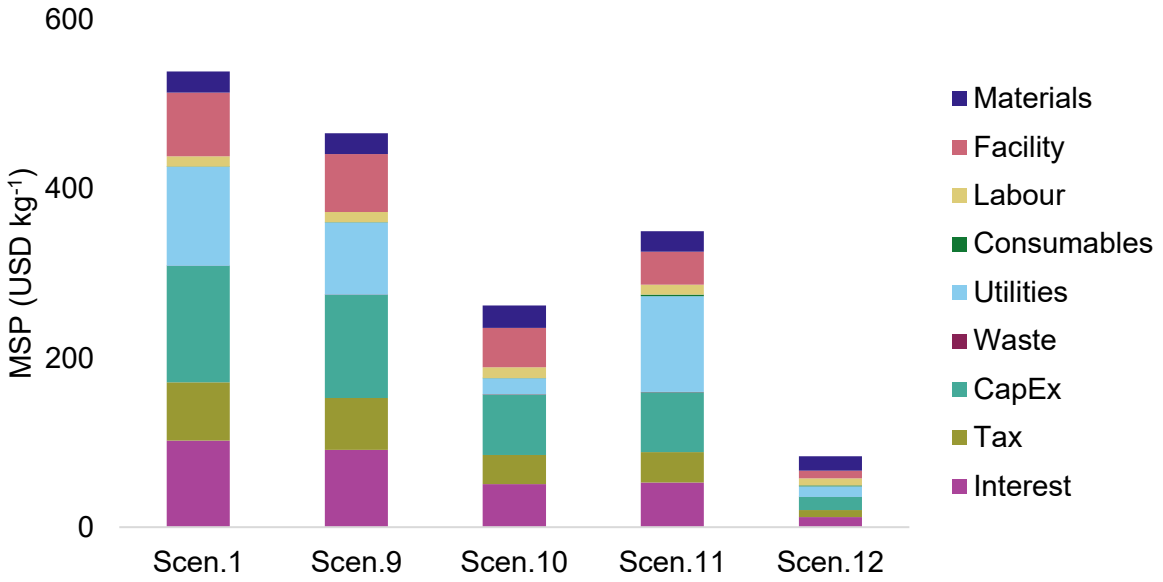


Figure 8-4 Effect of cultivation system on the minimum selling price (MSP, USD kg^{-1}) for the techno-economic assessment of an industrial extracellular polymeric substances (EPS) production process using the cyanobacterium *Calothrix brevissima*.Scenario 1 (baseline): indoor cultivation in tubular photobioreactors (PBRs) with artificial light. Scenario 9: outdoor cultivation in tubular PBRs with artificial and natural light. Scenario 10: outdoor cultivation in tubular PBRs with natural light. Scenario 11: indoor cultivation in bag PBRs with artificial light. Scenario 12: outdoor cultivation in bag PBRs with natural light. Costs are broken down into capital expenditure (CapEx), facility-dependent costs, labour-dependent costs, raw materials, utilities, consumables, waste, tax, and interest contributing to the minimum selling price (MSP, USD kg^{-1}).

The use of hanging bags instead of tubular PBRs was explored in scenario 11. Due to the much lower material cost for bag PBRs of 1,600,000 USD for support structure and 132,000 USD y^{-1} consumable costs for the bags, TCI reduced to 94,500,000 USD, representing a 46% reduction compared to the baseline scenario. Without tubular PBRs, the LED lights represented the most expensive equipment, costing 15,900,000

USD and making up 67% of MEC. Despite a considerable reduction in facility-dependent cost, they still made up 20% of total OpEx, as shown in Figure 8-5. Other costs remained the same, but the distribution changed accordingly. Utilities was still the largest contributor (60%) due to the high utility costs for lighting, heating/cooling and circulation of culture as described in section 8.3.1. Raw materials and labour made up 13% and 6%, respectively. Consumable costs were higher than in the baseline scenario due to the bag replacements, however, they only amounted to 179,000 USD y^{-1}, making up 1% of OpEx. This resulted in a MSP of 350 USD kg^{-1}, which was a 35% reduction compared to the baseline scenario.

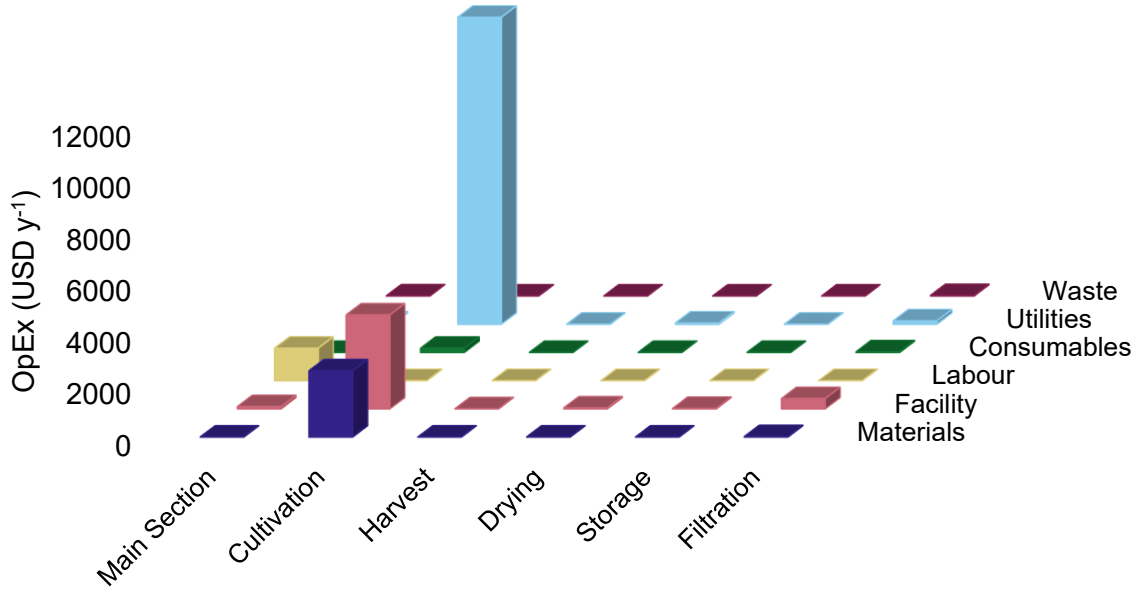


Figure 8-5 Itemised costs for indoor, phototrophic growth in bag photobioreactors (PBRs) with artificial lighting (scenario 11) for the techno-economic assessment of an industrial extracellular polymeric substances (EPS) production process using the cyanobacterium *Calothrix brevissima*.Costs are itemised by section (main section, cultivation, harvest, drying, storage, filtration) and cost type (facility-dependent costs, labour-dependent costs, raw materials, utilities, consumables, waste) contributing to the total operating expenditure (OpEx, USD y^{-1}).

A combination of the two scenarios with the most cost reduction was explored by investigating outdoor cultivation with natural light in PBR bags (scenario 12). This resulted in the strongest reduction of MSP of 84% to 84 USD kg^{-1}, which was close to

the target of 73 USD kg^{-1}. This reduction was a result of lower TCI and facility costs due to using bags and omitting LED lights, as well as lower utility costs from the lack of electricity for artificial lighting. TCI and OpEx of scenario 12 amounted to 29,700,000 USD and 7,250,000 USD y^{-1}, respectively, which represented the largest reduction compared to baseline with 83% and 72%, respectively. Within OpEx, facility-dependent costs and utilities were markedly reduced (83-89%) compared to the baseline scenario, amounting to 1,350,000 USD and 1,860,000 USD, respectively.

For the outdoor scenarios, it was assumed that the production titres from Exp. 2-9 can be achieved under outdoor conditions. However, this assumption is uncertain due to findings from Exp. 2-7, which showed that EPS production was negligible (<0.10 g L^{-1}, Figure 6-18*b*) when light duration and light intensity were below 16 hours and 25 µmol m^{-2} s^{-1}, respectively. Notably, the highest EPS production occurred under constant, high light conditions. Conversely, Exp. 2-8 indicated that EPS production also decreased at excessively high light irradiations. Despite the reduction in production costs and MSP for outdoor scenarios, the uncertainty surrounding EPS production remains a critical disadvantage. Strict control of temperature, light intensity, and light duration might be necessary to trigger EPS production effectively. Therefore, indoor cultivation using artificial lighting could be the only feasible option to ensure this level of control. To address this uncertainty, in-situ experiments at an outdoor facility would provide essential insights into the potential for EPS production under outdoor conditions. This could help clarify whether the production titres observed in Exp. 2-9 can be consistently replicated outdoors.

Table 8-7 Net present value (NPV) and profitability index (PI) of scenarios 9 to 12, which include different cultivation systems for industrial production of extracellular polymeric substances (EPS).An EPS minimum selling price (MSP) of 73 USD kg^{-1} and an interest rate of 8% were used. Scenario 1 (baseline): indoor cultivation in tubular photobioreactors (PBRs) with artificial light from *Calothrix brevissima*. Scenario 9: outdoor cultivation in tubular PBRs with artificial and natural light. Scenario 10: outdoor cultivation in tubular PBRs with natural light. Scenario 11: indoor cultivation in bag PBRs with artificial light. Scenario 12: outdoor cultivation in bag PBRs with natural light.

Scenario	**NPV**	**PI**
Scenario 9	-179,000,000	-0.1
Scenario 10	-80,800,000	0.2
Scenario 11	-130,000,000	-0.4
Scenario 12	-3,400,000	0.9

The NPV and PI of scenario 9 to 12 at an EPS selling price of 73 USD kg^{-1} are shown in Table 8-7. All different cultivation scenarios under photoautotrophic growth showed negative NPVs varying between -3,400,000 USD and -179,000,000 USD. This resulted in PIs between -0.4 and 0.9. This indicated that none of the cultivation scenarios was profitable, as all PIs were below 1.

8.4.4 Effect of Mixotrophic (Glucose) Growth Mode on MSP

As mentioned in section 6.9, the highest EPS titre was obtained in Exp. 2-6 under mixotrophic conditions (5 g L^{-1} glucose, 28 C and 150 µmol m^{-2} s^{-1}), resulting in 2.7 g L^{-1} EPS and 2.2 g L^{-1} biomass after 14 days. These parameters were applied to investigate the profitability of a mixotrophic scenario in indoor tubular PBRs (scenario 13), indoor bags (scenario 14) and outdoor bags with natural light (scenario 15).

Mixotrophic growth drastically decreased MSP in both, tubular PBRs and bag PBRs compared to phototrophic growth (Figure 8-6). Mixotrophic growth in tubular PBRs with artificial light (scenario 13), led to a 68% lower MSP of 172 USD kg^{-1} compared to the baseline scenario. This effect was even more pronounced using bag PBRs. The MSP of mixotrophic growth in bags with artificial light (scenario 14) was 80 USD kg^{-1}, which represented an 87% reduction from baseline scenario and an 80% reduction compared to phototrophic growth in bags (scenario 11). The most drastic decrease of MSP was

observed using a mixotrophic outdoor scenario with natural light in bag PBRs (scenario 15) resulting in an MSP of only 12 USD kg^{-1}. The main reason for the decreased MSP under mixotrophic conditions was the increased annual production of both EPS and biomass, impacting the revenues of the process. Despite the longer growth duration of 14 days, resulting in only 22 batches per year, the high EPS and biomass titre under mixotrophic conditions, resulted in annual production of 184,000 kg y^{-1} EPS and 173,000 biomass kg y^{-1}. Furthermore, the production costs were slightly lower compared to phototrophic growth, which will be explained further in the following paragraphs.

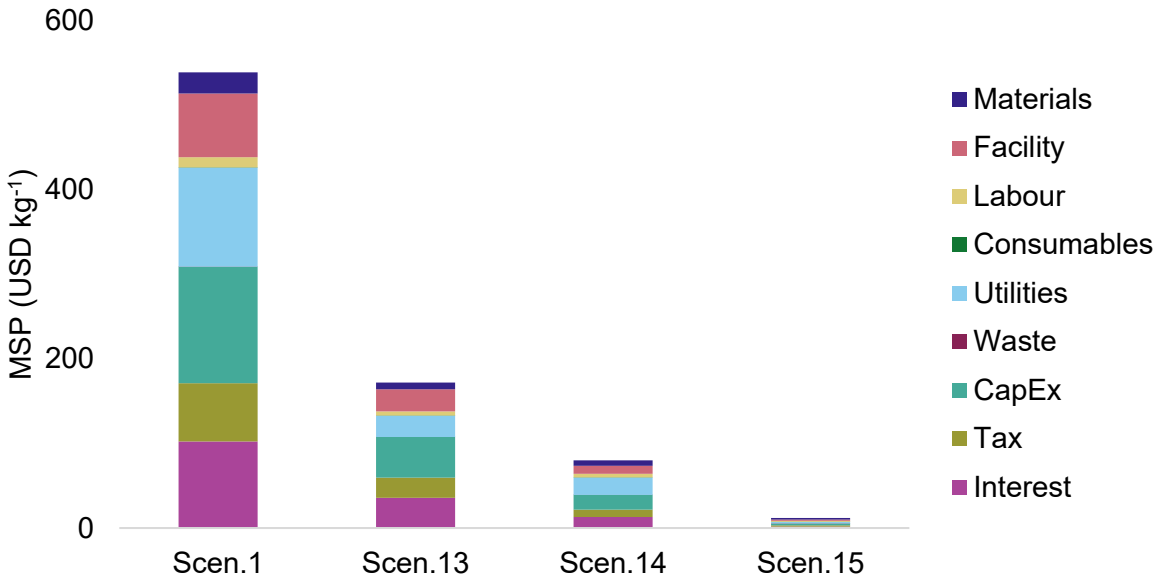


Figure 8-6 Effect of mixotrophic (glucose) growth mode on the minimum selling price (MSP, USD kg^{-1}) for the techno-economic assessment of an industrial extracellular polymeric substances (EPS) production process using the cyanobacterium *Calothrix brevissima*.Scenario 1 (baseline): indoor phototrophic cultivation in tubular photobioreactors (PBRs) with artificial light. Scenario 13: indoor, mixotrophic cultivation in tubular PBRs with artificial light. Scenario 14: indoor, mixotrophic cultivation in bag PBRs with artificial light. Scenario 15: outdoor, mixotrophic cultivation in bag PBRs with natural light. Costs are broken down into capital expenditure (CapEx), facility-dependent costs, labour-dependent costs, raw materials, utilities, consumables, waste, tax, and interest contributing to the MSP.

Mixotrophic growth in tubular PBRs (scenario 13) resulted in a reduction in TCI and OpEx (16,500,000 USD y^{-1}) compared to phototrophic growth in tubular PBRs (scenario 1) of 15% and 31%, respectively. The most impactful factor was replacement

of high intensity LEDs (up to 500 µmol m^{-2} s^{-1}) with cheaper, lower light intensity LEDs (up to 250 µmol m^{-2} s^{-1}), enabled by the lower light intensity used (150 µmol m^{-2} s^{-1}). These lights amounted to 9,810,000 USD, which was 56% lower than the high intensity LEDs in the baseline scenario. Furthermore, as mixotrophic growth only utilised air and glucose, the CO_2 supply unit was removed, which further reduced TCI, facility-dependent costs and utilities. This resulted in TCI, facility-dependent cost and utility cost of 150,000,000 USD, 6,660,000 USD and 6,490,000 USD, respectively. Despite the reduction, facility-dependent costs and utility costs were still the largest contributors to OpEx, making up 40% each, followed by raw materials (12%) and labour-dependent costs (8%). As shown in Figure 8-7, the cultivation section remained the most expensive section of the process, causing 87% of the total OpEx. Raw material costs of the mixotrophic scenario were 21% lower because the purchase cost of glucose (0.274 USD kg^{-1}) was 5-fold lower than for CO_2 (1.32 USD kg^{-1}) at a similar annual demand of about half a ton. Due to the lower light intensity used, electricity cost of the LEDs was halved, which resulted in a reduction of the total utility cost of the process by 46%. Additionally, due to the lower temperature (28°C), the process required more heating and less cooling compared to the baseline scenario. However, the overall cost for temperature control was similar due to the same price and similar total demand of heat transfer agents. This resulted in the distribution of utility costs of the PBR as 92% LEDs, 5% circulation pump, 3% hot water and 0.2% cooling water.

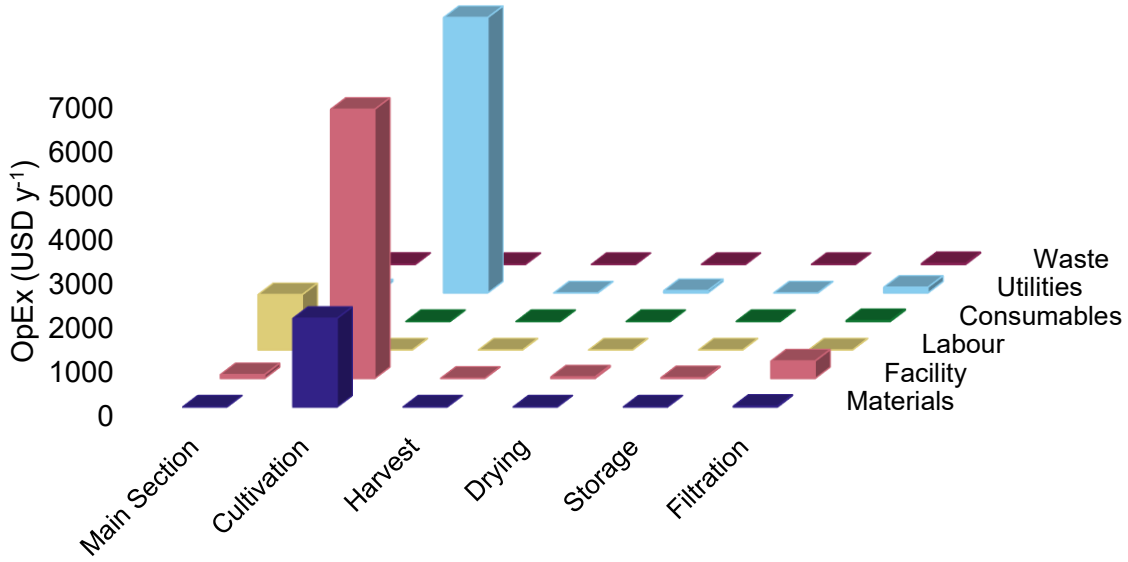


Figure 8-7 Itemised costs of indoor, mixotrophic growth in tubular photobioreactors (PBRs) with artificial lighting (scenario 13) for the techno-economic assessment of an industrial extracellular polymeric substances (EPS) production process using the cyanobacterium *Calothrix brevissima*.Costs are itemised by section (main section, cultivation, harvest, drying, storage, filtration) and cost type (facility-dependent costs, labour-dependent costs, raw materials, utilities, consumables, waste) contributing to the total operating expenditure (OpEx, USD y^{-1}).

In mixotrophic scenario 14, where tubular PBRs were replaced with bag PBRs, the effects of cheaper LED lights, lower electricity costs and cheaper carbon source costs was combined with lower material cost of the bag PBRs. As shown in Figure 8-8, the OpEx of the mixotrophic bag scenario (scenario 14) were mainly caused by utilities (50%) and facility-dependent costs (23%). Raw material, labour-dependent cost and consumables contributed 16%, 10% and 1%, respectively. Waste treatment / disposal costs were negligible (≤1%). It became evident that the cultivation stage was the costliest one, being responsible for 84% of total OpEx, whereas main section (labour), filtration, drying, storage and harvest, contributed 11%, 4%, 1%, 0.1% and 0.0%. Specifically, utilities and facility-dependent costs of the cultivation section amounted to 6,260,000 USD y^{-1} and 2,500,000 USD y^{-1}, respectively.

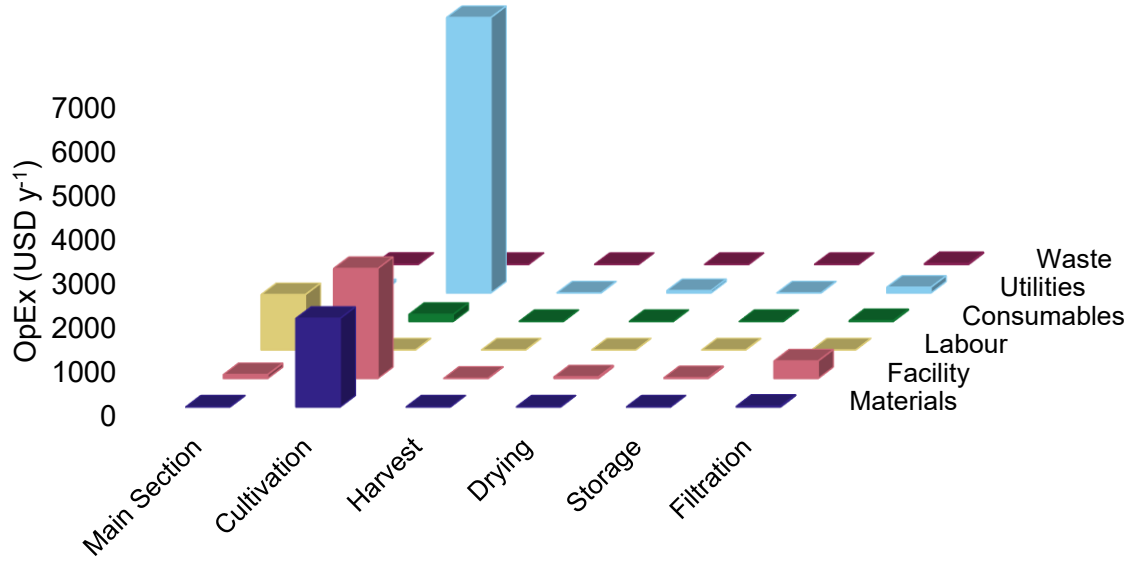


Figure 8-8 Itemised costs of indoor, mixotrophic growth in bag photobioreactors (PBRs) with artificial lighting (scenario 14) for the techno-economic assessment of an industrial extracellular polymeric substances (EPS) production process using the cyanobacterium *Calothrix brevissima*.Costs are itemised by section (main section, cultivation, harvest, drying, storage, filtration) and cost type (facility-dependent costs, labour-dependent costs, raw materials, utilities, consumables, waste) contributing to the total operating expenditure (OpEx, USD y^{-1}).

Despite reduction, the MSP of mixotrophic growth in indoor bags (scenario 14, 80 USD kg^{-1}) was still too high compared to the target of 73 USD kg^{-1}. This indicated that either lower production costs or higher revenues, through higher annual production or higher selling prices, were required to produce a profitable process.

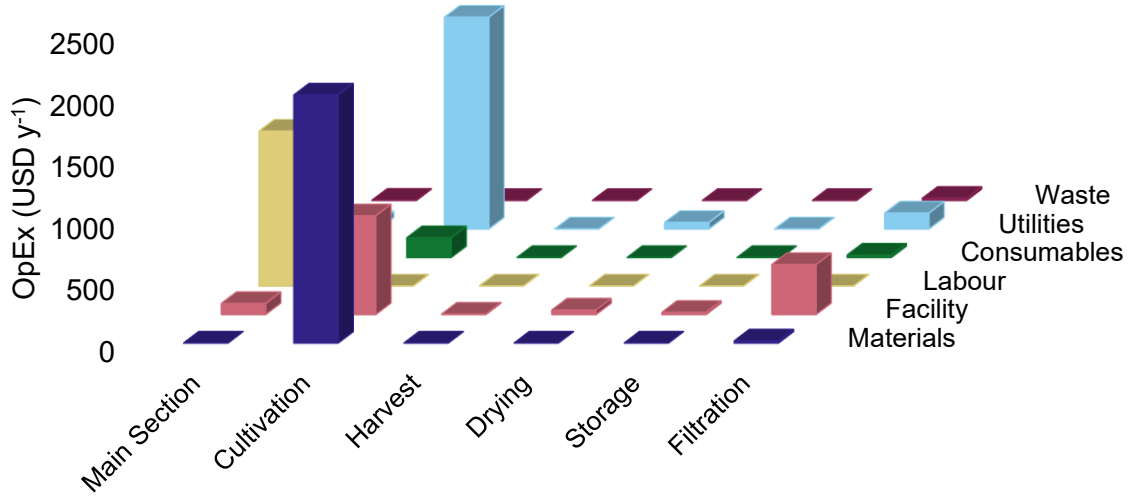


Figure 8-9 Itemised costs of outdoor, mixotrophic growth in bag photobioreactors (PBRs) with natural light (scenario 15) for the techno-economic assessment of an industrial extracellular polymeric substances (EPS) production process using the cyanobacterium *Calothrix brevissima*.Costs are itemised by section (main section, cultivation, harvest, drying, storage, filtration) and cost type (facility-dependent costs, labour-dependent costs, raw materials, utilities, consumables, waste) contributing to the total operating expenditure (OpEx, USD y^{-1}).

To reduce production costs further, a mixotrophic outdoor scenario with natural light in bag PBRs was explored (scenario 15). Due to the absence of LED lights, TCI, OpEx, facility-dependent costs and utility costs were further reduced to 29,700,000 USD, 6,790,000 USD, 1,350,000 USD y^{-1} and 1,950,000 USD y^{-1}, respectively. This is shown in Figure 8-9. Compared to indoor cultivation in bags with artificial lights (scenario 14), costs for outdoor cultivation in bags with natural lights (scenario 15) were nearly halved. This drastically reduced the MSP to 12 USD kg^{-1}.

Table 8-8 Net present value (NPV) and profitability index (PI) of scenarios 13 to 15, which include mixotrophic cultivation for industrial production of extracellular polymeric substances (EPS).An EPS minimum selling price (MSP) of 73 USD kg^{-1} and an interest rate of 8% were used. Scenario 1 (baseline): indoor phototrophic cultivation in tubular photobioreactors (PBRs) with artificial light from *Calothrix brevissima*. Scenario 13: indoor, mixotrophic cultivation in tubular PBRs with artificial light. Scenario 14: indoor, mixotrophic cultivation in bag PBRs with artificial light. Scenario 15: outdoor, mixotrophic cultivation in bag PBRs with natural light.

Scenario	**NPV**	**PI**
Scenario 13	-80,200,000	0.5
Scenario 14	-4,260,000	0.9
Scenario 15	42,600,000	2.4

The NPV and PI of the mixotrophic scenarios 13, 14 and 15 at an EPS selling price of 73 USD kg^{-1} are shown in Table 8-8. Indoor mixotrophic growth in tubular PBRs (scenario 13) or bag PBRs (scenario 14) with artificial lights was not profitable, resulting in negative NPVs of -80,200,000 and -4,260,000U SD, respectively, and PIs of 0.5 and 0.9, respectively. Outdoor mixotrophic conditions in bag PBRs with natural light combined production cost reduction with high revenues, resulting in a positive NPV of 42,600,000 USD and a PI of 2.4.

The cash flow of the only profitable scenario, scenario 15, at a target EPS selling price of 73 USD kg^{-1} is shown in Table 8-9. During operational years, the revenues amounted to 23 MM USD, which compensated for the OpEx of 9 MM USD, resulting in a gross profit of 14 MM USD. Considering 3 MM USD depreciation and 6 MM USD taxes, the net profit and NCF amounted to 11 MM USD annually. This resulted in DCFs between 3 and 8 MM USD annually, corresponding to an NPV of 43 MM USD.

Table 8-9 Cash flow (in million USD), net present value (NPV), and profitability index (PI) of scenario 15 for industrial production of extracellular polymeric substances (EPS).Scenario 15 comprises outdoor mixotrophic growth of cyanobacterium *Calothrix brevissima* in bag photobioreactors, with filtration for EPS downstream processing and use of the EPS as bio-emulsifier. An EPS minimum selling price (MSP) of 73 USD kg^{-1} and an interest rate of 8% were used. Abbreviations: CapEx, capital expenditure; Rev, revenues; OpEx, operating expenditure; GP, gross profit; Dep, depreciation; TI, taxable income; Tax, taxes; NP, net profit; NCF, net cash flow; DCF, discounted cash flow.

Year	CapEx	Rev	OpEx	GP	Dep	TI	Tax	NP	NCF	DCF
1	-8	0	0	0	0	0	0	0	-8	-8
2	-11	0	0	0	0	0	0	0	-11	-10
3	-8	4	6	-2	3	0	0	1	-7	-6
4	0	23	9	14	3	14	6	11	11	8
5	0	23	9	14	3	14	6	11	11	8
6	0	23	9	14	3	14	6	11	11	7
7	0	23	9	14	3	14	6	11	11	7
8	0	23	9	14	3	14	6	11	11	6
9	0	23	9	14	3	14	6	11	11	6
10	0	23	9	14	3	14	6	11	11	5
11	0	23	9	14	3	14	6	11	11	5
12	0	23	9	14	3	14	6	11	11	4
13	0	23	7	17	0	17	7	10	10	4
14	0	23	7	17	0	17	7	10	10	3
15	1	23	7	17	0	17	7	10	11	4
									NPV	43
									PI	2.4

All in all, it was revealed that at current production titres, the only profitable production scenario of a bioemulsifier with *C. brevissima* was outdoor cultivation without artificial lights in bag PBRs under mixotrophic conditions. However, it is uncertain whether the mixotrophic shake flask titres obtained with constant illumination in the laboratory, can be reproduced in outdoor PBR bags with natural light.

8.4.5 Alternative Species Scenario: *Nostoc foliaceum*

The effect of using an alternative species, *Nostoc foliaceum*, in mixotrophic mode can be seen in Figure 8-10. Similar to using *C. brevissima*, the MSP of *N. foliaceum* with tubular PBR was very high (470 USD kg^{-1}), which reduced drastically to 118 USD kg^{-1} when bag PBRs were used. Using *N. foliaceum* resulted in similar production costs compared to *C. brevissima.* Mixotrophic growth of Nostoc in tubular PBRs (scenario 16) led to similar TCI (149,000,000 USD) and OpEx (17,000,000 USD) as scenario 13. Similarly, the TCI and OpEx in PBR bags (scenario 17) were 68,500,000 USD and 13,600,000 USD, respectively, which was similar to scenario 14.

Main differences were the utility cost, which were 8% higher with *N. foliaceum*. This was due to the higher light intensity of 164 µmol m^{-2} s^{-1}, increasing the utility costs of the PBR by 9% compared to that of *C. brevissima* under mixotrophic growth (scenario 13). Due to the higher production costs, the MSP using *N. foliaceum* was higher than *C. brevissima* under mixotrophic conditions, despite *N. foliaceum* producing a total of 48,000 kg y^{-1} EPS and 344,000 kg y^{-1} DCW, which is 10% higher than the sum of products from *C. brevissima*.

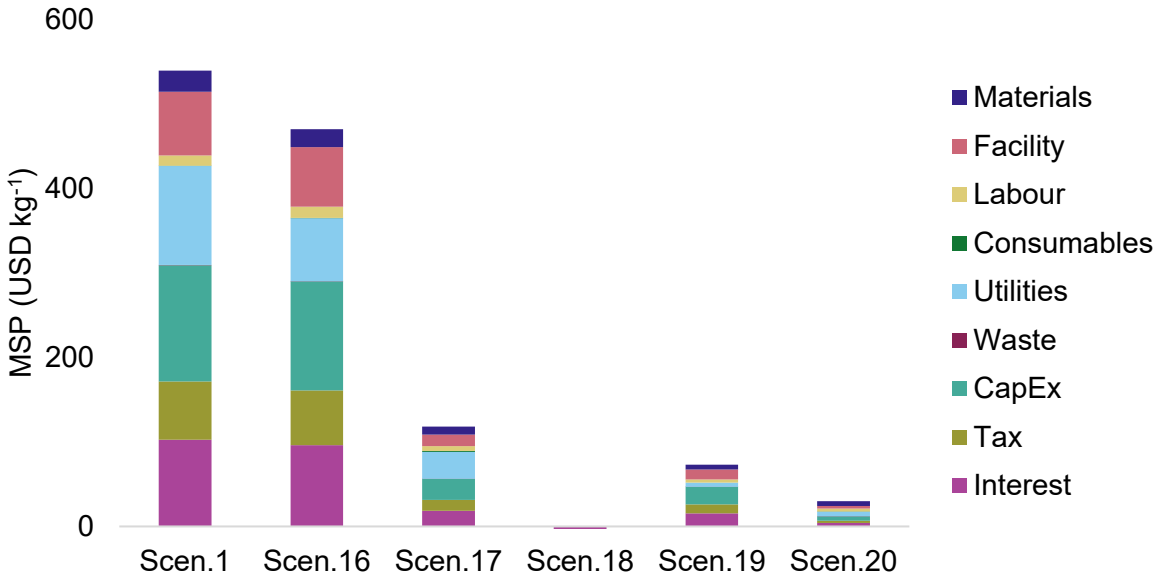


Figure 8-10 Minimum selling price (MSP, USD kg^{-1}) of scenarios using alternative cyanobacterial species (*Nostoc foliaceum*) for extracellular polymeric substances (EPS) and biomass production.Scenario 16: indoor cultivation in tubular photobioreactors (PBRs) with LED lights. Scenario 17: indoor cultivation in bag PBRs with LED lights. Scenario 18: outdoor cultivation in bag PBRs with natural light. MSP of scenario 18 (-155 USD kg^{-1}) is not displayed as the minimum of the y-axis was set to zero. For comparison, MSP of scenarios producing only biomass are shown: scenario 19 in tubular PBRs and scenario 20 in bag PBRs. Costs are broken down into capital expenditure (CapEx), facility-dependent costs, labour-dependent costs, raw materials, utilities, consumables, waste, tax, and interest contributing to the MSP.

However, applying the lowest production cost scenario, outdoor cultivation with natural light in bag PBRs (scenario 18), resulted in the lowest TCI and OpEx of 29,800,000 USD and 6,810,000 USD y^{-1}. The revenues of the biomass alone exceeded OpEx by far, amounting to 19,400,000 USD y^{-1}. This resulted in a negative MSP for EPS (-155 USD kg^{-1}, negative axis not displayed in Figure 8-10), indicating that the process was profitable from biomass alone. The NPV and PI of scenario 18 at an EPS selling price of 73 USD kg^{-1} is shown in Table 8-10. Scenario 18 generated a NPV of 41,000,000, resulting in a PI of 2.4, indicating a profitable scenario. The obtained NPV and PI values were similar to scenarios with *C. brevissima*. The same limitation with *C. brevissima* also applies to *N. foliaceum*. As described in section 6.10.1, it is unclear whether EPS production can be triggered without strict temperature and light intensity control. Additionally, according to the lab results in section 6.7, the EPS product of *N. foliaceum* showed worse performance than *C. brevissima*, with a 2.5-fold higher concentration being needed for the same emulsifying activity. This could mean a higher amount of product is required for the same effect, lowering the value of EPS from *N. foliaceum* compared to EPS from *C. brevissima.* This was not considered when applying the selling price for EPS from *N. foliaceum*.

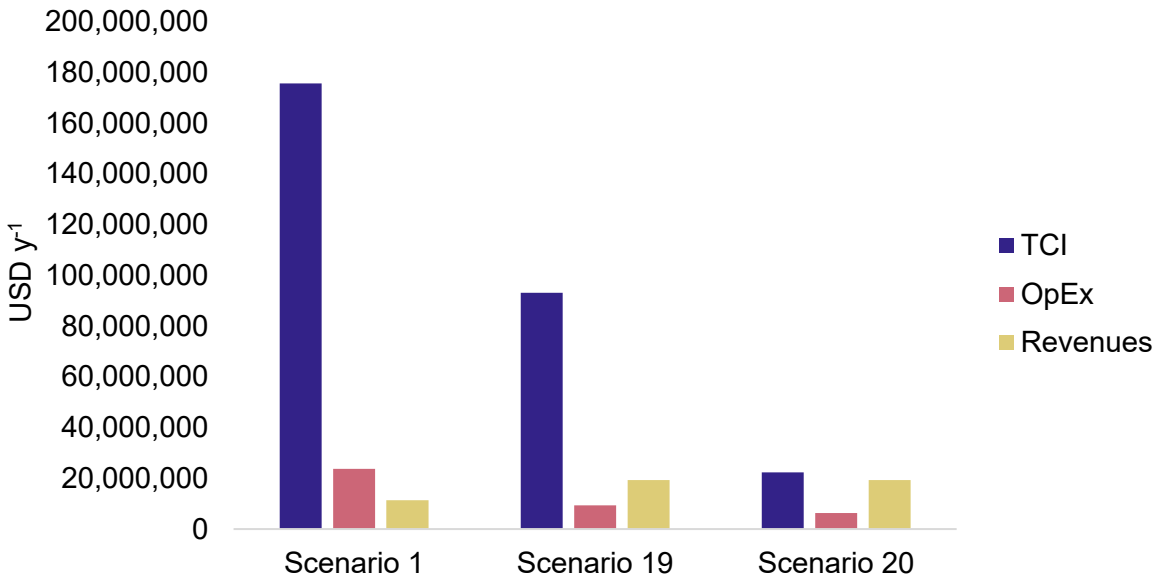


Figure 8-11 Total capital investment (TCI), operational expenditure (OpEx), and revenues of single-product (biomass) scenarios using *Nostoc foliaceum* compared to the baseline scenario.Scenario 19: single-product production of biomass in outdoor tubular photobioreactors (PBRs). Scenario 20: single-product production of biomass in outdoor bag PBRs. Costs and revenues are broken down into capital expenditure (CapEx), facility-dependent costs, labour-dependent costs, raw materials, utilities, consumables, waste, tax, and interest contributing to the total MSP (USD kg^{-1}).

Since *N. foliaceum* produced more biomass than EPS and it was unknown whether outdoor natural light production would trigger EPS, scenarios 19 and 20, producing biomass as a single product in tubular PBRs and bag PBRs, respectively, was explored. This resulted in MSPs for biomass of 73 and 30 USD kg^{-1} for tubular PBR and bag PBR scenario, respectively. TCI, facility-dependent and utility costs were lower due to less equipment being needed. However, also revenues were lower due to absence of revenues from EPS. Without EPS as product, purification equipment such as the filtration systems and flush tanks were omitted. Furthermore, the EPS storage tank was not required anymore, and consumables costs were reduced due to absence of membranes. Lastly, waste costs decreased due to reduced wastewater generation, as the process did not involve membranes requiring flushing or CIP. This also reduced raw materials costs, since less NaClO was required. As shown in Figure 8-11, this resulted in TCI, OpEx and revenues of the tubular PBR case of 93,100,000 USD, 9,340,000 USD y^{-1} and 19,300,000 USD y^{-1}, respectively. In the case of the bag

PBR case, TCI, OpEx and revenues amounted to 22,400,000 USD, 6,260,000 USD y^{-1} and 19,300,000 USD y^{-1}, respectively.

The NPV and PI values of scenarios 16 to 20 at an EPS selling price of 73 USD kg^{-1} are shown in Table 8-10. Similar to the results with *C. brevissima*, EPS production with *N. foliaceum* was only profitable in outdoor bag cultivation (scenario 18), resulting in NPV and PI of 41,000,000 USD and 2.4, respectively. Regarding single-product (biomass) production, use of tubular PBRs (scenario 19) was not profitable (PI of 0.8). However, single-product production in bag PBRs (scenario 20) was profitable with NPV and PI of 34,200,000 and 2.5, respectively. PIs of scenarios 20 and 18 were similar, suggesting that the additional revenues from generating EPS as product compensated for the added costs of EPS purification and other related expenses. However, the PI of scenario 20 was slightly higher than that of scenario 18, possibly indicating that producing only biomass with *N. foliaceum* could represent a more profitable route.

Table 8-10 Net present value (NPV) and profitability index (PI) of scenarios 16 to 20 for industrial production of extracellular polymeric substances (EPS) with *Nostoc foliaceum*.An EPS minimum selling price (MSP) of 73 USD kg^{-1} and an interest rate of 8% were used. Scenario 16: indoor cultivation in tubular photobioreactors (PBRs) with LED lights. Scenario 17: indoor cultivation in bag PBRs with LED lights. Scenario 18: outdoor cultivation in bag PBRs with natural light. Scenario 19: production of biomass as sole product, using outdoor cultivation in tubular PBRs with natural light. Scenario 20: production of biomass as sole product, using outdoor cultivation in bag PBRs with natural light.

Scenario	**NPV**	**PI**
Scenario 16	-85,700,000	0.4
Scenario 17	-7,900,000	0.9
Scenario 18	41,000,000	2.4
Scenario 19	-21,300,000	0.8
Scenario 20	34,200,000	2.5

All in all, it was revealed that using an alternative cyanobacterial species, *N. foliaceum,* in outdoor mixotrophic cultivation, led to similar economic performance than *C. brevissima*. However, biomass as sole product might represent a more profitable scenario using *N. foliaceum*, considering the lower EPS titre and worse bioemulsifier

performance. *N. foliaceum* biomass could potentially be even more valuable than assumed in this PhD thesis, as several *Nostoc* sp. are edible and contain bioactive compounds with antioxidant, anti-inflammatory or antitumor properties [333]. In 2013, the price of *Nostoc sphaeroides* biomass was as high as 3000 ¥ kg^{-1}, which corresponds to 521 USD kg^{-1} after currency conversion and HCIP adjustment [366]. Similarly to *C. brevissima*, it is uncertain whether the high biomass and EPS titres can be achieved using outdoor cultivation with natural light. Since *C. brevissima* was observed to produce biomass over larger culture condition ranges than EPS, it could be more likely that *N. foliaceum* will produce more consistent biomass titres than EPS titres using natural light. This is based on the assumption that *N. foliaceum* shows a similar response pattern. In-situ experiments monitoring EPS and DCW production under natural light conditions could provide further insight into the profitability of single-product compared to two-product production. One disadvantage of scenario 19 and 20 was uncertainty whether the supernatant was suitable for reuse for cultivation, or if it required a purification step such as MF to remove residual cells, debris or other impurities.

8.4.6 Alternative Product Scenario: Cosmeceutical Product

Production of an EPS-derived cosmeceutical from *C. brevissima* was explored as an alternative product scenario (scenario 21). Cosmeceuticals are cosmetic products that exhibit pharmaceutical therapeutic benefits, but not biological therapeutic benefits, and have become one of the fastest-growing sectors in the area of personal care cosmetics [367]. Based on the UV-protective and antioxidant properties of EPS from *C. brevissima*, they could be used as a day cream, a face cream with natural sunscreen. The combination of antioxidant and UV-protective properties is particularly useful as it protects from DNA mutation in skin cells caused by UVB, as well as ROS production caused by UVA which can cause mutations indirectly [147]. A consumer study found that 50% of participants prefer natural skincare products, 60% are willing to pay more for bio-based options, and most are aware of the harmful effects of synthetic ingredients on marine life [148]. There is already one algae-based commercial sunscreen product on the market, the UV-screening substance Helioguard-365 by Swiss company Mibelle AG Biotechnology. It contains the MAAs Porphyra-334 and shinorine and is sourced from red algae *Porphyra umbilicalis* [141, 368]. It is

commercially available as UV-protective day cream (SPF 25, 50mL) by the brand Ekseption for 44 GBP [310]. This corresponds to a selling price of 1,130 USD L^{-1}.

The highest UV absorbance obtained with *C. brevissima* (0.385 g L^{-1} EPS) was similar to 2000-fold diluted SPF30 (Appendix Figure 12-9), potentially indicating that EPS at a 2000-fold higher concentration (770 g EPS L^{-1}) could potentially offer similar protection level as SPF30. Based on the selling price of the solution of 1,130 USD L^{-1}, this would result in a selling price of 1,460 USD kg^{-1} EPS, which would generously compensate for the production costs. Scenario 21 was designed based on scenario 15, with the modification of replacing the spray dryer with a freeze dryer to preserve the bioactive properties [207].

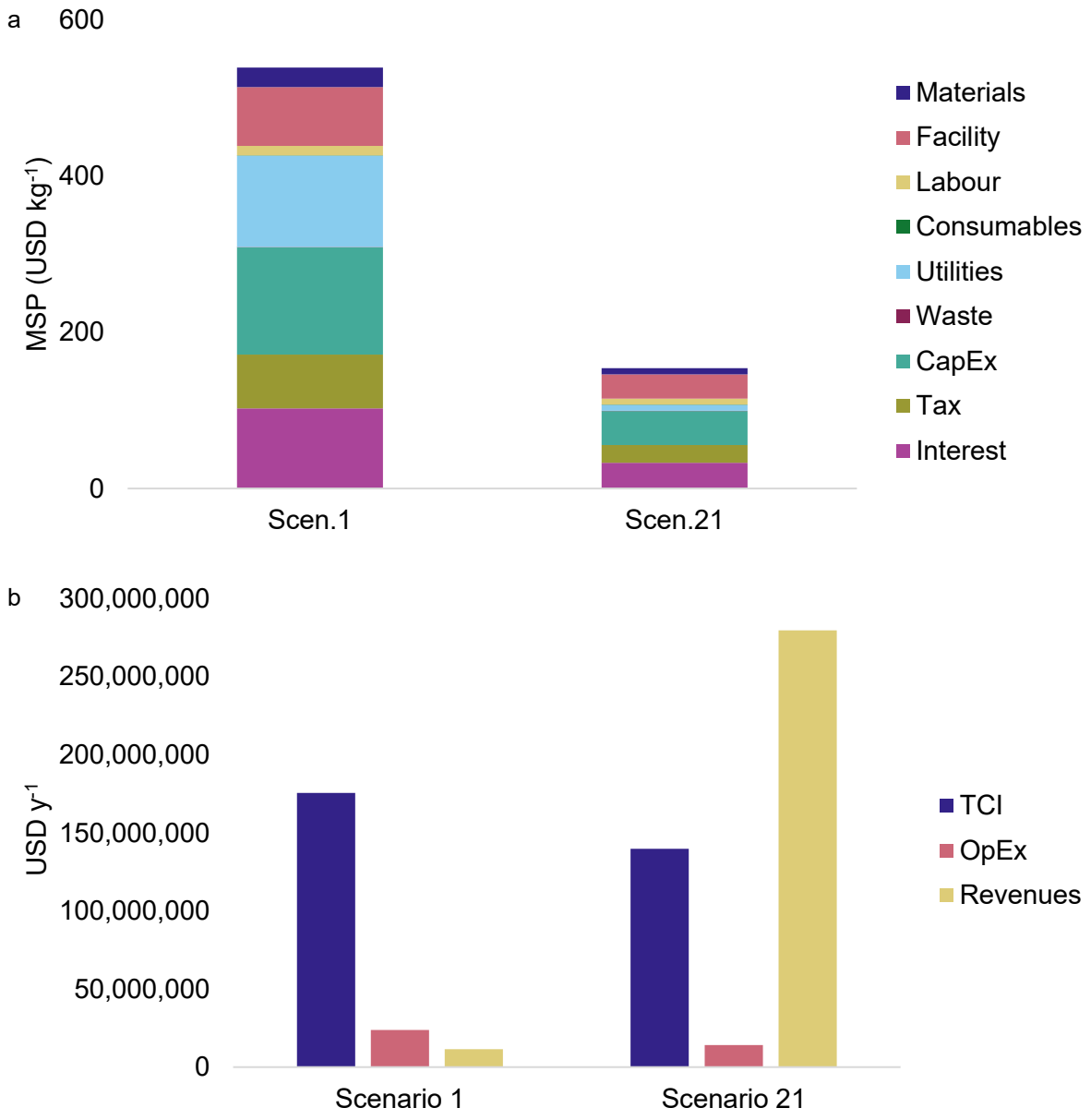


Figure 8-12 Comparison of cosmeceutical and bioemulsifier products for the techno-economic assessment of an industrial extracellular polymeric substances (EPS) production process using the cyanobacterium *Calothrix brevissima*.Scenario 21: production of a cosmeceutical product. Baseline scenario: production of a bioemulsifier. (a) Minimum selling price (MSP, USD kg^{-1}) of the cosmeceutical (scenario 21) compared to the bioemulsifier (baseline scenario). (b) Total capital investment (TCI), operational expenditure (OpEx), and revenues for bioemulsifier production (selling price 73 USD kg^{-1}) compared to cosmeceutical production (selling price 1,460 USD kg^{-1}). Costs are broken down into capital expenditure (CapEx), facility-dependent costs, labour-dependent costs, raw materials, utilities, consumables, waste, tax, and interest contributing to the MSP.

Production of a cosmeceutical (scenario 21) resulted in an MSP of 154 USD kg^{-1}, which was nearly 4-fold lower than the baseline scenario but higher than scenario 15 due to the use of a more expensive freeze dryer. TCI and OpEx amounted to 140,000,000 USD and 14,100,000 USD y^{-1} respectively (Figure 8-12*b*). Applying the selling price of 1460 USD kg^{-1}, revenues amounted to 280,000,000 USD, which was 24-fold higher than baseline scenario. The cash flow of scenario 21 is shown in Table 8-11. Due to the high EPS selling price of 1460 USD kg^{-1}, high revenues of 280 MM USD y^{-1} were generated during operational years. This resulted in net profits and NCF of about 166 MM USD annually. This corresponded to DCF of 52 to 122 MM USD per year, leading to a NPV of 892 MM USD. The PI (7.4) when producing a cosmeceutical (scenario 21) was nearly three times higher than the profitable bioemulsifier production scenario (scenario 15, PI=2.4). This indicated that a cosmeceutical represented a 3-fold higher profitable product than a bio-emulsifier or biomass.

Table 8-11 Cash flow (in million USD), net present value, and profitability index of scenario 21 for industrial production of extracellular polymeric substances (EPS).Scenario 21 comprises outdoor mixotrophic growth of cyanobacterium *Calothrix brevissima* in bag photobioreactors, with filtration for EPS downstream processing and use of the EPS as cosmeceutical. An EPS minimum selling price (MSP) of 1,460 USD kg^{-1} and an interest rate of 8% were applied. Abbreviations: CapEx, capital expenditure; Rev, revenues; OpEx, operating expenditure; GP, gross profit; Dep, depreciation; TI, taxable income; Tax, taxes; NP, net profit; NCF, net cash flow; DCF, discounted cash flow.

Year	CapEx	Rev	OpEx	GP	Dep	TI	Tax	NP	NCF	DCF
1	-40	0	0	0	0	0	0	0	-40	-40
2	-53	0	0	0	0	0	0	0	-53	-46
3	-40	47	23	24	14	24	9	28	-12	-9
4	0	280	27	253	14	253	101	166	166	122
5	0	280	27	253	14	253	101	166	166	113
6	0	280	27	253	14	253	101	166	166	104
7	0	280	27	253	14	253	101	166	166	97
8	0	280	27	253	14	253	101	166	166	90
9	0	280	27	253	14	253	101	166	166	83
10	0	280	27	253	14	253	101	166	166	77
11	0	280	27	253	14	253	101	166	166	71
12	0	280	27	253	14	253	101	166	166	66
13	0	280	14	266	0	266	106	159	159	59
14	0	280	14	266	0	266	106	159	159	54
15	7	280	14	266	0	266	106	159	166	52
									NPV	892
									PI	7.4

However, further tests such as characterisation of the UV-protective compounds (e.g. MAA), efficacy and toxicity tests would be necessary before EPS can be considered as a cosmeceutical, as described in section 5.5.5. Also, regulatory approval would be required before the EPS could be marketed as a cosmetic ingredient. While the EPS studied here are novel and not yet listed in the INCI database, similar ingredients are already used in cosmetics. Biomass and extracts from the cyanobacterium *A. platensis*, and oligosaccharides from algae such as *Gelidium* sp. are INCI-listed,

showing precedent for algae-derived compounds in skincare applications [369, 370]. Additionally, the suitability of the proposed DSP process would have to be tested, to ensure the UV-protective compounds are preserved and do not get washed out or degraded. Furthermore, optimisation must be repeated to maximise UV-protective compounds in EPS, reducing EPS concentration in the product to avoid excessive viscosity and ensure complete dissolution, as maximum solubility remains unknown. Alternatively, bioactivity of EPS can be enhanced by post-production modifications as described in section 2.2.3.3. However, these methods have drawbacks, including the use of toxic solvents, harsh conditions (e.g., strong acids for phosphorylation) that risk degrading or hydrolysing the polysaccharide, and low success rates under milder conditions [112]. Besides, this would require an additional processing step, necessitating a modification of the process design. These two points emphasize the advantage of adapting growth conditions to tailor the desired EPS, rather than post-production modifications. One promising observation that was made during the PhD project was that the supernatant showed high absorbance in the UV spectrum in both, shake flasks and PBR experiments (data not shown). Even liquid cultures left on a south-facing window sill with natural light and without agitation showed very high UV absorbance of the supernatant, similar to 1000-fold diluted SPF30 (data not shown). This could possibly indicate that, while it might be challenging to trigger EPS production in industrial-scale PBRs, enabling production of UV-protective compounds might be more feasible. If UV-protective compounds are produced in natural day/light cycle, this could also make the assumed titres for outdoor production without artificial lighting more attainable. However, whether this translates to industrial scale remains to be tested. In particular, the influence of PBR material on the production of UV-protective compounds warrants investigation. The PBR in this study was modelled as plastic, reflecting the real-world facility in Almería but plastics block most UV radiation [217, 288]. In contrast, glass allows transmission of UVA, which may support greater production of UV-responsive metabolites, though it comes with higher costs and structural demands [216, 217]. These trade-offs must be evaluated in future, more in-depth TEAs.

8.5 Sensitivity Analysis Results

A sensitivity analysis of four parameters, EPS titre (kg m^{-3}), scale (culture volume in m^3), purchase price of PBR with lights (USD per module) and electricity cost (USD

kWh^{-1}) was performed. As shown in Figure 8-13, all four tested parameters influenced the MSP. Increasing EPS titre and scale reduced MSP, whereas the purchase price of PBR with lights and the cost of electricity increased MSP. The most influential factor was EPS titre, which resulted in MSPs varying from values 2,750 USD kg^{-1} to 39 USD kg^{-1} when titre was set between 0.245 and 19.1 kg m^{-3} [55, 204]. The relationship between EPS titre and MSP followed inverse power-law distribution, with the effect being most pronounced at lower EPS titres (0.245 to 2.52 g L^{-1}), after which the graph flattens out asymptotically to the x-axis. The positive effect of the EPS titre on MSP was mostly caused by increased revenues. To a lesser extent, the higher CO_2 demand increased TCI and OpEx related to the CO_2 material cost and the CO_2 supply unit.

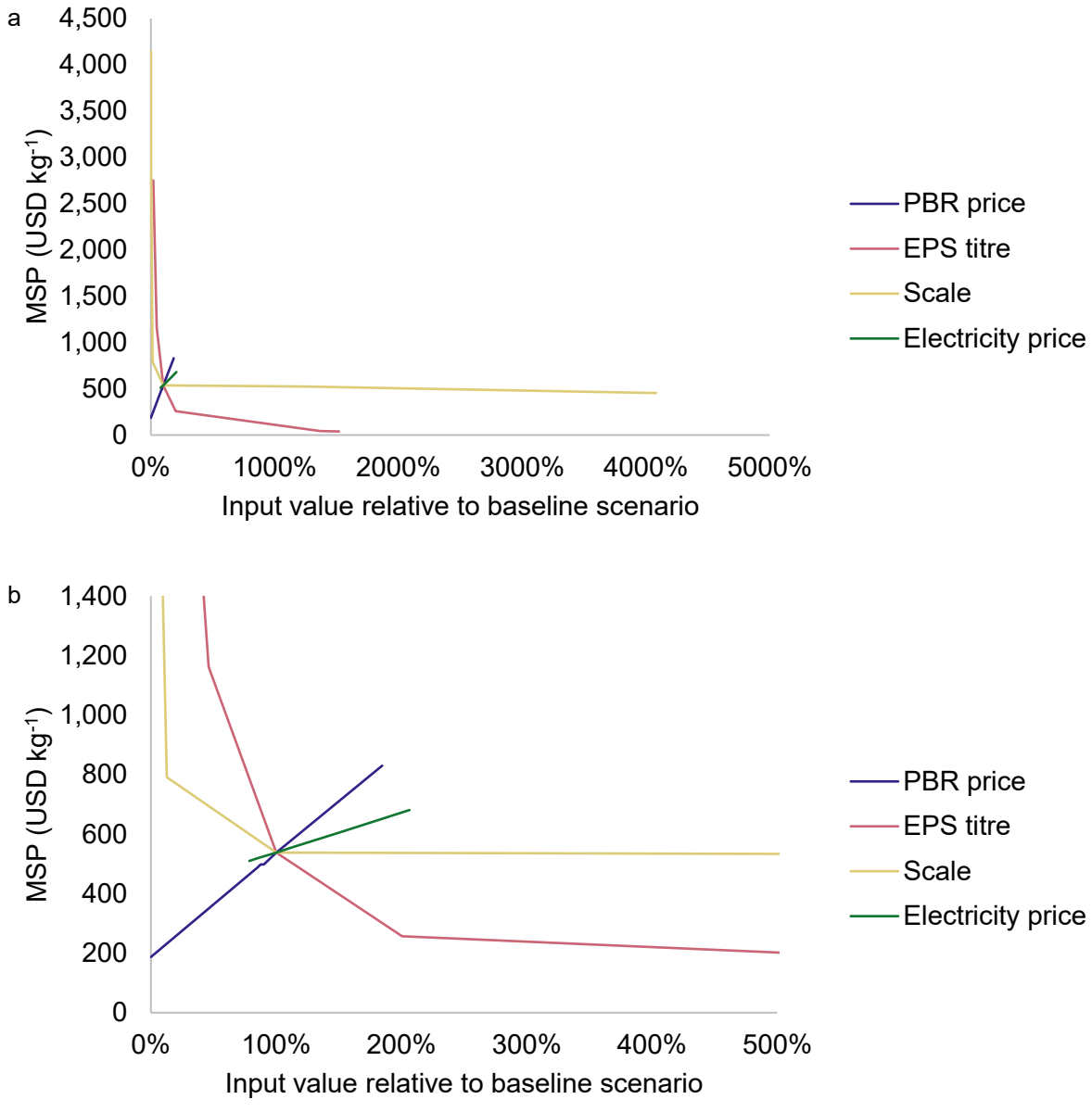


Figure 8-13 Sensitivity analysis of the baseline scenario for phototrophic growth in tubular photobioreactors (PBRs) with artificial lighting, for the techno-economic assessment of an industrial extracellular polymeric substances (EPS) production process using the cyanobacterium *Calothrix brevissima*.Parameters analysed include PBR purchase price (USD $unit^{-1}$), electricity price (USD kWh^{-1}), EPS titre (kg m^{-3}), and scale (PBR volume in m^3). (a) Minimum selling price (MSP, USD kg^{-1}) as a function of relative changes in PBR price, EPS titre, scale, and electricity price compared to the baseline scenario (%). (b) Zoomed view of the graph for enhanced visibility.

The effect of scale on MSP followed a similar trend, following inverse power-law distribution. However, the effect was less pronounced, with MSPs only varying from 2,939 USD kg^{-1} to 454 USD kg^{-1} when varying the scale from 30 to 122,000 m^3 [204, 259]. This effect was the most pronounced when increasing the scale from 30 to 3,000 m^3, which resulted in an 87% decrease in MSP, whereas further increase from 3,000 to 38,000 m^3 only reduced the MSP by 2%. After this point, the graph flattens out asymptotically to the x-axis. The drastic decrease of MSP in the range of 30 to 3,000 m^3 was largely caused by TCI not increasing at the same rate as the scale. Despite the scale increasing 100-fold from 30 to 3,000 m^3, TCI only increased by a factor of 22. This was due to the fact that the relationship between equipment price and capacity was not linear. The price increase of an equipment with size follows the power law (Equation 4-21), resulting in a lower price per capacity with increasing scale [291]. This is known as "*The Economies of Scale*" [371, 372]. For example, the purchase prices of NaClO tank and spray dryer increased 7-fold and 1.3-fold, despite the scale increasing 100-fold (from 30 m^3 to 3,000 m^3). Even more illustrative was the price of the centrifuge which remained at 404,000 USD for all PBR volumes, since even at the largest scale, the capacity of 9,000 m^3 h^{-1} was not reached. As facility-dependent costs were proportional to TCI, the increase of facility-dependent costs followed a similar trend. However, the most expensive equipment, namely PBRs, were designed with a scaling factor of 1 (section 4.4.3.2) due to their modular nature, meaning their price was proportional to the scale. When utilising a scaling factor (e.g. 0.8), the effect of scale could be even more pronounced [239]. Another influential factor were the labour-dependent costs (operating and laboratory), whereas other costs such as raw materials and waste treatment scaled nearly linear. Based on the design described in section 4.4.3.4, one operator was required per 1500 m^3 culture volume, with a

minimum of two operators present at all times. Due to this minimum requirement, labour-dependent costs were fixed at 1,090,000 USD y^{-1} for operators and 164,000 USD y^{-1} for laboratory, until a culture volume of 3000 m^3, after which they increased stepwise with each additional 1500 m^3. This resulted in labour making up 45% of total OpEx in smaller scale (30 m^3), which reduced to 19% (380 m^3) and 4% (3,000 to 122,000 m^3) on larger scale. This was comparable to literature, where labour-dependent costs reduced from 39% to 18% and 4% of OpEx, when scale increased ten-fold and 100-fold, respectively [250]. As a consequence, processes, in which the revenues are lower than the salaries of the operators will never be profitable. In the baseline scenario, the labour-dependent costs for operation and laboratory/QA/QC were 1,300,000 USD y^{-1}, meaning that a scale of at least 527 m^3 was needed to compensate for these costs alone. This was based on EPS titre, EPS selling price and number batches per year being 1.3 g L^{-1}, 73 USD kg^{-1} and 26, respectively.

The effect of PBR module price (incl. lights) and electricity price on MSP followed a linear pattern. MSP was more strongly influenced by the purchase cost of one PBR module (with lights) than that of electricity. This aligned with expectations, as PBR purchase cost was the most influential cost for TCI, as well as for OpEx through facility-dependent cost (section 8.3.2). MSP varied between 187 and 830 USD kg^{-1} when the PBR cost for one module (3 m^3) was varied between 0.345 USD and 64,400 USD [204, 306]. Electricity cost of 0.08 to 0.22 USD kWh^{-1} resulted in MSP between 510 and 681 USD kg^{-1} [305].

Chapter 9: Discussion

9.1 Chapter Overview

This chapter discusses the findings from the three experimental results chapters and the dry-lab techno-economic assessment. This chapter begins with a discussion of the findings from the screening of novel cyanobacteria for extracellular polymeric substances (EPS) with functional properties. It then examines the outcomes of the culture conditions optimisation, highlighting the strategies that enhanced EPS production. Thereafter, the chapter considers the challenges encountered during scale-up and their implications for reproducibility and industrial applicability. The physiological role of EPS with emulsifying properties and its implications for scaling up production are then discussed. Finally, the techno-economic assessment integrates the experimental results to evaluate whether the overarching aim of achieving a commercially viable EPS process has been met, and the chapter concludes with recommendations for future research to advance the commercialisation of cyanobacterial EPS.

9.2 Screening Novel Cyanobacteria for EPS with Functional Properties

This study set out to investigate the potential of cyanobacteria to produce EPS, given that only a small fraction of the many cyanobacterial species have been studied for this purpose. Based on their ecological and taxonomic diversity and the wide range of reported EPS yields (0.03 to 17 g L^{-1}), it was hypothesised that novel species might produce EPS at levels and with properties not yet documented [41, 181].

To compare the obtained EPS production results to literature values, Table 9-1 presents the maximum EPS concentrations from this study alongside literature values for cyanobacterial species of the same genera. Comparison was based on EPS productivity, which was calculated from EPS_{Max} concentration and respective growth duration according to Equation 2-1. The maximum obtained EPS concentrations and productivities of the novel cyanobacteria ranged from 0.11 ± 0.10 (n=3, *G. alpicola*) to 1.79 ± 0.15 g L^{-1} (n=2, *C. brevissima*), which corresponded to productivities of 1.9 ± 1.4 mg L^{-1} d^{-1} (n=3) to 29.9 ± 2.5 mg L^{-1} d^{-1} (n=2). The highest EPS productivity was

obtained by *C. brevissima*, which was significantly higher than the productivities of all other screened species ($p \leq 0.044$), except *A. oscillarioides*. This was likely due to the high standard deviation in the EPS_{Max} sample of *A. oscillarioides*, as other EPS concentrations between *A. oscillarioides* and *C. brevissima* were statistically significant, for example the previous sample (day 48, $p=0.029$).

Table 9-1 Maximum extracellular polymeric substances (EPS) concentration (C_{EPS}), growth duration at which the maximum EPS concentration was obtained, and the corresponding EPS productivity (P_{EPS}) of novel cyanobacteria in screening experiment compared to literature data.Data represent mean ± standard deviation of biological duplicates (n=2) or triplicates (n=3) as indicated in the second column. The conditions of the screening experiment were 25°C, constant illumination at 22 µmol m^{-2} s^{-1} and shaking at 250 RPM.

Species	**n**	**C_{EPS}** ($g\ L^{-1}$)	**Duration** (days)	**P_{EPS}** ($mg\ L^{-1}\ d^{-1}$)	**Source**
C. brevissima	2	1.79 ± 0.15	60	29.89 ± 2.45	This study
T. subtropicus	3	0.78 ± 0.18	60	12.96 ± 2.95	This study
N. longstaffi	3	0.77 ± 0.17	60	12.83 ± 2.86	This study
N. foliaceum	3	0.59 ± 0.08	48	12.25 ± 1.57	This study
A. platensis	2	0.51 ± 0.04	49	10.51 ± 0.83	This study
N. zetterstedtii	3	0.61 ± 0.12	60	10.14 ± 1.99	This study
O. rosea	3	0.22 ± 0.07	24	9.31 ± 2.97	This study
S. major	3	0.20 ± 0.02	22	8.94 ± 1.00	This study
A. oscillarioides	2	0.45 ± 0.46	60	7.53 ± 7.59	This study
T. bornetii	2	0.18 ± 0.05	24	7.29 ± 2.06	This study
A. marina	3	0.24 ± 0.07	36	6.63 ± 2.05	This study
S. reniformis	3	0.31 ± 0.09	49	6.24 ± 1.79	This study
F. diplosiphon	3	0.34 ± 0.02	60	5.64 ± 0.25	This study
P. keutzingianum	2	0.21 ± 0.01	48	4.36 ± 0.05	This study
P. breve	3	0.17 ± 0.03	56	2.98 ± 0.62	This study
G. alpicola	3	0.11 ± 0.08	56	1.88 ± 1.44	This study
Anabaena sp. ATCC 33047		17	5	3440.00	[181]

(continued on next page)

Table 9-1 (continued)

Species	n	C_{EPS} (g L^{-1})	Duration (days)	P_{EPS} (mg L^{-1} d^{-1})	Source
Spirulina sp. LEB-18		9.5	30	316.67	[64]
Anabaena sp. BTA992		1.7	30	56.67	[45]
Cyanothece sp. CCY 0110		1.77	42	42.10	[63]
A. platensis		0.2905	11	26.41	[195]
Nostoc sp. CCALA H06/21		8.085	1095	7.38	[50]
N. flagelliforme		0.106	20	5.30	[165]
A. platensis		0.0913	21	4.35	[166]
Trichormus variabilis		2.519	1098	2.29	[50]
Anabaena WSAF		0.056	28	2.00	[41]
Phormidium sp.		0.03	28	1.07	[41]
Nostoc punctiforme		0.579	1098	0.53	[50]

These values lie within the range of literature data (0.03 – 17 g L^{-1} and 1 - 3440 mg L^{-1} d^{-1}) [41, 181]. Compared to screening studies in literature, e.g. by Nicolaus, et al. [41] and Uhliariková, et al. [50], some of the novel cyanobacteria even exceeded the literature data in terms of EPS productivity. However, compared to the highest productivity obtained in literature, 3440 mg L^{-1} d^{-1} achieved by Moreno, et al. [181], the results obtained in this study are between 115-fold and 1829-fold lower. It should be noted that the value reported by Moreno, et al. [181] stands out as an outlier and should be interpreted with caution. In addition, as cultivation parameters differ considerably across studies, which may affect direct comparison with literature, since EPS production is highly variable based on culture conditions, as described in the literature review (section 2.3) [3]. Furthermore, the conditions in the screening experiment (25°C, constant illumination at 22 µmol m^{-2} s^{-1}, shaking at 250 RPM) were selected to be suitable for a wide range of species. This can lead to conditions being suboptimal for EPS production, resulting in lower EPS production compared to optimisation studies. Furthermore, one species, *O. rosea*, which performed well under room temperature

and ambient light conditions, failed to grow under the constant light, 25°C regime used here. This highlights the importance of tailored environmental parameters and suggests that the standardised screening conditions were suboptimal for this species.

Since EPS production is often stress-induced, some accumulation may reflect responses to media changes, as several strains were maintained in different media in culture collections than to the study. However, media compatibility tests (Appendix section 12.5) showed that for example *C. brevissima* grew similarly in BG-11 and its maintenance medium (MDM, p=0.46), suggesting limited media-related stress. Furthermore, *N. foliaceum* was already maintained in BG-11 in the culture collection (UTEX). EPS production may reflect broader adaptation to new conditions, and long-term studies are needed to assess whether it persists after acclimation.

EPS from all but one species contained substantial sugar fractions, consistent with polysaccharide-rich extracellular matrices. The average sugar content (41%$_{w/w}$) matched reported values from cyanobacterial EPS in literature (44%$_{w/w}$, section 2.2.1). Unusually low sugar content in *G. alpicola* and *O. rosea* (8 ± 2%, n=3), coupled with low overall EPS concentrations (< 0.20 g L^{-1}), suggests these samples may have been dominated by impurities co-precipitated during ethanol extraction. Protein was detected in six species, with *S. reniformis* containing the highest fractions (12 ± 5%$_{w/w}$, n=3). Sulphated EPS, which are correlated with bioactivity such as antioxidant or antimicrobial functions were found exclusively in marine species, which is known from literature [15, 19, 108, 260, 261]. The highest amount of sulphate was detected in *P. keutzingianum* (13 ± 2%$_{w/w}$, n=2). Monosaccharide analysis, using High-Performance Anion Exchange Chromatography with pulsed-amperometric detection (HPAEC-PAD) revealed a presence of up to nine different monosaccharides, with glucose as the dominant sugar (21%$_{w/w}$ on average), which is in accordance with literature [28]. The presence of deoxy sugars and uronic acids indicates complex structural heterogeneity. EPS from one species, *N. foliaceum*, showed three unidentified HPAEC-PAD peaks, possibly indicating the presence of novel monosaccharides, which could result in unique properties.

EPS from seven selected species were further examined for functional properties. EPS from *A. oscillarioides, C. brevissima*, and *T. subtropicus* demonstrated strong

emulsifying activity, comparable or superior to xanthan gum and matching Tween20. This aligns with prior literature showing that emulsifying activity is associated with amphiphilic components such as deoxy sugars and proteins and underscores the commercial potential of the novel EPS products [11]. Several EPS, particularly those produced by *A. oscillarioides*, *N. zetterstedtii*, and *C. brevissima*, showed indications of UV-protective properties. Their absorbance in the UVB and UVA regions suggests a reduced transmission of harmful wavelengths, implying potential UV-shielding capacity and suitability for bio-based sunscreen applications. These properties may be attributed to the presence of mycosporine-like amino acids (MAAs), which represent a promising natural alternative to conventional sunscreen agents [61]. Further structural elucidation and tests regarding efficacy for use in sunscreens are necessary. Antioxidant activity, measured via $ABTS^+$ and DPPH assays, showed that all tested EPS had radical scavenging potential. In the $ABTS^+$ assay, all species demonstrated radical scavenging activity, ranging from 88 ± 3% (n=3, *N. foliaceum*) to 97 ± 0% (n=3, *A. oscillarioides*) at an EPS concentration of 2 g L^{-1}. However, the positive control, ascorbic acid, achieved 97 ± 1% (n=3) scavenging at a concentration as low as 0.0625 g L^{-1}. In the DPPH assay, scavenging ranged from 20 ± 8% (n=2, *A. marina*) to 45 ± 6% (n=3, *N. longstaffi*) at 2 g L^{-1}, while ascorbic acid reached 95 ± 1% (n=3) at 0.5 g L^{-1}. Notably, cyanobacterial EPS reported in the literature have exhibited higher antioxidant activity than ascorbic acid [117, 118]. Iron-chelating activity was strongest in *A. oscillarioides* (78 ± 18%, n=2). However, the activities observed remained lower than those of the positive control, ethylenediaminetetraacetic acid (EDTA), whereas cyanobacterial EPS reported in the literature have exhibited higher iron-chelating activity than EDTA [118]. The flocculating activity of *T. subtropicus* (52 ± 9%, n=3) exceeded that of xanthan gum (33 ± 12%, n=3). *T. subtropicus* EPS also contained the highest content of uronic acids (13 ± 0.3%, n=3), which is correlated to flocculating activity [44]. However, practical issues with the flocculating assay limit the reliability of these results.

Supporting the hypothesis that EPS diversity in cyanobacteria is underexplored, the results reveal a wide range of EPS titres and functionalities across species. Although the target titre of <1 g L^{-1} was achieved, the two-month cultivation period required was considered too long, indicating the need for further optimisation. The next section examines how varying culture conditions enhanced EPS production.

9.3 Culture Conditions Optimisation

The initial screening phase identified *C. brevissima* and *N. foliaceum* as promising EPS producer, based on both, EPS quantity and quality, including emulsifying properties. Culture optimisation experiments highlighted the impact of environmental parameters on EPS productivity [3]: One-variable-at-a-time (OVAT) optimisation of light intensity during phototrophic cultivation improved EPS productivity two-fold to 81.8 ± 6.6 mg L^{-1} d^{-1} (n=2) in *C. brevissima* and to 20.2 ± 1.3 mg L^{-1} d^{-1} (n=2) in *N. foliaceum*. The most dramatic improvements were observed under mixotrophic conditions during multi-factor-optimisation, where the addition of glucose (5 g L^{-1}), elevated temperature (28°C) and light intensity (225 µmol m^{-2} s^{-1} for *C. brevissima*) increased EPS production to 2.65 ± 0.07 g L^{-1} (n=2, *C. brevissima*) and 0.70 ± 0.04 g L^{-1} (n=3, *N. foliaceum*). This represented an sixfold and fourfold increase of EPS productivity compared to the screening experiment, leading to EPS productivities of 189.3 ± 4.8 mg L^{-1} d^{-1} (n=2, *C. brevissima*) and 49.7 ± 2.8 mg L^{-1} d^{-1} (n=3, *N. foliaceum*). However, it should be noted that all three parameters reached the upper limits of the tested range, suggesting that the true optima may lie beyond the values examined. Therefore, more initial OVAT experiments would be useful to establish sufficiently broad ranges before moving to multi-factor optimisation.

Glucose's significance in influencing EPS production can be primarily attributed to its central role as carbon and energy source. Firstly, glucose is one of the main building blocks of EPS, making up 31 ± 6% (n=3) of *C. brevissima* EPS and 14 ± 3% (n=3) of *N. foliaceum* EPS (section 5.3.2). Furthermore, glucose can be utilised to generate ATP through glycolysis and cellular respiration, and NADPH through the pentose phosphate pathway, enhancing metabolic activity and the production of biomass or products such as EPS [373]. For *C. brevissima*, the combined effect of light intensity and temperature was statistically significant, possibly indicating an interaction effect between the two parameters. This was suggested by Trabelsi, et al. [168] to explain the combined effect of light intensity and temperature on *A. platensis*, without specific explanation for the underlying mechanisms. More generally, the authors suggested that EPS are released to prevent oxidative stress caused by inhibitory growth conditions [168]. Since the DCW optimum of *C. brevissima* was at a lower light intensity (75 µmol m^{-2} s^{-1}), EPS was initially suspected to be a response to light stress. However, as described in section 6.10.2, in further experiments, *C. brevissima* grew at light

intensities as high as 500 µmol m^{-2} s^{-1}, suggesting that while light stress could be a factor, the organism's ability to grow well under higher light levels indicates that EPS production may not be strictly related to light stress responses.

These findings suggest that carbon and light availability are major drivers of EPS biosynthesis, which is consistent with literature [33, 46]. However, such improvements may be accompanied by trade-offs in sustainability and axenicity, when used in commercial-scale production. Mixotrophic cultivation, while effective, requires glucose, which is derived from arable land and competes with food production [8]. Additionally, it increases the risk of contamination, thereby possibly compromising the axenicity of the system [199, 200]. Given the risk and sustainability concerns of glucose-based systems, phototrophic cultivation over a wider range of temperature (25-37°C) light intensities (25-500 µmol m^{-2} s^{-1}) was explored for *C. brevissima.* Although EPS production at the optimum of 31°C and 300 µmol m^{-2} s^{-1} (1.26 ± 0.03 g L^{-1}, n=2) was 34% lower than under mixotrophy (2.65 ± 0.07 g L^{-1}, n=2), it was still higher than most values found in literature (Table 9-1).

While the experiments showed clear improvements in EPS productivity, there are some limitations to the culture conditions and optimisation approach that should be considered. The Box–Behnken design was chosen because it is more time-efficient than other designs like full-factorial or central composite, as it uses fewer runs. However, its main drawback is that it may miss more complex interactions between variables [205, 206]. It might have been better to do more initial tests before applying this method, or to use a more detailed design like full-factorial or central composite design, especially if time and resources had allowed. Also, for some conditions, only duplicate runs were used due to time and equipment constraints. Using triplicates or more replicates would likely have improved the reliability of the model. In addition, only a small number of nutrients was tested ($CaCl_2$, magnesium, EDTA, glucose, acetate, and trace metal solution), but many other nutrients can also affect EPS production (section 2.3). It is possible that other nutrients not included here might have an even stronger influence on productivity. Finally, in the phototrophic experiment with *C. brevissima* (Experiment 2.9), EPS concentration (0.95 ± 0.02 g L^{-1}, n=2) was 2-fold higher than in an earlier experiment (0.44 ± 0.01 g L^{-1}, n=2), Experiment 2.8), despite the conditions being the same. This might be due to elevated CO_2 levels in the lab, as

the PBRs were running with CO_2 near the incubator that held the shake flasks. It would be worth testing different CO_2 concentrations in future experiments, as this appeared beneficial and could improve EPS productivity without the sustainability drawbacks of glucose. However, this was not possible with the shake flask setup used.

Overall, the results presented here support the initial hypothesis that culture conditions play a key role in enhancing EPS production. Both phototrophic and mixotrophic strategies led to increases in EPS concentration when parameters such as light intensity, temperature, and carbon availability were optimised. While some limitations in the optimisation approach were identified, the consistent improvements observed across different conditions and strains clearly show that environmental factors can be strategically adjusted to enhance EPS productivity. These findings highlight the potential of controlled culture conditions as a tool to improve the efficiency and commercial feasibility of microalgal EPS production systems.

9.4 Challenges Encountered During Scale-Up

Scale-up of *C. brevissima* cultivation in 1-litre photobioreactors (PBRs) resulted in higher DCW production but drastically reduced EPS production: In shake flasks, high EPS titres of up to 2.65 ± 0.07 g L^{-1} (n=2) were observed, whereas EPS production in PBRs was considerably lower (0.51 ± 0.23 g L^{-1}, n=2). DCW production was higher in PBRs (2.83 ± 0.65 g L^{-1}, n=2) than shake flasks (1.07 ± 0.03 g L^{-1}, n=2). EPS production remained low despite varying airflow from 1 to 4 L min^{-1}, CO_2 flow from zero to 100 mL min^{-1}, and light intensity from 50 to 950 µmol m^{-2} s^{-1}. Only three levels were tested for each parameter, so additional runs across a wider range, for example using a BBD or CCD, could yield a more thorough optimisation than the preliminary screening carried out here, but this was not feasible within the available timeframe. The reduction of EPS production during scale-up has been observed in literature. EPS production of *A. maxima* IFRPD 1183 in a 30 litre pond was 4 times lower than in a 200 mL culture tube [172]. Similarly, carbohydrate production of *Cyanothece* CCY 0110 was about three times lower in 10 L compared to 1 L [63]. However, in both of these cases, biomass growth and pigment production was decreased as well, which was not observed in the current study [63, 172].

The higher DCW could indicate that the PBRs represent more favourable conditions for growth for *C. brevissima*, which possibly alleviated the need for EPS production, in case EPS represent a stress response, e.g. for shear stress. A key distinction between the two systems was the mode of agitation and aeration: shaking in flasks versus bubbling in PBRs. This affected biofilm formation and cell distribution. In PBRs, cells mainly formed biofilm on the walls and accumulated at the top and bottom, leaving the liquid more transparent, indicating fewer suspended cells (Figure 7-7*a*-*b*). In contrast, shake flasks showed limited biofilm formation and a darker culture, suggesting more suspended cells (Figure 6-10*c*). Shaking may have induced shear stress that stimulated EPS production as a protective response, while bubbling possibly had a milder effect and less uniform mixing. Alternatively, EPS production may relate to biofilm and colony formation, which was hindered in shake flasks due to the glass surface, leading to higher EPS but lower DCW compared to PBRs. Further details are provided in the next section (section 9.5).

Alternatively, it was suspected that the additional biomass could originate from contaminating organisms, as the PBRs could not maintain sterility (section 7.6). However, an axenic PBR experiment also showed an increase in DCW_{Max} and a decrease in EPS compared to shake flasks (section 7.7). This indicated that the increase of biomass was due to higher *C. brevissima* growth and not originating from contaminating organisms. The EPS results from the axenic cultivation (Exp. 3-4) were still low (0.51 ± 0.23 g L^{-1}, n=2, day 11) compared to shake flask experiments (1.26 ± 0.03 g L^{-1}, n=2, day 11). Initially, it was suspected that contamination caused the low EPS titres, as the carbohydrate-rich EPS could serve as a carbon source for contaminating heterotrophs. However, it became clear that contamination was not responsible for the low EPS production. The complex nature of cyanobacterial EPS can protect them from degradation or consumption by other organisms. Degradation of cyanobacterial EPS requires a wide set of enzymes produced by different organisms, with condensed and insoluble fractions particularly resistant to enzymatic breakdown [374].

Another aspect initially suspected to result from contamination was the large variation between biological duplicates. The axenic PBR experiment showed that this variation was not caused by contamination. Instead, it appeared that the variation was more

likely to be caused by the equipment. Especially PBRs 1 and 2 showed much larger variation (Figure 7-9*a*) than PBRs 3 and 4 (Figure 7-9*b*). Initially, the gas board leak was suspected as cause for the variation, as described in section 7.2.2 and 7.6. However, in the axenic experiment, only gas board 2 was used for aeration, whereas gas board 1 was merely used to mix the water in the heat bath. Still, *C. brevissima* grown in PBR 2 behaved differently than expected, with the DCW average being only about half of that from a previous experiment under the same conditions (Exp. 3-1). It is unclear which part of the equipment could cause this issue. Light tiles have been ruled out by measuring the light intensity of each tile (section 7.2) and the thermometer was eliminated as an option by swapping it with another PBR. It could possibly be something that was not readily apparent, e.g. flickering of the LED tiles.

Another insight was the noticeable lag phase of 2 days in the PBRs supplied with CO_2 compared to those without (Figure 7-9*b*). This was likely caused by the inoculum being grown without CO_2. The results obtained with CO_2 in the previous sections might be underestimated due to the presence of a lag phase. It would be beneficial to cultivate the inoculum under the same conditions than the respective PBR to avoid a lag phase to occur and to obtain more accurate results. The available incubator (SciQuip Premium Compact) was not suitable to grow inoculum under the same conditions than the cultures, as controlling the CO_2 flow rate into each of the 20 shake flasks used to grow the inoculum would be challenging. Furthermore, the SciQuip incubator can only supply light intensities up to 220 µmol m^{-2} s^{-1}. Instead, the Duran bottle setup (Figure 4-3) could be used to grow the pre-cultures, the cultures, or both. In the latter case, six Duran bottles with foam traps and filters would have to be autoclaved, to use two bottles for pre-cultures and four additional bottles for the cultures. Another advantage of the autoclavable Duran bottles is the quicker turnover time, since they avoid the 48 hours downtime for sterilisation and neutralisation.

In summary, the scale-up experiments faced several challenges with the PBRs, including inconsistent reactor performance, technical issues, and difficulties maintaining axenicity. These issues affected the reliability of the results but also reflect common problems encountered during scale-up, such as microbial contamination, suboptimal mixing, and differences in vessel material and gas exchange compared to shake flasks [199, 200]. Furthermore, the substantial decrease of EPS production

during scale-up has direct implications for process economics, as reduced EPS titres impact the overall profitability of industrial production. The original hypothesis, that scale-up would sustain or improve EPS production while addressing industrial constraints, was not supported. These findings underline the need for dedicated scale-up studies to better understand and control the technical and biological factors affecting EPS production at larger volumes.

9.5 Physiological Role of EPS with Emulsifying Properties in *C. brevissima*

Production of emulsifying EPS by *C. brevissima*, as observed in this study, could be a dispersion or detachment/attachment strategy similar to that of production of *Emulcyan* by *Phormidum* J-1 as described in section 2.2.3.1 [26]. As described in the previous section (section 9.4), there were differences in culture homogeneity, DCW production and EPS production between shake flasks and PBRs. In shake flasks, the culture appeared relatively homogeneous, with some biofilm formation at the bottom and at the air–liquid interface on the walls. In contrast, cultures in PBRs were more heterogeneous, with biofilm concentrated on the vessel walls and bottom.

Based on the mechanism described in the literature review (section 2.2.3.1), the behaviour of *C. brevissima* could be explained by the following: The shake flasks conditions could be unfavourable for *C. brevissima*, resulting in the species to produce large amounts of emulsifying EPS, at the expense of biomass, to cover its hydrophobic sites, causing detachment from the surface with the aim to disperse into habitats with more favourable conditions. In the PBRs, conditions might be more favourable for *C. brevissima*, e.g. through less shear stress by growing in the corners, which are not reached by the disc shaped sparger, resulting in less need for EPS, and less need for dispersal. This assumption is based on the presumed hydrophobicity of *C. brevissima*. Fattom and Shilo [362] reported that benthic cyanobacteria, such as *Calothrix desertica*, are typically hydrophobic, whereas planktonic species are generally hydrophilic. Although the literature does not explicitly identify *C. brevissima* as hydrophobic or benthic, it is presumed hydrophobic since the genus *Calothrix* is generally described as benthic [375].

Alternatively, the aim of the production of EPS could be to attach to surfaces and/or to aggregate cells for colony formation. Attaching on the vessel wall might be beneficial to be closer to the light source. The shake flasks, which were made from borosilicate glass, might be harder to attach to due to the smooth and inert surface. Additionally, culture in shake flasks might be more rigorously mixed than the PBR, causing more EPS being washed and lost from cells, resulting in more EPS being needed. These two factors might make attachment more difficult, resulting in more EPS being produced at the expense of biomass. In the PBRs, the vessel was made out of acrylic plastic, which had a rougher surface that might be easier to attach to. Furthermore, aeration in the PBRs might be a less efficient form of mixing, resulting in cells growing in the corners, where the disc shaped sparger was less effective. Possibly, as attachment was easier, a lower amount of EPS was sufficient to cause the desired effect, thus cells could divert resources to biomass. However, in this case the mechanism is expected to differ from that described by Fattom and Shilo [26], as the aim of EPS is to attach to surfaces with its hydrophobic sites, as opposed to cover hydrophobic sites of the cell to cause detachment. Understanding the physiological role of *C. brevissima* to produce EPS could help identify the most effective method to induce EPS production in industrial-scale PBRs. Future research investigating the hypothesis that EPS were an attachment or dispersion strategy, could provide further insights. Testing whether the cells and EPS are hydrophobic could be an initial starting point, e.g. using a hexadecane-water biphasic system [26].

9.6 Techno-Economic Implications and Commercial Potential

It was hypothesised that techno-economic modelling could demonstrate the commercial feasibility of cyanobacterial EPS production, and that process design and cost analysis would help identify key factors for cost-effective implementation. The techno-economic assessment carried out in this study has shown that most EPS production scenarios remained economically unviable, mainly due to high capital and operating costs driven by tubular PBRs and artificial lighting, which caused 86% of equipment cost and 78% of the electricity costs in the baseline scenario. Similar observations were made in literature where a recent study showed that PBRs and lights made up 76% of total MEC and consumed 93% of the electrical energy [250].

Certain process designs, however, resulted in profitable outcomes: The use of bag PBRs in outdoor, mixotrophic, semi-continuous systems with natural light and filtration proved to be the most cost-effective configuration, resulting in a positive net present value (NPV, 42,600,000 USD) and profitability index (PI, 2.4). However, this profitability was dependent on achieving elevated EPS titres, which may not be realistic without controlled temperature and illumination.

Compared to competing products, the EPS-derived bioemulsifier from *C. brevissima* offers the advantage of being effective at a lower concentration while being priced similarly to its closest competitor, the seaweed-derived emulsifier SeaBalance2000. However, production costs could not be reduced sufficiently to match the cheaper bio-based emulsifier lecithin or the synthetic emulsifier Tween20, limiting its cost competitiveness in comparison to those products. Thus, the author of this PhD thesis agrees with the consensus in literature to focus on high-value EPS [11, 21]. An alternative product scenario was explored, where a high-value cosmeceutical, a day cream with UV-protective and antioxidant properties, was produced from the EPS-containing supernatant. This resulted in a highly profitable scenario with 3-fold higher PI (7.4) and 7-fold higher NPV (892,000,000 USD) than the most profitable bioemulsifier scenario. The results therefore partially support the hypothesis: techno-economic modelling was effective in identifying key cost drivers and viable process configurations, but widespread economic feasibility remains conditional on product value, achievable titres and PBR capital costs.

The TEA conducted in this study, while providing valuable insights, has several limitations and should be viewed as a preliminary screening-level analysis. The primary limitation is that the TEA relied on EPS and DCW titres obtained from shake flask experiments, despite these titres not being able to be replicated in the 1-litre PBRs (Chapter 7:). It is uncertain whether the biomass and EPS titres applied in the TEA can be achieved under the conditions of the most profitable scenario, which uses natural light, bag PBRs and glucose under mixotrophic cultivation. Firstly, it is uncertain whether natural light can trigger EPS production, as Exp. 2-7 revealed that light duration and intensity needed to exceed 16 hours and 25 µmol m^{-2} s^{-1} for *C. brevissima* to initiate EPS production (section 6.10.1). Furthermore, without strict light control, cells could receive too low light intensity due to self-shading, or too high light intensity at

lower cell densities, resulting in photoinhibition. In microalgal cultures, self-shading can occur with increasing cell density. This can lead to average irradiance in dense cultures being as low as 100 to 300 µmol m^{-2} s^{-1} despite solar irradiance reaching values up to 2000 µmol m^{-2} s^{-1} [341]. In general, production titres tend to decrease during scale-up compared to shake flask conditions due to challenges such as self-shading, suboptimal mass transfer or competition/inhibition by contamination of other microorganisms [199, 200]. These challenges were particularly evident in the 1-litre PBRs used in this study and are likely to be even more pronounced in larger systems. In particular, PBR bags, which are used as cost-reduction strategy, have been reported to have inadequate mixing [211]. This could lead to even lower EPS titres than observed in the lab-scale PBRs in this PhD thesis. Furthermore, the suitability of glucose use in industrial-scale PBRs remains uncertain due to contamination risks and sustainability concerns related to competition with food-producing arable land [8, 199]. A more sustainable alternative is purely phototrophic cultivation; however, this approach is expected to yield lower EPS titres (Exp. 2-6, section 6.9).

Several other factors related to process design, equipment, and economic assumptions also represent limitations of the current TEA. Firstly, PBR cost remains the largest driver of total expenses. Tubular PBRs and their associated lighting were the main contributors, and prices vary widely, strongly influencing profitability. While larger systems often benefit from economies of scale, this is not always true for modular PBRs. For example, an Lgem 45 m^3 PBR costs 526,500 USD, which is around 50% more per m^3 than the 3 m^3 unit used in this TEA priced at 21,700 USD [259, 306]. In this study, a linear cost increase was assumed due to the modular nature of equipment such as CO_2 units, air blowers, and LED lights. Economies of scale may only apply if bulk discounts are offered, which could reduce costs given the large number of units required (1,100 for the tubular PBR case). Secondly, equipment lifetime and process assumptions introduce uncertainty. For instance, while some studies report the lifetime of bag PBRs to range between 5 and 12 years [209, 376], others describe them as relatively fragile, with shorter lifespans, sometimes as low as one year, which would increase replacement frequency and overall cost [211, 217]. Similarly, the assumed EPS molecular weight (>50 kDa) affects filtration design. If smaller molecules are produced, alternative membranes with different costs, lifetimes, and energy demands may be required. Thirdly, operational and environmental factors

were simplified. Heating and cooling estimates did not include daily or seasonal temperature variations, potentially underestimating utility needs. Material and disposal costs may also be underestimated: sodium hypochlorite was excluded as a reactive input, extending unrealistically long recycling times, while wastewater disposal could become relevant under stricter regulations or higher discharge rates. Fourthly, product functionality uncertainties remain. The effect of spray drying on EPS functionality was not tested. If freeze-drying, which preserves bioactive properties, is required instead, the production costs are expected to be 35% higher (section 8.4.2) [207]. Furthermore, biofilm formation could complicate cleaning and harvesting, though one study reported it may simplify dewatering for *C. brevissima*, however it is uncertain whether this translates to industrial-scale PBRs [342]. A kill/spill tank, used to thermally inactivate or sterilise spent culture or contaminated fluids, particularly in systems handling GMOs or hazardous strains, was not included in this study [377]. As *C. brevissima* is a non-GMO, non-toxic species and all biomass is processed as product, a dedicated kill tank was not part of the base case design. Additionally, spray-drying the algal biomass and EPS at 80°C ensures that no viable biological material is released under normal conditions. However, future assessments should consider such system for crashed cultures, as they add to capital and operating costs, especially for heating, maintenance, and downtime [377]. Additionally, regional and economic assumptions add variability. The model is based on Spanish economic data and Lang factors for capital estimation, which may not reflect local differences in labour, materials, or construction [251]. Finally, marketing costs were excluded, which could further influence economic feasibility.

These limitations indicate that the TEA should be considered a screening-level analysis. While several uncertainties like the EPS titre were accounted for in the sensitivity analysis to mitigate the impact of these limitations, further research addressing these issues would provide a clearer and more reliable understanding of the techno-economics of EPS production using cyanobacteria. Despite limitations, this TEA can serve as a starting point for determining which production systems, titres, and growth modes are feasible, thereby guiding laboratory research from the outset toward economically viable strategies.

9.7 Future Research For Commercialising Cyanobacterial EPS

This PhD thesis provided valuable insight to guide future research on commercialising EPS production from cyanobacteria. Future research should focus on several aspects that contribute to the profitability of the process, which are listed in the following. As described in the previous section, the major challenge is to trigger EPS production in larger scales comparable to shake flask titres. As mentioned in section 9.5, EPS with emulsifying properties might be a strategy for detachment/attachment. It would have to be studied how to trigger the same response in larger-scale PBRs. For example, the effect of different materials (e.g. glass) or levels of shear stress in PBRs could be studied. EPS production would have to be tested in-situ to determine whether outdoor cultivation is suitable for EPS production. The impact of factors such as natural day/light cycles, light intensity, self-shading and contamination should be studied. If no suitable industrial-scale cultivation system can be found, a custom PBR, e.g. one that remains axenic, to achieve this specific aim might need to be designed. An axenic system could enable mixotrophic production, which resulted in the highest EPS titre obtained (0.51 ± 0.23 g L^{-1}, n=2, section 6.9). High EPS titre was the most relevant factor in the sensitivity analysis of the TEA (section 8.5). If mixotrophic conditions appear suitable for industrial-scale production, laboratory research into enhancing EPS and DCW titres even further would be beneficial. Possibly, EPS and DCW titres can be further enhanced with higher glucose concentrations, as the maximum was identified as the upper limit of the tested range (5 g L^{-1}, section 6.9). Additionally, diazotrophic growth instead of using sodium nitrate would be interesting to test, as this increased EPS production in *Anabaena* sp. ATCC 33047 8.6-fold to 17.2 g L^{-1} [181]. Also, the use of membrane PBRs could be explored as an option to produce EPS, as they can be used as an option to continuously separate extracellular metabolites [211]. However, since EPS are typically produced during the stationary phase, it is necessary to first investigate whether EPS production can be effectively triggered during continuous cultivation of the desired species.

One important consideration is that in most cases the DSP costs for EPS will be higher than those for biomass. Even in the simplest design (scenario 3), while biomass production requires a centrifuge and a spray dryer, EPS production necessitates not

only the same equipment but larger equipment (i.e., the spray dryer), leading to higher MEC, facility-dependent, and utility costs compared to biomass production alone. This is due to EPS being present in the supernatant of the centrifuge, which involves a larger volume compared to the pellet form (biomass). A proposed rule of thumb by the author of this PhD thesis is to consider EPS as main product only if the value is higher than that of biomass. Algal biomass selling prices can range from 27 USD kg^{-1} to 521 USD kg^{-1} [250, 333]. For lower value products such as bioemulsifiers, using a waste biomass resource might be more profitable as there are no production costs. One successful example is the seaweed-derived cosmetic emulsifier SeaBalance 2000 by biotech company Carbonwave. Similarly, while the film-like EPS observed in *C. brevissima* (section 6.2.2) might seem appealing for use as bio-plastic, its low value makes it unlikely to be economically viable.

If the titres during scale-up are too low to compensate for the production costs, another strategy is to focus on high-value products instead. In this case, screening experiments should be designed based on the final product or application in mind, e.g. obtaining EPS with bioactive properties. For example, in the case of sunscreen-containing cosmeceuticals, isolating cyanobacteria from extreme, high-UV environments could help identify EPS with optimal protective properties [176]. Furthermore, cultivating the species in the screening under specific conditions could further enhance the desired properties. For instance, MAA production can be enhanced by changing the growth parameters, such as quantity and quality of radiation, as well as nutrient availability (e.g. ammonium chloride) [160]. Another important factor to include in screening experiments is the management of contamination. Due to the high risk of contamination in PBRs, it would be beneficial to screen for maximum EPS production at conditions that hinder growth of other organisms [199]. In literature, *N. flagelliforme* was grown at pH 8–9, which prevented the contamination of other green alga [196].

In parallel, future research should consider the evolving environmental and legislative frameworks that govern large-scale algae production in Europe. In particular, the General Food Law Regulation (EC) 178/2002 and the Novel Food Regulation (EU) 2015/2283 establish strict safety, traceability, and authorisation requirements for novel microalgae-based food products. The European Food Safety Authority (EFSA) plays a central role in evaluating risks, requiring detailed assessments of production

processes, product composition, and environmental impacts [378]. Under the Environmental Impact Assessment Directive 2014/52/EU, large-scale algae operations are likely to trigger requirements under the Environmental Impact Assessment Directive 2014/52/EU, necessitating comprehensive assessments of ecological risks, mitigation strategies, and stakeholder engagement [379]. For industrial-scale operations, compliance with these legislative instruments is critical, especially as the EU introduces stricter transparency regulations and emphasises sustainability under the European Green Deal [378]. Life cycle assessment (LCA) would be useful to determine the sustainability of each process to include factors such as the sourcing of lecithin from soy beans which is associated with deforestation of the rain forest [359]. Similarly, glucose leads to competition with food resources for arable land [8]. To avoid this ethical dilemma, glucose could be sourced from lignocellulosic materials, which are non-edible plant residues such as sugar cane bagasse, corn stover and straw [380]. Similarly, the use of flue gas instead of pure CO_2 could be investigated to explore the process as a method for carbon sequestration. LCA would also be useful to assess the impact of using tubular PBRs compared to bag PBRs, as well as the impact of glucose compared to CO_2 as carbon source. Future research can build on the insights and challenges presented in this PhD thesis to advance the sustainable commercialisation of cyanobacterial EPS.

Chapter 10: Conclusions

This PhD thesis explored the potential of cyanobacteria to produce EPS for biotechnological applications, addressing the need for sustainable alternatives to petroleum-based materials. The research tackled key challenges in EPS production, including species identification, optimising titres, scale-up, and assessing the techno-economics of the process. Key findings offer valuable insights into the potential and limitations of cyanobacterial EPS, guiding future research and industrial applications.

This study aimed to identify novel wild type cyanobacteria capable of producing at least 1 g L^{-1} of EPS with relevant functional properties. Several strains met this criterion, with *C. brevissima* reaching 1.8 ± 0.10 g L^{-1} (day 60), exceeding the targeted concentration. The corresponding productivity of 29.9 ± 2.5 mg L^{-1} d^{-1} was higher than most screening studies, e.g. by Nicolaus, et al. [41] and Uhliariková, et al. [50] (Table 9-1). The screening also highlighted substantial biochemical diversity, with EPS containing nine monosaccharides, including rare sugars such as fucose and rhamnose, as well as sulphate and proteins. Functional analyses of seven promising EPS showed emulsifying, flocculating, UV-protective and antioxidant properties. Three EPS displayed emulsifying activity comparable to Tween20 and 2-3 times higher than xanthan gum. *C. brevissima* emerged as the most promising species, consistently producing the highest EPS titres with strong emulsifying, antioxidant and UV-protective characteristics. These findings underline the value of exploring the untapped cyanobacterial diversity.

The next stage assessed whether optimising cultivation conditions could improve titres and productivities. *C. brevissima* was the main focus, with *N. foliaceum* included for comparison. Single-factor optimisation demonstrated a strong influence of light intensity: under 150 µmol m^{-2} s^{-1} *C. brevissima* reached 1.72 ± 0.14 g L^{-1} on day 21, doubling productivity compared to the screening conditions. Mixotrophic multi-factor optimisation, combining light, temperature and glucose further increased titres to 2.65 ± 0.07 g L^{-1} in 14 days, with a productivity of 189.3 ± 4.8 mg L^{-1} d^{-1}. *N. foliaceum* also benefitted from multi factor optimisation, reaching 0.70 ± 0.04 g L^{-1} on day 14 with a fourfold productivity increase. These results show that tailored cultivation conditions can substantially enhance EPS production.

Following optimisation in shake flasks, *C. brevissima* was cultivated in 1-litre photobioreactors (PBRs) to assess scale up. While biomass productivity increased under CO_2 supplemented phototrophic growth, EPS productivity fell markedly to 17.0 mg L^{-1} d^{-1}, with a maximum of 0.1 g L^{-1}. Even after adjusting airflow, CO_2 and light colour, EPS titres remained below shake flask values. These results indicate scale- or equipment-dependent factors reduced EPS production at larger scale. EPS in *C. brevissima* may support surface attachment and colony formation, more critical in shake flasks due to higher shear stress. This underscores the challenges of scaling up cyanobacterial cultivation and the need for further research to address these limitations.

A techno economic assessment (TEA) based on shake flask data provided the first economic evaluation of phototrophic cyanobacterial EPS. PBRs and LED lighting were identified as the major cost drivers, accounting for approximately 86% of equipment costs and 78% of electricity usage. Only outdoor bag reactors using natural light combined with mixotrophic growth achieved profitability, with a Net Present Value (NPV) of 42.5 million USD and Profitability Index (PI) of 2.4. However, glucose use raises sustainability concerns due to competition with food for arable land. Phototrophic titres were too low for economic viability of lower value products such as bioemulsifiers. However, modelling high value products, such as cosmeceuticals with UV-protective and antioxidant properties, showed strong economic potential (NPV of 892 million USD and PI of 7.4). Therefore, the author of this PhD thesis aligns with the consensus in the literature that commercialisation of cyanobacterial EPS should focus on high value applications [11, 21].

In conclusion, this PhD project has addressed several challenges associated with cyanobacterial EPS production and laid important groundwork for further research into the commercialisation of cyanobacterial EPS. By identifying promising species, optimising cultivation conditions, illustrating scale-up challenges, and performing the first-of-its-kind TEA on phototrophic EPS production, this work advances the field and demonstrates the commercial potential of cyanobacterial EPS production, contributing to a sustainable bio-based economy.

Chapter 11: Bibliography

[1] J. Wang and W. Azam, "Natural resource scarcity, fossil fuel energy consumption, and total greenhouse gas emissions in top emitting countries," *Geoscience Frontiers,* vol. 15, no. 2, p. 101757, 2024.

[2] V. Beghetto *et al.*, "Plastics today: Key challenges and EU strategies towards carbon neutrality: A review," *Environmental Pollution,* p. 122102, 2023.

[3] D. Cruz, V. Vasconcelos, G. Pierre, P. Michaud, and C. Delattre, "Exopolysaccharides from cyanobacteria: strategies for bioprocess development," *Applied Sciences,* vol. 10, no. 11, p. 3763, 2020.

[4] A. J. Victoria, M. J. Astbury, and A. J. McCormick, "Engineering highly productive cyanobacteria towards carbon negative emissions technologies," *Current opinion in biotechnology,* vol. 87, p. 103141, 2024.

[5] D. Westlake, "Comparisons of plant productivity," *Biological Reviews,* vol. 38, no. 3, pp. 385-425, 1963.

[6] S. Paul, S. Bera, R. Dasgupta, S. Mondal, and S. Roy, "Review on the recent structural advances in open and closed systems for carbon capture through algae," *Energy Nexus,* vol. 4, p. 100032, 2021.

[7] K. M. Weyer, D. R. Bush, A. Darzins, and B. D. Willson, "Theoretical maximum algal oil production," *Bioenergy Research,* vol. 3, pp. 204-213, 2010.

[8] G. Markou and F. Monlau, "Nutrient recycling for sustainable production of algal biofuels," in *Biofuels from algae*: Elsevier, 2019, pp. 109-133.

[9] M. A. Borowitzka, "High-value products from microalgae—their development and commercialisation," *Journal of applied phycology,* vol. 25, pp. 743-756, 2013.

[10] L. Brennan and P. Owende, "Biofuels from microalgae—a review of technologies for production, processing, and extractions of biofuels and co-products," *Renewable and sustainable energy reviews,* vol. 14, no. 2, pp. 557-577, 2010.

[11] S. B. Pereira *et al.*, "Strategies to obtain designer polymers based on cyanobacterial extracellular polymeric substances (EPS)," *International journal of molecular sciences,* vol. 20, no. 22, p. 5693, 2019.

[12] A. P. S. Yadav, V. Dwivedi, S. Kumar, A. Kushwaha, L. Goswami, and B. S. Reddy, "Cyanobacterial extracellular polymeric substances for heavy metal removal: a mini review," *Journal of Composites Science,* vol. 5, no. 1, p. 1, 2020.

[13] L. Z. Chen, G. H. Wang, S. Hong, A. Liu, C. Li, and Y. D. Liu, "UV-B-induced oxidative damage and protective role of exopolysaccharides in desert cyanobacterium Microcoleus vaginatus," *Journal of Integrative Plant Biology,* vol. 51, no. 2, pp. 194-200, 2009.

[14] D. R. Hill, T. W. Keenan, R. F. Helm, M. Potts, L. M. Crowe, and J. H. Crowe, "Extracellular polysaccharide of Nostoc commune (Cyanobacteria) inhibits fusion of membrane vesicles during desiccation," *Journal of Applied Phycology,* vol. 9, pp. 237-248, 1997.

[15] G. Colica and R. D. Philippis, "Exopolysaccharides from cyanobacteria and their possible industrial applications," *Cyanobacteria: an economic perspective,* pp. 197-207, 2014.

[16] R. M. Abed, S. Dobretsov, and K. Sudesh, "Applications of cyanobacteria in biotechnology," *Journal of applied microbiology,* vol. 106, no. 1, pp. 1-12, 2009.

[17] I. Anestopoulos *et al.*, "Marine-derived surface active agents: Health-promoting properties and blue biotechnology-based applications," *Biomolecules,* vol. 10, no. 6, p. 885, 2020.

[18] I. W. Sutherland, "Structure-function relationships in microbial exopolysaccharides," *Biotechnology advances,* vol. 12, no. 2, pp. 393-448, 1994.

[19] R. De Philippis and M. Vincenzini, "Exocellular polysaccharides from cyanobacteria and their possible applications," *FEMS Microbiology Reviews,* vol. 22, no. 3, pp. 151-175, 1998.

[20] S. Pereira, A. Zille, E. Micheletti, P. Moradas-Ferreira, R. De Philippis, and P. Tamagnini, "Complexity of cyanobacterial exopolysaccharides: composition, structures, inducing factors and putative genes involved in their biosynthesis and assembly," *FEMS microbiology reviews,* vol. 33, no. 5, pp. 917-941, 2009.

[21] G. Pierre *et al.*, "What is in store for EPS microalgae in the next decade?," *Molecules,* vol. 24, no. 23, p. 4296, 2019.

[22] Market Research Future. "Global Emulsifiers Market Overview." https://www.marketresearchfuture.com/reports/emulsifiers-market-1717and (accessed July 12, 2024.

[23] N. R. Ngatu *et al.*, "Anti-inflammatory effects of sacran, a novel polysaccharide from Aphanothece sacrum, on 2, 4, 6-trinitrochlorobenzene–induced allergic dermatitis in vivo," *Annals of Allergy, Asthma & Immunology,* vol. 108, no. 2, pp. 117-122. e2, 2012.
[24] K. Hayashi, T. Hayashi, and I. Kojima, "A natural sulfated polysaccharide, calcium spirulan, isolated from Spirulina platensis: in vitro and ex vivo evaluation of anti-herpes simplex virus and anti-human immunodeficiency virus activities," *AIDS research and human retroviruses,* vol. 12, no. 15, pp. 1463-1471, 1996.
[25] K. Kanekiyo *et al.*, "Isolation of an antiviral polysaccharide, nostoflan, from a terrestrial cyanobacterium, Nostoc f lagelliforme," *Journal of natural products,* vol. 68, no. 7, pp. 1037-1041, 2005.
[26] A. Fattom and M. Shilo, "Production of emulcyan by Phormidium J-1: its activity and function," *FEMS Microbiology Letters,* vol. 31, no. 1, pp. 3-9, 1985.
[27] M. Šutovská *et al.*, "The chemical profile and pharmacodynamic properties of extracellular Wollea saccata biopolymer," *International journal of biological macromolecules,* vol. 103, pp. 863-869, 2017.
[28] C. Gaignard *et al.*, "Screening of marine microalgae: Investigation of new exopolysaccharide producers," *Algal Research,* vol. 44, p. 101711, 2019.
[29] N. Prybylski *et al.*, "Bioactive polysaccharides from microalgae," in *Handbook of microalgae-based processes and products*: Elsevier, 2020, pp. 533-571.
[30] M. Jha, G. Venkataraman, and B. Kaushik, "Response of Westiellopsis prolifica and Anabaena sp. to salt stress," *MIRCEN journal of Applied Microbiology and Biotechnology,* vol. 3, pp. 307-317, 1987.
[31] J. Hou *et al.*, "Effects of CeO 2, CuO, and ZnO nanoparticles on physiological features of Microcystis aeruginosa and the production and composition of extracellular polymeric substances," *Environmental Science and Pollution Research,* vol. 24, pp. 226-235, 2017.
[32] D. Borah *et al.*, "Biolubricant potential of exopolysaccharides from the cyanobacterium Cyanothece epiphytica," *Applied microbiology and biotechnology,* vol. 102, pp. 3635-3647, 2018.
[33] A. Otero and M. Vincenzini, "Nostoc (cyanophyceae) goes nude: Extracellular polysaccharides serve as a sink for reducing power under unbalanced c/n metabolism 1," *Journal of Phycology,* vol. 40, no. 1, pp. 74-81, 2004.
[34] Z.-X. Wu and L.-R. Song, "Physiological comparison between colonial and unicellular forms of Microcystis aeruginosa Kütz.(Cyanobacteria)," *Phycologia,* vol. 47, no. 1, pp. 98-104, 2008.
[35] Y. Liu *et al.*, "Structural characterization of a bioactive water-soluble heteropolysaccharide from Nostoc sphaeroids kütz," *Carbohydrate Polymers,* vol. 200, pp. 552-559, 2018.
[36] Z. Yang and F. Kong, "Abiotic factors in colony formation: effects of nutrition and light on extracellular polysaccharide production and cell aggregates of Microcystis aeruginosa," *Chinese Journal of Oceanology and Limnology,* vol. 31, no. 4, pp. 796-802, 2013.
[37] R. L. Oliver, "Floating and sinking in gas-vacuolate cyanobacteria," *Journal of phycology,* vol. 30, no. 2, 1994.
[38] Y. Li and D. Li, "Physiological variations of bloom-forming Microcystis (Cyanophyceae) related to colony size changes during blooms," *Phycologia,* vol. 51, no. 6, pp. 599-603, 2012.
[39] R. De Philippis, M. C. Margheri, R. Materassi, and M. Vincenzini, "Potential of unicellular cyanobacteria from saline environments as exopolysaccharide producers," *Applied and Environmental Microbiology,* vol. 64, no. 3, pp. 1130-1132, 1998.
[40] C. Delattre, G. Pierre, C. Laroche, and P. Michaud, "Production, extraction and characterization of microalgal and cyanobacterial exopolysaccharides," *Biotechnology advances,* vol. 34, no. 7, pp. 1159-1179, 2016.
[41] B. Nicolaus *et al.*, "Chemical composition and production of exopolysaccharides from representative members of heterocystous and non-heterocystous cyanobacteria," *Phytochemistry,* vol. 52, no. 4, pp. 639-647, 1999.
[42] R. Chug and S. Mathur, "Extracellular polymeric substances from cyanobacteria: Characteristics, isolation and biotechnological applications-A," *International Journal of Engineering, Science and Technology,* vol. 3, pp. 49-53, 2013.
[43] F. Di Pippo *et al.*, "Characterization of exopolysaccharides produced by seven biofilm-forming cyanobacterial strains for biotechnological applications," *Journal of applied phycology,* vol. 25, pp. 1697-1708, 2013.
[44] O. N. Tiwari, R. Khangembam, M. Shamjetshabam, A. S. Sharma, G. Oinam, and J. J. Brand, "Characterization and optimization of bioflocculant exopolysaccharide production by cyanobacteria Nostoc sp. BTA97 and Anabaena sp. BTA990 in culture conditions," *Applied biochemistry and biotechnology,* vol. 176, pp. 1950-1963, 2015.

[45] R. Khangembam, O. N. Tiwari, and M. Kalita, "Production of exopolysaccharides by the cyanobacterium Anabaena sp. BTA992 and application as bioflocculants," *J. Appl. Biol. Biotechnol,* vol. 4, no. 1, pp. 008-011, 2016.
[46] M. Phélippé, O. Gonçalves, G. Thouand, G. Cogne, and C. Laroche, "Characterization of the polysaccharides chemical diversity of the cyanobacteria Arthrospira platensis," *Algal Research,* vol. 38, p. 101426, 2019.
[47] C. Laroche, "Exopolysaccharides from microalgae and cyanobacteria: diversity of strains, production strategies, and applications," *Marine drugs,* vol. 20, no. 5, p. 336, 2022.
[48] R. d. Philippis and M. Vincenzini, "Outermost polysaccharidic investments of cyanobacteria: nature, significance and possible applications," 2003.
[49] L. Liu, G. Pohnert, and D. Wei, "Extracellular metabolites from industrial microalgae and their biotechnological potential," *Marine drugs,* vol. 14, no. 10, p. 191, 2016.
[50] I. Uhliariková, B. Chválová, M. Matulová, V. Cepák, J. Lukavský, and P. Capek, "Extracellular biopolymers produced by freshwater cyanobacteria: A screening study," *Chemical Papers,* vol. 73, pp. 771-776, 2019.
[51] V. Vicente-García, E. Ríos-Leal, G. Calderón-Domínguez, R. O. Cañizares-Villanueva, and R. Olvera-Ramírez, "Detection, isolation, and characterization of exopolysaccharide produced by a strain of Phormidium 94a isolated from an arid zone of Mexico," *Biotechnology and bioengineering,* vol. 85, no. 3, pp. 306-310, 2004.
[52] H.-W. Chen, W.-J. Huang, T.-H. Wu, and C.-L. Hon, "Effects of extracellular polymeric substances on the bioaccumulation of mercury and its toxicity toward the cyanobacterium Microcystis aeruginosa," *Journal of Environmental Science and Health, Part A,* vol. 49, no. 12, pp. 1370-1379, 2014.
[53] R. M. Zampieri *et al.*, "Anti-inflammatory activity of exopolysaccharides from Phormidium sp. ETS05, the most abundant cyanobacterium of the therapeutic Euganean thermal muds, using the zebrafish model," *Biomolecules,* vol. 10, no. 4, p. 582, 2020.
[54] A. Parikh and D. Madamwar, "Partial characterization of extracellular polysaccharides from cyanobacteria," *Bioresource Technology,* vol. 97, no. 15, pp. 1822-1827, 2006.
[55] C. Su, Z. Chi, and W. Lu, "Optimization of medium and cultivation conditions for enhanced exopolysaccharide yield by marine Cyanothece sp. 113," *Chinese Journal of Oceanology and Limnology,* vol. 25, pp. 411-417, 2007.
[56] Y. Chisti, "Biodiesel from microalgae," *Biotechnology advances,* vol. 25, no. 3, pp. 294-306, 2007.
[57] H. Barberousse *et al.*, "Capsular polysaccharides secreted by building façade colonisers: characterisation and adsorption to surfaces," *Biofouling,* vol. 22, no. 6, pp. 361-370, 2006.
[58] J. L. Plude *et al.*, "Chemical characterization of polysaccharide from the slime layer of the cyanobacterium Microcystis flos-aquae C3-40," *Applied and environmental microbiology,* vol. 57, no. 6, pp. 1696-1700, 1991.
[59] H. Sudo, J. G. Burgess, H. Takemasa, N. Nakamura, and T. Matsunaga, "Sulfated exopolysaccharide production by the halophilic cyanobacterium Aphanocapsa halophytia," *Current Microbiology,* vol. 30, pp. 219-222, 1995.
[60] C. Hu, Y. Liu, B. S. Paulsen, D. Petersen, and D. Klaveness, "Extracellular carbohydrate polymers from five desert soil algae with different cohesion in the stabilization of fine sand grain," *Carbohydrate polymers,* vol. 54, no. 1, pp. 33-42, 2003.
[61] L. Trabelsi, N. H. M'sakni, H. Ben Ouada, H. Bacha, and S. Roudesli, "Partial characterization of extracellular polysaccharides produced by cyanobacterium Arthrospira platensis," *Biotechnology and Bioprocess Engineering,* vol. 14, pp. 27-31, 2009.
[62] M. H. Hussein, R. A. Hamouda, A. M. A. Elhadary, M. A. Abuelmagd, S. Ali, and M. Rizwan, "Characterization and chromium biosorption potential of extruded polymeric substances from Synechococcus mundulus induced by acute dose of gamma irradiation," *Environmental Science and Pollution Research,* vol. 26, pp. 31998-32012, 2019.
[63] R. Mota *et al.*, "Production and characterization of extracellular carbohydrate polymer from Cyanothece sp. CCY 0110," *Carbohydrate Polymers,* vol. 92, no. 2, pp. 1408-1415, 2013.
[64] C. S. de Jesus *et al.*, "Pilot-scale isolation and characterization of extracellular polymeric substances (EPS) from cell-free medium of Spirulina sp. LEB-18 cultures under outdoor conditions," *International journal of biological macromolecules,* vol. 124, pp. 1106-1114, 2019.
[65] V. K. Sangar and P. R. Dugan, "Polysaccharide produced by Anacystis nidulans: its ecological implication," *Applied microbiology,* vol. 24, no. 5, pp. 732-734, 1972.
[66] M. Ahmed, T. C. Moerdijk-Poortvliet, A. Wijnholds, L. J. Stal, and S. Hasnain, "Isolation, characterization and localization of extracellular polymeric substances from the cyanobacterium

Arthrospira platensis strain MMG-9," *European Journal of Phycology,* vol. 49, no. 2, pp. 143-150, 2014.
[67] I. Chentir *et al.*, "Enhancement of extracellular polymeric substances (EPS) production in Spirulina (Arthrospira sp.) by two-step cultivation process and partial characterization of their polysaccharidic moiety," *International journal of biological macromolecules,* vol. 105, pp. 1412-1420, 2017.
[68] D. Fischer, U. Schlösser, and P. Pohl, "Exopolysaccharide production by cyanobacteria grown in closed photobioreactors and immobilized using white cotton towelling," *Journal of applied phycology,* vol. 9, pp. 205-213, 1997.
[69] R. Mota *et al.*, "Cyanoflan: A cyanobacterial sulfated carbohydrate polymer with emulsifying properties," *Carbohydrate polymers,* vol. 229, p. 115525, 2020.
[70] H. Ge, L. Xia, X. Zhou, D. Zhang, and C. Hu, "Effects of light intensity on components and topographical structures of extracellular polysaccharides from the cyanobacteria Nostoc sp," *Journal of Microbiology,* vol. 52, no. 2, pp. 179-183, 2014.
[71] Q. Wang and Y. Fang, "Analysis of sugars in traditional Chinese drugs," *Journal of Chromatography b,* vol. 812, no. 1-2, pp. 309-324, 2004.
[72] A. Decamp *et al.*, "A new, quick, and simple protocol to evaluate microalgae polysaccharide composition," *Marine drugs,* vol. 19, no. 2, p. 101, 2021.
[73] I. Uhliariková, M. Matulová, and P. Capek, "Optimizing acid hydrolysis for monosaccharide compositional analysis of Nostoc cf. linckia acidic exopolysaccharide," *Carbohydrate Research,* vol. 508, p. 108400, 2021.
[74] K. A. Taylor and J. G. Buchanan-Smith, "A colorimetric method for the quantitation of uronic acids and a specific assay for galacturonic acid," *Analytical Biochemistry,* vol. 201, no. 1, pp. 190-196, 1992.
[75] N. Blumenkrantz and G. Asboe-Hansen, "New method for quantitative determination of uronic acids," *Analytical biochemistry,* vol. 54, no. 2, pp. 484-489, 1973.
[76] M. Dubois, K. Gilles, J. Hamilton, P. Rebers, and F. Smith, "A colorimetric method for the determination of sugars," *Nature,* vol. 168, no. 4265, pp. 167-167, 1951.
[77] R. G. Spiro, "[1] Analysis of sugars found in glycoproteins," in *Methods in enzymology*, vol. 8: Elsevier, 1966, pp. 3-26.
[78] D. Strieth, A. Schwarz, J. Stiefelmaier, N. Erdmann, K. Muffler, and R. Ulber, "New procedure for separation and analysis of the main components of cyanobacterial EPS," *Journal of Biotechnology,* vol. 328, pp. 78-86, 2021.
[79] Y. Zhou *et al.*, "Microalgal extracellular polymeric substances (EPS) and their roles in cultivation, biomass harvesting, and bioproducts extraction," *Bioresource Technology,* p. 131054, 2024.
[80] P. B. Torres, A. Nagai, C. E. P. Jara, J. P. Santos, F. Chow, and D. Y. A. C. d. Santos, "Determination of sulfate in algal polysaccharide samples: a step-by-step protocol using microplate reader," *Ocean and Coastal Research,* vol. 69, p. e21021, 2021.
[81] J. Park *et al.*, "Easy and rapid quantification of lipid contents of marine dinoflagellates using the sulpho-phospho-vanillin method," *Algae,* vol. 31, no. 4, pp. 391-401, 2016.
[82] S. Debnath *et al.*, "Engineering strategies and applications of cyanobacterial exopolysaccharides: A review on past achievements and recent perspectives," *Carbohydrate Polymers,* p. 121686, 2023.
[83] S.-G. Shen *et al.*, "Comparisons of functional properties of polysaccharides from Nostoc flagelliforme under three culture conditions," *Polymers,* vol. 11, no. 2, p. 263, 2019.
[84] E. D. Ngouémazong, S. Christiaens, A. Shpigelman, A. Van Loey, and M. Hendrickx, "The emulsifying and emulsion-stabilizing properties of pectin: A review," *Comprehensive Reviews in Food Science and Food Safety,* vol. 14, no. 6, pp. 705-718, 2015.
[85] Q. Tang and G. Huang, "Improving method, properties and application of polysaccharide as emulsifier," *Food chemistry,* vol. 376, p. 131937, 2022.
[86] E. Dickinson, "Hydrocolloids at interfaces and the influence on the properties of dispersed systems," *Food hydrocolloids,* vol. 17, no. 1, pp. 25-39, 2003.
[87] E. Dickinson, "Emulsion stabilization by polysaccharides and protein-polysaccharide complexes," *FOOD SCIENCE AND TECHNOLOGY-NEW YORK-MARCEL DEKKER-,* pp. 501-501, 1995.
[88] H. Zhang *et al.*, "Mechanistic understanding of the relationships between molecular structure and emulsification properties of octenyl succinic anhydride (OSA) modified starches," *Food Hydrocolloids,* vol. 74, pp. 168-175, 2018.
[89] D. Kavitake, S. Balyan, P. B. Devi, and P. H. Shetty, "Evaluation of oil-in-water (O/W) emulsifying properties of galactan exopolysaccharide from Weissella confusa KR780676," *Journal of food science and technology,* vol. 57, pp. 1579-1585, 2020.

[90] I. M. Banat, R. S. Makkar, and S. S. Cameotra, "Potential commercial applications of microbial surfactants," *Applied microbiology and biotechnology,* vol. 53, pp. 495-508, 2000.
[91] M. Fuji, "3.4 ADSORPTION PROPERTIES AND WETTABILITY OF NANOPARTICLE SURFACE," *Nanoparticle Technology Handbook,* p. 121, 2018.
[92] S. Bonilla T and D. G. Allen, "Flocculation with Lysozyme: A Non-Enzymatic Application," *The Canadian Journal of Chemical Engineering,* vol. 94, no. 2, pp. 231-237, 2016.
[93] C. S. Lee, J. Robinson, and M. F. Chong, "A review on application of flocculants in wastewater treatment," *Process safety and environmental protection,* vol. 92, no. 6, pp. 489-508, 2014.
[94] T. Kuroiwa, I. Kobayashi, A. M. Chuah, M. Nakajima, and S. Ichikawa, "Formulation and stabilization of nano-/microdispersion systems using naturally occurring edible polyelectrolytes by electrostatic deposition and complexation," *Advances in Colloid and Interface Science,* vol. 226, pp. 86-100, 2015.
[95] F. Roselet, D. Vandamme, M. Roselet, K. Muylaert, and P. C. Abreu, "Screening of commercial natural and synthetic cationic polymers for flocculation of freshwater and marine microalgae and effects of molecular weight and charge density," *Algal research,* vol. 10, pp. 183-188, 2015.
[96] J. Gregory and C. R. O'Melia, "Fundamentals of flocculation," *Critical Reviews in Environmental Science and Technology,* vol. 19, no. 3, pp. 185-230, 1989.
[97] J. Caskey and R. Primus, "The effect of anionic polyacrylamide molecular conformation and configuration on flocculation effectiveness," *Environmental progress,* vol. 5, no. 2, pp. 98-103, 1986.
[98] B. Bolto and J. Gregory, "Organic polyelectrolytes in water treatment," *Water research,* vol. 41, no. 11, pp. 2301-2324, 2007.
[99] M. Razali, Z. Ahmad, M. Ahmad, and A. Ariffin, "Treatment of pulp and paper mill wastewater with various molecular weight of polyDADMAC induced flocculation," *Chemical Engineering Journal,* vol. 166, no. 2, pp. 529-535, 2011.
[100] M. Lapointe and B. Barbeau, "Understanding the roles and characterizing the intrinsic properties of synthetic vs. natural polymers to improve clarification through interparticle Bridging: A review," *Separation and Purification Technology,* vol. 231, p. 115893, 2020.
[101] J. Labille, F. Thomas, M. Milas, and C. Vanhaverbeke, "Flocculation of colloidal clay by bacterial polysaccharides: effect of macromolecule charge and structure," *Journal of colloid and interface science,* vol. 284, no. 1, pp. 149-156, 2005.
[102] J. C. Zambrano and T. A. Vilgis, "Tunable oleosome-based oleogels: influence of polysaccharide type for polymer bridging-based structuring," *Food Hydrocolloids,* vol. 137, p. 108399, 2023.
[103] B. S. Gupta and J. E. Ako, "Application of guar gum as a flocculant aid in food processing and potable water treatment," *European Food Research and Technology,* vol. 221, pp. 746-751, 2005.
[104] E. Baldev, D. MubarakAli, R. Shriraman, D. Pandiaraj, N. Alharbi, and N. Thajuddin, "Extraction and partial characterization of exopolysaccharides from marine cyanobacteria and their flocculation property," 2015.
[105] A. Banerjee *et al.*, "Optimization and characterization of a novel exopolysaccharide from Bacillus haynesii CamB6 for food applications," *Biomolecules,* vol. 12, no. 6, p. 834, 2022.
[106] D.-P. Xu *et al.*, "Natural antioxidants in foods and medicinal plants: Extraction, assessment and resources," *International journal of molecular sciences,* vol. 18, no. 1, p. 96, 2017.
[107] M. Andrew and G. Jayaraman, "Structural features of microbial exopolysaccharides in relation to their antioxidant activity," *Carbohydrate research,* vol. 487, p. 107881, 2020.
[108] L. Parwani, M. Bhatnagar, A. Bhatnagar, and V. Sharma, "Antioxidant and iron-chelating activities of cyanobacterial exopolymers with potential for wound healing," *Journal of applied phycology,* vol. 26, pp. 1473-1482, 2014.
[109] P. He, L. Geng, J. Wang, Z. Wang, D. Mao, and C. Xu, "Purification, characterization and bioactivity of an extracellular polysaccharide produced from Phellinus igniarius," *Annals of microbiology,* vol. 62, pp. 1697-1707, 2012.
[110] L. Meng, S. Sun, R. Li, Z. Shen, P. Wang, and X. Jiang, "Antioxidant activity of polysaccharides produced by Hirsutella sp. and relation with their chemical characteristics," *Carbohydrate Polymers,* vol. 117, pp. 452-457, 2015.
[111] J.-Q. Zheng, J.-Z. Wang, C.-W. Shi, D.-B. Mao, P.-X. He, and C.-P. Xu, "Characterization and antioxidant activity for exopolysaccharide from submerged culture of Boletus aereus," *Process Biochemistry,* vol. 49, no. 6, pp. 1047-1053, 2014.
[112] S. Li *et al.*, "Molecular modification of polysaccharides and resulting bioactivities," *Comprehensive Reviews in Food Science and Food Safety,* vol. 15, no. 2, pp. 237-250, 2016.

[113] S. B. Majee, D. Avlani, and G. R. Biswas, "Molecular modification of marine sulfated polysaccharides," in *Enzymatic Technologies for Marine Polysaccharides*: CRC Press, 2019, pp. 395-416.
[114] Y. Wu, M. Ye, Z. Du, L. Jing, M. M. Surhio, and L. Yang, "Carboxymethylation of an exopolysaccharide from Lachnum and effect of its derivatives on experimental chronic renal failure," *Carbohydrate polymers,* vol. 114, pp. 190-195, 2014.
[115] X. Du, J. Zhang, Z. Lv, L. Ye, Y. Yang, and Q. Tang, "Chemical modification of an acidic polysaccharide (TAPA1) from Tremella aurantialba and potential biological activities," *Food chemistry,* vol. 143, pp. 336-340, 2014.
[116] H. Sashiwa and S.-i. Aiba, "Chemically modified chitin and chitosan as biomaterials," *Progress in polymer science,* vol. 29, no. 9, pp. 887-908, 2004.
[117] W. Gongi, N. Cordeiro, J. L. G. Pinchetti, and H. B. Ouada, "Functional, rheological, and antioxidant properties of extracellular polymeric substances produced by a thermophilic cyanobacterium Leptolyngbya sp," *Journal of Applied Phycology,* vol. 34, no. 3, pp. 1423-1434, 2022.
[118] W. Gongi, J. L. Gomez Pinchetti, N. Cordeiro, and H. B. Ouada, "Extracellular polymeric substances produced by the Thermophilic Cyanobacterium Gloeocapsa gelatinosa: Characterization and assessment of their antioxidant and metal-chelating activities," *Marine Drugs,* vol. 20, no. 4, p. 227, 2022.
[119] C. Leyva-Porras, M. Román-Aguirre, P. Cruz-Alcantar, J. T. Pérez-Urizar, and M. Z. Saavedra-Leos, "Application of antioxidants as an alternative improving of shelf life in foods," *Polysaccharides,* vol. 2, no. 3, pp. 594-607, 2021.
[120] P. Adegbola, I. Aderibigbe, W. Hammed, and T. Omotayo, "Antioxidant and anti-inflammatory medicinal plants have potential role in the treatment of cardiovascular disease: a review," *American journal of cardiovascular disease,* vol. 7, no. 2, p. 19, 2017.
[121] J. Pokorny, N. Yanishlieva, and M. H. Gordon, *Antioxidants in food: practical applications*. CRC press, 2001.
[122] V. Raikos, "Natural antioxidants for food applications: challenges and recent developments," *EC Nutrition,* 2017.
[123] H. Verhagen, P. A. Schilderman, and J. C. Kleinjans, "Butylated hydroxyanisole in perspective," *Chemico-biological interactions,* vol. 80, no. 2, pp. 109-134, 1991.
[124] R. S. Lanigan and T. A. Yamarik, "Final report on the safety assessment of BHT (1)," *International journal of toxicology,* vol. 21, pp. 19-94, 2002.
[125] M. Taghvaei and S. M. Jafari, "Application and stability of natural antioxidants in edible oils in order to substitute synthetic additives," *Journal of food science and technology,* vol. 52, pp. 1272-1282, 2015.
[126] J. Morone, A. Alfeus, V. Vasconcelos, and R. Martins, "Revealing the potential of cyanobacteria in cosmetics and cosmeceuticals—A new bioactive approach," *Algal Research,* vol. 41, p. 101541, 2019.
[127] H. Bayr, "Reactive oxygen species," *Critical care medicine,* vol. 33, no. 12, pp. S498-S501, 2005.
[128] C. F. Liu, K. C. Tseng, S. S. Chiang, B. H. Lee, W. H. Hsu, and T. M. Pan, "Immunomodulatory and antioxidant potential of Lactobacillus exopolysaccharides," *Journal of the Science of Food and Agriculture,* vol. 91, no. 12, pp. 2284-2291, 2011.
[129] V. A. Timoshnikov, T. V. Kobzeva, N. E. Polyakov, and G. J. Kontoghiorghes, "Redox interactions of vitamin C and iron: Inhibition of the pro-oxidant activity by deferiprone," *International journal of molecular sciences,* vol. 21, no. 11, p. 3967, 2020.
[130] R. C. Lindsay, "Food additives," in *Fennema's food chemistry*: CRC Press, 2007, pp. 701-762.
[131] Y. V. Yuan, D. E. Bone, and M. F. Carrington, "Antioxidant activity of dulse (Palmaria palmata) extract evaluated in vitro," *Food chemistry,* vol. 91, no. 3, pp. 485-494, 2005.
[132] I. Uhliariková, M. Matulová, Z. Košťálová, J. Lukavský, and P. Capek, "Lactylated acidic exopolysaccharide produced by the cyanobacterium Nostoc cf. linckia," *Carbohydrate Polymers,* vol. 276, p. 118801, 2022.
[133] H. El Khadem, *Carbohydrate chemistry: monosaccharides and their oligomers*. Elsevier, 2012.
[134] A. Kastin, *Handbook of biologically active peptides*. Academic press, 2013.
[135] S. Eckert *et al.*, "From the free ligand to the transition metal complex: FeEDTA–formation seen at ligand K-edges," *Inorganic Chemistry,* vol. 61, no. 27, pp. 10321-10328, 2022.
[136] C. Oviedo and J. Rodríguez, "EDTA: the chelating agent under environmental scrutiny," *Quimica Nova,* vol. 26, pp. 901-905, 2003.

[137] R. P. Rastogi, D. Madamwar, H. Nakamoto, and A. Incharoensakdi, "Resilience and self-regulation processes of microalgae under UV radiation stress," *Journal of Photochemistry and Photobiology C: Photochemistry Reviews,* vol. 43, p. 100322, 2020.
[138] S. Gabros, T. A. Nessel, and P. M. Zito, "Sunscreens and photoprotection," 2019.
[139] M. Martínez-Ruiz *et al.*, "Microalgae bioactive compounds to topical applications products—a review," *Molecules,* vol. 27, no. 11, p. 3512, 2022.
[140] N. Shaath and M. Shaath, "Recent sunscreen market trends," *Sunscreens, regulations and commercial development, 3rd edn. Taylor & Francis, Boca Raton,* pp. 929-940, 2005.
[141] D. Schmid, C. Schürch, and F. Zülli, "Mycosporine-like amino acids from red algae protect against premature skin-aging," *Euro Cosmet,* vol. 9, pp. 1-4, 2006.
[142] N. Serpone, D. Dondi, and A. Albini, "Inorganic and organic UV filters: Their role and efficacy in sunscreens and suncare products," *Inorganica chimica acta,* vol. 360, no. 3, pp. 794-802, 2007.
[143] E. Manová, N. von Goetz, U. Hauri, C. Bogdal, and K. Hungerbühler, "Organic UV filters in personal care products in Switzerland: a survey of occurrence and concentrations," *International journal of hygiene and environmental health,* vol. 216, no. 4, pp. 508-514, 2013.
[144] M. Avenel-Audran *et al.*, "Octocrylene, an emerging photoallergen," *Archives of dermatology,* vol. 146, no. 7, pp. 753-757, 2010.
[145] D. Oral, A. Yirun, and P. Erkekoglu, "Safety concerns of organic ultraviolet filters: special focus on endocrine-disrupting properties," *Journal of Environmental Pathology, Toxicology and Oncology,* vol. 39, no. 3, 2020.
[146] M. M. Tsui *et al.*, "Occurrence, distribution and ecological risk assessment of multiple classes of UV filters in surface waters from different countries," *Water research,* vol. 67, pp. 55-65, 2014.
[147] V. Castro, R. Oliveira, and A. C. Dias, "Microalgae and cyanobacteria as sources of bioactive compounds for cosmetic applications: A systematic review," *Algal Research,* p. 103287, 2023.
[148] N. Sajinčič, O. Gordobil, A. Simmons, and A. Sandak, "An exploratory study of consumers' knowledge and attitudes about lignin-based sunscreens and bio-based skincare products," *Cosmetics,* vol. 8, no. 3, p. 78, 2021.
[149] W. Bandaranayake, "Mycosporines: are they nature's sunscreens?," *Natural Product Reports,* vol. 15, no. 2, pp. 159-172, 1998.
[150] L. Núñez-Pons, C. Avila, G. Romano, C. Verde, and D. Giordano, "UV-protective compounds in marine organisms from the Southern Ocean," *Marine drugs,* vol. 16, no. 9, p. 336, 2018.
[151] R. P. Sinha, S. P. Singh, and D.-P. Häder, "Database on mycosporines and mycosporine-like amino acids (MAAs) in fungi, cyanobacteria, macroalgae, phytoplankton and animals," *Journal of Photochemistry and Photobiology B: Biology,* vol. 89, no. 1, pp. 29-35, 2007.
[152] S. Bhatia, K. Sharma, A. G. Namdeo, B. Chaugule, M. Kavale, and S. Nanda, "Broad-spectrum sun-protective action of Porphyra-334 derived from Porphyra vietnamensis," *Pharmacognosy research,* vol. 2, no. 1, p. 45, 2010.
[153] D. Ručová *et al.*, "Photoprotective and antioxidant properties of scytonemin isolated from Antarctic cyanobacterium Nostoc commune Vaucher ex Bornet & Flahault and its potential as sunscreen ingredient," *Journal of Applied Phycology,* vol. 35, no. 6, pp. 2839-2850, 2023.
[154] F. de la Coba *et al.*, "UVA and UVB photoprotective capabilities of topical formulations containing mycosporine-like amino acids (MAAs) through different biological effective protection factors (BEPFs)," *Marine drugs,* vol. 17, no. 1, p. 55, 2019.
[155] R. P. Sinha, M. Klisch, A. Vaishampayan, and D.-P. Häder, "Biochemical and spectroscopic characterization of the cyanobacterium Lyngbya sp. inhabiting Mango (Mangifera indica) trees: presence of an ultraviolet-absorbing pigment, scytonemin," *Acta Protozool,* vol. 38, no. 4, pp. 291-298, 1999.
[156] F. Garcia-Pichel and R. W. Castenholz, "Characterization and biological implications of scytonemin, a cyanobacterial sheath pigment 1," *Journal of Phycology,* vol. 27, no. 3, pp. 395-409, 1991.
[157] R. P. Rastogi and A. Incharoensakdi, "Characterization of UV-screening compounds, mycosporine-like amino acids, and scytonemin in the cyanobacterium Lyngbya sp. CU2555," *FEMS microbiology ecology,* vol. 87, no. 1, pp. 244-256, 2014.
[158] C. Hu, G. Völler, R. Süßmuth, E. Dittmann, and J. C. Kehr, "Functional assessment of mycosporine-like amino acids in M icrocystis aeruginosa strain PCC 7806," *Environmental microbiology,* vol. 17, no. 5, pp. 1548-1559, 2015.
[159] D. Joshi, C. Mohandass, and M. Dhale, "Effect of UV-B radiation and desiccation stress on photoprotective compounds accumulation in marine Leptolyngbya sp," *Applied biochemistry and biotechnology,* vol. 184, pp. 35-47, 2018.

[160] D. K. Singh *et al.*, "Response of a rice-field cyanobacterium Anabaena sp. HKAR-7 upon exposure to ultraviolet-B radiation and ammonium chloride," *Environmental Sustainability,* vol. 4, no. 1, pp. 95-105, 2021.
[161] H. Yoshimura, S. Okamoto, Y. Tsumuraya, and M. Ohmori, "Group 3 sigma factor gene, sigJ, a key regulator of desiccation tolerance, regulates the synthesis of extracellular polysaccharide in cyanobacterium Anabaena sp. strain PCC 7120," *DNA research,* vol. 14, no. 1, pp. 13-24, 2007.
[162] C. Whitfield and K. Larue, "Stop and go: regulation of chain length in the biosynthesis of bacterial polysaccharides," *Nature structural & molecular biology,* vol. 15, no. 2, pp. 121-123, 2008.
[163] M. Santos *et al.*, "Absence of KpsM (Slr0977) impairs the secretion of extracellular polymeric substances (EPS) and impacts carbon fluxes in Synechocystis sp. PCC 6803," *Msphere,* vol. 6, no. 1, pp. 10.1128/msphere. 00003-21, 2021.
[164] J.-B. Vergnes, V. Gernigon, P. Guiraud, and C. Formosa-Dague, "Bicarbonate concentration induces production of exopolysaccharides by Arthrospira platensis that mediate bioflocculation and enhance flotation harvesting efficiency," *ACS Sustainable Chemistry & Engineering,* vol. 7, no. 16, pp. 13796-13804, 2019.
[165] H. Yu, S. Jia, and Y. Dai, "Accumulation of exopolysaccharides in liquid suspension culture of Nostoc flagelliforme cells," *Applied Biochemistry and Biotechnology,* vol. 160, no. 2, pp. 552-560, 2010.
[166] M. B. Silva, E. G. Azero, C. M. Teixeira, and C. T. Andrade, "Influence of culture conditions on the production of extracellular polymeric substances (EPS) by Arthrospira platensis," *Bioresources and bioprocessing,* vol. 7, no. 1, p. 47, 2020.
[167] H. El-Baky, K. H. El-Baz, and S. El-Latife, "Induction of sulfated polysaccharides in Spirulina platensis as response to nitrogen concentration and its biological evaluation," 2014.
[168] L. Trabelsi, H. Ben Ouada, H. Bacha, and M. Ghoul, "Combined effect of temperature and light intensity on growth and extracellular polymeric substance production by the cyanobacterium Arthrospira platensis," *Journal of Applied Phycology,* vol. 21, pp. 405-412, 2009.
[169] B. Gris, E. Sforza, T. Morosinotto, A. Bertucco, and N. La Rocca, "Influence of light and temperature on growth and high-value molecules productivity from Cyanobacterium aponinum," *Journal of Applied Phycology,* vol. 29, pp. 1781-1790, 2017.
[170] L. Kratky, T. Jirout, and V. Belohlav, "Economic feasibility study for artificial lighting of microalgal flat-panel photobioreactors," *International Journal of Environmental Science and Technology,* vol. 20, no. 11, pp. 12089-12100, 2023.
[171] J. Kvíderová, D. Kumar, J. Lukavský, P. Kaštánek, and S. P. Adhikary, "Estimation of growth and exopolysaccharide production by two soil cyanobacteria, Scytonema tolypothrichoides and Tolypothrix bouteillei as determined by cultivation in irradiance and temperature crossed gradients," *Engineering in Life Sciences,* vol. 19, no. 3, pp. 184-195, 2019.
[172] M. Dejsungkranont, Y. Chisti, and S. Sirisansaneeyakul, "Optimization of production of C-phycocyanin and extracellular polymeric substances by Arthrospira sp," *Bioprocess and biosystems engineering,* vol. 40, no. 8, pp. 1173-1188, 2017.
[173] A. Otero and M. Vincenzini, "Extracellular polysaccharide synthesis by Nostoc strains as affected by N source and light intensity," *Journal of Biotechnology,* vol. 102, no. 2, pp. 143-152, 2003.
[174] P.-p. Han, S.-g. Shen, H.-Y. Wang, Y. Sun, Y.-j. Dai, and S.-r. Jia, "Comparative metabolomic analysis of the effects of light quality on polysaccharide production of cyanobacterium Nostoc flagelliforme," *Algal Research,* vol. 9, pp. 143-150, 2015.
[175] W. Hill, "Effects of light," *Algal ecology: freshwater benthic ecosystems,* pp. 121-148, 1996.
[176] X. Gao, "Scytonemin plays a potential role in stabilizing the exopolysaccharidic matrix in terrestrial cyanobacteria," *Microbial ecology,* vol. 73, no. 2, pp. 255-258, 2017.
[177] P.-p. Han, Y. Sun, S.-r. Jia, C. Zhong, and Z.-l. Tan, "Effects of light wavelengths on extracellular and capsular polysaccharide production by Nostoc flagelliforme," *Carbohydrate polymers,* vol. 105, pp. 145-151, 2014.
[178] J. Khattar *et al.*, "Isolation and characterization of exopolysaccharides produced by the cyanobacterium Limnothrix redekei PUPCCC 116," *Applied biochemistry and biotechnology,* vol. 162, pp. 1327-1338, 2010.
[179] P.-p. Han *et al.*, "Applying the strategy of light environment control to improve the biomass and polysaccharide production of Nostoc flagelliforme," *Journal of Applied Phycology,* vol. 29, no. 1, pp. 55-65, 2017.
[180] N. Jindal, D. Singh, and J. Khattar, "Kinetics and physico-chemical characterization of exopolysaccharides produced by the cyanobacterium Oscillatoria formosa," *World Journal of Microbiology and Biotechnology,* vol. 27, pp. 2139-2146, 2011.

[181] J. Moreno, M. A. Vargas, H. Olivares, J. n. Rivas, and M. G. Guerrero, "Exopolysaccharide production by the cyanobacterium Anabaena sp. ATCC 33047 in batch and continuous culture," *Journal of Biotechnology,* vol. 60, no. 3, pp. 175-182, 1998.
[182] V. Shah, N. Garg, and D. Madamwar, "Exopolysaccharide production by a marine cyanobacterium Cyanothece sp. Application in dye removal by its gelation phenomenon," *Applied Biochemistry and Biotechnology,* vol. 82, no. 2, pp. 81-90, 1999.
[183] R. De Philippis, M. C. Margheri, E. Pelosi, and S. Ventura, "Exopolysaccharide production by a unicellular cyanobacterium isolated from a hypersaline habitat," *Journal of Applied Phycology,* vol. 5, no. 4, pp. 387-394, 1993.
[184] L. Lama, B. Nicolaus, V. Calandrelli, M. C. Manca, I. Romano, and A. Gambacorta, "Effect of growth conditions on endo-and exopolymer biosynthesis in Anabaena cylindrica 10 C," *Phytochemistry,* vol. 42, no. 3, pp. 655-659, 1996.
[185] Z. Chi and S. Zhao, "Optimization of medium and cultivation conditions for pullulan production by a new pullulan-producing yeast strain," *Enzyme and Microbial Technology,* vol. 33, no. 2-3, pp. 206-211, 2003.
[186] R. De Philippis, C. Sili, G. Tassinato, M. Vincenzini, and R. Materassi, "Effects of growth conditions on exopolysaccharide production by Cyanospira capsulata," *Bioresource Technology,* vol. 38, no. 2-3, pp. 101-104, 1991.
[187] X. Ma, M. Li, E. Jiang, B. Pan, and L. Gao, "Humic acid inhibits colony formation of the cyanobacterium Microcystis at high level of iron," *Chemosphere,* vol. 281, p. 130742, 2021.
[188] P. Mateo, I. Bonilla, E. Fernandez-Valiente, and E. Sanchez-Maeso, "Essentiality of boron for dinitrogen fixation in Anabaena sp. PCC 7119," *Plant Physiology,* vol. 81, no. 2, pp. 430-433, 1986.
[189] R. Asthana and S. Singh, "Calcium-boron interaction in exopolysaccharide production by the cyanobacterium, Nostoc spongiaeforme," *Journal of microbiology and biotechnology,* vol. 10, no. 3, pp. 381-385, 2000.
[190] L. Z. Chen, D. H. Li, L. R. Song, C. X. Hu, G. H. Wang, and Y. D. Liu, "Effects of salt stress on carbohydrate metabolism in desert soil alga Microcoleus vaginatus Gom," *Journal of Integrative Plant Biology,* vol. 48, no. 8, pp. 914-919, 2006.
[191] S. Ozturk and B. Aslim, "Modification of exopolysaccharide composition and production by three cyanobacterial isolates under salt stress," *Environmental Science and Pollution Research,* vol. 17, no. 3, pp. 595-602, 2010.
[192] R. De Philippis, C. Sili, and M. Vincenzini, "Response of an exopolysaccharide-producing heterocystous cyanobacterium to changes in metabolic carbon flux," *Journal of Applied Phycology,* vol. 8, no. 4, pp. 275-281, 1996.
[193] E. J. Phlips, C. Zeman, and P. Hansen, "Growth, photosynthesis, nitrogen fixation and carbohydrate production by a unicellular cyanobacterium, Synechococcus sp.(Cyanophyta)," *Journal of Applied Phycology,* vol. 1, no. 2, pp. 137-145, 1989.
[194] Z. Chen *et al.*, "Isolation of a novel strain of Cyanobacterium sp. with good adaptation to extreme alkalinity and high polysaccharide yield," *Journal of Oceanology and Limnology,* vol. 39, no. 3, pp. 1131-1142, 2021.
[195] L. Trabelsi, H. Ben Ouada, F. Zili, N. Mazhoud, and J. Ammar, "Evaluation of Arthrospira platensis extracellular polymeric substances production in photoautotrophic, heterotrophic and mixotrophic conditions," *Folia microbiologica,* vol. 58, no. 1, pp. 39-45, 2013.
[196] N. Tan, S. R. Jia, P. P. Han, W. Guo, and Y. J. Dai, "The open culture of Nostoc flagelliforme with a 25 L open pond," *Advanced Materials Research,* vol. 554, pp. 1009-1012, 2012.
[197] J. Dharmaraja, S. Shobana, M. Huy, A. K. Vatland, V. Ashokkumar, and G. Kumar, "Design and scale-up of photobioreactors," in *Current Developments in Biotechnology and Bioengineering*: Elsevier, 2023, pp. 11-32.
[198] P. Benner, L. Meier, A. Pfeffer, K. Krüger, J. E. Oropeza Vargas, and D. Weuster-Botz, "Lab-scale photobioreactor systems: principles, applications, and scalability," *Bioprocess and biosystems engineering,* vol. 45, no. 5, pp. 791-813, 2022.
[199] D. M. Arias, J. García, and E. Uggetti, "Production of polymers by cyanobacteria grown in wastewater: Current status, challenges and future perspectives," *New biotechnology,* vol. 55, pp. 46-57, 2020.
[200] T. L. da Silva and A. Reis, "Scale-up problems for the large scale production of algae," in *Algal biorefinery: An integrated approach*: Springer, 2015, pp. 125-149.
[201] R. Svane and N. T. Eriksen, "Exopolysaccharides are partly growth associated products in Microcystis flos-aquae," *Journal of Applied Phycology,* vol. 27, no. 1, pp. 163-170, 2015.
[202] V. Shah, A. Ray, N. Garg, and D. Madamwar, "Characterization of the extracellular polysaccharide produced by a marine cyanobacterium, Cyanothece sp. ATCC 51142, and its

exploitation toward metal removal from solutions," *Current microbiology,* vol. 40, no. 4, pp. 274-278, 2000.
[203] D. S. V. Pereyra and S. G. Ferrari, "Extracellular polymeric substance (EPS) production by Nostoc minutum under different laboratory conditions," *Advances in microbiology,* vol. 6, no. 05, p. 374, 2016.
[204] A. T. Koçer, B. İnan, S. Kaptan Usul, D. Özçimen, M. T. Yılmaz, and İ. Işıldak, "Exopolysaccharides from microalgae: production, characterization, optimization and techno-economic assessment," *Brazilian Journal of Microbiology,* vol. 52, no. 4, pp. 1779-1790, 2021.
[205] S. Narukulla *et al.*, "Comparative study between the Full Factorial, Box–Behnken, and Central Composite Designs in the optimization of metronidazole immediate release tablet," *Microchemical Journal,* vol. 207, p. 111875, 2024.
[206] F. Rodrigues *et al.*, "Response Surface Methodology Applied to Cyanobacterial EPS Production: Steps and Statistical Validations," *Processes,* vol. 12, no. 8, p. 1733, 2024.
[207] H. Li *et al.*, "Pilot-scale isolation of bioactive extracellular polymeric substances from cell-free media of mass microalgal cultures using tangential-flow ultrafiltration," *Process biochemistry,* vol. 46, no. 5, pp. 1104-1109, 2011.
[208] S. B. Pereira, R. Mota, C. P. Vieira, J. Vieira, and P. Tamagnini, "Phylum-wide analysis of genes/proteins related to the last steps of assembly and export of extracellular polymeric substances (EPS) in cyanobacteria," *Scientific reports,* vol. 5, no. 1, p. 14835, 2015.
[209] Y. Zhu, S. B. Jones, and D. B. Anderson, "Algae farm cost model: Considerations for photobioreactors," Pacific Northwest National Lab.(PNNL), Richland, WA (United States), 2018.
[210] T. M. Mata, A. A. Martins, and N. S. Caetano, "Microalgae for biodiesel production and other applications: a review," *Renewable and sustainable energy reviews,* vol. 14, no. 1, pp. 217-232, 2010.
[211] B. Wang, C. Q. Lan, and M. Horsman, "Closed photobioreactors for production of microalgal biomasses," *Biotechnology advances,* vol. 30, no. 4, pp. 904-912, 2012.
[212] C. Wang and C. Q. Lan, "Effects of shear stress on microalgae–A review," *Biotechnology Advances,* vol. 36, no. 4, pp. 986-1002, 2018.
[213] Y. Xu, I. M. Ibrahim, C. I. Wosu, A. Ben-Amotz, and P. J. Harvey, "Potential of new isolates of Dunaliella salina for natural β-carotene production," *Biology,* vol. 7, no. 1, p. 14, 2018.
[214] S. Pourkarimi, A. Hallajisani, A. Alizadehdakhel, A. Nouralishahi, and A. Golzary, "Factors affecting production of beta-carotene from Dunaliella salina microalgae," *Biocatalysis and Agricultural Biotechnology,* vol. 29, p. 101771, 2020.
[215] C. B. Grewe and O. Pulz, "The biotechnology of cyanobacteria," in *Ecology of cyanobacteria II: Their diversity in space and time*: Springer, 2012, pp. 707-739.
[216] Q. Huang, F. Jiang, L. Wang, and C. Yang, "Design of photobioreactors for mass cultivation of photosynthetic organisms," *Engineering,* vol. 3, no. 3, pp. 318-329, 2017.
[217] R. Hijazi, J. R. Mounsef, and H. Y. Kanaan, "Design considerations for photo-bioreactors: A review," in *2020 5th International Conference on Renewable Energies for Developing Countries (REDEC)*, 2020: IEEE, pp. 1-7.
[218] J. Beardall, P. Heraud, S. Roberts, K. Shelly, and S. Stojkovic, "Effects of UV-B radiation on inorganic carbon acquisition by the marine microalga Dunaliella tertiolecta (Chlorophyceae)," *Phycologia,* vol. 41, no. 3, pp. 268-272, 2002.
[219] A. P. Lopes, F. M. Santos, T. F. Silva, V. J. Vilar, and J. C. Pires, "Outdoor cultivation of the microalga Chlorella vulgaris in a new photobioreactor configuration: The effect of ultraviolet and visible radiation," *Energies,* vol. 13, no. 8, p. 1962, 2020.
[220] H. Jiang and B. Qiu, "Inhibition of photosynthesis by UV-B exposure and its repair in the bloom-forming cyanobacterium Microcystis aeruginosa," *Journal of Applied Phycology,* vol. 23, pp. 691-696, 2011.
[221] G. S. Babu, P. Joshi, and P. Viswanathan, "UVB-induced reduction in biomass and overall productivity of cyanobacteria," *Biochemical and biophysical research communications,* vol. 244, no. 1, pp. 138-142, 1998.
[222] C. Wong, M. Teoh, S. Phang, and W. Chu, "Effect of ultraviolet radiation (UVR) on the tropical microalga Chlorella vulgaris," *Malaysian Journal of Science,* vol. 30, no. 1, pp. 3-15, 2011.
[223] Y.-J. Moon, S. I. Kim, and Y.-H. Chung, "Sensing and responding to UV-A in cyanobacteria," *International journal of molecular sciences,* vol. 13, no. 12, pp. 16303-16332, 2012.
[224] M. Ehling-Schulz, W. Bilger, and S. Scherer, "UV-B-induced synthesis of photoprotective pigments and extracellular polysaccharides in the terrestrial cyanobacterium Nostoc commune," *Journal of Bacteriology,* vol. 179, no. 6, pp. 1940-1945, 1997.

[225] D. Vandamme, I. Foubert, and K. Muylaert, "Flocculation as a low-cost method for harvesting microalgae for bulk biomass production," *Trends in biotechnology,* vol. 31, no. 4, pp. 233-239, 2013.
[226] A. K. Patel *et al.*, "Separation and fractionation of exopolysaccharides from Porphyridium cruentum," *Bioresource technology,* vol. 145, pp. 345-350, 2013.
[227] J. P. Chen, H. Mou, L. K. Wang, T. Matsuura, and Y. Wei, "Membrane separation: basics and applications," *Membrane and desalination technologies,* pp. 271-332, 2011.
[228] H. Ennaceri, K. Fischer, A. Schulze, and N. R. Moheimani, "Membrane fouling control for sustainable microalgal biodiesel production: A review," *Renewable and Sustainable Energy Reviews,* vol. 161, p. 112335, 2022.
[229] B. B. Fogler and R. V. Kleninschmidt, "Spray drying," *Industrial & Engineering Chemistry,* vol. 30, no. 12, pp. 1372-1384, 1938.
[230] K. R. Ward and P. Matejtschuk, "The principles of freeze-drying and application of analytical technologies," *Cryopreservation and freeze-drying protocols,* pp. 99-127, 2021.
[231] F. Fasaei, J. Bitter, P. Slegers, and A. Van Boxtel, "Techno-economic evaluation of microalgae harvesting and dewatering systems," *Algal research,* vol. 31, pp. 347-362, 2018.
[232] S. Zapata-Boada, M. Gonzalez-Miquel, M. Jobson, and R. Cuellar-Franca, "Solvent screening methodology considering techno-economic and environmental sustainability criteria for algae lipid extraction," in *Computer aided chemical engineering*, vol. 49: Elsevier, 2022, pp. 1039-1044.
[233] G. d. S. Costa *et al.*, "Advances in Biomass and Microbial Lipids Production: Trends and Prospects," *Processes,* vol. 12, no. 12, p. 2903, 2024.
[234] G. Karabulut, A. Purkiewicz, and G. Goksen, "Recent developments and challenges in algal protein and peptide extraction strategies, functional and technological properties, bioaccessibility, and commercial applications," *Comprehensive Reviews in Food Science and Food Safety,* vol. 23, no. 3, p. e13372, 2024.
[235] E. Nunes, K. Odenthal, N. Nunes, T. Fernandes, I. A. Fernandes, and M. A. P. de Carvalho, "Protein extracts from microalgae and cyanobacteria biomass. Techno-functional properties and bioactivity: A review," *Algal Research,* p. 103638, 2024.
[236] F. Pagels, R. N. Pereira, A. A. Vicente, and A. C. Guedes, "Extraction of pigments from microalgae and cyanobacteria—A review on current methodologies," *Applied Sciences,* vol. 11, no. 11, p. 5187, 2021.
[237] I. Fatima, M. Munir, R. Qureshi, U. Hanif, N. Gulzar, and A. A. Sheikh, "Advanced methods of algal pigments extraction: A review," *Critical Reviews in Food Science and Nutrition,* vol. 64, no. 27, pp. 9771-9788, 2024.
[238] L. Wang *et al.*, "Efficient membrane microalgal harvesting: Pilot-scale performance and techno-economic analysis," *Journal of cleaner production,* vol. 218, pp. 83-95, 2019.
[239] G. Thomassen, U. Egiguren Vila, M. Van Dael, B. Lemmens, and S. Van Passel, "A techno-economic assessment of an algal-based biorefinery," *Clean Technologies and Environmental Policy,* vol. 18, pp. 1849-1862, 2016.
[240] D. Chittora, M. Meena, T. Barupal, P. Swapnil, and K. Sharma, "Cyanobacteria as a source of biofertilizers for sustainable agriculture," *Biochemistry and biophysics reports,* vol. 22, p. 100737, 2020.
[241] N. I. Krinsky, "Antioxidant functions of carotenoids," *Free Radical Biology and Medicine,* vol. 7, no. 6, pp. 617-635, 1989.
[242] C. Vílchez, E. Forján, M. Cuaresma, F. Bédmar, I. Garbayo, and J. M. Vega, "Marine carotenoids: biological functions and commercial applications," *Marine drugs,* vol. 9, no. 3, pp. 319-333, 2011.
[243] E. Rueda *et al.*, "Challenges, progress, and future perspectives for cyanobacterial polyhydroxyalkanoate production," *Reviews in Environmental Science and Bio/Technology,* pp. 1-30, 2024.
[244] F. Garcia-Pichel and R. W. Castenholz, "Occurrence of UV-absorbing, mycosporine-like compounds among cyanobacterial isolates and an estimate of their screening capacity," *Applied and Environmental Microbiology,* vol. 59, no. 1, pp. 163-169, 1993.
[245] E. P. Balskus and C. T. Walsh, "The genetic and molecular basis for sunscreen biosynthesis in cyanobacteria," *Science,* vol. 329, no. 5999, pp. 1653-1656, 2010.
[246] C. A. Llewellyn and R. L. Airs, "Distribution and abundance of MAAs in 33 species of microalgae across 13 classes," *Marine drugs,* vol. 8, no. 4, pp. 1273-1291, 2010.
[247] G. Chi *et al.*, "Production of polyunsaturated fatty acids by Schizochytrium (Aurantiochytrium) spp," *Biotechnology advances,* vol. 55, p. 107897, 2022.

[248] J. Wynn, P. Behrens, A. Sundararajan, J. Hansen, and K. Apt, "Production of single cell oils by dinoflagellates," in *Single cell oils*: Elsevier, 2010, pp. 115-129.
[249] S. Y. W. Chai, F. J. F. Phang, L. S. Yeo, L. H. Ngu, and B. S. How, "Future era of techno-economic analysis: Insights from review," *Frontiers in Sustainability,* vol. 3, p. 924047, 2022.
[250] B. Vázquez-Romero *et al.*, "Techno-economic analysis of microalgae production for aquafeed in Norway," *Algal Research,* vol. 64, p. 102679, 2022.
[251] B. Vázquez-Romero, J. A. Perales, H. Pereira, M. Barbosa, and J. Ruiz, "Techno-economic assessment of microalgae production, harvesting and drying for food, feed, cosmetics, and agriculture," *Science of the Total Environment,* vol. 837, p. 155742, 2022.
[252] A. E. Ramírez-Partida, T. García-Cayuela, L. F. Amador-Castro, H. S. Alper, and D. Carrillo-Nieves, "Towards a biorefinery processing Sargassum seaweed: Techno-economic assessment of alginate and fucoidan production through SuperPro Designer® process simulation," *Environmental Technology & Innovation,* vol. 34, p. 103587, 2024.
[253] E. Bergman, "Evaluation of the software SuperPro Designer through simulation of a biohydrogen production process," 2016.
[254] A. Saltelli *et al.*, *Global sensitivity analysis: the primer*. John Wiley & Sons, 2008.
[255] F. Subakti, R. Noguchi, A. Diharmi, J. Miyasaka, K. Ohdoi, and A. Ito, "Techno-economical assessment of Kappaphycus alvarezii carrageenan extraction plant," *Journal of Applied Phycology,* pp. 1-18, 2025.
[256] J. Barlow, R. C. Sims, and J. C. Quinn, "Techno-economic and life-cycle assessment of an attached growth algal biorefinery," *Bioresource technology,* vol. 220, pp. 360-368, 2016.
[257] J. S. Saral, A. R. Satheesh, and P. Ranganathan, "Economic and environmental analysis of algal biorefinery for the production of renewable fuels and co-product," *Energy Conversion and Management: X,* vol. 14, p. 100189, 2022.
[258] G. Penloglou and C. Kiparissides, "Techno-Economic Analysis of Multiple Scenarios for the Production of Microalgal Chemicals and Polymers," in *Handbook of Algal Technologies and Phytochemicals*: CRC Press, 2019, pp. 133-143.
[259] F. Acién, J. Fernández, J. Magán, and E. Molina, "Production cost of a real microalgae production plant and strategies to reduce it," *Biotechnology advances,* vol. 30, no. 6, pp. 1344-1353, 2012.
[260] F. Ascencio, N. Gama, R. De Philippis, and B. Ho, "Effectiveness of Cyanothece spp. and Cyanospira capsulata exocellular polysaccharides as antiadhesive agents for blocking attachment of Helicobacter pylori to human gastric cells," *Folia microbiologica,* vol. 49, pp. 64-70, 2004.
[261] V. D. Mendhulkar, L. A. Shetye, and O. Khot, "Modulation of the anti-cancer activity of sulfated polysaccharides, synthesized in spirulina platensis, due to varying degree of sulfation induced by nutrient and physical stress," *Journal of Biologically Active Products from Nature,* vol. 10, no. 4, pp. 275-284, 2020.
[262] N. K. Sarker and P. Kaparaju, "Microalgal Bioeconomy: A Green Economy Approach Towards Achieving Sustainable Development Goals," *Sustainability (2071-1050),* vol. 16, no. 24, 2024.
[263] A. Olabi *et al.*, "Role of microalgae in achieving sustainable development goals and circular economy," *Science of The Total Environment,* vol. 854, p. 158689, 2023.
[264] University of Texas at Austin Culture Collection of Algae. "Enriched Seawater Medium." https://utex.org/products/enriched-seawater-medium?variant=30991770124378 (accessed 23 April, 2021).
[265] University of Texas at Austin Culture Collection of Algae. "BG-11 Medium." https://utex.org/products/bg-11-medium?variant=30991786868826 (accessed 23 April, 2021).
[266] C. Kourmentza *et al.*, "Occurrence of non-toxic bioemulsifiers during polyhydroxyalkanoate production by Pseudomonas strains valorizing crude glycerol by-product," *Bioresource technology,* vol. 281, pp. 31-40, 2019.
[267] A. Khvataeva-Domanov and S. Mabic, "Four Ways to Better Water Quality in LC-MS," ed: R&D Magazine, 2015.
[268] M. M. Bradford, "A rapid and sensitive method for the quantitation of microgram quantities of protein utilizing the principle of protein-dye binding," *Analytical biochemistry,* vol. 72, no. 1-2, pp. 248-254, 1976.
[269] H. Kaplan Can, F. Gurbuz, and M. Odabaşı, "Partial characterization of cyanobacterial extracellular polymeric substances for aquatic ecosystems," *Aquatic Ecology,* vol. 53, pp. 431-440, 2019.
[270] Thermo Fisher Scientific Inc. *Instructions for Coomassie Plus (Bradford) Assay Reagent*. (2012).

[271] G. Yakubov *et al.*, "Origins of polysaccharide conformation and viscoelasticity in miscible heterogeneous solvent," 2023.
[272] D. G. Cooper and B. G. Goldenberg, "Surface-active agents from two Bacillus species," *Applied and environmental microbiology,* vol. 53, no. 2, pp. 224-229, 1987.
[273] R. Kurane, K. Toeda, K. Takeda, and T. Suzuki, "Culture conditions for production of microbial flocculant by Rhodococcus erythropolis," *Agricultural and biological chemistry,* vol. 50, no. 9, pp. 2309-2313, 1986.
[274] K. Shimada, K. Fujikawa, K. Yahara, and T. Nakamura, "Antioxidative properties of xanthan on the autoxidation of soybean oil in cyclodextrin emulsion," *Journal of agricultural and food chemistry,* vol. 40, no. 6, pp. 945-948, 1992.
[275] R. Re, N. Pellegrini, A. Proteggente, A. Pannala, M. Yang, and C. Rice-Evans, "Antioxidant activity applying an improved ABTS radical cation decolorization assay," *Free radical biology and medicine,* vol. 26, no. 9-10, pp. 1231-1237, 1999.
[276] L. Chun-hui, W. Chang-hai, X. Zhi-liang, and W. Yi, "Isolation, chemical characterization and antioxidant activities of two polysaccharides from the gel and the skin of Aloe barbadensis Miller irrigated with sea water," *Process Biochemistry,* vol. 42, no. 6, pp. 961-970, 2007.
[277] M. O. Elnahas, M. A. Amin, M. M. Hussein, V. C. Shanbhag, A. E. Ali, and J. D. Wall, "Isolation, characterization and bioactivities of an extracellular polysaccharide produced from Streptomyces sp. MOE6," *Molecules,* vol. 22, no. 9, p. 1396, 2017.
[278] J. Chou, T. J. Robinson, and H. Doan, "Rapid comparison of UVB absorption effectiveness of various sunscreens by UV-Vis spectroscopy," *Journal of analytical & bioanalytical techniques,* vol. 8, no. 2, 2017.
[279] D. K. Lee, J. In, and S. Lee, "Standard deviation and standard error of the mean," *Korean journal of anesthesiology,* vol. 68, no. 3, pp. 220-223, 2015.
[280] I. Guideline, "Validation of analytical procedures Q2 (R2)," *ICH: Geneva, Switzerland,* 2022.
[281] R. Naffa, G. Holmes, W. Zhang, C. Maidment, I. Shehadi, and G. Norris, "Comparison of liquid chromatography with fluorescence detection to liquid chromatography-mass spectrometry for amino acid analysis with derivatisation by 6-aminoquinolyl-N-hydroxysuccinimidyl-carbamate: Applications for analysis of amino acids in skin," *Arabian Journal of Chemistry,* vol. 13, no. 2, pp. 3997-4008, 2020.
[282] A. Kavathia and M. Misra, "Development and validation of RP-HPLC and UV-spectrophotometric methods for rapid simultaneous estimation of amlodipine and benazepril in pure and fixed dose combination," *Arabian journal of chemistry,* vol. 10, pp. S3021-S3028, 2017.
[283] M. Arayne, N. Sultana, M. Zuberi, and F. Siddiqui, "Spectrophotometric quantitation of metformin in bulk drug and pharmaceutical formulations using multivariate technique," *Indian journal of pharmaceutical sciences,* vol. 71, no. 3, p. 331, 2009.
[284] S. M. Ross, *Introduction to probability and statistics for engineers and scientists*. Academic press, 2020.
[285] L. Wu *et al.*, "Co-exposure effects of urinary polycyclic aromatic hydrocarbons and metals on lung function: mediating role of systematic inflammation," *BMC Pulmonary Medicine,* vol. 24, no. 1, p. 386, 2024.
[286] H. Seo and T. A. Hatton, "Electrochemical direct air capture of CO2 using neutral red as reversible redox-active material," *Nature Communications,* vol. 14, no. 1, p. 313, 2023.
[287] R. Dormido, J. Sánchez, N. Duro, S. Dormido-Canto, M. Guinaldo, and S. Dormido, "An interactive tool for outdoor computer controlled cultivation of microalgae in a tubular photobioreactor system," *Sensors,* vol. 14, no. 3, pp. 4466-4483, 2014.
[288] A. Solimeno, F. G. Acíen, and J. García, "Mechanistic model for design, analysis, operation and control of microalgae cultures: calibration and application to tubular photobioreactors," *Algal research,* vol. 21, pp. 236-246, 2017.
[289] E. M. Grima, "ALGAE BIOMASS IN SPAIN: A CASE STUDY," University of Almeria, 18-21 May 2010, 2010.
[290] D. d. G. Saint Cyr, C. Wisniewski, L. Schrive, E. Farhi, and C. Rivasseau, "Feasibility study of microfiltration for algae separation in an innovative nuclear effluents decontamination process," *Separation and Purification Technology,* vol. 125, pp. 126-135, 2014.
[291] INTELLIGEN INC., "SuperPro Designer®User Guide, Version 11," 2326 Morse Avenue - Scotch Plains, NJ 07076 - USA, 2018. Accessed: 12th July 2024. [Online]. Available: https://www.intelligen.com/wp-content/uploads/2020/05/SuperPro_ManualForPrinting_v11.pdf
[292] F. Acién Fernández, J. Fernández Sevilla, and E. Molina Grima, "Photobioreactors for the production of microalgae," *Reviews in Environmental Science and Bio/Technology,* vol. 12, pp. 131-151, 2013.

[293] J. Hegedüs, G. Hantos, and A. Poppe, "Lifetime modelling issues of power light emitting diodes," *Energies,* vol. 13, no. 13, p. 3370, 2020.
[294] S. S. Pumps, *Centrifugal pump handbook*. Butterworth-Heinemann, 2010.
[295] E. S. Umdu, I. Kahraman, N. Yildirim, and L. Bilir, "Optimization of microalgae panel bioreactor thermal transmission property for building façade applications," *Energy and Buildings,* vol. 175, pp. 113-120, 2018.
[296] European Commission. "Photovoltaic Geographical Information System (PVGIS)." https://re.jrc.ec.europa.eu/pvg_tools/en/#MR (accessed September 18, 2024).
[297] T. L. Bergman, *Fundamentals of heat and mass transfer*. John Wiley & Sons, 2011.
[298] J. W. Richardson, M. D. Johnson, and J. L. Outlaw, "Economic comparison of open pond raceways to photo bio-reactors for profitable production of algae for transportation fuels in the Southwest," *Algal Research,* vol. 1, no. 1, pp. 93-100, 2012.
[299] G. Panis and J. R. Carreon, "Commercial astaxanthin production derived by green alga Haematococcus pluvialis: A microalgae process model and a techno-economic assessment all through production line," *Algal research,* vol. 18, pp. 175-190, 2016.
[300] A. de Souza Rangel, J. C. de Souza Santos, and J. R. F. Savoia, "Modified profitability index and internal rate of return," *Journal of International Business and Economics,* vol. 4, no. 2, pp. 13-18, 2016.
[301] Simply Ingredients. "SeaBalance 2000 by Carbonwave [Product Page]." https://simply-ingredients.com/products/seabalance-2000-by-carbonwave?variant=42449640947898 (accessed July 15, 2024.
[302] Eurostat. "Harmonized Index of Consumer Prices (HICP) [Database]." https://ec.europa.eu/eurostat/databrowser/view/tec00027/default/table?lang=en&category=t_prc.t_prc_hicp (accessed July 24, 2024).
[303] S. K. Ram, L. Kumar, R. D. Tyagi, and P. Drogui, "Techno-economic evaluation of simultaneous production of extra-cellular polymeric substance (EPS) and lipids by Cloacibacterium normanense NK6 using crude glycerol and sludge as substrate," *Water Science and Technology,* vol. 77, no. 9, pp. 2228-2241, 2018.
[304] J. Pruvost, J. Cornet, F. Le Borgne, V. Goetz, and J. Legrand, "Theoretical investigation of microalgae culture in the light changing conditions of solar photobioreactor production and comparison with cyanobacteria," *Algal Research,* vol. 10, pp. 87-99, 2015.
[305] Eurostat. Electricity prices for non-household consumers - bi-annual data (from 2007 onwards) [Online] Available: https://ec.europa.eu/eurostat/databrowser/view/nrg_pc_205/default/table?lang=en&category=nrg.nrg_price.nrg_pc
[306] Lgem, "Personal Communication with Rupert Wieger from Lgem, 21 August 2024," ed, 2023.
[307] R. Gogar, S. Viamajala, P. A. Relue, and S. Varanasi, "Techno-economic assessment of mixed-furan production from diverse biomass hydrolysates," *ACS Sustainable Chemistry & Engineering,* vol. 9, no. 9, pp. 3428-3438, 2021.
[308] G. A. Colusse, M. E. R. Duarte, J. C. de Carvalho, and M. D. Noseda, "Media effects on laboratory scale production costs of Haematococcus pluvialis biomass," *Bioresource Technology Reports,* vol. 7, p. 100236, 2019.
[309] C.-S. Huang and J. J. Ciesla, "Lessons Learned from the On-Site Distillation of Used Solvents Generated by Health Care Facilities," *Journal of Environmental Health,* pp. 26-30, 1992.
[310] Pandora's Box Beauty. "Ekseption All Day Shield Fluid (50ml) [Product Page]." https://www.pandorasboxbeauty.com/product-page/ekseption-all-day-shield-fluid-50ml (accessed September 18, 2024).
[311] J. Huang, N. Graham, M. Templeton, Y. Zhang, C. Collins, and M. Nieuwenhuijsen, "A comparison of the role of two blue–green algae in THM and HAA formation," *Water Research,* vol. 43, no. 12, pp. 3009-3018, 2009.
[312] M. Song and O.-M. Lee, "A study of newly recorded genera and species of filamentous blue-green algae (Cyanophyceae, cyanobacteria) in Korea," *Journal of Ecology and Environment,* vol. 38, no. 4, pp. 619-627, 2015.
[313] S. Pereira *et al.*, "Using extracellular polymeric substances (EPS)-producing cyanobacteria for the bioremediation of heavy metals: do cations compete for the EPS functional groups and also accumulate inside the cell?," *Microbiology,* vol. 157, no. 2, pp. 451-458, 2011.
[314] S. Jia, H. Yu, Y. Lin, and Y. Dai, "Characterization of extracellular polysaccharides from Nostoc flagelliforme cells in liquid suspension culture," *Biotechnology and Bioprocess Engineering,* vol. 12, pp. 271-275, 2007.
[315] Z. Chi, C. Su, and W. Lu, "A new exopolysaccharide produced by marine Cyanothece sp. 113," *Bioresource technology,* vol. 98, no. 6, pp. 1329-1332, 2007.

[316] S. Felz, P. Vermeulen, M. C. van Loosdrecht, and Y. M. Lin, "Chemical characterization methods for the analysis of structural extracellular polymeric substances (EPS)," *Water Research,* vol. 157, pp. 201-208, 2019.
[317] C. Le and D. C. Stuckey, "Colorimetric measurement of carbohydrates in biological wastewater treatment systems: a critical evaluation," *Water research,* vol. 94, pp. 280-287, 2016.
[318] P. Gupta and B. Diwan, "Bacterial exopolysaccharide mediated heavy metal removal: a review on biosynthesis, mechanism and remediation strategies," *Biotechnology Reports,* vol. 13, pp. 58-71, 2017.
[319] T. Neu, T. Dengler, B. Jann, and K. Poralla, "Structural studies of an emulsion-stabilizing exopolysaccharide produced by an adhesive, hydrophobic Rhodococcus strain," *Microbiology,* vol. 138, no. 12, pp. 2531-2537, 1992.
[320] R. Shepherd, J. Rockey, I. W. Sutherland, and S. Roller, "Novel bioemulsifiers from microorganisms for use in foods," *Journal of Biotechnology,* vol. 40, no. 3, pp. 207-217, 1995.
[321] S.-k. Kam and J. Gregory, "Charge determination of synthetic cationic polyelectrolytes by colloid titration," *Colloids and Surfaces A: Physicochemical and Engineering Aspects,* vol. 159, no. 1, pp. 165-179, 1999.
[322] P. Sun *et al.*, "Revealing the characteristics of a novel bioflocculant and its flocculation performance in Microcystis aeruginosa removal," *Scientific Reports,* vol. 5, no. 1, p. 17465, 2015.
[323] J. de Jesús Paniagua-Michel, J. Olmos-Soto, and E. R. Morales-Guerrero, "Algal and microbial exopolysaccharides: new insights as biosurfactants and bioemulsifiers," *Advances in food and nutrition research,* vol. 73, pp. 221-257, 2014.
[324] O. M. Abdel-Salam, N. M. Shaffie, E. A. Omara, and N. N. Yassen, "Citric acid an antioxidant in liver," in *The liver*: Elsevier, 2018, pp. 183-198.
[325] B. Li *et al.*, "In vitro and in vivo evaluation of an exopolysaccharide produced by Lactobacillus helveticus KLDS1. 8701 for the alleviative effect on oxidative stress," *Food & function,* vol. 10, no. 3, pp. 1707-1717, 2019.
[326] T. H. N. Vu *et al.*, "Genome mining associated with analysis of structure, antioxidant activity reveals the potential production of levan-rich exopolysaccharides by food-derived Bacillus velezensis VTX20," *Applied Sciences,* vol. 11, no. 15, p. 7055, 2021.
[327] B. Jiang *et al.*, "Separation, structural characteristics and biological activity of lactic acid bacteria exopolysaccharides separated by aqueous two-phase system," *Lwt,* vol. 147, p. 111617, 2021.
[328] K. Han, K. V. Naveen, X. Zhang, A. Sathiyaseelan, and H.-Y. Kim, "Cellular Antioxidant Potential and Cytotoxic Activities of Extracellular Polysaccharides Isolated from Lactobacillus graminis Strain KNUAS018," *Polysaccharides,* vol. 6, no. 2, p. 33, 2025.
[329] A. Krężel and W. Bal, "Structure–function relationships in glutathione and its analogues," *Organic & biomolecular chemistry,* vol. 1, no. 22, pp. 3885-3890, 2003.
[330] C. S. Yentsch and C. M. Yentsch, "The attenuation of light by marine phytoplankton with specific reference to the absorption of near-UV radiation," in *The role of solar ultraviolet radiation in marine ecosystems*: Springer, 1982, pp. 691-700.
[331] J. Cao *et al.*, "Exploring marine algae-derived phycocyanin nanoparticles as a safe and effective adjuvant for sunscreen systems," *Discover Applied Sciences,* vol. 6, no. 1, p. 24, 2024.
[332] S. Schiavo, M. Oliviero, A. Philippe, and S. Manzo, "Nanoparticles based sunscreens provoke adverse effects on marine microalgae Dunaliella tertiolecta," *Environmental Science: Nano,* vol. 5, no. 12, pp. 3011-3022, 2018.
[333] D. Han, Z. Deng, F. Lu, and Z. Hu, "Biology and biotechnology of edible Nostoc," *Handbook of microalgal culture: Applied phycology and biotechnology,* pp. 433-444, 2013.
[334] Algenuity Ltd, "Personal communication with Andrew Spicer from Algenuity Ltd, 5 October 2021," Personal communication with Andrew Spicer from Algenuity Ltd, 5 October 2021 ed, 2021.
[335] G. Yakubov, "Personal communication with Gleb Yakubov from University of Nottingham, 20 April 2023," Personal communication with Gleb Yakubov from University of Nottingham, 20 April 2023 ed, 2023.
[336] M. Mullan, "Controlling the hardness of ice cream, gelato and similar frozen desserts," *Food Science and Technology. https://doi. org/10.1002/fsat. 3510_3. x (unpublished data),* 2023.
[337] P. Ramasamy and X. Zhang, "Effects of shear stress on the secretion of extracellular polymeric substances in biofilms," *Water Science and Technology,* vol. 52, no. 7, pp. 217-223, 2005.
[338] K. D. Demadis, A. Ketsetzi, and E.-M. Sarigiannidou, "Catalytic effect of magnesium ions on silicic acid polycondensation and inhibition strategies based on chelation," *Industrial & engineering chemistry research,* vol. 51, no. 26, pp. 9032-9040, 2012.

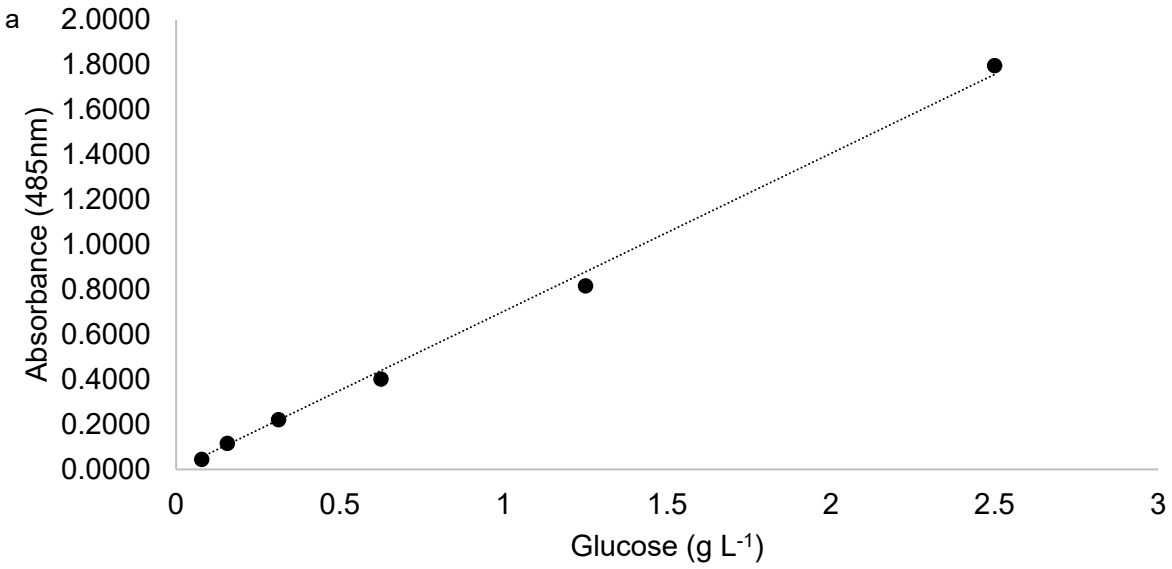
[339] S. Ursi, M. Guimarães, and E. M. Plastino, "Deleterious effect of TRIS buffer on growth rates and pigment content of Gracilaria birdiae Plastino & EC Oliveira (Gracilariales, Rhodophyta)," *Acta Botanica Brasilica,* vol. 22, pp. 891-896, 2008.
[340] T. Zavřel *et al.*, "Quantitative insights into the cyanobacterial cell economy," *Elife,* vol. 8, p. e42508, 2019.
[341] T. Costache, F. G. Acien Fernandez, M. Morales, J. Fernández-Sevilla, I. Stamatin, and E. Molina, "Comprehensive model of microalgae photosynthesis rate as a function of culture conditions in photobioreactors," *Applied microbiology and biotechnology,* vol. 97, pp. 7627-7637, 2013.
[342] W. Jurkowski, M. Paper, and T. B. Brück, "Isolation and investigation of natural rare earth metal chelating agents from Calothrix brevissima-a step towards unraveling the mechanisms of metal biosorption," *Frontiers in Bioengineering and Biotechnology,* vol. 10, p. 833122, 2022.
[343] D. Alim, S. Sircaik, and S. L. Panwar, "The significance of lipids to biofilm formation in Candida albicans: an emerging perspective," *Journal of Fungi,* vol. 4, no. 4, p. 140, 2018.
[344] I. K. Hong, S. I. Kim, and S. B. Lee, "Effects of HLB value on oil-in-water emulsions: Droplet size, rheological behavior, zeta-potential, and creaming index," *Journal of industrial and engineering chemistry,* vol. 67, pp. 123-131, 2018.
[345] Xanthella Ltd, "Personal communication with Alyn McKenzie from Xanthella Ltd, 27 October 2023," Personal communication with Alyn McKenzie from Xanthella Ltd, 27 October 2023 ed, 2023.
[346] N. T. THANH, Y. UEMURA, N. OSMAN, and L. ISMAIL, "The effect of aeration rate on the growth of Scenedesmus quadricauda in column photobioreactor," *Journal of the Japan Institute of Energy,* vol. 94, no. 2, pp. 177-180, 2015.
[347] M. Bonnans *et al.*, "Blue light: Friend or foe?," *Journal of Photochemistry and Photobiology B: Biology,* vol. 212, p. 112026, 2020.
[348] F. Wang and M. Chen, "Chromatic acclimation processes and their relationships with phycobiliprotein complexes," *Microorganisms,* vol. 10, no. 8, p. 1562, 2022.
[349] S. S. Golden, "Light-responsive gene expression in cyanobacteria," *Journal of bacteriology,* vol. 177, no. 7, pp. 1651-1654, 1995.
[350] F. Pagels, G. Lopes, V. Vasconcelos, and A. C. Guedes, "White and red LEDs as two-phase batch for cyanobacterial pigments production," *Bioresource technology,* vol. 307, p. 123105, 2020.
[351] K. Sałek and S. R. Euston, "Sustainable microbial biosurfactants and bioemulsifiers for commercial exploitation," *Process Biochemistry,* vol. 85, pp. 143-155, 2019.
[352] N. J. Krog and F. V. Sparso, "Food emulsifiers: their chemical and physical properties," *Food emulsions,* vol. 12, 2004.
[353] Global Market Insights. "Food Emulsifiers Market Size." https://www.gminsights.com/industry-analysis/food-emulsifiers-market (accessed July 7, 2024.
[354] X. Hong, Q. Zhao, Y. Liu, and J. Li, "Recent advances on food-grade water-in-oil emulsions: Instability mechanism, fabrication, characterization, application, and research trends," *Critical reviews in food science and nutrition,* vol. 63, no. 10, pp. 1406-1436, 2023.
[355] Mordor Intelligence. "Emulsifiers Market Size." https://www.mordorintelligence.com/industry-reports/emulsifier-market (accessed July 10, 2024).
[356] J. Xue and Q. Zhong, "Thyme oil nanoemulsions coemulsified by sodium caseinate and lecithin," *Journal of agricultural and food chemistry,* vol. 62, no. 40, pp. 9900-9907, 2014.
[357] William Reed Ltd. "Q&A Carbonwave expands seaweed emulsifier as demand grows." https://www.cosmeticsdesign.com/Article/2023/05/24/Q-A-Carbonwave-expands-seaweed-emulsifier-as-demand-grows (accessed July 11 2024.
[358] S. Naimi, E. Viennois, A. T. Gewirtz, and B. Chassaing, "Direct impact of commonly used dietary emulsifiers on human gut microbiota," *Microbiome,* vol. 9, pp. 1-19, 2021.
[359] A. Itó Corrêa, "Environmental, social and economic impacts of organic, Fairtrade soybean production in Brazil: risk assessment study for Paraná state," A. Itó Corrêa, 2018.
[360] E. Potrich *et al.*, "Replacing hexane by ethanol for soybean oil extraction: Modeling, simulation, and techno-economic-environmental analysis," *Journal of Cleaner Production,* vol. 244, p. 118660, 2020.
[361] The Soapery. "Polysorbate 20 [Product Page]." https://www.thesoapery.co.uk/products/polysorbate-20?variant=39941153161310 (accessed September 11, 2024).
[362] A. Fattom and M. Shilo, "Hydrophobicity as an adhesion mechanism of benthic cyanobacteria," *Applied and Environmental Microbiology,* vol. 47, no. 1, pp. 135-143, 1984.

[363] M. Shilo and A. Fattom, "Polymeric substance and method of separating and culturing bacteria," Patent US5250201A, 1991.
[364] I. Jagadeeswaran and H. Sriram, "EU 1907/2006–Registration, Evaluation, Authorisation and Restriction of Chemicals," in *Medical Device Guidelines and Regulations Handbook*: Springer, 2022, pp. 237-260.
[365] E. Economics, "Evaluation of the Council Directive 92/83/EEC on the harmonisation of the structures of excise duties on alcohol and alcoholic beverages," 2016.
[366] H. Qin, J. Lu, Z. Wang, and D. Li, "The influence of soil and water physicochemical properties on the distribution of Nostoc sphaeroides (Cyanophyceae) in paddy fields and biochemical comparison with indoor cultured biomass," *Journal of applied phycology,* vol. 25, pp. 1737-1745, 2013.
[367] L. Pachuau, N. Das, R. Nath, J. Sutradhar, and M. K. Das, "Natural polymer-based nanocarriers for advanced cosmeceutical application," in *Nanocosmeceuticals*: Elsevier, 2022, pp. 431-452.
[368] A. Gupta *et al.*, "Natural sun-screening compounds and DNA-repair enzymes: Photoprotection and photoaging," *Catalysts,* vol. 13, no. 4, p. 745, 2023.
[369] SpecialChem. "INCI Ingredient Algae Oligosaccharides." https://cosmetics.specialchem.com/inci-ingredients/algae-oligosaccharides (accessed April 21, 2025).
[370] SpecialChem. "INCI Ingredient Spirulina platensis Extract." https://cosmetics.specialchem.com/inci-ingredients/spirulina-platensis-extract (accessed April 21, 2025).
[371] L. Bruni, "Internal economies of scale with a given technique," *The Journal of Industrial Economics,* pp. 175-190, 1964.
[372] G. S. Patience and D. C. Boffito, "Distributed production: Scale-up vs experience," *Journal of Advanced Manufacturing and Processing,* vol. 2, no. 2, p. e10039, 2020.
[373] S. Shinde *et al.*, "Glycogen metabolism jump-starts photosynthesis through the oxidative pentose phosphate pathway (OPPP) in cyanobacteria," *bioRxiv,* p. 657304, 2019.
[374] F. Rossi and R. De Philippis, "Role of cyanobacterial exopolysaccharides in phototrophic biofilms and in complex microbial mats," *Life,* vol. 5, no. 2, pp. 1218-1238, 2015.
[375] L. M. Sihvonen *et al.*, "Strains of the cyanobacterial genera Calothrix and Rivularia isolated from the Baltic Sea display cryptic diversity and are distantly related to Gloeotrichia and Tolypothrix," *FEMS microbiology ecology,* vol. 61, no. 1, pp. 74-84, 2007.
[376] J. N. Clippinger and R. E. Davis, "Techno-economic analysis for the production of algal biomass via closed photobioreactors: future cost potential evaluated across a range of cultivation system designs," National Renewable Energy Lab.(NREL), Golden, CO (United States), 2019.
[377] T. Allman, "Bioreactors: design, operation, and applications," in *Fermentation Microbiology and Biotechnology, Fourth Edition*: CRC Press, 2018, pp. 283-308.
[378] J. D. Cruz and V. Vasconcelos, "Legal aspects of microalgae in the European food sector," *Foods,* vol. 13, no. 1, p. 124, 2023.
[379] H. Keller, S. Gärtner, G. Reinhardt, and N. Rettenmaier, "Environmental assessment of Dunaliella-based algae biorefinery concepts," *D-factory project reports,* 2017.
[380] S. Nanda, R. Azargohar, A. K. Dalai, and J. A. Kozinski, "An assessment on the sustainability of lignocellulosic biomass for biorefining," *Renewable and Sustainable Energy Reviews,* vol. 50, pp. 925-941, 2015.
[381] Culture Collection of Algae and Protozoa, "Algaculture for Biotechnology," Course, 2021.
[382] J. B. Waterbury, "The cyanobacteria—isolation, purification and identification," *The prokaryotes,* vol. 4, pp. 1053-1073, 2006.
[383] B. Hopkins, "Personal communication with Bradley Hopkins from University of Nottingham, 22 October 2024," ed, 2024.
[384] M. Martinho de Brito *et al.*, "Properties of exopolymeric substances (EPSs) produced during cyanobacterial growth: potential role in whiting events," *Biogeosciences,* vol. 20, no. 15, pp. 3165-3183, 2023.
[385] L. Robertson, "Personal Communication with Lorelei Robertson, 9 October 2024," ed, 2024.
[386] K. Kourmentza, "Personal communication with Konstantina Kourmentza from University of Nottingham, 30 September 2024," ed, 2024.
[387] D. Cobon, "Personal communication with Darell Cobon from University of Nottingham, 6 November 2024," 6 November 2024.

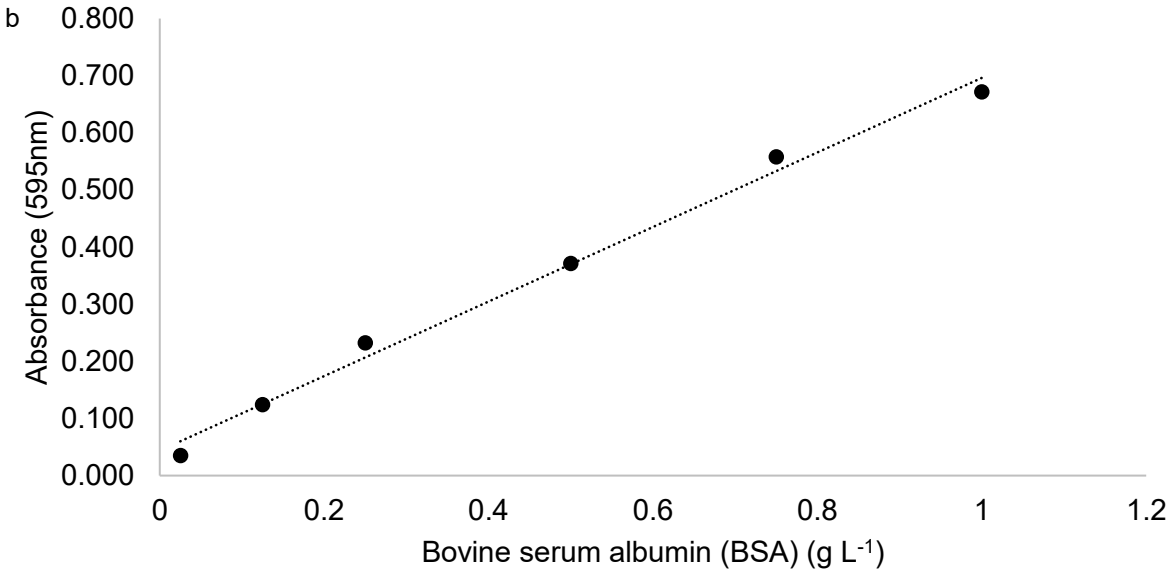
Chapter 12: Appendix

12.1 Calibration Curves of Detection of EPS composition and properties assays

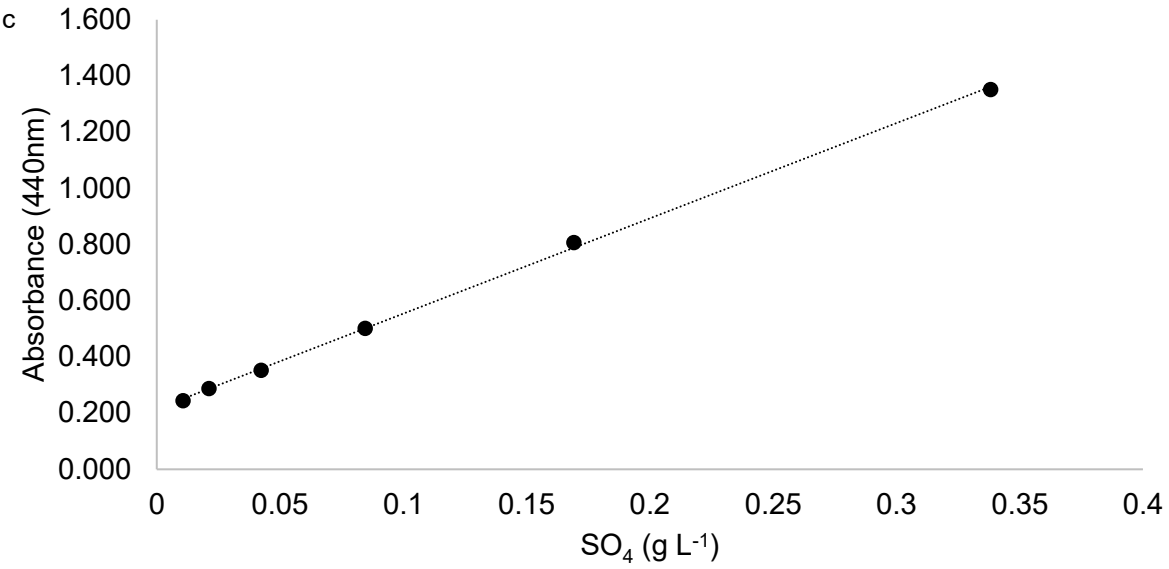
a



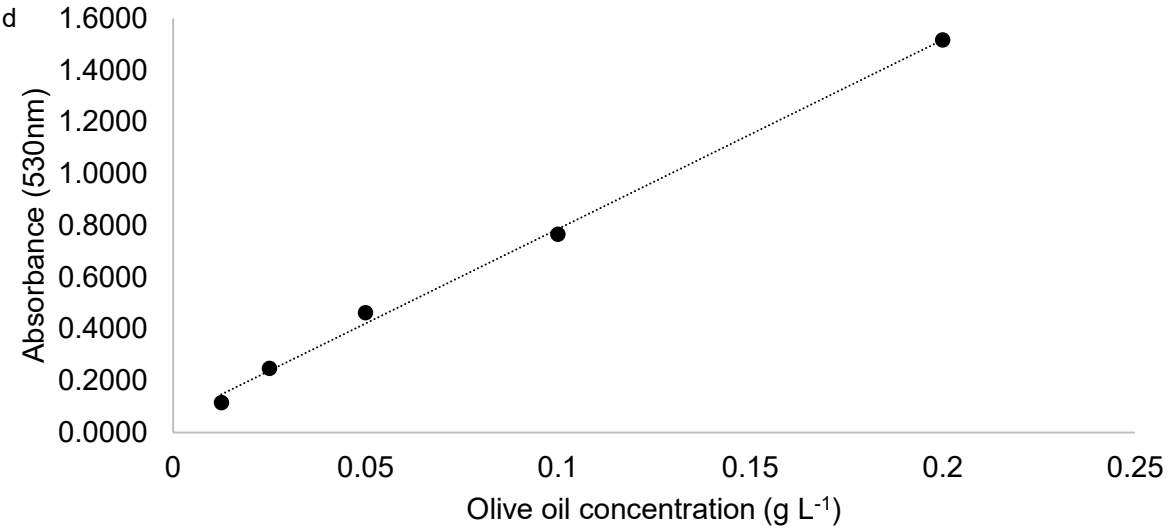
b



c


1.600
1.400
1.200
1.000
0.800
0.600
0.400
0.200
0.000
Absorbance (440nm)
0
0.05
0.1
0.15
0.2
0.25
0.3
0.35
0.4
SO4 (g L-1)

d


1.6000
1.4000
1.2000
1.0000
0.8000
0.6000
0.4000
0.2000
0.0000
Absorbance (530nm)
0
0.05
0.1
0.15
0.2
0.25
Olive oil concentration (g L-1)

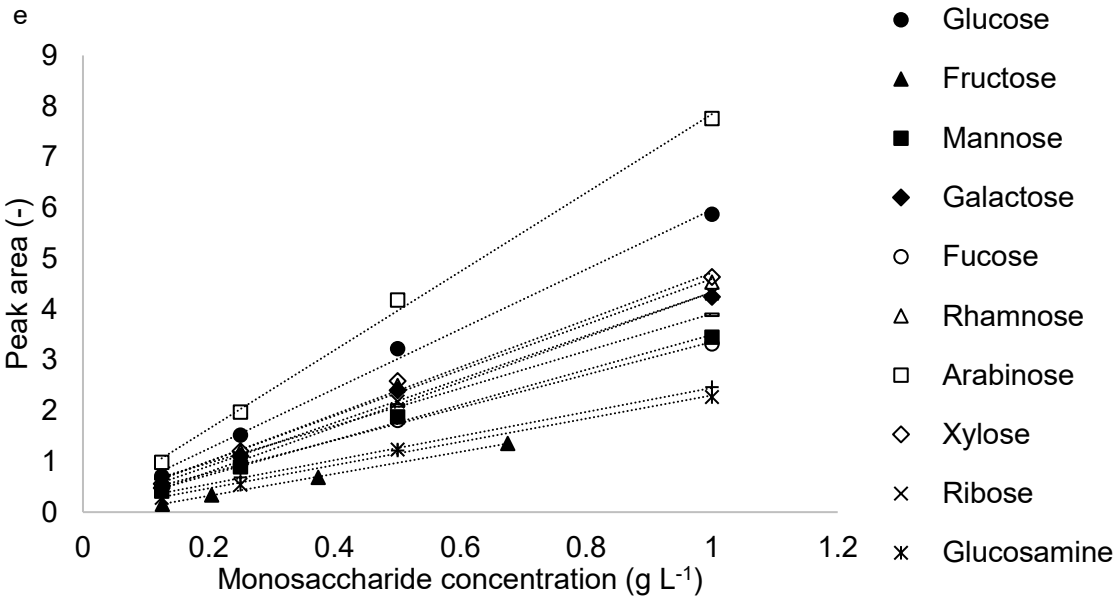
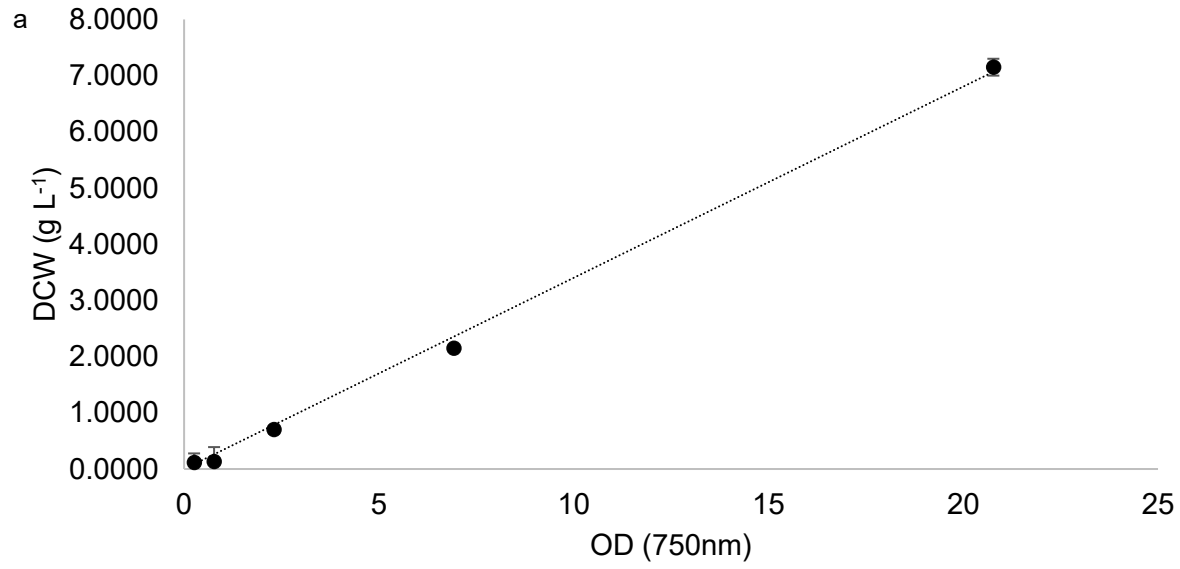
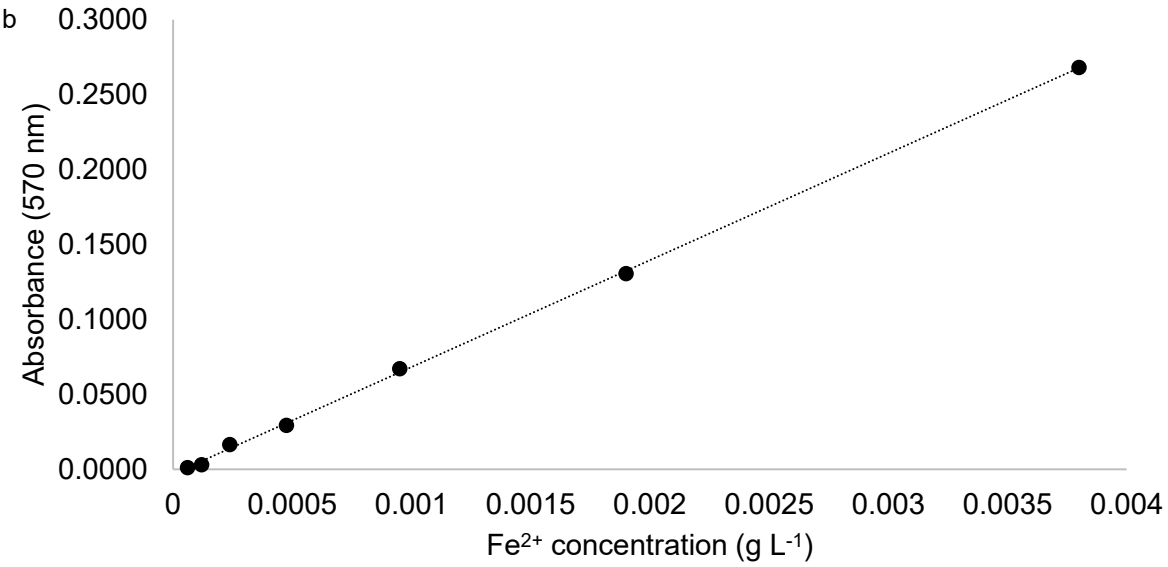


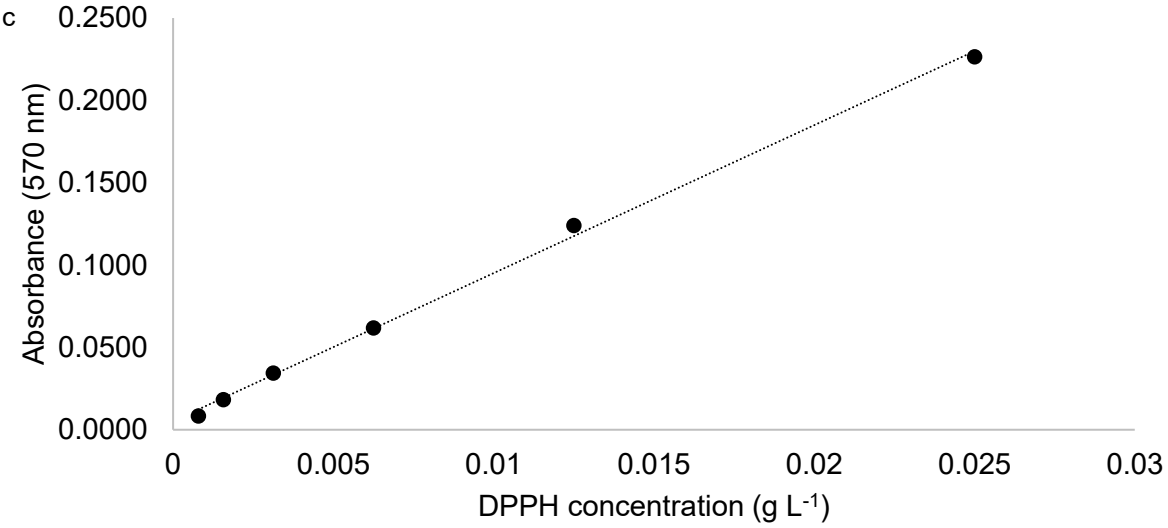
Figure 12-1 Standard curves for extracellular polymeric substances (EPS) composition assays.(a) Phenol sulfuric acid method for total carbohydrate content estimation. (b) Bradford assay for total protein content estimation. (c) Barium chloride gelatine test for total sulphate ion content estimation. (d) Phospho-vanillin method for total lipid content estimation. (e) High-Performance Anion Exchange Chromatography with pulsed-amperometric detection (HPAEC-PAD) for monosaccharide identification and quantification.



b


Absorbance (570 nm)
0.3000
0.2500
0.2000
0.1500
0.1000
0.0500
0.0000
0
0.0005
0.001
0.0015
0.002
0.0025
0.003
0.0035
0.004
Fe2+ concentration (g L-1)

c


Absorbance (570 nm)
0.2500
0.2000
0.1500
0.1000
0.0500
0.0000
0
0.005
0.01
0.015
0.02
0.025
0.03
DPPH concentration (g L-1)

d

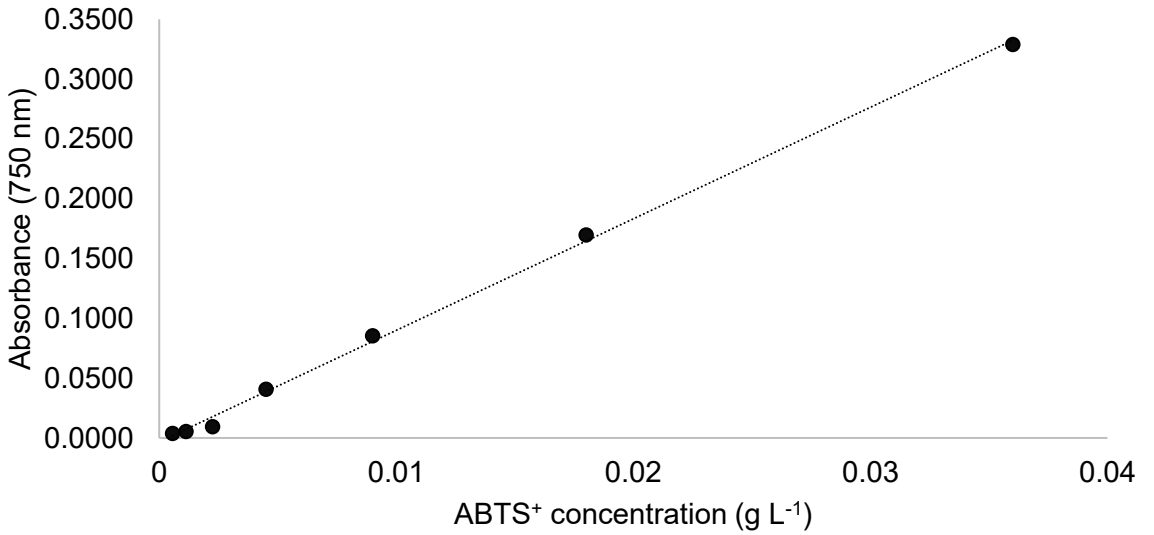

Absorbance (750 nm)
0.3500
0.3000
0.2500
0.2000
0.1500
0.1000
0.0500
0.0000
0
0.01
0.02
0.03
0.04
ABTS+ concentration (g L-1)

Figure 12-2 Standard curves for dry cell weight (DCW) from optical density (OD) estimation, and extracellular polymeric substances (EPS) properties assays.(a) Relationship between OD_{750nm} and DCW based on *Anabaena oscillarioides* culture. Values show mean ± 1 standard deviation (n=3). (b) Standard curve of iron-chelating assay. (c) Standard curve for 2,2-diphenyl-1-picrylhydrazyl (DPPH) scavenging assay. (d) Standard curve of 2,2'-azino-bis(3-ethylbenzothiazoline-6-sulfonic acid) cation ($ABTS^{+}$) scavenging assay.

12.2 Trendline Equations and Limit of Detection of EPS composition and properties assays

Table 12-1 Trendline equations, R^2 values, standard deviation (σ) of blanks, limits of detection (LOD), and limits of saturation (LOS) for standard curves used in extracellular polymeric substances (EPS) composition and property assays.In the equations, x denotes analyte concentration and y denotes absorbance (for colorimetric and turbidimetric assays) or peak area (for high-performance anion-exchange chromatography with pulsed-amperometric detection, HPAEC-PAD). Abbreviations: BSA, bovine serum albumin.

Assay	Analyte	Trendline equation	R^2 value	σ	LOD	LOS	Unit
Phenol-sulfuric acid method	Glucose	y = 0.7027x	0.998	0.021	0.100	2.500	g L^{-1}
Bradford assay	BSA	y = 0.6524x + 0.0437	0.992	0.014	0.069	1.000	g L^{-1}
$BaCl_2$ gelatine test	SO_4	y = 3.3902x + 0.215	0.999	0.007	0.007	0.338	g L^{-1}
Phospho-vanillin assay	Olive oil	y = 7.3061x + 0.0559	0.997	0.016	0.007	0.200	g L^{-1}
HPAEC-PAD (glucose)	Glucose	y = 5.93x + 0.0426	0.997	0.143	0.079	2.000	g L^{-1}
HPAEC-PAD (fructose)	Fructose	y = 2.0536x - 0.0583	0.994	0.056	0.089	2.000	g L^{-1}
HPAEC-PAD (mannose)	Mannose	y = 3.4791x + 0.0229	0.997	0.158	0.150	2.000	g L^{-1}
HPAEC-PAD (arabinose)	Arabinose	y = 7.8075x + 0.0516	0.998	0.037	0.016	2.000	g L^{-1}
HPAEC-PAD (galactose)	Galactose	y = 4.3135x + 0.0275	0.994	0.117	0.090	2.000	g L^{-1}
HPAEC-PAD (fucose)	Fucose	y = 3.3046x + 0.0709	0.997	0.111	0.111	2.000	g L^{-1}
HPAEC-PAD (glucosamine)	Glucosamine	y = 2.2966x + 0.0059	0.997	0.043	0.061	2.000	g L^{-1}
HPAEC-PAD (glucuronic acid)	Glucuronic acid	y = 3.8165x + 0.1334	0.996	0.058	0.050	2.000	g L^{-1}
HPAEC-PAD (galacturonic acid)	Galacturonic acid	y = 2.341x + 0.0981	0.999	0.148	0.208	2.000	g L^{-1}

(continued on next page)

Table 12-1 (continued)

Assay	Analyte	Trendline equation	R^2 value	σ	LOD	LOS	Unit
HPAEC-PAD (rhamnose)	Rhamnose	y = 4.5568x + 0.0572	0.997	0.052	0.037	2.000	g L^{-1}
HPAEC-PAD (xylose)	Xylose	y = 4.6887x + 0.0392	0.996	0.173	0.122	2.000	g L^{-1}
HPAEC-PAD (ribose)	Ribose	y = 4.3679x - 0.0551	0.999	0.102	0.077	2.000	g L^{-1}
$ABTS^+$ scavenging activity	$ABTS^+$	y = 9.3431x - 0.0038	0.998	0.003	0.001	0.036	g L^{-1}
DPPH scavenging activity	DPPH	y = 8.9848x + 0.0053	0.998	0.003	0.001	0.025	g L^{-1}
Iron-chelating activity	Fe-complex	y = 71.292x - 0.0031	1.000	0.003	0.000	0.004	g L^{-1}
Estimation of DCW from OD_{750}	DCW	y = 0.3402x	0.998	0.071	0.686	7.150	g L^{-1}

Table 12-2 Retention times (minutes) and peak numbers of monosaccharides in high-performance anion-exchange chromatography with pulsed-amperometric detection (HPAEC-PAD) used for monosaccharide identification and quantification of extracellular polymeric substances (EPS).

Monosaccharide	Retention time (min)	Method	Peak number
Fucose	2.575	Method 1	1
Rhamnose	3.042	Method 2	2
Arabinose	3.358	Method 2	3
Galactose	4.483	Method 1	4
Glucose	4.767	Method 1	5
Xylose	5.367	Method 1	6
Mannose	6.308	Method 1	7
Glucosamine	7.433	Method 1	8
Fructose	8.358	Method 1	9
Ribose	8.792	Method 1	10
Galacturonic acid	24.100	Method 1	11
Glucuronic acid	24.575	Method 1	12

12.3 Establishing Axenic Cultures

Multiple species used for the experiments were obtained as xenic cultures from culture collections. Axenisation was performed prior to cultivation to avoid alteration of EPS measurements caused by consumption or production of EPS by contaminating microorganisms. The methods used were re-streaking and serial dilution. Both methods were performed aseptically in a microbial safety cabinet (MSC). To purify the species by re-streaking, cultures were grown on agar plates with species-appropriate medium. The method taught in the course ‘CCAP Algaculture for Biotechnology’ was used with modifications. Cyanobacterial cells were added to the centre of an agar plate and streaked outwards in an asterisk-shaped pattern with an inoculation loop. Agar plates were incubated at 30°C with constant light (40 µmol m^{-2} s^{-1}). As soon as green colonies were visible, single colonies that appeared to be free of contamination were transferred to a new agar plate, using an inoculation loop or scalpel. This process was repeated until the plate was free of contaminant colonies [381]. As alternative method,

liquid culture was serially diluted (eight dilutions of factor 10) in microcentrifuge tubes (Eppendorf) containing BG-11 [382]. Of each dilution, 100 µL was plated on agar plates with suitable medium. As soon as green colonies were visible, they were transferred to new agar plates with an inoculation loop or by cutting the colonies cut out with a scalpel, placing onto a new agar plate and streaking out half of the colony.

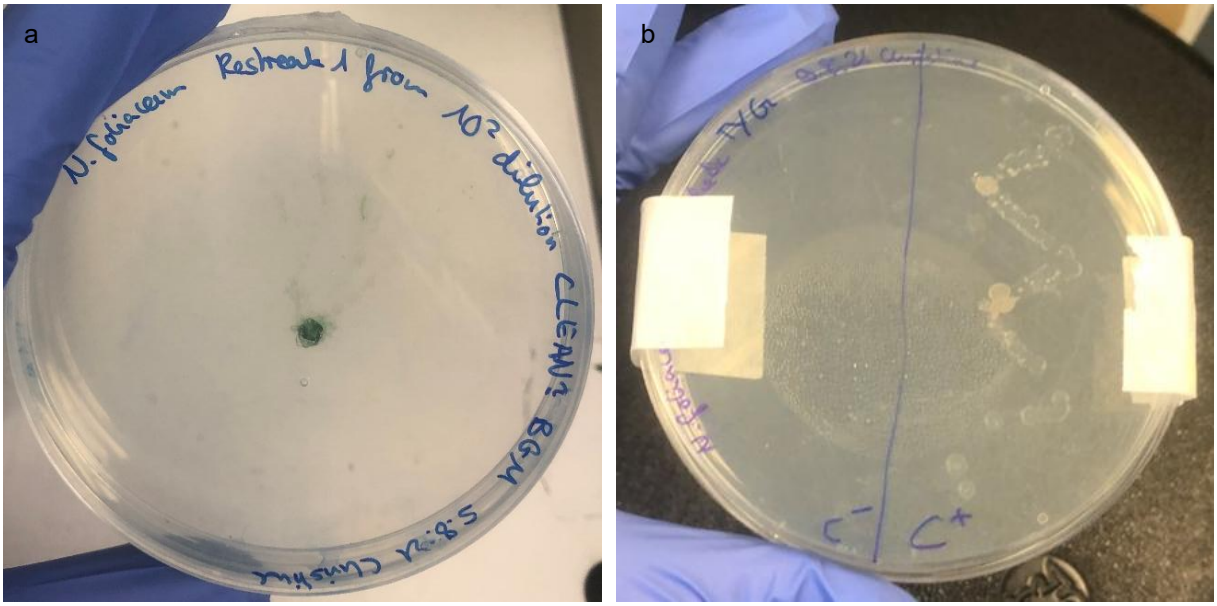


Figure 12-3 Photos of agar plates of axenisation of *Nostoc foliaceum*.(a) Axenic *Nostoc foliaceum* colony obtained by serial dilution.(b) LB plate shows absence of growth from re-streak of the axenic plate (C^-) and presence of growth of previous (contaminated) plate (C^+).

Axenic cultures were verified by visual inspection of agar plates for absence of contaminating colonies, and absence of fungi or bacteria in microscopies. Besides, colonies from the plate were used to inoculate a negative control (C^-) of an agar plate, containing 25 g L^{-1} Lysogeny broth (LB) and 12.5 g L^{-1} agar (Bacteriological agar, Oxoid). A positive control (C^+) was performed by inoculating LB medium with colonies from a previous (contaminated) plate. The negative and positive control were incubated at 30°C for 7 days. Confirmation of axenic cultures was based on absence of growth in the negative control and presence of growth in the positive control. Similarly, contamination checks throughout the experiments were performed by plating cultures on LB plates. Re-streaking was successful as purification method of *A. oscillarioides*. Axenic culture was confirmed by visual inspection of agar plates and microscopies, as well as absence of growth in negative control and presence of growth

in positive control. Serial dilution proved to be a simple and effective purification method for *N. foliaceum*. A colony cut out from the 10^{-2} dilution plate (Figure 12-3*a*) was confirmed as axenic (Figure 12-3*b*).

12.4 Media Compositions

Table 12-3 Composition of marine media (ASN-III, ESM, L1-Si) used for cultivation of marine cyanobacteria.Values are given as concentrations of salts and nutrients (g L^{-1}).

Enriched seawater medium (ESM)		**Artificial seawater medium (ASN-III)**		**L1 Medium without Silicate (L1-Si)**	
Based on UTEX collection		Based on CCAP collection		Based on CCAP collection	
Compound	**g L^{-1}**	**Compound**	**g L^{-1}**	**Compound**	**g L^{-1}**
Seawater	980.0000	NaCl	25.0000	Seawater	950.0000
$NaNO_3$	0.0470	$MgSO_4.7H_2O$	3.5000	$NaNO_3$	0.74966
Na_2glycerophosphate•$5H_2O$	0.0070	$MgCl_2.6H_2O$	2.0000	$NaH_2PO_4 \cdot H_2O$	0.04995
HEPES buffer	0.0650	$CaCl_2.2H_2O$	0.5000	$Na_2EDTA \cdot 2H_2O$	0.04355
$Fe(NH_4)2(SO_4)2$•$6H_2O$	0.0023	KCl	0.5000	$Fe_3 \cdot 6H_2O$	0.03163
Na_2EDTA•$2H_2O$	0.0052	Citric acid	0.0030	$MnCl_2 \cdot 4\ H_2O$	0.00178
H_3BO_3	0.0037	Fe-Amm-citrate	0.0030	$ZnSO_4 \cdot 7H_2O$	0.00023
Fe_3•$6H_2O$	0.0002	Na_2 EDTA.$2H_2O$	0.0005	$CoCl_2 \cdot 6H_2O$	0.00012
$MnSO_4$•H_2O	0.0005	$NaNO_3$	0.7500	$CuSO_4 \cdot 5H_2O$	0.00002

(continued on next page)

Table 12-3 (continued)

Enriched seawater medium (ESM)		**Artificial seawater medium (ASN-III)**		**L1 Medium without Silicate (L1-Si)**	
Based on UTEX collection		Based on CCAP collection		Based on CCAP collection	
Compound		**g L^{-1}**		**Compound**	
$ZnSO_4 \cdot 7H_2O$	0.0001	K_2HPO_4	0.5724	$Na_2MoO4 \cdot 2H_2O$	0.00020
$CoCl_2 \cdot 6H_2O$	0.0000	Na_2CO3	0.0234	H_2SeO_3	0.00001
Vitamin B12	0.0000041	H_3BO_3	0.002860	$NiSO_4 \cdot 6H_2O$	0.00003
Biotin	0.0000008	$MnCl_2.4H_2O$	0.001810	Na_3VO_4	0.00002
Thiamine	0.0000101	$ZnSO_4.7H_2O$	0.000220	K_2CrO_4	0.00002
		$Na_2MoO4.2H_2O$	0.000390	thiamine	0.00110
		$CuSO_4.5H_2O$	0.000079	biotin	0.00001
		$Co(NO_3)2.6H_2O$	0.00005	cyanocobalamin	0.00001
		Vitamin B12	0.00001		

Table 12-4 Composition of freshwater media (BG-11, BG-11_0, CB, MDM, SOT) used for cultivation of freshwater cyanobacteria.Values are given as concentrations of salts and nutrients (g L^{-1}).

Blue Green Algae Medium 11 (BG-11) Based on UTEX collection		**BG-11 Medium without nitrogen (BG-11_0)** Based on UTEX collection		**Modified Detmer Medium (MDM)** Based on NIES collection		**Soil-Extract Medium (SOT)** Based on NIES collection		**Cyanobacteria Broth Medium (CB)** Based on NIES collection	
Compound	g L^{-1}	Compound	g L^{-1}	Compound	g L^{-1}	Compound	g L^{-1}	Compound	g L^{-1}
$NaNO_3$	1.500	K_2HPO_4	0.0400	KNO_3	1.0000	NaHCO3	16.8000	$Ca(NO_3)2 \cdot 4H_2O$	0.1500
K_2HPO_4	0.0400	$MgSO_4.7H_2O$	0.0750	$MgSO_4 \cdot 7H_2O$	0.2500	K_2HPO_4	0.5000	KNO_3	0.1000
$MgSO_4.7H_2O$	0.0750	$CaCl_2.2H_2O$	0.0360	K_2HPO_4	0.2500	$NaNO_3$	2.5000	β-Na_2glyceroph	0.0500
$CaCl_2.2H_2O$	0.0360	Citric acid	0.0060	NaCl	0.1000	$K2SO_4$	1.0000	$MgSO_4 \cdot 7H_2O$	0.0400
Citric acid	0.0060	Ammonium ferric citrate	0.0060	$CaCl_2 \cdot 2H_2O$	0.0100	NaCl	1.0000	Vitamin B12	0.000001
Ammonium ferric citrate	0.0060	$EDTANa_2.2H_2O$	0.0010	$FeSO_4 \cdot 7H_2O$	0.0020	$MgSO_4 \cdot 7H_2O$	0.2000	Biotin	0.000001
$EDTANa_2.2H_2O$	0.0010	Na_2CO3	0.0200	Conc $H2SO_4$	0.0003	$CaCl_2 \cdot 2H_2O$	0.0400	Thiamine HCl	0.00001

(continued on next page)

Table 12-4 (continued)

Blue Green Algae Medium 11 (BG-11)		**BG-11 Medium without nitrogen (BG-11$_0$)**		**Modified Detmer Medium (MDM)**		**Soil-Extract Medium (SOT)**		**Cyanobacteria Broth Medium (CB)**	
Based on UTEX collection		Based on UTEX collection		Based on NIES collection		Based on NIES collection		Based on NIES collection	
Compound		g L^{-1}		Compound		g L^{-1}		Compound	
Na_2CO3	0.0200	H_3BO_3	0.00286 0	H_3BO_3	0.002860	$FeSO_4 \cdot 7H_2O$	0.01	$Na_2EDTA \cdot 2H_2O$	0.0030
H_3BO_3	0.00286 0	$MnCl_2.4H_2O$	0.00181 0	$MnSO_4 \cdot 7H_2O$	0.002500	$Na_2EDTA \cdot 2H_2O$	0.08	$Fe_3 \cdot 6H_2O$	0.000588
$MnCl_2.4H_2O$	0.00181 0	$ZnSO_4.7H_2O$	0.00022 0	$ZnSO_4 \cdot 7H_2O$	0.000222	H_3BO_3	0.002860 0	$MnCl_2 \cdot 4H_2O$	0.000108
$ZnSO_4.7H_2O$	0.00022 0	$Na_2MoO4.2H_2O$	0.00039 0	$CuSO_4 \cdot 5H_2O$	0.000079	$MnSO_4 \cdot 7H_2O$	0.002500 0	$ZnSO_4 \cdot 7H_2O$	0.000066
$Na_2MoO4.2H_2O$	0.00039 0	$CuSO_4.5H_2O$	0.00007 9	$Na_2MoO4 \cdot 2H_2O$	0.000021	$ZnSO_4 \cdot 7H_2O$	0.000222 0	$CoCl_2 \cdot 6H_2O$	0.000012
$CuSO_4.5H_2O$	0.00007 9	$Co(NO_3)2.6H_2O$	0.00004 9			$CuSO_4 \cdot 5H_2O$	0.000079 0	$Na_2MoO_4 \cdot 2H_2O$	0.000007 5
$Co(NO_3)2.6H_2O$	0.00004 9					$Na_2MoO4.2H_2O$	0.000021 0	Tris (hydroxymeth	0.5000

12.5 Media Compatibility Testing

Each species has its own maintenance medium recommended by its culture collection. To identify a single medium that could support all species and avoid effects from differing nutrient compositions (section 0), every species was grown in all maintenance media (marine: ASN-III, ESM, L1-Si; freshwater: BG-11, BG-11_0, CB, MDM, SOT). Media compositions can be found in Table 12-3 and Table 12-4 in the appendix. Pre-culture (50µL) of each species were added aseptically to 250µL medium in 96-well-plates. The cyanobacteria were cultivated under ambient temperature and light conditions. Absorbance at 750 nm was measured twice per week to analyse growth.

Prior to the EPS screening experiment, the compatibility of the cyanobacterial species with different media was tested. Table 12-5 shows the growth of freshwater cyanobacteria based on five different media (BG-11, BG-11_0, MDM, CB and SOT medium) as a heatmap. The majority of the species (6 out of 10 species) grew strongest in BG-11, reaching OD_{750} values of up to 1.638 ± 0.017 (*A. platensis*). *N. foliaceum* and *N. zetterstedtii* grew best in CB medium (OD_{750} of 0.579 ± 0.036 and 0.569 ± 0.025, respectively). *N. longstaffi* grew most in MDM medium (OD_{750} of 0.243 ± 0.170), and *C. brevissima* showed highest growth in BG-11_0 (OD_{750} of 0.552 ± 0.088). Interestingly, this species grew better in BG-11_0 than BG-11, indicating that it is a nitrogen-fixing species. This agrees with literature [342]. SOT medium resulted in the least growth for almost all freshwater species. The only exception was *A. platensis*, which was maintained in this medium in the culture collection (NIES). Based on these observations, BG-11 was selected as the growth medium, since it was suitable for all freshwater species and is widely used in literature.

Table 12-5 Growth of novel freshwater cyanobacterial species depending on different freshwater media (BG-11, BG-11_0, CB, MDM, SOT).Table displays absorbance value (OD_{750}) after 44 days of growth in microplates under ambient light and temperature conditions. Results colour-coded for most (green) and least (red) growth of species. Values show mean ± 1 standard deviation (n=3). Abbreviations: G.a.: *Gloeocapsa alpicola*; A.o.: *Anabaena oscillarioides*; N.f.: *Nostoc foliaceum*; N.l.: *Nostoc longstaffi*; N.z.: *Nostoc zetterstedtii*; T.s.: *Trichormus subtropicus*; C.b.: *Calothrix brevissima*; F.d.: Fremyella diplosiphon; S.r.: *Sphaerospermopsis reniformis*; A.p.: *Arthrospira platensis*.

	BG-11	**BG-11_0**	**MDM**	**CB**	**SOT**
G. a.	1.016 ± 0.086	0.854 ± 0.012	0.347 ± 0.049	0.463 ± 0.096	0.072 ± 0.023
A. o.	1.479 ± 0.002	0.954 ± 0.057	1.377 ± 0.025	0.127 ± 0.001	0.078 ± 0.028
N. f.	0.376 ± 0.378	0.484 ± 0.088	0.209 ± 0.011	0.579 ± 0.036	0.163 ± 0.103
N. l.	0.098 ± 0.002	0.226 ± 0.026	0.243 ± 0.170	0.008 ± 0.073	0.077 ± 0.011
N. z.	0.454 ± 0.081	0.240 ± 0.031	0.364 ± 0.227	0.569 ± 0.025	0.089 ± 0.024
T. s.	1.221 ± 0.168	0.759 ± 0.270	1.138 ± 0.400	0.457 ± 0.147	0.566 ± 0.295
C. b.	0.304 ± 0.155	0.552 ± 0.088	0.393 ± 0.079	0.112 ± 0.007	-0.02 ± 0.005
F. d.	0.557 ± 0.053	0.485 ± 0.067	0.410 ± 0.072	0.356 ± 0.176	0.032 ± 0.024
S. r.	0.324 ± 0.019	0.153 ± 0.034	0.010 ± 0.005	0.026 ± 0.021	0.014 ± 0.012
A. p.	1.638 ± 0.017	1.356 ± 0.011	1.180 ± 0.004	0.003 ± 0.028	1.245 ± 0.113
C-	-0.11 ± 0.145	0.009 ± 0.008	0.041 ± 0.008	0.022 ± 0.012	0.039 ± 0.002

The growth of marine cyanobacteria in different marine media (ESM, ASN-III, L1-Si) is depicted in Table 12-6. Half of the species grew the strongest in ESM, whereas *P. breve*, *O. rosea* and *P. keutzingianum* grew better in L1-Si or ASN-III. However, these species still showed acceptable growth in ESM, which is why this medium was selected for the screening experiment, as it appeared to be suitable for all marine species.

Table 12-6 Growth of novel marine cyanobacterial species *Phormidium breve*, *Phormidium keutzingianum*, *Spirulina major*,*Acaryochloris marina*, *Oscillatoria rosea* and *Tychonema bornetii* in different marine media (ASN-III, ESM, L1-Si).Table displays absorbance value (OD_{750}) after 38 days of growth in microplates under ambient light and temperature conditions. Results colour-coded for most (green) and least (red) growth of species. Values show mean ± 1 standard deviation (n=3).

	ESM	**ASN-III**	**L1-Si**
P. breve	0.058 ± 0.017	0.046 ± 0.037	0.103 ± 0.007
P. keutzingianum	0.359 ± 0.357	0.713 ± 0.049	0.132 ± 0.073
S. major	0.547 ± 0.022	0.214 ± 0.084	0.250 ± 0.022
A. marina	0.625 ± 0.012	0.393 ± 0.022	0.501 ± 0.004
O. rosea	0.967 ± 0.008	1.033 ± 0.028	0.282 ± 0.003
T. bornetii	0.228 ± 0.030	0.108 ± 0.013	0.077 ± 0.007
C-	0.004 ± 0.005	0.021 ± 0.003	-0.01 ± 0.011

12.6 Thermal Degradation Behaviour of Novel Cyanobacteria

Thermogravimetric analysis (TGA) is used to assess the thermal behaviour and stability of EPS, revealing distinct degradation phases. These typically include the loss of bound water molecules in Phase I, depolymerization and bond breakage in Phase II, and the formation of graphitic carbon in the final phase [54, 269]. The residual EPS content, such as uronic acids, sulfate groups, and cations, can hinder complete decomposition [269]. TGA results are beneficial for understanding the thermal stability and potential applications of polysaccharides.

Thermogravimetric analysis (TGA) was carried out under nitrogen atmosphere with a heating rate of 20 °C min^{-1}. The temperature ranged from 30°C to 670°C. Around 5.5 mg of sample was placed in a platinum pan and the TGA system calibrated in terms of weight and temperature (four standard Curie points) prior to sample analysis [383].[28]

[28] TGA was performed by Bradley Hopkins (University of Nottingham).

TGA was performed to determine the thermal behaviour and stability of the novel EPS. As shown in Figure 12-4, thermal degradation took place in three phases. In the first phase, between 30°C and 100°C, a minor decrease in weight was observed across all species, with a weight loss of around 10-15%. After this phase, the weight remained stable between 100°C and approximately 250°C, where changes in weight were as low as 2% to 9%. A second major degradation phase began around 250°C and extended to 350°C. For all species, this was the major degradation phase, with species losing between 34% and 55% of their weight. EPS from *N. longstaffi* showed the strongest weight loss, only retaining 27% of its weight at 350°C. EPS from *C. brevissima* retained only about 34% of its original weight by 350°C. EPS from three species, *A. oscillarioides, N. zetterstedtii* and *T. subtropicus* showed a rapid reduction, with only around 40% weight remaining by 350°C. EPS from *N. zetterstedtii* lost the least weight in phase II, with 47% residual weight at 350°C. The third phase of degradation occurred approximately between 350°C and 500°C. The novel EPS lost between 9% and 25%. EPS from *C. brevissima* lost the most weight during the third degradation phase, retaining only 9% of the original weight by 500°C. Least degradation in the third phase was observed in EPS from *N. longstaffi*, which retained 20% of its residual weight by 500°C. EPS from *A. oscillarioides, N. zetterstedtii* and *T. subtropicus* lost around 15% each in this phase, resulting in 23%, 32% and 26% of the initial weight remaining, respectively. Between 500°C and 600°C, some species continued to degrade, though the weight loss was less pronounced. The residual weight at 600°C showed variation across species. EPS from *C. brevissima and N. foliaceum* exhibited almost complete degradation, leaving -1% and 10% residual weight, respectively. EPS from *N. longstaffi, T. subtropicus*, and *A. oscillarioides* retain about 20% of their initial weight, while EPS from *N. zetterstedtii* retains 29%, showing the highest residual weight among all species.

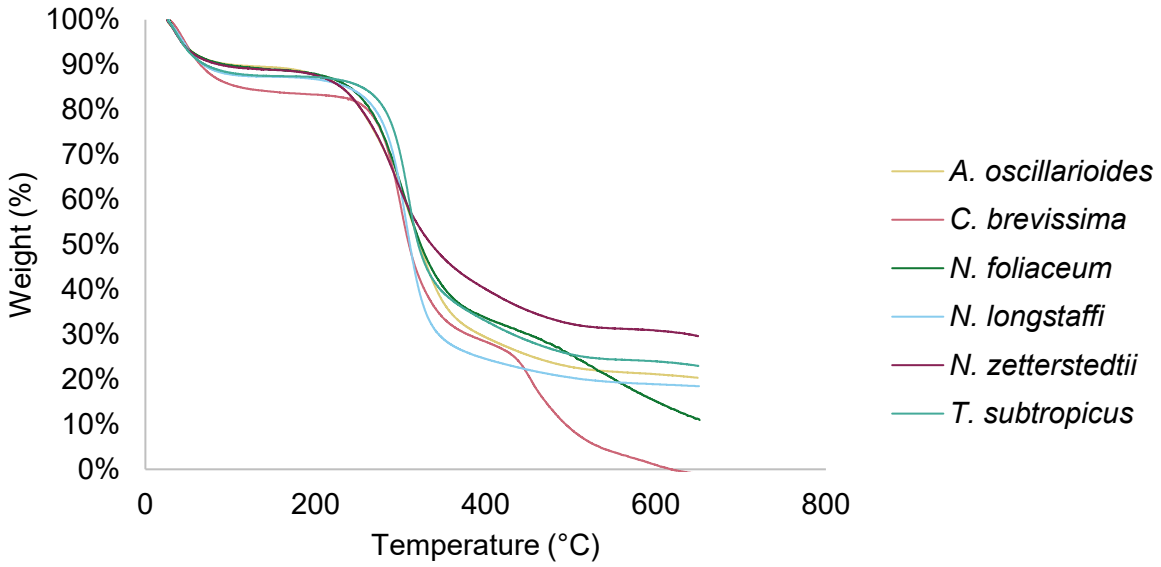


Figure 12-4 Thermal degradation profile obtained with Thermogravimetric Analysis of novel extracellular polymeric substances from *Anabaena oscillarioides, Calothrix brevissima, Nostoc foliaceum, Nostoc longstaffi, Nostoc zetterstedtii* and *Trichormus subtropicus*.Analysis was performed with n=1 per species, without biological replicates.

Three well-differentiated thermal degradation steps have been observed for several EPS from cyanobacteria in literature [54, 269]. Phase I involves loss of physically absorbed or bound water molecules [269]. Phase II marks depolymerization accompanied by the breakage of C–O and C–C bonds in the ring units resulting in the release of CO, CO_2 and H_2O [54, 269]. The final phase includes formation of graphitic carbon and polynuclear aromatic structures [54]. The residual EPS content can be attributed to uronic acids, sulphate groups and cations, which prevent complete decomposition [269].

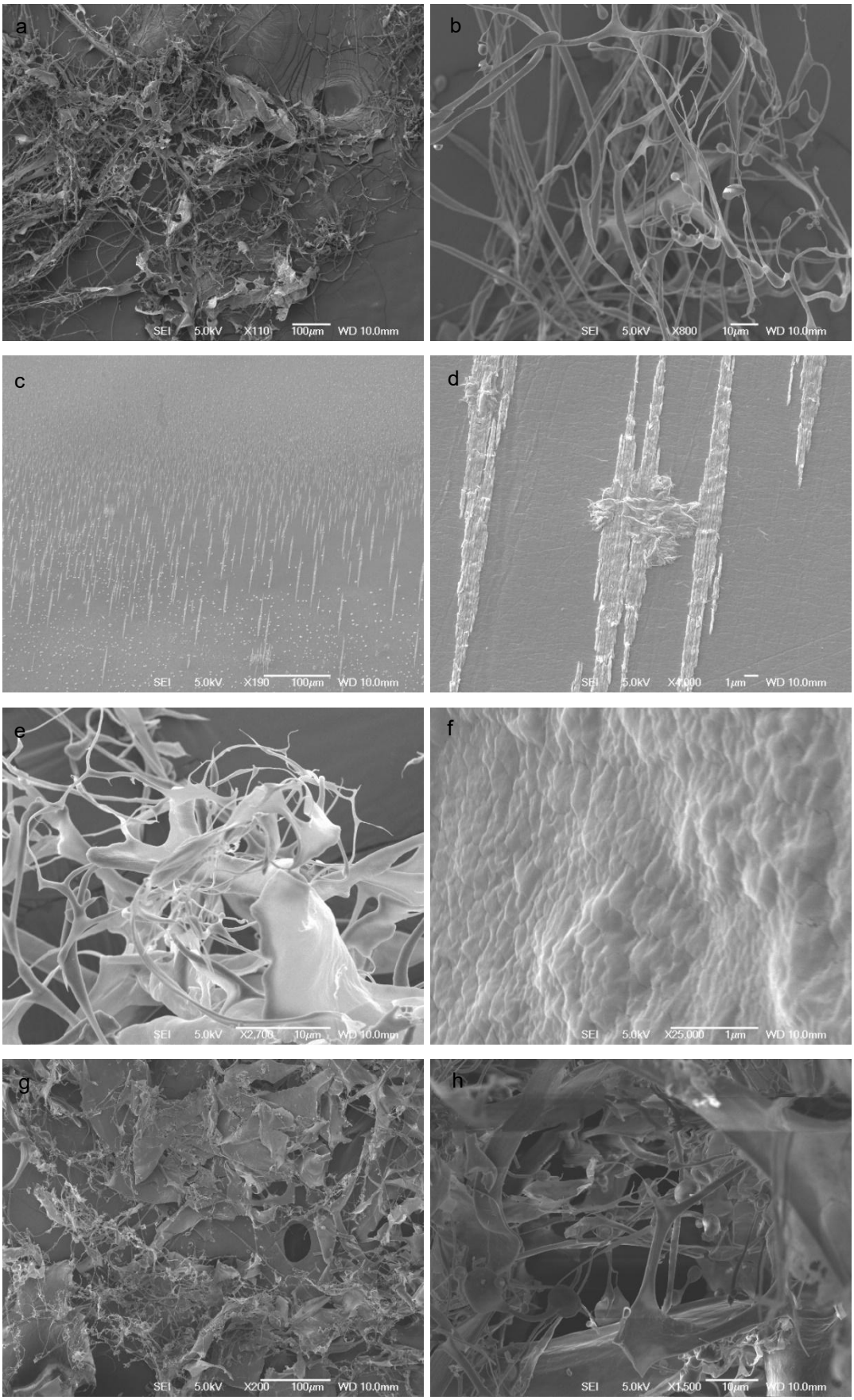
The thermal behaviour and stability of a polysaccharide determine its applicability [269]. The results indicate that EPS from *N. zetterstedtii*, *A. oscillarioides*, *N. longstaffi* and *T. subtropicus* exhibit higher thermal stability, possibly due to a higher content of thermally resistant compounds, such as minerals or highly cross-linked polysaccharides. This makes them more suitable for applications requiring heat resistance. In contrast, EPS from *C. brevissima* and *N. foliaceum* show lower thermal

stability, indicated by their earlier decomposition onset and lower residual weight, suggesting a greater proportion of easily degradable organic components.

12.7 Scanning Electron Microscopy (SEM) Pictures Novel Cyanobacteria

Scanning electron microscopy (SEM) provides detailed images of the morphology, which is particularly useful for observing crystalline structures or fibril width [384]. The samples were cut down to size and placed onto aluminium specimen stubs using carbon double-sided adhesive tape. They were then coated with roughly 10 nm of iridium to create a conductive surface to allow for imaging in the SEM. The SEM used was a JEOL 7000 Field Emission Gun Scanning Electron microscope. The samples were imaged at a working distance of 10 mm using an acceleration voltage of 5 kV.[29] Fibril width of EPS was estimated using the Analyze Feature of ImageJ software [385]. The width of ten different fibres was analysed, and the average was calculated using MS Excel [386]. The fibril widths of the novel EPS were analysed using scanning electron microscopy (SEM). As shown in Figure 12-5, EPS from all species were fibrous, except *A. marina*, which was film-like. The fibril width was analysed, and the results are shown in Table 12-7.

[29] SEM was performed by Lorelei Robertson (University of Nottingham).


a
SEI 5.0kV X110 100μm WD 10.0mm
b
SEI 5.0kV X800 10μm WD 10.0mm
c
SEI 5.0kV X190 100μm WD 10.0mm
d
SEI 5.0kV X4,000 1μm WD 10.0mm
e
SEI 5.0kV X2,700 10μm WD 10.0mm
f
SEI 5.0kV X25,000 1μm WD 10.0mm
g
SEI 5.0kV X200 100μm WD 10.0mm
h
SEI 5.0kV X1,500 10μm WD 10.0mm

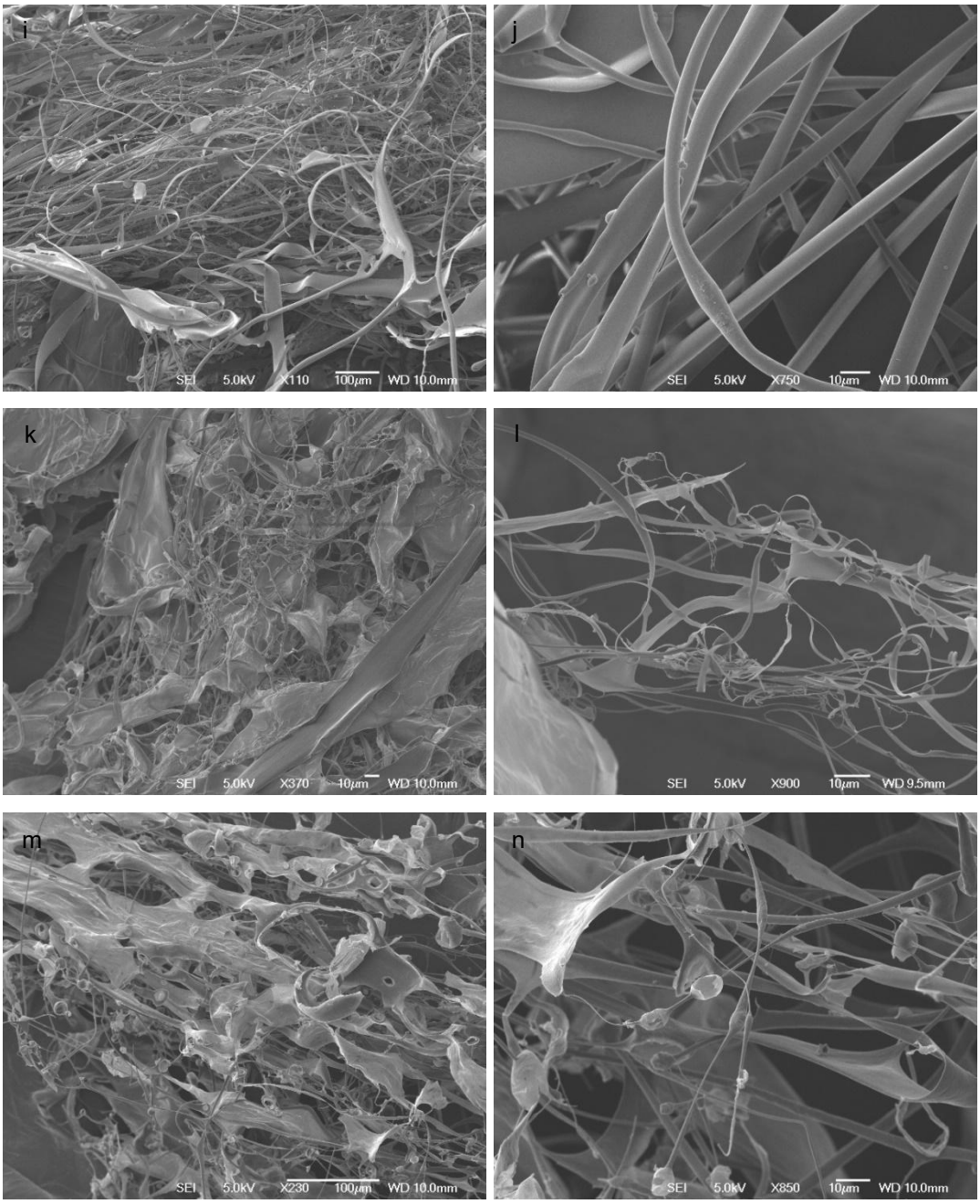


Figure 12-5 Scanning Electron Microscopy (SEM) pictures of EPS from seven novel cyanobacterial species.(a-b) *Anabaena oscillarioides*; (c-d) *Acaryochloris marina*; (e-f) *Calothrix brevissima*; (g-h) *Nostoc foliaceum*; (i-j) *Nostoc longstaffi*; (k-l) *Nostoc zetterstedtii*; (m-n) *Trichormus subtropicus*.

As shown in Table 12-7, the average fibril width of EPS from *A. oscillarioides* was 1.68 ± 0.86 µm (n=10), with a range from 0.63 to 3.39 µm. EPS from *C. brevissima* had an average width of 0.69 ± 0.42 µm (n=10), ranging between 0.22 and 1.65 µm, while EPS from *N. foliaceum* displayed an average of 1.08 ± 0.61 µm (n=10), with values

from 0.25 to 2.04 µm. The EPS fibrils of *N. longstaffi* were the thickest, averaging 5.99 ± 2.26 µm (n=10), and varied from 2.36 to 9.52 µm. For EPS from *N. zetterstedtii*, the average width was 1.73 ± 0.74 µm (n=10), ranging from 0.73 to 2.98 µm.

Table 12-7 Fibril width of extracellular polymeric substances (EPS) from seven novel cyanobacterial species.Values are presented as mean ± standard deviation of technical replicates (n=10).

Species	**Fibril width (µm)**
A. oscillarioides	1.68 ± 0.86
A. marina	No fibrils (film)
C. brevissima	0.69 ± 0.42
N. foliaceum	1.08 ± 0.61
N. longstaffi	5.99 ± 2.26
N. zetterstedtii	1.73 ± 0.74
T. subtropicus	2.25 ± 1.32

EPS from *T. subtropicus* showed an average fibril width of 2.25 ± 1.32 µm (n=10), with a range of 0.55 to 3.63 µm. No fibril width data was available for *A. marina*, as the EPS formed a film without distinct fibrils. EPS from *N. longstaffi* exhibited the largest fibril widths, while *C. brevissima* had the smallest.

12.8 Comparative Analysis of Film-like and Cotton-like Appearance of *C. brevissima* EPS

12.8.1 Thermogravimetric Analysis (TGA)

Thermal degradation profiles (Figure 12-6*b*), showed similar results for both EPS. The EPS followed the typical three-step degradation described in section 12.6. The main difference was a higher thermal stability and higher residual content of the shiny-film EPS, which was 34% compared to 26%. This could be a result of the presence of uronic acids in the shiny film EPS [269]. This was also different from the TGA results of *C. brevissima* EPS in the screening experiment (section 12.6), which underwent complete degradation, leaving -1% residual weight. All in all, it is unclear, which compositional or structural feature resulted in the different appearances.

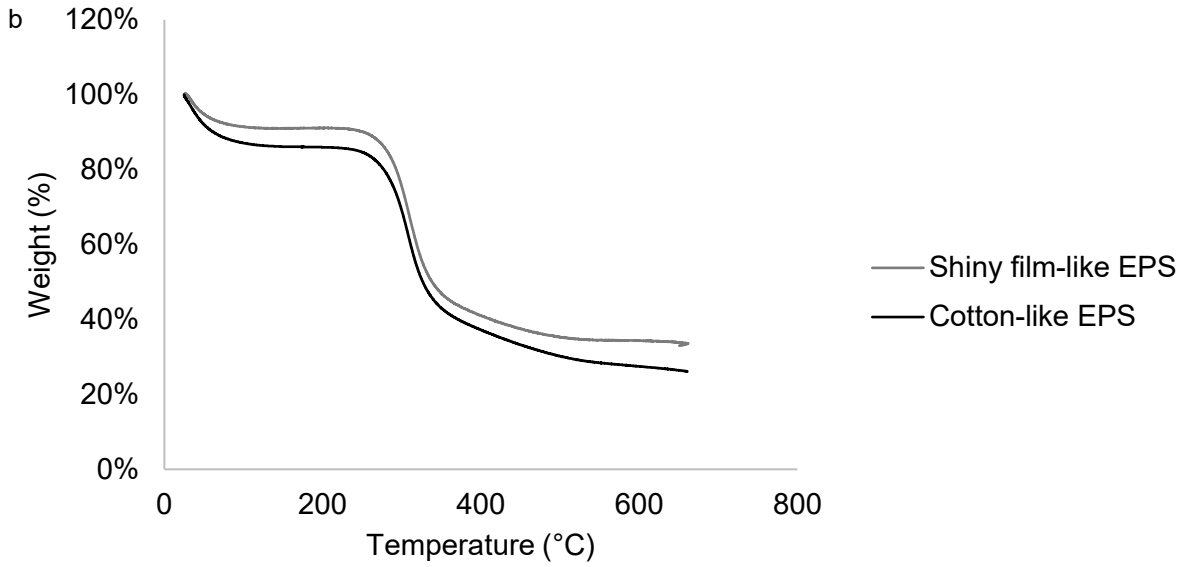


Figure 12-6 Thermal degradation profile of shiny film-like and cotton-like extracellular polymeric substances (EPS) from *Calothrix brevissima* based on Thermogravimetric Analysis.

12.8.2 Scanning Electron Microscopy (SEM)

Additionally, Scanning Electron Microscopy (SEM) pictures were taken, and the fibril width was analysed. The SEM pictures are shown in Figure 12-7. The fibril width of the cotton-like EPS of *C. brevissima* was 3.55 ± 1.81 µm, ranging from 1.39 to 6.26 µm. This was significantly different (p=0.0007) from the width of this species measured in the screening experiment (section 12.7), which was considerably lower (0.69 ± 0.42 µm). The earlier samples (shiny film-like) also appeared as a film on the SEM pictures, leading to no fibril width being determined.

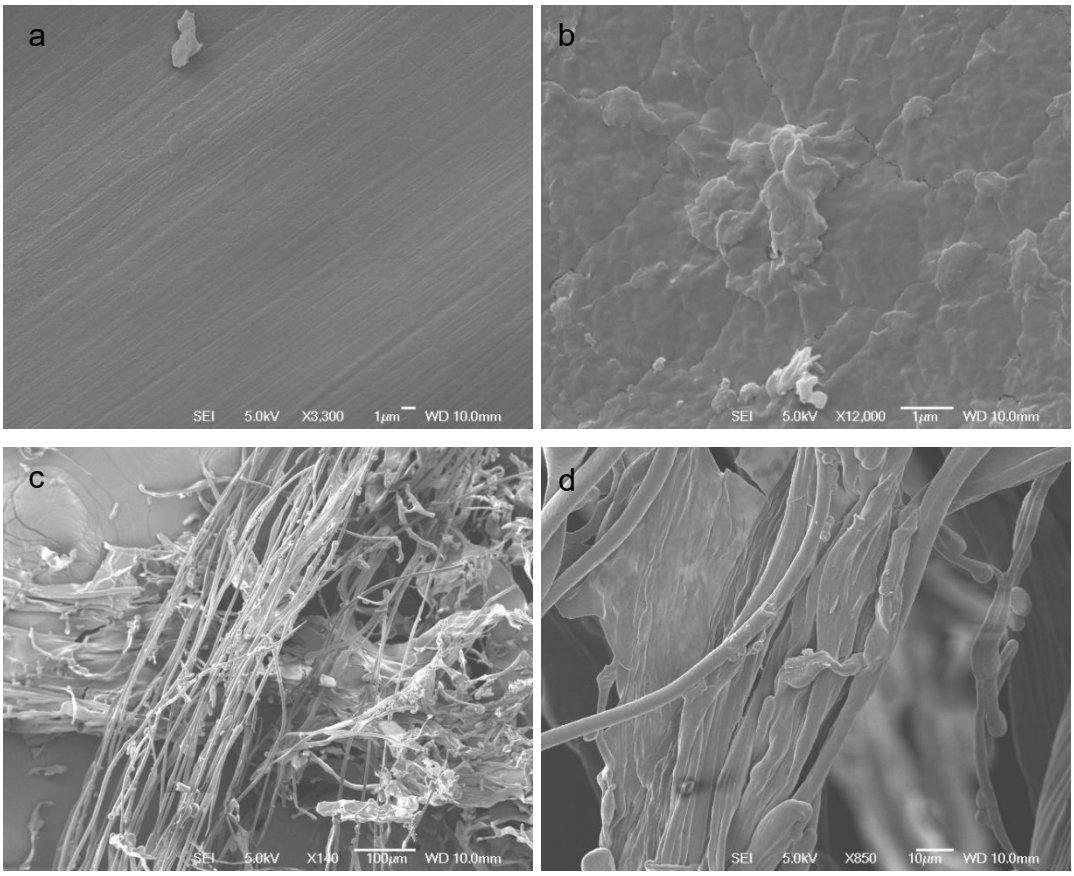


Figure 12-7 Scanning Electron Microscopy (SEM) pictures of extracellular polymeric substances (EPS) from *Calothrix brevissima*.(a) SEM pictures of early EPS samples (day 14 and 28) appearing shiny film-like. (b) SEM pictures of later EPS samples (day 42 and 56) appearing cotton-like.

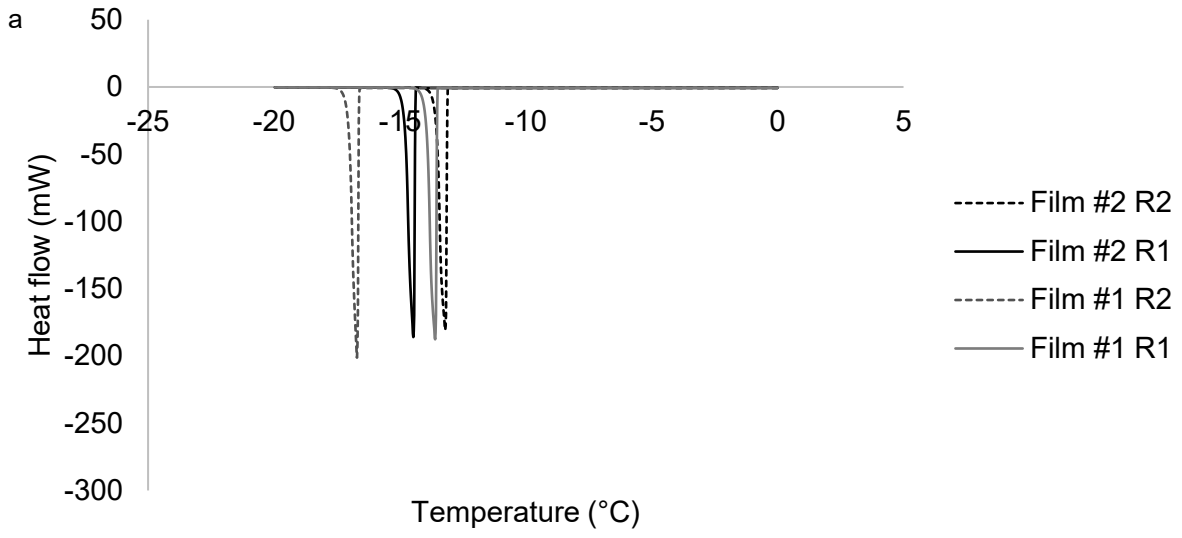
12.8.1 Differential Scanning Calorimetry (DSC)

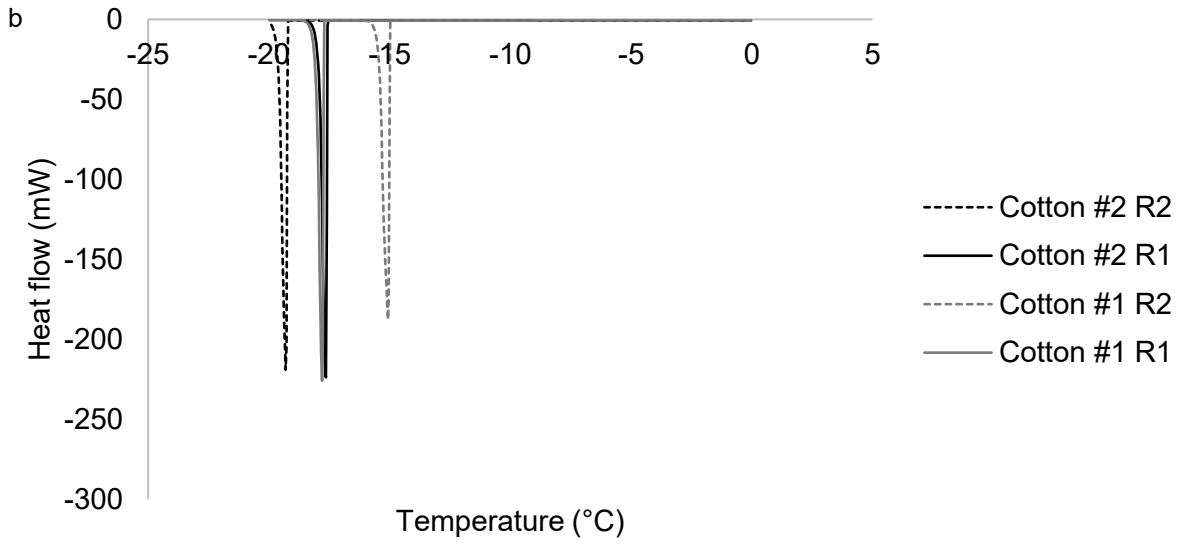
Differential scanning calorimetry (DSC) can characterize the thermal properties, indicating whether the EPS is amorphous or crystalline [63]. DSC was performed using a cyclic temperature method under nitrogen purge (N_2, 25.0 mL min^{-1}) with data collected at 1.0-second intervals. The cycle began with equilibration at 20.0°C for 2.0 minutes, followed by cooling from 20.0°C to -20.0°C at a rate of -1.0 K min^{-1}, a hold at -20.0°C for 2.0 minutes, and then heating back to 20.0°C at 1.0 K min^{-1}. This sequence was repeated with an additional hold at 20.0°C for 2.0 minutes before the second cooling and heating cycle [387]. Biological duplicates of the samples were analysed in technical duplicates. Each sample was run for two cycles of heating and freezing.

Locust bean gum and water in technical duplicates were used as positive and negative control, respectively.[30]

The DSC results of the film-like and cotton-like EPS samples are presented in Figure 12-8. The shiny film-like EPS exhibited an exothermic peak between -12°C and -17°C, whereas the cotton-like EPS showed an exothermic peak at a slightly lower temperature, in the range of -15°C to -20°C. Each sample was performed in biological duplicates and technical duplicates, resulting in four peaks for cotton-like EPS and four peaks for shiny film-like EPS. For both types of EPS, there was a larger difference between the technical replicates than the biological replicates, possibly indicating inaccuracy stemming from the equipment. In most samples, the temperature of the exothermic peak remained consistent across repeated heating and cooling cycles, with the second cycle closely matching the initial peak temperature (second cycle data not shown). The exothermic peak of the positive control, locust bean gum, and the solvent, water, also occurred at low temperatures of -17°C to -19°C. This was much lower than expected given the typical freezing point of water. There were additional issues, including instances where several replicates exhibited a flat line, such as the second replicate of water. The cause for these problems is unknown.

[30] DSC was conducted by Darrell Cobon (University of Nottingham).


a
50
0
-25
-20
-15
-10
-5
0
5
-50
-100
-150
-200
-250
-300
Heat flow (mW)
Temperature (°C)
Film #2 R2
Film #2 R1
Film #1 R2
Film #1 R1


b
0
-25
-20
-15
-10
-5
0
5
-50
-100
-150
-200
-250
-300
Heat flow (mW)
Temperature (°C)
Cotton #2 R2
Cotton #2 R1
Cotton #1 R2
Cotton #1 R1

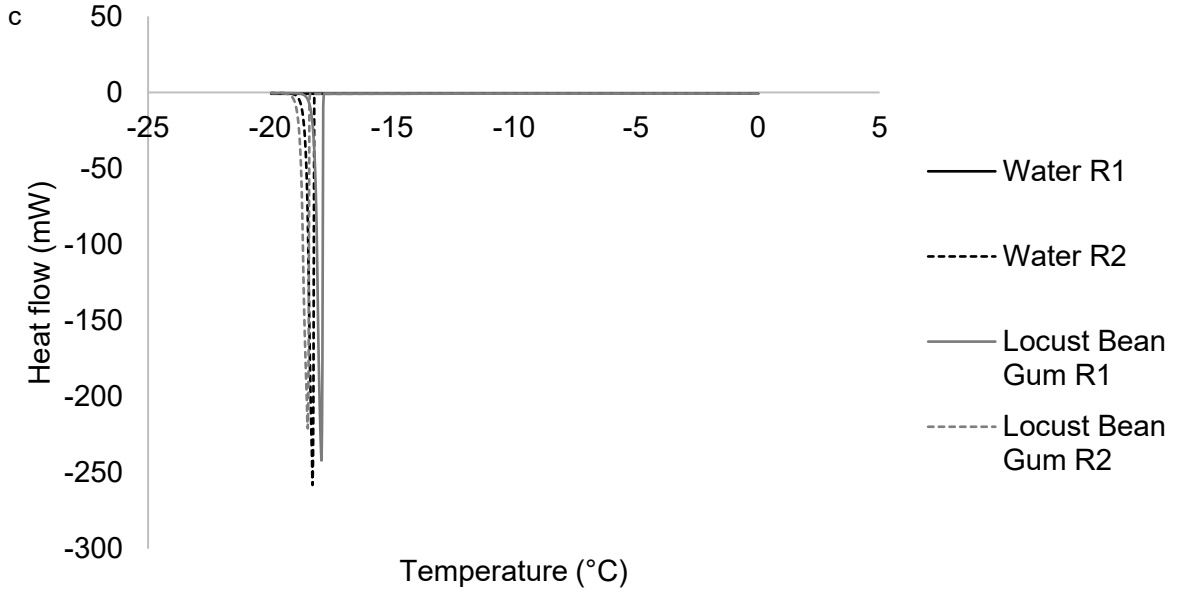

c
50
0
-25
-20
-15
-10
-5
0
5
-50
-100
-150
-200
-250
-300
Heat flow (mW)
Temperature (°C)
Water R1
Water R2
Locust Bean Gum R1
Locust Bean Gum R2

Figure 12-8 Differential Scanning Calorimetry (DSC) of *Calothrix brevissima* extracellular polymeric substances (EPS), locust bean gum (positive control, C^+) and water (negative control, C^-).(a) DSC of early EPS samples (day 14 and 28) appearing shiny film-like. (b) DSC of later EPS samples (day 42 and 56) appearing cotton-like. Abbreviations: #: number of biological replicate; R: technical replicate.

A summary of onset, peak and endset temperatures (°C) of film-like and cotton-like EPS, water and locust gum are shown in Table 12-8. Overall, there were no statistically significant differences between the sample types across all three temperature parameters ($p>0.05$). Since the second replicate of water showed a flat line, statistical analysis of differences to EPS and locust bean gum were not possible. A repetition of the analysis could not be performed due to time constraints. Since film-like EPS appeared to show a slightly higher freezing point than cotton-like EPS and the difference was not statistically significant, this suggests that the visual differences between the EPS types were not due to significantly different freezing behaviours.

Table 12-8 Onset, peak, and endset temperatures (°C) during Differential Scanning Calorimetry (DSC) of extracellular polymeric substances (EPS) from *Calothrix brevissima*, water (negative control, C^-), and locust bean gum (positive control, C^+).Cultures were grown under 50 µmol m^{-2} s^{-1}, 25°C, 150 RPM shaking, and 60% working volume (30 mL culture in 50 mL Erlenmeyer flasks). Early EPS samples (day 14) show a shiny film-like appearance, whereas later samples (day 56) appear cotton-like. Values show mean of replicates ± one standard deviation (n=2). Standard deviation of water could not be determined as the second replicate failed.

Sample	**Onset (°C)**	**Peak (°C)**	**Endset (°C)**
Film-like EPS	-14.3 ± 1.5	-3.9 ± 1.3	-13.2 ± 1.6
Cotton-like EPS	-17.2 ± 1.7	-5.7 ± 1.3	-15.8 ± 1.5
Water	-18.1	-4.5	-16.4
Locust bean gum	-17.9 ± 0.6	-5.8 ± 1.2	-16.5 ± 0.7

12.9 UV-absorbance of EPS from *Calothrix brevissima* Cultivated Under High Light

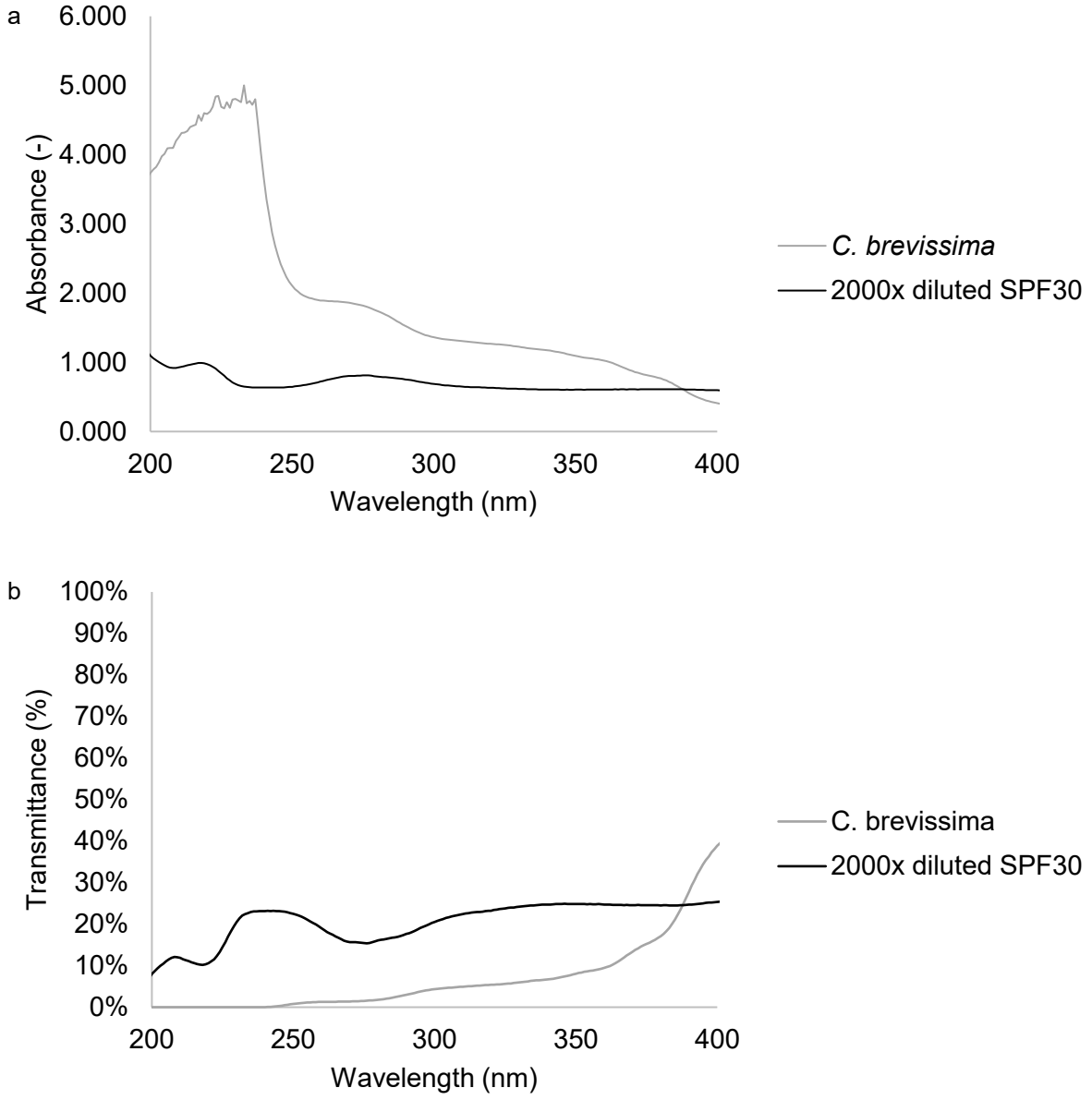


Figure 12-9 Absorbance and transmittance of the supernatant (0.385 g EPS L^{-1}) of *Calothrix brevissima* grown for 7 days at 31°C and 450 µmol m^{-2} s^{-1}, and of 2000x diluted sunscreen (SPF30, 0.5 g L^{-1}).(a) UV/vis absorbance spectrum depending on wavelength. (b) Transmittance depending on wavelength.

12.10 Sterilisation and Inoculation Procedures for PBRs

The sterilisation and inoculation procedures are shown in Figure 12-10. PBR vessels and lids with all components, except the pH sensor, were wiped down with Isopropyl alcohol (IPA) and placed upside down in the MSC. The PBRs were exposed to UV light for 5 min, flipped and exposed to UV light for another 5 min to sterilise the inside and outside (Figure 12-10*a*). Sterile MQ water (1 L) and 0.236 mL sodium hypochlorite (14%) were added, and the PBRs were closed by placing the lid on the vessel. All other components were connected aseptically: The pH sensor was sterilised with IPA and fitted into the lid. The autoclaved inlet filter was fitted on the gas inlet. The autoclaved foam trap was connected to the PBR vent. An autoclaved silicon tube (1mm I.D x 2mm O.D) was connected to the sampling port via a male-luer-to-barb connector. The other end of the silicon tube was fitted with a female-luer-to-barb connector and closed with a luer lock plug. The PBRs were taken out of the MSC, left to soak for 2 hours and subsequently aerated for 24 hours. After 24 hours of sterilisation, the ends of the sampling tubes were sterilised with IPA and placed in the MSC (Figure 12-10*b*). Filter-sterilised sodium thiosulphate (10 mL, 3.63 g L^{-1}) was added with syringes through the sampling port (Figure 12-10*c*). The PBRs were left to soak for 2 hours and subsequently aerated for 24 hours for neutralisation.



Figure 12-10 Sterilisation and inoculation protocol Xanthella MicroPharos photobioreactors (PBRs).(a) Assembly of PBRs in Microbial Safety Cabinet (MSC). (b-c) After 24 hours of sterilisation with sodium hypochlorite, neutralisation reagent was added via sampling port tubing placed in MSC. (d) After 24 hours of neutralisation, PBRs were pumped empty. (e) Foam trap was placed in MSC and swapped with Duran bottle containing inoculum. (f) Inoculum was pumped through the vent into the PBR.

The sterilised and neutralised PBRs were pumped empty by placing the ends of the sampling tubes into a sterile bottle in the MSC (Figure 12-10*d*). The foam trap bottle was placed in the MSC and swapped with the bottle containing the inoculum (Figure 12-10*e*). Inoculum was pumped through the vent into the PBR (Figure 12-10*f*). Contamination checks were performed of the sterilised PBRs, the inoculum and each sample.

12.11 Conference Presentations and Posters

12.11.1 Oral Presentations

Christine Steffen, Dr. Yanming Wang, Prof. Jon McKechnie, Dr. Konstantina Kourmentza (2023). Oral Presentation. Renewable Resources and Biorefineries, Riga, Latvia.

12.11.2 Conference Posters

Christine Steffen, Dr. Yanming Wang, Prof. Jon McKechnie, Dr. Konstantina Kourmentza (2024). Conference Poster. Biomass Biorefinery Network, Sheffield, UK.

Christine Steffen, Dr. Yanming Wang, Prof. Jon McKechnie, Dr. Konstantina Kourmentza (2023). Conference Poster. A Festival of Algae, Manchester, UK.

Christine Steffen, Dr. Yanming Wang, Prof. Jon McKechnie, Dr. Konstantina Kourmentza (2023). Conference Poster. Environmental Biotechnology Network, Edinburgh, UK. (Third place for Best Poster Award).

Christine Steffen, Dr. Yanming Wang, Prof. Jon McKechnie, Dr. Konstantina Kourmentza (2022). Conference Poster. Engineering Showcase, Nottingham, UK. (Runner-up for Best Poster Award).

Christine Steffen, Dr. Yanming Wang, Prof. Jon McKechnie, Dr. Konstantina Kourmentza (2022). Conference Poster. Carbon Recycling Network, Nottingham, UK.